WAVE OBSTACLE INTERACTION FOR A SUBMERGED HORIZONTAL CIRCULAR CYLINDER

BY

D.J. LACEY, B.Sc.

Thesis submitted to The City University
for the Degree of Doctor of Philosophy
in the Department of Civil Engineering

October, 1983

SYNOPSIS

Theoretical and numerical investigations have been completed for the solution of the potential theory problem of wave scattering by the method of integral equations. It has been demonstrated that a distribution of sources over a boundary which is distinct from the fluid boundary results in a Fredholm integral equation of the first kind with a regular kernel. This is an alternative to the conventional integral equation formulations which are Fredholm equations of the second kind with singular kernels.

Application of the regular kernel method with a distribution of wave sources to the problem of waves interacting with a submerged circular obstacle in a two dimensional domain gives numerical results which are more accurate than the conventional methods for equivalent discretisation schemes. It has been found that the implementation of refinements to the discretisation scheme is only occasionally beneficial.

The experimental investigation of waves interacting with a submerged circular cylinder includes the measurement of the wave motion in the near-field and far-field and the measurement of pressures on the cylinder surface. The objective of the study is to determine whether the linear potential theory predictions are in agreement with the measured values. The experimental programme was designed to establish the importance of finite wave height and the extent to which measurements obtained for steeper waves and shallower cylinder submergence depart from the predictions of small amplitude theory.

Consideration has been given to the possibility of developing an appropriate non-linear theoretical model by reference to the alternative methods which are currently being investigated and the experimental results obtained in this study.

ACKNOWLEDGEMENTS

The work reported in this thesis was carried out in the Civil Engineering Department of The City University, London. Dr. K. Arumugam's supervision of the work has been greatly appreciated and the assistance of colleagues at The City University has been of considerable value. The author wishes to thank [redacted] in particular for his assistance in the early stages of the study.

[redacted] and [redacted] were responsible for the development of the software which has been employed in this study for the collection and analysis of experimental data. Mr. K.J. Williams carried out the experiments for the determination of a wave probe dynamic calibration correction factor and kindly supplied figure 5.3.2. [redacted] was responsible for the construction of the laboratory models and thanks are also extended to [redacted] for his help in the laboratory.

The writer gratefully acknowledges the work of [redacted] who typed the manuscript.

This work was made possible by the award of maintenance and support grants by the Science and Engineering Research Council.

CONTENTS

LIST OF FIGURES

LIST OF TABLES

CHAPTER 1 - INTRODUCTION

1.1 General Introduction

Offshore structures and marine vehicles must be designed to withstand the most demanding ocean conditions and to perform specific functions under the full range of environmental conditions. The theoretical and experimental investigation of wave motion and wave structure interaction spans a considerable range of topics and contributions to the development and application of the science have been made by applied mathematicians, naval architects and engineers from a number of disciplines.

The investigation of the motion of gravity waves has been studied by the applied mathematician since the nineteenth century and currently a variety of wave theories are available. The first applications of the classical wave theories to problems of engineering significance were concerned with the problem of the motion of ships and ever since the naval architect has been a major contributor to the development of the theoretical and physical understanding of wave structure interaction. More recently coastal and offshore engineering problems have received considerable research attention and the continued exploitation of offshore energy resources guarantees that a more complete understanding of wave structure interaction will be sought.

A number of mechanisms give rise to wave induced forces on fixed structural elements and the particular mechanisms which govern are determined by the geometry and location of the element

and the size of the element relative to the incident wave field. For elements with a characteristic dimension which is small compared with the incident wave the force imposed is made up of an inertia and a drag component with a transverse or lift force. Under these conditions the drag and lift forces are due to the existance of an oscillating fluid wake. As the relative size of the object increases the extent of this wake diminishes and, if the element has no sharp corners, eventually vanishes so that the magnitude of the drag and lift forces is sufficiently small to be neglected.

If the size of the structural element is large enough to deform the ambient wave field the element is subjected to the inertia force plus a diffraction force. It is assumed that for such an element the drag force may be neglected and a potential theory problem formulated. If an oscillating wake is introduced by any corners on the element the viscous effects are assumed to be local and are excluded from the analysis. The solution of the boundary value problem which may be posed for the diffraction or scattered wave potential permits the evaluation of the hydrodynamic pressure and thus the wave induced force. If additionally the structure is in motion a boundary value problem is posed for each degree of freedom and the potentials required to complete the analysis are the radiation potentials.

A number of alternative methods have been employed to provide potential theory formulations and solutions for these problems, but with the exception of very simple geometrical configurations no exact solutions are available and the solutions required must be obtained by numerical means. In recent years the finite element method (f.e.m.)

has been applied to obtain solutions for problems in wave hydrodynamics but the two methods with a greater tradition in the analysis of wave structure interaction are Ursell's multipole method and the method of integral equations both of which require the introduction of fluid singularities and the numerical solution of a system of linear algebraic equations.

The method of integral equations has been applied in a variety of ways and is referred to variously as the source distribution method, the boundary integral equation method (B.I.E.M.) or the boundary element method (b.e.m.) and the 'Frank Close Fit' method is included in this category. It is now possible to obtain the prediction of wave loads on offshore structures and marine vehicles by performing a three dimensional analysis and a number of computer packages have been developed for commercial use including NMIWAVE and MATTHEW. However, the principle method in the analysis of marine vehicles is the use of two-dimensional modelling with an appropriate strip theory.

A possible limitation of the above mentioned methods is concerned with the assumption of small amplitude waves which is necessary for the application of linear wave theory. In the ocean environment the waves incident upon a structure or vehicle may be steep and this has led to the suggestion that the finite amplitude of the waves should be accounted for by the development of a nonlinear theory for wave diffraction and radiation problems. The inclusion of the steady horizontal force based on an analysis of the transportation of momentum by gravity waves is straightforward since

only the reflected and transmitted wave heights are required and these may be obtained from the linear analysis. The evaluation of the non-linear oscillatory forces is not simple and while the subject has been considered by a number of researchers the only known case for which solutions have been obtained is for the vertical circular cylinder and this has been achieved by analytical rather than numerical means.

Experimental investigations of wave structure interaction effects are numerous and have been carried out for a number of purposes. For objects which are small compared with the ambient wave motion a vast number of model tests have been performed to establish the force mechanisms which are significant for a range of problems and also to provide data for the application of semi-empirical formulae. Many of these tests have been performed for analogous problems such as the oscillating cylinder in still water or the fixed cylinder in a U-tube and this analogous flow approach, while it suffers obvious limitations, has a number of distinct advantages over model tests for wave flows: firstly the variable parameters which are used to describe the wave motion may be varied independently and secondly it is possible to achieve satisfactory Reynolds' number scaling.

The motivation for model tests for problems in which the structural element spans a significant portion of the incident wavelength is different and is concerned with the validation of the theoretical predictions based on the solution of the potential theory problem. In particular the model test has proved particularly useful in determining whether and under what circumstances the assumptions of small amplitude wave theory and fluid inviscidity

are inappropriate.

The understanding of wave structure interactions and the development of suitable theoretical models which provide the basis for reliable design have clearly made great advances in recent decades. Much of the work has, however, been concerned with two particular types of structure or vehicle, namely the ship hull and the offshore platform. The bulk of research has therefore been geared to provide information relating to these geometric configurations and generally speaking the naval architect has been concerned with a single elongated obstacle located in the free surface and the engineer has been concerned with different types of structure located on the ocean bottom and spanning the entire water depth. More recently activity within the offshore industry has demanded the application of the established theory and understanding to a new variety of problems. Some notable examples are the estimation of wave induced forces on the hulls of a new breed of drilling platform, floating breakwaters andwave energy devices.

1.2 Introduction to the present study

A study has been made of wave diffraction by a horizontal circular cylinder submerged in water of finite depth. The thesis includes the results of a theoretical and numerical investigation of the application of the integral equation method to obtain the solution of wave hydrodynamics problems in a two dimensional domain and an experimental investigation designed for the validation of the numerical predictions.

The application of the method of integral equations to obtain the solutions of potential theory problem may take a number of alternative forms each of which is based on a result due to Green's theorem. The two methods which have been applied most frequently in the solution of wave hydrodynamics problems employ a singular solution of an associated potential theory problem which is referred to as the Green's function, the wave function or the wave source. The first of these methods employs a surface distribution of wave sources and double sources and the integral equation is solved to obtain the unknown potential. This method has therefore been called the direct method to distinguish it from the second method which employs a surface distribution of sources only with an initially unknown variation of density. In this method application of the kinematic boundary condition on the object gives rise to an integral equation for the source density function and the solution may then be applied to obtain the value of the unknown potential. The second method has been called the indirect method.

In this study the solution of the linear diffraction boundary value problem by the indirect boundary value problem has been discussed in detail. It has been demonstrated that an integral equation may be formulated in which the scattered wave velocity potential is expressed as a continuous distribution of sources over a fictitious boundary outside the fluid domain. This approach in which the kernel of the integral equation is regular may not be applied in the direct method.

The formulation of a second-order diffraction boundary value problem in integral equation form has been presented and it has been demonstrated that the indirect method is to be preferred

to the direct method in this case on the basis of efficiency. In deriving expressions for the second-order wave profile for the diffraction problem it has been shown that two distinct second-order corrections must be included. The first is similar to the correction in the second-order Stokes wave and is referred to as a fixed second order component. The second correction, due entirely to the presence of the object, is quite distinct and may be regarded as the inclusion of a free wave oscillating at twice the incident wave frequency travelling with a wave speed which is independent of the incident wave speed.

The numerical investigation has two aspects. The first and major aim is to determine whether the regular kernel integral equation formulation is amenable to numerical solution and the second is to examine the effect of refining the numerical techniques employed in the discretisation of the integral equations. A diffraction computer program has been written which includes the option of the conventional singular kernel method in addition to the regular kernel method and results have been presented for both cases for a range of problems. The alternative discretisation schemes incorporated in the program permit the selection of an assumed constant, linear or quadratic variation of source density on an element with a quadrature formula of a specified order. The choice of element type and quadrature formula have been varied in order to establish the most suitable scheme for the particular problems considered.

An experimental programme has been designed and carried out for the validation of the predictions of small amplitude, inviscid theory. In particular the tests have been concerned with a

cylinder which is located at small depths of submergence since it is for obstacles in this region that the physical mechanisms of wave structure interaction are least well understood. The tests have also been designed to establish the effects of finite wave height and therefore to determine the value of a non-linear solution of the diffraction problem for this particular problem.

The experimental programme has been carried out in two stages. The first stage is concerned with the comparison of the linear diffraction predictions for the wave motion with the measurements obtained in the laboratory. The purpose of this work was firstly to identify the mechanisms which might be significant in inducing a force on the obstacle, secondly to determine whether the wave object interaction resulted in any dissipation of wave energy and thirdly to establish the order of the free waves identified in previous laboratory tests and predicted by second-order diffraction theory. The second stage is concerned with the measurement of pressure at points on the object boundary and comparison of the results with the values predicted by the linear diffraction program.

CHAPTER 2 - LITERATURE SURVEY

2.1 Introduction

The literature devoted to the theoretical and experimental investigation of wave motion and wave structure interaction is vast and spans a considerable range of topics. A number of comprehensive reviews have been written from the perspective of the naval architect (Wehausen, 1971 and Odabasi and Hearn, 1977) and the marine engineer (Hogben, 1977 and Sarpkaya and Isaacson, 1981) and the scope of this literature survey has therefore been restricted to include only those articles which are directly relevent to the subject matter of this thesis or investigations which include developments and results which are of significance to this study.

The evaluation of the forces imposed by waves on the elements which comprise an offshore structure is a particularly demanding problem requiring drastic simplification of the real sea conditions if an approximation to the force is to be obtained. If flow separation effects are a feature no mathematical solutions are available even for the simplest problems and if diffraction effects are significant solutions are only generally possible by means of a computer program for an inviscid, linear wave formulation of the relevent potential theory problem. The use of semi-empirical formulae in the design of offshore structures has therefore proved to be advantageous in a number of simplified wave structure interaction problems and Morison's equation with a similar formula for the transverse or lift force are basic design tools.

A considerable range of engineering problems have been formulated and solved by means of potential theory. The methods which have been chosen for the solution of such problems vary according to the type of formulation and exact solutions are only available for a limited number of problems so that in many cases a numerical solution procedure is required. If the potential theory formulation can be rewritten in integral equation form a discretisation procedure may be employed to give numerical results. This approach has been extensively used for the solution of the wave hydrodynamics problems of scattering and radiation and a number of computer programs have been written and tested for a range of obstacle configurations.

A major feature of the solution of potential theory problems in wave hydrodynamics is the application of a linearised boundary condition at the free surface boundary. The assumption of linearity is only strictly valid for waves which are of small amplitude and therefore the steeper waves encountered under real sea conditions are not fully accounted for. This has resulted in the investigation of the possibility of extending the potential theory formulation and solution to a higher-order.

If the solutions of the potential theory problems for wave scattering and radiation are to be used withconfidence in the design of offshore structures the physical conditions under which the predictions are valid must be established. Many experimental studies have been completed for this purpose for different problems of engineering significance and in general good agreement with the potential theory results is obtained but under certain

circumstances it is necessary to include higher-order terms in the analysis to achieve satisfactory agreement.

2.2 Semi-Empirical Wave Force Prediction

Experimental studies for obstacles in steady flow have indicated that the formation of a wake due to the separation of the fluid is a complicated process in which the location of separation points is variable for a smooth body contour. The separated flow gives rise to a drag force which has been represented by a semi-empirical formula in which the coefficient of drag varies with the Reynolds' number. For one dimensional oscillatory flow the processes are more difficult since for smooth obstacles the locations of the separation points are variable and, for obstacles of any shape, vortices formed or partially formed in one half-cycle may affect those generated in the subsequent half-cycle. For steady and oscillatory flows the forces induced may be evaluated analytically by the simulation of separated vortex sheets by discrete vortex elements (Graham, 1979). However, for problems in waves there is further complication due to the variables associated with the motion of vortices which have been shed and it is therefore not surprising that no mathematical solution has been obtained and that semi-empirical formulae are used. The most widely used formula of this type is the so-called Morison equation introduced by Morison, O'Brien, Johnson and Schaaf (1950) in response to the demand for a design formula for offshore structures in which the verical cylindrical pile is the most important structural element. Working on the analogous problem of a cylinder submerged under a standing wave Keulegan and

Carpenter (1958) demonstrated the dependence of the coefficients of Morison's equation upon a period parameter which has since been referred to as the Keulegan-Carpenter number.

Subsequent to the introduction of the Morison equation framework for the evaluation of wave induced forces on small bodies and the correlation of the force coefficients with the Keulegan-Carpenter number a considerable number of laboratory investigations have been performed to establish values of the empirical coefficients which might be employed in the design of offshore structures. Much of this work is discussed in the reviews cited above and in general is concerned with the vertical circular cylinder or cylinders in analogous oscillatory flows. However, the assumption of a uni-directional but oscillatory velocity vector in wave structure interaction problems for small structural elements is not universally applicable. For the submerged horizontal circular cylinder these conditions only arise for shallow water conditions and for deeper water the element responds to a rotating velocity vector which, in the limiting case of deep water, has a constant magnitude. Koterayama (1979) has performed a series of laboratory tests in order to evaluate the coefficients of a slightly modified Morison equation for the horizontal and vertical components of the force in deep water.

For cylinders in steady and oscillatory flows and for vertical cylinders in waves a transverse force occurs which is due to asymmetry in the wake. For the case of the vertical circular cylinder in waves Bidde (1971) and Isaacson and Maull (1976)

have investigated the variation of the lift force with the Keulegan-Carpenter number demonstrating the dependence of the force on the form of the wake.

If flow separation effects are significant for the submerged horizontal circular cylinder use of Morison's equation for the horizontal and vertical components of force excludes any measure of the effects of asymmetry in the wake. Using the technique of spectral analysis with the results of flow visualisation experiments Maull and Norman (1979) demonstrated the importance of the motion of the vortices in influencing the magnitude of the force components for a horizontal cylinder.

As an alternative to the Morison equation a single force coefficient may be employed if viscous effects are negligible. Chakrabarti (1973) proposed the use of a single force coefficient with the Froude Krylov force for a number of submerged objects of symmetry in order that the effects of wave diffraction might be included without recourse to a full diffraction analysis be means of a computer package.

In it's original form Morison's equation does not include the effects of finite wave height and it is common practice in design to replace the expressions for velocity and acceleration by expressions obtained from a higher-order wave theory (such as Stokes 5^{th}). This procedure lacks any theoretical basis but is regarded as convenient in estimating wave loads for design purposes. Lighthill (1979) has criticised the use of the Morison equation framework on the grounds

that it fails to represent properly the mechanisms responsible for the wave induced force and demonstrated that the non-linearity associated with the finite height of the waves contributes a second-order irrotational flow component which is not insignificant for the case of the vertical circular cylinder.

Morison, O'Brien, Johnson and Schaaf (1950) assumed that the interaction of a progressive wave with a cylindrical object extending from the bottom through the free surface induces a force which may be expressed as the sum of two components. Assuming quasi-steady conditions the drag force was taken in a similar form to the steady flow representation and it was proposed that the drag coefficient should have substantially the same value as for steady flow. The inertia force was assumed to be proportional to the accelerative force exerted on the mass of water displaced by the pile thereby introducing a second coefficient generally referred to as the inertia coefficient. This expression may be criticised for a number of reasons. Perhaps the most obvious criticism is concerned with the representation of the drag force in a manner which predicts that this component makes no contribution to the total force at points in the cycle at which the particle velocity is zero. This is physically unreasonable for an oscillatory flow since the convection of vorticity must introduce a history effect which within this framework would be attributed to inertia effects. However, the results presented using coefficients derived from the measured moment at points of zero velocity and acceleration demonstrate good agreement with the measured moment.

In spite of a number of shortcomings the Morison equation has been adopted almost universally as the representation of wave induced forces for circular cylindrical elements for which separation effects are significant and since it's introduction it has been the subject of a quite considerable and occasionally mis-directed research effort. The majority of studies have been associated with the need to establish suitable values of the coefficients for use in design and a significant problem is encountered in such work because the Reynolds' number range which occurs under real sea conditions cannot be reproduced in wave tests at model scale. Much work has therefore been concerned with the evaluation of coefficients for the simplified but analogous oscillatory flows produced by oscillation of a cylinder in still water or oscillation of the fluid in a U-tube. Theselater studies provide valuable information but in isolation might be regarded as deficient since they fail to include three dimensional effects, non-linear effects and free surface effects. A full account of the research into the Morison equation may be obtained by referring to Sarpkaya and Isaacson (1981) and a number of the reviews cited therein.

One particular study of considerable significance was conducted by Keulegan and Carpenter (1958) and since the fluid motion in their study is essentially uni-directional and oscillatory this work may be catagorised with the oscillating cylinder and U-tube experiments performed subsequently. The main result of this paper is the demonstration of the dependence of the force coefficients on the period parameter. The authors were also able to propose a physical explanation of the results obtained suggesting that the maximum value of the drag coefficient and the minimum value of the

inertia coefficient which occur at approximately the same value of the period parameter correspond to the formation and separation of a single eddy in each cycle. In the original paper the results obtained were not correlated with the Reynolds' number and it was concluded that such a correlation did not appear to exist. However, it has subsequently been demonstrated that if the results are replotted (Sarpkaya, 1976) Reynolds' number dependence is of significance. These replots demonsrate two features of particular note. Firstly, the reduction of the drag coefficient with Reynolds' number for any value of the Keulegan-Carpenter number suggests that the values of coefficients obtained in tests at lower Reynolds' numbers are not applicable in predicting forces at higher Reynolds' numbers particularly if boundary layer conditions differ between model and prototype Reynolds' number regimes as the results for steady flow suggest. The second feature of the replotting relates to the variation of the inertia coefficient with Reynolds' number at higher values of the Keulegan-Carpenter numbers and this confirms that viscous effects are being interpreted incorrectly in the application of the Morison equation.

The application of the Morison equation to cylinders of different orientation to the particle motion should not be regarded as straightforward if fluid separation is significant since the behaviour of the wake might be considerably different.
For the horizontal cylinder Koterayama (1979) has evaluated the Morison's equation coefficients in deep water waves so that the cylinder responds to a rotating velocity vector of constant magnitude. This work is subject to the criticism of laboratory studies emphasised above in that the range of Reynolds' numbers is small and

of no practical significance for design purposes. However, the study is of some value and comparison of results for both the coefficients varying with the Keulegan-Carpenter number give smaller values than the corresponding results for oscillatory flow and explanations based on the convection of vortices might be advanced to account for this difference. It would be dangerous to argue that increasing the Reynolds' number for this configuration would lead to a further reduction in the drag coefficient since the form of the wake is quite different from that which occurs in steady or oscillatory flows.

An unusual feature of the analysis employed by Koterayama which is of significance at smaller values of the Keulegan-Carpenter number is the subtraction of the velocity component of the diffraction forces from the measured forces so that the drag component may be evaluated accurately. Since such forces are only of the order of 10% of the drag force this measure may be regarded as unnecessary but does indicate another failure of the Morison equation to properly model the physics of the interaction.

Koterayama has also correlated the second-order forces with the Keulegan-Carpenter number and attributes forces which are as much as 30% of the first-order forces to separation effects. This is improbable at smaller values of the Keulegan-Carpenter number and an alternative explanation must be proposed based on considerations of non-linear interaction.

It might also be expected that if the submerged cylinder is located at smaller depths below the wave the adequacy of the Morison

equation would be further diminished and the results of these tests would cease to be valid particularly for steeper waves since the physics of diffraction, inertia and separation effects would all be modified.

Bidde (1971) was the first to study transverse forces on a cylinder in waves. The measurement of in-line and transverse forces with the results of a flow visualisation permit a number of conclusions to be drawn concerning the magnitude of the lift force and the mechanics which give rise to such forces. The flow visualisation experiments demonstrate that a number of so-called eddy shedding regimes may be identified and a classification made on the basis of the Keulegan-Carpenter number. In view of this relationship between the wake flow and the Keulegan-Carpenter number it is not surprising that the ratio of lift to longitudinal force correlates with this paremeter. The on-set of the lift force is associated with the development of an asymmetric wake and increasing the Keulegan-Carpenter number permits the development and separation of increasing numbers of vortices with the identification of a Von Karman vortex street at larger values. At the very largest values of the Keulegan-Carpenter number extreme turbulence is identified due to the interaction of eddies shed in the previous half cycle with those being formed and it is for this regime that the maximum ratio of lift to longitudinal force occurs reaching a value of as much as 60%. Two important points have been noted by Issacson and Maull (1976) concerning the work of Bidde. Firstly, that the Keulegan-Carpenter values are averaged over the depth and therefore appear to be smaller than those generally quoted and secondly that the turbulence identified for larger values of the

Keulegan-Carpenter number does not exist and is due to the inadequacy of the flow visualisation technique.

It is suggested by Isaacson and Maull (1976) that their investigation of the transverse forces on vertical cylinders in waves might be considered as an extension of Biddes investigation and certainly this study provides a clarification of the main results of the earlier study. One important result which was not demonstrated in the earlier study was the dependence of the lift force on the water depth parameter in addition to the Keulegan-Carpenter number.

This study, reported more fully in the doctoral thesis of Isaacson (1974), serves to advance the understanding of the relationship between the form of the oscillatory wake and the transverse force induced by the fluid motion. The results of a study of an oscillating cylinder in still water have been used to determine the eddy shedding regimes and to explain the mechanisms which give rise to the oscillation of the lift force at different multiples of the frequency of oscillation. An important result discovered in this preparatory study is that the vortex which most clearly influences the force on the cylinder is that vortex which having fully developed has not yet been shed and if this eddy is shed it's influence is reduced. It has also been demonstrated that if the flow reverses prior to complete separation, or perhaps advanced development of a vortex the dissipation of this vortex gives rise to a preferential growth on one side of the cylinder for the next half cycle.

For the cylinder in a wave the measurement of the pressure distribution on the cylinder at several depths and at different instants

was used to demonstrate two features. By comparison of the measured pressures with the potential theory predictions and flow visualisation results the influence of a single vortex was demonstrated and the correlation of the vortex with depth was established.

It was concluded that there is a general agreement among the results of the study of transverse forces which show that onset of assymetry and therefore lift occurs at a Keulegan-Carpenter number of approximately 5.

Although the oscillation of the lift force was noticed to be an exact multiple (N+1, where N is the number of eddies shed per cycle) of the fundamental wave frequency Isaacson and Maull do not comment on the effect of the assymetry, which gives rise to this relationship, on the in-line force. A component of the drag force which oscillates at twice the fundamental frequency can not be accomodated within the framework of the Morison equation but is suggested by the work on transverse forces and has been identified for the particular case of the submerged horizontal cylinder by Koterayama (1979). The paper presented at the Symposium of Wave-Induced Forces on Cylinders, Bristol 1978 by Maull and Norman (1979) reports the results of a thorough investigation of the vortex induced wave forces on a submerged horizontal cylinder. Significant oscillations of both the components of the force are recorded at twice the fundamental frequency for waves which approach the deep water limit and flow visualisation is used to demonstrate how this occurs.

The results of the study of Maull and Norman emphasise the variation of the vertical component of the force, referred to as the

lift force, with the eccentricity of the partical orbit. It is demonstrated that the occurence of a rotational velocity vector gives results for both components of the force which differ from those obtained for a one dimensional oscillatory flow and these differences are explained qualitatively by referring to Blasius' equation. It was suggested that additional assymetry in the wake due to the rotational nature of the flow is the mechanism responsible for the occurrence of this assymetry at a lower number of the Keulegan-Carpenter value than in the oscillatory flow problems. For a fuller understanding of the viscous induced wave forces on a submerged circular cylinder it is suggested that the work of Maull and Norman should be extended to include a greater range of the Keulegan-Carpenter number and also to include cylinders at small depths of immersion where freesurface effects may result in a modified flow.

Each of the works cited above in which the forces are related to the form of the wake are subject to the same criticism that has been levelled at the use of model tests on cylinders in waves to provide coefficients for prediction of forces using Morison's equation. This criticism relates to the range of the Reynolds' number for which the tests are carried out and the considerable differences in the form of the wake which are suspected for higher ranges of Reynolds' number.

The proposal of an equation with a single coefficient made by Chakrabarti (1973) with the associated recommendation of suitable coefficients for objects of symmetry resembles the use of Morison's equation with the drag component excluded and is intended for

application in cases when diffraction effects are of some significance but may be regarded as proportional to the Froude Krylov force. This method of approximate prediction is similar to the use of a diffraction coefficient which is described in Sarpkaya and Isaacson (1981: 387) with the exception that a single coefficient value is recommended and that this value of the coefficient is based upon experimental data.

For the horizontal circular cylinder Chakrabarti has used the experimental results of Schiller (1971) to evaluate the horizontal and vertical coefficients and then uses these coefficients to demonstrate excellent agreement of the proposed theory with the same results. The results obtained, in spite of the agreement between semi-empirical theory and experiment, are deficient in that they have not been tested for a range of data and it is suggested that for different values of the water depth parameter the results would vary due to the change in the flow about the cylinder. It is also questionable whether the results will apply to cylinder located at different depths in the wave and it must therefore be concluded that the agreement which has been obtained between theory and experiment may prove to be superficial.

In the opening address of the BOSS '79 * conference Lighthill (1979) presented an excellent exposition of the different physical mechanisms which underly the main methods used for estimating wave loads. Having clarified a number of the fundamentals

---

* Proceedings 2nd International Conf. on the behaviour of off-shore structures, BOSS '79, London.

of wave structure interaction suggestions of possible improvements in estimation techniques were presented. It was emphasised in the lecture that non-linear irrotational flow effects must be included if a more accurate modelling of wave structure interaction effects is to be achieved and that the framework of Morison's equation is unsuitable since it interprets these effects as the result of viscous mechanisms. Lighthill identified three distinct sources of non-linear (second-order) irrotational flow wave loading. The first, which was demonstrated to be more significant for problems in which scattering is significant, is associated with the quadratic correction to the velocity potential. The other two sources, the dynamic pressure and the finite wave height, give rise to significant contributions for the problems for which Morison's equation has been traditionally used. This has been demonstrated by taking the example of the vertical circular cylinder, adding an irrotational flow term to the conventional Morison equation and for typical wave data indicating that the conventional and suggested estimation techniques require considerably different drag coefficients to predict the same total force. This effect may prove to be less pronounced for submerged elements such as the horizontal cylinder since 80% of the contribution to the non-linear irrotational flow term in Lighthill's example is due to the additional force obtained by integrating the pressure to the elevated free surface position. This second-order term due to finite wave height acts at the still water level and is clearly only relevant for surface piercing cylinders. However, for submerged horizontal cylinders additional non-linear effects might prove to be significant for small depths of submergence giving similar results to those obtained by Lighthill. Such effects should

be investigated for this problem so that viscous effects are not over-emphasised particularly at small Keulegan-Carpenter numbers.

2.3 The Integral Equation Method

The integral equation method is the basis for a considerable number of computer programs written for the numerical solution of the wave scattering (diffraction) and wave radiation problems of hydrodynamics. The original formulations of these problems in integral equation form are due to John (1950) and Ursell (1953) and these studies prepared the way for the subsequently computed numerical solutions which are reviewed at the end of this section.

The integral equation method is a classical method in potential theory and has been applied to problems in many branches of physics and engineering. For many problems of physical significance the exact solution of integral equation formulations are not available and therefore the numerical solution techniques introduced by Jaswon (1964) and Symm (1964) are particularly valuable tools which have been widely used and form the basis of the boundary element method. For an account of developments in the application of this method Jaswon and Symm (1977), Banerjee and Butterfield (1979) and Banerjee and Shaw (1982) should be consulted.

The application of this method involves the assumption that a continuous distribution of sources may be assumed to exist throughout the domain and over it's boundary which results in the representation of the unknown potential as a distribution of sources over the boundary of the domain. A number of studies have been

made in which the resulting representation of the potential is due to a continuous distribution of sources over an auxiliary or fictitious boundary which lies outside the physically significant domain. The first of these is due to Oliveira (1968) in which solutions are presented for several stress analysis problems.

An alternative formulation in which Green's boundary formula is used has been proposed by Patterson and Sheikh (1982). It may be demonstrated quite simply that the theoretical formulation employed is incorrect which is surprising in view of the good results obtained by application of the method which the authors refer to as a regular boundary element method. Coates (1982) using the same type of formulation as Oliveira applied the separated boundary method to obtain solutions for a number of simple potential theory problems and concluded that the results obtained are more accurate than the results obtained by the methods in which sources are distributed over the domain boundary.

The integral equation method has been used extensively in the solution of wave hydrodynamics problems to obtain predictions for the design of offshore structures. The majority of applications differ from the usual way in which the boundary element techniques are used because a singular solution, or Green's function, is included in place of the simple source. Three recent studies by Hearn and Donati (1981) Eatock Taylor (1982) and Hearn, Donati and Mahendran (1982) indicate that in spite of the fact that a considerable number of studies have been completed for this particular application of the integral equation method there are still subsidiary topics which demand fuller consideration if the method is to be employed efficiently and reliably. In fact it is quite clear that the application of the method for the design of offshore structures is not necessarily straightforward and requires an appreciation of the effects of different descretisation schemes.

The formulation of John (1950) for floating bodies in waves might be regarded as the combination of two methods of potential theory since the integral equation formulation includes the use of a Green's function. In this classical paper any function which satisfies the governing differential equation throughout the fluid domain and the prescribed boundary conditions at the bottom boundary and the free surface of the fluid is referred to as a "wave function" and the study is concerned with finding such a function which determines the motion of the fluid from the conditions on the object and at infinity. The required wave function is separated into two components the first of which is called the "primary" wave function and corresponds to the motion of a wave in the absence of an obstacle and the second is a wave function which, having been "caused" by the presence of the obstacle, will behave like an outgoing progressive wave at large distances from the obstacle.

The Green's function chosen behaves like an outgoing progressive cylindrical wave at large distances and is used with the wave function which determines the fluid motion in the application of Green's theorem. It is the expression of the Green's function in series form, introduced by the author, which provides more detailed information about the components of the wave function. It is demonstrated that the second component may be represented as the sum of a "secondary" wave

component corresponding to the first term in the series expression of the Green's function and satisfying the Sommerfield radiation condition and a "local" wave component which vanishes at infinity and is given by the remaining terms of the series.

Having analysed the behaviour of the wave function at infinity an integral equation formulation is obtained by locating the singular point on the obstacle surface. John derives a fundamental uniqueness theorem and consequently, for the decomposition of the wave function described above, states the theorem: "A wave function in uniquely determined by it's primary component and by its values or the values of it's normal derivative on the obstacle surface". This uniqueness theorem is only applicable for a floating body with prescribed harmonic motion.

The study is carried out for three dimensional motion due to the interaction of a wave with a bounded obstacle. It is pointed out that exactly analogous uniqueness theorems can be proved for two dimensional motions and that the same decomposition of the wave function is possible. In the two dimensional case the secondary wave component can be thought of as consisting of two components one which progresses in the direction opposite to the primary wave (reflected wave) and one which combines with the primary wave to give the transmitted wave.

Concerning the solution of the integral equation two sources of difficulty are identified. The first is associated with the existence of eigenfunctions at certain frequencies and the second is due to the existence of a strong singularity in the kernel for points of intersection of the obstacle and the free surface. The second problem makes it difficult to establish the validity of the Fredholm theorem for the integral equation but this problem is less troublesome for an orthogonal intersection of the surfaces. These difficulties occur for the same restricted class of problems for which uniqueness was proved but for obstacles which are completely submerged there are no essential difficulties in the solution of integral equations.

John's study is particularly thorough and the decomposition of the wave motion, the integral equation formulation and the derivation of a series form for the Green's function are basic to many subsequent studies of wave scattering and radiation. However, no solutions are obtained and it would appear that the first solutions evaluated for this class of problems are those obtained by Ursell (1953). The motivation for this study was the failure, under certain conditions, of the multipole method introduced by the same author in an earlier paper (Ursell, 1949). The initial integral equation formulation takes the same form as that which was presented by John, namely the Green's theorem, but the formulation is reduced to a respresentation of the required potential as a distribution of sources only and solutions are then obtained by an iterative procedure.

The introduction of the method of integral equations to obtain numerical solutions for potential theory problems may be

attributed to Jaswon (1964) and Symm (1964). The formulation of problems using Green's theorem resembles the integral equation of John and it is the numerical procedures introduced in the second part of this two part paper that have been used in the computer programs written for problems of wave hydrodynamics. Additionally, it is these same techniques which form the basis of what has been called the boundary element method (b.e.m.).

The paper by Jaswon includes a theoretical study of the Fredholm integral equation of the first kind performed with a view to it's numerical exploitation and emphasises the value of the Green's theorem which is referred to as Green's boundary formula.

The second paper by Symm explains the numerical discretisation techniques required for the solution of integral equations and presents results for a number of problems, some of which would not be amenable to any other treatment. The considerable flexibility of the method is apparent from the results presented for problems in which Fredholm's first equation, Fredholm's second equation and coupled integral equations are exploited to give solutions for problems in which the domain geometries are not simple.

The first use of an auxiliary or fictitious boundary which is distinct from the boundary of the domain would appear to be by Oliveira (1968). The author of this work classifies the method as an integral equation method but presents the theory as a matrix equation which is derived by the linear superposition of independent

elementary solutions. The preliminary testing of the method with different locations of the auxiliary boundary indicated some failure for a boundary which was remote from the domain boundary and therefore the method was subsequently used with the auxiliary boundary close to the real boundary. The application of the method to several problems and comparison of results firstly with those of a finite element analysis and then with the results of photoelasticity tests demonstrates that the accuracy achieved is satisfactory and it is concluded that this accuracy is achieved because the logarithmic singularity of conventional integral equation methods is avoided by the use of an auxiliary boundary.

The regular boundary element method introduced by Patterson and Sheikh (1982) and applied to the problem of flow past an obstacle in an open channel includes an elementary theoretical error in the application of Green's theorem. The mistake occurs due to the failure to distinguish between the field point and the source point in the derivation of the theory and this results in a formulation in which it is required that the boundary conditions are applied on the separated boundary. This does not appear to be appreciated by the authors and with the separated boundary chosen to be very close to the real boundary good results were obtained. It might be assumed that the successful numerical solution of a number of test problems is made possible because of the similarity between the density variations of the source distributions on the fictitious boundary and the variation of the boundary conditions on the problem boundary. The regular boundary element method should therefore be regarded as an approximate method and it is suggested that any benefits associated with the ficititious boundary approach are best sought by distributing simple sources only since this method is mathematically correct.

Coates (1982) studied the solution of a number of potential theory problems by using a distribution of sources on a separate fictitious boundary. The first problem solved is an interior boundary value problem subject to a Dirichlet condition and before testing the separated boundary method the conventional integral equation method is shown to give errors which are more significant at points on and near the boundary of the domain than for points within the interior. Implementation of the separate source method for this problem gives a considerable improvement in accuracy particularly at points on and near the boundary and this result is confirmed by comparison of results with those of Symm (1964) for an L-shaped domain. This result is of importance because in many problems it is solutions for points on the boundary of the domain which are required so that quantities of physical significance such as pressures can be evaluated. By repeated solution of the exterior Neumann problem of flow past a circular cylinder near a plane boundary it is demonstrated that the best location of the fictitious boundary is at a sufficient distance from the real boundary to eliminate the considerable variation of the kernel function due to source node interaction but not too remote because this introduces ill-conditioning problems.

Many papers have been published in the last two decades reporting results obtained from computer programs written for the solution of the problems of wave hydrodynamics by the discretisation of alternative integral equation formulations. The problems to which this method has been applied are wide

ranging and include two and three dimensional obstacles which may be submerged or located in the free surface and may be either fixed or in motion. The testing of the numerical results has been equally comprehensive and includes comparison with exact solutions if the geometry of the problem permits or results of the finite element or multipole methods for other problems.

The earliest applications of the integral equation method to these problems all employed an integral equation formulation which is based on the representation of the unknown potential as a distribution of wave sources or Green's functions over the obstacle boundary. This resembles the final formulation of Ursell (1953) which has been mentioned above but the first solutions of this type of formulation by the discretisation procedure appear to be due to Kim (1965). Similar applications of the method by Frank (1967), Garrison and Chow (1972) and Hogben and Standing (1974) followed. The method used by Frank has subsequently been referred to by naval architects as the close fit method and the program developed by Hogben and Standing has since been called NMIWAVE. One interesting variation on the close fit method has been published by Maeda (1974) in which the problem is solved by making use of stream functions.

The popularity of this method is surprising for two reasons. Firstly, because the method requires the solution of an integral equation for a function which has no physical significance before evaluating the unknown pontential by a back-substitution and secondly, because this formulation differs from the formulation

presented by John (1950) in which Green's theorem is employed. The Green's theorem formulation in which the unknown potential is represented as the sum of a distribution of wave sources and double sources yields the required solution directly and has been used by Naftzger and Chakrabarti (1979) and Hearn and Donati (1980) and the three dimensional program developed by Hearn has been called MATTHEW.

A feature of these conventional integral equation methods is that under certain conditions the method fails. This is due to the existence of eigen values for the homogeneous Fredholm equation corresponding to the Fredholm integral equation of the second kind and is therefore absent if the separated source boundary method is employed since this method requires the solution of a Fredholm integral equation of the first kind. In wave hydrodynamics problems this phenomenon is referred to as the irregular frequency problem and for the vertical circular cylinder problem Murphy (1978) has obtained the values at which this effect occurs. This breakdown has been encountered by Naftzger and Chakrabarti (1979) and Hearn and Donati (1981) and has been avoided by use of the separated source boundary by Van Oortmersson (1972) and Coates (1982). This is an advantage of secondary importance and if the separated source boundary method is to be used in preference to the conventional method for any type of problem the method must be demonstrated to give an improved accuracy for reduced computational effort without any loss of reliability.

The problems of wave hydrodynamics have also been solved by the application of Green's theorem with simple sources and double sources distributed over the entire boundary of the fluid domain. This application of the method initiated by Jaswon (1964) and Symm (1964) was first made by Bai and Yeung (1974) and has more recently been exploited by Au and Brebbia (1982) and Bird and Shepherd (1982). The simple source methods have not however, been greatly used and recent work on the solution of these problems has employed one of the alternative formulations in which the Green's function is used.

It is convenient to review the papers by Hearn and Donati (1981) and Hearn, Donati and Mahendran (1982) together since they are both concerned with the application of integral equation methods to solve wave hydrodynamics problems for various bodies in motion. It is stated that the first of these papers was prepared with the intention of making sea-keeping theories more comprehensible to the practicing naval architect and, taken with the second paper which reports the results of analyses performed in preparation for an experimental study of wave energy devices, demonstrates that the application of the three dimensional integral equation method and the two dimensional integral equation method with a strip theory is not a straigthforward process.

The first paper reports the application of methods to two ships, a warship and a merchant vessel and the study is particularly concerned with problems of numerical stability including the

occurence of breakdown at irregular frequencies. In discussing the application of the two alternative methods it is noted that if different discretisations are employed different results will be obtained due to the improved representation of the geometry or the improved numerical stability of the system of algebraic equations. It is also noted that a discretisation may prove to be more acceptable for some motions than others. The problem of irregular frequencies is also identified by the onset of numerical instability but this type of problem can not be averted by improving the discretisation and requires a smoothing process based on results for frequencies either side of the irregular frequency. In the study two irregular frequencies were identified in the two dimensional analysis of the merchant vessel.

The second paper includes a hydrodynamic analysis of two structures, the rigid body form of the Lancaster Flexible Bag and an articulated Cockerell raft system. The difficulties encountered emphasise that the utilization of integral equation methods in design requires considerable experience and expertise and that a greater understanding of possible sources of numerical failure is necessary. Results for the rigid structure, which has a simple geometry, confirm several simple facts concerning numerical stability and discretisation but the analysis of the articulated system resulted in considerable numerical instability due to discretisation problems in the viscinity of the hinge. Because the analysis of the articulated structure requires that all possible

configurations of the raft system are considered the three dimensional program was extended to permit a simultaneous solution of twenty radiation and ten diffraction problems. The program was run interactively so that failures might be identified and modifications to the discretisation introduced. By this method it was established that satisfactory results could only be achieved with a detailed discretisation and on comparison with the results of a two dimensional analysis the later proved to be unacceptable. In concluding the study the authors stated that advanced numerical methods when properly applied can be relied upon to provide good results but that it is evident that proper application is by no means a trivial matter.

In a brief review of the analysis of hydrodynamic loads by boundary element methods Eatock Taylor (1982) explains how the integral equation method may be used in combination with the finite element method. The author calls this the boundary element coupled method and it has been referred to elsewhere as a hybrid element method. The finite element method is particularly well suited to the solution of problems in small domains with complicated geometries but is not easily applied to exterior problems in which the domain, or part of it, extends to infinity. However, the integral equation method in which the Green's function is included is ideal for such problems since the conditions at infinity are automatically satisfied. It is therefore suggested that this method combines the advantages of each of the methods. It is also demonstrated that careful choice of the dimensions of the interior domain in which the finite element method is used eliminates the irregular frequency problem.

2.4 Non-Linear Analysis of Wave Obstacle Interaction

Analysis of wave obstacle interaction, whether semi-empirical or mathematical, has been developed on the assumption that the incident wave may be described as a small amplitude periodic motion, that any motion is itself of small amplitude and that the interaction between the wave and the obstacle is a linear process. Viscous effects are, strictly speaking, non-linear but for the interaction of waves with obstacles which span a significant portion of the wavelength the assumption of an inviscid fluid may for most problems be justified. For smaller obstacles flow separation is of significance and the drag component in Morison's equation is non-linear but is modified to obtain a linear representation.

For wave obstacle interaction under ocean conditions the assumption of small amplitude motion is often violated and it is therefore important to consider the significance of non-linearity. There are two means by which the importance of non-linear effects may be established. The first method, which is the subject of this section, involves the extension of the theoretical model to a higher-order of approximation and this procedure, if possible, gives an indication of the theoretical adequacy of the linear solution. This theoretical refinement does not however guarantee that the mathematical model provides an adequate representation of the physics of the problem and the second method involves the use of model tests for conditions where non-linear behaviour is expected to diminish the validity of the linear solution.

The mathematical problem associated with progressive gravity waves includes a non-linear free surface conditionwhich is so intractable that progress is very difficult unless simplifying assumptions are made. If wave height is significant the reduction of this condition to a linear condition at the still water level is inadequate and therefore a number of theoretical models have been derived which describe the wave motion in the absence of any obstacle. It may be noted that the inclusion of finite wave height effects in the Morison's equation method is achieved by using these higher-order wave theories to provide expressions for the particle velocity and acceleration. This procedure lacks rigour and is a poor model of the physics of interaction (Lighthill, 1979) but has proved to be a useful means of extending the semi-empirical theory for use in design.

The extension of the theoretical model for the problems of wave scattering and wave radiation is particularly demanding and has recently been investigated in a number of studies. Some indication of the importance of the non-linear free surface condition is obtained by reference to the study of Tuck (1965) in which the problem of flow past a cylinder submerged at small depths below a free surface was investigated. However, the problem for progressive gravity waves is quite different and Tuck's results cannot be taken to apply even when problems are geometrically similar.

Higher-order solutions of potential theory wave obstacle interaction problems, which are the main subject of this section of the literature survey, may be obtained by a formulation which employs

the perturbation procedure as used in the Stokes' wave theory. By this method the second-order correction to the first approximation consists of two components. The first and most easily evaluated component is the steady or mean force which has been obtained by the multipolemethod (Ogilvie, 1963), the momentum method (Longuet-Higgins, 1977) and by the numerical solution of the integral equation formulation (Standing, Dacunha and Matten, 1981). This component is of physical significance in a wide range of engineering problems in which structures are required to be anchored. The second component is the oscillatory component which fluctuates at twice the frequency of the fundamental oscillation and the only problem for which solutions are known to have been obtained is for the case of the vertical circular cylinder. These solutions have been the subject of a series of investigations in which attempts have been made to extend the method of MacCamy and Fuchs (1954) to obtain second-order solutions and a number of mistakes in the various formulations have been identified.

For the same problem of a vertical circular cylinder but for shallow water conditions Isaacson (1977a) has obtained solutions for the wave scattering problem by application of cnoidal wave theory. The results of this study may be taken as an indication that under some conditions the results of a sinusoidal diffraction theory may prove to be inadequate.

The utilization of well established numerical methods for the evaluation of fluctuating second-order quantities has not been investigated in spite of the fact that two quite feasible suggestions have been made. The first suggestion was made by Salvesen (1974)

who in discussing the work of Bai and Yeung (1974) enquired whether their methods could be extended with a perturbation scheme to obtain non-linear solutions to ship-wave problems. This suggestion has not been implemented nor has the suggestion made by Lighthill (1979) in which a linear diffraction program would be used to obtain non-linear (second-order) solutions by using the principle of reciprocity.

A different possibility is that of extending a computational wave theory, such as the one developed by Longuet-Higgins and Cokelet (1976), to include an obstacle. This method would provide a complete non-linear solution and Lau (1983) has obtained preliminary solutions which are currently being tested for the problem of a fixed circular cylinder submerged in water of finite depth.

The motion of progressive gravity waves of finite height may be described by a number of theories and a recent review which includes many references to studies in this branch of the science is included in Sarpkaya and Isaacson (1981). The earliest formulation is due to Stokes (1847) who employed a perturbation procedure to obtain successively higher-order approximations to the exact solution. An account of this approach with the quotation of the principal results may be found in Wehausen and Laitone (1960). The perturbation procedure is only formally valid for conditions which in shallow water place a servere restriction on the wave height and therefore the cnoidal wave theory, first developed by Korteweg and de Vries (1895), is preferable for waves of finite height in the shallow water range.

A more recent development in the theory of finite height waves is the introduction of the stream function theory by Dean (1965). This is a numerical method in which a stream function expression is introduced which satisfies the governing differential equation and the condition on the bottom boundary plus the kinematic free surface condition. The dynamic free surface condition is then the only condition to be satisfied and this is achieved by an iterative procedure.

Another numerical method which has been developed only very recently is reported by Longuet-Higgins and Cokelet (1976). In this method an integral equation is solved for the normal velocity of marked particles in the free surface of the wave and by employing a time-stepping procedure the progress of the wave may be followed. Excellent agreement of the results of this method for the free surface profile with results obtained by Stokes' series indicate that this method is valid for waves of finite height moving with constant form but the main value of this method is for the mathematical modelling of unsteady waves. Numerical computations have been obtained for waves which steepen and overturn and it has been demonstrated that the surface remains rounded for time-stepping which continues after the overturning of the wave crest. One particularly interesting possibility in the application of this method is suggested by the authors. This is the possibility of using this method to give an insight into the energy and momentum lost in wave breaking and to gauge the transfer of momentum from waves to surface currents.

The theoretical study undertaken by Tuck (1965) is concerned with the effect of non-linearity at the free surface on

flow past a submerged cylinder. Although free surface waves occur as a result of the flow past a submerged cylinder this is a different class of problem to the geometrically similar problem which is the subject of this thesis. However, the similarity is sufficient for the results to be of interest and indeed the author introduces the study by considering the justification for the assumption of linearity in a number of wave problems relevant to the prediction of ship motion.

The formulation of a consistent second-order theory in which the condition at the free surface is satisfied to this order gives results for the force on a cylinder located near the free surface which are considerably different from results obtained with a linear free surface condition. The results differ by as much as a factor of two or three for shallow submergence but the author states that this does not imply the inadequacy of linear theoretical analysis of ship behaviour. The results of this study should however be taken as a warning that non-linear free surface effects may be of importance in the mathematical solution of a wide variety of wave obstacle interaction problems.

One further important point noted by Tuck concerns the relevance of the non-linear solution to the physical flow. The study does not include model tests to provide a validation of the potential theory results and it is commented that the conditions under which non-linear effects become mathematically significant are precisely the same as the conditions for which mathematical solutions are least likely to be an adequate representation of the physics of the flow, even if higher-order approximations to the solutions are obtainable.

Oglivie (1963) evaluated the time-averages of the second-order force for circular cylinders submerged in water of infinite depth. Results were given for a fixed cylinder in a sinusoidal wave, a cylinder forced to oscillate sinusoidally in otherwise calm water and a neutrally bouyant cylinder permitted to respond to first-order oscillatory forces. The knowledge of the first-order potential was sufficient to obtain these mean second-order forces and computations were carried out and graphical results presented by use of Ursell's multipole method. For the cylinder in a wave the steady horizontal forces are found to be zero but values of the steady vertical force are evaluated and plotted.

The prediction of zero mean horizontal force for a submerged horizontal circular cylinder in deep water is in agreement with the result of an alternative method of mean force evaluation explained by Longuet-Higgins (1977). The alternative formula is obtained by consideration of the horizontal flux of momentum and assuming momentum to be conserved when a wave interacts with a body the mean horizontal force is obtained by summing the momentum flux of the incident, reflected and transmitted waves. Since the linear theory predicts no reflection of waves by a submerged cylinder (Dean, 1948 and Ursell, 1950b) but transmission of the incident wave with a phase shift the wave scattering process does not result in a redistribution of the wave momentum and there is therefore no mean force. For more general problems in two dimensions measurement of reflection and transmission coefficients or evaluation by a linear diffraction theory therefore permits an estimation of the mean force. The former option is probably advantageous since the prediction of wave reflection and transmission characteristics excludes both the

possibility of energy absorption or dissipation and the inclusion of higher harmonies in the formula.

The linear diffraction computer program NMIWAVE has been extended to include the facility for the evaluation of second-order drift forces for three dimensional bodies and this work is reported by Standing, Dacunha and Matten (1981). Two methods are developed and tested by comparison with simple theories (based on transportation of momentum), each other and then with the results of specially designed experiments.

The first method is the far field method and is based on the momentum method. Because the diffraction program is an indirect formulation, numerical solution of the integral equation for the source distribution function permits the evaluation of free surface elevation in the far field. It is therefore possible to write expressions for the mean forces which include integrals over the obstacle surface and may be evaluated quite straightforwardly if the values of the source distribution function have been determined at the nodal points.

Although the far field method is simpler and much less computationally demanding than the second method it may only be used to evaluate second-order mean values in the horizontal plane. The near field method may be used to obtain steady values for three components of force and three components of the moment. In a general formulation of this method six terms must be included to give values for the components of force or moment and they may be listed as

1) The additional pressures acting between the structure's mean waterline and instantaneous free surface.

2) The integrated second-order dynamic pressure.

3) The change in force due to first-order motions throughout the pressure field.

4) Hydrostatic pressures acting between the mean waterline and instantaneous free surface.

5) Changes in the bouyancy force due to second-order motions.

6) A contribution due to the set-down of the regular incident wave.

The authors note that the evaluation of the mean force by this near field method requires careful location of the fluid singularities employed in the numerical model if errors are to be avoided for evaluation of the relevent quantities at points near the obstacle free surface junction.

The results obtained by both methods have been found to agree well with each other and have been confirmed by experiment. Comparison with the results obtained by the simple theories, which are commonly used for evaluation of mean forces in design of mooring systems, indicate that the extended computer program is a necessary improvement if mean forces are to be evaluated with reasonable accuracy for a range of conditions.

Extension of the linear diffraction analysis of MacCamy and Fuchs (1954) to obtain analytical second-order results for the vertical circular cylinder has been the subject of a number of investigations in recent years and the various approaches are reviewed in the most recent series of papers by Hunt and Baddour (1980a, 1980b, 1981). One particular problem which has given rise to the suggestion, made by Isaacson (1977b), that no second-order solution can be obtained is concerned with the existence of an irregularity at the intersection of the free surface and obstacle boundaries. Such a conclusion would obviously be relevent to a wide class of wave scattering and radiation problems but the difficulty has been resolved by Miloh (1980) who presented an analysis by which the irregularity is isolated.

Results for this problem computed recently by Hunt and Baddour (1982) are indicative of the importance of this study for problems which give rise to significant wave scattering. The second-order steady and oscillatory force components are evaluated and combined with the first-order forces to demonstrate that linear theory underestimates the total horizontal force on the cylinder by a small amount for small values of the diffraction parameter but by a significant amount for larger cylinders.

It must be recognized that if linear diffraction results are to be extended to a second-order by the perturbation scheme the results will only be valid for the same range of waves as the Stokes' waves in an unbounded ocean and will therefore not be suitable for problems in the shallow water depth range.

For a vertical circular cylinder located in water of finite depth interacting with waves in the shallow water range Isaacson (1977a) has obtained results by a cnoidal diffraction theory. The results are demonstrated by plotting the ratio of cnoidal force prediction to sinusoidal force prediction against the Ursell number, which is a measure of wave non-linearity, for a range of the diffraction parameter, ka. For longer waves the cnoidal diffraction theory predictions are as much as two or three times the sinusoidal diffraction theory predictions for waves in which non-linear effects are more pronounced. These results are of importance because under these conditions the application of the traditionally used techniques for evaluation of wave scattering and radiation quantities, which are all based on sinusoidal wave theory, do not give adequate results for finite height waves. It may therefore be infered that there are other problems for which similar results might be obtained and that the extension of the linear diffraction theory to a higher-order merits further investigation.

For the wave scattering and radiation problems Bai and Yeung (1974) were the first to apply the finite element method and the fundamental singularity method to problems in which the free surface extends to infinity. In the discussion of this work Salvesen (1974) suggests that the most significant application of the two methods may be in solving non-linear body-wave problems. The approach suggested would involve the use of a perturbation scheme and it is estimated that the solution of second-order or third-order problems would take approximately the same time as the linear solution whereas the evaluation of the second-order solution by the Green's function method may take as much as ten times the time required to compute the linear solution.

In reply to this suggestion the authors state that both methods could quite easily be extended to solve second-order problems and that the modifications for use of the methods with a perturbation scheme are only minor. As an alternative approach to the non-linear problem it was pointed out that a finite element formulation in which the exact free surface condition is applied would result in a system of non-linear algebraic equations which could be solved by an iterative scheme.

It would appear from the literature published since this discussion that none of these possibilities have been investigated. It may also be noted that the simplicity and computational efficiency of the extension of Bai and Yeung's methods by a perturbation scheme has been overstated. In a perturbation scheme the condition at the free surface for higher-order solutions is written as a linear differential equation which resembles the first-order equation with an additional pressure term which is applied over the entire free surface. This pressure distribution may be evaluated by knowledge of the lower-order solutions and it is the complexity of these evaluations and consequently the large demand on computational resources which increases the difficulty of this approach.

In considering the second-order problem for a fixed obstacle in a wave Lighthill (1979) identified three components in the second-order force which have already been stated in this literature survey (section 2.2). The dynamic pressure component and the waterline component due to finite wave height may be evaluated quite straightforwardly in a diffraction analysis but the third component, due to the quadratic correction to the velocity potential appears

at first to require a solution of the second-order problem. However, Lighthill has demonstrated first by application of the reciprocity principle and secondly by application of Green's theorem that the second-order force due to wave scattering may be evaluated by solution of a linear radiation problem. No solutions appear to have been evaluated by this method in spite of the fact that a considerable number of programs are available for the solution of the radiation problem which would only require the inclusion of additional subroutines for the evaluation of a free surface integral.

An additional possibility for the solution of non-linear wave obstacle interaction problems is currently being investigated by Lau (1983). This method is similar to the method of Lunguet-Higgins and Cokelet (1976) in that the non-linear free surface condition is applied on the moving free surface and an integral equation is repeatedly solved in the application of a sophisticated time-stepping process.

In extending this type of method to include an obstacle additional complications are introduced by the necessity to solve the integral equation subject to the radiation condition at large distances from the obstacle. This has been achieved by solving two problems in parallel and since the Laplace equation is linear these solutions may be added to give the final solution. This is not however the most difficult aspect of this problem. The passage of a wave over a submerged obstacle results in a temporary change in wave speed and therefore wavelength which results in the phase shift in the transmitted wave. The inclusion of this variation

of wavelength in the numerical model is the most difficult problem in the application of this method and is essential if meaningful results are to be obtained.

2.5 Experimental Validation of Potential Theory Results for Wave Obstacle Interaction

The linear potential theory formulation of wave scattering and radiation problems is well established and numerical solutions may be obtained by a variety of computer programs so that the form of the wave and the response of the obstacle may be predicted. The linear theory requires modification if waves of finite height are to be included in an analysis and methods by which the steady second-order forces have been calculated were outlined in the previous section. It was also explained that it might be possible to obtain higher-order oscillatory force values by several different methods and it is expected that results will be published in the following years which confirm that the suggested methods are workable.

If the various theoretical models are to be of practical significance it is essential that comparison with experimental measurements are obtained for a comprehensive range of problems so that the validity of the theory can be established. The various features which distinguish between the different problems include whether the obstacle is fixed or in motion, whether it is entirely submerged or surface piercing and whether the problem is two- or three-dimensional. It must be stressed that validation of linear

theory results under any one particular set of conditions does not necessarily guarantee the validity for a different problem and this is particularly true if examination of non-linear effects is included in the experimental programme.

If a set of experiments is designed and carried out for the validation of the theoretical model the experimental conditions must be such that there are no substantial violations of the boundary value problem as posed. Such experiments may be distinguished from others in which the physical conditions are deliberately chosen to be different from those upon which the simplified linear theory is based. This second type of study is of particular value in the continued absence of any general and complete higher-order theory for wave obstacle interaction problems and for any particular problem will indicate the limits of validity of the linear theory.

The studies reviewed in this section of the literature survey include both types of study and in general good agreement is achieved between experimental and theoretical results under favourable conditions. Before considering in detail the experimental studies which most closely resemble the study reported in this thesis a number of additional studies may be mentioned which are concerned with the validation of potential theory results by experiment for related problems of wave obstacle interaction.

Several experimental studies have been conducted to determine whether the linear diffraction theory provides satisfactory predictions for the force on a surface piercing vertical circular cylinder. The most recent publications in which these studies have

been reviewed are Sarpkaya and Isaacson (1981) and Coates (1982) and a number of general observations can be made concerning the results of these studies.

For the vertical circular cylinder it has been suggested that diffraction effects become significant if the diameter of the cylinder spans more than one-fifth of the wavelength, ($D/L>0.2$, Hogben, 1974). It may therefore be noted that much of the data obtained for forces on vertical cylinders is for conditions under which the cylinder responds to a purely inertial loading. Examination of the force results of Hogben and Standing (1974) and Mogridge and Jamieson (1975) reproduced by Sarpkaya and Isaacson indicate that the experimental results obtained for waves interacting with a cylinder when wave scattering is of significance depart more considerably from the theoretical results than those for inertial loading. This is an important observation if the linear theory is to be used for problems in which diffraction effects do genuinely dominate.

Isaacson and Sarpkaya noted that on the basis of all the available evidence it may be stated that reasonable agreement between theory and experiment is generally obtained and Coates has observed that measurements of pressure demonstrate less satisfactory agreement than measurements of force. One further feature identified by Sarpkaya and Isaacson is that the bulk of the data has been obtained for waves of small steepness and in general the waves do not exceed half of the maximum steepness. The available information therefore provides good evidence for the value of linear water wave theory for this particular problem but does not indicate whether the

application of linear theory would provide an adequate modelling of interaction with the steeper waves which would be encountered under ocean conditions.

A study which perhaps more closely resembles the study which is reported in this thesis was conducted by Salvesen (1969). The resemblence is found in the submergence of the obstacle at a small depth below a free surface. This study has been conducted for an obstacle in a steady flow which gives rise to free surface waves. The results obtained demonstrate that for a small depth of submergence non-linear free surface effects are important and the linear theory gives a poor representation of the wave resistance. This result can not be directly applied to the problem of the present study but may be used as an indication of the importance of free surface effects and consequently the necessity for investigation of wave obstacle interaction for submerged bodies just below a free surface.

A number of important experimental studies have been completed for the interaction of waves with a fixed two dimensional obstacle of simple geometry and for the generation of waves by the forced sinusoidal oscillation of an obstacle. Ursell, Dean and Yu (1960) investigated the generation of waves by a piston wave maker and Yu and Ursell (1961) performed a similar study for a circular cylinder oscillating in the free surface. These studies were stated by the authors to provide much needed evidence for the practical values of the linearized theory of water waves. A study of similar relevence was conducted by Dean and Ursell (1959) for a fixed semi-immersed circular cylinder in waves and this study has been repeated

recently by Martin and Dixon (1983). All these studies are important because they permit the examination of linear wave theory under controlled conditions. There are, however, important differences between each of the above problems and that of submerged horizontal circular cylinders in waves.

The author is only aware of three studies in which force measurements have been made for fixed submerged circular cylinders in waves when inertia or diffraction effects predominate. Chakrabarti (1973) reports the experimental study conducted by Schiller (1971) for deeply submerged cylinders and these may be interpreted as an indication of good agreement between experiment and theory. The study conducted by Koterayama (1979), which has already been considered in this literature survey, also includes results which demonstrate good agreement between experiment and theory. The cylinder in this study is not so remote from the free surface as in the previously cited study but is not close enought to test whether free surface effects are important or not. Therefore, the experiments conducted by Jeffrey, Richmond, Salter and Taylor (1976) are of interest because they include results for forces on cylinders at small depths of submergence.

There are two additional publications which include experimental studies of wave obstacle interaction for a horizontal circular cylinder submerged at small depths below the free surface. The doctoral thesis of Dixon (1980) includes measurements of the reflection coefficient and a few measurements of the drift force for a circular cylinder in and just below the free surface. A more comprehensive study of the drift force on a circular cylinder

submerged below the free surface has been conducted by Longuet-Higgins (1977) and this study is particularly illuminating because quite plausible explanations were proposed to account for the discrepancies between theory and experiment.

The experimental study of Ursell, Dean and Yu (1960) is the first confirmation of the accuracy of linear wave theory for forced motions. The theoretical formulation of the wave motion due to a piston-type wave maker is due to Havelock (1929) and the expression for the velocity potential is in the form of a local wave which vanishes at a distance of a few wavelengths away from the wave maker and a harmonic wave travelling away from the wavemaker. The experimental procedure was designed to eliminate tank reflections and two sets of experiments were completed. The first set of results were obtained for waves of small steepness ($0.002 < H/L < 0.03$) and the measurement of wave height indicated an average error of 3.4% with the measured values lying on a curve below the theoretical values. In order to establish the importance of wave steepness a second set of experiments were performed for finite height waves. This second set of measurements for larger wave steepness ($0.045 < H/L < 0.048$) indicated a systematic discrepancy with the measured values being on average 10% below the theoretical ones. The authors conclude that the results obtained confirm the validity of small amplitude wave theory.

The study completed by Yu and Ursell (1961) for the comparison of theoretical and experimental values for the surface waves generated by the vertical oscillation of a circular cylinder on water of finite

depth was seen by the authors as a sequel to the previously reviewed study. The theoretical predictions were obtained by extending Ursell's (1949) multipole method to accommodate waves in finite water depths. Experiments were only performed for small amplitude oscillations of the cylinder resulting in the generation of waves of small steepness only. The discrepancy between theory and experiment was again small with experimental values being consistently smaller than the theoretical predictions with the magnitude of the error being generally less than 5% of the measured value.

The studies of Dean and Ursell (1959) and Martin and Dixon (1983) may be considered in two parts. In the first parts the measured values of the horizontal and vertical components of force are compared with theory and in the second parts the form of the diffracted wave is compared with the theoretical predictions. In both studies the multipole method is applied to the problem of waves interacting with a fixed semi-immersed circular cylinder to provide the theoretical predictions. The earlier study has been completed for waves of small steepness so that the boundary conditions of the potential theory problem are essentially satisfied with regard to the amplitude of the motion. The second study by Dixon has been designed to give an indication of the variation of the measured values with wave steepness.

Comparison of measured force values with theoretical predictions by Dean and Ursell demonstrated good agreement but Dixon's results for the variation of wave steepness at a single frequency indicate that force values depart significantly from the theoretical values for steeper waves. For these measurements the

maximum wave steepness is approximately 0.05 and the wave height is always less than the cylinder diameter.

For measurements of the reflection coefficient in the first of these studies the average difference between theory and experiment was 14% with the measured value always being the smaller. The second study also demonstrates significant discrepancies for waves of small steepness and the magnitude of the discrepancy does not show any consistent variation with wave steepness.

In the study of Dean and Ursell measurements of the transmission coefficient were also made and excellent agreement with theory was discovered. This indicated a loss of energy in the system with the deficit being in the reflected wave. Dean and Ursell suggested two mechanisms which account for this loss of energy: the first suggestion is that the wave maker oscillation includes higher harmonics and the second is that there is the possibility of vorticity in the reflection process.

The results reproduced by Chakrabarti (1973) from the study of the wave forces on a completely submerged horizontal circular cylinder by Schiller (1971) have been obtained for a deeply submerged cylinder at a sufficient distance from the bed to avoid inducement of higher velocities below the cylinder. The results presented for this situation may be interpreted as the response of the cylinder to a purely inertial loading because the cylinder is located at a depth at which the amplitudes of particle motion have considerably decayed even for interaction with waves in finite depths of water. Chakrabarti was able to demonstrate good agreement between measured and

theoretical values for the vertical component of force with an equation which is the same as the expression for the theoretical inertia force and good agreement was also obtained for the horizontal force by applying a coefficient which increased the inertia force prediction by 5%. It may therefore be concluded that the measured values are in close agreement with the theoretical predictions.

The experiments conducted by Koterayama (1979) for the interaction of waves with a fixed submerged circular cylinder in deep water include a set of results for small values of the Keulegan-Carpenter number. These force results have been obtained for conditions under which neither separation or wave scattering effects are thought to be of significance. The cylinder is located at a depth which is sufficiently remote from the free surface to avoid significant non-linear free surface effects and therefore the experiments for small amplitude waves will indicate whether or not there is agreement with the potential theory results.

The results are presented in two alternative but equivalent forms both of which indicate that in general good agreement is obtained between potential theory and experiment. The first presentation shows that the measured inertia coefficients for the horizontal and vertical components of force are approximately equal to the theoretical value of 2 and the second presentation in which the measured values of the horizontal force are compared with the potential theory force values demonstrates the same agreement.

It may be noted that for larger values of the diffraction

parameter there is a significant discrepancy between theory and experiment. This discrepancy may be due to the failure of the mathematical model to predict forces when wave scattering becomes significant and resembles the results for the vertical circular cylinder discussed previously.

Analysis of the data collected in these experiments provides information concerning the harmonic composition of the force components. The results of the analysis demonstrate that there is a component which fluctuates at twice the wave frequency which the author attributes to viscous effects. This explanation is adequate for larger values of the Keulegan-Carpenter number when flow separation is of significance but for inertial wave loading these fluctuations may be regarded as evidence for non-linear wave obstacle interaction.

The tests for waves interacting with a horizontal circular cylinder conducted by Jeffrey, Richmond, Salter and Taylor (1976) in conjunction with experiments on Salter's duck do not include a comparison between experimental and theoretical values and are primarily concerned with the problem of surface piercing bodies. However, some experimental results are presented for completely submerged bodies and for results obtained at larger values of wave steepness the fluctuations of the forces depart from the predicted simple harmonic form. It is suggested that theoretical results for the experimental data might be obtained by application of a diffraction computer program and this would give additional evidence concerning the validity of small amplitude wave theory for the problems for

which the results are obtained, and in particular for the problem of the cylinder submerged at small depths below the free surface.

The study conducted by Dixon (1980) for the reflection of waves by a circular cylinder in the free surface includes several measurements for the case of complete submergence. These results, for the cylinder at four different locations, have been obtained for waves at three different frequencies and for each frequency wave steepness is varied. The measurement technique employed means that the measurement of the reflection coefficient, R, includes tank reflection and is therefore subject to an error of approximately 5%. Because the value of R is generally less than 0.05 the results may be taken to indicate that the linear potential theory result of no reflection has been confirmed experimentally.

Dixon also presents several measurements of mean force for the range of cylinder locations. For the case of a completely submerged cylinder the potential theory prediction of zero mean horizontal force is not confirmed by the experimental results and it is noted that although the magnitude of the discrepancy is small compared with the oscillatory forces it is significant for the design of mooring systems. The experimental study conducted by Longuet-Higgins (1977) is also concerned with the examination of mean forces exerted by waves on floating or submerged bodies. The theoretical prediction of the mean force is obtained by a formula derived by satisfying the principle of momentum conservation and application of this formula requires the measurement of incident and reflected wave heights. The predicted values, when compared with measurements

of the mean force obtained for models of a Cockerell wave raft and a Salter 'duck', demonstrate that the simple theory is valid for waves of small steepness. However, for steeper waves the theoretical force overestimates the measured value and the author conducted a series of model tests on a submerged horizontal circular cylinder to determine the extent of the discrepancy and the mechanisms which are significant for a range of wave steepnesses.

The experiments for the cylinder with small amplitude waves again demonstrates good agreement between theory and experiment but for steeper waves the measured force was smaller than the predicted value. For the steeper waves the presence of an appreciable second harmonic in the transmitted wave was visually identified and the author states that the ratio of wave height to local fluid depth and the ratio of local particle velocity to wave speed both imply the occurence of such non-linear behaviour. A formula for the mean force exerted by a wave which included a second harmonic was then derived and tested. The new formula predicted the occurence of a reduced force and even a negative force for a sufficiently large second harmonic content but the tests indicated that this formula accounted for some but not all of the reduction or reversal which was identified in the measured mean force values.

The agreement between the theory and the measured values was less satisfactory for breaking waves. The author suggested that the passage of the wave over the cylinder gives rise to a change in the mean water level such as that which occurs when waves approach a simple beach. The cylinder is therefore considered to act as a double beach and if wave 'set-up' or 'set-down' produce an asymmetric

change in hydrostatic pressure above the cylinder a mean horizontal force is produced. It is argued that the occurence of wave breaking is delayed by the rapid change in depth and always occurs beyond the mid point of the cylinder giving rise to a significant wave set-up and therefore a mean horizontal force upstream. It is also demonstrated that such changes in mean water level give rise to mean vertical forces.

This paper is a unique contribution of the understanding of wave induced forces on submerged obstacles since it identifies the importance of non-linear effects and suggests how such affects occur.

CHAPTER 3 - WAVE HYDRODYNAMICS

3.1 Introduction

The governing equations of irrotational motion are presented and boundary value problems are formulated and solutions written for surface waves. For the sake of clarity much detailed proof and derivation is avoided and reference is made to standard texts.

The theory of integral equations is introduced and applied to obtain a formulation for the linear diffraction boundary value problem. It is demonstrated that the continuous distribution of sources or double sources over a fictitious boundary external to the fluid domain results in a regular kernel integral equation formulation. The singular and regular kernel integral equations written for continuous surface distributions of wave sources form the basis for the numerical investigations of the following chapters.

The application of the integral equation method to the second-order diffraction boundary value problem indicates that the problem may prove amenable to a numerical approach.

The chapter closes with the application of Bernoulli's equation to obtain expressions for pressure and free surface displacement. The pressures are integrated to obtain expressions for forces and the free surface displacements in the far field are employed to obtain expressions for the reflection and transmission coefficients.

3.2 Potential Theory

The vector field $\underline{u} = (u,v,w)$ is said to be irrotational if

$$\text{curl } \underline{u} = \nabla \times \underline{u} = \underline{0} \qquad 3.2.1$$

where $\nabla = (\partial/\partial x, \partial/\partial y, \partial/\partial z)$.

For a fluid motion characterized by the velocity vector $\underline{u}$ equation 3.2.1 is a statement of zero vorticity. A necessary and sufficient condition that curl $\underline{u} = 0$ is that we can find a scalar function $\Phi(x,y,z)$ such that

$$\underline{u} = \nabla\Phi \qquad 3.2.2$$

The fundamental equations of motion for an inviscid, incompressible fluid with constant density are the continuity equation

$$\text{div } \underline{u} = \nabla \cdot \underline{u} = 0 \qquad 3.2.3$$

and Euler's equations which, written in vector notation, are

$$\underline{u}_t + (\underline{u}\nabla) \cdot \underline{u} = -\frac{1}{\rho} \nabla(p + \rho g y) \qquad 3.2.4$$

where p is the fluid pressure, ρ is the fluid density, g is the acceleration of gravity and y is the vertical coordinate and is positive in the upward direction.

For irrotational motion the substitution $\underline{u} = \nabla\Phi$ (equation 3.2.2) in the continuity equation (3.2.3) results in the Laplace equation

$$\nabla^2\Phi = 0 \qquad 3.2.5$$

Integration of Euler's equations gives rise to Bernoulli's equation

$$\frac{p}{\rho} + \Phi_t + \frac{1}{2}(\nabla\Phi)^2 + gy = F(t) \qquad 3.2.6$$

in which F(t) is an arbitrary function of time only and may for most purposes be absorbed into the velocity potential since the gradient of the scalar function is unaffected. Witham (1962) indicates that F(t) is important in certain non-linear water wave problems.

The Laplace equation and the Bernoulli equation must be satisfied at all points in the fluid domain. The particular motion in the domain is determined by the conditions imposed on the boundaries.

The kinematic boundary condition for an impermeable surface, defined by $S(x,y,z,t) = 0$, is that the substantial derivative is zero

$$\frac{DS}{Dt} = S_t + \underline{u} \cdot \nabla S = 0 \qquad 3.2.7$$

The significance of the kinematic boundary condition is that the velocity of any point on the impermeable surface must be identical to the velocity of the fluid particle adjacent to that point. For a boundary with unspecified position and velocity an additional dynamic boundary condition is required. If the pressure, p, may be prescribed, Bernoulli's equation (3.2.6) is applied on this portion of the fluid boundary.

In a properly posed boundary value problem the boundary conditions are sufficient to determine the fluid motion uniquely.

In the subsequent sections the fundamental equations, stated above, and introduced comprehensively in Lamb (1932), are applied to surface waves. Proofs of uniqueness are cited when available. The remainder of the chapter will consider motion of a fluid in a two dimensional domain only.

3.3 Surface Waves

Consider the motion of a fluid in two dimensions for a finite depth of fluid, h. If the free surface is defined by $y = \eta(x,t)$, the velocity potential $\Phi(x,y,t)$ satisfies Laplace's equation and the boundary conditions on Φ are

$$\left.\begin{aligned} \Phi_t + \frac{1}{2}(\nabla\Phi)^2 + g\eta &= 0, \\ \eta_t + \Phi_x\eta_x - \Phi_y &= 0, \end{aligned}\right\} \text{ at } y = \eta(x,t) \qquad 3.3.1$$

$$\Phi_y = 0 \quad \text{at } y = -h \qquad 3.3.2$$

where the dynamic boundary condition includes the assumption of constant pressure on the free surface.

The condition on Φ at $y = \eta(x,t)$ is highly non-linear and an exact solution of the boundary value problem is not possible. In addition the free surface boundary conditions are prescribed at an initially unknown location. An approximation to Φ is therefore required which satisfies a modified form of the exact boundary value problem.

Assuming small amplitude wave motion the boundary condition on Φ at the free surface is linearised. Relocation of the free

surface at the still water level results in errors of the same order as those already neglected. Solution of the linearised boundary value problem provides a first approximation to the fluid motion.

For waves of finite height a perturbation procedure may be employed in which Φ and η are expanded in a perturbation series in some parameter ε.

$$\Phi = \varepsilon\Phi^{(1)} + \varepsilon^2\Phi^{(2)} + \varepsilon^3\Phi^{(3)} + \ldots\ldots$$
$$\eta = \varepsilon\eta^{(1)} + \varepsilon^2\eta^{(2)} + \varepsilon^3\eta^{(3)} + \ldots\ldots \qquad 3.3.3$$

It is then assumed that the value of $\Phi(x,y,t)$ at the free surface can be expressed in terms of a Taylor series expansion about the undisturbed position $y = 0$.

$$\Phi(x,\eta,t) = \Phi(x,0,t) + \eta(\Phi_y)_{y=0} + \frac{1}{2}\eta^2(\Phi_{yy})_{y=0} + \ldots. \qquad 3.3.4$$

Algebraic manipulation of equations 3.2.5, 3.3.1 to 3.3.4 and collection of terms in ε, ε^2,..... results in the following boundary value problem

$$\nabla^2\Phi^{(p)} = 0 \quad \text{for } -h < y < 0, \quad (p = 1,2,\ldots) \qquad 3.3.5$$

$$\Phi_y^{(p)} = 0 \quad \text{on} \quad y = -h \qquad (p = 1,2,\ldots) \qquad 3.3.6$$

$$\Phi_{tt}^{(1)} + g\Phi_y = 0 \quad \text{on } y = 0, \qquad 3.3.7a$$

$$\Phi_{tt}^{(2)} + g\Phi_y^{(2)} = -2\nabla\Phi^{(1)}.\nabla\Phi_t^{(1)} + \frac{1}{g}\Phi_t^{(1)}\Phi_{tty}^{(1)} + \Phi_t^{(1)}\Phi_{yy}^{(1)} \text{ on } y = 0 \qquad 3.3.7b$$

etc.

The boundary value problem for $\Phi^{(1)}$ is the same as that which is obtained by assuming small wave amplitude. The inclusion of successive terms in the perturbation series results in progressively higher order approximations to the exact value of Φ.

The method of separation of variables is employed to obtain analytical solutions to the boundary value problems. Solutions of the successive higher-order problems are found, with additional labour, from the solution of the preceding problem. The principle results of the first- and second-order problems for progressive waves may be written in the form

$$\Phi = \frac{\omega H}{2k} \frac{\cosh k(h+y)}{\sinh kh} \sin(kx-\omega t) + \frac{3}{32} \omega H^2 \frac{\cosh 2k(h+y)}{\sinh^4 kh} \sin 2(kx-\omega t) + O(\varepsilon^3) \qquad 3.3.8$$

$$\eta = \frac{H}{2} \cos(kx-\omega t) + \frac{kH^2}{16} \frac{\cosh kh}{\sinh^3 kh} (2 + \cosh 2kh)\cos 2(kx-\omega t) + O(\varepsilon^3) \qquad 3.3.9$$

$$\frac{\omega^2}{g} = k \tanh kh + O(\varepsilon^3) \qquad 3.3.10$$

where H is the wave height, ω the angular frequency and k the wave number. Equation 3.3.10 is the dispersion equation and equations 3.3.8 to 3.3.10 are the equations for a Stokes' second-order wave.

Finite amplitude wave theory is treated in detail by Wehausen and Laitone (1960) who cite the classical papers. Existence of an exact solution to which the results of the perturbation analysis converge has seldom been demonstrated and the relevant work is

discussed by Wehausen and Laitone (1960) who conclude that this mathematical shortcoming is of no major significance.

3.4 Singular Solutions

The fundamental solution of Laplace's equation (3,2,5) for a two-dimensional domain may be written

$$\phi(\underline{x},\underline{\xi}) = -\frac{\sigma}{2\pi} \log R \qquad 3.4.1$$

The physical flow represented by this potential is that of a fluid source. The point $\underline{x} = (x,y)$ is referred to as the field point and $\underline{\xi} = (\xi,\eta)$ as the source point and $R = |\underline{x}-\underline{\xi}|$. The flux outward across a circle surrounding the source point $\underline{\xi}$ is

$$-\frac{\partial\phi}{\partial R}\, 2\pi R = \sigma \qquad 3.4.2$$

where σ is a measure of source output which may be positive or negative and is referred to as the strength of the source or the source density. The source potential is a mathematical concept which requires the continual creation or annihilation of fluid. Continuity is therefore violated and the motion is physically unacceptable, however, the fundamental solution proves valuable in the construction of solutions to problems which are not generally amenable to exact solution.

Multipoles may be constructed by placing additional sources in the vicinity of the point $\underline{\xi}$ and permitting the distance between the sources to vanish. In the current study the simple source and the doublet are adequate. The doublet may be written

$$\phi(\underline{x},\underline{\xi}) = -\frac{\mu}{2\pi}\frac{\partial}{\partial S}(\log R) \qquad 3.4.3$$

where $\partial/\partial S$ indicates a space-differentiation in the direction of the doublet axis and μ is called the doublet moment.

We shall now consider the formulation and solution of the linear surface wave problem in which a simple source is located at a single point in the fluid domain. The exercise is that of constructing a singular solution of Laplace's equation, i.e. a Green's function $G(\underline{x}, \underline{\xi}, t)$, which satisfies the following conditions

$$\nabla^2 G = 0 \quad \text{for } -h < y < 0, \quad \underline{x} \neq \underline{\xi}, \qquad 3.4.4$$

$$G_y = 0 \quad \text{on } y = -h, \qquad 3.4.5$$

$$\nu G + G_y = 0 \quad \text{on } y = 0, \qquad 3.4.6$$

where $\nu = \omega^2/g$,

$$G - (\log R)\cos\omega t \text{ is regular for } -h < y < 0 \qquad 3.4.7$$

and for large values of $r\ (=x-\xi)$,

$$G \text{ represents a diverging wave.} \qquad 3.4.8$$

Equation 3.4.8, the radiation condition, is significant in that it imposes a uniqueness which would otherwise be absent. The solution may be obtained by methods which require the use of complex variables or Fourier transforms. Both methods are followed through in Wehausen and Laitone, the former for the problem outlined above and the latter for the analogous three dimensional problem.

The singular solution, G, refered to by John (1950) as "a wave function corresponding to a wave in a liquid of constant depth h issuing from the point (x,y)" may be written in complex form as

$$G(\underline{x}, \underline{\xi}, t) = g(\underline{x}, \underline{\xi}) \exp(-i\omega t) \qquad 3.4.9$$

with $$g = g_1 + ig_2 \qquad 3.4.10$$

where

$$g_1 = \frac{1}{2\pi} \log \frac{R}{h} + \frac{1}{2\pi} \log \frac{R_2}{h}$$

$$- \frac{1}{\pi} PV \int_0^{\infty} \left[\frac{(\mu+\nu)\exp(-\mu h)\cosh\mu(h+y)\cosh\mu(h+\eta)\cos\mu(x-\xi)}{\mu(\mu\sinh\mu h - \nu\cosh\mu h)} + \frac{\exp(-\mu h)}{\mu} \right] d\mu \qquad 3.4.11$$

$$g_2 = - g_o \cosh(x - \xi) \qquad 3.4.12$$

where $R_2^2 = (x-\xi)^2 + (y+2h + \eta)^2$ is the distance between the field point and the image of the source point in the bottom boundary $y = -h$ and

$$g_o = \frac{\nu}{k} \frac{\cosh k(y+h)\cosh k(\eta+h)}{\nu h + \sinh^2 kh} \qquad 3.4.13$$

The integral in equation 3.4.11 is interpreted as a Cauchy principle value and the path of integration is indented at the positive real root $\mu=k$ of the denominator. Thorne (1953) states that "The significance of taking an integral other than the principle value is to introduce a standing wave at infinity".

An alternative expression for the real part of the Green's function, g_1, is derived by John (1950). The source and image source potentials are included in the integral by using identities for logarithmic functions and a portion of the integrand is represented by its partial fraction expansion. The result is then integrated term by term and the expression obtained may be written

$$g_1 = g_o \sin k|x-\xi| \qquad 3.4.14$$

$$- \sum_{i=1}^{\infty} \frac{1}{c_i} C_i \cos c_i(y+h)\cos c_i(\eta+h)\exp(-c_i|x-\xi|)$$

where $$C_i = \frac{c_i^2 + \nu^2}{c_i^2 h + \nu^2 h - \nu} \qquad 3.4.15$$

and $c_i, i \geq 1$, are the real positive roots of the equation

$$c\tan ch = -\nu \qquad 3.4.16$$

In addition to the singular solutions derived and stated in Wehausen and Laitone (1960) solutions for higher-order singularities in two and three dimensions are obtained by Thorne (1953).

3.5 Wave Diffraction

The boundary value problems discussed in the preceding sections are for a fluid domain bounded only by the moving free surface and the boundary at a depth $y = -h$. In this section we consider the boundary value problem for such a domain into which a fixed obstacle, defined by $\Gamma_o(x,y) = 0$, is introduced. The definition sketch is given in figure 3.5.1.

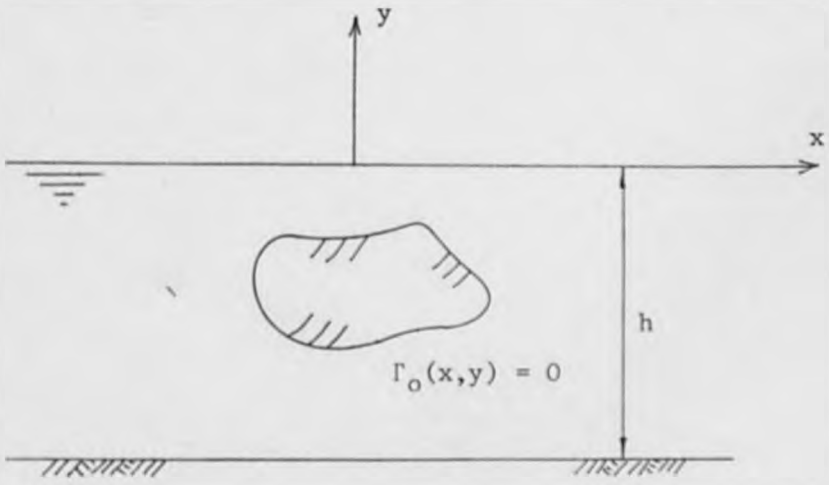

Figure 3.5.1 Definition sketch for diffraction problem

The additional boundary conditions are the kinematic condition on the boundary Γ_o and the radiation condition.

In order to obtain a second-order diffraction theory we adopt the perturbation series equation 3.3.3 and the boundary condition on Γ_o may then be expressed as

$$\phi_m^{(p)} = 0 \quad \text{on } \Gamma_o, \quad (p = 1,2) \tag{3.5.1}$$

where the subscript m indicates the normal gradient on Γ_o. Equation 3.5.1 with equations 3.3.5 to 3.3.7 and a suitable radiation condition compose the boundary value problem for wave diffraction to the second-order.

Since Laplace's equation is linear we may express the velocity potential Φ as the sum of two potentials

$$\Phi = \Phi_w + \Phi_s \tag{3.5.2}$$

where Φ_w is the incident wave potential and Φ_s is the scattered wave potential. The potentials Φ_w and Φ_s are expanded in a perturbation series in ε and substituted into the boundary value problem. Φ_w, the incident wave potential is chosen to be identical to the potential stated in equation 3.3.8, therefore the problem is that of finding Φ_s subject to the conditions

$$\nabla^2\phi_s^{(p)} = 0 \quad \text{for } -h < y < 0, \quad (p = 1,2) \tag{3.5.3}$$

$$\phi_{s_y}^{(p)} = 0 \quad \text{on } y = -h, \qquad (p = 1,2) \tag{3.5.4}$$

$$\phi_{s_{tt}}^{(1)} + g\phi_{s_y}^{(1)} = 0 \quad \text{on } y = 0, \tag{3.5.5a}$$

$$\phi_{tt}^{(2)} + g\phi_y^{(2)} = -2\nabla\phi^{(1)}\cdot\nabla\phi_t^{(1)} + \frac{1}{g}\phi_t^{(1)}\phi_{tty}^{(1)} + \phi_t^{(1)}\phi_{yy}^{(1)} \quad \text{on } y = 0 \qquad 3.5.5b$$

$$\phi_{s_m}^{(p)} = -\phi_{w_m}^{(p)} \quad \text{on } \Gamma_o \ (p = 1,2) \qquad 3.5.6$$

and $$\phi_s^{(p)} = i\frac{k^2}{\omega}\phi_{s_r}^{(p)} \quad \text{for} \quad r \to \infty \ (p = 1,2) \qquad 3.5.7$$

where $r = |x|$.

It may be noted that the lack of linearity in equation 3.5.5b deprives us of the opportunity of eliminating the incident wave potential and that equation 3.5.7 is the radiation condition for progressive wave motion in a two dimensional domain.

The discussion of the non-linear diffraction boundary value problem is postponed and we now consider the linear problem. The uniqueness problem has been treated in great detail by John (1950) who provides a proof which is valid subject to certain geometrical restrictions on the obstacle surface, Γ_o, namely that Γ_o intersects the free surface perpendicularly. This restriction excludes obstacles which are completely submerged. However, for the particular case of a circular two dimensional obstacle submerged in water of infinite depth Ursell (1950b) has proved uniqueness. John concludes his discussion of the uniqueness problem by stating that the absence of a general uniqueness proof for the linear wave diffraction boundary value problem should not be taken to imply the absence of a solution which determines the fluid motion uniquely.

For two dimensional obstacles no analytical solution exists. It is therefore necessary to obtain a solution by the application of numerical techniques to the problem as stated or to an alternative formulation.

The first option would be to apply finite element or finite difference techniques to obtain a solution to the boundary value problem as stated in equations 3.5.3, 3.5.4, 3.5.5a, 3.5.6 and 3.5.7 with p=1. Since application of the finite element method requires that the entire fluid domain is discretized consideration must be given to the application of the radiation condition. It seems that the most suitable approach is to apply a hybrid element method in which the fluid domain is divided into exterior and interior domains and the finite element method is applied in the interior domain and an alternative method in the external domain. This direct numerical approach may prove advantageous when attempting to solve the second-order problem as stated in equations 3.5.3 to 3.5.7.

The second option, with a greater tradition in the solution of potential theory problems, involves the introduction of fluid singularities. The singularities may be introduced either as a system of multipoles at the centre of the obstacle or as continuous surface distributions of singularities. The multipole method was applied by Ursell (1950a) to the problem for a submerged circular cylinder in water of finite depth. The multipoles which vanish at very large distances from their location may be chosen to satisfy the free surface and bottom boundary conditions. The radiation condition is satisfied by inclusion of a suitable harmonic function which satisfies the same boundary conditions as the multipoles. The potential is expressed as a power series with unknown coefficients which must be determined by applying the boundary condition on the surface of the obstacle. Values for the coefficients are obtained by solving a system of simultaneous linear algebraic equations.

The multipole method suffers two limitations. Firstly, for objects of more complicated geometry, a conformal transformation is required to map the object onto an arc of a circle and the method is not generally applicable to problems which include more than one obstacle. Therefore, the method is best suited to single objects of simple geometry. Secondly, the assumptions inherent in the formulation do not permit an application of the method to obtain a solution to the second-order boundary value problems.

In the subsequent sections the method of integral equations is introduced and it is demonstrated that the wave diffraction boundary value problem may be rewritten in integral equation form.

3.6 Integral Equations

Many problems in potential theory may be solved by the formulation and numerical solution of an integral equation subject to certain prescribed boundary conditions. A brief theoretical introduction to the Fredholm integral equation is included in appendix A.1. In this section we are concerned with the introduction of integral equation formulations for potential theory problems in hydrodynamics, therefore the scope of this section will be sufficient to permit application of the method to a boundary value problem in a doubly-connected domain with mixed boundary conditions. It may be noted that application of the method to problems in two dimensional domains, may, under certain conditions, introduce difficulties which are absent in three dimensional potential theory. These are concerned with possible logarithmic behaviour at infinity and the possible existence of a Γ-contour (Jaswon, 1964).

The formulation of an integral equation for the solution of a potential theory problem requires the introduction of surface distributions of singularities. Lamb (1932:Art 56) stated that the singularities of equations 3.4.1 and 3.4.3 may be imagined to be continuously distributed over lines, surfaces or volumes. If we imagine a singular harmonic function, ϕ^*, distributed over a Liapunov surface, Γ, with a continuously varying strength, σ, then the distribution is written

$$\int_\Gamma \sigma(\underline{\xi})\phi^*(\underline{x},\underline{\xi})d\Gamma \qquad 3.6.1$$

$\phi^*(\underline{x},\underline{\xi})$ will be referred to as the source potential at the field point, $\underline{x}$, due to the location of the source at the source point, $\underline{\xi}$, where $\underline{\xi} \in \Gamma$. We may also write a similar integral for a double layer of sources over Γ

$$\int_\Gamma \mu(\underline{\xi}) \frac{\partial \phi^*}{\partial n} (\underline{x},\underline{\xi})d\Gamma \qquad 3.6.2$$

where μ is the density of the double source and $\partial/\partial n$ indicates space-differentiation in the direction of the double source axis.

We now proceed, in a similar fashion to Lamb (1932: Art 57,58), to prove that a potential, ϕ, may be regarded as due to a distribution of single sources, ϕ^*, and double sources, $\partial\phi^*/\partial n$, over the boundary of the domain, Γ, or alternatively as a distribution of single or double sources only.

For a domain, Ω, bounded by a surface, Γ, in which ϕ and ψ are two potential functions, Green's theorem may be written in the form

$$\int_\Omega (\phi\nabla^2\psi - \psi\nabla^2\phi)d\Omega = \int_\Gamma (\phi\nabla\psi - \psi\nabla\phi)d\Gamma \qquad 3.6.3$$

The function ϕ is chosen to be harmonic in $\Omega+\Gamma$ and the potential ψ is chosen as the potential due to a surface distribution of sources ϕ^* throughout the domain Ω and over the boundary of the domain Γ, where

$$\phi^*(\underline{x},\underline{\xi}) = \log|\underline{x}-\underline{\xi}| + \phi_o^*(\underline{x},\underline{\xi}) \qquad 3.6.4$$

with ϕ_o^* a regular harmonic function within $\Omega+\Gamma$.

We may now write

$$\nabla^2\phi = 0 \qquad 3.6.5$$

$$\nabla^2\phi^* = 2\pi\delta(\underline{x}-\underline{\xi}) \qquad 3.6.6$$

where equation 3.6.5 is Laplace's equation and equation 3.6.6 is Poisson's equation where the Dirac delta function is defined by

$$\delta(\underline{x}-\underline{\xi}) = 0 \qquad \underline{x} \neq \underline{\xi}, \qquad 3.6.7a$$

$$\delta(\underline{x}-\underline{\xi}) = \infty \qquad \underline{x} = \underline{\xi}, \qquad 3.6.7b$$

For $\underline{x} \neq \underline{\xi}$ we may reduce Green's theorem

$$0 = \int_\Gamma \phi \frac{\partial\phi^*}{\partial n}\, d\Gamma - \int_\Gamma \phi^* \frac{\partial\phi}{\partial n}\, d\Gamma \qquad 3.6.8$$

where the change of notation is to aid in distinguishing between the gradient of the source axis and a normal to a physical boundary which will be introduced later in this section.

The integrals in equation 3.6.8 must now be evaluated with consideration for the possible locations of the field point $\underline{x}$. If the field point is located at a point within the domain equation 3.6.8 cannot be applied throughout the whole of the domain since $\nabla^2\phi^* \neq 0$ as $\underline{x} \to \underline{\xi}$. This difficulty is eliminated by describing a small circular surface, Γ_ε, about $\underline{x}$ as centre (figure 3.6.1a) and the

integrals in equation 3.6.8 are evaluated over $\Gamma + \Gamma_\varepsilon$. Substituting for ϕ^* from equation 3.6.4 equation 3.6.8 is rewritten

$$\int_\Gamma \phi \frac{\partial}{\partial n}(\phi_o^* + \log R)d\Gamma - \int_\Gamma (\phi_o^* + \log R)\frac{\partial \phi}{\partial n} d\Gamma \qquad 3.6.9$$

$$= -\int_{\Gamma_\varepsilon} \phi \frac{\partial}{\partial n}(\phi_o^* + \log R)d\Gamma_\varepsilon + \int_{\Gamma_\varepsilon} (\phi_o^* + \log R)\frac{\partial \phi}{\partial n} d\Gamma_\varepsilon$$

where $R = |\underline{x}-\underline{\xi}|$. The boundary Γ_ε is of length $2\pi R$ and $\partial/\partial n\ (\log R) = -\partial/\partial R(\log R) = -1/R$ (where the normal is taken to be positive when pointing out of Ω). Evaluation of the integral on the righthand side of equation 3.6.9 which includes the simple dipole will result in a finite limit for $\varepsilon \to 0$. The integrals for the weaker singularity and the functions ϕ_o^* and $\partial\phi_o^*/\partial n$ vanish as $\varepsilon \to 0$. Equation 3.6.9 may now be written

$$\frac{1}{2\pi}\int_\Gamma \phi \frac{\partial \phi^*}{\partial n} d\Gamma - \frac{1}{2\pi}\int_\Gamma \phi^* \frac{\partial \phi}{\partial n} d\Gamma = \phi(\underline{x}) \qquad 3.6.10$$

for $\underline{x} \in \Omega$. If $\underline{x}$ is located on the boundary Γ (figure 3.6.1b)

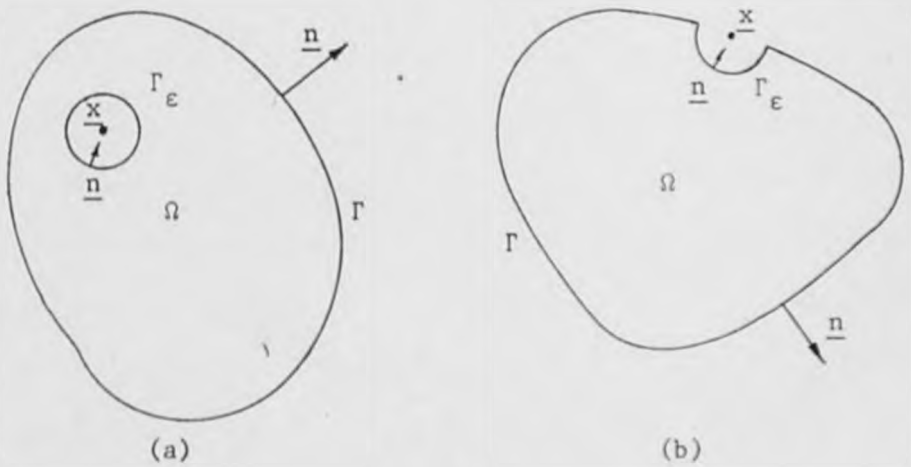

Figure 3.6.1 Exclusion of singular point from domain

a circular arc, Γ_ε, is introduced which has a length, $2\Pi\alpha$, where α is dependent upon the curvature of the surface Γ at the point $\underline{x}$. In this case the integrals over the boundary Γ must be evaluated in the Cauchy principal value sense. The third and final alternative is that $\underline{x}$ is located outside the domain and its boundary in which case there is no singular term. Equation 3.6.10 may now be written in a more general form

$$-\frac{1}{2\Pi}\int_\Gamma \phi\,\frac{\partial\phi^*}{\partial n}\,d\Gamma + \frac{1}{2\Pi}\int_\Gamma \phi^*\,\frac{\partial\phi}{\partial n}\,d\Gamma = \beta\phi(\underline{x}) \qquad 3.6.11$$

where $\beta = 0 \qquad \underline{x} \notin \Omega + \Gamma$ 3.6.12a

$\beta = \alpha \qquad \underline{x} \in \Gamma$ 3.6.12b

$\beta = 1 \qquad \underline{x} \in \Omega$ 3.6.12c

Comparison with integrals in equation 3.6.1 and 3.6.2 indicates that the value of ϕ for $\underline{x} \in \Omega + \Gamma$ is given by the sum of two potentials, the first is the velocity potential due to a surface distribution of sources with a density $-\partial\phi/\partial n$ per unit length and the second is due to a surface distribution of double sources with axes normal to the surface and density ϕ.

For a domain which extends to infinity in all directions the surface integrals in equation 3.6.11 may be taken to apply to the internal boundary alone. The potential due to a dipole vanishes as $|\underline{x}-\underline{\xi}|$ becomes large but consideration must be given to the behaviour of the logarithmic singularity at infinity. It may be demonstrated (Jaswon, 1964) that a potential function exists which is bounded at infinity and which includes an additive constant which it is convenient to neglect. We also require that ϕ_o^* is chosen such that the remaining integrals vanish.

We now consider a doubly-connected domain, Ω, bounded by $\Gamma = \Gamma_1 + \Gamma_2$. The domains Ω_1 and Ω_2 fill the remainder of the infinite domain with the domain Ω_2 bounded by a circle of infinite radius centred at $\underline{x}$ which is located in Ω (figure 3.6.2). The potentials ϕ, ϕ_1 and ϕ_2 refer to the domains Ω, Ω_1 and Ω_2 respectively and the normals drawn into the domains are $\partial/\partial n$, $\partial/\partial n_1$ and $\partial/\partial n_2$ respectively. Since $\underline{x}$ is internal to Ω it is therefore external to $\Omega_1 + \Omega_2$ and by application of equation 3.6.12 we have

$$\phi(\underline{x}) = \frac{1}{2\pi}\int_\Gamma \phi^* \frac{\partial\phi}{\partial n}\, d\Gamma - \frac{1}{2\pi}\int_\Gamma \phi \frac{\partial\phi^*}{\partial n}\, d\Gamma \qquad 3.6.13a$$

$$0 = \frac{1}{2\pi}\int_{\Gamma_1} \phi^* \frac{\partial\phi_1}{\partial n_1} d\Gamma - \frac{1}{2\pi}\int_{\Gamma_1} \phi_1 \frac{\partial\phi^*}{\partial n_1}\, d\Gamma \qquad 3.6.13b$$

$$0 = \frac{1}{2\pi}\int_{\Gamma_2} \phi^* \frac{\partial\phi_2}{\partial n_2} d\Gamma - \frac{1}{2\pi}\int_{\Gamma_2} \phi_2 \frac{\partial\phi^*}{\partial n_2}\, d\Gamma \qquad 3.6.13c$$

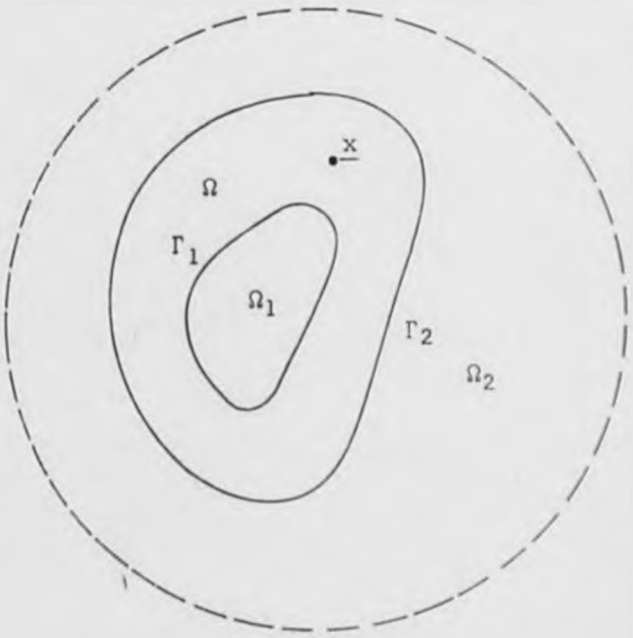

Figure 3.6.2 Doubly-connected domain

By the definitions of the normals on Γ_1 and Γ_2 we may substitute $\partial/\partial n_1 = -\partial/\partial n$ on Γ_1 and $\partial/\partial n_2 = -\partial/\partial n$ on Γ_2. Addition of equations 3.6.13 gives

$$\phi(\underline{x}) = \frac{1}{2\pi}\int_{\Gamma_1} \phi^* \frac{\partial}{\partial n}(\phi - \phi_1)\, d\Gamma - \frac{1}{2\pi}\int_{\Gamma_1} (\phi - \phi_1)\frac{\partial \phi^*}{\partial n}\, d\Gamma$$

$$+ \frac{1}{2\pi}\int_{\Gamma_2} \phi^* \frac{\partial}{\partial n}(\phi - \phi_2)\, d\Gamma - \frac{1}{2\pi}\int_{\Gamma_2} (\phi - \phi_2)\frac{\partial \phi^*}{\partial n} d\Gamma \qquad 3.6.14$$

Clearly the same result would be obtained for $\underline{x} \in \Gamma_1$ or $\underline{x} \in \Gamma_2$.

The functions ϕ_1 and ϕ_2 are determined by the values of ϕ_1, $\partial\phi_1/\partial n_1$ and ϕ_2, $\partial\phi_2/\partial n_2$ on the boundaries Γ_1 and Γ_2 respectively. If we set $\phi_1 = \phi$ on Γ_1 and $\phi_2 = \phi$ on Γ_2 equation 3.6.14 is reduced to the form

$$\phi(\underline{x}) = \frac{1}{2\pi}\int_{\Gamma_1} \phi^* \frac{\partial}{\partial n}(\phi - \phi_1) d\Gamma + \frac{1}{2\pi}\int_{\Gamma_2} \phi^* \frac{\partial}{\partial n}(\phi - \phi_2) d\Gamma \qquad 3.6.15$$

That is, the potential is determined by a distribution of sources over Γ with an unknown density

$$\frac{\partial}{\partial n}(\phi - \phi_1) \quad \text{on} \quad \Gamma_1 \qquad 3.6.16a$$

$$\frac{\partial}{\partial n}(\phi - \phi_2) \quad \text{on} \quad \Gamma_2 \qquad 3.6.16b$$

It is convenient to rewrite equation 3.6.11 in the form

$$\phi(\underline{x}) = \frac{1}{2\pi}\int \sigma(\underline{\xi})\, \phi^*(\underline{x},\underline{\xi}) d\Gamma \qquad 3.6.17$$

where σ denotes the source density function.

Alternatively, if the normal velocities on Γ_1 and Γ_2 are chosen such that $\partial\phi_1/\partial n_1 = -\partial\phi/\partial n$ on Γ_1 and $\partial\phi_2/\partial n_2$ on Γ_2, the reduced form of equation 3.6.10 is

$$\phi(\underline{x}) = \frac{1}{2\Pi}\int_{\Gamma_1}(\phi - \phi_1)\frac{\partial\phi^*}{\partial n}\,d\Gamma - \frac{1}{2\Pi}\int_{\Gamma_2}(\phi - \phi_2)\frac{\partial\phi^*}{\partial n}\,d\Gamma \qquad 3.6.18$$

in which the potential is determined by a distribution of double sources over Γ with unknown density

$$-(\phi - \phi_1) \quad \text{on} \quad \Gamma_1 \qquad 3.6.19a$$

$$-(\phi - \phi_2) \quad \text{on} \quad \Gamma_2 \qquad 3.6.19b$$

Equation 3.6.14 is rewritten

$$\phi(\underline{x}) = \frac{1}{2\Pi}\int_{\Gamma}\mu(\underline{\xi})\frac{\partial\phi^*}{\partial n}(\underline{x},\underline{\xi})\,d\Gamma \qquad 3.6.20$$

It has been shown that the potential function $\phi(\underline{x})$ may be represented by any one of three integral equations for $\underline{x} \in \Gamma_1 + \Omega + \Gamma_2$. However, the domain, Ω, considered in the preceding paragraphs with associated surface and boundary distributions of sources through the domain and over the boundary, Γ, are abstract mathematical concepts. Introduction of a fluid domain, Ω_F, attaches a physical significance to the potential function, ϕ, which may be determined if appropriate boundary conditions are prescribed on the physical boundaries of the fluid domain, Γ_F. The possible boundary conditions may be classified as follows:

$$\phi(\underline{x}) = \bar{\phi}(\underline{x}) \;,\; \underline{x} \in \Gamma_D, \qquad 3.6.21a$$

$$\frac{\partial\phi}{\partial n}(\underline{x}) = \frac{\partial\bar{\phi}}{\partial n}(\underline{x}), \underline{x} \in \Gamma_N, \qquad 3.6.21b$$

$$\alpha(\underline{x})\phi(\underline{x}) + \beta(\underline{x})\frac{\partial\phi}{\partial n}(\underline{x}) + \gamma(\underline{x}) = 0 \;,\; \underline{x} \in \Gamma_M, \qquad 3.6.21c$$

where α, β and γ are known functions, $\Gamma_F = \Gamma_D + \Gamma_N + \Gamma_M$ (figure 3.6.3) and the over-bar indicates a prescribed value. The first and second type of condition are the Dirichlet and Neumann conditions, respectively, which are particular cases of the linear relation stated in the third equation.

If the physical boundary, Γ_F, is taken to coincide with the boundary of the doubly-connected domain, Γ, an integral equation may be formulated for the fluid potential in $\Omega_F(\Omega)$. This results in a coupled integral equation which may be reduced by a suitable choice of the regular harmonic function ϕ_o^*.

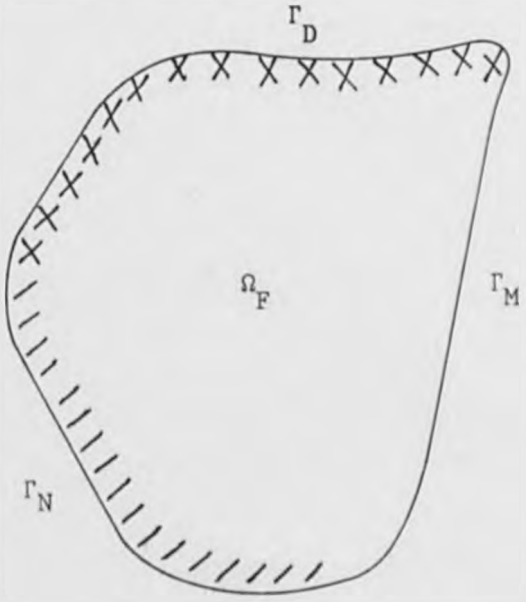

Figure 3.6.3 Boundary conditions for fluid domain

3.7 Linear Wave Diffraction

We are now in a position to formulate an integral equation for the scattered velocity potential $\phi_s^{(1)}$. It is convenient to express the first-order potential $\bar{\Phi}^{(1)}$ $(= \phi_w^{(1)} + \phi_s^{(1)})$ in complex notation with the superscript supressed , that is

$$\Phi = \phi \exp(-i\omega t) \qquad 3.7.1$$

where $$\phi = (\phi_s + \phi_w) \qquad 3.7.2$$

We now proceed to obtain an integral equation representation for the spatial potential ϕ_s subject to the appropriate boundary conditions as stated in equations 3.5.4, 3.5.5a, 3.5.6 and 3.5.7 with p = 1. A number of alternative integral equations may be written depending upon the source distributions on the domain boundary and the choice of the source potential ϕ^*.

If the integral equation is chosen as a distribution of sources and double sources in the form of equation 3.6.11 with $\underline{x} \in \Gamma$ it may be demonstrated that the solution of the integral equation yields the value of $\phi_s(\underline{x})$ for $\underline{x} \in \Gamma$ which may in turn be used to obtain values of $\phi_s(\underline{x})$ for $\underline{x} \in \Omega$. This formulation for the linear wave diffraction was employed by Bai and Yeung (1974) who employed distributions of simple sources and double sources ($\phi^* = \log|\underline{x}-\underline{\xi}|$). More recently Naftzger and Chakrabarti (1979) employed the two dimensional wave function written in equations 3.4.9 to 3.4.16 to reduce the integral equation. Both alternatives result in a Fredholm integral equation of the second kind for which an analytical solution is unavailable. There is a well established general theory for integral equations of the second kind, however, the classical theory does not, strictly speaking, apply to

equations with singular kernels. For equations in which the kernels are weakly singular the general theory is taken to apply and a numerical solution is sought. Since in these methods the value of the unknown potential, ϕ_s, is evaluated by solution of the integral equation as written, the method is often referred to as a direct method.

As an alternative the scattered potential may be written as a distribution of sources or double sources only in the same form as equation 3.6.13 or 3.6.16. The latter proves advantageous for problems in which the physical boundary, or a portion of it, is a thin impermeable membrane which divides the fluid domain. However, the general approach is similar for either distribution and we proceed to consider the case of a distribution of sources only.

The diffraction problem does not appear to have been solved by a distribution of simple sources or simple doublets only. However, for problems in two and three dimensions this type of representation with ϕ^* chosen to be the appropriate Green's function has proved to be most popular. The popularity of this method may at first sight appear surprising since the unknown source density function must be determined before the physically significant quantities may be evaluated. This method is consequently referred to as an indirect integral method.

For the two dimensional wave diffraction boundary value problem the scattered potential, ϕ_s, may be generated by a distribution of sources over the boundary Γ.

$$\phi_s(\underline{x}) = \int_\Gamma \sigma(\underline{\xi})\phi^*(\underline{x},\underline{\xi})d\Gamma, \quad \underline{x} \in \Omega + \Gamma \qquad 3.7.3$$

Before the boundary conditions may be applied an expression is required for the gradient of the potential. If the gradient is required at the point $\underline{x} \in \Omega + \Gamma$ in the direction specified by $\partial/\partial m$ we may write

$$\frac{\partial \phi_s(\underline{x})}{\partial m} = \int_\Gamma \sigma(\underline{\xi}) \frac{\partial \phi^*}{\partial m}(\underline{x},\underline{\xi}) d\Gamma, \quad \underline{x} \in \Omega + \Gamma \qquad 3.7.4$$

It must be noted that $\partial/\partial m$ may bear no relationship to the axis of a double source. For a point $\underline{x} \in \Omega$ this representation is adequate, however, for $\underline{x} \in \Gamma$ the behaviour of the kernel must be considered for $\underline{x} \to \underline{\xi}$. The approach adopted is similar to that described previously in which a small arc, Γ_ε, of length $2\Pi\alpha$, is described about the point $\underline{x} = \underline{\xi}$. The resulting expression for the gradient may be written

$$\frac{\partial \phi_s(\underline{x})}{\partial m} = \int_\Gamma \sigma(\underline{\xi}) \frac{\partial \phi^*}{\partial m}(\underline{x},\underline{\xi}) d\Gamma + \beta\sigma(\underline{x}) \qquad 3.7.5$$

where $\beta = 0 \qquad \underline{x} \in \Omega \qquad 3.7.6a$

$\beta = \alpha \qquad \underline{x} \in \Gamma \qquad 3.7.6b$

Application of the boundary conditions (equations 3.5.4, 3.5.5a, 3.5.6, 3.5.7 with p = 1) on the various portion of the fluid boundary results in the following integral equation formulation.

$$0 = \int_\Gamma \sigma \frac{\partial \phi^*}{\partial y} d\Gamma + \beta\sigma, \quad \underline{x} \in \Gamma_B, \qquad 3.7.7a$$

$$0 = \nu \int_\Gamma \sigma\phi^* d\Gamma - \int_\Gamma \sigma \frac{\partial \phi^*}{\partial y} d\Gamma - \beta\sigma, \quad \underline{x} \in \Gamma_s, \qquad 3.7.7b$$

$$0 = \frac{\partial \phi_w}{\partial m} + \int_\Gamma \sigma \frac{\partial \phi^*}{\partial m} d\Gamma + \beta\sigma, \quad \underline{x} \in \Gamma_o, \qquad 3.7.7c$$

$$0 = \int_\Gamma \sigma \frac{\partial \phi^*}{\partial r} d\Gamma + \beta\sigma - \frac{ik^2}{\omega} \int_\Gamma \sigma\phi^* d\Gamma, \quad \underline{x} \in \Gamma_R + \Gamma_L \qquad 3.7.7d$$

where $r = |x-\xi|$ and $\Gamma = \Gamma_B + \Gamma_S + \Gamma_o + \Gamma_R + \Gamma_L$. (figure 3.7.1). Since $\underline{x} \in \Gamma$ and the boundaries Γ_B, Γ_S, Γ_R and Γ_L are straight lines $\beta = \alpha = 1$ in equations 3.7.7a, b and d provided $\underline{x}$ is not at a corner point. For $\underline{x} \in \Gamma_o$ we may in general write $\beta = \alpha = \frac{1}{2}$ on the understanding that there are no corners in Γ_o. However, Γ is no longer a Liapunov surface and consideration must be given to the behaviour at corner points.

If ϕ^* is chosen to be the Green's function written in equations 3.4.9 to 3.4.16 the conditions 3.7.7a, b and d are automatically satisfied and the integral equation reduces to the form

$$0 = \frac{\partial \phi_w}{\partial m} + \int_\Gamma \sigma \frac{\partial g}{\partial m} \, d\Gamma + \frac{\sigma}{2} \qquad 3.7.8$$

The problem for the doubly-connected domain has therefore been reduced to an exterior Neumann problem.

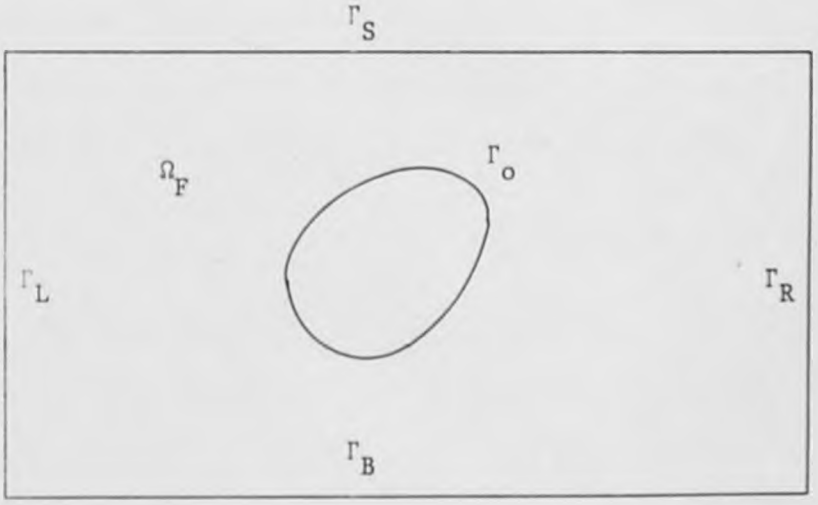

Figure 3.7.1 Fluid domain for diffraction problem

Again the integral equations are Fredholm integral equations of the second kind, however, equation 3.7.7 or 3.7.8 must be solved for the unknown source density function, σ, which may then be substituted in equation 3.7.3 to determine the potential function ϕ_s at any point $\underline{x} \in \Omega + \Gamma$.

3.8 Integral Equation Formulations with Regular Kernels

In choosing the physical boundaries of the fluid domain to be coincident with the source distribution boundaries and the fluid domain to be coincident with the surface distribution of sources each integral equation formulated for the linear diffraction problem includes a singular kernel. This is a feature of the integral equation method for potential theory problems and we may refer to these equations as singular kernel integral equations. The equations required to evaluate the potential or its gradient at a point within the domain do not contain singular kernels and may therefore be referred to as regular kernel equations. In this section it is demonstrated that a regular kernel integral equation may be formulated for the solution of potential theory problems and the method is applied to obtain formulations for the linear diffraction problem.

The basis of the regular kernel integral equation is in the choice of two distinct domains, the fluid domain Ω_F, bounded by Γ_F and the fictitious domain Ω, bounded by Γ. The domain Ω, as previously, has an imagined surface distribution of sources and the boundary, Γ, has an associated line distribution which gives rise to the expressions for the potential function written in equations 3.6.11, 3.6.17 and

3.6.20. The potential function $\phi(\underline{x})$ is taken to be regular and harmonic throughout the infinite domain and to have physical significance attached to it within the fluid domain and on the fluid boundary ($\underline{x} \in \Omega_F + \Gamma_F$). A simple example of this approach is the representation of the motion of a fluid past a circle in the infinite domain by the superposition of the uniform flow and doublet potentials. The distinction is that the doublet potential is singular at its origin but the similarities may be emphasised. Firstly, that the boundary condition is satisfied over a particular boundary and secondly that physical significance is then attached to this boundary and the potential function is taken to represent the fluid motion on the boundary and in the region exterior to it.

We now concern ourselves with the possible relationships between the physical and fictitious domains. We first consider the two dimensional doubly-connected domain as introduced in section 3.6 in which the physical domain Ω_F is located (figure 3.8.1).

The choice of Green's boundary formula (equation 3.6.11) under these circumstances proves unsuitable. Since the field point, $\underline{x}$, lies within the domain, Ω, the value of β is set to unity. We might therefore attempt to apply the boundary conditions for $\underline{x} \in \Gamma_F$ but examination of the equation indicates that unless the potential and its gradient are prescribed on the fictitious boundary the equation is indeterminate. It is therefore clear that this approach only results in a suitable formulation if Γ and Γ_F are chosen to be coincident.

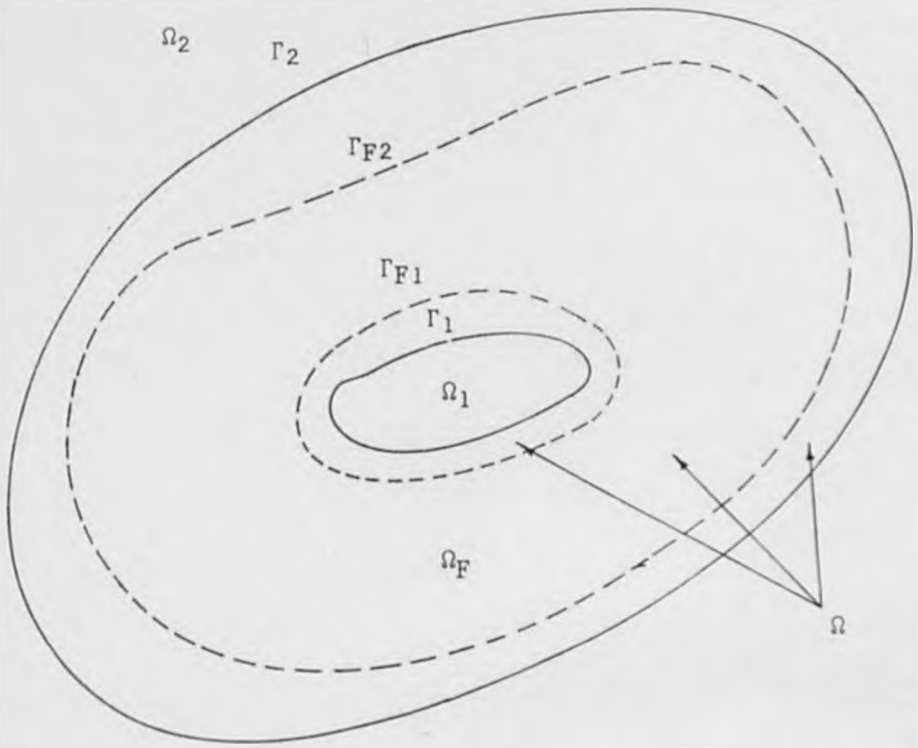

Figure 3.8.1 Doubly-connected domain containing physical domain

We now pursue a formulation by representing the potential function as a distribution of sources only on the understanding that a similar argument holds for a distribution of double sources. The significance of the choice of domain locations is best indicated by prescribing boundary conditions on $\Gamma_F = \Gamma_{F1} + \Gamma_{F2}$ to obtain an integral equation formulation and the linear diffraction problem is therefore re-examined.

It has been demonstrated that the formulation of an integral equation in this problem depends not only on the representation of the scattered potential in integral form but also on a similar representation of the potential gradient (equations 3.7.3 and 3.7.5). With the physical boundary separated from the fictitious boundary the boundary conditions may be applied for the field point on the fluid boundary

$\underline{x} \in \Gamma_F$. The kernels in equation 3.7.3 and 3.7.5 are now non-singular and we therefore set β equal to zero. The appropriate formulation is therefore implicit in equations 3.7.7 and we may rewrite equation 3.7.8 in the more general form

$$0 = \frac{\partial \phi_w}{\partial m}(\underline{x}) + \int_\Gamma \sigma(\underline{\xi}) \frac{\partial g}{\partial m}(\underline{x},\underline{\xi}) d\Gamma + \beta\sigma(\underline{x}) \qquad 3.8.1$$

with β as specified in equations 3.7.6.

The source distributions are fictitious concepts. We may therefore, as an alternative, imagine that for a doubly connected domain there is a surface distribution of sources throughout the rest of infinite space, $\Omega_1 + \Omega_2$, and over the domain boundaries, $\Gamma_1 + \Gamma_2$, but not within the domain, Ω. The fluid domain, Ω_F, is again located within the fictitious domain, Ω (figure 3.8.1).

Under these circumstances the choice of the Green's boundary formula (equation 3.6.11) requires that the constant β is set to zero but the method proves to be unsuitable for the same reasons as stated above. This is the approach which most closely resembles the "regular boundary element method" proposed by Patterson and Sheikh (1982).

This alternative relationship between the fluid domain and the fictitious domain does not alter the regular kernel integral equation formulations stated in equations 3.7.7 and 3.8.1 since the representations for the potential (equation 3.7.3) and the potential gradient (equation 3.7.5) hold throughout the infinite domain.

It has now been demonstrated that the regular kernel integral equation, generated by the distribution of sources over fictitious boundaries external to the domain in which the fluid is contained, may be employed in potential theory. In particular the regular kernel integral equation formulation for the linear diffraction boundary value problem has been stated. The integral equations are Fredholm integral equations of the first kind for which no general theory is available. However, for a number of problems in which physical significance is attached to the potential function, the formulation and solution of singular and regular kernel Fredholm equations of the first kind has yielded satisfactory results (Symm, 1964; Oliveira, 1968; Coates, 1982). The regular kernel integral equation together with its singular kernel counterpart as stated in equation 3.8.1 forms the basis for the numerical investigations of the next chapter.

3.9 Second-Order Diffraction Theory

The second-order diffraction boundary value problem is included in equations 3.5.3 to 3.5.7 and this section is concerned with the formulation of an integral equation for the problem as stated. It has been demonstrated that potential theory problems may be formulated as integral equations by representing the unknown potential as a distribution of sources and double sources over a domain boundary. Alternatively, a formulation is obtained for sources or double sources distributed over a boundary which may be chosen to coincide with the domain boundary or may be located outside the domain. The following formulation is carried out for

the case of a distribution of sources only but it may be noted that any one of the alternative representations might have been chosen. The unknown second-order scattered wave potential is given in its spatial form by

$$\phi_s^{(2)}(\underline{x}) = \int_\Gamma \sigma(\underline{\xi})\phi^*(\underline{x},\underline{\xi})\, d\Gamma \qquad 3.9.1$$

where again the boundary Γ may or may not coincide with the physical boundaries of the fluid domain and the gradient at a point is given by

$$\frac{\partial \phi_s^{(2)}}{\partial m} = \int_\Gamma \sigma(\underline{\xi}) \frac{\partial \phi^*}{\partial m}(\underline{x},\underline{\xi}) d\Gamma + \beta\sigma(\underline{x}) \qquad 3.9.2$$

where β is given in equation 3.7.6.

It is now necessary to apply the boundary conditions on $\phi_s^{(2)}$ to obtain a formulation in the same form as equation 3.7.7. The equations 3.7.7a and 3.7.7d require no modification since the form of the bottom boundary and radiation boundary conditions are the same for the first- and second-order problems. The modification for the statement of the condition on the object boundary is simple and it is required only that the incident wave normal velocity $\partial\phi_w/\partial m$ is replaced by the second-order expression $\partial\phi_w^{(2)}/\partial m$ which may be obtained from the second-term in equation 3.3.8. The application of the free surface boundary condition is, however, more difficult and this difficulty is associated with the evaluation of the right hand side of equation 3.5.5b in which it is necessary to include the total potential $\Phi(\underline{x},t)$.

The first-order potential is given by equations 3.7.1 and 3.7.2 and therefore if a solution is obtained for the first-order boundary value problem stated in equation 3.7.7 the source density function may then be applied to obtain the value of the potential or potential gradient using equations 3.7.3 and 3.7.5. This approach may be extended to include the evaluation of the potential gradients included in the right hand side of equation 3.5.5b and if the left hand side of equation 3.5.5b is written as the sum of the scattered wave and incident wave second-order potentials the equation may be rewritten in the general form

$$\frac{\partial^2 \phi_s^{(2)}}{\partial t^2}(\underline{x},t) + g \frac{\partial \phi_s^{(2)}}{\partial y}(\underline{x},t) = Q(\underline{x},t) \qquad 3.9.3$$

where Q is obtained by substitution of the expressions given in Appendix A.2 in the right hand side of equation 3.5.5b and includes the second-order incident wave terms. The function Q will consist of a constant term and a term fluctuating at twice the incident wave frequency and the second-order scattered wave potential will be of the same form, therefore, considering the fluctuating parts only

$$Q(\underline{x},t) = q(\underline{x}) \exp(-2\, i\omega t) \qquad 3.9.4$$

$$\phi_s^{(2)}(\underline{x},t) = \phi_s^{(2)}(\underline{x}) \exp(-2\, i\omega t) \qquad 3.9.5$$

and equation 3.9.3 may be written

$$\frac{\partial \phi_s^{(2)}}{\partial y} - V\phi_s^{(2)} = \frac{1}{g} q \qquad 3.9.6$$

where $$V = \frac{4\omega^2}{g} = 4\nu. \qquad 3.9.7$$

It has been demonstrated that the second-order boundary condition at the free surface may be reduced to a non-homogenous linear differential equation of the same form as the homogenous equation in the first-order problem. The final equation in the integral equation formulation of the second-order problem may therefore be written

$$\frac{q}{g} = -V \int_\Gamma \sigma\phi^* d\Gamma + \int_\Gamma \sigma \frac{\partial \phi^*}{\partial y} d\Gamma + \beta\sigma, \quad \underline{x}\epsilon\Gamma_s \qquad 3.9.8$$

and equation 3.9.8 together with equations 3.7.7a and d and the modified form of equation 3.7.7c constitute the required integral equation formulation.

In this case the introduction of the Green's function written in equations 3.4.9 to 3.4.16 may prove to be less suitable but it must be noted that if this approach is adopted the Green's function will be of the same form but with equation 3.4.9 replaced by

$$G(\underline{x},\underline{\xi},t) = g(\underline{x},\underline{\xi})\exp(-2i\omega t) \qquad 3.9.9$$

and the value of the wave number, k, determined by solution of the dispersion equation in the form

$$V = k\tanh kh \qquad 3.9.10$$

The appropriate integral equation formulation may then be written

$$0 = \frac{\partial \phi_w^{(2)}}{\partial m} + \int_\Gamma \sigma \frac{\partial g}{\partial m} d\Gamma + \beta\sigma, \quad \underline{x}\epsilon\Gamma_o \qquad 3.9.11a$$

$$\frac{q}{g} = -V \int_{\Gamma} \sigma g d\Gamma + \int_{\Gamma} \sigma \frac{\partial g}{\partial y} d\Gamma + \beta\sigma, \quad \underline{x} \epsilon \Gamma_s \qquad 3.9.11b$$

where Γ may, in this case, be either the boundary $\Gamma_o + \Gamma_s$ or a geometrically similar boundary outside the fluid domain.

A similar procedure may be followed in order to provide a formulation based on the Green's boundary formula and again this type of formulation results in an integral equation which must be solved for the required potential itself rather than the source density function. However, this alternative introduces additional labour in the evaluation of the function q in equation 3.9.6 since the number of integrals for the evaluation of the potential gradients of the type written in Appendix A.2 is doubled.

3.10 Pressures, Forces and Wave Motion

A vector field is completely described if the potential is known at all points within and on the boundaries of the fluid domain. The preceding sections provide expressions for the scattered wave potential, which, together with the incident wave potential stated earlier, describe the motion of the fluid due to interaction with a submerged obstacle. Application of Bernoulli's equation (equation 3.2.6) permits the evaluation of the hydrodynamic pressure at points within the fluid domain and in particular on the boundary of the obstacle. Bernoulli's equation takes the form

$$p(\underline{x},t) = -\rho \, \Phi_t(\underline{x},t) - \frac{\rho}{2} \, (\nabla\Phi(\underline{x},t))^2 \qquad 3.10.1$$

For a linear analysis the potential Φ is given in equation 3.7.1 and substitution in equation 3.10.1 gives

$$p(\underline{x},t) = \mathrm{Re}(p(\underline{x})\exp(-i\omega t)) \qquad 3.10.2$$

where $$p(\underline{x}) = i\omega\rho\phi(\underline{x}) \qquad 3.10.3$$

and the total pressure p may be expressed in the same form as equation 3.7.2

$$p(\underline{x}) = p_w(\underline{x}) + p_s(\underline{x}) \qquad 3.10.4$$

where p_w is the incident wave pressure and p_s the scattered wave pressure.

If the pressure on the obstacle is described in this way the horizontal and vertical components of force per unit length may be obtained by integration over the submerged obstacle boundary. The components of the Froude Krylov force, defined as that force which would act in the absence of the obstacle boundary, are given by

$$f_{kx} = \int_{\Gamma_o} p_w \; n_x \; d\Gamma_o, \qquad 3.10.5a$$

$$f_{ky} = \int_{\Gamma_o} p_w \; n_y \; d\Gamma_o. \qquad 3.10.5b$$

where n_x and n_y are the direction cosines. The total force components are given by

$$f_x = \int_{\Gamma_o} p \; n_x \; d\Gamma_o, \qquad 3.10.6a$$

$$f_y = \int_{\Gamma_o} p \; n_y \; d\Gamma_o. \qquad 3.10.6b$$

Application of Bernoulli's equation at the still water level gives an expression for the free surface displacement

$$\eta(\underline{x},t) = -\frac{1}{g}\phi_t(\underline{x},t) - \frac{1}{2g}(\nabla\phi(\underline{x},t))^2 \qquad 3.10.7$$

where $\underline{x} = (x,0)$ and for a linear analysis

$$\eta(\underline{x},t) = \mathrm{Re}\ (\eta(\underline{x})\exp(-i\omega t)) \qquad 3.10.8$$

where $$\eta(\underline{x}) = \frac{i\omega\phi(\underline{x})}{g} \qquad 3.10.9$$

and the free surface displacement may be expressed in the form

$$\eta = \eta_w + \eta_s \qquad 3.10.10$$

where η_w is the incident wave surface displacement and η_s is the scattered wave surface displacement.

The reflection and transmission coefficients R and T are given by

$$\eta^-(\underline{x},t) = \frac{H}{2}\,\mathrm{Re}\ \{\ i\ \exp(i(kx-\omega t)) + i\ R\ \exp(-i(kx+\omega t))\} \qquad 3.10.11$$

$$\eta^+(\underline{x},t) = \frac{H}{2}\,\mathrm{Re}\ \{i\ T\ \exp(i(kx-\omega t))\} \qquad 3.10.12$$

where R and T are complex and η^- and η^+ are the free surface displacements far upstream and far downstream of the obstacle. Adopting the form stated in equation 3.10.8 the displacement far upstream is written

$$\eta^-(\underline{x}) = \frac{H}{2}\,i\,\exp(ikx) + \frac{H}{2}\,i\,R\,\exp(-ikx) \qquad 3.10.13$$

where the first term is the incident wave surface displacement, η_w, and by application of equation 3.10.10

$$\eta_s^-(\underline{x}) = \frac{H}{2} i R \exp(-ikx) \qquad 3.10.14$$

hence $$|\eta_s^-(\underline{x})| = \frac{H}{2} |R| \qquad 3.10.15$$

The free surface displacement far downstream is given by

$$\eta^+(\underline{x}) = \frac{H}{2} i T \exp(ikx) \qquad 3.10.16$$

and by equating 3.10.10 and 3.10.16

$$\eta_s^+(\underline{x}) = \frac{H}{2} i T \exp(ikx) - \eta_w = \frac{H}{2}(T-1) i \exp(ikx) \qquad 3.10.17$$

hence $$|\eta_s^+(\underline{x})| = \frac{H}{2} |T-1| \qquad 3.10.18$$

The reflection and transmission coefficients may therefore be obtained from the scattered wave free surface displacements.

The second-order horizontal drift force may be stated in the form

$$f_d = \frac{1}{16} \rho g \left[1 + \frac{2kh}{\sinh(2kh)} \right] (1 + R^2 - T^2) H^2 \qquad 3.10.19$$

and for the motion of an inviscid fluid the principle of energy conservation which may be written

$$R^2 + T^2 = 1 \qquad 3.10.20$$

must be satisfied. Therefore the formula for the drift force is reduced to

$$f_d = \frac{1}{8}\rho g\left[1 + \frac{2kh}{\sinh(2kh)}\right]R^2H^2 \qquad 3.10.21$$

The evaluation of the second-order fluctuating forces requires integrations similar to those written in equations 3.10.6 but it must be noted that the second-order pressure consists of two components. The first component is the dynamic pressure

$$-\frac{\rho}{2}\left(\nabla\phi^{(1)}(\underline{x},t)\right)^2 \qquad 3.10.22$$

which may be evaluated from the solution of the first-order problem. The second component is the pressue due to the second-order potential

$$-\rho\,\phi_t^{(2)}(\underline{x},t) \qquad 3.10.23$$

If the immersed obstacle is surface piercing an additional term is required to account for the finite height of the wave. In vertical plane problems this force per unit length is given by

$$-n_x\int_o^\eta p\,dy = -n_x\int_o^\eta (\rho g(\eta-y) + O(\varepsilon^3))dy \qquad 3.10.24$$

$$= -\frac{\rho g}{2}(\eta^{(1)})^2 + O(\varepsilon^3)$$

$$= -\frac{\rho}{2g}\left(\phi_t^{(1)}(\underline{x},t)\right)^2 + O(\varepsilon^3)$$

and the force acts at the still water level, y = 0.

It has been demonstrated that the pressures on the boundary of an immersed or partially immersed obstacle, and therefore the components of force, consist of a steady component and components fluctuating at the incident wave frequency and at twice the incident wave frequency. If the analysis were extended to a higher-order additional components would be included fluctuating at higher multiples of the incident wave frequency and of diminishing magnitude.

The second-order Stokes' wave written in equations 3.3.8 to 3.3.10 indicate that a wave motion in the absence of an obstacle is made up of components fluctuating at the wave frequency and at twice the wave frequency. The introduction of the obstacle modifies the wave motion but since the governing equation is linear, the total potential is given by the linear superposition of the incident and scattered potentials. The total potential will therefore be similar to the second-order Stokes'wave but it must be noted that the second-order component in this case will consist of two terms. The first term must be similar to the Stokes' second-order terms included in equations 3.3.8 and 3.3.9 and is characterized by the fact that the wave number k is given by equation 3.3.10. The significance of this is that the second-order component is "locked" into the first-order component and may be referred to as a fixed second-order wave and that the wave profile is therefore of constant form. The second-order free surface displacement obtained from equation 3.10.7 for a diffracted wave is of the form

$$\eta^{(2)}(\underline{x},t) = -\frac{1}{g}\phi_t^{(2)}(\underline{x},t) - \frac{1}{2g}(\nabla\phi^{(1)}(\underline{x},t))^2 \qquad 3.10.25$$

and the first term may be written in the form

$$-\frac{1}{g}\left(\phi_{s_t}^{(2)} + \phi_{w_t}^{(2)}\right) \qquad 3.10.26$$

where the second term is a fixed second-order wave identical to the term in the second-order Stokes' wave. The scattered wave term in equation 3.10.26 may be obtained by solution of any one of the integral equation formulations discussed in section 3.9 and therefore this term will differ from the incident wave term in that the dispersion equation to be satisfied is of the form written in equation 3.9.10. The wave number, and therefore the wavelength, is different from the incident wave value and therefore the second-order scattered wave is not locked into the first-order wave and may therefore be referred to as a free wave.

The second-order wave motion due to the interaction of a wave with an immersed obstacle may be regarded as the superposition of two second-order waves, the first being similar to the Stoke's wave and the second having different dispersive qualities and therefore being similar to a linear wave.

CHAPTER 4 - NUMERICAL ANALYSIS

4.1 Introduction

It has been demonstrated that the velocity potential of a fluid motion may be represented by continuous distributions of sources over a boundary which is essentially fictitious. If this fictitious boundary is chosen to coincide with the physical boundaries of the fluid a number of integral equation formulations may be written each of which is a Fredholm integral equation of the second kind with a singular kernel. The kernels may be chosen to be simple sources or Green's functions and the formulations may be classified as direct or indirect integral equation methods. In the direct method the potential is expressed as the sum of potentials due to continuous distributions of sources and double sources and the integral equation is solved to obtain the unknown potential. The indirect method requires that the potential is expressed as a continuous distribution of sources only or double sources only and the integral equation is solved to obtain the unknown source density function before the unknown potential may be evaluated.

As an alternative the fictitious boundary may be located outside the fluid domain. The resulting integral equation formulations are of the first kind and the kernel remains regular over the entire fluid boundary as well as within the fluid domain. Again the kernel function may be chosen to be a simple source or a Green's function but the direct formulation is inappropriate.

This chapter is concerned with the numerical solution of the regular kernel integral equation formulation of the linear diffraction boundary value problem for an obstacle in a two dimensional domain. The techniques employed are, however, suitable for the numerical solution of many potential theory problems and Coates (1982) has demonstrated that for certain problems in which an exact solution is available the regular kernel method provides more accurate results than the conventional singular kernel method. It is suggested that the numerical results obtained by Patterson and Sheikh (1982) demonstrate the numerical robustness of a 'regular boundary element method' since the boundary conditions are prescribed in an approximate manner.

The numerical analysis of an integral equation reduces the problem to that of obtaining the solution of a system of linear algebraic equations by requiring that the boundary conditions are satisfied at a discrete number of points on the boundary of the fluid domain and that there is a distribution of a number of discrete sources over the fictitious boundary. If the simple source is chosen as the kernel of the integral equation the coefficients of the resulting system of equations are easily evaluated. However, the system of equations required to obtain an adequate solution may prove to be of considerable magnitude. Introduction of an appropriate Green's function reduces the boundary value problem since the conditions on certain boundaries are automatically satisfied. The order of the system of equations is therefore reduced considerably which may be of particular value in obtaining numerical solutions for integral equations of the first kind with regular kernels since the possibility of ill-conditioning is reduced. For the linear wave diffraction

problem in a two dimensional domain with a bottom boundary at a finite depth the appropriate Green's function has been written in the previous chapter and will be referred to as the wave function. The details of the numerical discretisation techniques required to evaluate the coefficients of the system of equations are given in this chapter along with the details of the numerical evaluation of the wave function.

A computer program has been written for the indirect wave function formulation of the linear diffraction boundary value problem. The solution is obtained and applied to evaluate pressures on the object and the horizontal and vertical components of force. The free surface displacement is also evaluated and the far-field results are employed to give the reflection and transmission coefficients. An unfortunate feature of the wave diffraction problem in a two-dimensional domain is that no exact solutions exist and program testing may only be achieved by comparison of results with predictions obtained by numerical means. In order to facilitate comparison of program results with previously published work, and to provide theoretical values for the experimental study, a circular cylindrical object is chosen and as an aid to program testing both the singular and regular kernel options have been incorporated.

4.2 The Integral Equation

The numerical solution of the Fredholm integral equations is now considered. Alternative numerical formulations are outlined and the subroutines written for the compilation and solution of the

system of equations are described. In the indirect formulation adopted in this study the results of solution have no physical significance and the testing of these subroutines is bound up with the testing of the diffraction computer program.

The discretisation procedure was introduced by Fredholm (1903) to demonstrate the existence of solutions for integral equations but it was not appreciated that the technique could be applied to obtain the solutions of the equations. Symm (1964) indicated that for a number of simple potential theory problems the discretisation procedure yields satisfactory numerical results. The approach adopted by Symm and by many others since has been to divide the boundary into a number of elements each with a centrally located node at which the appropriate boundary condition must be applied. The unknown function and the kernel of the integral equation are assumed to have a constant value on any element which may be regarded as being equivalent to the location of a discrete source of unknown strength at each of the nodal points. Having effected this discretisation procedure a linear equation may be written for each application of the boundary conditions. The system of equations may be written in matrix form as

$$(\underline{A} - \beta\, \underline{I})\underline{x} = \underline{b} \qquad 4.2.1$$

where, if n is the number of nodes, the kernel matrix $\underline{A}$ and the unit matrix $\underline{I}$ have dimensions nxn and the known vector $\underline{b}$ and the unknown vector $\underline{x}$ have dimensions nx1. The constant β has a given value for the Fredholm equation of the second kind and is zero for the Fredholm equation of the first kind.

Discretisation procedures have been successfully applied to obtain solutions for Fredholm equations of the second kind with weakly singular kernels but particular care must be taken for problems which are formulated as Fredholm equations of the first kind since the resulting system of equations may prove to be ill-conditioned. For equations with weakly singular kernels this may not prove significant however, if the kernel is an everywhere regular function the problem becomes more significant. The matrix equation corresponding to the Fredholm equation of the first kind,

$$\underline{A}\,\underline{x} = \underline{b} \qquad 4.2.2$$

is said to be ill-conditioned if a small change in the vector $\underline{b}$ results in a large change in the solution vector $\underline{x}$. For an equation which is not too ill-conditioned an iterative procedure may be employed which permits the solution to be obtained to full machine accuracy.

The ill-conditioning of a system of equations is associated with loss of diagonal dominance in the kernel matrix $\underline{A}$ and accounts for the lack of a general theory for Fredholm equations of the first kind and for the reluctance of many workers to formulate potential theory problems in this form. For the weakly singular kernel diagonal dominance is achieved by the discretisation procedure described above which accounts for the satisfactory numerical results obtained by Symm (1964). It has, however, been found that as the discretisation becomes more precise such systems of equations do become ill-conditioned since diagonal dominance is insufficiently strong and the dominance identified for a coarse discretisation is dissipated within a diagonal band.

For an equation with a regular kernel diagonal dominance may never be achieved. However, in the particular type of problem with which this study is concerned, it may be possible to achieve diagonal dominance by locating the source distribution on a boundary which is concentric with the physical boundary and which is sufficiently close to ensure a maximum coefficient in the kernel matrix, $\underline{A}$, for the interaction of corresponding nodes and sources. A discretisation for such a problem is indicated in Figure 4.2.1 for an external problem in the domain $\Omega + \Gamma_o$ with discrete sources located on the boundary Γ which is not included in $\Omega + \Gamma_o$.

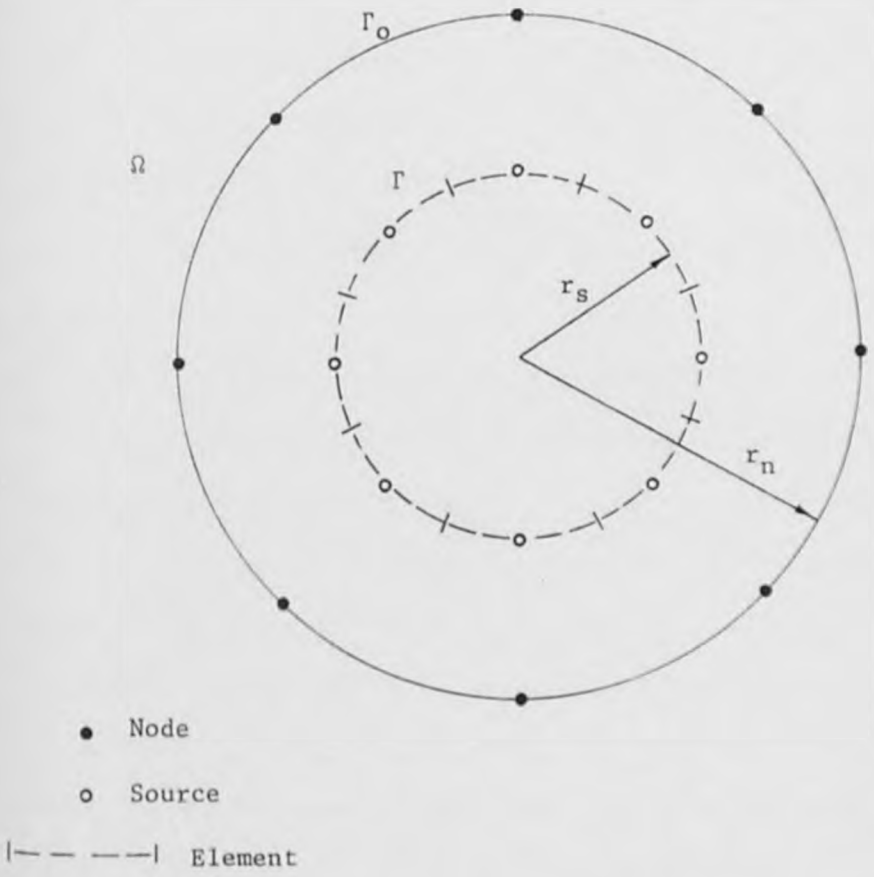

Figure 4.2.1 Discretisation Scheme for Proposed Method

The discretisation is similar to that which has been outlined except that it is the source boundary which is divided into elements and the position of this boundary is determined by assuming a constant value for the ratio of the distances from the chosen origin to corresponding node and source locations, denoted by r_n and r_s respectively. This type of method was first successfully adopted by Oliveira (1968) for the solution of stress analysis problems.

The discretisation scheme discussed above (and adapted to the separate boundary formulation) has been employed in most published diffraction programs with the notable exception of the two dimensional simple source formulations of Au and Brebbia (1982) and Bird and Shepherd (1982) and the three dimensional wave function formulation of Coates (1982). Alternative discretisation schemes may be employed to compile the system of linear equations in which the numerical assumptions are less restrictive.

These alternative schemes originated with the finite element method and are often referred to as boundary element methods. The advance is achieved by introducing higher-order elements within which the unknown function is given by a Lagrangian interpolation. The advantage gained by employing such higher-order elements is that the same accuracy may be achieved for fewer nodes with a consequent reduction in the order of the resulting system of equations. This reduction may prove to be of particular significance for systems of equations in which ill-conditioning may occur and in general reduces the computational requirements for compilation and solution. A further numerical refinement which may be included in the numerical analysis is that of permitting the kernel function to vary over each element. This is equivalent to locating more than one discrete source

on an element and requires the introduction of suitable numerical quadrature formulae for evaluation of the element integrations.

If a solution to an integral equation is achieved for any of the above-mentioned discretisation schemes the same schemes may be adopted for the evaluation of integrals. An integral evaluation may be written in matrix form as

$$\underline{x} = \underline{A}\,\underline{b} \qquad 4.2.3$$

where in this case $\underline{x}$, the unknown vector, is to be obtained by multiplication of the kernel matrix, $\underline{A}$, compiled by the appropriate scheme, by the vector, $\underline{b}$, obtained by solution of the original system of equations. In the direct method this permits the evaluation of the potential function at points within the domain and in the indirect method at points on the boundary and within the domain.

The discretisation employed in the diffraction computer program is now considered in more detail. The main concern of this investigation is to establish whether the system of equations obtained by discretisation of the regular kernel integral equation is amenable to numerical solution. However, since the program includes the conventional singular kernel method the subsequent numerical analysis is performed for the Fredholm equation of the second kind. For the Fredholm equation of the first kind with a regular kernel the equations are obtained by exclusion of the singular term. It is emphasised that whichever method is adopted integrations apply to the fictitious source boundary.

The equation to be solved for the wave function formulation of the linear diffraction boundary value problem has been written in general form in equation 3.8.1. As stated the first step is to require that the boundary condition is satisfied at a finite number of nodal points, say n. We therefore write

$$0 = \frac{\partial \phi_w}{\partial m}(\underline{x}_i) + \beta\sigma(\underline{x}_i) + \int_\Gamma \frac{\partial g}{\partial m}(\underline{x}_i, \underline{\xi})\sigma(\underline{\xi})d\Gamma \qquad 4.2.4$$

which is valid for i=1,....n, where β is given in 3.7.6. The next step is to divide the boundary, Γ, into a discrete number of elements $\Delta\Gamma$. The consequence of this subdivision is to reduce the integral equation 4.2.4 to a sum of a series of element integrations. We write

$$0 = \frac{\partial \phi_w}{\partial m}(\underline{x}_i) + \beta\sigma(\underline{x}_i) + \int_{\Delta\Gamma_\ell} \frac{\partial g}{\partial m}(\underline{x}_i, \underline{\xi})\sigma(\underline{\xi})d\Gamma \qquad 4.2.5$$

where the repeated index ℓ=1,....q implies summation. The variation of the unknown function, σ, is approximated on each element by the Lagrangian interpolation formula

$$\sigma(\underline{\xi}) = N_k(\underline{\xi})\sigma(\underline{\xi}_k), \quad k=1,....p \qquad 4.2.6$$

where the repeated index, k, implies summation and (p-1) indicates the order of the Lagrange interpolation polynomials, N_k. Since the interpolation polynomials have the same form on each individual element we may write equation 4.2.5 in the form

$$0 = \frac{\partial \phi_w}{\partial m}(\underline{x}_i) + \beta\sigma(\underline{x}_i) + \sigma(\underline{\xi}_{k\ell}) \int_{\Delta\Gamma_\ell} \frac{\partial g}{\partial m}(\underline{x}_i, \underline{\xi})N_k(\underline{\xi})d\Gamma \qquad 4.2.7$$

If the points at which the boundary condition is satisfied are referred to as boundary nodes and the points on the elements at which the value of σ are required are referred to as element nodes the order of the polynomials and the number of elements are chosen to give an equal number of boundary and element nodes. For the Fredholm equation of the second kind the locations of the boundary and element nodes are identical but for the regular kernel Fredholm equation of the first kind the boundary and element nodes are located on two distinct but corresponding boundaries.

The simplest technique for the evaluation of the integrals in equation 4.2.7 is to assume that the variation of the kernel function, $\partial g/\partial m$, may be adequately modelled by locating a single source at the central point on each element. Evaluation of each integral is then reduced to a simple multiplication. If, however, the element length is too large for the variation of the kernel function to be small the integrals may be evaluated by locating a number of discrete sources on the element. The integrals may then be evaluated by applying a quadrature formula of the type

$$\int_{-1}^{+1} I(\mu)\, d\mu = H_i I(\mu_j), \quad j=1,....m \qquad 4.2.8$$

where H_j, the weights, are given for the abscissas μ_j and the repeated index, j, implies summation. For the evaluation of the integrals in equations 4.2.7 the abscissas correspond to the locations of the discrete sources and equation 4.2.8 written for the local element coordinate system must be rewritten for the element within the global cartesian coordinate system. Equations 4.2.7 become

$$0 = \frac{\partial \phi_w}{\partial m}(\underline{x}_i) + \beta\sigma(\underline{x}_i) + \sigma(\underline{\xi}_{k\ell})H_j \frac{\partial g}{\partial m}(\underline{x}_i, \underline{\xi}_j)N_k(\xi_j)|J| \qquad 4.2.9$$

where the Jacobian, $|J|$, effects the transformation from the local element coordinate system into the global cartesian system. Evaluation of each quadrature in turn permits the compilation of a matrix equation in the form of equation 4.2.1.

Equations 4.2.9 are a general expression for the discretisation scheme employed in the writing of the diffraction program. The detail is now considered and a brief description of the subroutines written for inclusion in the diffraction program is given.

Since the object chosen for the present study is a circular cylinder the elements are chosen as arcs of equal length. The program includes the option of constant, linear or quadratic variation of source density on the elements and details of the Lagrange interpolation formulae are given in Appendix A.3.1. The choice of element type results in the location of one, two or three nodes on each element.

Simpson's rule may be regarded as a particular example of the general quadrature formula written in equation 4.2.8. Adopting Simpson's rule would require the location of discrete sources at the extremes of each element and at an odd number of equally spaced points within the element. However, it may prove convenient to avoid location of the sources at the extremes or at the centre of the element since it is for such points that the interpolation polynomial may have a zero value. The Legendre-Gauss quadrature

formula is therefore chosen since it avoids these unsuitable features and provides a higher degree of accuracy. Details of the formula and its application are found in Appendix A.3.2.

The location of boundary nodes, elements and sources for a constant variation of source density on an element and a single point quadrature has been given in Figure 4.2.1. Alternative discretisation schemes for the circular cylinder with sources located on the separate boundary are given in Figure 4.2.2 in which the number of sources is chosen to be identical to the number of nodes.

In order to prepare for the assembly of the matrix equation the subroutines VARN, GAUSSDAT and COORDS have been written. Subroutine GAUSSDAT has been written to set the Gauss weights and abscissas for single-point, two-point, three-point and four-point quadrature, where the type of quadrature to be set is determined by the input to the program. Subroutines VARN and COORDS both require the locations of the abscissas on the element. The evaluations of the Lagrangian polynomials for each of the abscissas are carried out in VARN and the nodal and source coordinates within the global cartesian system are generated in COORDS. These subroutines along with the other subroutines considered in this section are listed in Appendix A.4.

Compilation of the matrix equation also requires evaluation of the normal gradient of the spacial part of the incident wave potential, ϕ_w. It is convenient to obtain the output of the diffraction program in non-dimensional form and therefore the potential ϕ_w is expressed in non-dimensional form as

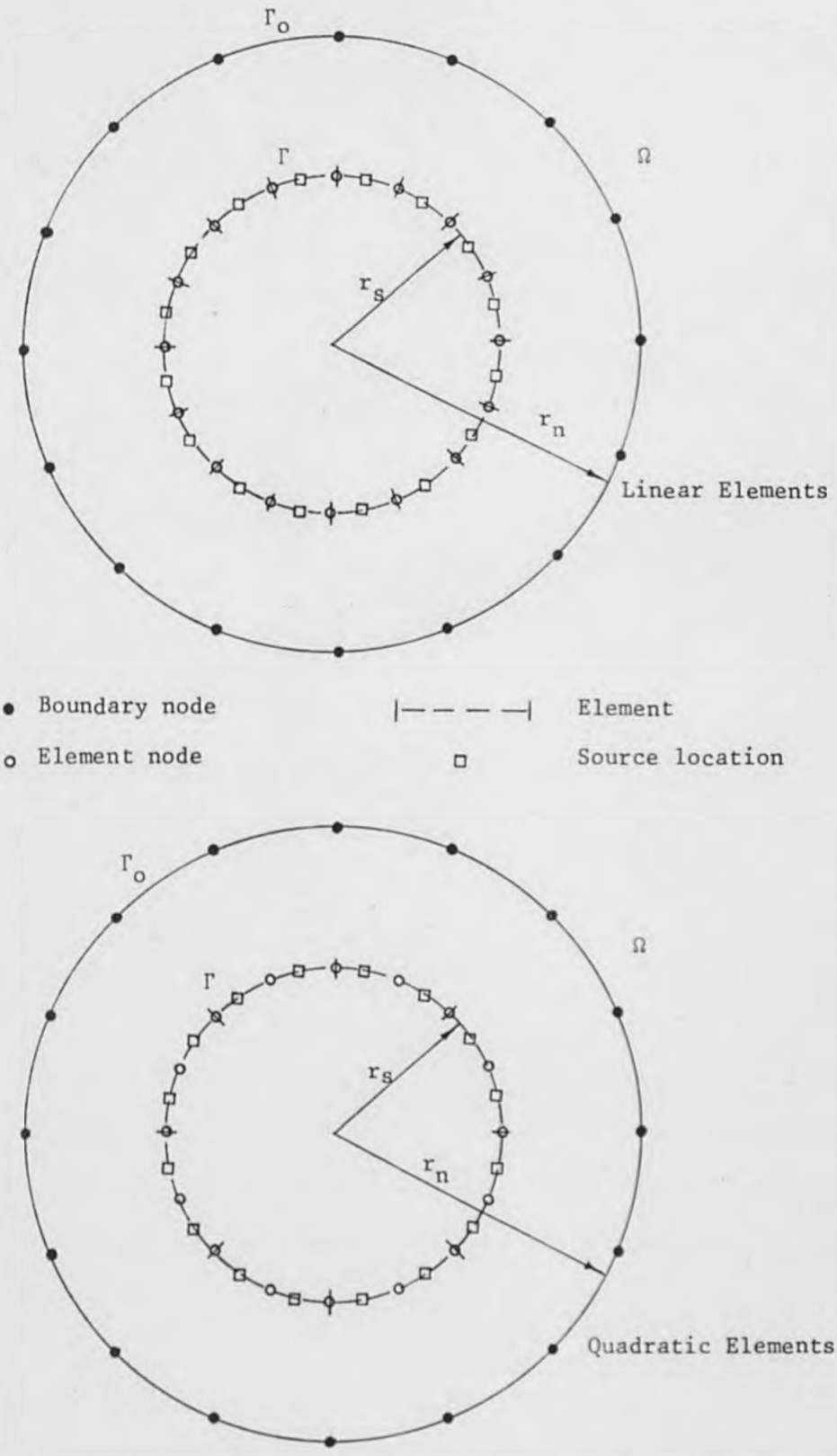

Figure 4.2.2 Linear and Quadratic Elements

$$\bar{\phi}_w = \phi_w/(gH/2\omega) \qquad 4.2.10$$

where $$\phi_w = \frac{gH}{2\omega} \frac{\cosh k(y+h)}{\cosh kh} \exp(ikx) \qquad 4.2.11$$

In non-dimensional form, with the over-bar suppressed, we write

$$\frac{\partial \phi_w}{\partial m} = \frac{\partial \phi_w}{\partial x} \frac{\partial x}{\partial m} + \frac{\partial \phi_w}{\partial y} \frac{\partial y}{\partial m} \qquad 4.2.12$$

where $$\frac{\partial \phi_w}{\partial x} = i\,k \frac{\cosh k(y+h)}{\cosh kh} \exp(ikx) \qquad 4.2.13a$$

$$\frac{\partial \phi_w}{\partial y} = \frac{k \sinh k(y+h)}{\cosh kh} \exp(ikx) \qquad 4.2.13b$$

and each of the terms in equation 4.2.9 will therefore have dimensions L^{-1} but the integral

$$\int_\Gamma \sigma(\underline{\xi}) g(\underline{x}, \underline{\xi}) d\Gamma \qquad 4.2.14$$

required for the evaluation of pressures and free surface displacements, will be non-dimensional. The evaluation of equation 4.2.12 for the nodal points on the object boundary gives the complex vector $\underline{b}$ of equations 4.2.1 and 4.2.2. The evaluations are carried out in subroutine INCWAVE.

The quadratures written in equation 4.2.9 are evaluated in either subroutine CSRCDEN or SRCDEN and the result of each quadrature is located at the appropriate point in the kernel matrix $\underline{A}$. The discretisation scheme adopted in subroutine CSRCDEN is that outlined at the beginning of this section, namely, constant element variation

of the source density function and a single source located at the element node. The purpose for including CSRCDEN is to provide comparison with the higher order elements included in the subroutine SCRDEN. Two points must be noted with regard to the assembly of the matrix equation in subroutines CSRCDEN and SRCDEN. Firstly, for coincidence of the object and source boundaries care must be taken in evaluation of the integral of the type written in equation 4.2.7 when the sources are located on the same element as the boundary nodes. It is shown in Appendix A.2.3 that the result of an exact integration of $\partial/\partial m$ (log R) for this case is self-cancelling and therefore the quadrature for this term may be excluded in the assembly of the matrix equation.

The second point to be noted is that the wave function, the source density function and the known vector due to the incident wave potential normal gradient are complex quantities. Equation 4.2.1 may therefore be rewritten by making the substitutions

$$\underline{A} = \underline{A}_1 + i\,\underline{A}_2 \qquad 4.2.15a$$

$$\underline{x} = \underline{x}_1 + i\,\underline{x}_2 \qquad 4.2.15b$$

$$\underline{b} = \underline{b}_1 + i\,\underline{b}_2 \qquad 4.2.15c$$

and equation 4.2.1 becomes

$$(\underline{A}_1 - \beta\underline{I})\underline{x}_1 - \underline{A}_2\underline{x}_2 = \underline{b}_1 \qquad 4.2.16a$$

$$(\underline{A}_1 - \beta\underline{I})\underline{x}_2 + \underline{A}_2\underline{x}_1 = \underline{b}_2 \qquad 4.2.16b$$

Equations 4.2.16 may be rearranged to eliminate the imaginary part of the unknown vector and evaluate the real part and then the imaginary part is evaluated by back-substitution. This approach has not, however, been adopted in the computer program and the equations 4.2.16 have been assembled in the same form as equation 4.2.1 which is partitioned as

$$\left[\begin{array}{c|c} \underline{A}_1 - \beta\underline{I} & -\underline{A}_2 \\ \hline \underline{A}_2 & \underline{A}_1 - \beta\underline{I} \end{array}\right] \left[\begin{array}{c} \underline{x}_1 \\ \hline \underline{x}_2 \end{array}\right] = \left[\begin{array}{c} \underline{b}_1 \\ \hline \underline{b}_2 \end{array}\right] \qquad 4.2.17$$

The subroutine SOLN written for the solution of matrix equation 4.2.17 employs the Gaussian elimination method with pivoting and scaling to minimize round-off errors. While it is recognized that this is not the most efficient method the choice was made in an attempt to preserve the diagonal dominance of the matrices to be inverted in the regular kernel Fredholm equation formulation.

The discretisation schemes employed (and the associated subroutines) have been described and a flow diagram of this first stage of the diffraction program, with subroutines in parenthesis, is given in Figure 4.2.3. However, the implementation of these operations requires that the kernel function of the integral equation is evaluated and the next section is concerned with the evaluation of the wave function and its normal gradient on the object boundary.

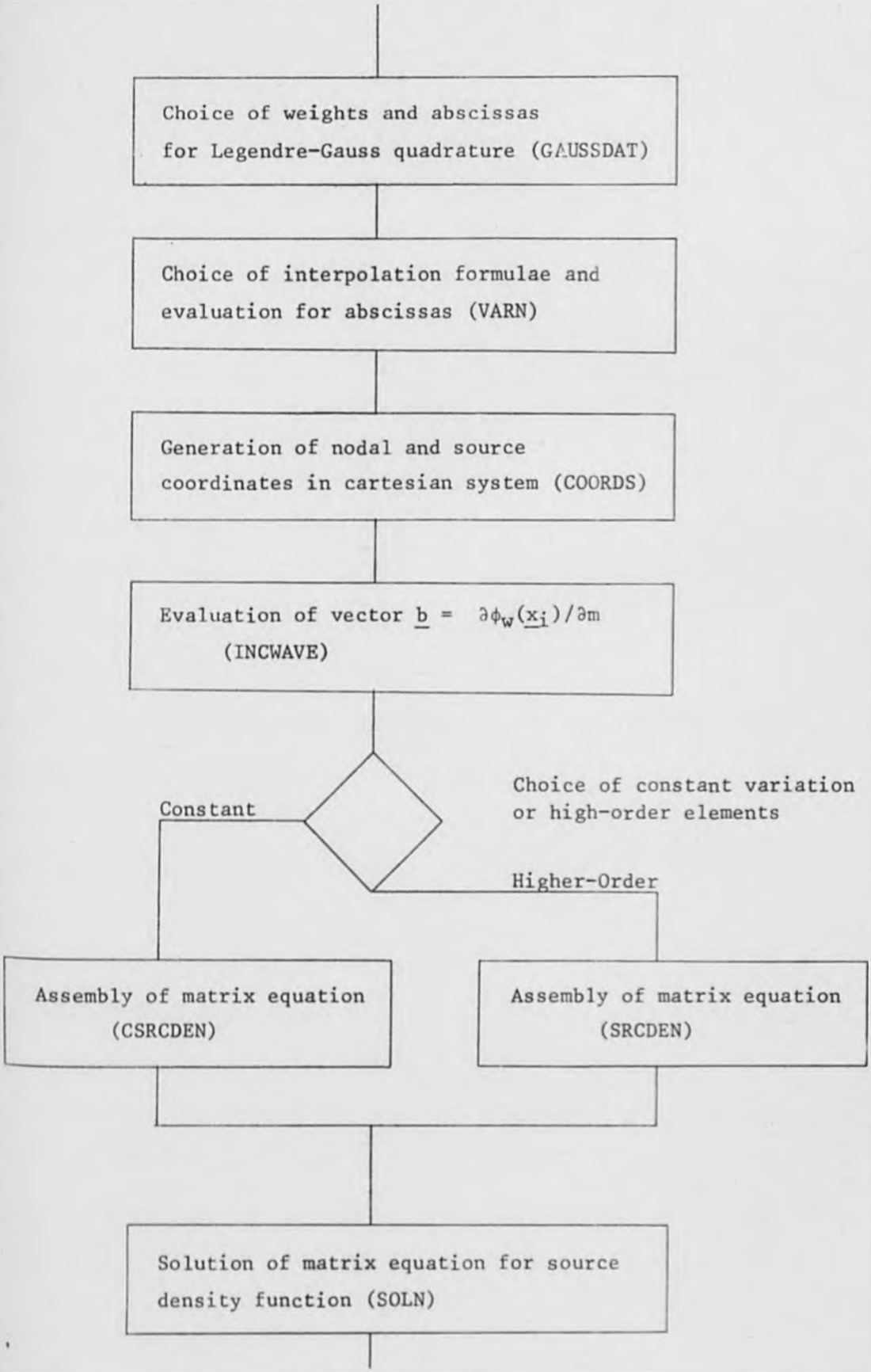

Figure 4.2.3 Assembly and Solution of Matrix Equation

4.3 The Wave Function

The evaluation of the wave function and the normal gradient of the wave function at the specified nodal points on the object boundary due to the location of a fluid singularity at a point on the fictitious source distribution boundary is basic to the formulation employed in the diffraction program. Each of the alternative numerical approaches outlined in the previous section require that a discrete number of singularities are located on the source boundary and that the Neumann condition on the object boundary is satisfied at a discrete number of nodal points. The resulting system of linear algebraic equations is written as a matrix equation in which the elements of the square matrix are obtained by integration of the evaluations of the potential gradients due to the discrete fluid singularities. Similar techniques are employed in compiling the matrix equation for evaluation of the scattered velocity potential for which the potentials due to the singularities are required.

In general we are concerned with an object located in a two dimensional fluid domain bounded by the free water surface and an impermeable fixed bottom boundary at a specified depth. A suitable wave function for such a domain has been written in equations 3.4.9 to 3.4.16 and we require that the corresponding expressions for the normal gradient of the function at a nodal point are written. For the spacial wave function, $g(\underline{x},\underline{\xi})$, the normal gradient is written

$$\frac{\partial g}{\partial m} = \frac{\partial g}{\partial x} \cdot \frac{\partial x}{\partial m} + \frac{\partial g}{\partial y} \cdot \frac{\partial y}{\partial m} \qquad 4.3.1$$

where $\partial/\partial m$ indicates the normal gradient on the object boundary at

the nodal point, $\underline{x}$. It must be emphasised that this function is distinct from the double source discussed in the previous chapter. Adopting the same approach as in section 3.4 we may write the function $\partial g/\partial m$ in complex form as

$$\frac{\partial g}{\partial m} = \frac{\partial g_1}{\partial m} + i \frac{\partial g_2}{\partial m} \qquad 4.3.2$$

The imaginary part in equation 4.3.2 is, in component form

$$\frac{\partial g_2}{\partial x} = -kg_0 \sin k(x-\xi) \qquad 4.3.3a$$

$$\frac{\partial g_2}{\partial y} = kg_0 \tanh k(y+h) \cos k(x-\xi) \qquad 4.3.3b$$

and the alternative expressions for $\partial g_1/\partial x$, $\partial g_1/\partial y$ are written in the subsequent sub-sections.

The remainder of this section is concerned with the numerical evaluation of the wave function and its normal gradient. The subroutines are listed in appendix A.5 in the order in which they occur in this section and numerical results for test cases are given in appendix A.6. The imaginary parts of the wave function and it's normal gradient are evaluated in subroutines IMGRN and IMDGRN respectively.

4.3.1 The series form

The series form for the real part of the wave function,

$g(\underline{x},\underline{\xi})$, is written in equations 3.4.14 to 3.4.16. The horizontal and vertical gradients may therefore be written

$$\frac{\partial g_1}{\partial x} = kg_0 \cos k|x-\xi| + \sum_{i=1}^{\infty} C_i \cos c_i(y+h)\cos c_i(\eta+h)\exp(-c_i|x-\xi|) \qquad 4.3.4a$$

$$\frac{\partial g_1}{\partial y} = \frac{\partial g_0}{\partial y} \sin k|x-\xi| + \sum_{i=1}^{\infty} C_i \sin c_i(y+h)\cos c_i(\eta+h)\exp(-c_i|x-\xi|) \qquad 4.3.4b$$

where, c_i and C_i are specified in equations 3.4.15 and 3.4.16 and

$$\frac{\partial g_0}{\partial y} = \nu \frac{\sinh k(y+h)\cosh k(\eta+h)}{\nu h + \sinh^2 kh} \qquad 4.3.5$$

The evaluation of the series in equations 3.4.14 and 4.3.4 for a point $\underline{x}$ due to a source at the point $\underline{\xi}$ requires firstly that the wave data is specified and secondly that the roots of the dispersion equation are evaluated. The diffraction program has been written for a wave of unit height and therefore specification of the water depth, h, and the wavelength, $L(= 2\pi/k)$, with the acceleration due to gravity is adequate for the description of a particular wave.

The subroutine DISP has been written for evaluation of the roots of the dispersion equation using the Newton-Raphson iterative method and details are given in appendix A.3.4. It is

also convenient to include within subroutine DISP the evaluation and storage of the function C_i and it may be noted that the function g_0 has been expressed in an alternative form to equation 3.4.13

$$g_o = \frac{1}{c_o} C_o \cosh c_o(\eta+h)\cosh c_o(y+h) \qquad 4.3.6$$

where $c_o = k$ and

$$C_o = \frac{k^2 - \nu^2}{hk^2 - h\nu^2 + \nu} \qquad 4.3.7$$

and the evaluation of C_o is also contained within DISP.

Examination of the form of the series written in equations 3.4.14 and 4.3.4 indicates that convergence will depend largely on the behaviour of the exponential term. Therefore, for a given horizontal separation of the field point $\underline{x}$ and the source point $\underline{\xi}$ the choice of a maximum number of series terms to be evaluated will determine the extent of the convergence to the required value and for a fixed number of terms the convergence is more complete for a larger value of $|x-\xi|$. Subroutines GRNSER and DGRNSER contain the series evaluations of the functions g_1 and $\partial g_1/\partial m$ respectively to a specified accuracy.

The statement of the series form of the gradient of the wave function in equation 4.3.4 is adequate for the evaluation of the magnitude of $\partial g_1/\partial m$ but not, however, the vector quantity. This difficulty is due to the inclusion of the modulus function $|x-\xi|$ which results in the specification of the horizontal component of

the gradient as a positive quantity for all $(x-\xi)$. This feature might be avoided by eliminating the modulus and taking the negative roots of the dispersion equation for $(x-\xi)<0$ in equation 4.3.1 However, in the program (subroutine DGRNSER) it is convenient to avoid this problem by testing $(x-\xi)$ to establish the relative locations of the source and field points and the to impart the correct direction.

4.3.2 The Integral Form

The integral equation form of the wave function has been written in equation 3.4.11 and the horizontal and vertical components of the normal gradient at a point on the object boundary are

$$\frac{\partial g_1}{\partial x} = \frac{1}{2\Pi}\frac{(x-\xi)}{R^2} + \frac{1}{2\Pi}\frac{(x-\xi)}{R_2^2} + \frac{1}{\Pi}\,PV\int_0^\infty I(\mu)\cosh\mu(y+h)\sin\mu(x-\xi)\,d\mu \qquad 4.3.8a$$

$$\frac{\partial g_1}{\partial y} = \frac{1}{2\Pi}\frac{(y-\eta)}{R^2} + \frac{1}{2\Pi}\frac{(2h+y+\eta)}{R_2^2} - \frac{1}{\Pi}\,PV\int_0^\infty I(\mu)\sinh\mu(y+h)\cos\mu(x-\xi)\,d\mu \qquad 4.3.8b$$

where $I(\mu) = \dfrac{(\mu+\nu)\exp(-\mu h)\cosh\mu(\eta+h)}{\mu\sinh\mu h - \nu\cosh\mu h}$ 4.3.9

The scheme adopted for the evaluation of the principal value integrals in equations 3.4.11 and 4.3.8 closely resembles the method used by Monacella (1966). However, it may be noted that alternative expressions for the wave function might be written which are equivalent to equation 3.4.11 and that this approach has been adopted for two dimensional problems by Kim (1965), Frank (1967) and more recently by Hearn and Donati (private communication).

For the case of the two dimensional wave function the decay of the integrand is less rapid than in the analogous three dimensional function and it therefore becomes advantageous to evaluate the infinite integral in the form

$$PV \int_0^{\infty} f(\mu)d\mu \sim PV \int_0^{\mu_1} f(\mu)d\mu + \int_{\mu_1}^{\mu_{max}} f(\mu)d\mu \qquad 4.3.9$$

where $f(\mu)$ may be taken to represent the integral and in any of the equations 3.4.11 or 4.3.8 , μ_1 is the change over value and μ_{max} is the maximum value of μ included in the integration.

The difficulty associated with the evaluation of the principal value integral is due to the integrand singularity at $\mu=k$ which becomes obvious when the denominator of I_1 is rewritten in the form of the dispersion equation

$$\mu\sinh\mu h - \nu\cosh\mu h = \cosh\mu h(\mu\tanh\mu h - \nu) \qquad 4.3.10$$

The general scheme for the removal of the singular behaviour is as

follows. For an integrand $f(\mu)$ with a simple pole at $\mu=k$ the integrand may be written as $f(\mu) = g(\mu)/h(\mu)$. The principal value integral may then be written

$$PV \int_0^{\mu_1} f(\mu)d\mu = \int_0^{\mu_1} f(\mu)d\mu - \int_0^{\mu_1} \frac{g(k)}{h'(k)(\mu-k)} d\mu$$

$$+ \frac{g(k)}{h'(k)} \log \left| \frac{\mu_1 - k}{k} \right| \qquad 4.3.11$$

where the prime denotes differentiation with respect to μ.

The subroutines written for the evaluation of the wave function and it's normal gradient by the integral expressions are GRNIN and DGRNIN respectively. Subroutine GRNIN calls three subroutines, LOGTERM which evaluates the logarithmic term, INT1 which evaluates the principal value integral and INT3 which evaluates the remainder integral. Subroutine DGRNIN is similar and calls subroutines DLOGTERM, INT2 and INT4. Subroutines LOGTERM and DLOGTERM are straightforward and include measures to avoid singular behaviour. The integrations in subroutines INT1, INT2, INT3 and INT4 are carried out by an iterative form of Simpson's rule in which the interval is divided into successively smaller divisions and tests are included to obtain convergence to the required accuracy. Attempts have been made to replace the Simpson's rule iterative method with a Gauss Lageurre quadrature method for an infinite interval in subroutines INT3 and INT4. However, the results were in general inadequate and have therefore been abandoned.

4.3.3 Evaluation for the Diffraction Program

The diffraction program requires that the wave function and the normal gradient of the wave function at points on the object boundary are evaluated to a specified accuracy. It is required in this case that the accuracy to which the wave function evaluations are made is sufficient to guarantee that no errors are introduced into the final results of the diffraction program and the results of tests performed to determine suitable accuracy limits have been included in Appendix A.6. The significance of this requirement is that if it is known that no errors are introduced due to the wave function evaluations then the variations in the final results for a given problem obtained by alternative discretisation schemes is due solely to these different numerical techniques.

The results obtained from wave function testing have also been used to determine the conditions under which the series or integral evaluation subroutines are to be preferred. The tests which have been employed to determine the most suitable alternative are based on the tests employed in the series evaluations (equations A.6.1 and A.6.2) and these tests require that the integral evaluation scheme is chosen if the specified accuracy is unattainable for a maximum number of terms in the series. Since this test may, for a more coarse discretisation, choose the series alternative for a source on the same element as the node an additional test has been included to ensure that under such circumstances the integral alternative is always chosen. The subroutines written to effect these selection tests are GRNFN for

the wave function and DGRNFN for the normal gradient and a flow diagram for the wave function evaluation is given in Figure 4.3.1 in which only the subroutine names are given and the corresponding subroutines for evaluation of the gradient are given in parenthesis.

4.4 The Diffraction Program

If the matrix equation of the type written in equation 4.2.1 is solved to obtain the unknown source density function vector a matrix evaluation of the same form as equation 4.2.3 may be performed to obtain the scattered velocity potential. The matrix equation corresponds to the integral equation written in equation 3.8.1 and the matrix evaluation corresponds to the representation of the scattered potential as a surface distribution of wave sources

$$\phi_s(\underline{x}) = \frac{1}{2\Pi} \int_\Gamma \sigma(\underline{\xi}) g(\underline{x},\underline{\xi}) d\Gamma \qquad 4.4.1$$

The numerical procedure adopted for the assembly of the kernel matrix is the same as that adopted for the integral equation and therefore equation 4.4.1 may be rewritten

$$\phi_s(\underline{x}_i) = \sigma(\underline{\xi}_{k\ell}) H_j g(\underline{x}_i,\underline{\xi}_j) N_k(\xi_j) |J| \qquad 4.4.2$$

The subroutines GAUSSDAT, VARN and COORDS are therefore also required for the evaluation of equation 4.4.2 but one feature of the matrix compilation differs. It has been demonstrated in Appendix A.3.3

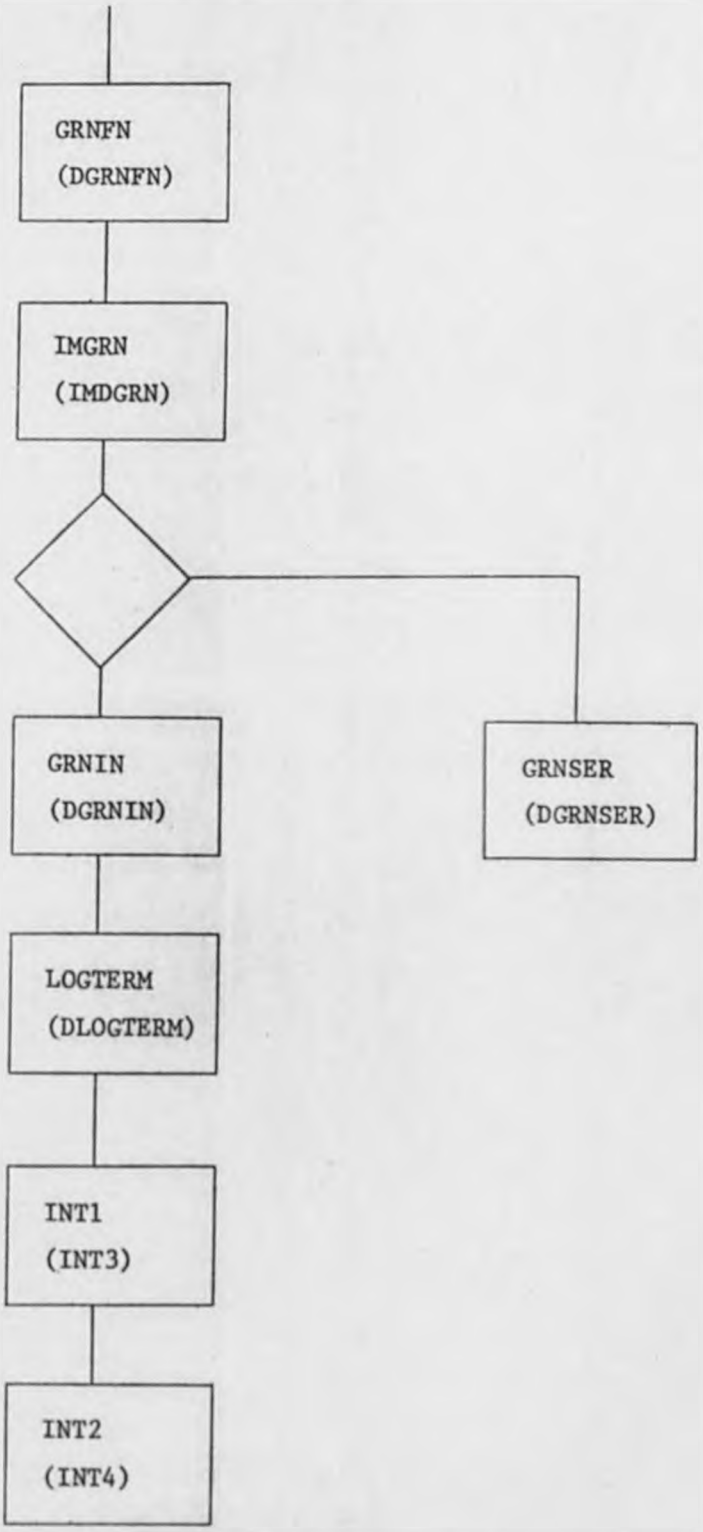

Figure 4.3.1 Wave Function Evaluation

that for a source on an element the integration of the normal gradient of the logarithmic singularity vanishes. In this case the logarithmic singularity does not vanish when integrated and is not accurately evaluated by a simple quadrature and therefore an exact integration is carried out, the details of which are given in Appendix A.3.5. The results of the analytical integrations are included in subroutine ELINT which is listed in Appendix A.7 along with the other subroutines described in this section.

The scattered potential ϕ_s is never evaluated since it is more meaningful to evaluate the quantities which have physical significance, namely the pressure on the object boundary and the free surface displacement. Expressions of the same form as equation 4.4.2 may, by application of Bernoulli's equation, be written for these quantities since

$$p_s(\underline{x}_i) = i\omega\rho\ \phi_s(\underline{x}_i) \qquad 4.4.3$$

and

$$\eta_s(\underline{x}_i) = \frac{i\omega}{g}\ \phi_s(\underline{x}_i) \qquad 4.4.4$$

In the diffraction program the results of evaluating equation 4.4.2 are in non-dimensional form and therefore equations 4.4.3 and 4.4.4 are rewritten

$$\bar{p}_s(\underline{x}_i) = i\ \bar{\phi}_s(\underline{x}_i) \qquad 4.4.5$$

$$\bar{\eta}_s(\underline{x}_i) = i\ \bar{\phi}_s(\underline{x}_i) \qquad 4.4.6$$

where the overbar indicates a non-dimensional quantity and

$$\bar{p}_s(\underline{x}_i) = p_s(\underline{x}_i)/(\rho g H/2) \qquad 4.4.7$$

$$\bar{\eta}_s(\underline{x}_i) = \eta_s(\underline{x}_i)/(H/2) \qquad 4.4.8$$

The subroutines written for the evaluation of equation 4.4.5 and 4.4.6 are named CPRESS, PRESS and CWAVE, WAVE, where as in the integral equation subroutines the prefixed letter C indicates that a constant element, single source discretisation scheme is employed. The pressure evaluation subroutines give the incident wave and total wave pressures and the results are integrated in subroutine FORCE to obtain the components of the Froude Krylov force and the total force as given in equations 3.10.5 and 3.10.6. The integrations are achieved by application of Simpson's rule for which the subroutine SIMPSON has been written and it may be noted that this subroutine is written specifically for a closed boundary since the initial and final interval points are taken to coincide. The subroutine FORCE also includes the evaluation of the diffraction coefficients which are defined by

$$C_x = \frac{f_x}{f_{kx}} \quad , \quad C_y = \frac{f_y}{f_{ky}} \quad . \qquad 4.4.9$$

The reflection and transmission coefficients might have been evaluated by application of the relations given in equations 3.10.14, 3.10.15, 3.10.17 and 3.10.18, however, a more straightforward approach has been adopted based on the expressions for the wave

function at large distances from the source location. The details of this procedure are included in Appendix A.3.6 and the subroutines written for the implementation of this scheme are CREFL and REFL.

Each of the subroutines mentioned above have been written for the evaluation of the results in complex form and therefore for each quantity the modulus and the argument of the complex number give the maximum amplitude of the fluctuating quantity and its phase. A final flow diagram for the diffraction program is given in Figure 4.4.1 and the remainder of the chapter is devoted to the testing of the program and the theoretical investigation of the diffraction problem based on numerical predictions. A number of the facilities within the diffraction program are not used until the following chapter in which the numerical predictions are compared with the results of laboratory tests.

4.5 Numerical Results

A test programme has been devised and carried out to investigate the numerical solution of the linear diffraction boundary value problem by the integral equation method for a submerged circular obstacle in water of finite depth. The results of these tests, which have been designed for the investigation of two distinct problems, are presented in this section.

The primary objective is to determine whether the regular kernel integral equation formulation is amenable to numerical solution and the secondary objective is to establish whether, for either the

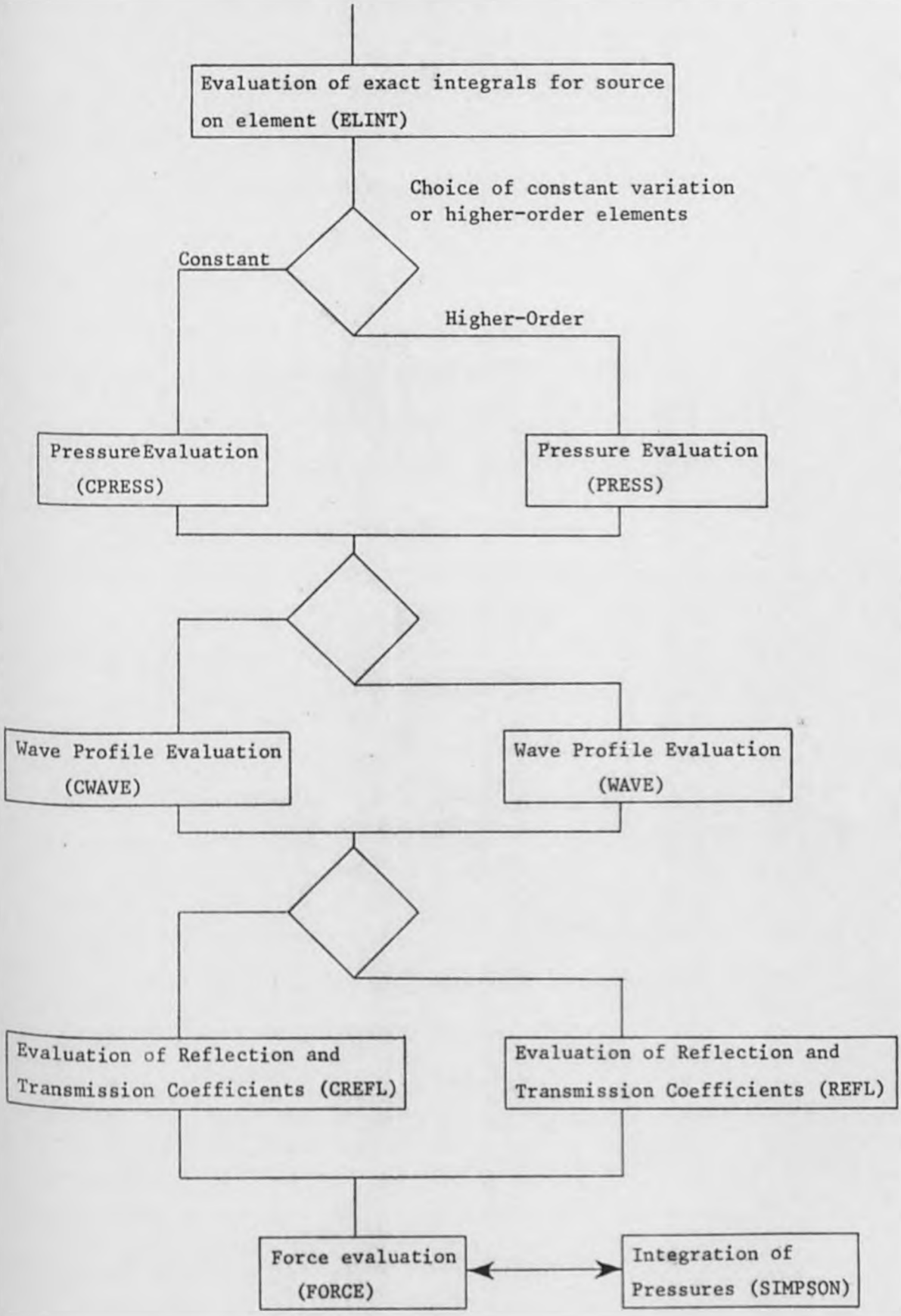

Figure 4.4.1 Results of Diffraction Program

regular or singular kernel method, the use of higher-order discretisation techniques is advantageous. The study of these two problems has largely been carried out in parallel and the same two criteria have been employed to evaluate the suitability of the methods for application to obtain solutions for diffraction problems. The alternative methods which have been investigated in this series of tests may only be accepted as suitable alternatives to the conventional methods if firstly they prove to be reliable and secondly if the results are obtained by a more computationally efficient means.

The regular kernel integral equation formulation has been used by Van Oortmerssen (1972) and Coates (1982) for the diffraction problem in a three dimensional domain. The results obtained by Van Oortmerssen (1972) and later by Boreel (1974) using the same numerical model are not compared with solutions which are known to be correct for the problems considered and the comparison with experimental results suggests that the numerical results might be regarded with some suspicion. Coates (1982) has applied the regular kernel formulations to obtain predictions for the force on a surface piercing circular cylinder in water of constant finite depth. The choice of this geometry permits comparison of numerical results with the exact solution obtained by the method introduced by Havelock (1940) and extended to the problem of wave diffraction in finite water depths by MacCamy and Fuchs (1954). The results presented do not appear to do justice to the method since disagreement with the exact solution may in general be attributed either to errors in the wave function evaluation or to the coarse discretisations which have been

employed. However, it has been demonstrated that the solutions obtained are not particularly sensitive to the location of the source boundary except when this boundary approaches the object boundary.

The majority of published numerical results for wave diffraction problems obtained by the integral equation method have employed simple discretisation techniques. The numerical formulation for "higher-order elements" was given by Bai and Yeung (1974) but results were only obtained using the conventional constant element method. Eatock Taylor (1982) also presents the required numerical formulation for application of higher-order elements but results have only been obtained using what are referred to as constant source panels.

The aim of refining the numerical discretisation techniques is primarily to achieve an increased computational efficiency. If the integral equation method is employed for surface distributions of simple sources and double sources higher-order elements may be used with Gaussian quadrature formulae without much regard to the number of Gauss points which are required. However, if the wave function is to be used in either the direct or indirect formulation increasing the number of Gauss points increases the number of wave function evaluations which has a considerable effect on the computational resources required to achieve a solution. Therefore, if higher-order elements are to be used for such problems it must first be demonstrated that the improvement in the numerical modelling permits a more coarse discretisation with a reduction in the total

number of wave function evaluations.

Numerical results for the solution of a number of diffraction and radiation problems in two dimensional domains using simple source distributions have been published by Au and Brebbia (1982) and Bird and Shepherd (1982). Both works employ higher-order discretisations and the later study was initiated by Brebbia, co-author of the first paper cited. While successfully applying linear and quadratic elements with a four point Gaussian quadrature to obtain solutions to three different problems Bird and Shepherd (1982) do not attempt to demonstrate that these methods are an improvement to the conventional constant element approach. The results presented by Au and Brebbia appear a little more instructive since the constant, linear and quadratic element results are compared and the number of nodes used are specified. The results obtained for a bottom-seated semi-circular obstruction are taken to indicate that the implementation of quadratic elements provides a more rapid convergence to the correct solution and it is suggested that this is due to the better representation of the geometry of the obstruction. However, caution must be exercised in accepting this result since the correct solution due to Chakrabarti (1973) is only in fact correct for an obstruction submerged in deep water and the results presented do not extend into this range but are restricted to waves in water of finite depth. Further examination of the results presented gives evidence that the numerical results do not converge to the assumed correct solution however precise the discretisation and reinterpretation on these grounds might suggest that the accuracy and efficiency of the constant element results are not improved upon.

The only known application of higher-order discretisation techniques to a wave function formulation is due to Coates (1982). It is indicated that by application of two dimensional quadratic elements satisfactory results (less than 1% error) are obtained for 56 nodes compared with the 96 used by Hogben and Standing (1974) and the 120 used by Garrison and Chow (1972). However, these results are again inconclusive since the superior rate of convergence obtained may be due to the use of a separate source boundary.

As an initial test for the diffraction program the results must be compared with data which is known to be correct. It is preferable when testing a numerical method to choose a simple geometry for which an exact solution is known and to establish that the method and the program written to execute the method achieve satisfactory accuracy. For two dimensional problems this approach is not possible since no exact solution is available and it therefore becomes necessary to compare results with established numerical results. In this section the results of the diffraction program for the range of element locations and discretisations are first compared with the results published by Naftzger and Chakrabarti (1979). These comparative tests are intended only to give a first impression for the alternative schemes and are followed by a more detailed examination. As an additional test results have been obtained for the case of a semi-immersed circular obstacle in water of infinite depth and comparison has been made with the results of Martin and Dixon (1983). These results are presented in Appendix A.8.

The results obtained by Naftzger and Chakrabarti for the case of a submerged circular obstacle in water of finite depth have been achieved using the direct integral equation formulation with the same form of the wave function as that which has been used in the present study. Two tests have been used to establish the accuracy of the results. The first, which is more valid in the case of the direct formulation than the indirect, requires a check on the conservation of energy in a similar manner to the method described in Appendix A.3.6. The second is only valid for the small portion of the data which approximates to the infinite water depth problem for which it has been demonstrated that the results do agree well with those of Ogilvie (1963) who used the multipole method. The only details of the constant element discretisation required to achieve the results presented is that about 100 elements are required to give results accurate to within 1% but that more elements are required if the obstacle is close to the free surface or bottom boundary.

The results given in this section are intended to give a full comparison of the alternative schemes outlined in this chapter and it has been ensured that the results are not obscured by variations in the numerical results for the wave function and its normal gradient. Initial tests have indicated that the source boundary location parameter RAT = r_s/r_n may be set to 0.7 to achieve satisfactory results and therefore tests have been performed for this setting before investigating the effects of varying RAT. Before presenting the results it may be noted that in the assembly of the matrix equations two different numerical variations are treated. The first is that of the source density function and the program has been written to

include assumed constant, linear and quadratic variation and these alternatives are often referred to as constant, linear and quadratic elements. The second is concerned with the evaluation of the integrals on each element and therefore relates to the variation of the wave function or the gradient of the wave function over the element. The numerical treatment of this second type of variation is determined by the choice of quadrature formula and the initial approach has been to choose this formula so that the total number of quadrature points (sources) is equal to the total number of nodes. The significance of this choice is that with a reduction of the element length both types of numerical variation will be modelled more closely.

The first set of results presented in Figures 4.5.1 to 4.5.3 and Tables 4.5.1 to 4.5.3 are obtained by the conventional singular kernel indirect integral equation formulation with a constant element single source discretisation. The results are presented for a range of the parameter ka which in this case must be regarded as a diffraction refraction parameter and since the water depth parameter h/a = 2.5 and the cylinder depth parameter y_o/a = 1.25 are set the range of ka includes shallow, intermediate and deep water depths. In assessing these results for the horizontal and vertical components of force and the reflection coefficient plus those results which are presented subsequently two indications of convergence may be identified: the proximity of the results to those of Naftzger and Chakrabarti and the grouping of the results for the different discretisations. For this first set of graphs it is clear that the results are better for larger values of the alternative water depth parameter h/L.

For an assumed linear variation of source density the results presented in Figures 4.5.4 to 4.5.6 and Tables 4.5.4 to 4.5.6 give conflicting and therefore inconclusive evidence for the horizontal and vertical components of force and the reflection coefficient and therefore a more detailed investigation of the comparative rates of convergence is required. However, examination of the results for an assumed quadratic variation of source density given in Figures 4.5.7 to 4.5.9 and Tables 4.5.7 to 4.5.9 are clearly less satisfactory than those achieved by the constant and linear element discretisations for smaller values of the parameter h/L.

The results for the regular kernel method for the same discretisation scheme as was used in Figures 4.5.1 to 4.5.3 have been given in Figures 4.5.10 to 4.5.12 and Tables 4.5.10 to 4.5.12. These graphs give a preliminary indication that the results obtained by this alternative method are not only satisfactory but are superior to the results of the conventional singular kernel method. Application of the higher-order discretisation techniques to the regular kernel method affect the convergence adversely as is demonstrated in Figures 4.5.13 to 4.5.18 and Tables 4.5.13 to 4.5.18 but in all cases the method yields satisfactory results for the more precise discretisation schemes.

Examination of the residual values (RES) in Tables 4.5.1 to 4.5.18 indicates that this measure of energy conservation is no more than a useful indicator of the accuracy of the results achieved. This test must be viewed with additional caution because it only checks the evaluations of the first stage of the program, namely the solution stage.

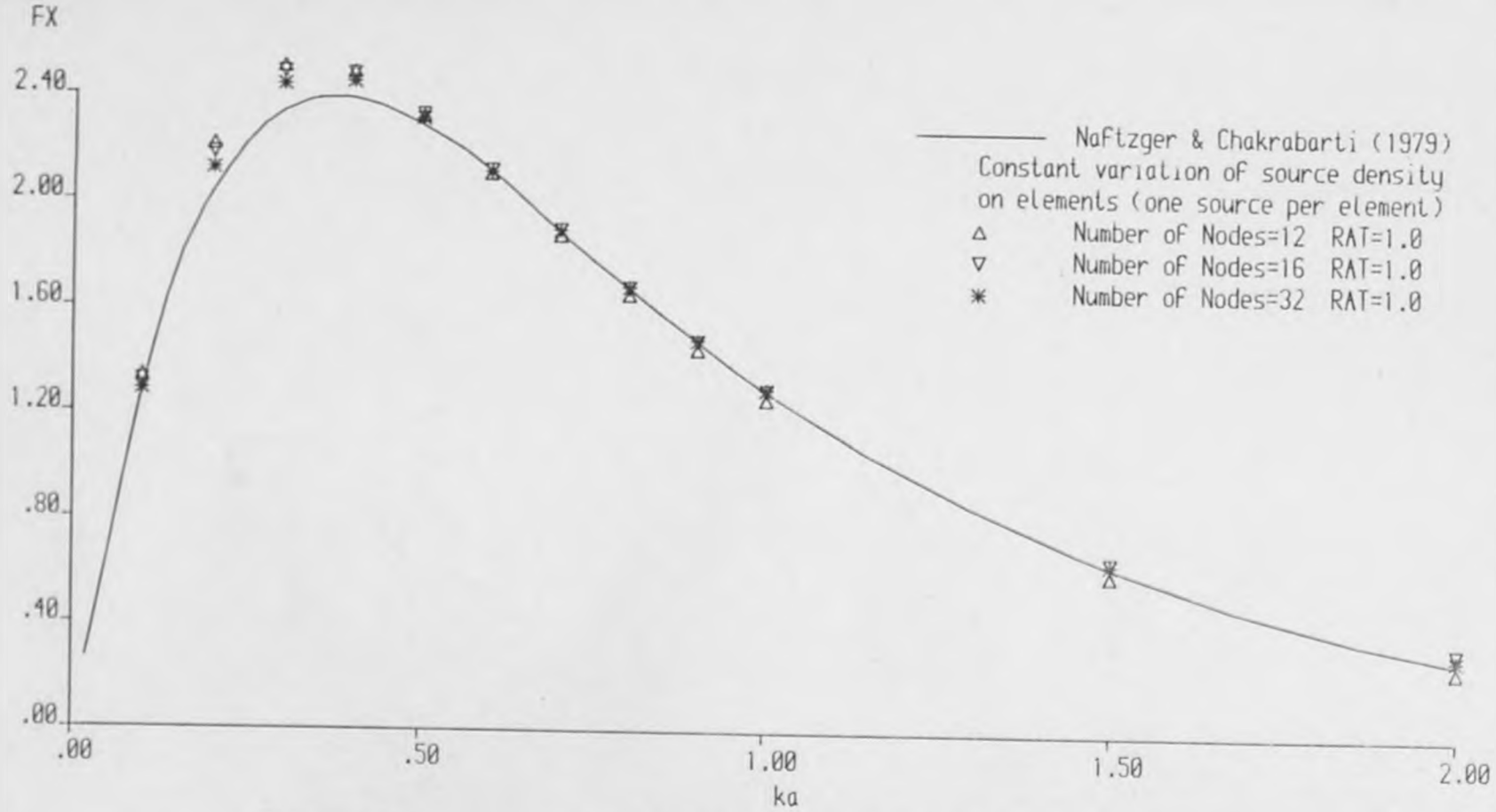

Figure 4.5.1 Maximum horizontal force on a submerged cylinder

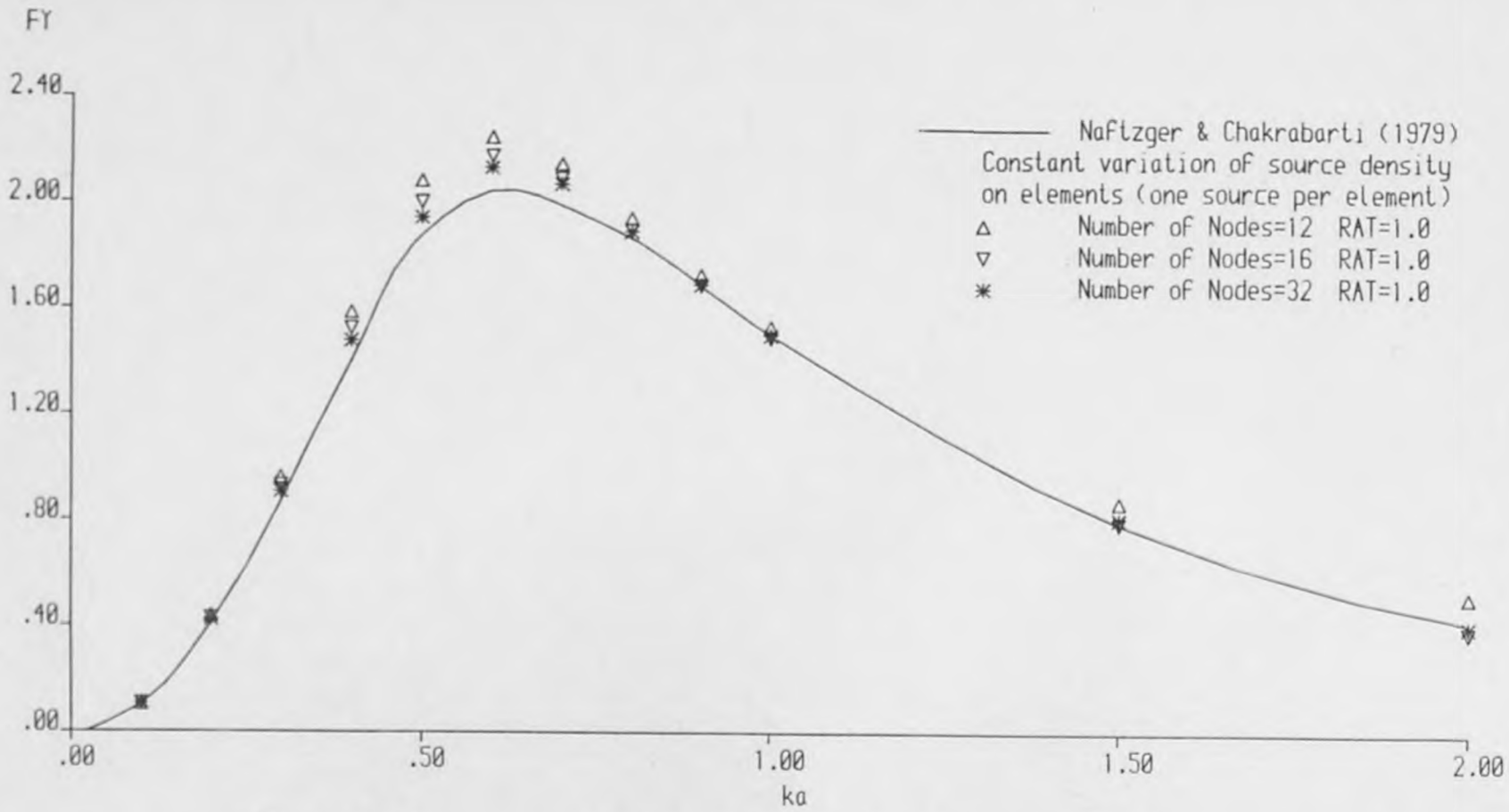

Figure 4.5.2 Maximum vertical force on a submerged cylinder

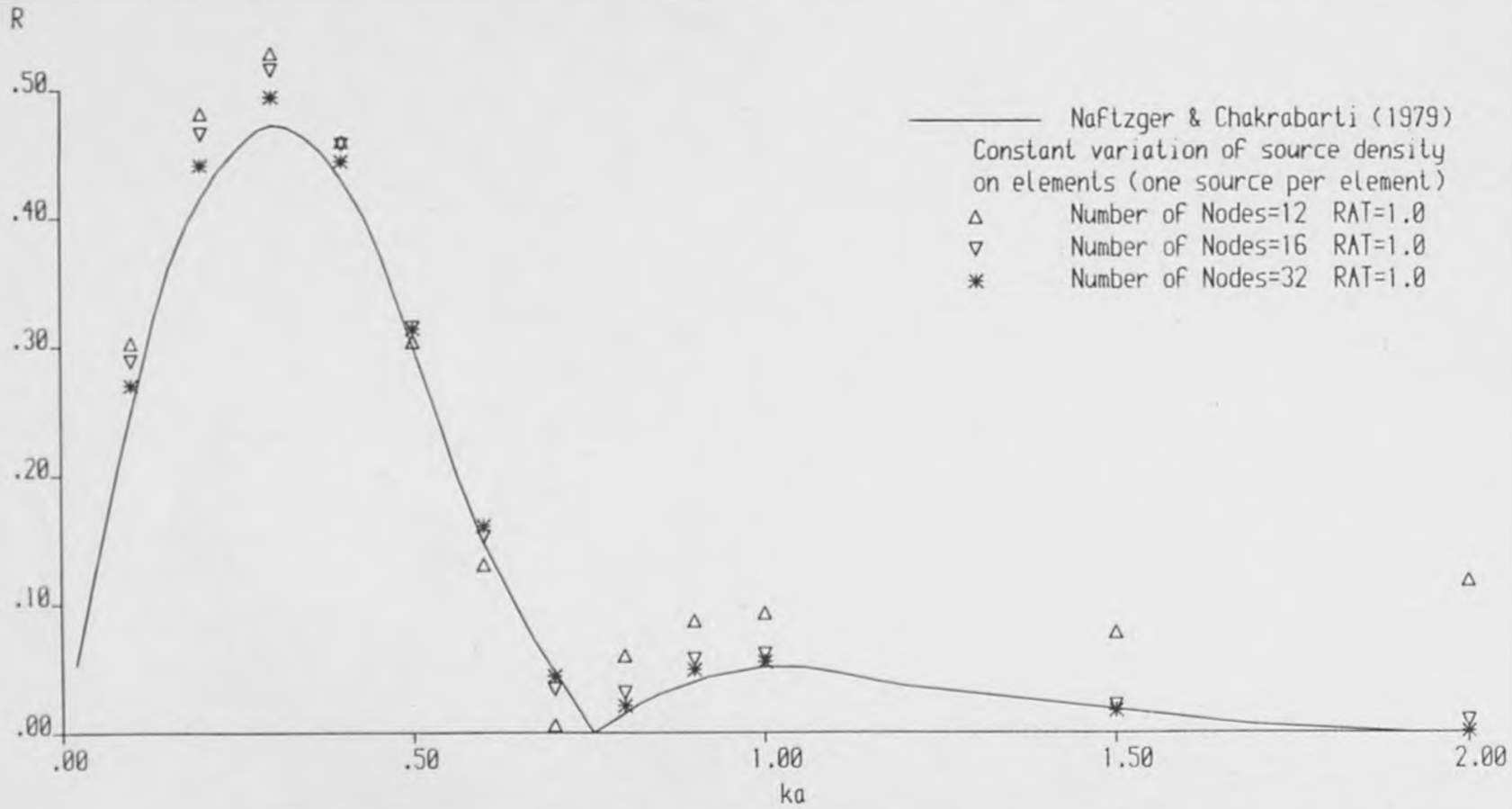

Figure 4.5.3 Reflection coefficient for a submerged cylinder

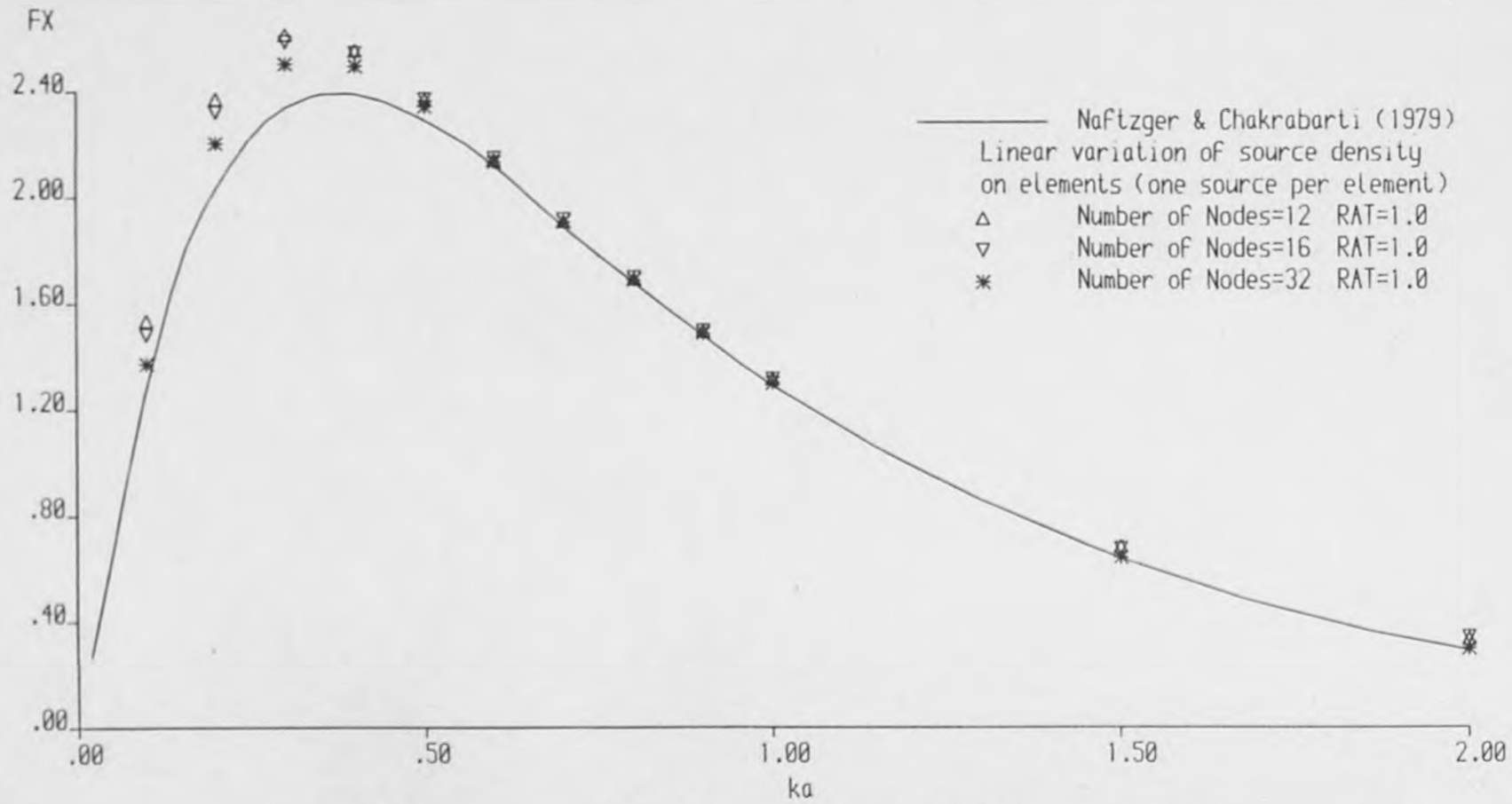

Figure 4.5.4 Maximum horizontal force on a submerged cylinder

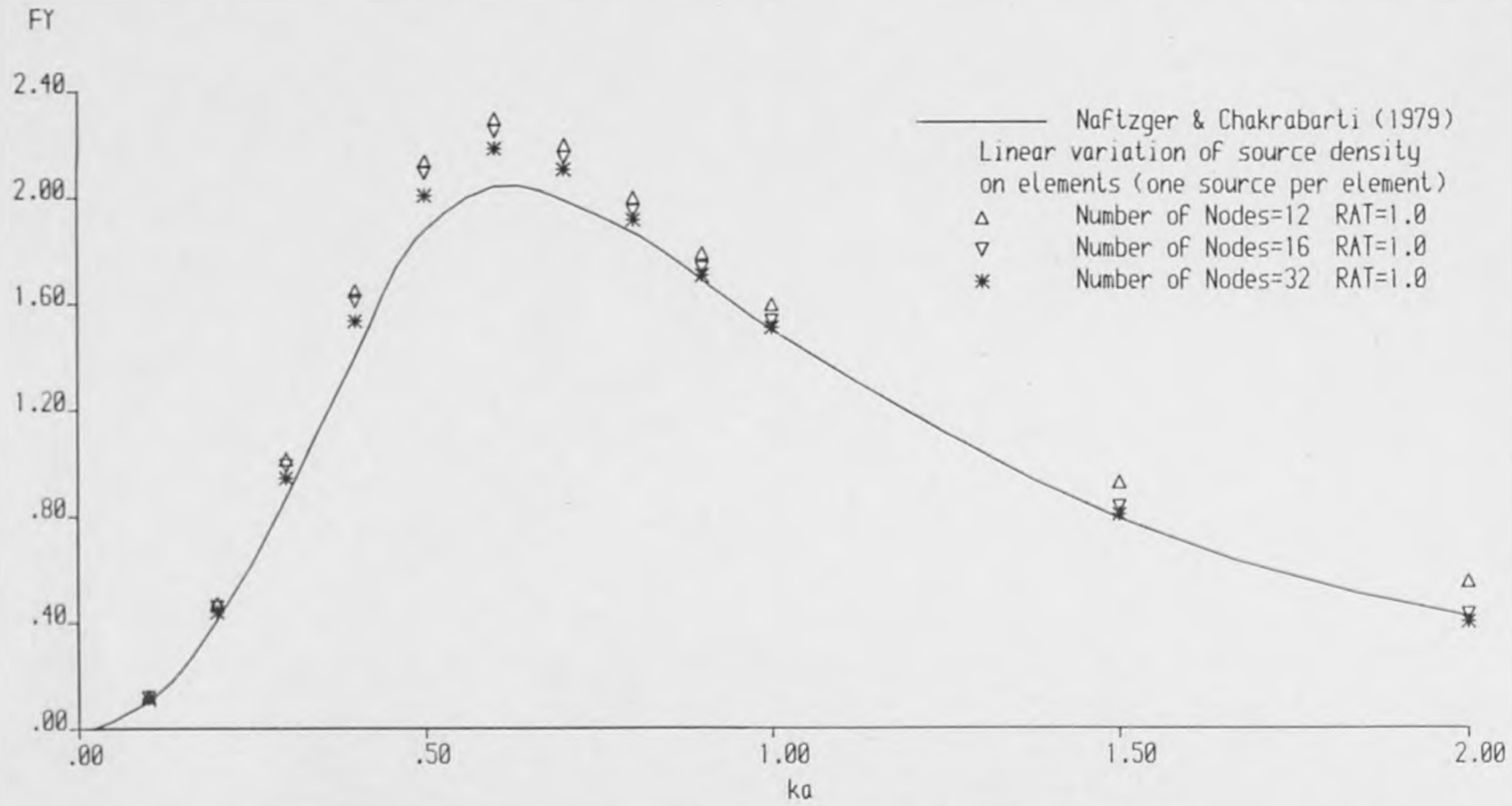

Figure 4.5.5 Maximum vertical force on a submerged cylinder

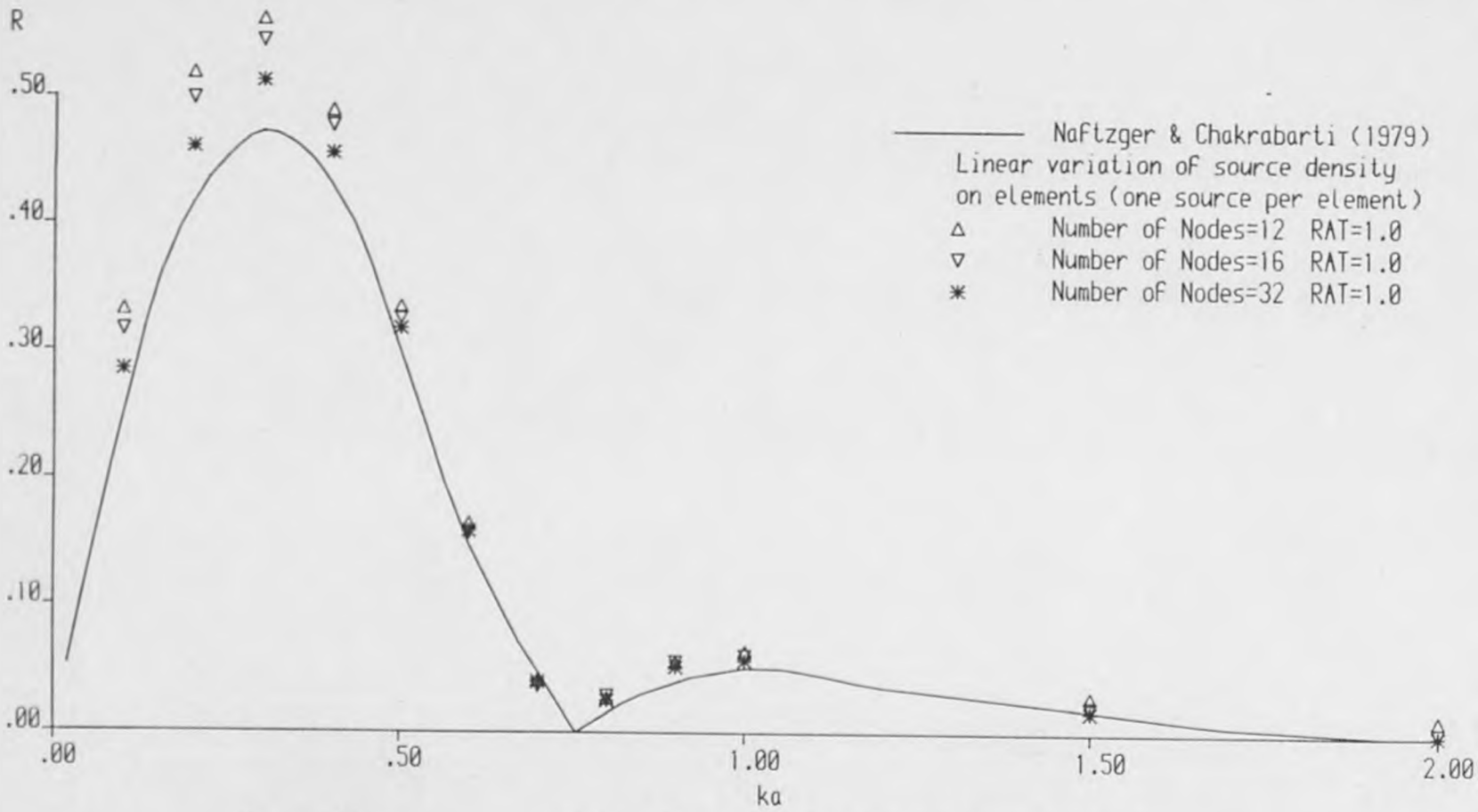

Figure 4.5.6 Reflection coefficient for a submerged cylinder

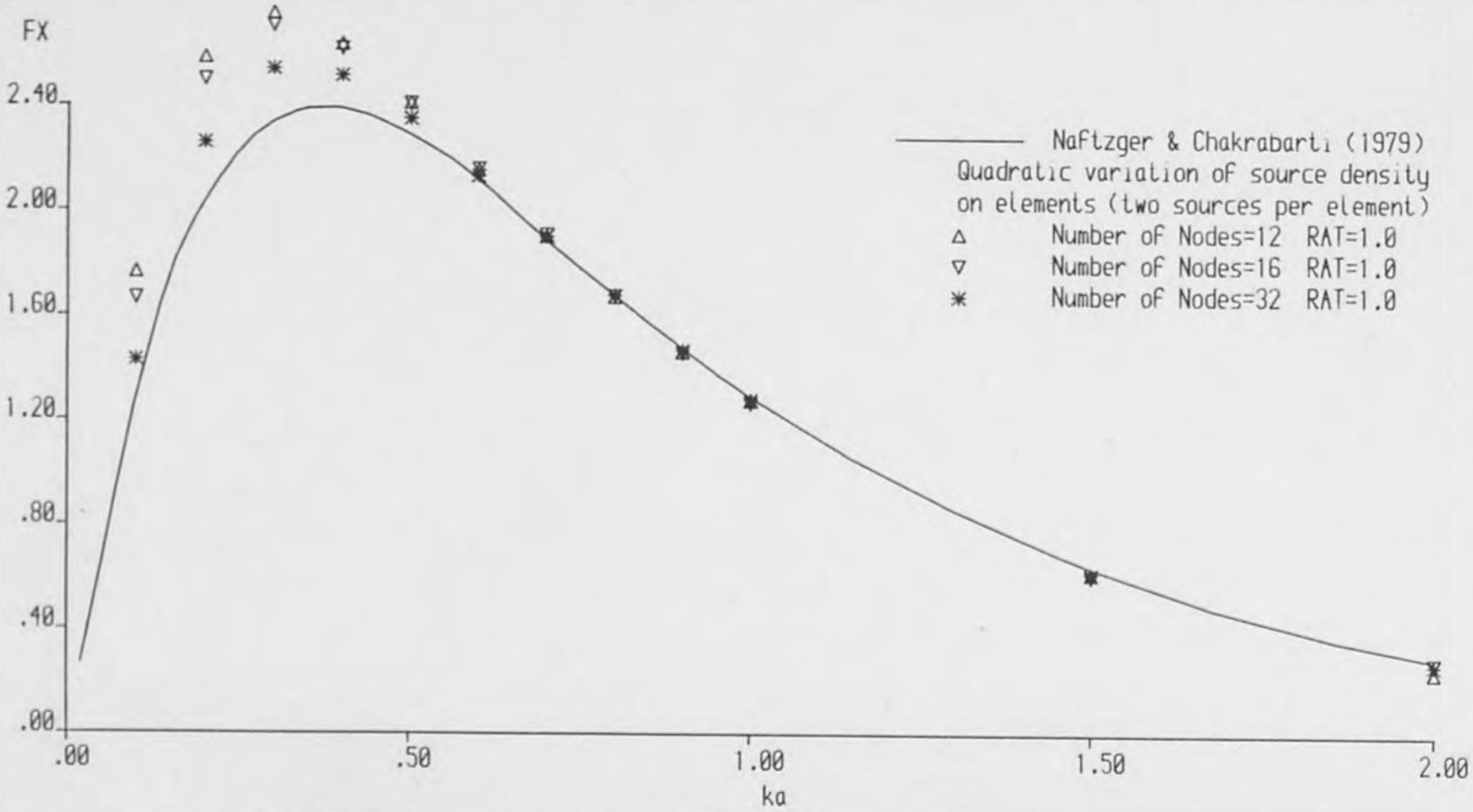

Figure 4.5.7 Maximum horizontal force on a submerged cylinder

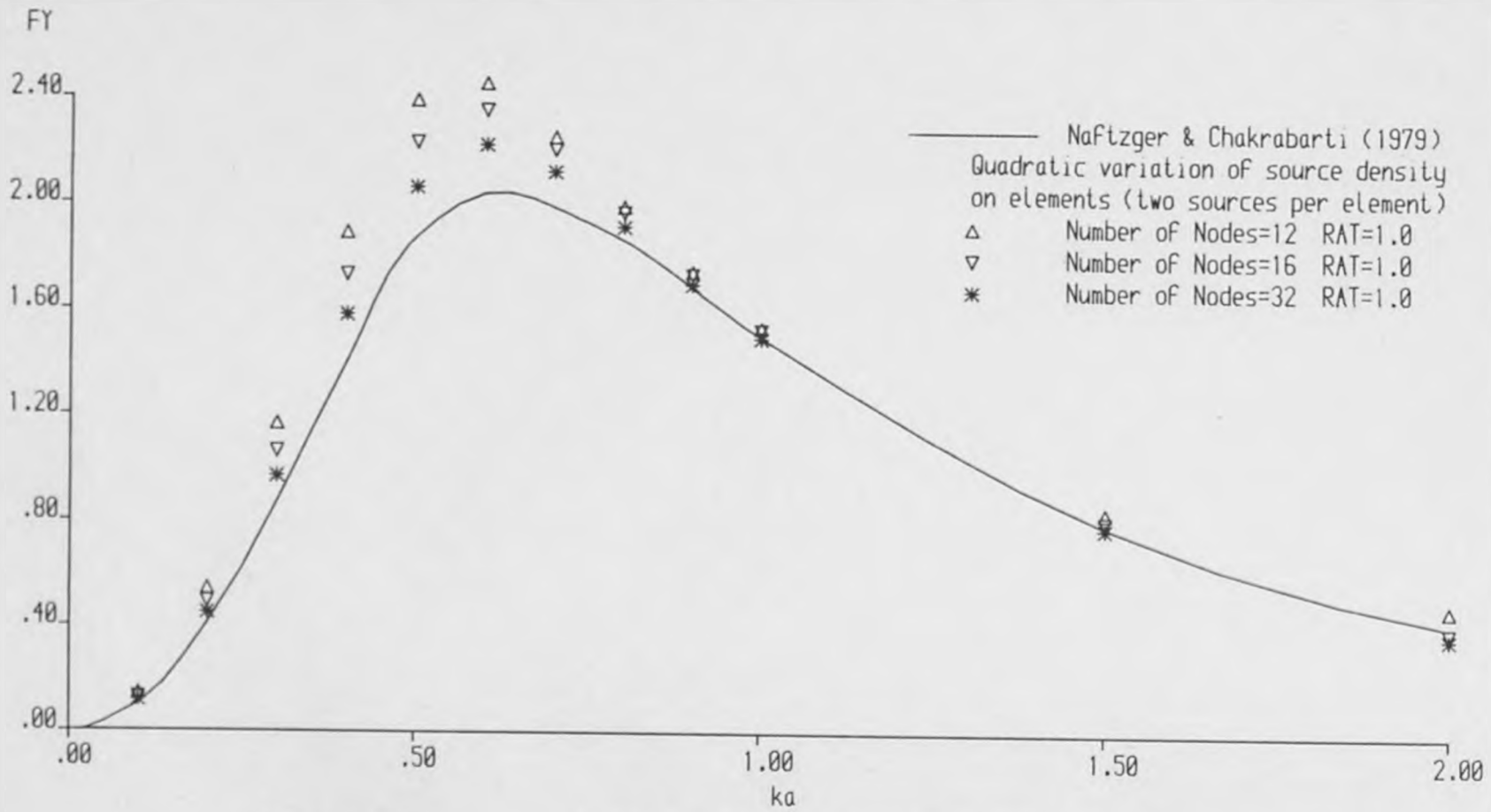

Figure 4.5.8 Maximum vertical force on a submerged cylinder

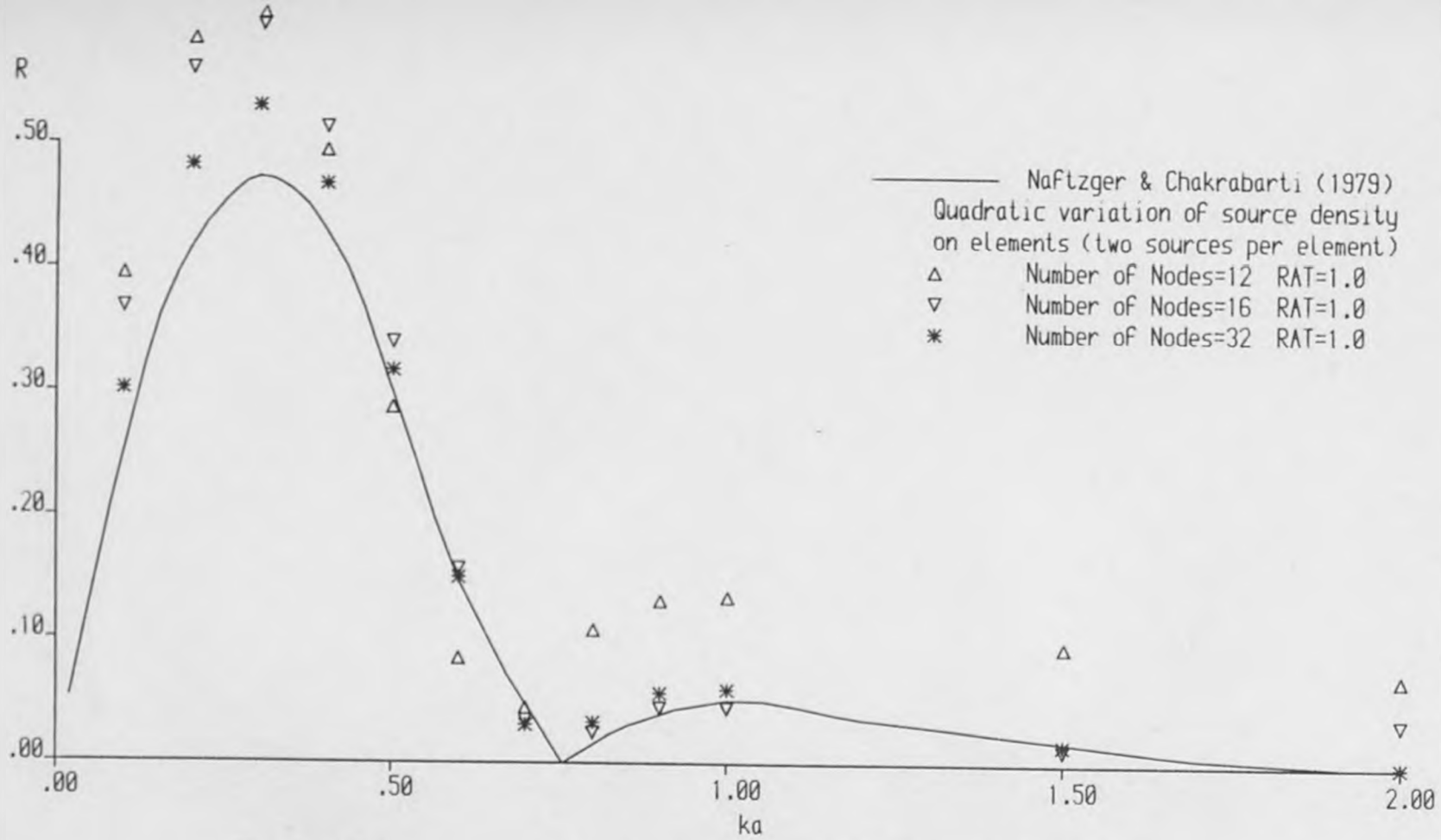

Figure 4.5.9 Reflection coefficient for a submerged cylinder

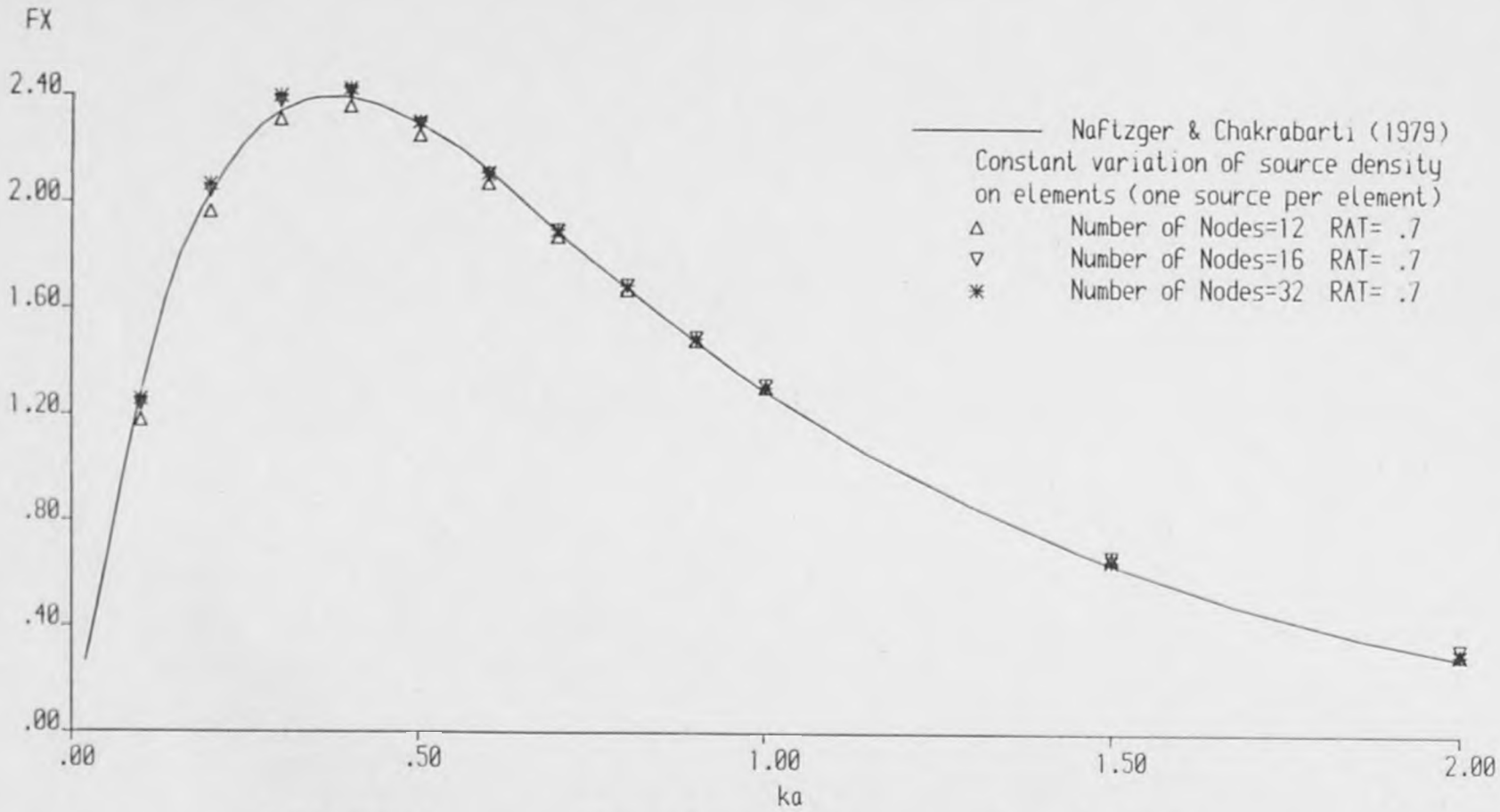

Figure 4.5.10 Maximum horizontal force on a submerged cylinder

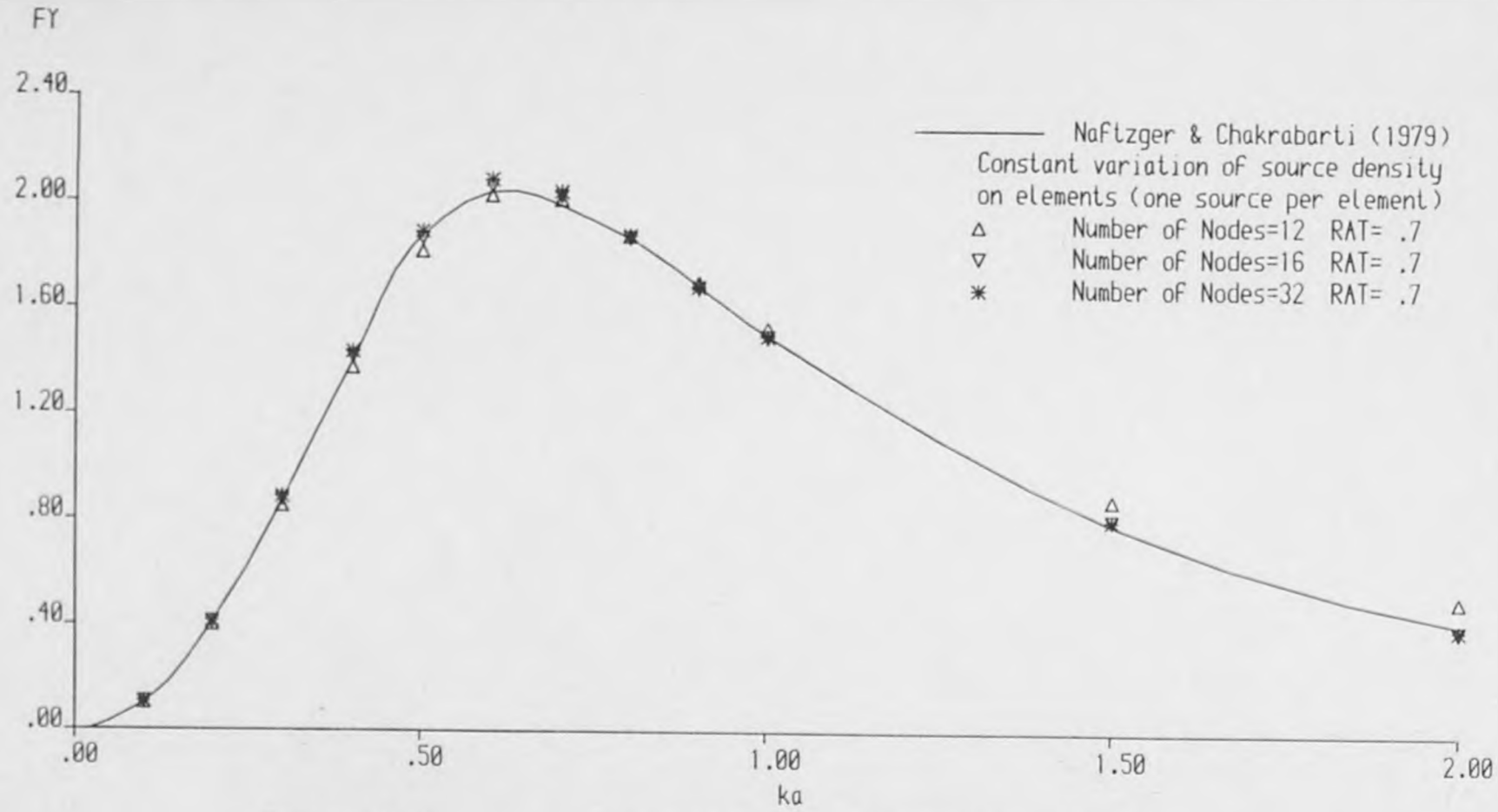

Figure 4.5.11 Maximum vertical force on a submerged cylinder

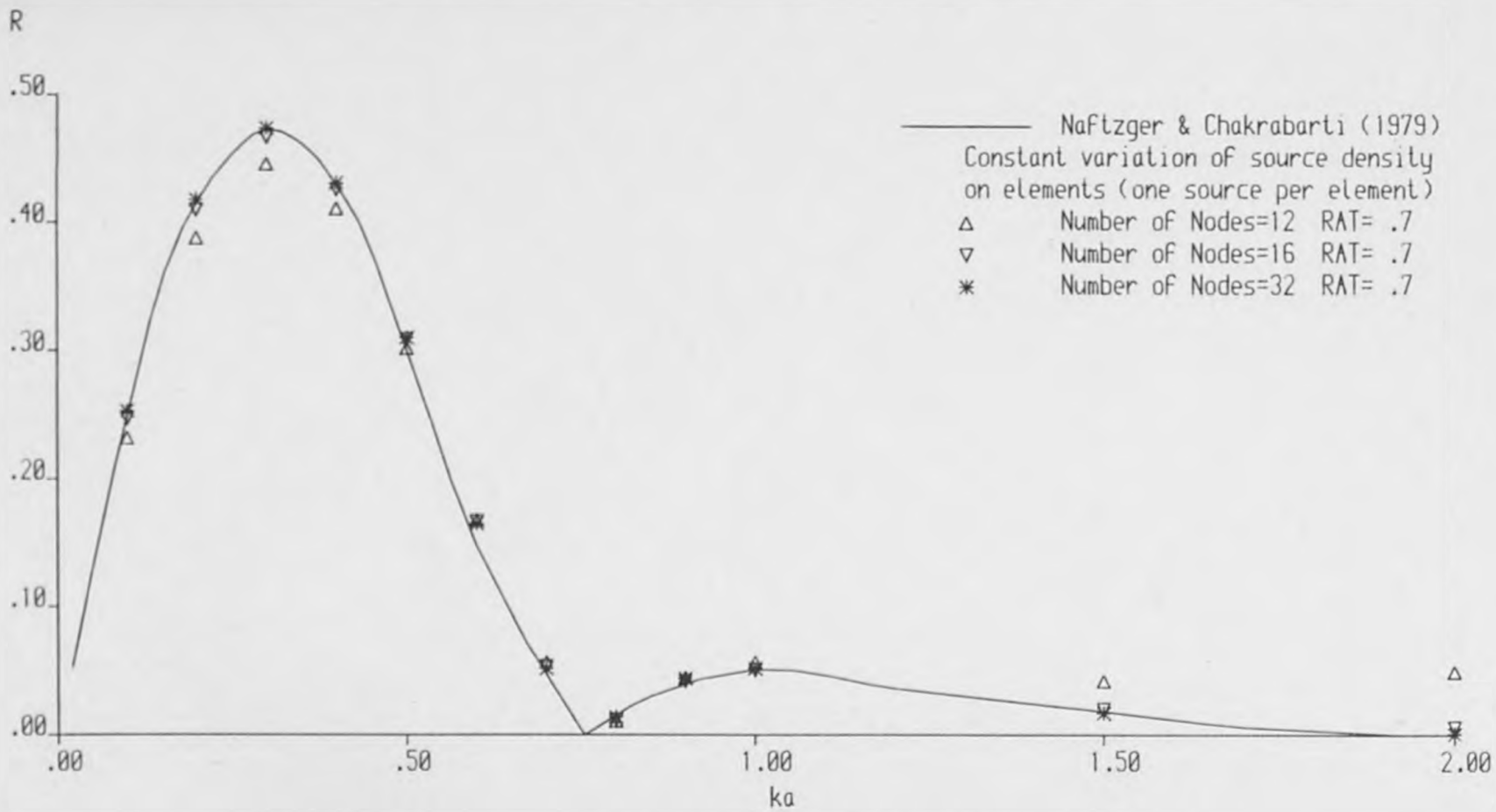

Figure 4.5.12 Reflection coefficient for a submerged cylinder

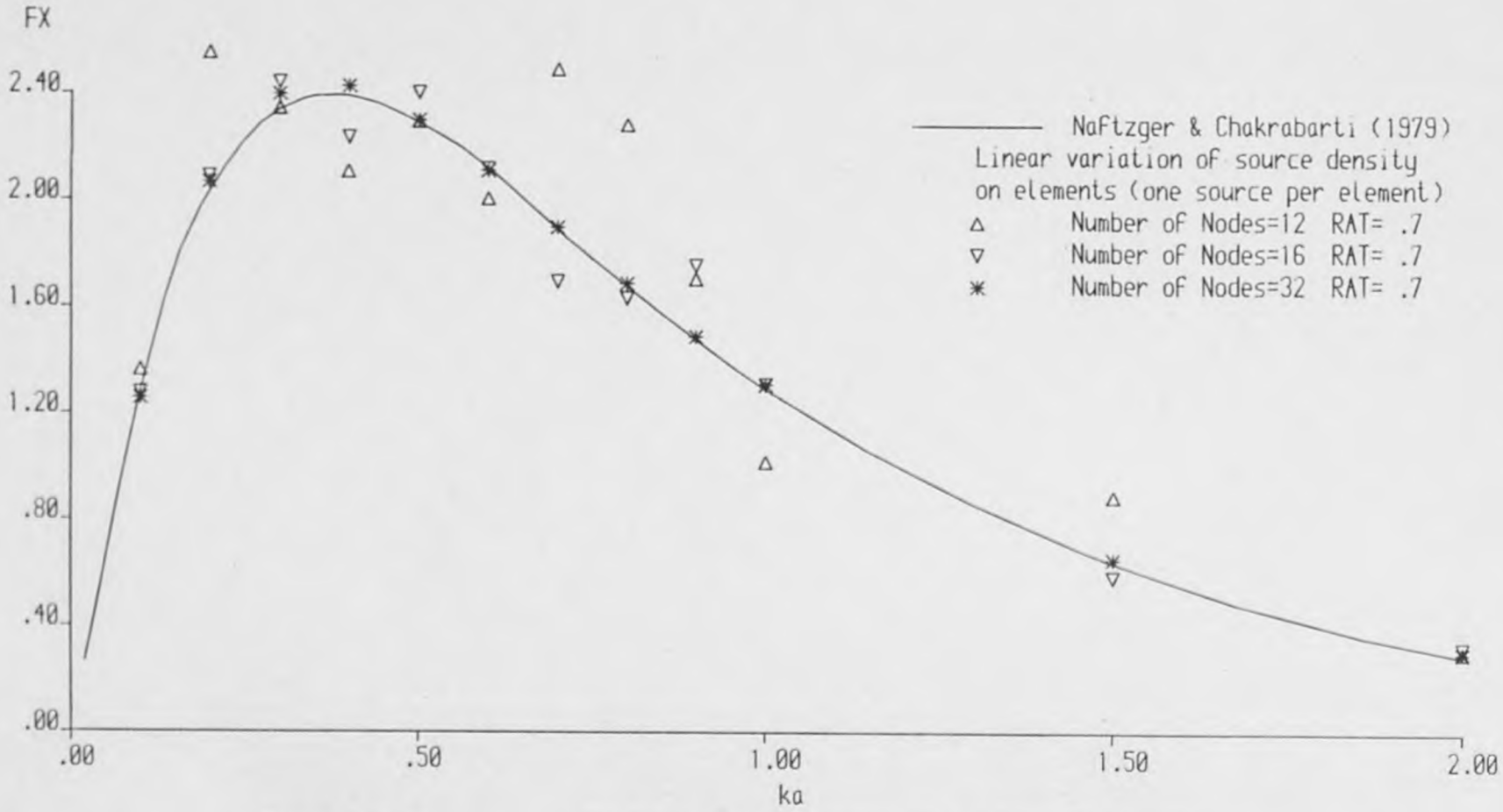

Figure 4.5.13 Maximum horizontal force on a submerged cylinder

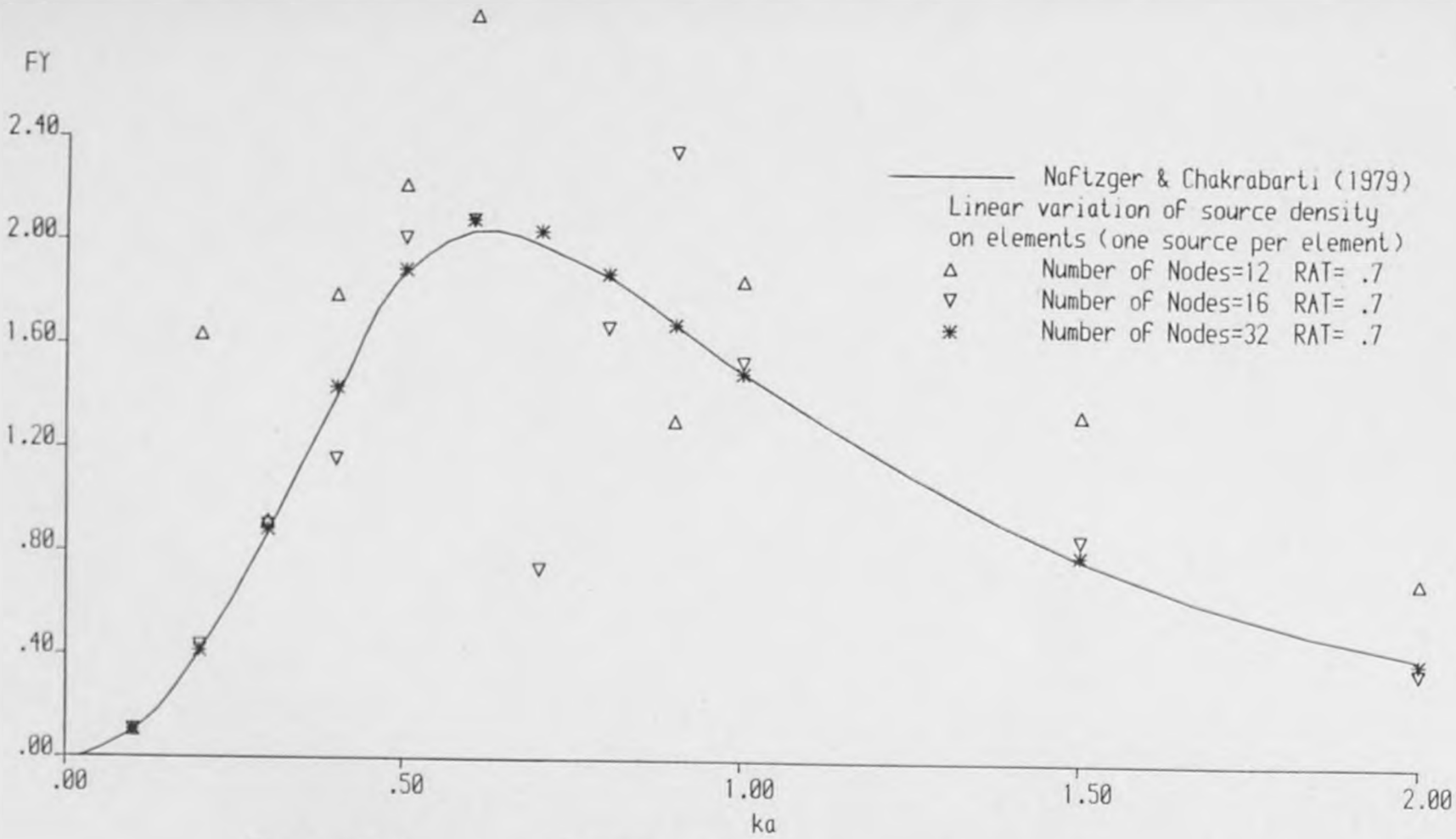

Figure 4.5.14 Maximum vertical force on a submerged cylinder

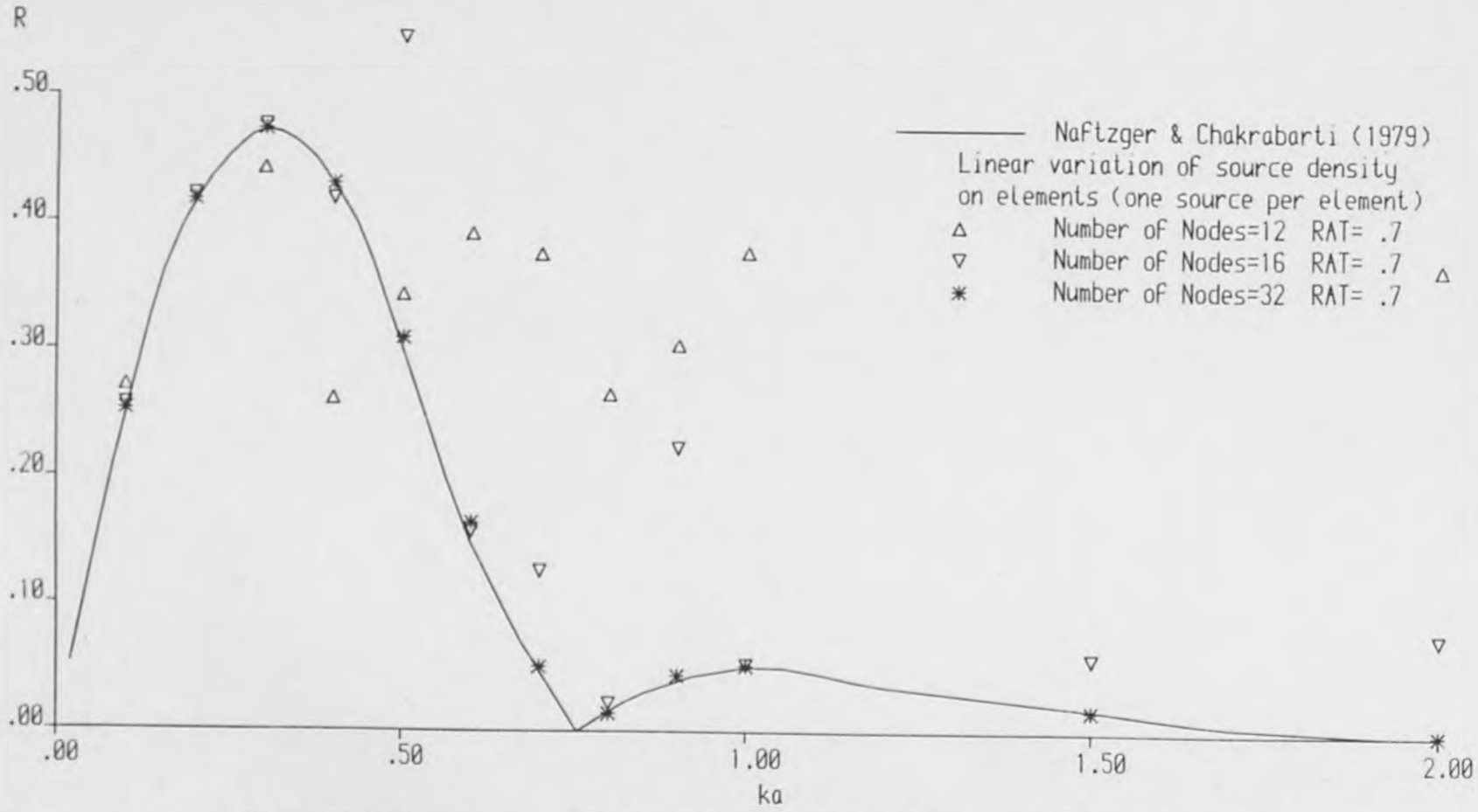

Figure 4.5.15 Reflection coefficient for a submerged cylinder

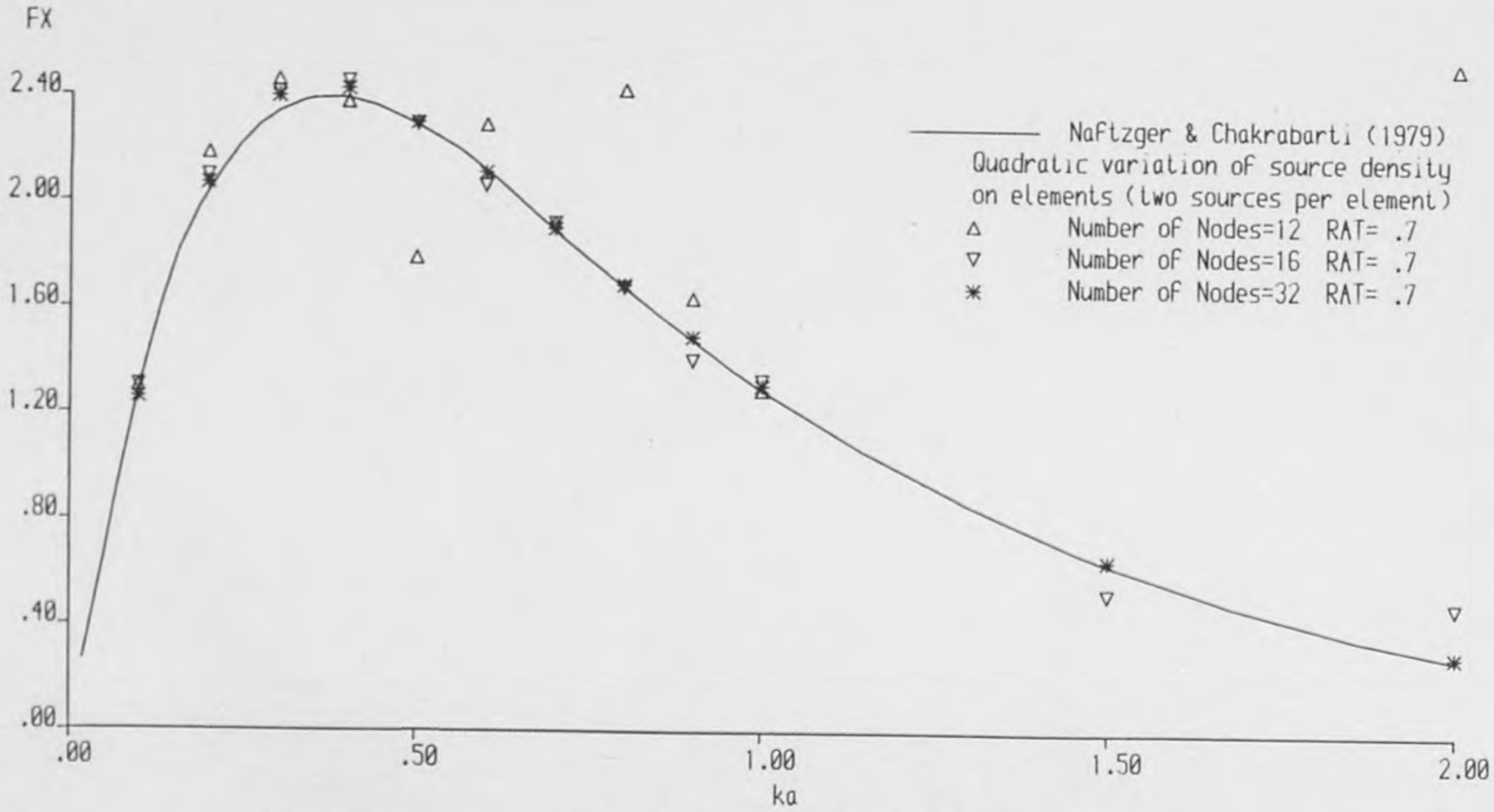

Figure 4.5.16 Maximum horizontal force on a submerged cylinder

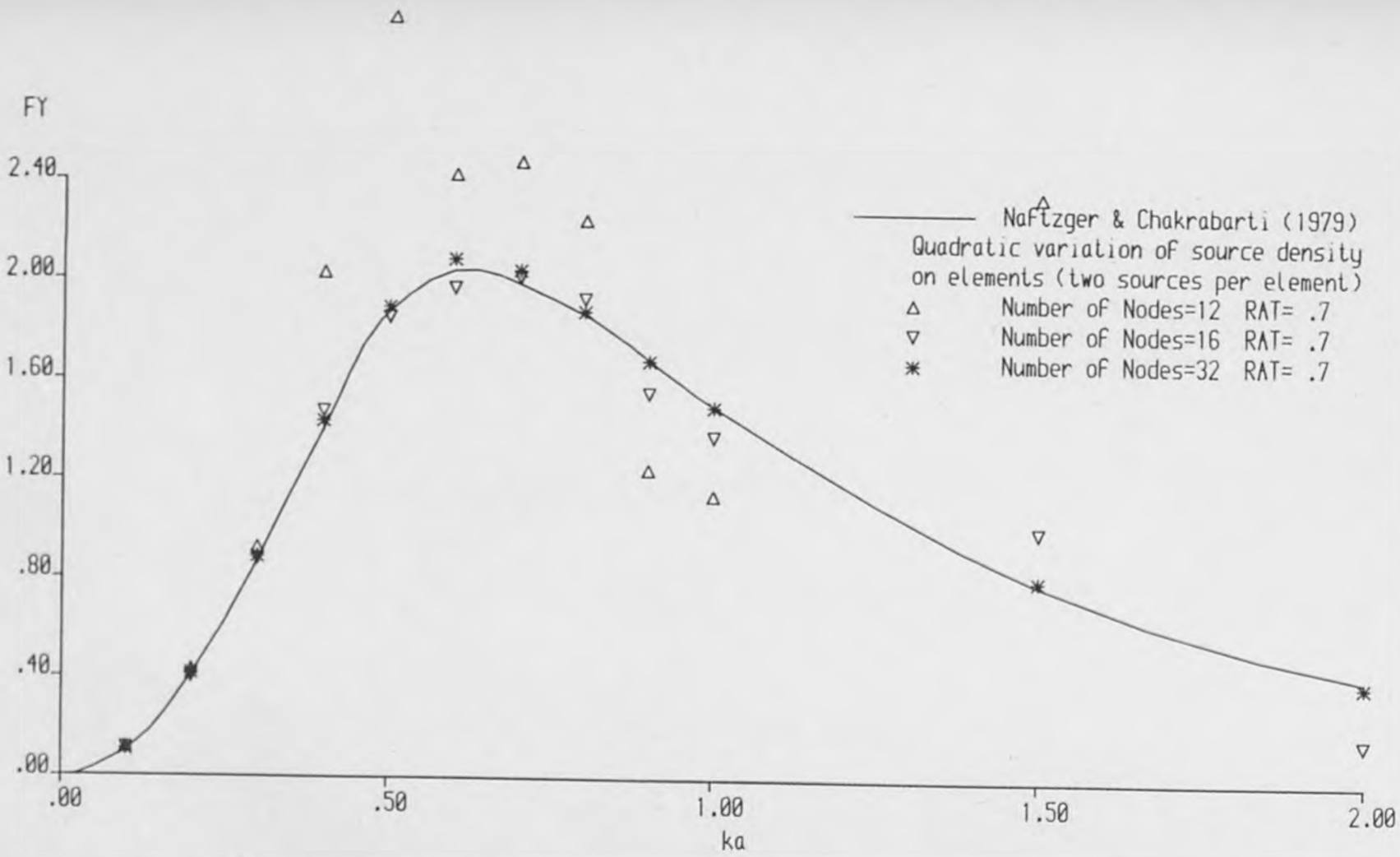

Figure 4.5.17 Maximum vertical force on a submerged cylinder

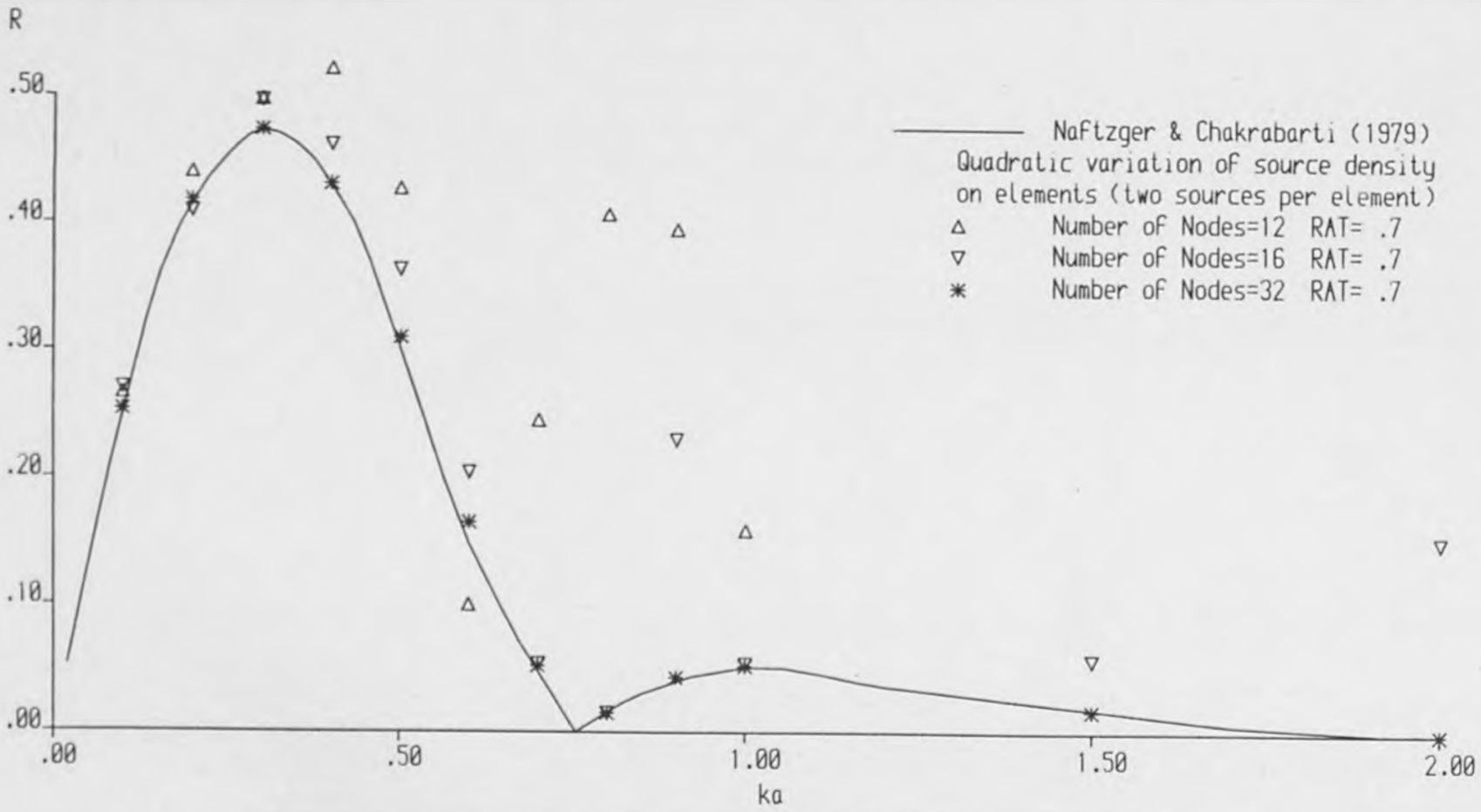

Figure 4.5.18 Reflection coefficient for a submerged cylinder

SOURCES DISTRIBUTED ON CYLINDER BOUNDARY
NO NODES= 12 (CONSTANT ELEMENTS)
ONE-POINT GAUSS QUADRATURE

ka	h/L	Mod(R)	Arg(R)	RES	Mod(Fx)	Arg(Fx)	Mod(Fy)	Arg(Fy)
0.10	0.04	0.303	-0.400	0.3E-07	1.337	0.311	0.104	-1.567
0.20	0.08	0.482	-0.319	0.3E-07	2.215	0.537	0.436	-1.537
0.30	0.12	0.529	-0.250	0.3E-07	2.511	0.672	0.961	-1.456
0.40	0.16	0.460	-0.177	0.5E-07	2.491	0.747	1.584	-1.302
0.50	0.20	0.304	-0.096	0.1E-07	2.327	0.789	2.079	-1.091
0.60	0.24	0.131	-0.024	0.7E-08	2.109	0.813	2.246	-0.889
0.70	0.28	0.006	0.024	0.7E-08	1.879	0.826	2.145	-0.751
0.80	0.32	0.060	0.049	0.3E-07	1.656	0.832	1.941	-0.679
0.90	0.36	0.087	0.058	0.6E-07	1.450	0.834	1.726	-0.650
1.00	0.40	0.093	0.058	0.1E-06	1.263	0.830	1.531	-0.647
1.50	0.60	0.078	0.011	0.7E-07	0.609	0.763	0.872	-0.730
2.00	0.80	0.118	-0.046	0.7E-07	0.266	0.653	0.520	-0.799

Processor time=0.0272

Table 4.5.1 Diffraction Results for a Submerged Cylinder

SOURCES DISTRIBUTED ON CYLINDER BOUNDARY
NO NODES= 16 (CONSTANT ELEMENTS)
ONE-POINT GAUSS QUADRATURE

ka	h/L	Mod(R)	Arg(R)	RES	Mod(Fx)	Arg(Fx)	Mod(Fy)	Arg(Fy)
0.10	0.04	0.289	-0.404	0.2E-07	1.317	0.297	0.104	-1.567
0.20	0.08	0.466	-0.326	0.1E-07	2.181	0.516	0.427	-1.540
0.30	0.12	0.516	-0.259	0.2E-07	2.490	0.650	0.931	-1.463
0.40	0.16	0.458	-0.188	0.6E-08	2.485	0.727	1.523	-1.319
0.50	0.20	0.315	-0.111	0.3E-07	2.333	0.771	1.999	-1.120
0.60	0.24	0.153	-0.042	0.3E-07	2.123	0.797	2.174	-0.928
0.70	0.28	0.034	0.006	0.1E-07	1.900	0.812	2.089	-0.793
0.80	0.32	0.031	0.032	0.1E-06	1.682	0.820	1.896	-0.720
0.90	0.36	0.057	0.042	0.2E-07	1.480	0.823	1.686	-0.691
1.00	0.40	0.061	0.043	0.4E-07	1.297	0.822	1.490	-0.688
1.50	0.60	0.021	-0.004	0.7E-07	0.660	0.768	0.793	-0.782
2.00	0.80	0.009	-0.064	0.8E-07	0.333	0.681	0.386	-0.881

Processor time=0.0378

Table 4.5.2 Diffraction Results for a Submerged Cylinder

SOURCES DISTRIBUTED ON CYLINDER BOUNDARY
NO NODES= 32 (CONSTANT ELEMENTS)
ONE-POINT GAUSS QUADRATURE

ka	h/L	Mod(R)	Arg(R)	RES	Mod(Fx)	Arg(Fx)	Mod(Fy)	Arg(Fy)
0.10	0.04	0.270	-0.411	0.2E-07	1.285	0.277	0.105	-1.567
0.20	0.08	0.441	-0.336	0.2E-08	2.121	0.486	0.421	-1.541
0.30	0.12	0.495	-0.271	0.6E-07	2.442	0.619	0.908	-1.469
0.40	0.16	0.444	-0.202	0.5E-07	2.454	0.698	1.477	-1.334
0.50	0.20	0.314	-0.128	0.1E-07	2.316	0.744	1.941	-1.146
0.60	0.24	0.161	-0.061	0.5E-07	2.116	0.771	2.129	-0.962
0.70	0.28	0.044	-0.013	0.7E-08	1.898	0.787	2.067	-0.828
0.80	0.32	0.021	0.013	0.1E-07	1.684	0.796	1.890	-0.754
0.90	0.36	0.049	0.025	0.5E-07	1.484	0.800	1.689	-0.722
1.00	0.40	0.055	0.026	0.6E-07	1.301	0.799	1.499	-0.717
1.50	0.60	0.017	-0.018	0.7E-07	0.653	0.749	0.809	-0.805
2.00	0.80	0.001	-0.076	0.2E-06	0.310	0.666	0.409	-0.904

Processor time=0.1157

Table 4.5.3 Diffraction Results for a Submerged Cylinder

SOURCES DISTRIBUTED ON CYLINDER BOUNDARY
NO NODES= 12 (LINEAR ELEMENTS)
ONE-POINT GAUSS QUADRATURE

ka	h/L	Mod(R)	Arg(R)	RES	Mod(Fx)	Arg(Fx)	Mod(Fy)	Arg(Fy)
0.10	0.04	0.332	-0.390	0.6E-08	1.536	0.343	0.121	-1.566
0.20	0.08	0.519	-0.306	0.1E-07	2.372	0.578	0.471	-1.538
0.30	0.12	0.562	-0.239	0.5E-08	2.615	0.708	1.015	-1.459
0.40	0.16	0.490	-0.171	0.3E-07	2.555	0.774	1.647	-1.310
0.50	0.20	0.335	-0.098	0.4E-07	2.369	0.802	2.135	-1.110
0.60	0.24	0.165	-0.036	0.5E-07	2.141	0.811	2.296	-0.925
0.70	0.28	0.041	0.001	0.7E-08	1.911	0.808	2.197	-0.804
0.80	0.32	0.027	0.017	0.5E-07	1.694	0.798	1.998	-0.746
0.90	0.36	0.056	0.017	0.5E-07	1.496	0.784	1.788	-0.731
1.00	0.40	0.064	0.008	0.5E-07	1.318	0.767	1.596	-0.741
1.50	0.60	0.029	-0.076	0.7E-07	0.685	0.651	0.928	-0.891
2.00	0.80	0.013	-0.163	0.6E-07	0.334	0.523	0.554	-1.035

Processor time=0.0328

Table 4.5.4 Diffraction Results for a Submerged Cylinder

SOURCES DISTRIBUTED ON CYLINDER BOUNDARY
NO NODES= 16 (LINEAR ELEMENTS)
ONE-POINT GAUSS QUADRATURE

ka	h/L	Mod(R)	Arg(R)	RES	Mod(Fx)	Arg(Fx)	Mod(Fy)	Arg(Fy)
0.10	0.04	0.316	-0.395	0.1E-07	1.483	0.325	0.117	-1.567
0.20	0.08	0.499	-0.313	0.3E-07	2.322	0.555	0.459	-1.538
0.30	0.12	0.545	-0.246	0.2E-07	2.588	0.688	0.991	-1.460
0.40	0.16	0.478	-0.176	0.2E-07	2.547	0.759	1.609	-1.311
0.50	0.20	0.326	-0.100	0.1E-07	2.372	0.794	2.091	-1.109
0.60	0.24	0.158	-0.035	0.3E-07	2.149	0.810	2.250	-0.920
0.70	0.28	0.037	0.007	0.4E-07	1.919	0.815	2.149	-0.793
0.80	0.32	0.029	0.027	0.5E-07	1.700	0.813	1.947	-0.729
0.90	0.36	0.056	0.031	0.3E-07	1.498	0.806	1.732	-0.709
1.00	0.40	0.061	0.026	0.1E-06	1.317	0.796	1.534	-0.714
1.50	0.60	0.021	-0.044	0.8E-08	0.678	0.707	0.835	-0.843
2.00	0.80	0.003	-0.120	0.5E-07	0.341	0.595	0.429	-0.973

Processor time=0.0440

Table 4.5.5 Diffraction Results for a Submerged Cylinder

SOURCES DISTRIBUTED ON CYLINDER BOUNDARY
NO NODES= 32 (LINEAR ELEMENTS)
ONE-POINT GAUSS QUADRATURE

ka	h/L	Mod(R)	Arg(R)	RES	Mod(Fx)	Arg(Fx)	Mod(Fy)	Arg(Fy)
0.10	0.04	0.285	-0.406	0.9E-08	1.373	0.293	0.112	-1.567
0.20	0.08	0.461	-0.328	0.1E-07	2.203	0.510	0.439	-1.540
0.30	0.12	0.513	-0.262	0.7E-08	2.504	0.643	0.944	-1.465
0.40	0.16	0.456	-0.192	0.1E-07	2.496	0.720	1.533	-1.324
0.50	0.20	0.318	-0.117	0.7E-09	2.343	0.763	2.006	-1.131
0.60	0.24	0.159	-0.049	0.3E-08	2.133	0.787	2.183	-0.943
0.70	0.28	0.040	-0.003	0.5E-07	1.909	0.801	2.104	-0.810
0.80	0.32	0.025	0.022	0.1E-07	1.690	0.807	1.914	-0.739
0.90	0.36	0.052	0.031	0.8E-07	1.487	0.808	1.705	-0.711
1.00	0.40	0.057	0.031	0.9E-07	1.301	0.805	1.509	-0.708
1.50	0.60	0.017	-0.020	0.9E-07	0.644	0.745	0.806	-0.809
2.00	0.80	0.001	-0.083	0.4E-06	0.298	0.654	0.401	-0.916

Processor time=0.1199

Table 4.5.6 Diffraction Results for a Submerged Cylinder

SOURCES DISTRIBUTED ON CYLINDER BOUNDARY
NO NODES= 12 (QUADRATIC ELEMENTS)
TWO-POINT GAUSS QUADRATURE

ka	h/L	Mod(R)	Arg(R)	RES	Mod(Fx)	Arg(Fx)	Mod(Fy)	Arg(Fy)
0.10	0.04	0.395	-0.367	0.3E-07	1.765	0.412	0.142	1.452
0.20	0.08	0.585	-0.275	0.2E-07	2.587	0.667	0.542	-1.570
0.30	0.12	0.606	-0.204	0.1E-07	2.756	0.793	1.167	-1.449
0.40	0.16	0.495	-0.126	0.3E-07	2.639	0.850	1.891	-1.253
0.50	0.20	0.288	-0.041	0.6E-07	2.413	0.873	2.392	-1.003
0.60	0.24	0.085	0.027	0.2E-07	2.156	0.877	2.457	-0.791
0.70	0.28	0.045	0.063	0.3E-07	1.906	0.870	2.255	-0.667
0.80	0.32	0.108	0.075	0.7E-07	1.674	0.857	1.993	-0.616
0.90	0.36	0.132	0.072	0.1E-06	1.465	0.840	1.748	-0.608
1.00	0.40	0.135	0.060	0.1E-06	1.278	0.819	1.536	-0.623
1.50	0.60	0.095	-0.033	0.4E-08	0.618	0.693	0.844	-0.783
2.00	0.80	0.071	-0.126	0.1E-06	0.245	0.556	0.486	-0.937

Processor time=0.0494

Table 4.5.7 Diffraction Results for a Submerged Cylinder

SOURCES DISTRIBUTED ON CYLINDER BOUNDARY
NO NODES= 16 (QUADRATIC ELEMENTS)
TWO-POINT GAUSS QUADRATURE

ka	h/L	Mod(R)	Arg(R)	RES	Mod(Fx)	Arg(Fx)	Mod(Fy)	Arg(Fy)
0.10	0.04	0.368	-0.378	0.2E-07	1.664	0.381	0.126	1.535
0.20	0.08	0.561	-0.289	0.8E-08	2.502	0.630	0.491	-1.550
0.30	0.12	0.597	-0.219	0.1E-07	2.710	0.762	1.063	-1.456
0.40	0.16	0.514	-0.145	0.5E-07	2.621	0.829	1.732	-1.286
0.50	0.20	0.341	-0.063	0.8E-07	2.411	0.862	2.233	-1.061
0.60	0.24	0.158	0.006	0.2E-07	2.162	0.878	2.356	-0.857
0.70	0.28	0.035	0.049	0.5E-07	1.912	0.884	2.207	-0.727
0.80	0.32	0.025	0.068	0.1E-06	1.677	0.884	1.970	-0.666
0.90	0.36	0.045	0.072	0.7E-07	1.462	0.879	1.736	-0.650
1.00	0.40	0.045	0.066	0.1E-06	1.269	0.871	1.527	-0.658
1.50	0.60	0.012	-0.004	0.5E-07	0.608	0.788	0.809	-0.795
2.00	0.80	0.035	-0.082	0.1E-06	0.280	0.674	0.400	-0.927

Processor time=0.0709

Table 4.5.8 Diffraction Results for a Submerged Cylinder

SOURCES DISTRIBUTED ON CYLINDER BOUNDARY
NO NODES= 32 (QUADRATIC ELEMENTS)
TWO-POINT GAUSS QUADRATURE

ka	h/L	Mod(R)	Arg(R)	RES	Mod(Fx)	Arg(Fx)	Mod(Fy)	Arg(Fy)
0.10	0.04	0.302	-0.400	0.4E-09	1.428	0.311	0.115	-1.566
0.20	0.08	0.483	-0.319	0.6E-08	2.261	0.536	0.449	-1.538
0.30	0.12	0.531	-0.251	0.1E-07	2.544	0.671	0.970	-1.460
0.40	0.16	0.468	-0.180	0.4E-08	2.518	0.746	1.580	-1.311
0.50	0.20	0.318	-0.101	0.4E-07	2.353	0.789	2.061	-1.106
0.60	0.24	0.151	-0.031	0.5E-07	2.134	0.812	2.224	-0.910
0.70	0.28	0.031	0.016	0.1E-06	1.903	0.826	2.122	-0.776
0.80	0.32	0.033	0.041	0.1E-07	1.679	0.833	1.916	-0.705
0.90	0.36	0.057	0.050	0.9E-07	1.471	0.835	1.698	-0.678
1.00	0.40	0.060	0.050	0.6E-07	1.282	0.833	1.496	-0.677
1.50	0.60	0.016	-0.001	0.1E-07	0.618	0.775	0.784	-0.779
2.00	0.80	0.001	-0.033	0.4E-03	0.274	0.689	0.378	-0.889

Processor time=0.1720

Table 4.5.9 Diffraction Results for a Submerged Cylinder

SOURCES DISTRIBUTED ON INTERNAL BOUNDARY,RS= 0.70*CA
NO NODES= 12 (CONSTANT ELEMENTS)
ONE-POINT GAUSS QUADRATURE

ka	h/L	Mod(R)	Arg(R)	RES	Mod(Fx)	Arg(Fx)	Mod(Fy)	Arg(Fy)
0.10	0.04	0.232	-0.423	0.2E-07	1.178	0.237	0.103	-1.568
0.20	0.08	0.388	-0.356	0.6E-09	1.964	0.425	0.401	-1.544
0.30	0.12	0.446	-0.296	0.9E-08	2.309	0.552	0.852	-1.481
0.40	0.16	0.411	-0.233	0.3E-08	2.358	0.631	1.374	-1.363
0.50	0.20	0.302	-0.166	0.1E-07	2.250	0.678	1.813	-1.200
0.60	0.24	0.168	-0.105	0.1E-07	2.073	0.705	2.025	-1.034
0.70	0.28	0.057	-0.060	0.2E-07	1.873	0.720	2.011	-0.908
0.80	0.32	0.011	-0.034	0.5E-08	1.673	0.726	1.875	-0.833
0.90	0.36	0.045	-0.023	0.8E-07	1.483	0.727	1.702	-0.799
1.00	0.40	0.057	-0.021	0.8E-07	1.308	0.724	1.530	-0.790
1.50	0.60	0.042	-0.067	0.1E-07	0.666	0.659	0.884	-0.870
2.00	0.80	0.049	-0.129	0.8E-07	0.308	0.558	0.511	-0.963

Processor time=0.0165

Table 4.5.10 Diffraction Results for a Submerged Cylinder

SOURCES DISTRIBUTED ON INTERNAL BOUNDARY,RS= 0.70*CA
NO NODES= 16 (CONSTANT ELEMENTS)
ONE-POINT GAUSS QUADRATURE

ka	h/L	Mod(R)	Arg(R)	RES	Mod(Fx)	Arg(Fx)	Mod(Fy)	Arg(Fy)
0.10	0.04	0.247	-0.418	0.3E-08	1.238	0.253	0.106	-1.567
0.20	0.08	0.410	-0.348	0.2E-07	2.042	0.451	0.410	-1.543
0.30	0.12	0.467	-0.285	0.2E-07	2.379	0.581	0.876	-1.476
0.40	0.16	0.426	-0.220	0.2E-08	2.413	0.661	1.416	-1.351
0.50	0.20	0.309	-0.149	0.2E-07	2.292	0.708	1.863	-1.177
0.60	0.24	0.167	-0.085	0.4E-07	2.105	0.736	2.062	-1.003
0.70	0.28	0.054	-0.038	0.7E-08	1.897	0.752	2.025	-0.873
0.80	0.32	0.012	-0.011	0.3E-07	1.690	0.761	1.868	-0.797
0.90	0.36	0.042	0.000	0.1E-06	1.495	0.765	1.679	-0.763
1.00	0.40	0.051	0.003	0.9E-07	1.316	0.764	1.495	-0.756
1.50	0.60	0.020	-0.040	0.1E-08	0.671	0.712	0.809	-0.839
2.00	0.80	0.006	-0.099	0.1E-06	0.327	0.627	0.400	-0.938

Processor time=0.0264

Table 4.5.11 Diffraction Results for a Submerged Cylinder

SOURCES DISTRIBUTED ON INTERNAL BOUNDARY,RS= 0.70*CA
NO NODES= 32 (CONSTANT ELEMENTS)
ONE-POINT GAUSS QUADRATURE

ka	h/L	Mod(R)	Arg(R)	RES	Mod(Fx)	Arg(Fx)	Mod(Fy)	Arg(Fy)
0.10	0.04	0.253	-0.417	0.1E-07	1.257	0.259	0.107	-1.567
0.20	0.08	0.418	-0.345	0.2E-07	2.066	0.459	0.415	-1.543
0.30	0.12	0.474	-0.281	0.1E-07	2.398	0.590	0.887	-1.474
0.40	0.16	0.431	-0.215	0.1E-06	2.426	0.670	1.435	-1.346
0.50	0.20	0.310	-0.144	0.2E-07	2.301	0.717	1.889	-1.169
0.60	0.24	0.165	-0.078	0.2E-06	2.110	0.746	2.086	-0.991
0.70	0.28	0.052	-0.031	0.3E-06	1.898	0.763	2.041	-0.859
0.80	0.32	0.014	-0.003	0.5E-09	1.688	0.773	1.878	-0.784
0.90	0.36	0.044	0.009	0.7E-08	1.490	0.777	1.685	-0.750
1.00	0.40	0.052	0.011	0.1E-06	1.309	0.777	1.499	-0.742
1.50	0.60	0.017	-0.030	0.9E-07	0.655	0.730	0.808	-0.824
2.00	0.80	0.001	-0.086	0.1E-06	0.305	0.650	0.404	-0.920

Processor time=0.0939

Table 4.5.12 Diffraction Results for a Submerged Cylinder

SOURCES DISTRIBUTED ON INTERNAL BOUNDARY,RS= 0.70*CA
NO NODES= 12 (LINEAR ELEMENTS)
ONE-POINT GAUSS QUADRATURE

ka	h/L	Mod(R)	Arg(R)	RES	Mod(Fx)	Arg(Fx)	Mod(Fy)	Arg(Fy)
0.10	0.04	0.272	-0.413	0.1E-02	1.364	0.278	0.107	1.366
0.20	0.08	0.667	-0.221	0.7E 00	2.553	0.716	1.637	-0.538
0.30	0.12	0.443	-0.238	0.5E-01	2.345	0.693	0.920	-1.455
0.40	0.16	0.262	-0.316	0.4E 00	2.107	0.704	1.790	-0.923
0.50	0.20	0.344	0.003	0.5E 00	2.295	0.739	2.220	-1.174
0.60	0.24	0.392	0.002	0.2E 00	2.005	0.869	2.878	-0.767
0.70	0.28	0.376	-0.230	0.1E 02	2.491	1.319	4.485	0.681
0.80	0.32	0.266	-0.151	0.7E 00	2.284	0.820	3.198	1.487
0.90	0.36	0.305	0.452	0.3E-01	1.706	0.875	1.316	-0.954
1.00	0.40	0.378	0.496	0.8E-01	1.019	0.881	1.854	-0.666
1.50	0.60	0.664	0.130	0.9E 00	0.891	0.415	1.349	-1.244
2.00	0.80	0.369	-0.325	0.4E 00	0.306	-0.282	0.717	1.124

Processor time=0.0155

Table 4.5.13 Diffraction Results for a Submerged Cylinder

SOURCES DISTRIBUTED ON INTERNAL BOUNDARY,RS= 0.70*CA
NO NODES= 16 (LINEAR ELEMENTS)
ONE-POINT GAUSS QUADRATURE

ka	h/L	Mod(R)	Arg(R)	RES	Mod(Fx)	Arg(Fx)	Mod(Fy)	Arg(Fy)
0.10	0.04	0.257	-0.415	0.7E-03	1.277	0.264	0.107	-1.566
0.20	0.08	0.422	-0.341	0.8E-02	2.088	0.463	0.434	-1.540
0.30	0.12	0.477	-0.272	0.7E-02	2.442	0.600	0.904	-1.481
0.40	0.16	0.419	-0.193	0.4E 00	2.236	0.551	1.158	1.193
0.50	0.20	0.546	-0.293	0.2E 00	2.403	0.473	2.013	-1.202
0.60	0.24	0.158	-0.062	0.3E-01	2.118	0.750	2.085	-0.967
0.70	0.28	0.127	-0.112	0.7E-02	1.696	1.031	0.738	-0.620
0.80	0.32	0.022	0.353	0.2E 00	1.634	0.839	1.670	-0.733
0.90	0.36	0.224	0.180	0.7E 00	1.755	0.942	2.356	-0.813
1.00	0.40	0.053	0.147	0.3E-01	1.310	0.795	1.541	-0.717
1.50	0.60	0.058	0.119	0.2E 00	0.587	0.775	0.866	-0.838
2.00	0.80	0.076	0.120	0.1E 00	0.324	0.639	0.366	-1.013

Processor time=0.0256

Table 4.5.14 Diffraction Results for a Submerged Cylinder

SOURCES DISTRIBUTED ON INTERNAL BOUNDARY,RS= 0.70*CA
NO NODES= 32 (LINEAR ELEMENTS)
ONE-POINT GAUSS QUADRATURE

ka	h/L	Mod(R)	Arg(R)	RES	Mod(Fx)	Arg(Fx)	Mod(Fy)	Arg(Fy)
0.10	0.04	0.253	-0.416	0.3E-05	1.257	0.259	0.107	-1.568
0.20	0.08	0.418	-0.345	0.6E-04	2.066	0.459	0.415	-1.543
0.30	0.12	0.474	-0.281	0.5E-05	2.398	0.590	0.887	-1.474
0.40	0.16	0.431	-0.215	0.5E-04	2.427	0.670	1.435	-1.346
0.50	0.20	0.310	-0.144	0.4E-03	2.300	0.718	1.889	-1.169
0.60	0.24	0.165	-0.078	0.1E-03	2.110	0.746	2.086	-0.991
0.70	0.28	0.051	-0.034	0.1E-02	1.898	0.763	2.042	-0.859
0.80	0.32	0.014	-0.001	0.4E-03	1.689	0.773	1.878	-0.784
0.90	0.36	0.044	0.009	0.4E-04	1.490	0.777	1.685	-0.750
1.00	0.40	0.052	0.011	0.5E-03	1.309	0.777	1.499	-0.742
1.50	0.60	0.017	-0.019	0.1E-03	0.655	0.730	0.807	-0.824
2.00	0.80	0.001	0.189	0.5E-03	0.305	0.651	0.404	-0.917

Processor time=0.0940

Table 4.5.15 Diffraction Results for a Submerged Cylinder

SOURCES DISTRIBUTED ON INTERNAL BOUNDARY,RS= 0.70*CA
NO NODES= 12 (QUADRATIC ELEMENTS)
TWO-POINT GAUSS QUADRATURE

ka	h/L	Mod(R)	Arg(R)	RES	Mod(Fx)	Arg(Fx)	Mod(Fy)	Arg(Fy)
0.10	0.04	0.266	-0.397	0.5E-02	1.300	0.298	0.116	1.366
0.20	0.08	0.440	-0.335	0.1E-02	2.180	0.490	0.432	1.470
0.30	0.12	0.498	-0.267	0.2E-01	2.459	0.620	0.924	-1.448
0.40	0.16	0.522	0.023	0.1E 00	2.377	0.775	2.030	-1.402
0.50	0.20	0.427	0.446	0.2E 00	1.786	0.646	3.060	-0.770
0.60	0.24	0.100	-0.107	0.3E 00	2.291	0.727	2.428	-0.687
0.70	0.28	0.245	0.326	0.2E 00	1.921	0.812	2.481	-0.843
0.80	0.32	0.407	-0.365	0.1E 01	2.425	0.893	2.248	-0.706
0.90	0.36	0.395	0.277	0.2E 00	1.638	0.931	1.247	-0.506
1.00	0.40	0.159	0.258	0.2E 00	1.292	0.844	1.142	-0.654
1.50	0.60	3.605	-0.419	0.3E 02	3.410	-0.858	2.352	-0.514
2.00	0.80	4.426	-0.466	0.2E 02	2.525	-0.063	4.649	0.959

Processor time=0.0148

Table 4.5.16 Diffraction Results for a Submerged Cylinder

SOURCES DISTRIBUTED ON INTERNAL BOUNDARY,RS= 0.70*CA
NO NODES= 16 (QUADRATIC ELEMENTS)
TWO-POINT GAUSS QUADRATURE

ka	h/L	Mod(R)	Arg(R)	RES	Mod(Fx)	Arg(Fx)	Mod(Fy)	Arg(Fy)
0.10	0.04	0.270	-0.417	0.5E-02	1.301	0.262	0.112	1.505
0.20	0.08	0.409	-0.352	0.2E-01	2.094	0.442	0.403	1.520
0.30	0.12	0.497	-0.297	0.1E-02	2.413	0.601	0.878	-1.476
0.40	0.16	0.462	-0.225	0.8E-01	2.454	0.643	1.474	-1.389
0.50	0.20	0.363	-0.089	0.1E 00	2.296	0.743	1.852	-1.220
0.60	0.24	0.204	0.154	0.3E-01	2.061	0.844	1.970	-0.885
0.70	0.28	0.054	0.099	0.4E-01	1.920	0.781	2.016	-0.837
0.80	0.32	0.015	-0.205	0.4E-01	1.680	0.789	1.930	-0.768
0.90	0.36	0.230	0.024	0.1E 00	1.404	0.736	1.554	-0.634
1.00	0.40	0.054	-0.140	0.2E-02	1.327	0.792	1.379	-0.620
1.50	0.60	0.057	0.037	0.1E 00	0.527	0.661	1.003	-0.901
2.00	0.80	0.151	0.343	0.3E-01	0.486	0.940	0.168	-0.519

Processor time=0.0257

Table 4.5.17 Diffraction Results for a Submerged Cylinder

SOURCES DISTRIBUTED ON INTERNAL BOUNDARY,RS= 0.70*CA
NO NODES= 32 (QUADRATIC ELEMENTS)
TWO-POINT GAUSS QUADRATURE

ka	h/L	Mod(R)	Arg(R)	RES	Mod(Fx)	Arg(Fx)	Mod(Fy)	Arg(Fy)
0.10	0.04	0.253	-0.416	0.1E-04	1.257	0.259	0.107	-1.568
0.20	0.08	0.418	-0.345	0.3E-04	2.066	0.459	0.415	-1.543
0.30	0.12	0.474	-0.281	0.1E-03	2.398	0.590	0.887	-1.474
0.40	0.16	0.431	-0.215	0.9E-04	2.426	0.670	1.435	-1.346
0.50	0.20	0.310	-0.144	0.2E-02	2.300	0.717	1.893	-1.168
0.60	0.24	0.165	-0.078	0.7E-03	2.110	0.746	2.086	-0.991
0.70	0.28	0.052	-0.027	0.1E-03	1.898	0.763	2.042	-0.859
0.80	0.32	0.015	0.001	0.5E-03	1.688	0.773	1.879	-0.784
0.90	0.36	0.043	0.018	0.1E-02	1.492	0.779	1.684	-0.749
1.00	0.40	0.052	0.011	0.1E-02	1.308	0.777	1.498	-0.742
1.50	0.60	0.017	-0.026	0.5E-03	0.655	0.731	0.808	-0.824
2.00	0.80	0.000	-0.242	0.1E-02	0.304	0.647	0.401	-0.915

Processor time=0.0942

Table 4.5.18 Diffraction Results for a Submerged Cylinder

Each of the tables presented up to this point have included the total processor time required for the execution of the jobs submitted to obtain the results given. A significant portion of the processor time is required for the evaluation of the wave function values and therefore increasing the order of the equations increases the number of evaluations and therefore the execution time considerably. Additionally the time required for the compilation and solution of the matrix equations is proportional to the square of the matrix dimensions and therefore if any one of the methods tested above achieves the same accuracy for a coarser discretisation this method promises the most significant improvement in efficiency. The preliminary indication is that the only possible improvement of this type over the conventional singular kernel constant element method would be due to the regular kernel constant element method. Conclusions of this nature are postponed until after a more detailed investigation but it may be noted that even for an equivalent discretisation the regular kernel alternative results in an improved efficiency which is more marked for higher-order discretisation schemes. For the constant element discretisation schemes the saving in processor time is in the order of 25% and may be attributed to a saving in the evaluation of the wave function values.

In order to provide a more detailed examination of the convergence of results achieved by the different methods for this geometric configuration three values of the parameter ka have been chosen: ka = 0.2 has been chosen because it approaches the shallow water range, ka = 1.0 because it approaches the deep water range and ka = 0.5 as an intermediate value. Evidence from figures 4.5.1 to 4.5.18 indicates that in general better agreement with the results

of Naftzger and Chakrabarti and more rapid convergence to this solution are obtained for the deeper water problem whichever discretisation scheme is used. Results for the components of force have been given in Figures 4.5.19 to 4.5.24 and Tables 4.5.19 to 4.5.24 and each graph includes the full range of schemes employed in the previously presented results. It must be emphasised that it is not possible to establish a solution which is precisely correct and the aim of presenting the results in this form is to establish whether the alternative methods give results which are in reasonable agreement as the discretisations become more precise and to determine whether any of the alternative schemes gives more rapid convergence to a "final" solution. Each of these graphs and those subsequently given in this form include only those results which lie within a range of approximately $\pm$ 10% of this "final" solution.

The first conclusion which may be drawn from these graphs which was suspected from those previously presented is that this implementation of higher-order variation of source density with sources distributed over the object boundary affects convergence adversely particularly for the problems in which the presence of the fluid bottom is of more significance. These results also demonstrate conclusively that the regular kernel integral equation formulation is amenable to numerical solution and suggest that the results achieved are more accurate and converge to the final solution more rapidly than the conventional singular kernel method and this is again more relevent for shallower water depths. It may also be noted that these results give no evidence of ill-conditioning for larger numbers of nodes. The use of higher-order variations of

source density for elements on the separated source boundary does not have such a detrimental affect as in the case of sources distributed on the object boundary, but it would appear again that the assumed constant variation of source density is the most reliable numerical formulation.

Before concluding that the use of higher-order elements is unsuitable for the solution of these problems the use of higher-order Gaussian quadrature has been implemented to determine whether the loss of accuracy identified in the above results is due to the inadequacy of the numerical integration techniques. These results are given in Figures 4.5.25 to 4.5.27 and Tables 4.5.25 to 4.5.30 for the horizontal component of force only and it may be noted that for approximately the same computational effort (based on the number of wave function evaluations) the results for the sources distributed on the object boundary are poorer than those achieved previously. For the sources distributed on the separated boundary the results are also less accurate for similar computational effort.

The final tests which have been performed for this particular set of data are designed to determine whether or not the results are sensitive to the choice of location of the source boundary. The higher-order discretisation techniques have not been employed in these tests and the results are given in Figures 4.5.28 to 4.5.30 and Tables 4.5.31 to 4.5.34. On the basis of these graphs it would appear that convergence to the final solution is increased as the source boundary is moved further from the object boundary. In particular the results obtained for RAT = 0.9 are least satisfactory at the coarser discretisations for which the solutions have been

obtained and this may be attributed to the failure of the numerical quadrature formula when the source is located close to a node. The results obtained for RAT = 0.5 suggest that the regular kernel method may be used with an even coarser discretisation than that suggested by the results for RAT = 0.7 with a further improvement in the computational efficiency, but it is more probable that ill-conditioning will occur for sources located on more remote separated boundaries.

It has therefore been demonstrated that for this particular problem the numerical solution of the linear diffraction boundary value problem by the integral equation method is achieved reliably and most efficiently by the regular kernel formulation using a simple discretisation scheme provided the source boundary is located at a sufficient distance from the object boundary to eliminate errors due to inadequate numerical quadrature.

These conclusions can not however be taken as final because the problem which has been tested has a circular cylinder located at a fixed depth given by $y_o/h = 0.5$ so that the important problem of cylinders located near the still water level has not been considered. The tests presented subsequently have been carried out for wave and geometric data which resembles the experimental data of the next chaper so that the numerical results presented in this section may be used to determine the accuracy with which theoretical predictions are made for comparison with measured results. This data is different from that which has been tested previously for two further reasons: firstly, refraction effects are essentially absent (h/L =.5) and secondly the cylinder spans only a small portion of the

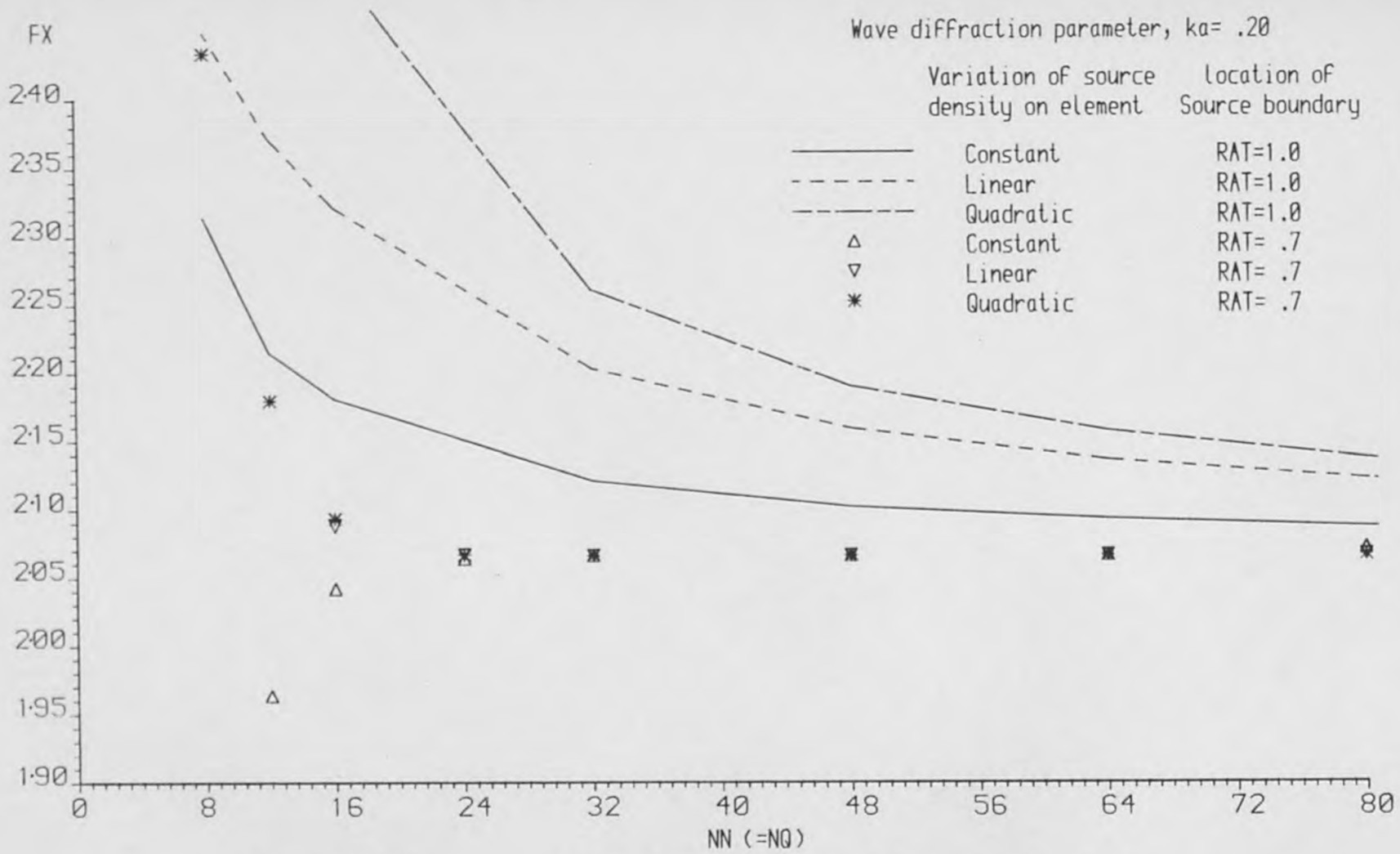

Figure 4.5.19 Maximum horizontal force on a submerged cylinder

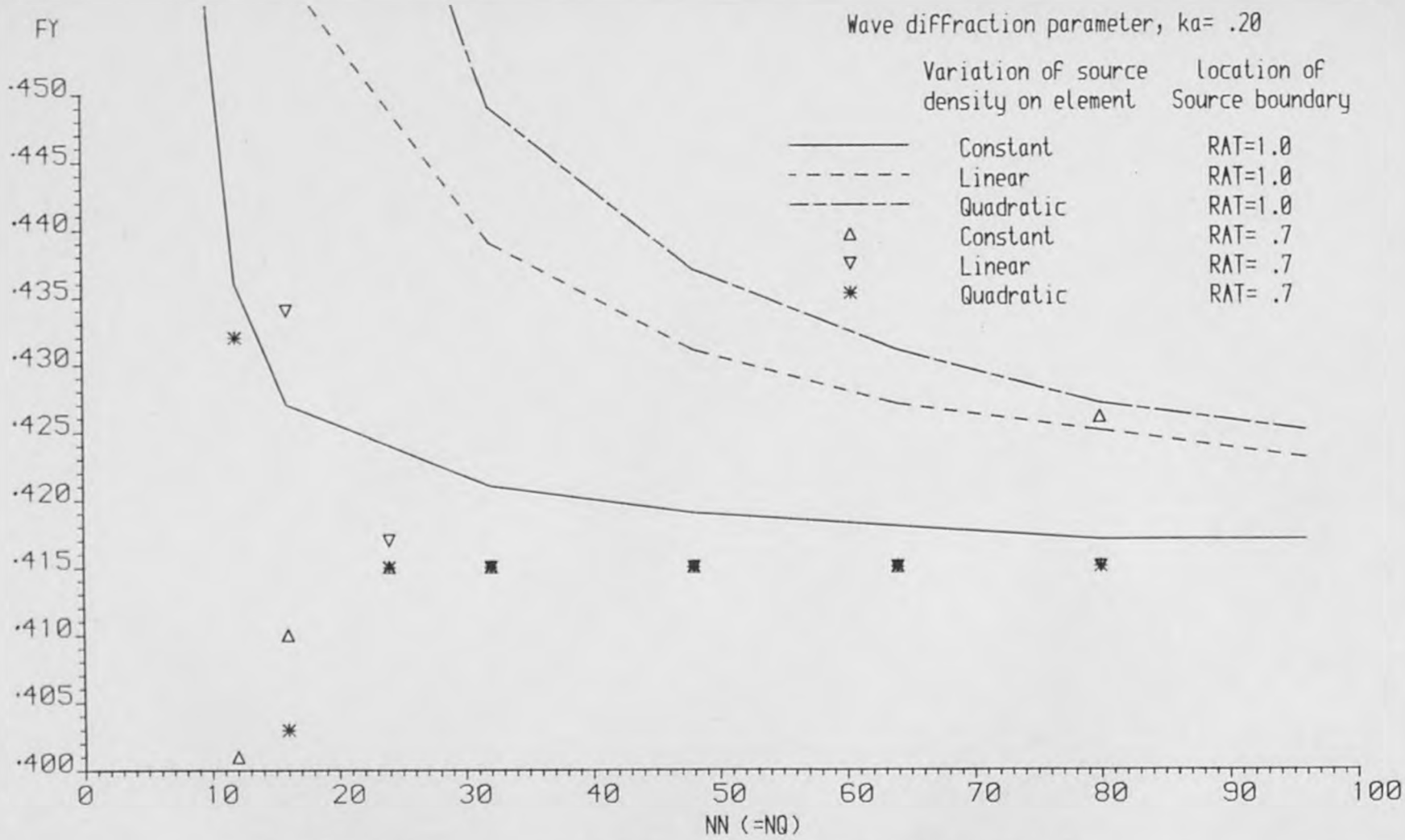

Figure 4.5.20 Maximum vertical force on a submerged cylinder

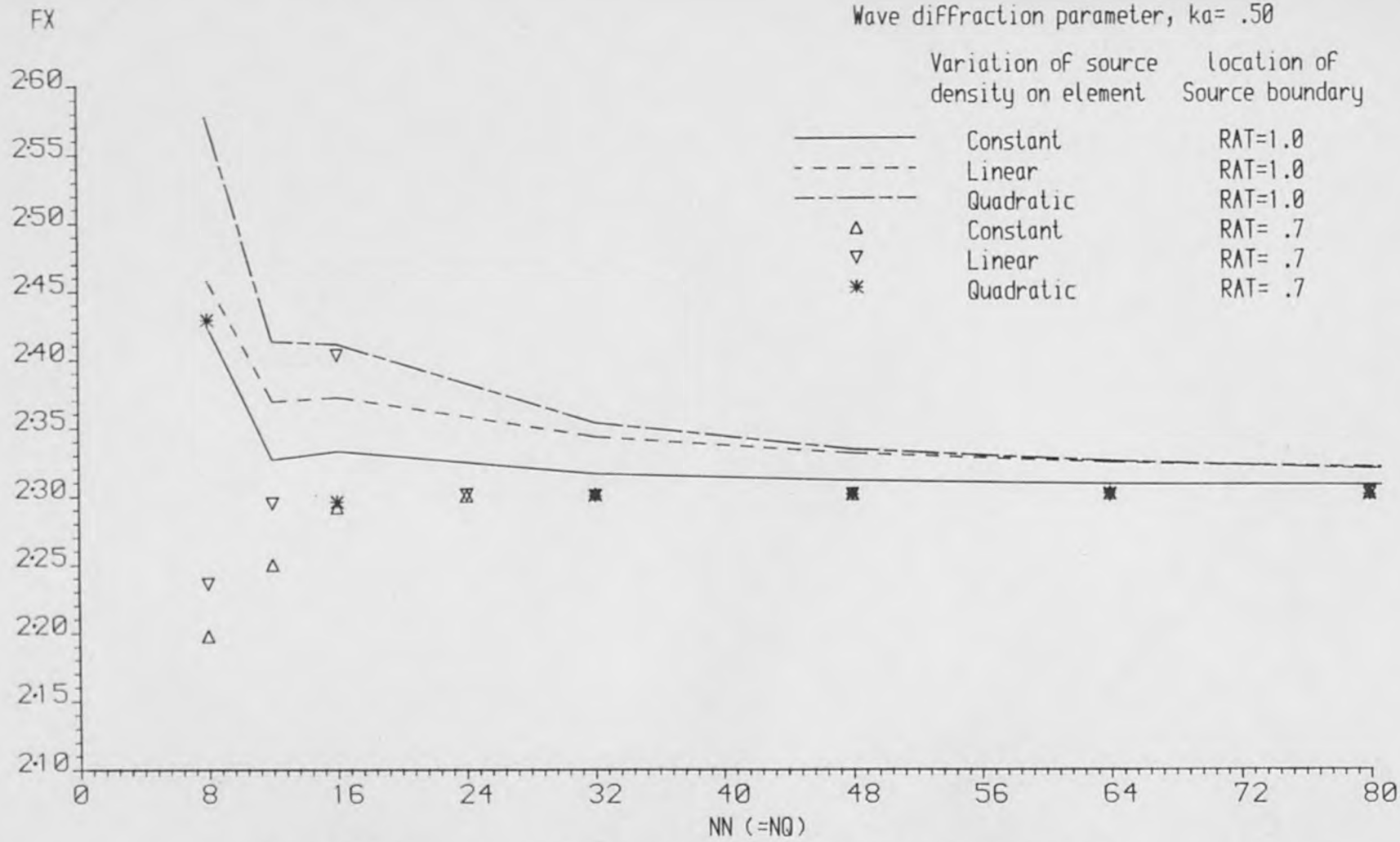

Figure 4.5.21 Maximum horizontal Force on a submerged cylinder

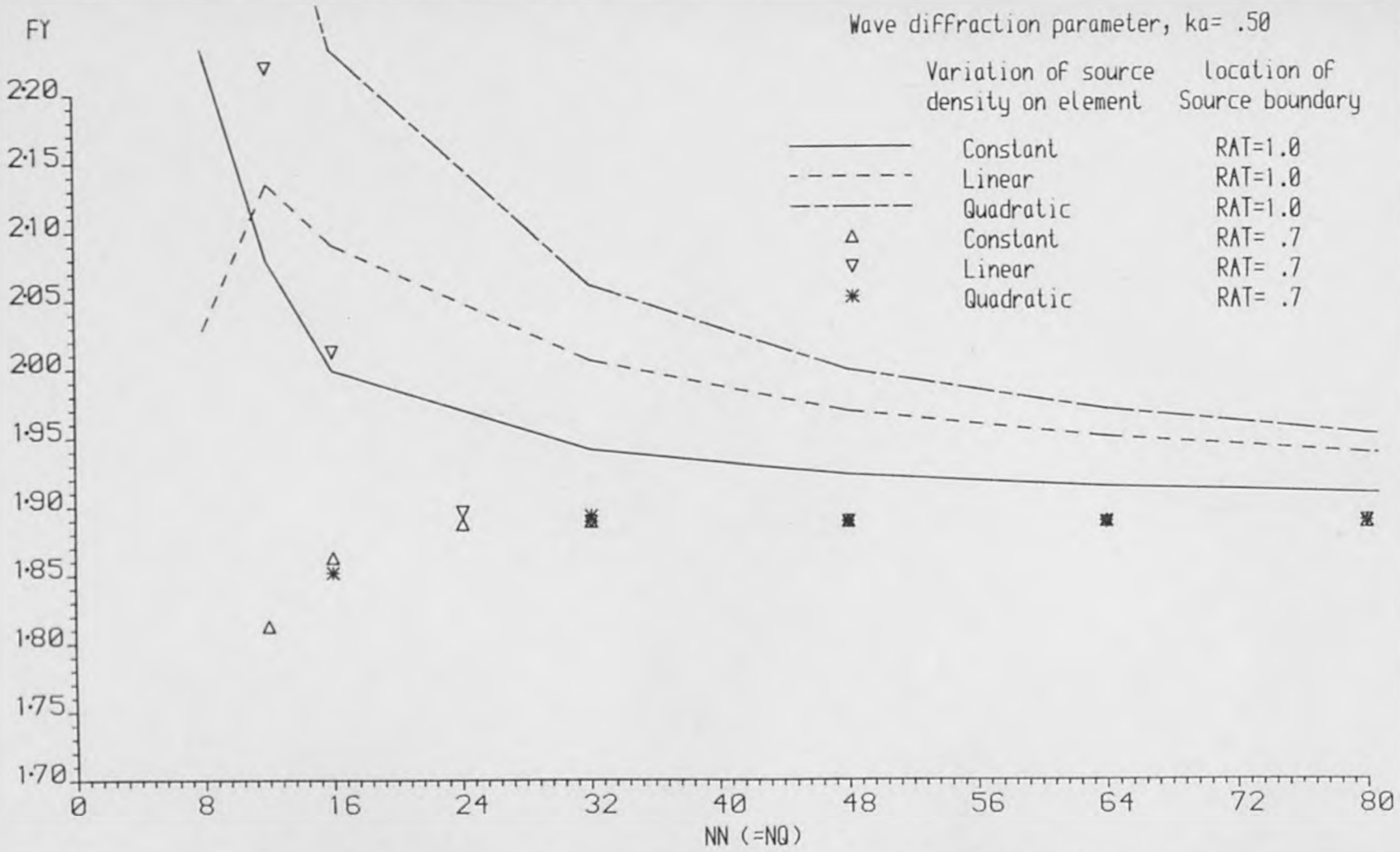

Figure 4.5.22 Maximum vertical force on a submerged cylinder

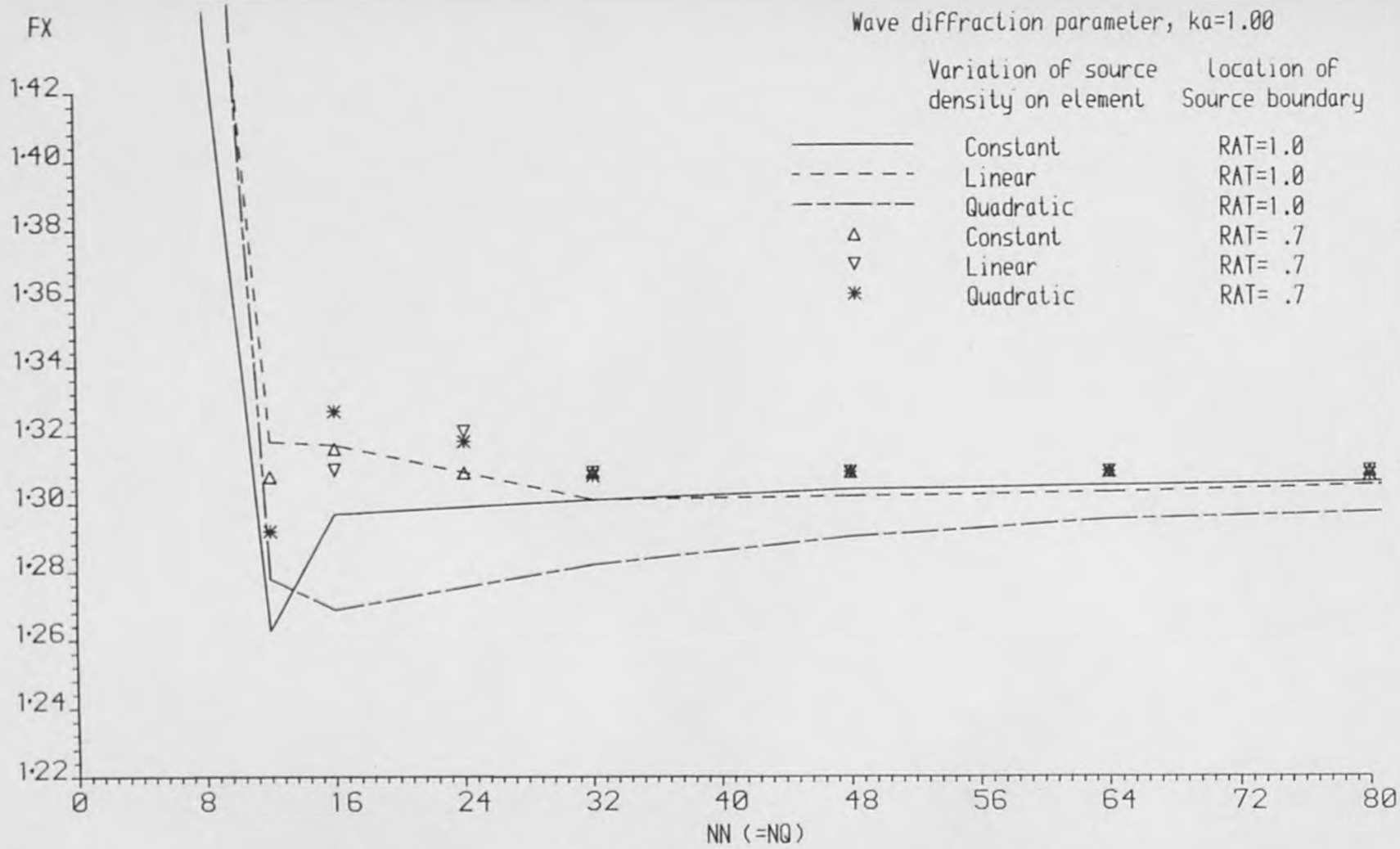

Figure 4.5.23 Maximum horizontal force on a submerged cylinder

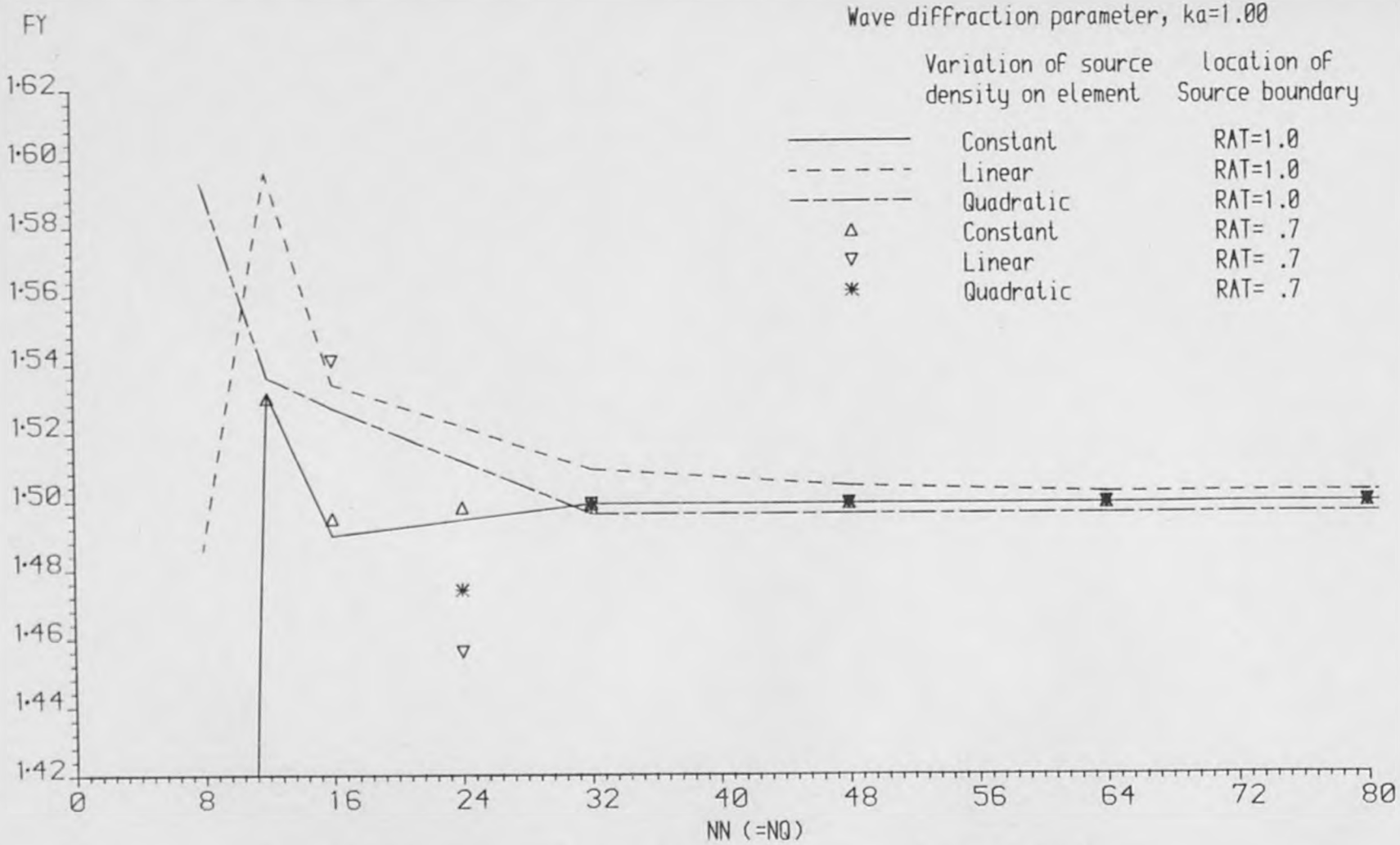

Figure 4.5.24 Maximum vertical force on a submerged cylinder

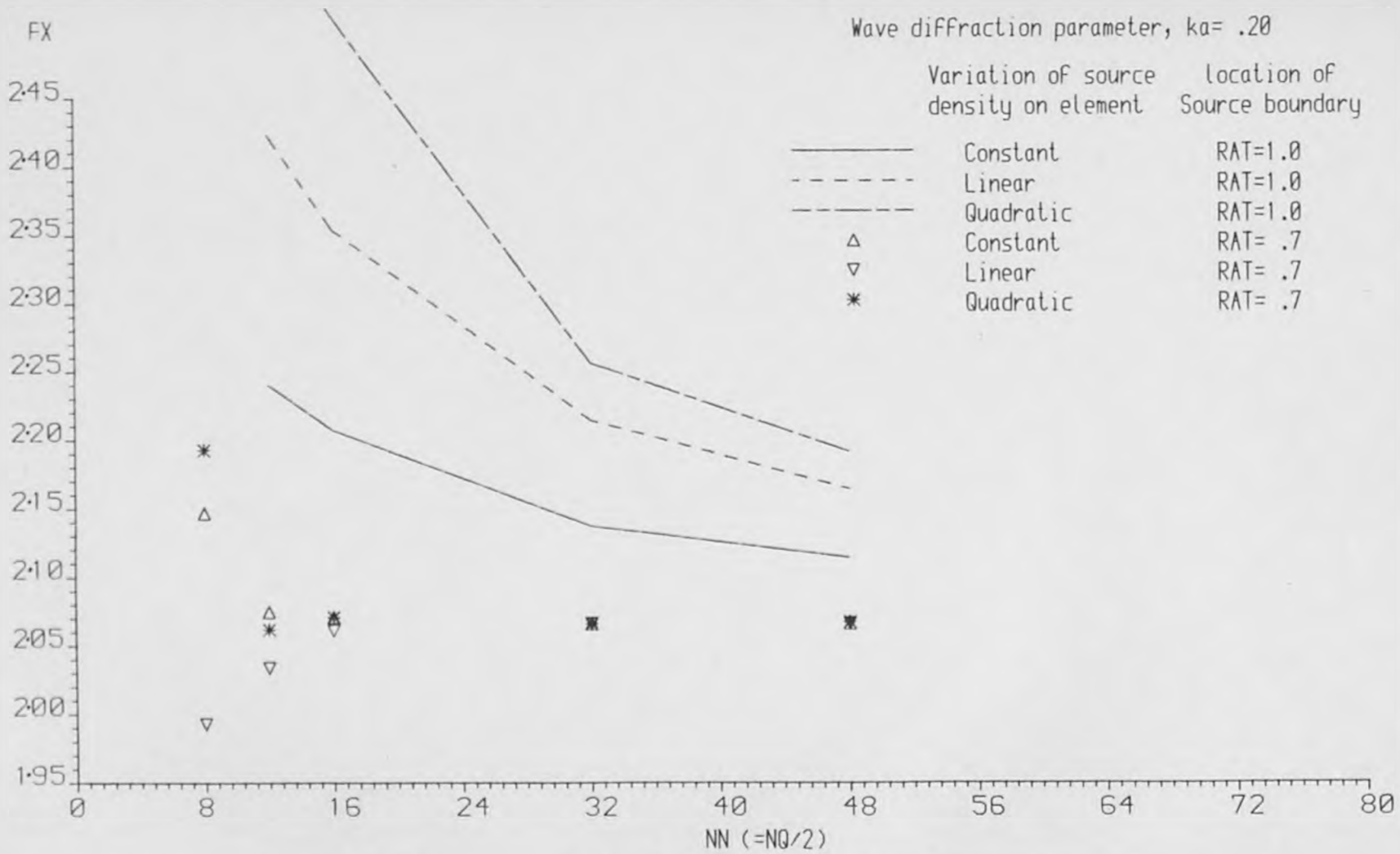

Figure 4.5.25 Maximum horizontal force on a submerged cylinder

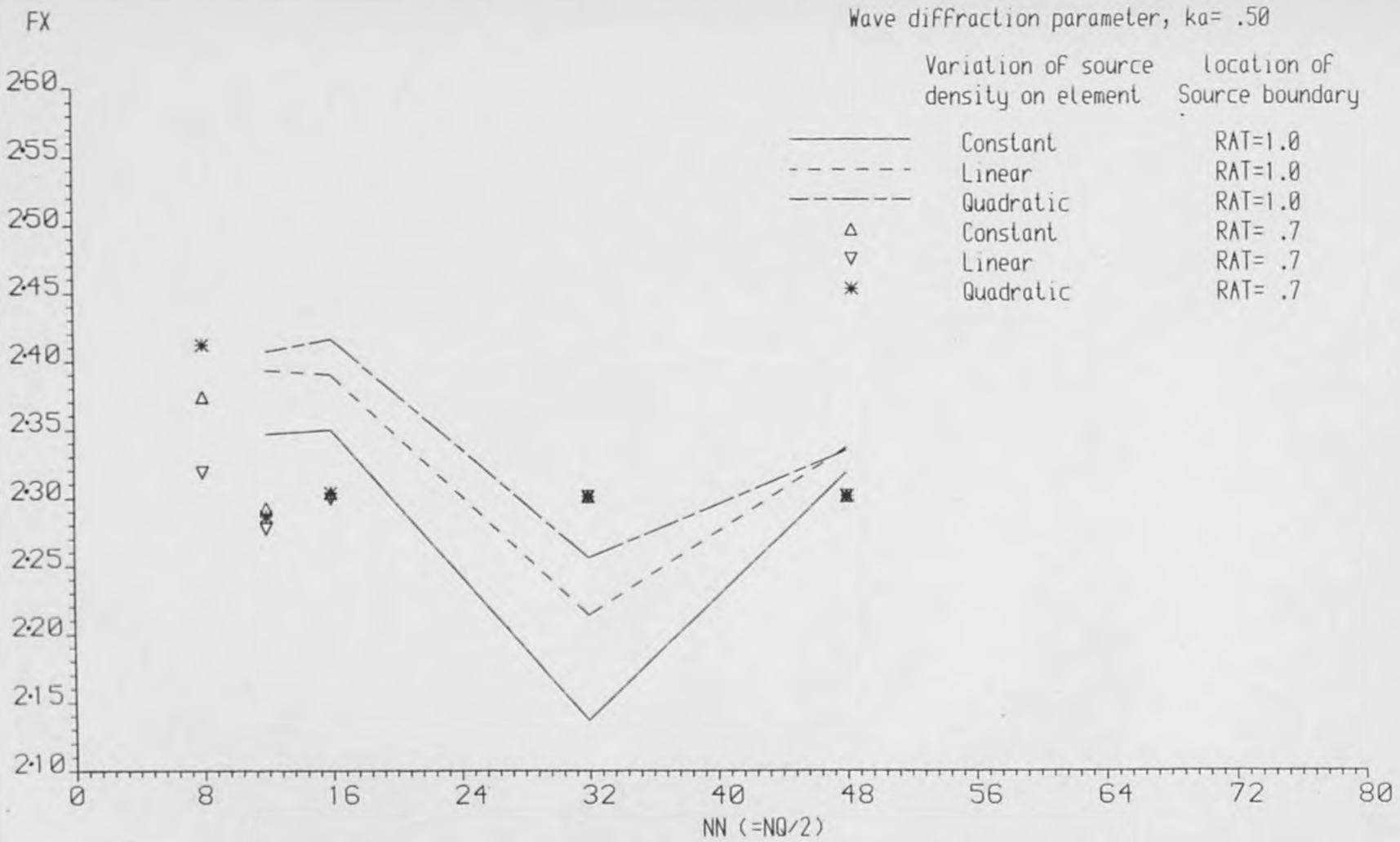

Figure 4.5.26 Maximum horizontal Force on a submerged cylinder

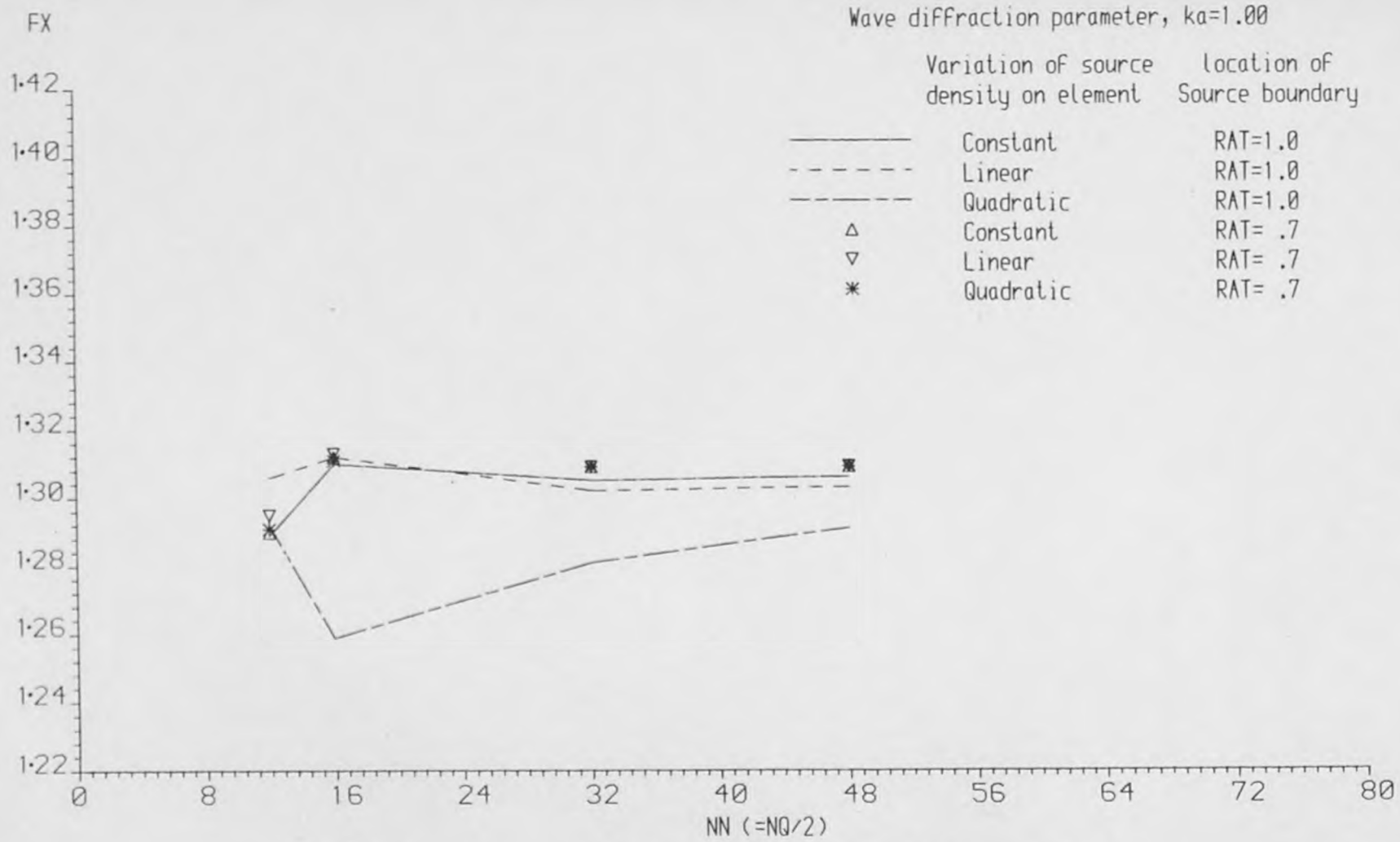

Figure 4.5.27 Maximum horizontal force on a submerged cylinder

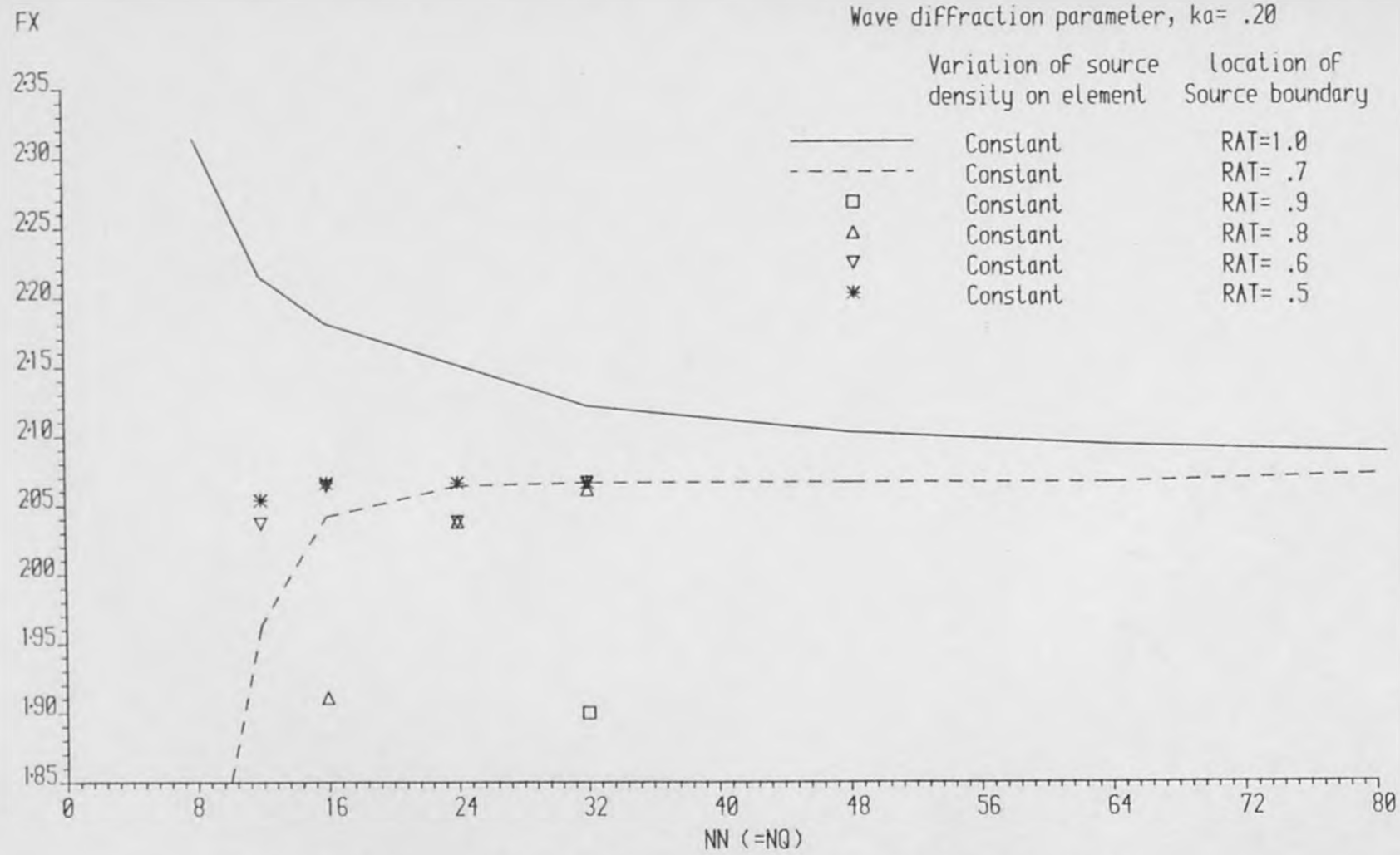

Figure 4.5.28 Maximum horizontal force on a submerged cylinder

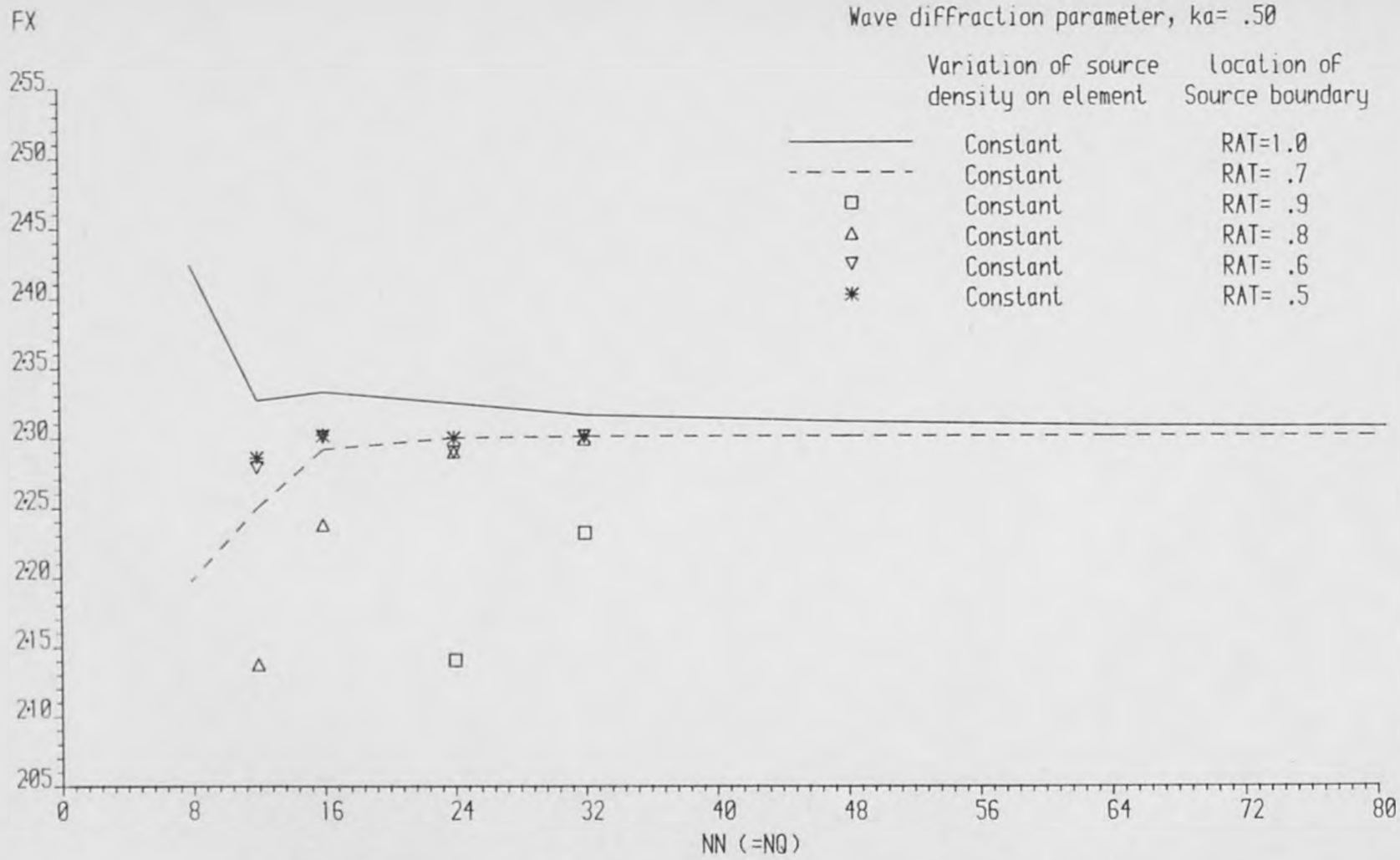

Figure 4.5.29 Maximum horizontal force on a submerged cylinder

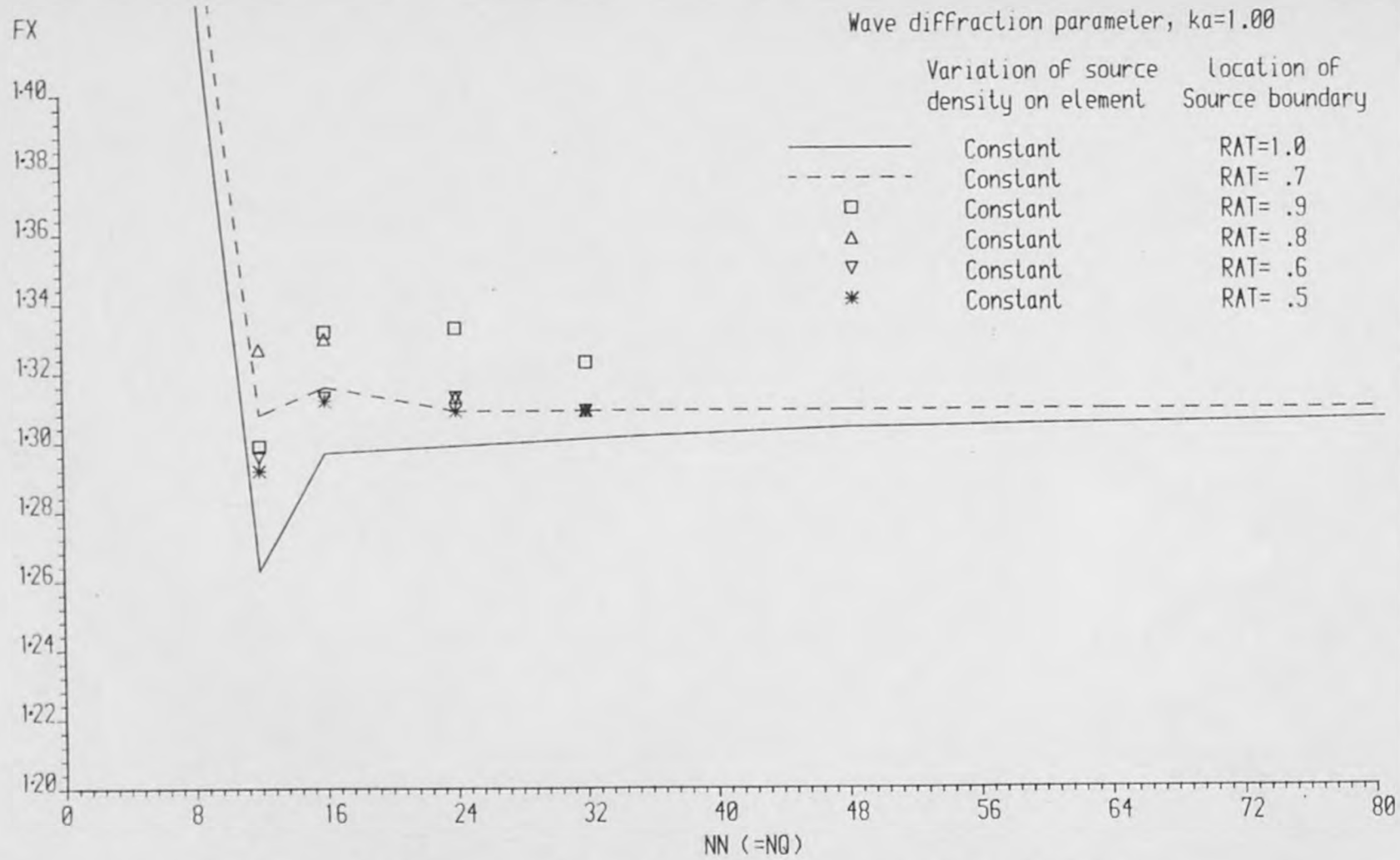

Figure 4.5.30 Maximum horizontal force on a submerged cylinder

SOURCES DISTRIBUTED ON CYLINDER BOUNDARY
CONSTANT VARIATION OF SOURCE DENSITY ON ELEMENT
ONE-POINT GUASS QUADRATURE
DIFRACTION PARAMETER,ka=0.2

NN	Mod(R)	Arg(R)	RES	Mod(Fx)	Arg(Fx)	Mod(Fy)	Arg(Fy)
8	0.495	-0.302	0.2E-08	2.314	0.570	0.474	-1.518
12	0.482	-0.319	0.3E-07	2.215	0.537	0.436	-1.537
16	0.466	-0.326	0.1E-07	2.181	0.516	0.427	-1.540
24	0.449	-0.333	0.5E-08	2.140	0.495	0.423	-1.541
32	0.441	-0.336	0.2E-08	2.121	0.486	0.421	-1.541
48	0.433	-0.339	0.7E-08	2.102	0.477	0.419	-1.542
64	0.429	-0.341	0.2E-07	2.093	0.472	0.418	-1.542
80	0.427	-0.341	0.4E-07	2.087	0.470	0.417	-1.542
96	0.425	-0.342	0.2E-03	2.084	0.468	0.417	-1.542

Table 4.5.19a Diffraction Results for a Submerged Cylinder

SOURCES DISTRIBUTED ON CYLINDER BOUNDARY
CONSTANT VARIATION OF SOURCE DENSITY ON ELEMENT
ONE-POINT GUASS QUADRATURE
DIFRACTION PARAMETER,ka=0.5

NN	Mod(R)	Arg(R)	RES	Mod(Fx)	Arg(Fx)	Mod(Fy)	Arg(Fy)
8	0.110	-0.024	0.1E-07	2.424	0.803	2.233	-0.878
12	0.304	-0.096	0.1E-07	2.327	0.789	2.079	-1.091
16	0.315	-0.111	0.3E-07	2.333	0.771	1.999	-1.120
24	0.315	-0.123	0.2E-07	2.321	0.753	1.960	-1.138
32	0.314	-0.128	0.1E-07	2.316	0.744	1.941	-1.146
48	0.313	-0.133	0.1E-07	2.311	0.735	1.923	-1.154
64	0.312	-0.136	0.3E-07	2.308	0.730	1.914	-1.158
80	0.312	-0.138	0.5E-07	2.307	0.728	1.909	-1.160
96	0.312	-0.139	0.3E-04	2.306	0.726	1.906	-1.162

Table 4.5.19b Diffraction Results for a Submerged Cylinder

SOURCES DISTRIBUTED ON CYLINDER BOUNDARY
CONSTANT VARIATION OF SOURCE DENSITY ON ELEMENT
ONE-POINT GUASS QUADRATURE
DIFRACTION PARAMETER,ka=1.0

NN	Mod(R)	Arg(R)	RES	Mod(Fx)	Arg(Fx)	Mod(Fy)	Arg(Fy)
8	0.449	0.138	0.2E-06	1.444	0.770	0.992	-0.335
12	0.093	0.058	0.1E-06	1.263	0.830	1.531	-0.647
16	0.061	0.043	0.4E-07	1.297	0.822	1.490	-0.688
24	0.056	0.031	0.4E-07	1.299	0.806	1.498	-0.708
32	0.055	0.026	0.6E-07	1.301	0.799	1.499	-0.717
48	0.054	0.021	0.3E-07	1.304	0.792	1.499	-0.725
64	0.053	0.019	0.1E-06	1.305	0.788	1.499	-0.730
80	0.053	0.017	0.1E-06	1.306	0.786	1.499	-0.732
96	0.053	0.016	0.7E-07	1.306	0.784	1.499	-0.734

Table 4.5.19c Diffraction Results for a Submerged Cylinder

SOURCES DISTRIBUTED ON CYLINDER BOUNDARY
LINEAR VARIATION OF SOURCE DENSITY ON ELEMENT
ONE-POINT GUASS QUADRATURE
DIFRACTION PARAMETER,ka=0.2

NN	Mod(R)	Arg(R)	RES	Mod(Fx)	Arg(Fx)	Mod(Fy)	Arg(Fy)
8	0.527	-0.304	0.3E-07	2.449	0.586	0.463	-1.540
12	0.519	-0.306	0.1E-07	2.372	0.578	0.471	-1.538
16	0.499	-0.313	0.3E-07	2.322	0.555	0.459	-1.538
24	0.475	-0.323	0.2E-07	2.246	0.526	0.446	-1.539
32	0.461	-0.328	0.1E-07	2.203	0.510	0.439	-1.540
48	0.447	-0.334	0.2E-07	2.159	0.493	0.431	-1.541
64	0.440	-0.336	0.3E-07	2.136	0.485	0.427	-1.541
80	0.435	-0.338	0.2E-07	2.122	0.480	0.425	-1.542
96	0.432	-0.339	0.2E-07	2.113	0.476	0.423	-1.542

Table 4.5.20a Diffraction Results for a Submerged Cylinder

SOURCES DISTRIBUTED ON CYLINDER BOUNDARY
LINEAR VARIATION OF SOURCE DENSITY ON ELEMENT
ONE-POINT GUASS QUADRATURE
DIFRACTION PARAMETER,ka=0.5

NN	Mod(R)	Arg(R)	RES	Mod(Fx)	Arg(Fx)	Mod(Fy)	Arg(Fy)
8	0.348	-0.115	0.5E-07	2.458	0.783	2.029	-1.144
12	0.335	-0.098	0.4E-07	2.369	0.802	2.135	-1.110
16	0.326	-0.100	0.1E-07	2.372	0.794	2.091	-1.109
24	0.320	-0.110	0.3E-07	2.354	0.776	2.039	-1.121
32	0.318	-0.117	0.7E-09	2.343	0.763	2.006	-1.131
48	0.315	-0.125	0.7E-07	2.331	0.749	1.969	-1.142
64	0.314	-0.129	0.5E-08	2.324	0.742	1.950	-1.148
80	0.313	-0.132	0.1E-06	2.320	0.737	1.938	-1.152
96	0.313	-0.134	0.5E-07	2.317	0.734	1.930	-1.155

Table 4.5.20b Diffraction Results for a Submerged Cylinder

SOURCES DISTRIBUTED ON CYLINDER BOUNDARY
LINEAR VARIATION OF SOURCE DENSITY ON ELEMENT
ONE-POINT GUASS QUADRATURE
DIFRACTION PARAMETER,ka=1.0

NN	Mod(R)	Arg(R)	RES	Mod(Fx)	Arg(Fx)	Mod(Fy)	Arg(Fy)
8	0.080	-0.051	0.3E-07	1.526	0.666	1.486	-0.825
12	0.064	0.008	0.5E-07	1.318	0.767	1.596	-0.741
16	0.061	0.026	0.1E-06	1.317	0.796	1.534	-0.714
24	0.059	0.032	0.7E-07	1.303	0.806	1.516	-0.705
32	0.057	0.031	0.9E-07	1.301	0.805	1.509	-0.708
48	0.056	0.027	0.3E-07	1.302	0.799	1.504	-0.716
64	0.055	0.024	0.2E-06	1.303	0.795	1.502	-0.721
80	0.054	0.024	0.4E-03	1.305	0.792	1.502	-0.724
96	0.054	0.020	0.6E-07	1.305	0.790	1.501	-0.727

Table 4.5.20c Diffraction Results for a Submerged Cylinder

SOURCES DISTRIBUTED ON CYLINDER BOUNDARY
QUADRATIC VARIATION OF SOURCE DENSITY ON ELEMENT
TWO-POINT GUASS QUADRATURE
DIFRACTION PARAMETER,ka=0.2

NN	Mod(R)	Arg(R)	RES	Mod(Fx)	Arg(Fx)	Mod(Fy)	Arg(Fy)
8	0.698	-0.238	0.4E-08	2.924	0.799	0.603	1.454
12	0.585	-0.275	0.2E-07	2.587	0.667	0.542	-1.570
16	0.561	-0.289	0.8E-08	2.502	0.630	0.491	-1.550
32	0.483	-0.319	0.6E-08	2.261	0.536	0.449	-1.538
48	0.460	-0.328	0.2E-07	2.190	0.508	0.437	-1.540
64	0.449	-0.333	0.1E-07	2.157	0.495	0.431	-1.540
80	0.442	-0.335	0.2E-07	2.137	0.488	0.427	-1.541
96	0.438	-0.337	0.5E-08	2.124	0.483	0.425	-1.541

Table 4.5.21a Diffraction Results for a Submerged Cylinder

SOURCES DISTRIBUTED ON CYLINDER BOUNDARY
QUADRATIC VARIATION OF SOURCE DENSITY ON ELEMENT
TWO-POINT GUASS QUADRATURE
DIFRACTION PARAMETER,ka=0.5

NN	Mod(R)	Arg(R)	RES	Mod(Fx)	Arg(Fx)	Mod(Fy)	Arg(Fy)
8	0.489	-0.060	0.5E-07	2.577	0.952	2.300	-1.164
12	0.288	-0.041	0.6E-07	2.413	0.873	2.392	-1.003
16	0.341	-0.063	0.8E-07	2.411	0.862	2.233	-1.061
32	0.318	-0.101	0.4E-07	2.353	0.789	2.061	-1.106
48	0.316	-0.116	0.6E-07	2.334	0.764	1.999	-1.128
64	0.315	-0.123	0.8E-05	2.325	0.752	1.970	-1.139
80	0.314	-0.127	0.8E-05	2.319	0.745	1.952	-1.145
96	0.314	-0.130	0.1E-06	2.316	0.740	1.941	-1.149

Table 4.5.21b Diffraction Results for a Submerged Cylinder

SOURCES DISTRIBUTED ON CYLINDER BOUNDARY
QUADRATIC VARIATION OF SOURCE DENSITY ON ELEMENT
TWO-POINT GUASS QUADRATURE
DIFRACTION PARAMETER,ka=1.0

NN	Mod(R)	Arg(R)	RES	Mod(Fx)	Arg(Fx)	Mod(Fy)	Arg(Fy)
8	0.033	-0.007	0.7E-07	1.555	0.800	1.593	-0.819
12	0.135	0.060	0.1E-06	1.278	0.819	1.536	-0.623
16	0.045	0.066	0.1E-06	1.269	0.871	1.527	-0.658
32	0.060	0.050	0.6E-07	1.282	0.833	1.496	-0.677
48	0.058	0.037	0.1E-06	1.290	0.815	1.496	-0.698
64	0.056	0.031	0.4E-07	1.295	0.805	1.496	-0.709
80	0.055	0.027	0.5E-07	1.297	0.800	1.496	-0.715
96	0.055	0.023	0.2E-03	1.299	0.796	1.496	-0.720

Table 4.5.21c Diffraction Results for a Submerged Cylinder

SOURCES DISTRIBUTED ON INTERNAL BOUNDARY,RS=0.7*CA
CONSTANT VARIATION OF SOURCE DENSITY ON ELEMENT
ONE-POINT GUASS QUADRATURE
DIFRACTION PARAMETER,ka=0.2

NN	Mod(R)	Arg(R)	RES	Mod(Fx)	Arg(Fx)	Mod(Fy)	Arg(Fy)
8	0.308	-0.385	0.2E-09	1.740	0.338	0.356	-1.546
12	0.388	-0.356	0.6E-09	1.964	0.425	0.401	-1.544
16	0.410	-0.348	0.2E-07	2.042	0.451	0.410	-1.543
24	0.417	-0.345	0.1E-07	2.064	0.459	0.415	-1.543
32	0.418	-0.345	0.2E-07	2.066	0.459	0.415	-1.543
48	0.418	-0.345	0.1E-07	2.066	0.459	0.415	-1.543
64	0.418	-0.345	0.2E-08	2.066	0.459	0.415	-1.543
80	0.430	-0.330	0.5E-01	2.071	0.460	0.426	1.485

Table 4.5.22a Diffraction Results for a Submerged Cylinder

SOURCES DISTRIBUTED ON INTERNAL BOUNDARY,RS=0.7*CA
CONSTANT VARIATION OF SOURCE DENSITY ON ELEMENT
ONE-POINT GUASS QUADRATURE
DIFRACTION PARAMETER,ka=0.5

NN	Mod(R)	Arg(R)	RES	Mod(Fx)	Arg(Fx)	Mod(Fy)	Arg(Fy)
8	0.251	-0.219	0.3E-07	2.198	0.568	1.553	-1.256
12	0.302	-0.166	0.1E-07	2.250	0.678	1.813	-1.200
16	0.309	-0.149	0.2E-07	2.292	0.708	1.863	-1.177
24	0.310	-0.144	0.2E-07	2.300	0.717	1.887	-1.169
32	0.310	-0.144	0.2E-07	2.301	0.717	1.889	-1.169
48	0.310	-0.144	0.9E-07	2.301	0.718	1.889	-1.169
64	0.310	-0.144	0.2E-07	2.301	0.718	1.889	-1.169
80	0.311	-0.144	0.7E-05	2.301	0.718	1.888	-1.169

Table 4.5.22b Diffraction Results for a Submerged Cylinder

SOURCES DISTRIBUTED ON INTERNAL BOUNDARY,RS=0.7*CA
CONSTANT VARIATION OF SOURCE DENSITY ON ELEMENT
ONE-POINT GUASS QUADRATURE
DIFRACTION PARAMETER,ka=1.0

NN	Mod(R)	Arg(R)	RES	Mod(Fx)	Arg(Fx)	Mod(Fy)	Arg(Fy)
8	0.142	-0.087	0.1E-06	1.470	0.577	1.311	-0.851
12	0.057	-0.021	0.8E-07	1.308	0.724	1.530	-0.790
16	0.051	0.003	0.9E-07	1.316	0.764	1.495	-0.756
24	0.051	0.011	0.7E-07	1.309	0.776	1.498	-0.743
32	0.052	0.011	0.1E-06	1.309	0.777	1.499	-0.742
48	0.051	0.011	0.1E-04	1.309	0.777	1.499	-0.742
64	0.051	0.011	0.1E-06	1.309	0.777	1.499	-0.742
80	0.051	0.011	0.1E-05	1.309	0.777	1.499	-0.742

Table 4.5.22c Diffraction Results for a Submerged Cylinder

SOURCES DISTRIBUTED ON INTERNAL BOUNDARY,RS=0.7*CA
LINEAR VARIATION OF SOURCE DENSITY ON ELEMENT
ONE-POINT GUASS QUADRATURE
DIFRACTION PARAMETER,ka=0.2

NN	Mod(R)	Arg(R)	RES	Mod(Fx)	Arg(Fx)	Mod(Fy)	Arg(Fy)
8	0.504	-0.244	0.1E-01	2.545	0.632	0.540	-1.205
12	0.667	-0.221	0.7E 00	2.553	0.716	1.637	-0.538
16	0.422	-0.341	0.8E-02	2.088	0.463	0.434	-1.540
24	0.419	-0.346	0.2E-04	2.067	0.459	0.417	-1.546
32	0.418	-0.345	0.6E-04	2.066	0.459	0.415	-1.543
48	0.418	-0.345	0.5E-07	2.066	0.459	0.415	-1.543
64	0.418	-0.345	0.3E-05	2.066	0.459	0.415	-1.543
80	0.418	-0.345	0.4E-04	2.066	0.459	0.415	-1.543

Table 4.5.23a Diffraction Results for a Submerged Cylinder

SOURCES DISTRIBUTED ON INTERNAL BOUNDARY,RS=0.7*CA
LINEAR VARIATION OF SOURCE DENSITY ON ELEMENT
ONE-POINT GUASS QUADRATURE
DIFRACTION PARAMETER,ka=0.5

NN	Mod(R)	Arg(R)	RES	Mod(Fx)	Arg(Fx)	Mod(Fy)	Arg(Fy)
8	0.307	0.390	0.2E 00	2.236	0.897	1.360	-0.480
12	0.344	0.003	0.5E 00	2.295	0.739	2.220	-1.174
16	0.546	-0.293	0.2E 00	2.403	0.473	2.013	-1.202
24	0.311	-0.140	0.1E-02	2.301	0.720	1.896	-1.168
32	0.310	-0.144	0.4E-03	2.300	0.718	1.889	-1.169
48	0.310	-0.144	0.3E-05	2.301	0.718	1.889	-1.169
64	0.310	-0.143	0.2E-04	2.300	0.718	1.888	-1.169
80	0.310	-0.144	0.3E-03	2.301	0.717	1.889	-1.169

Table 4.5.23b Diffraction Results for a Submerged Cylinder

SOURCES DISTRIBUTED ON INTERNAL BOUNDARY,RS=0.7*CA
LINEAR VARIATION OF SOURCE DENSITY ON ELEMENT
ONE-POINT GUASS QUADRATURE
DIFRACTION PARAMETER,ka=1.0

NN	Mod(R)	Arg(R)	RES	Mod(Fx)	Arg(Fx)	Mod(Fy)	Arg(Fy)
8	0.445	-0.061	0.5E 00	1.178	1.255	0.688	-0.440
12	0.378	0.496	0.8E-01	1.019	0.881	1.854	-0.666
16	0.053	0.147	0.3E-01	1.310	0.795	1.541	-0.717
24	0.043	0.273	0.5E-02	1.321	0.801	1.456	-0.771
32	0.052	0.011	0.5E-03	1.309	0.777	1.499	-0.742
48	0.052	0.011	0.3E-05	1.309	0.777	1.499	-0.742
64	0.051	0.011	0.5E-04	1.309	0.777	1.499	-0.742
80	0.052	0.011	0.5E-04	1.309	0.777	1.499	-0.742

Table 4.5.23c Diffraction Results for a Submerged Cylinder

SOURCES DISTRIBUTED ON INTERNAL BOUNDARY, RS=0.7*CA
QUADRATIC VARIATION OF SOURCE DENSITY ON ELEMENT
TWO-POINT GUASS QUADRATURE
DIFRACTION PARAMETER, ka=0.2

NN	Mod(R)	Arg(R)	RES	Mod(Fx)	Arg(Fx)	Mod(Fy)	Arg(Fy)
8	0.619	-0.181	0.2E 00	2.434	0.688	0.833	-1.505
12	0.440	-0.335	0.1E-02	2.180	0.490	0.432	1.470
16	0.409	-0.352	0.2E-01	2.094	0.442	0.403	1.520
24	0.418	-0.345	0.8E-04	2.067	0.460	0.415	-1.545
32	0.418	-0.345	0.3E-04	2.066	0.459	0.415	-1.543
48	0.418	-0.345	0.4E-05	2.066	0.459	0.415	-1.543
64	0.418	-0.345	0.5E-05	2.066	0.459	0.415	-1.543
80	0.418	-0.345	0.1E-04	2.066	0.459	0.415	-1.543

Table 4.5.24a Diffraction Results for a Submerged Cylinder

SOURCES DISTRIBUTED ON INTERNAL BOUNDARY, RS=0.7*CA
QUADRATIC VARIATION OF SOURCE DENSITY ON ELEMENT
TWO-POINT GUASS QUADRATURE
DIFRACTION PARAMETER, ka=0.5

NN	Mod(R)	Arg(R)	RES	Mod(Fx)	Arg(Fx)	Mod(Fy)	Arg(Fy)
8	0.221	0.141	0.4E 00	2.429	0.508	0.982	-1.468
12	0.427	0.446	0.2E 00	1.786	0.646	3.060	-0.770
16	0.363	-0.089	0.1E 00	2.296	0.743	1.852	-1.220
24	0.594	-0.469	0.5E 00	1.991	0.677	1.271	-1.247
32	0.310	-0.144	0.2E-04	2.300	0.717	1.889	-1.168
48	0.310	-0.144	0.6E-03	2.301	0.718	1.889	-1.169
64	0.310	-0.144	0.2E-04	2.301	0.718	1.889	-1.169
80	0.310	-0.144	0.2E-05	2.300	0.718	1.889	-1.169

Table 4.5.24b Diffraction Results for a Submerged Cylinder

SOURCES DISTRIBUTED ON INTERNAL BOUNDARY, RS=0.7*CA
QUADRATIC VARIATION OF SOURCE DENSITY ON ELEMENT
TWO-POINT GUASS QUADRATURE
DIFRACTION PARAMETER, ka=1.0

NN	Mod(R)	Arg(R)	RES	Mod(Fx)	Arg(Fx)	Mod(Fy)	Arg(Fy)
8	1.616	0.382	0.4E 01	1.817	-0.733	1.335	-0.768
12	0.159	0.258	0.2E 00	1.292	0.844	1.142	-0.654
16	0.054	-0.140	0.2E-02	1.327	0.792	1.379	-0.620
24	0.049	0.100	0.7E-02	1.318	0.773	1.474	-0.746
32	0.051	0.011	0.4E-03	1.309	0.777	1.499	-0.742
48	0.051	0.011	0.2E-04	1.309	0.777	1.499	-0.742
64	0.051	0.011	0.1E-04	1.309	0.777	1.499	-0.742
80	0.051	0.011	0.1E-04	1.308	0.777	1.499	-0.742

Table 4.5.24c Diffraction Results for a Submerged Cylinder

SOURCES DISTRIBUTED ON CYLINDER BOUNDARY
CONSTANT VARIATION OF SOURCE DENSITY ON ELEMENT
TWO-POINT GUASS QUADRATURE
DIFRACTION PARAMETER,ka=0.2

NN	Mod(R)	Arg(R)	RES	Mod(Fx)	Arg(Fx)	Mod(Fy)	Arg(Fy)
8	0.482	-0.316	0.1E-07	2.339	0.540	0.459	-1.534
12	0.472	-0.323	0.2E-08	2.240	0.523	0.450	-1.539
16	0.460	-0.328	0.3E-07	2.207	0.509	0.439	-1.540
32	0.439	-0.336	0.2E-07	2.137	0.484	0.427	-1.541
48	0.432	-0.339	0.1E-07	2.114	0.476	0.423	-1.542

Table 4.5.25a Diffraction Results for a Submerged Cylinder

SOURCES DISTRIBUTED ON CYLINDER BOUNDARY
CONSTANT VARIATION OF SOURCE DENSITY ON ELEMENT
TWO-POINT GUASS QUADRATURE
DIFRACTION PARAMETER,ka=0.5

NN	Mod(R)	Arg(R)	RES	Mod(Fx)	Arg(Fx)	Mod(Fy)	Arg(Fy)
8	0.259	-0.093	0.7E-07	2.450	0.770	2.064	-1.063
12	0.316	-0.111	0.1E-07	2.347	0.772	2.063	-1.120
16	0.318	-0.118	0.8E-07	2.350	0.762	2.005	-1.132
32	0.314	-0.130	0.2E-09	2.326	0.741	1.951	-1.149
48	0.313	-0.134	0.9E-08	2.318	0.734	1.931	-1.155

Table 4.5.25b Diffraction Results for a Submerged Cylinder

SOURCES DISTRIBUTED ON CYLINDER BOUNDARY
CONSTANT VARIATION OF SOURCE DENSITY ON ELEMENT
TWO-POINT GUASS QUADRATURE
DIFRACTION PARAMETER,ka=1.0

NN	Mod(R)	Arg(R)	RES	Mod(Fx)	Arg(Fx)	Mod(Fy)	Arg(Fy)
8	0.243	0.040	0.1E-06	1.478	0.725	1.264	-0.601
12	0.074	0.030	0.1E-06	1.289	0.796	1.555	-0.701
16	0.058	0.029	0.1E-06	1.310	0.801	1.508	-0.711
32	0.055	0.023	0.4E-07	1.305	0.794	1.504	-0.722
48	0.054	0.020	0.7E-07	1.306	0.789	1.502	-0.728

Table 4.5.25c Diffraction Results for a Submerged Cylinder

SOURCES DISTRIBUTED ON CYLINDER BOUNDARY
LINEAR VARIATION OF SOURCE DENSITY ON ELEMENT
TWO-POINT GUASS QUADRATURE
DIFRACTION PARAMETER,ka=0.2

NN	Mod(R)	Arg(R)	RES	Mod(Fx)	Arg(Fx)	Mod(Fy)	Arg(Fy)
8	0.549	-0.289	0.2E-07	2.542	0.622	0.507	-1.530
12	0.530	-0.300	0.1E-07	2.423	0.593	0.484	-1.536
16	0.506	-0.310	0.2E-07	2.354	0.563	0.466	-1.538
32	0.462	-0.327	0.2E-07	2.214	0.511	0.441	-1.540
48	0.447	-0.333	0.5E-07	2.164	0.494	0.432	-1.541

Table 4.5.26a Diffraction Results for a Submerged Cylinder

SOURCES DISTRIBUTED ON CYLINDER BOUNDARY
LINEAR VARIATION OF SOURCE DENSITY ON ELEMENT
TWO-POINT GUASS QUADRATURE
DIFRACTION PARAMETER,ka=0.5

NN	Mod(R)	Arg(R)	RES	Mod(Fx)	Arg(Fx)	Mod(Fy)	Arg(Fy)
8	0.272	-0.067	0.2E-07	2.482	0.818	2.249	-1.028
12	0.324	-0.082	0.3E-07	2.393	0.821	2.210	-1.080
16	0.324	-0.093	0.3E-07	2.390	0.804	2.127	-1.096
32	0.317	-0.115	0.2E-07	2.351	0.766	2.016	-1.128
48	0.315	-0.124	0.5E-08	2.336	0.750	1.975	-1.141

Table 4.5.26b Diffraction Results for a Submerged Cylinder

SOURCES DISTRIBUTED ON CYLINDER BOUNDARY
LINEAR VARIATION OF SOURCE DENSITY ON ELEMENT
TWO-POINT GUASS QUADRATURE
DIFRACTION PARAMETER,ka=1.0

NN	Mod(R)	Arg(R)	RES	Mod(Fx)	Arg(Fx)	Mod(Fy)	Arg(Fy)
8	0.207	0.019	0.9E-07	1.493	0.711	1.407	-0.651
12	0.079	0.035	0.7E-07	1.306	0.801	1.586	-0.691
16	0.064	0.040	0.4E-07	1.312	0.816	1.530	-0.691
32	0.058	0.034	0.6E-07	1.302	0.810	1.511	-0.703
48	0.056	0.028	0.8E-07	1.303	0.802	1.506	-0.713

Table 4.5.26c Diffraction Results for a Submerged Cylinder

SOURCES DISTRIBUTED ON CYLINDER BOUNDARY
QUADRATIC VARIATION OF SOURCE DENSITY ON ELEMENT
FOUR-POINT GUASS QUADRATURE
DIFRACTION PARAMETER,ka=0.2

NN	Mod(R)	Arg(R)	RES	Mod(Fx)	Arg(Fx)	Mod(Fy)	Arg(Fy)
12	0.577	-0.275	0.5E-07	2.575	0.662	0.560	-1.564
16	0.564	-0.289	0.2E-07	2.509	0.632	0.483	-1.552
32	0.481	-0.320	0.4E-07	2.256	0.534	0.449	-1.538
48	0.460	-0.328	0.3E-07	2.191	0.508	0.437	-1.540

Table 4.5.27a Diffraction Results for a Submerged Cylinder

SOURCES DISTRIBUTED ON CYLINDER BOUNDARY
QUADRATIC VARIATION OF SOURCE DENSITY ON ELEMENT
FOUR-POINT GUASS QUADRATURE
DIFRACTION PARAMETER,ka=0.5

NN	Mod(R)	Arg(R)	RES	Mod(Fx)	Arg(Fx)	Mod(Fy)	Arg(Fy)
12	0.224	-0.025	0.6E-07	2.407	0.865	2.496	-0.945
16	0.354	-0.065	0.5E-07	2.416	0.868	2.199	-1.070
32	0.317	-0.101	0.8E-07	2.350	0.787	2.061	-1.106
48	0.316	-0.116	0.9E-07	2.334	0.764	2.000	-1.128

Table 4.5.27b Diffraction Results for a Submerged Cylinder

SOURCES DISTRIBUTED ON CYLINDER BOUNDARY
QUADRATIC VARIATION OF SOURCE DENSITY ON ELEMENT
FOUR-POINT GUASS QUADRATURE
DIFRACTION PARAMETER,ka=1.0

NN	Mod(R)	Arg(R)	RES	Mod(Fx)	Arg(Fx)	Mod(Fy)	Arg(Fy)
12	0.251	0.082	0.9E-07	1.292	0.794	1.483	-0.530
16	0.013	0.070	0.4E-07	1.259	0.893	1.508	-0.668
32	0.061	0.049	0.8E-07	1.281	0.832	1.496	-0.677
48	0.058	0.037	0.2E-06	1.291	0.815	1.496	-0.698

Table 4.5.27c Diffraction Results for a Submerged Cylinder

SOURCES DISTRIBUTED ON INTERNAL BOUNDARY,RS=0.7*CA
CONSTANT VARIATION OF SOURCE DENSITY ON ELEMENT
TWO-POINT GUASS QUADRATURE
DIFRACTION PARAMETER,ka=0.2

NN	Mod(R)	Arg(R)	RES	Mod(Fx)	Arg(Fx)	Mod(Fy)	Arg(Fy)
8	0.429	-0.337	0.3E-07	2.147	0.478	0.427	-1.537
12	0.422	-0.343	0.2E-07	2.075	0.465	0.420	-1.542
16	0.419	-0.344	0.8E-08	2.071	0.461	0.415	-1.542
32	0.418	-0.345	0.5E-08	2.066	0.459	0.415	-1.543
48	0.418	-0.345	0.5E-05	2.066	0.459	0.415	-1.543

Table 4.5.28a Diffraction Results for a Submerged Cylinder

SOURCES DISTRIBUTED ON INTERNAL BOUNDARY,RS=0.7*CA
CONSTANT VARIATION OF SOURCE DENSITY ON ELEMENT
TWO-POINT GUASS QUADRATURE
DIFRACTION PARAMETER,ka=0.5

NN	Mod(R)	Arg(R)	RES	Mod(Fx)	Arg(Fx)	Mod(Fy)	Arg(Fy)
8	0.256	-0.125	0.1E-07	2.374	0.718	1.913	-1.112
12	0.307	-0.140	0.2E-07	2.293	0.721	1.920	-1.162
16	0.310	-0.143	0.5E-07	2.304	0.719	1.890	-1.167
32	0.310	-0.144	0.3E-06	2.301	0.718	1.889	-1.169
48	0.310	-0.144	0.2E-07	2.301	0.718	1.889	-1.169

Table 4.5.28b Diffraction Results for a Submerged Cylinder

SOURCES DISTRIBUTED ON INTERNAL BOUNDARY,RS=0.7*CA
CONSTANT VARIATION OF SOURCE DENSITY ON ELEMENT
TWO-POINT GUASS QUADRATURE
DIFRACTION PARAMETER,ka=1.0

NN	Mod(R)	Arg(R)	RES	Mod(Fx)	Arg(Fx)	Mod(Fy)	Arg(Fy)
8	0.212	0.014	0.2E-06	1.456	0.700	1.265	-0.657
12	0.066	0.011	0.9E-07	1.290	0.770	1.529	-0.735
16	0.053	0.011	0.4E-07	1.312	0.777	1.494	-0.741
32	0.051	0.011	0.9E-07	1.309	0.777	1.499	-0.742
48	0.051	0.011	0.1E-06	1.309	0.777	1.499	-0.742

Table 4.5.28c Diffraction Results for a Submerged Cylinder

SOURCES DISTRIBUTED ON INTERNAL BOUNDARY,RS=0.7*CA
LINEAR VARIATION OF SOURCE DENSITY ON ELEMENT
TWO-POINT GUASS QUADRATURE
DIFRACTION PARAMETER,ka=0.2

NN	Mod(R)	Arg(R)	RES	Mod(Fx)	Arg(Fx)	Mod(Fy)	Arg(Fy)
8	0.382	-0.356	0.4E-08	1.993	0.423	0.400	-1.540
12	0.410	-0.348	0.2E-07	2.034	0.450	0.413	-1.543
16	0.416	-0.346	0.3E-07	2.061	0.457	0.414	-1.543
32	0.418	-0.345	0.1E-07	2.066	0.459	0.415	-1.543
48	0.418	-0.345	0.1E-07	2.066	0.459	0.415	-1.543

Table 4.5.29a Diffraction Results for a Submerged Cylinder

SOURCES DISTRIBUTED ON INTERNAL BOUNDARY,RS=0.7*CA
LINEAR VARIATION OF SOURCE DENSITY ON ELEMENT
TWO-POINT GUASS QUADRATURE
DIFRACTION PARAMETER,ka=0.5

NN	Mod(R)	Arg(R)	RES	Mod(Fx)	Arg(Fx)	Mod(Fy)	Arg(Fy)
8	0.256	-0.159	0.2E-07	2.319	0.666	1.780	-1.164
12	0.305	-0.149	0.8E-07	2.278	0.706	1.883	-1.175
16	0.310	-0.145	0.9E-08	2.300	0.715	1.881	-1.171
32	0.310	-0.144	0.7E-06	2.301	0.718	1.889	-1.169
48	0.310	-0.144	0.1E-07	2.301	0.718	1.889	-1.169

Table 4.5.29b Diffraction Results for a Submerged Cylinder

SOURCES DISTRIBUTED ON INTERNAL BOUNDARY,RS=0.7*CA
LINEAR VARIATION OF SOURCE DENSITY ON ELEMENT
TWO-POINT GUASS QUADRATURE
DIFRACTION PARAMETER,ka=1.0

NN	Mod(R)	Arg(R)	RES	Mod(Fx)	Arg(Fx)	Mod(Fy)	Arg(Fy)
8	0.191	-0.015	0.1E-06	1.462	0.665	1.277	-0.714
12	0.063	0.002	0.1E-06	1.295	0.757	1.528	-0.751
16	0.052	0.009	0.2E-06	1.313	0.773	1.494	-0.745
32	0.051	0.011	0.1E-06	1.309	0.777	1.499	-0.742
48	0.051	0.011	0.1E-07	1.309	0.777	1.499	-0.742

Table 4.5.29c Diffraction Results for a Submerged Cylinder

SOURCES DISTRIBUTED ON INTERNAL BOUNDARY,RS=0.7*CA
QUADRATIC VARIATION OF SOURCE DENSITY ON ELEMENT
FOUR-POINT GUASS QUADRATURE
DIFRACTION PARAMETER,ka=0.2

NN	Mod(R)	Arg(R)	RES	Mod(Fx)	Arg(Fx)	Mod(Fy)	Arg(Fy)
8	0.451	-0.335	0.5E-07	2.193	0.493	0.409	-1.547
12	0.417	-0.344	0.3E-07	2.062	0.460	0.422	-1.541
16	0.419	-0.344	0.3E-07	2.071	0.461	0.415	-1.543
32	0.418	-0.345	0.2E-08	2.066	0.459	0.415	-1.543
48	0.418	-0.345	0.8E-03	2.067	0.459	0.415	-1.541

Table 4.5.30a Diffraction Results for a Submerged Cylinder

SOURCES DISTRIBUTED ON INTERNAL BOUNDARY, RS=0.7*CA
QUADRATIC VARIATION OF SOURCE DENSITY ON ELEMENT
FOUR-POINT GUASS QUADRATURE
DIFRACTION PARAMETER, ka=0.2

NN	Mod(R)	Arg(R)	RES	Mod(Fx)	Arg(Fx)	Mod(Fy)	Arg(Fy)
8	0.367	-0.138	0.3E-07	2.412	0.756	1.834	-1.191
12	0.292	-0.139	0.4E-07	2.287	0.715	1.930	-1.152
16	0.312	-0.143	0.4E-07	2.304	0.719	1.888	-1.169
32	0.310	-0.144	0.5E-07	2.301	0.718	1.889	-1.169
48	0.310	-0.144	0.4E-07	2.301	0.718	1.889	-1.169

Table 4.5.30b Diffraction Results for a Submerged Cylinder

SOURCES DISTRIBUTED ON INTERNAL BOUNDARY, RS=0.7*CA
QUADRATIC VARIATION OF SOURCE DENSITY ON ELEMENT
FOUR-POINT GUASS QUADRATURE
DIFRACTION PARAMETER, ka=1.0

NN	Mod(R)	Arg(R)	RES	Mod(Fx)	Arg(Fx)	Mod(Fy)	Arg(Fy)
8	0.073	0.009	0.6E-07	1.446	0.763	1.383	-0.735
12	0.096	0.016	0.2E-07	1.291	0.763	1.512	-0.712
16	0.049	0.012	0.1E-06	1.311	0.780	1.495	-0.743
32	0.051	0.011	0.1E-06	1.309	0.777	1.499	-0.742
48	0.051	0.011	0.2E-07	1.309	0.777	1.499	-0.742

Table 4.5.30c Diffraction Results for a Submerged Cylinder

SOURCES DISTRIBUTED ON INTERNAL BOUNDARY, RS=0.9*CA
CONSTANT VARIATION OF SOURCE DENSITY ON ELEMENT
ONE-POINT GUASS QUADRATURE
DIFRACTION PARAMETER, ka=0.2

NN	Mod(R)	Arg(R)	RES	Mod(Fx)	Arg(Fx)	Mod(Fy)	Arg(Fy)
12	0.163	-0.440	0.3E-08	1.199	0.176	0.266	-1.558
16	0.221	-0.419	0.9E-08	1.399	0.239	0.300	-1.555
24	0.313	-0.385	0.4E-08	1.715	0.341	0.354	-1.549
32	0.368	-0.364	0.1E-07	1.900	0.402	0.386	-1.546

Table 4.5.31a Diffraction Results for a Submerged Cylinder

SOURCES DISTRIBUTED ON INTERNAL BOUNDARY, RS=0.9*CA
CONSTANT VARIATION OF SOURCE DENSITY ON ELEMENT
ONE-POINT GUASS QUADRATURE
DIFRACTION PARAMETER, ka=0.5

NN	Mod(R)	Arg(R)	RES	Mod(Fx)	Arg(Fx)	Mod(Fy)	Arg(Fy)
12	0.187	-0.340	0.2E-07	1.772	0.345	1.128	-1.414
16	0.232	-0.291	0.2E-07	1.940	0.444	1.296	-1.360
24	0.281	-0.219	0.3E-07	2.141	0.584	1.576	-1.272
32	0.310	-0.145	0.6E-08	2.299	0.716	1.884	-1.170

Table 4.5.31b Diffraction Results for a Submerged Cylinder

SOURCES DISTRIBUTED ON INTERNAL BOUNDARY, RS=0.9*CA
CONSTANT VARIATION OF SOURCE DENSITY ON ELEMENT
ONE-POINT GUASS QUADRATURE
DIFRACTION PARAMETER, ka=1.0

NN	Mod(R)	Arg(R)	RES	Mod(Fx)	Arg(Fx)	Mod(Fy)	Arg(Fy)
12	0.002	-0.234	0.2E-07	1.299	0.418	1.344	-1.152
16	0.011	-0.166	0.2E-07	1.332	0.520	1.398	-1.040
24	0.032	-0.074	0.4E-07	1.333	0.654	1.470	-0.886
32	0.043	-0.027	0.5E-07	1.323	0.721	1.490	-0.807

Table 4.5.31c Diffraction Results for a Submerged Cylinder

SOURCES DISTRIBUTED ON INTERNAL BOUNDARY, RS=0.8*CA
CONSTANT VARIATION OF SOURCE DENSITY ON ELEMENT
ONE-POINT GUASS QUADRATURE
DIFRACTION PARAMETER, ka=0.2

NN	Mod(R)	Arg(R)	RES	Mod(Fx)	Arg(Fx)	Mod(Fy)	Arg(Fy)
12	0.314	-0.384	0.1E-07	1.720	0.342	0.358	-1.549
16	0.371	-0.363	0.4E-08	1.911	0.405	0.388	-1.546
24	0.409	-0.348	0.2E-07	2.038	0.449	0.410	-1.543
32	0.416	-0.345	0.7E-08	2.061	0.458	0.414	-1.543

Table 4.5.32a Diffraction Results for a Submerged Cylinder

SOURCES DISTRIBUTED ON INTERNAL BOUNDARY,RS=0.8*CA
CONSTANT VARIATION OF SOURCE DENSITY ON ELEMENT
ONE-POINT GUASS QUADRATURE
DIFRACTION PARAMETER,ka=0.5

NN	Mod(R)	Arg(R)	RES	Mod(Fx)	Arg(Fx)	Mod(Fy)	Arg(Fy)
12	0.280	-0.220	0.8E-08	2.138	0.582	1.592	-1.273
16	0.301	-0.178	0.2E-07	2.238	0.658	1.744	-1.218
24	0.309	-0.150	0.1E-08	2.290	0.707	1.863	-1.178
32	0.310	-0.145	0.6E-08	2.299	0.716	1.884	-1.170

Table 4.5.32b Diffraction Results for a Submerged Cylinder

SOURCES DISTRIBUTED ON INTERNAL BOUNDARY,RS=0.8*CA
CONSTANT VARIATION OF SOURCE DENSITY ON ELEMENT
ONE-POINT GUASS QUADRATURE
DIFRACTION PARAMETER,ka=1.0

NN	Mod(R)	Arg(R)	RES	Mod(Fx)	Arg(Fx)	Mod(Fy)	Arg(Fy)
12	0.039	-0.083	0.6E-07	1.327	0.636	1.506	-0.896
16	0.043	-0.031	0.9E-07	1.330	0.715	1.492	-0.813
24	0.050	0.004	0.6E-07	1.313	0.766	1.499	-0.755
32	0.051	0.010	0.4E-07	1.309	0.775	1.499	-0.744

Table 4.5.32c Diffraction Results for a Submerged Cylinder

SOURCES DISTRIBUTED ON INTERNAL BOUNDARY,RS=0.6*CA
CONSTANT VARIATION OF SOURCE DENSITY ON ELEMENT
ONE-POINT GUASS QUADRATURE
DIFRACTION PARAMETER,ka=0.2

NN	Mod(R)	Arg(R)	RES	Mod(Fx)	Arg(Fx)	Mod(Fy)	Arg(Fy)
12	0.411	-0.347	0.1E-07	2.037	0.451	0.414	-1.543
16	0.417	-0.345	0.2E-07	2.064	0.458	0.414	-1.543
24	0.409	-0.348	0.2E-07	2.038	0.449	0.410	-1.543
32	0.418	-0.345	0.2E-07	2.066	0.459	0.415	-1.543

Table 4.5.33a Diffraction Results for a Submerged Cylinder

SOURCES DISTRIBUTED ON INTERNAL BOUNDARY,RS=0.6*CA
CONSTANT VARIATION OF SOURCE DENSITY ON ELEMENT
ONE-POINT GUASS QUADRATURE
DIFRACTION PARAMETER,ka=0.5

NN	Mod(R)	Arg(R)	RES	Mod(Fx)	Arg(Fx)	Mod(Fy)	Arg(Fy)
12	0.306	-0.149	0.4E-07	2.279	0.707	1.884	-1.175
16	0.310	-0.144	0.5E-07	2.301	0.716	1.884	-1.170
24	0.309	-0.150	0.1E-08	2.290	0.707	1.863	-1.178
32	0.310	-0.144	0.3E-07	2.301	0.718	1.889	-1.169

Table 4.5.33b Diffraction Results for a Submerged Cylinder

SOURCES DISTRIBUTED ON INTERNAL BOUNDARY, RS=0.6*CA
CONSTANT VARIATION OF SOURCE DENSITY ON ELEMENT
ONE-POINT GUASS QUADRATURE
DIFRACTION PARAMETER, ka=1.0

NN	Mod(R)	Arg(R)	RES	Mod(Fx)	Arg(Fx)	Mod(Fy)	Arg(Fy)
12	0.063	0.001	0.9E-07	1.296	0.755	1.529	-0.753
16	0.053	0.010	0.3E-07	1.313	0.774	1.494	-0.744
24	0.050	0.004	0.6E-07	1.313	0.766	1.499	-0.755
32	0.051	0.011	0.9E-07	1.309	0.777	1.499	-0.742

Table 4.5.33c Diffraction Results for a Submerged Cylinder

SOURCES DISTRIBUTED ON INTERNAL BOUNDARY, RS=0.5*CA
CONSTANT VARIATION OF SOURCE DENSITY ON ELEMENT
ONE-POINT GUASS QUADRATURE
DIFRACTION PARAMETER, ka=0.2

NN	Mod(R)	Arg(R)	RES	Mod(Fx)	Arg(Fx)	Mod(Fy)	Arg(Fy)
12	0.416	-0.345	0.2E-07	2.054	0.457	0.417	-1.542
16	0.418	-0.345	0.3E-07	2.066	0.459	0.414	-1.543
24	0.418	-0.345	0.2E-07	2.066	0.459	0.415	-1.543
32	0.418	-0.345	0.6E-07	2.066	0.459	0.415	-1.543

Table 4.5.34a Diffraction Results for a Submerged Cylinder

SOURCES DISTRIBUTED ON INTERNAL BOUNDARY, RS=0.5*CA
CONSTANT VARIATION OF SOURCE DENSITY ON ELEMENT
ONE-POINT GUASS QUADRATURE
DIFRACTION PARAMETER, ka=0.5

NN	Mod(R)	Arg(R)	RES	Mod(Fx)	Arg(Fx)	Mod(Fy)	Arg(Fy)
12	0.306	-0.144	0.3E-07	2.286	0.714	1.902	-1.168
16	0.310	-0.144	0.1E-03	2.302	0.717	1.886	-1.169
24	0.310	-0.144	0.7E-08	2.300	0.718	1.889	-1.169
32	0.311	-0.144	0.6E-07	2.301	0.718	1.888	-1.169

Table 4.5.34b Diffraction Results for a Submerged Cylinder

SOURCES DISTRIBUTED ON INTERNAL BOUNDARY, RS=0.5*CA
CONSTANT VARIATION OF SOURCE DENSITY ON ELEMENT
ONE-POINT GUASS QUADRATURE
DIFRACTION PARAMETER, ka=1.0

NN	Mod(R)	Arg(R)	RES	Mod(Fx)	Arg(Fx)	Mod(Fy)	Arg(Fy)
12	0.065	0.008	0.2E-06	1.292	0.766	1.527	-0.740
16	0.052	0.011	0.1E-06	1.312	0.776	1.494	-0.742
24	0.052	0.011	0.8E-07	1.309	0.777	1.500	-0.742
32	0.051	0.011	0.2E-06	1.309	0.778	1.498	-0.742

Table 4.5.34c Diffraction Results for a Submerged Cylinder

water depth (h/a = 10.1). One wave is chosen so that the diffraction parameter is fixed at ka = 0.3 and numerical results are obtained for two of the cylinder locations for which experimental results are obtained, $(y_o - a)/L = 0.05, 0.10$.

The results of these numerical tests are presented in figures 4.5.31 to 4.5.36 and tables 4.5.36 to 4.5.41. In these graphs and tables the values of the diffraction coefficient for the horizontal component of force, as defined in equation 4.4.9, is obtained for a range of discretisation schemes. In order to obtain a comparison of the results for various locations of the source boundary the results for different types of element are plotted separately. Figures 4.5.31 and 4.5.32 are results obtained for an assumed constant variation of source density with one source located on each element; figures 4.5.33 and 4.5.34 are for an assumed linear variation of source density and again a single source is located on each element but for the results for an assumed quadratic variation of source density, given in figures 4.5.35 and 4.5.36, two sources are located on each element. Each graph includes results for $RAT(r_s/r_n) = 1.0, 0.9, 0.7$ and 0.5.

Previous results indicated that for the same discretisation scheme the results obtained for a separate source boundary were obtained more rapidly than for sources located on the boundary of the obstacle. In order to determine whether this feature is repeated for the present results the processor time has been noted for program runs with 32 nodes for the two sets of data tested here. The values are given in table 4.5.35 and it is observed that although the removal of sources from the obstacle boundary does result in a small

improvement in efficiency the differences are less pronounced than for the previous example. Efficiency will only therefore be significantly improved if the regular kernel option gives a consistently more rapid convergence to the final solution than the singular kernel method.

Variation of source density on element	Processor time RAT = 1.0	RAT = 0.9	RAT = 0.7	RAT = 0.5
Constant	.0606	.0520	.0585	.0572
Linear	.0539	.0492	.0472	.0457
Quadratic	.0773	.0514	.0477	.0458

Table 4.5.35 Comparison of program efficiency

The first observation which may be made from the results presented in figures 4.5.31 and 4.5.32 and tables 4.5.36 and 4.5.37 is that the results obtained by the conventional singular kernel method with an assumed constant variation of source density have not converged to the final solution. The tabulated results do indicate that the result is converging slowly as the discretisation becomes more precise but results for as many as 96 nodes are poor when compared with each of the alternatives tested in this section. These results may be compared with those of Naftzger and Chakrabarti who commented, without giving details, that for cylinders located near the boundaries of the fluid somewhat more than 100 nodes are required to obtain a final solution.

The failure of the conventional method to achieve convergence for this problem at the same level of discretisation as the alternative schemes makes the more detailed examination of this set of results of greater significance. Examination of the results for assumed linear and quadratic variations of source density on the element with sources located on the obstacle boundary indicates that similar results are obtained and that the assumed linear variation gives more rapid convergence for both examples. These results contradict those of the previously tested example and indicate that under certain conditions higher-order elements may be employed to improve the numerical model and to achieve solution more efficiently than the traditionally used constant element.

The final tests performed for the previous example (figures 4.5.28 to 4.5.30) indicated that for a greater separation of the source boundary from the obstacle boundary a more rapid convergence to the final solution is obtained. The results currently under consideration confirm this trend, give results which are similar for each of the three discretisation schemes and also indicate the breakdown of the method for more precise discretisations. The breakdowns are somewhat erratic in nature, have only been encountered for RAT = .7 and RAT = .5 with NN > 48 and are due to the occurence of ill-conditioning in the system of algebraic equations which is demonstrated by failure to satisfy the energy criterion. It is therefore evident that although a separated source boundary located near to the obstacle boundary gives slow convergence to the final solution this option is the most reliable one for more precise discretisations.

Consideration of the sets of results obtained in this numerical study provides evidence to suggest that for submerged two dimensional obstacles the regular kernel integral equation method is amenable to numerical solution and if used with care will provide reliable results more efficiently than the conventional singular kernel method with an assumed constant variation of source density and a single source located centrally on each element. Because the results obtained for the application of higher-order elements with sources on the obstacle boundary are contradictory and because the choice of element does not greatly affect results for separated source boundaries it may also be suggested that the implementation of these numerical refinements is unnecessary.

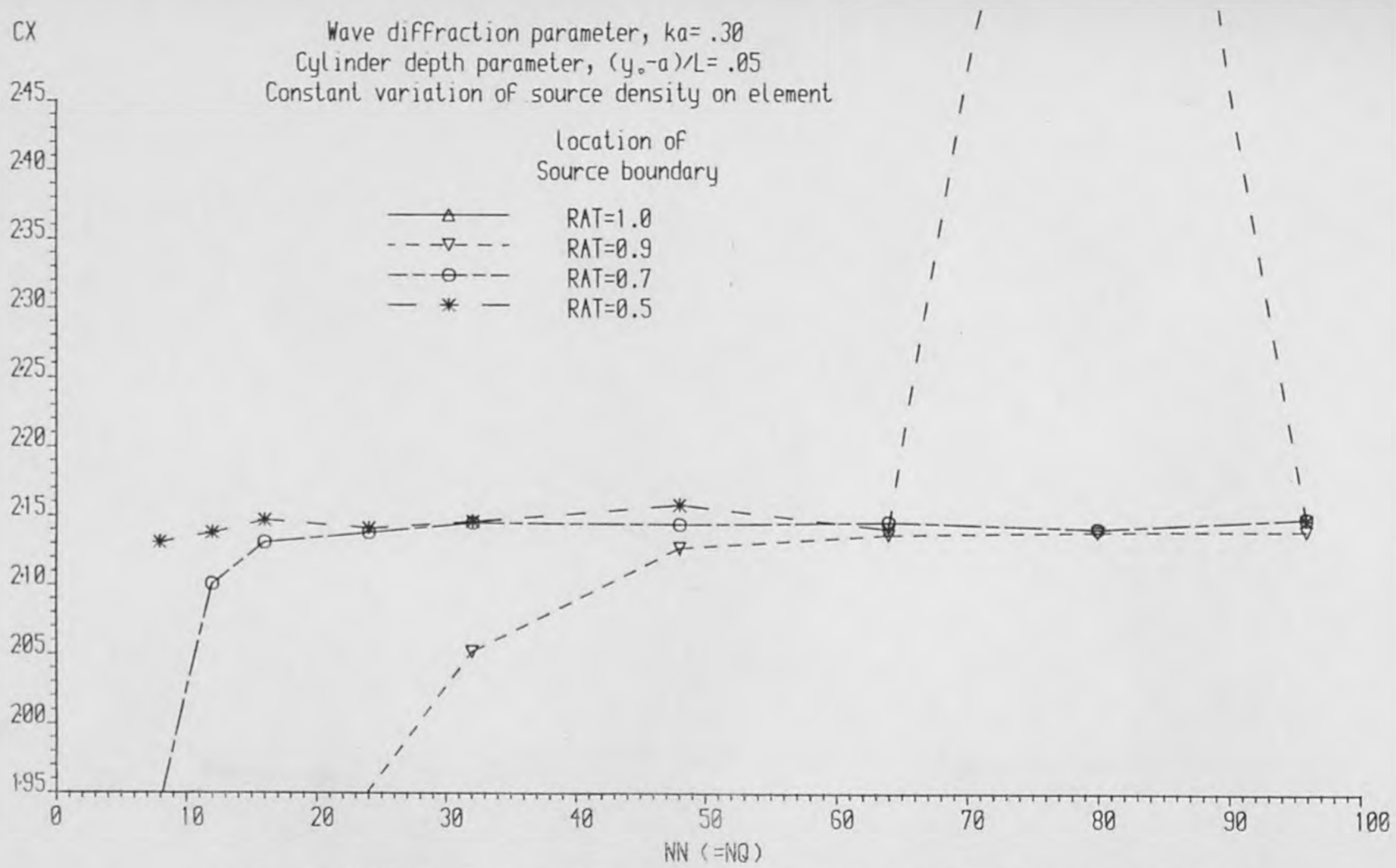

Figure 4.5.31 Diffraction coefficient for the horizontal force on a submerged cylinder

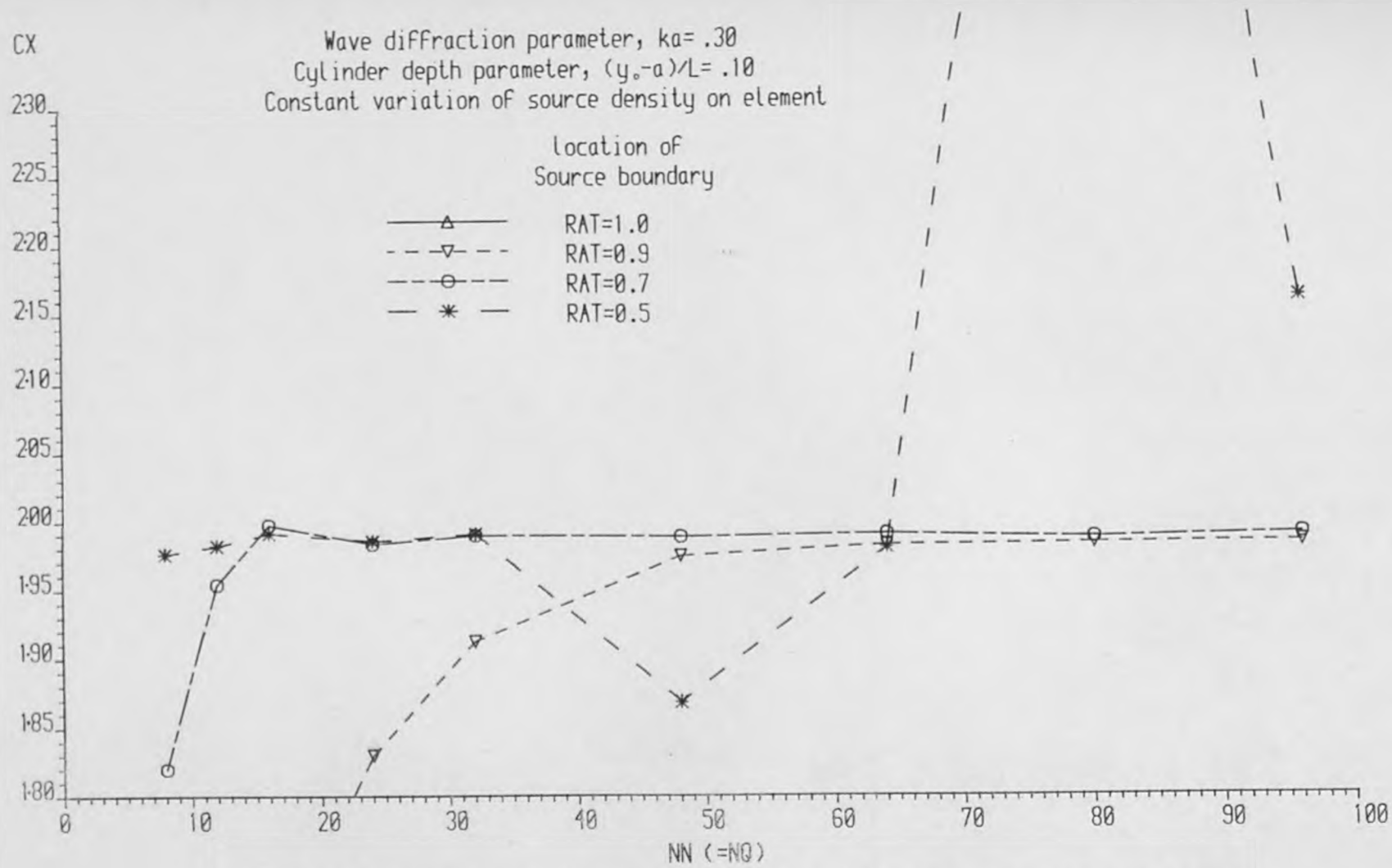

Figure 4.5.32 Diffraction coefficient for the horizontal force on a submerged cylinder

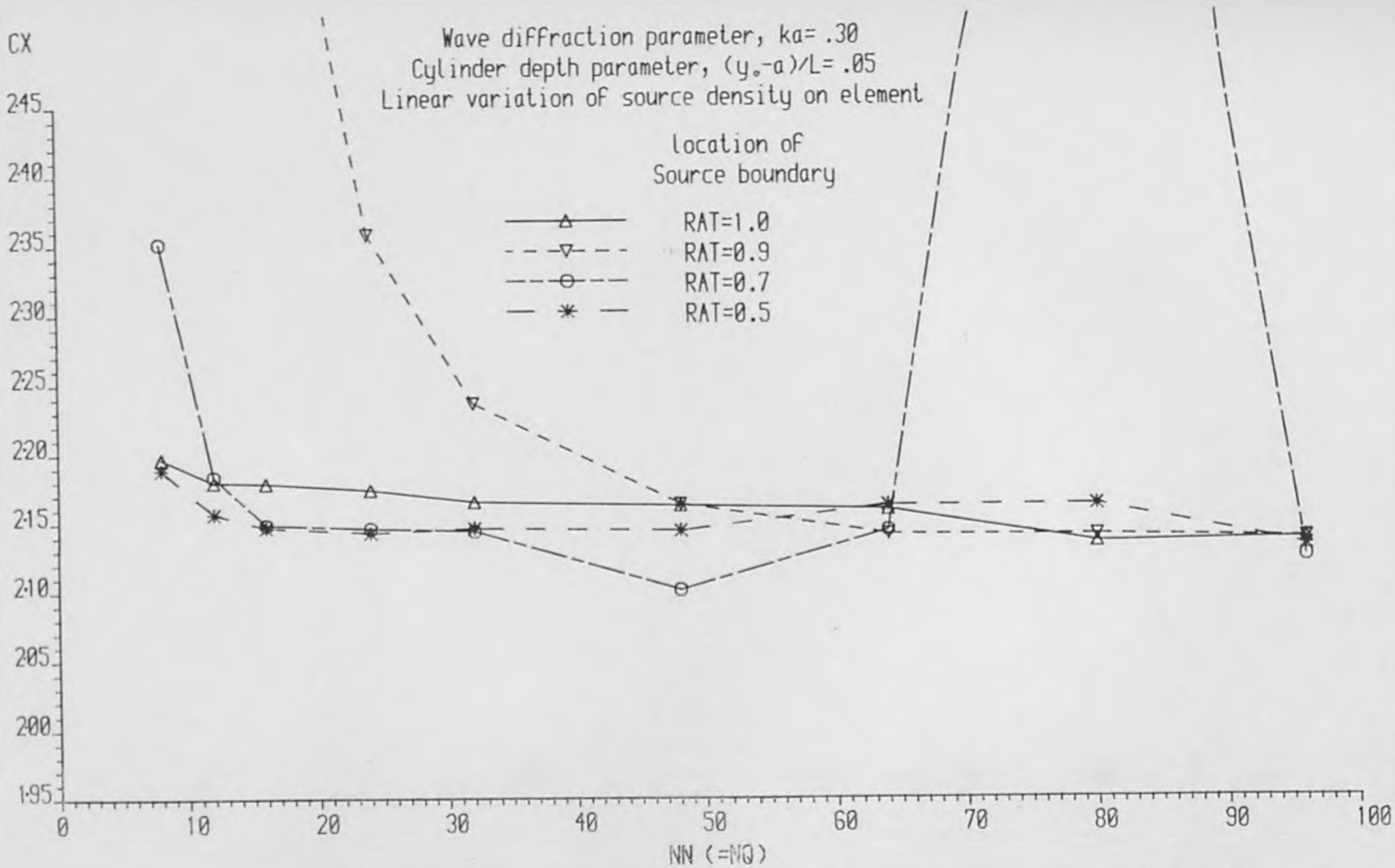

Figure 4.5.33 Diffraction coefficient for the horizontal force on a submerged cylinder

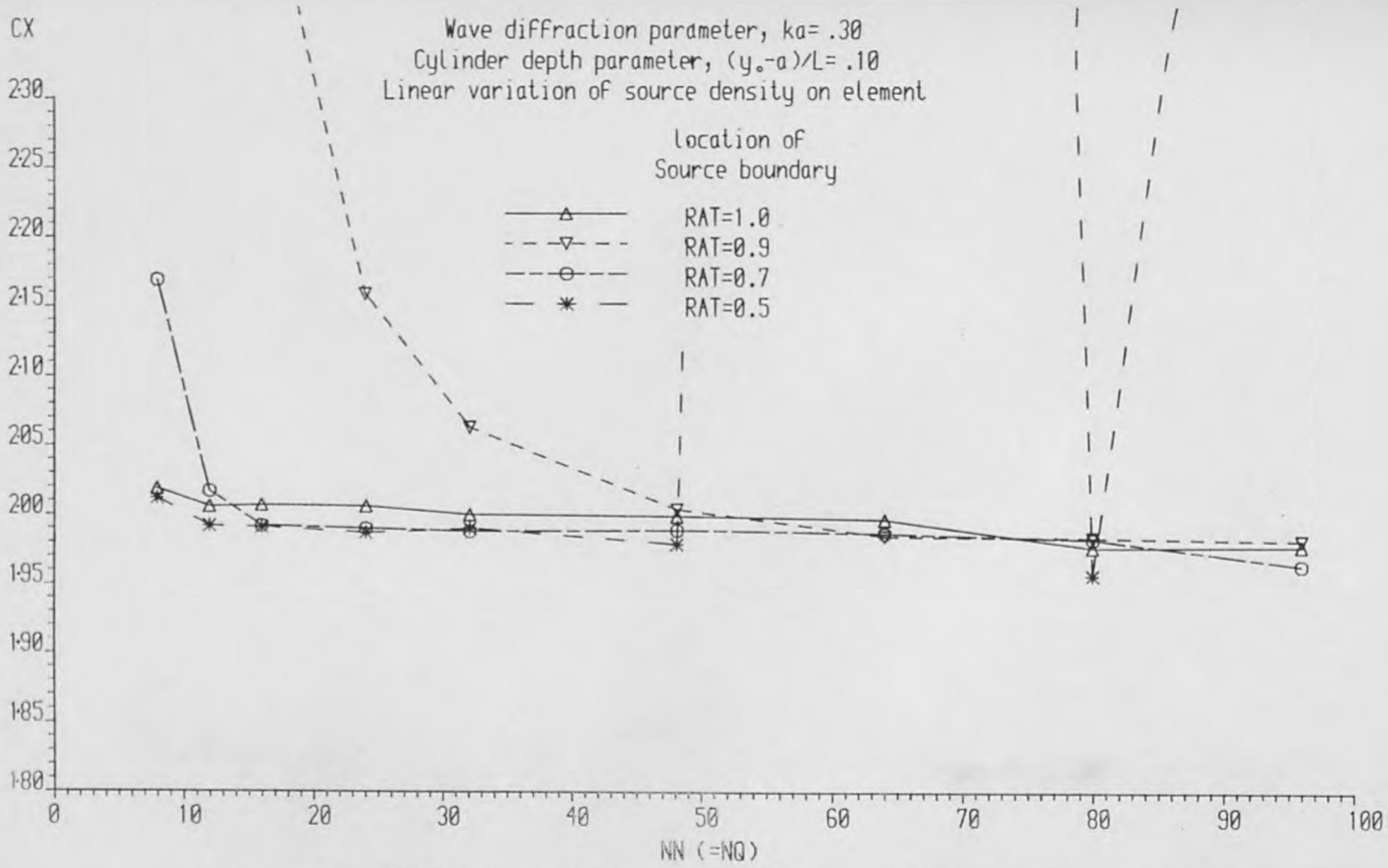

Figure 4.5.34 Diffraction coefficient for the horizontal force on a submerged cylinder

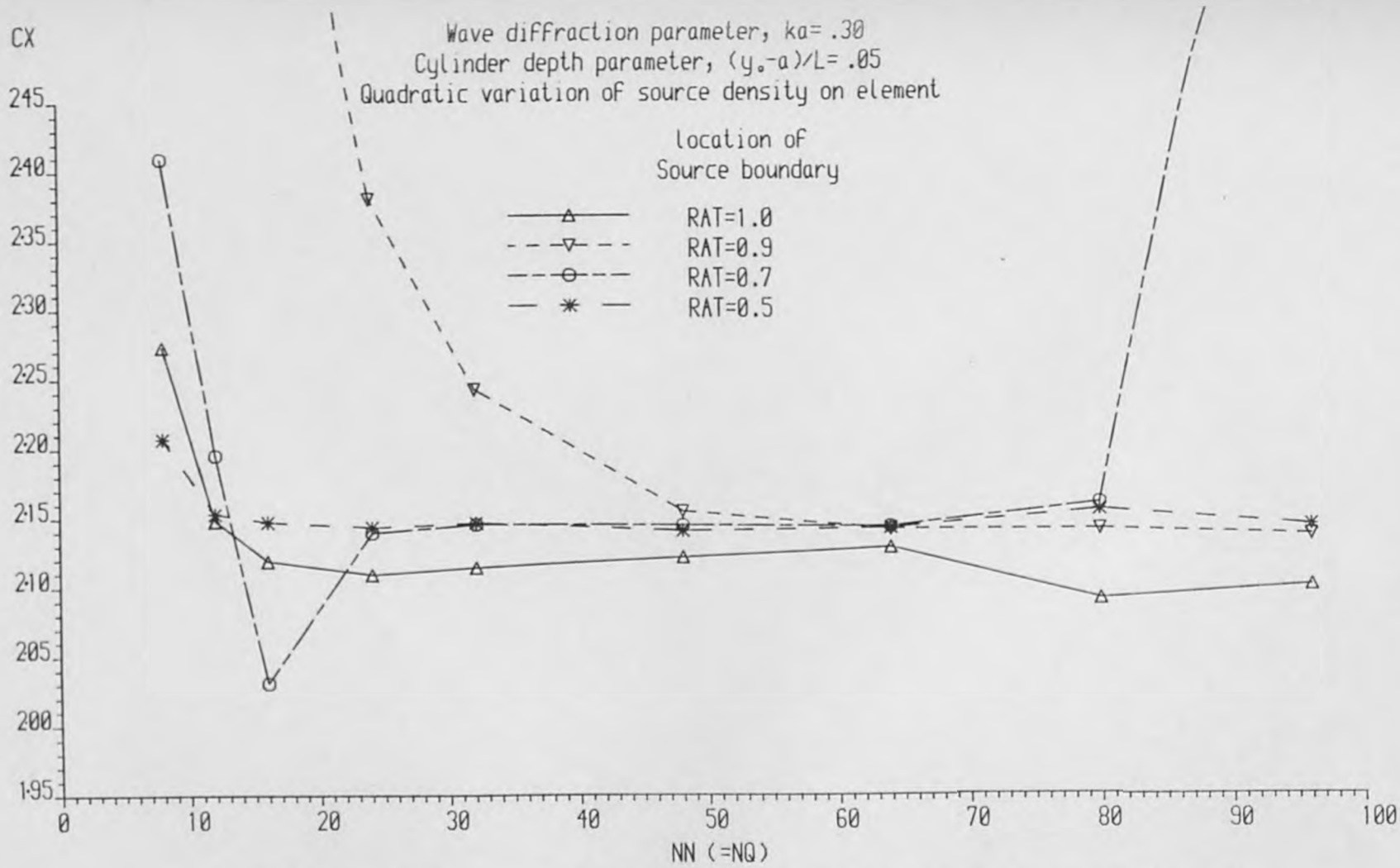

Figure 4.5.35 Diffraction coefficient for the horizontal force on a submerged cylinder

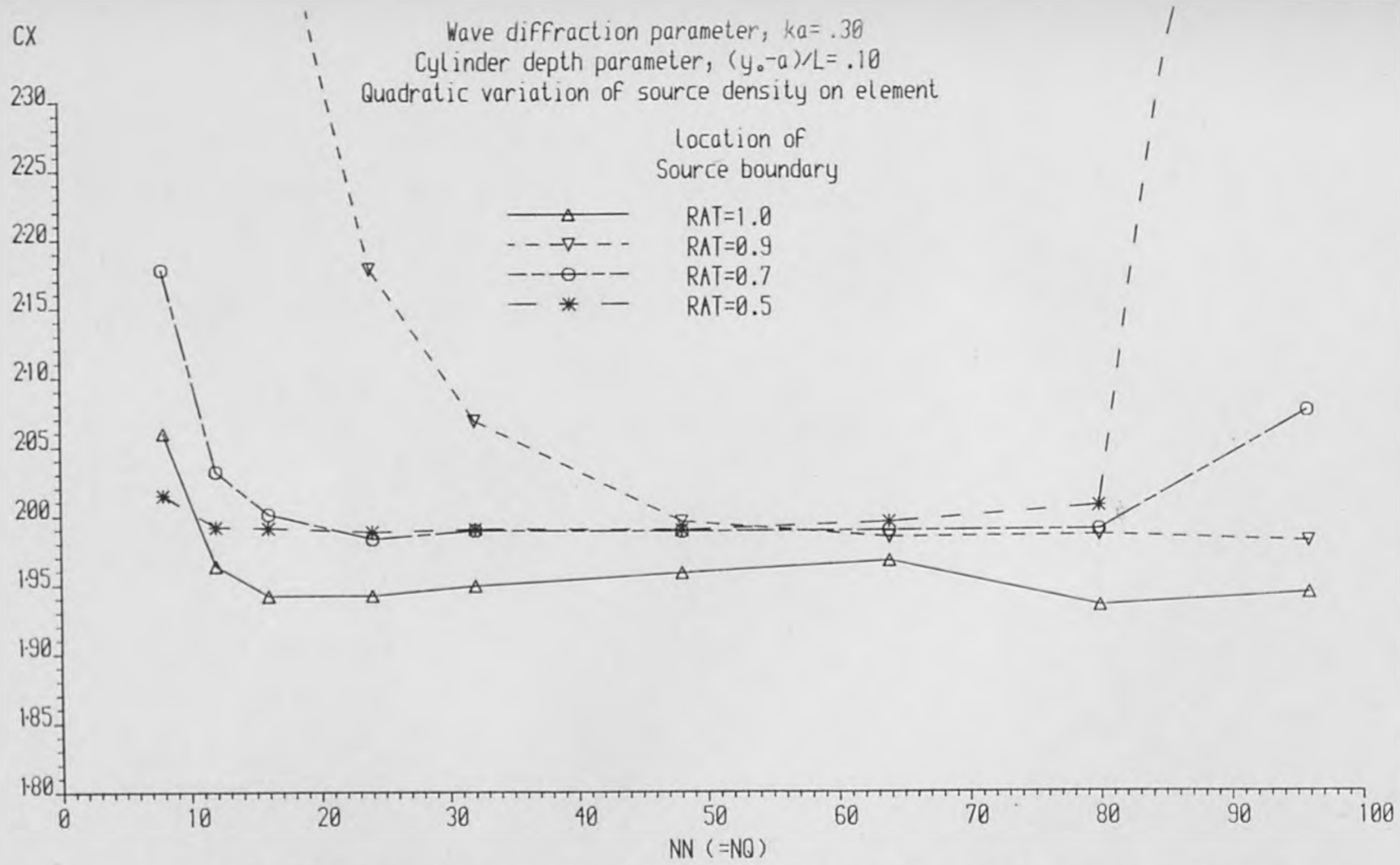

Figure 4.5.36 Diffraction coefficient for the horizontal force on a submerged cylinder

CONSTANT VARIATION OF SOURCE DENSITY ON ELEMENT
ONE-POINT GUASS QUADRATURE
DIFRACTION PARAMETER, ka=0.305
CYLINDER DEPTH PARAMETER, $(y_o - a)/L$=0.05
DIFFRACTION COEFFICIENT FOR HORIZONTAL COMPONENT OF FORCE

NN	RAT=1.0	RAT=0.9	RAT=0.7	RAT=0.5
8	3.621	1.485	1.944	2.131
12	1.447	1.631	2.101	2.138
16	0.492	1.768	2.131	2.147
24	0.431	1.952	2.138	2.141
32	0.873	2.052	2.145	2.146
48	1.309	2.127	2.144	2.158
64	1.519	2.137	2.146	2.141
80	1.647	2.139	2.141	3.000
96	1.725	2.140	2.149	2.148

Table 4.5.36 Diffraction Results for a Submerged Cylinder

CONSTANT VARIATION OF SOURCE DENSITY ON ELEMENT
ONE-POINT GUASS QUADRATURE
DIFRACTION PARAMETER, ka=0.305
CYLINDER DEPTH PARAMETER, $(y_o - a)/L$=0.10
DIFFRACTION COEFFICIENT FOR HORIZONTAL COMPONENT OF FORCE

NN	RAT=1.0	RAT=0.9	RAT=0.7	RAT=0.5
8	3.332	1.440	1.820	1.976
12	1.357	1.563	1.954	1.982
16	0.470	1.679	1.997	1.991
24	0.389	1.830	1.983	1.985
32	0.800	1.912	1.989	1.990
48	1.207	1.974	1.988	1.868
64	1.403	1.982	1.990	1.980
80	1.522	1.983	1.987	3.000
96	1.585	1.984	1.990	2.161

Table 4.5.37 Diffraction Results for a Submerged Cylinder

LINEAR VARIATION OF SOURCE DENSITY ON ELEMENT
ONE-POINT GUASS QUADRATURE
DIFRACTION PARAMETER, ka=0.305
CYLINDER DEPTH PARAMETER, $(y_o - a)/L$=0.05
DIFFRACTION COEFFICIENT FOR HORIZONTAL COMPONENT OF FORCE

NN	RAT=1.0	RAT=0.9	RAT=0.7	RAT=0.5
8	2.197	4.203	2.352	2.189
12	2.180	3.052	2.184	2.157
16	2.179	2.757	2.149	2.147
24	2.174	2.358	2.146	2.143
32	2.165	2.236	2.144	2.146
48	2.162	2.163	2.101	2.144
64	2.159	2.141	2.144	2.162
80	2.135	2.140	3.065	2.162
96	2.137	2.137	2.124	2.132

Table 4.5.38 Diffraction Results for a Submerged Cylinder

LINEAR VARIATION OF SOURCE DENSITY ON ELEMENT
ONE-POINT GUASS QUADRATURE
DIFRACTION PARAMETER,ka=0.305
CYLINDER DEPTH PARAMETER,$(y_o - a)/L$=0.10
DIFFRACTION COEFFICIENT FOR HORIZONTAL COMPONENT OF FORCE

NN	RAT=1.0	RAT=0.9	RAT=0.7	RAT=0.5
8	2.019	3.588	2.169	2.012
12	2.006	2.686	2.017	1.992
16	2.007	2.475	1.992	1.991
24	2.006	2.159	1.990	1.987
32	2.000	2.063	1.988	1.990
48	1.999	2.004	1.989	1.979
64	1.997	1.985	1.987	6.651
80	1.977	1.984	1.983	1.957
96	1.978	1.982	1.964	3.000

Table 4.5.39 Diffraction Results for a Submerged Cylinder

QUADRATIC VARIATION OF SOURCE DENSITY ON ELEMENT
TWO-POINT GUASS QUADRATURE
DIFRACTION PARAMETER,ka=0.305
CYLINDER DEPTH PARAMETER,$(y_o - a)/L$=0.05
DIFFRACTION COEFFICIENT FOR HORIZONTAL COMPONENT OF FORCE

NN	RAT=1.0	RAT=0.9	RAT=0.7	RAT=0.5
8	2.273	5.479	2.409	2.207
12	2.148	3.225	2.195	2.153
16	2.119	2.766	2.031	2.147
24	2.109	2.380	2.139	2.143
32	2.114	2.242	2.145	2.146
48	2.121	2.154	2.144	2.140
64	2.128	2.141	2.143	2.142
80	2.091	2.141	2.160	2.155
96	2.100	2.136	2.873	2.143

Table 4.5.40 Diffraction Results for a Submerged Cylinder

QUADRATIC VARIATION OF SOURCE DENSITY ON ELEMENT
TWO-POINT GUASS QUADRATURE
DIFRACTION PARAMETER,ka=0.305
CYLINDER DEPTH PARAMETER,$(y_o - a)/L$=0.10
DIFFRACTION COEFFICIENT FOR HORIZONTAL COMPONENT OF FORCE

NN	RAT=1.0	RAT=0.9	RAT=0.7	RAT=0.5
8	2.060	3.697	2.178	2.015
12	1.964	2.846	2.032	1.992
16	1.942	2.483	2.001	1.991
24	1.942	2.178	1.983	1.988
32	1.949	2.068	1.989	1.990
48	1.958	1.995	1.988	1.989
64	1.967	1.984	1.989	1.995
80	1.934	1.985	1.989	2.006
96	1.943	1.980	2.074	3.000

Table 4.5.41 Diffraction Results for a Submerged Cylinder

CHAPTER 5 - EXPERIMENTAL INVESTIGATION

5.1 Introduction

An experimental study has been performed for the investigation of the interaction of regular waves with a horizontal circular cylindrical model in a laboratory wave flume. This study is in some ways similar to studies which have already been completed (for example Longuet-Higgins, 1976 and Koterayama, 1979) but it is thought to be the only study in which detailed measurements of the wave motion in both the far-field and near-field are obtained for a submerged obstacle. This also appears to be the only published study in which pressure measurements have been made on the surface of a submerged horizontal circular cylinder.

The major purpose of the experimental study is the validation of the results of the linear diffraction analysis. The experimental programme has been designed by determining the conditions under which wave scattering will occur for the range of waves which may be generated in the laboratory facility. For the range of waves chosen the wave steepness and cylinder location are varied and these variations are introduced because increasing wave steepness and reducing cylinder submergence both imply a non-linear interaction and therefore suggest that measured results may depart from the predictions of a linear analysis.

The theory which is being tested in this study, if extended to a higher-order of approximation, is characterized by the linear summation of values which oscillate at multiples of the wave

frequency. The analysis of measurements in this study has therefore been achieved by making use of the technique of spectralanalysis to obtain the components in the Fourier series.

5.2 Theoretical Considerations

5.2.1 Dimensional Analysis

A problem with the design of an experimental programme for a wave hydrodynamics problem is the large number of variables which are inerrelated and affect the measurements which are being studied. In the present study the method of dimensional analysis is of value for two reasons. Firstly, the results of the dimensional analysis may be employed to determine which parameters are sufficient to describe the problem completely and therefore which parameter variations must be included in the experimental programme and secondly the dimensional analysis is required to determine whether or not the scaling of model test results is valid.

A dimensional analysis of the problem of wave diffraction by a submerged cylindrical obstacle in water of finite depth has been given in Appendix A.9. It is clear that there is a certain flexibility in the choice of parameters and for the experimental study it is convenient to commence with the expression

$$\frac{F}{\rho g D H \ell} = f(D/L,\ H/L,\ h/L,\ y_o/h,\ R_e/\sqrt{F_r}) \qquad 5.2.1$$

The first parameter, D/L, is the diffraction parameter and is equivalent to the parameter ka(= πD/L). For problems in water of finite depth this parameter might be referred to as a diffraction refraction parameter since the location of the fluid bottom will affect the form of the resulting wave motion. This parameter may be used to describe the conditions for which wave diffraction is a significant feature in wave loading problems and the value of D/L > 0.2 has been proposed by Hogben (1974) for the particular case of the surface piercing vertical circular cylinder. However, Martin and Dixon (1983) indicated that this value is unsuitable for cylinders located in the free surface since the theoretically derived reflection and transmission coefficients predict that significant wave scattering will occur at lower values of D/L.

The parameter H/L is the wave steepness parameter and gives an indication of the degree of non-linearity of a progressive wave. Since no general non-linear diffraction theory is available increasing the wave steepness may lead to a significant departure of measured values from those which are obtained by the available theoretical models.

The water depth parameter h/L describes the extent to which the fluid bottom affects wave motion and it is conventional to define shallow water depth(h/L < .05), intermediate water depth (.05 < h/L < 0.5) and deep water depth (h/L > 0.5) ranges.

A parameter is required which, together with the other parameters, describes the location of the obstacle relative to the field of motion. The parameter y_o/h is a possible choice and

y_o/L a suitable alternative but the parameter $(y_o-a)/L$ has been chosen for the present study because it is similar in form to the water depth parameter h/L. This parameter then gives an indication of the "instantaneous shallow water" region above the cylinder and also, together with the wave steepness parameter, H/L, gives an alternative indication of the importance of non-linear effects since the parameter $H/(y_o-a)$ is similar in form to the parameter which is used for this purpose in shallow water problems.

The final non-dimensional group $R_e/\sqrt{F_r}$ will give a measure of the importance of viscous and free surface effects. Problems associated with Reynolds' and Froude scaling are well known and in model tests for wave problems it is not possible to obtain dynamic similarity for either. However, for wave diffraction problems viscous effects are not generally important and the variation of results with the Froude number does not appear to have been considered. This group is therefore excluded, but because the investigation of free surface effects is an important part of the present experimental study it is noted that the scaling of model tests to prototype scale without achieving Froude similarity may lead to errors.

5.2.2 Linear Diffraction Analysis

For a linear potential theory formulation of the wave diffraction problem it is assumed that an inviscid fluid makes only small amplitude oscillatory motions. The dimensional equation may therefore be reduced to the form

$$\frac{F}{\rho g a\, H/2} = f(ka,\ h/L,\ (y_o-a)/L) \qquad 5.2.2$$

where the denominator of the left hand side has been modified to agree with the non-dimensional group employed in the diffraction program and F is now the force per unit length.

The objective of the experimental study reported in this chapter is to validate the results of the diffraction program for the particular problem of a submerged horizontal circular cylinder and before commencing an account of this study it is important to establish an indication of the importance of wave scattering for the range of parameters for which the laboratory tests have been performed. For some wave diffraction problems the form of the diffracted wave may be taken as evidence of wave scattering, however, for the circular cylinder submerged in deep water the reflection and transmission coefficients have theoretical values of zero and unity respectively. Even if the form of the diffracted wave gives evidence of wave scattering the choice of a criterion based on reflection and transmission coefficient values would exclude local diffracted wave effects (John,1950) and therefore could only give a partial indication of the importance of diffraction in wave loading.

The use of the diffraction coefficients, as defined in equation 4.4.9, provides a better means of determining the onset of, or the importance of,wave scattering effects and a dimensional equation may be written in the form

$$C_x = f(ka,\ h/L,\ (y_o-a)/L). \qquad 5.2.3$$

If h/L is chosen so that the fluid bottom is effectively absent the diffraction coefficients will not be modified by the

effects of refraction and the coefficient values will be identical to the theoretical inertia coefficient results at small values of the diffraction parameter. For a circular cylinder the theoretical value of the diffraction coefficients at small ka is therefore 2.0 and departures from this value indicate that wave scattering effects are important.

The diffraction computer program may be used to give the diffraction coefficients for the range of data for which the experimental study has been conducted and an indication of the importance of diffraction effects may therefore be established. Application of the diffraction program in this way also provides an additional test of the program accuracy by comparison with the theoretical inertia coefficient result at small ka.

The experimental results reported in this chapter have been obtained for a single cylinder of radius a = .055 m and a range of waves in water of depth, h = .555m at three frequencies f_o = 0.977, 1.172, 1.367 Hz. The value of the diffraction coefficient is therefore within the range $0.2 < ka < 0.5$. The cylinder is located at three depths of submergence for the sets of waves at each frequency corresponding to $(y_o-a)/L$ = 0.05, 0.10, 0.15. As an indication of the importance of wave scattering for this range of data the diffraction computer program has been used to obtain a plot of the diffraction coefficients against the diffraction parameter by varying the cylinder radius at each of the depths of submergence for the frequency f_o = 1.172Hz. The results obtained are for a 32 node linear element discretisation with sources located on a separate

source boundary with radius $r_s = 0.7a$. This discretisation scheme has been shown in Chapter 4 to give numerical results which are within $\pm 2\%$ of the final solution.

The results presented in Figure 5.2.1 demonstrate that at the value of the diffraction coefficient corresponding to the experimental set up (ka = .305) diffraction effects are of some significance particularly at smaller depths of submergence. The results for the vertical component of force give values of the diffraction coefficient which approach the theoretical inertia coefficient value of 2.0 at small ka but the horizontal component does not. The computed results obtained at the lower ka values were therefore checked by alternative discretization schemes. All numerical results obtained are in close agreement with the results plotted and it may therefore be necessary to conclude that the numerical model gives results at small ka which are in error for this set of data.

5.2.3 Non-Linear Diffraction Analysis

For the submerged horizontal circular cylinder the only non-linear forces which have been predicted theoretically are the horizontal and vertical components of the second-order steady force. For cylinders in deep water linear theory predicts the absence of any reflected wave and therefore, by the momentum flux method with energy conservation, no horizontal drift force is predicted. For waves in finite water depth no theoretical values are known to have been evaluated by means other than the momentum flux formula although the method adopted by Ogilvie (1963) could be applied. The theoretical evaluation of the drift force only requires the knowledge of the first-

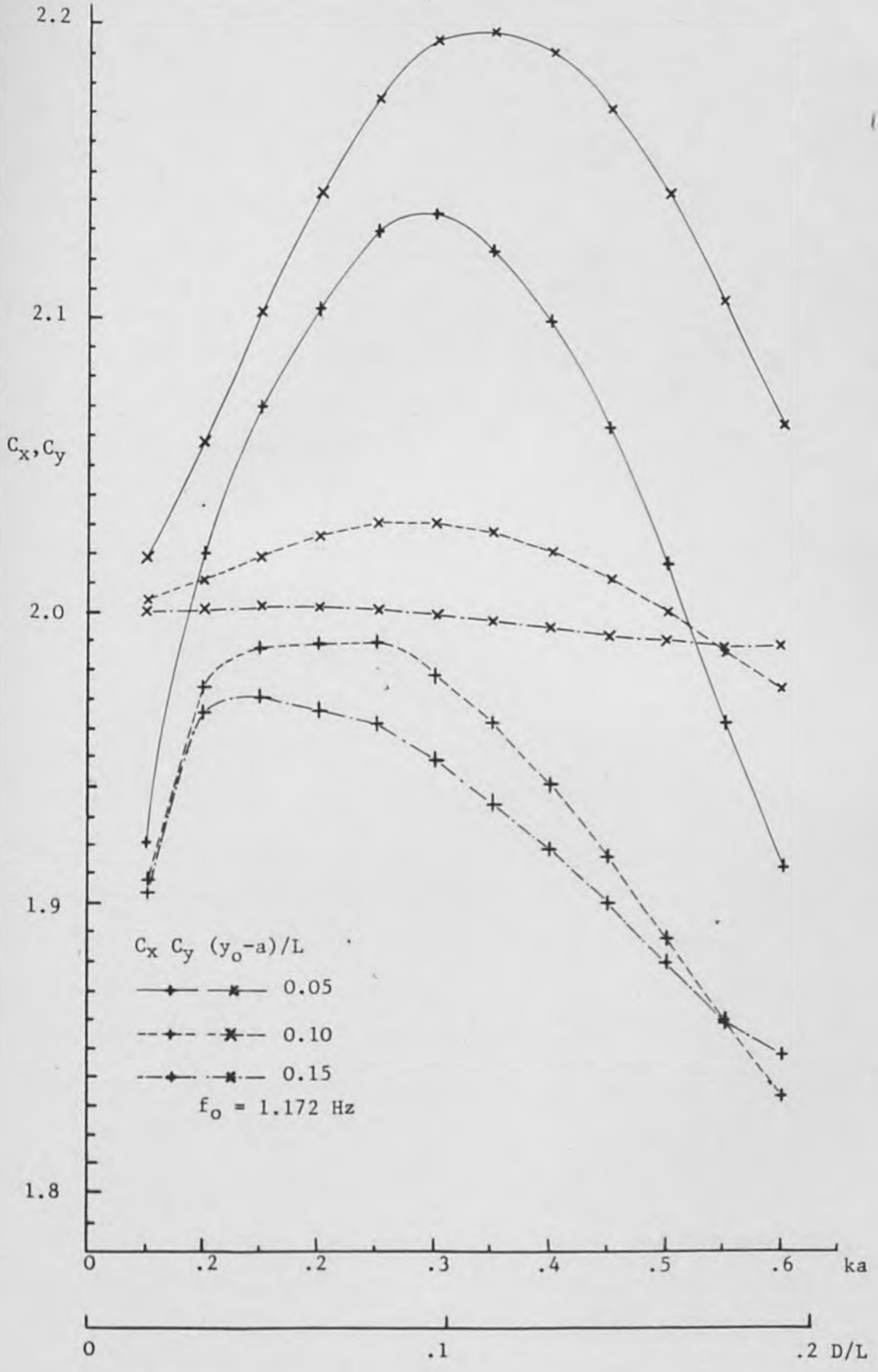

Figure 5.2.1 Diffraction Coefficients

order potential and therefore might be accomplished by the integral equation method as well as the multipole method and both of these methods would be superior to the momentum flux method because they also yield the vertical component of the steady force.

Although no non-linear theoretical results have been obtained for the problem of a cylinder submerged in waves it is possible to provide a framework for the non-linear interaction by referring to the formulation of the second-order boundary value problem and by analogy with other wave problems as well as by citing the results of experimental studies.

Studies of the importance of non-linear free surface effects for the similar problem of a submerged obstacle at small depths in a steady flow by Tuck (1965) and Salvesen (1969) provide theoretical and experimental evidence to suggest that non-linear conditions become increasingly important as the depth of submergence is reduced. The second-order diffraction boundary value problem has been formulated in Chapter 3 of this thesis and this indicates that pressures and therefore forces will occur which oscillate at twice the wave frequency. Without computations to provide quantitative evidence it is not possible to determine whether these predicted oscillations at a higher frequency will give increased total force components. However, it may be noted that if the second-order oscillatory quantities are going to affect the magnitude of the total components of force they must exceed 20% of the values obtained by a linear analysis and that this can be established by experimental means. The perturbation analysis also indicates that the diffracted wave will contain a free wave which oscillates at twice the wave frequency

and this free wave has been identified in experiments conducted by Longuet-Higgins (1977) who demonstrated that it's presence affects the mean force exerted by the wave on a submerged cylinder. The only study in which oscillatory second-order forces have been measured for the horizontal circular cylinder has been conducted by Koterayama (1979) but these results are not a major part of his study and only give an indication that non-linear effects are of some importance.

If the submerged horizontal circular cylinder is considered as a double beach the importance of nonlinear effects is implied. For waves of small steepness interacting with a cylinder at small depths of submergence the majority of the energy is transmitted through the region above the cylinder which might therefore be regarded as an instantaneous shallow water region. For increasing wave steepness the wave height become significant compared with the local water depth and the local partical velocities are a significant fraction of the wave speed so that the importance of non-linear effects might be suspected. It may be noted at this point that cnoidal diffraction results (Isaacson, 1977a) for waves of finite height in shallow water gives results which differ from those of sinusoidal wave theory so that measured quantities obtained in this experimental study for shallow depths of submergence might be expected to depart from the results obtained by the linear diffraction computer program.

If waves are sufficiently steep wave breaking will be induced by the presence of the cylinder and under such conditions the importance of non-linearity is obvious and might be expected to result in induced forces which are considerably different from predictions

obtained by a linear or even a second-order analysis.

5.2.4 Objectives of Experimental Study

The primary purpose of the experimental study is to determine whether and under what conditions the results of laboratory tests depart from those predicted by the linear wave diffraction analysis. The quantities used to test the theoretical results are the spatial variation of the wave height upstream and downstream of the cylinder and the pressures at four points on the cylinder boundary.

The discussion of the previous sections indicates that two different effects are expected to give rise to non-linear interaction and the experimental programme has therefore been designed to include a range of cylinder locations and for each location the wave steepness is varied. For waves of small steepness interacting with cylinders at larger depths of submergence the assumptions of the linear potential theory formulation are essentially satisfied and therefore agreement of theory with experiment might be expected. However, if wave steepness or local shallow water effects are of significance the assumptions of a linear analysis are violated and it is necessary to determine the importance of the exclusion of non-linear effects from the theoretical model.

In the absence of higher-order theoretical predictions the experimental test is the only means of determining the importance of non-linear effects. In the context of this thesis the experimental results will provide information which will indicate whether the

numerical solution of the second-order formulation will provide a suitable refinement to the theoretical model or alternatively whether a more complete non-linear potential theory analysis such as that due to Lau (1983) is required.

One possible source of departure of the experimental results from those of the linear diffraction program which can not be accounted for by improvement of the potential theory formulation is associated with the occurrence of viscous effects either in the interaction with the cylinder or the transmission of the wave. The experimental study has therefore been designed to include a test of the conservation of energy so that energy losses can be identified.

5.3 Experimental Apparatus and Procedure

5.3.1 Wave Flume, Generator and Beach

Experimental results have been obtained for a horizontal circular cylinder located in a glass-sided flume of approximate length 17m, width 0.75m with an effective maximum water depth of 0.555m. The waves are generated by the vertical oscillation of a triangular cross-sectioned wedge and absorbed by a three-legged beach at the other end of the flume.

Detailed studies of the waves in the flume have been made by Coates (1982) and Ellix and Arumugam (1983) and it is therefore only necessary to give a brief account here.

No simple theory is available for this type of generator but Coates (1982) applied the linear theory for waves generated by the small oscillation of a vertical plane (Havelock, 1929, Ursell, Dean and Yu, 1960) to give an indication of the generator efficiency. It was concluded that backflow under the wedge results in an 18% loss of efficiency based on measured wave height and wedge stroke values for a range of waves. This loss of efficiency is significant in the present study because it is required that steep non-linear waves are generated and it is therefore necessary to restrict the range of waves to those which are sufficiently short to give a rapid decay of particle motion with depth. This restriction minimizes the back flow under the generator but the maximum wave steepnesses attainable under stable conditions are no greater than 0.1 which is only about two thirds of the maximum wave steepness generally expressed as

$$H/L = 0.142 \tanh(kh) \qquad 5.3.1$$

In the theoretical considerations of section 3.10 it was demonstrated that the second-order diffraction theory predicts a wave motion which is composed of a wave of similar form to the Stokes second-order wave and an additional second-order free wave with dispersive properties which are independent of the primary motion. The formulation which gave rise to this prediction may be applied to the problem of bodies in motion of which the oscillating wedge is an example and therefore it might be suggested that the free waves identified in the above mentioned studies are not as first thought due to imperfections in the wedge oscillation but are a result of the fluid wedge interaction. Since no results are available for

for the theoretical predictions these suggestions can not as yet be verified quantitatively.

In a particularly thorough study of the waves generated by the wedge Ellix and Arumugam (1983) have employed the fast Fourier transform technique to distinguish between the second-order free and second-order fixed waves. The free surface oscillations at twice the fundamental frequency at a location are separated into those which are in phase and those which are in quadrature with the fundamental oscillation. By measurement of these components at a number of locations over several wavelengths and plotting the results the amplitudes of the two distinct waves at this frequency are identified. The results for the Stokes second-order wave are in reasonable agreement with the theoretical values for a range of waves up to a steepness of H/L = 0.06 and the ratio of second-order free and fixed wave amplitudes plotted against wave steepness indicates that the free wave is more of a feature for long small amplitude waves which are not chosen in the present study.

In the time between the two studies referred to in this section the absorbing beach was reconstructed to improve the dissipative properties and therefore to reduce the reflection of wave energy. The beach now consists of three lengths the first extending from the bottom of the tank to a "knee" at an intermediate depth is 2.44 m long and the second length which extends from this location to the still water level is 3.13 m long. For the studies reported in this thesis the inclinations of these first two lengths were 7.7^{o} and 4.2^{o} respectively and the reflection coefficient is generally restricted to less than 3% and never exceeds 5%. Energy is

dissipated by inducing wave breaking as the wave enters shallow water and any remaining energy is either reflected or absorbed by friction on the final horizontal section of the beach which 1.26m long.

One feature often misunderstood in wave flume experiments is the reflection of waves incident upon the generator. These waves which may be the result of reflection from the beach or reflection from a model located in the flume are reflected with minimal energy loss but, provided that this process is not highly non-linear, the only effect of this process is to give a small modification to the amplitude and phase of the waves propogating from the wedge.

It may be concluded that the steeper shorter waves chosen for the present study may be described as Stokes second-order waves with neglible free wave and reflected wave components.

5.3.2 Measurement of free surface elevation

The oscillation of the free surface at a fixed location is measured by using resistance wave probes with a purpose built amplifier based on a design developed at the Hydraulics Research Station. The probes are calibrated statically before each set of experiments by displacing the probe through a sequence of known distances in still water and recording the voltage output. Comprehensive initial results for this calibration procedure are given in figure 5.3.1 and the excellent linearity of the response to changes in immersed length permits a less detailed calibration for subsequent tests.

A feature of this measurement system which has only recently

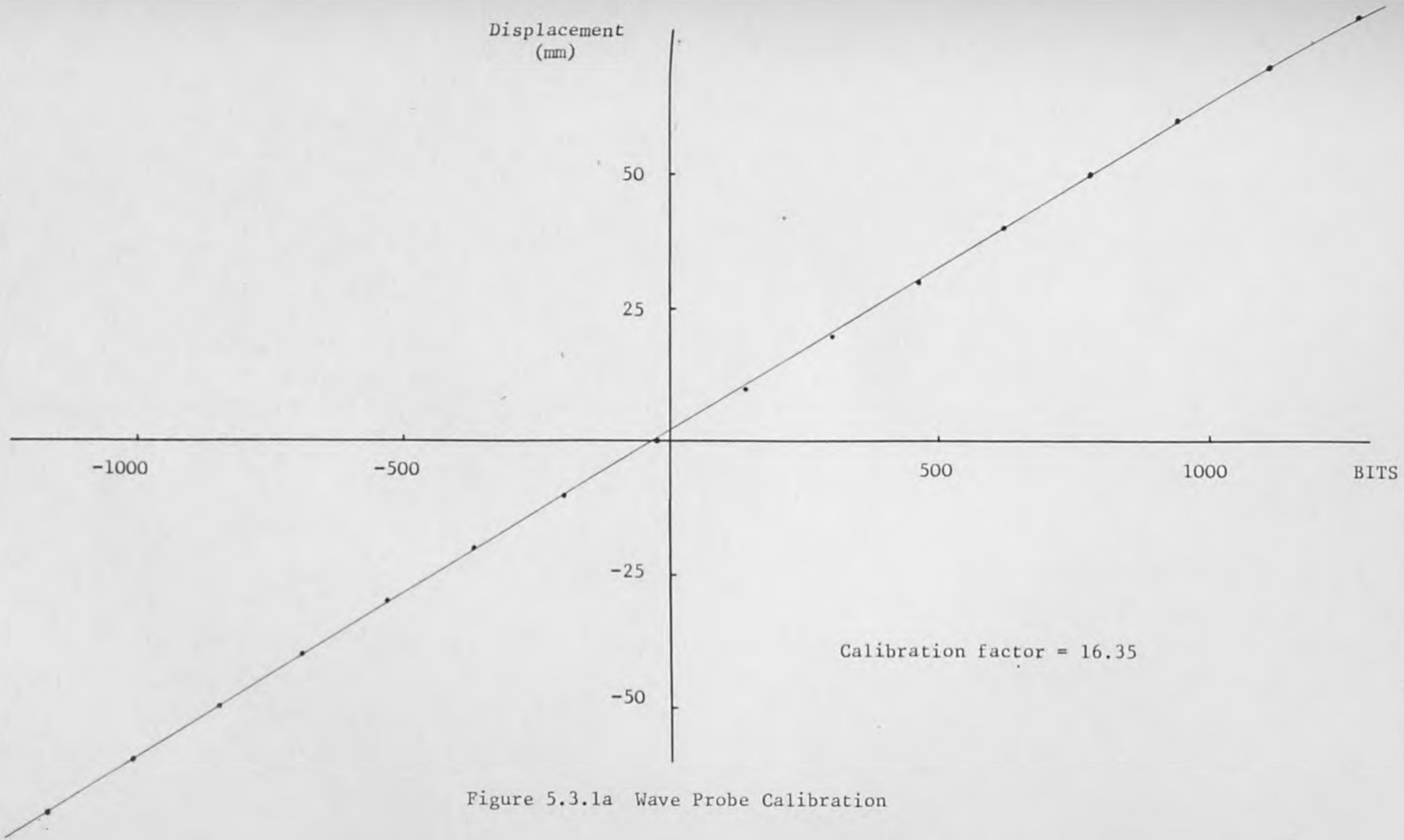

Figure 5.3.1a Wave Probe Calibration

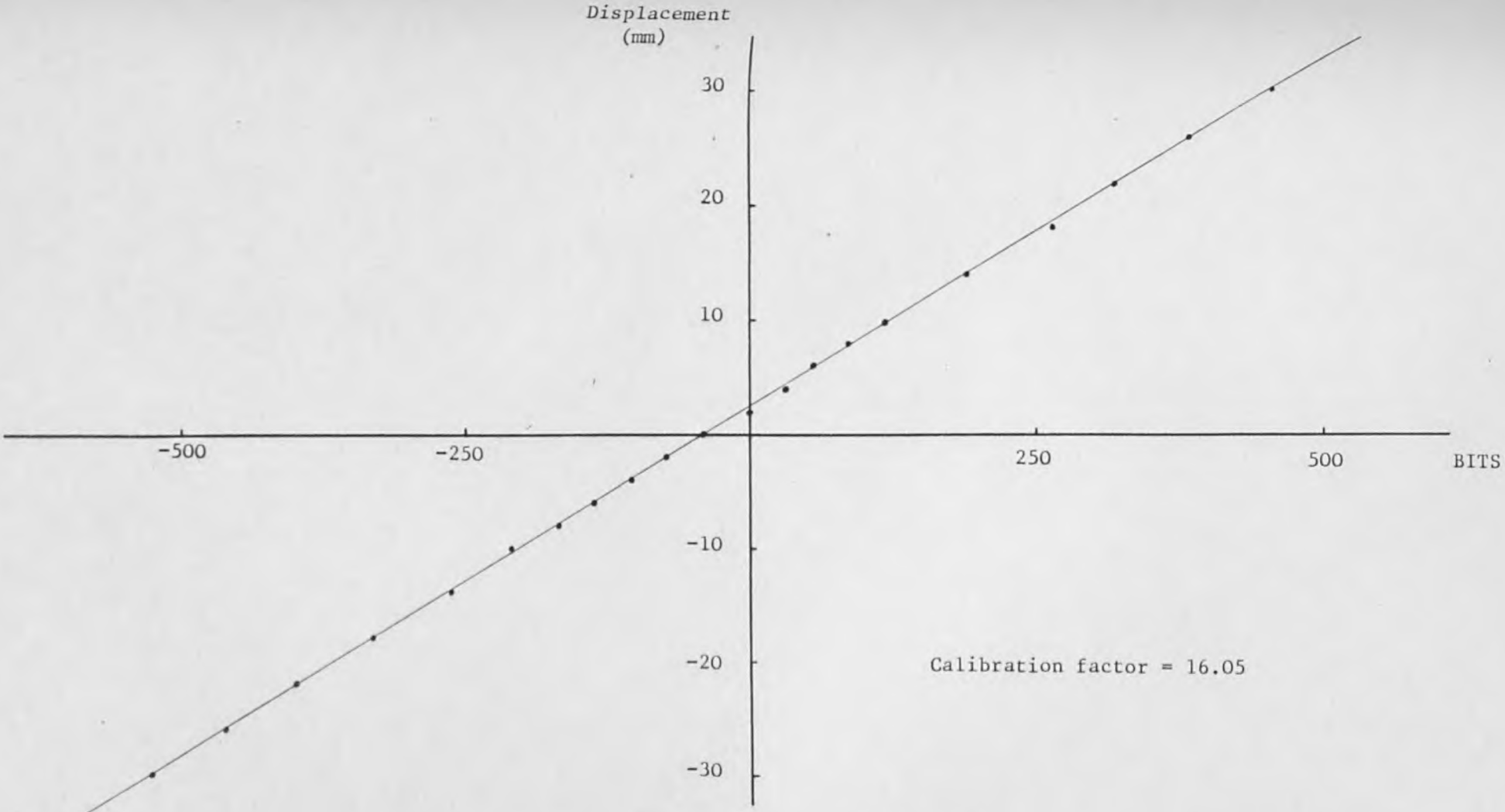

Figure 5.3.1b Wave Probe Calibration

been appreciated is that the results of a dynamic calibration differ from those obtained by the equivalent static calibration. This is thought to be due to the amplifier characteristics and if ignored results in errors in amplitude and phase measurement which are too large to be neglected. The present study is only concerned with the measurement of free surface displacement and these measurements must be made using the results of the static calibration factor with a dynamic amplification factor which is both frequency and amplitude dependent. All measurements of wave height in this study are obtained by the Fast Fourier transform technique, the use of which is discussed later. Two points are relevent here: firstly the measured amplitude, $H_m/2$, at the wave frequency, f_o, is obtained by the empirical equation

$$\frac{H_m(f_o)}{H_s(f_o)} = (1 + 0.0113\ f_o^{2.40} + 0.0037\ f_o^{2.51} \log(H_s(f_o))) \qquad 5.3.2$$

where $H_s/2$ is the scanned wave amplitude obtained by application of the static calibration constant obtained by the procedure outlined above, and secondly the value of $H_m/2$ obtained by this means is the true wave amplitude provided oscillations at three times the wave frequency or higher are negligible.

The calibration equation 5.3.2 has been obtained by fitting a curve to a set of data obtained by oscillating a wave probe through a known distance in still water and for all tests the measured value lies within $\pm$ 1% of the value predicted. These results are reproduced in figure 5.3.2. Because the range of frequencies and

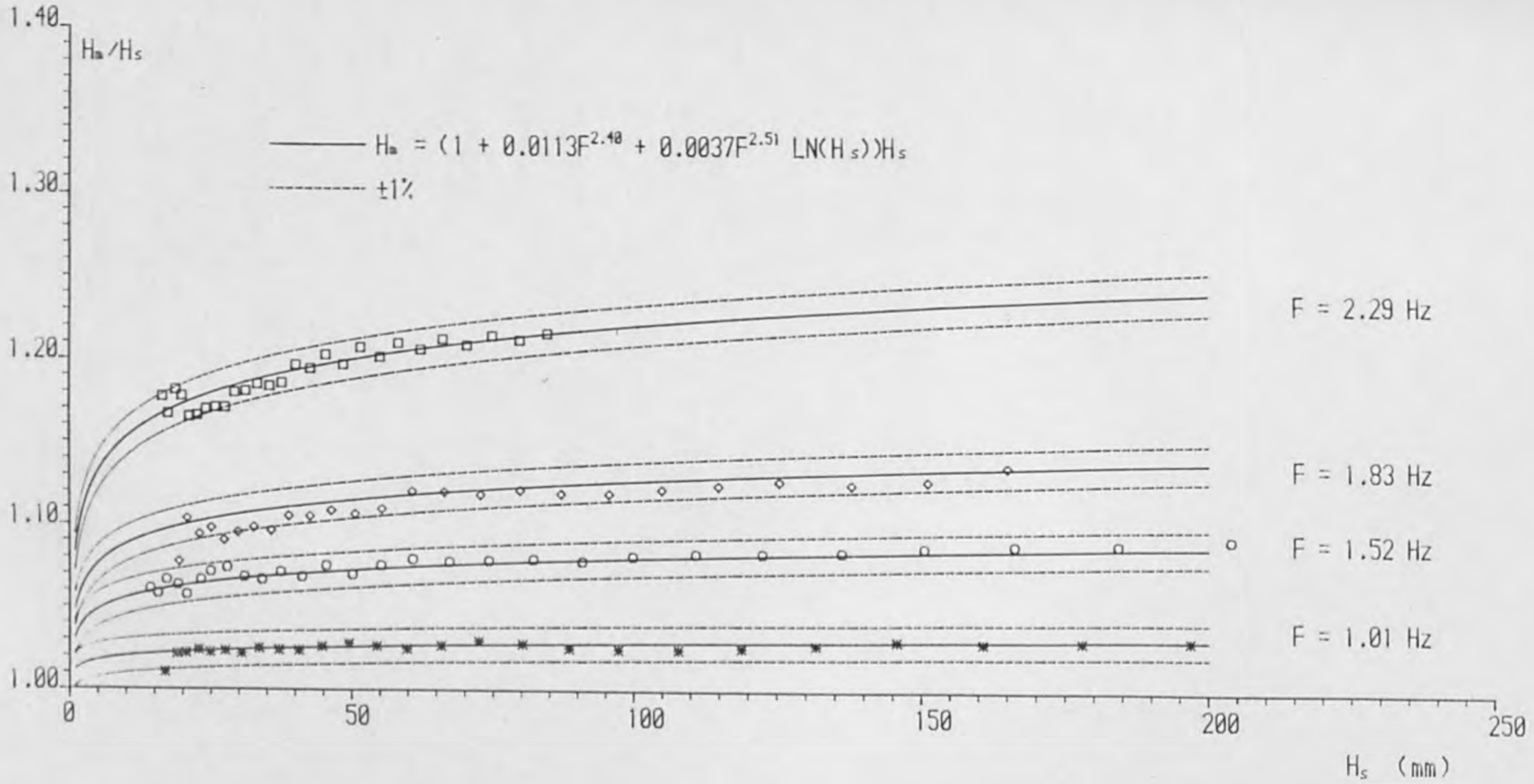

Figure 5.3.2 Wave probe dynamic calibration

wave heights which occur in the experimental study lie within the range of frequencies and amplitudes from which equation 5.3.2 is derived the equation can be applied with some confidence, however, the correction of oscillations at higher frequencies is problematic. If the same formula is used it must be extrapolated to smaller amplitudes of oscillation than those for which the formula is known to apply. In the absence of any alternative this procedure is employed but it is noted that the measured amplitudies of oscillation at multiples of the wave frequency may be subject to errors of unknown magnitude.

5.3.3 Measurement of Pressure

Pressures have been measured using a number of low range Bell and Howell transducers (BHL 4054-10, 35 mbar) with a SE Labs bridge conditioning unit (SE 995).

The pressure measurements have been obtained for two different problems: firstly for a preliminary study of the pressure field under a wave in the absence of any obstacle and secondly for the study of the pressures on a submerged circular cylinder. The transducers have been located outside the wave flume on a purpose built rack and therefore two problems must be considered. The first is a problem which is absent in the measurement of pressures on surface piercing obstacles and is concerned with the possible modification of the pressure signal due to the passage of tubing from the pressure tapping to the transducer through the moving free surface. To avoid this problem, rigidly fixed, small

bore metal piping has been used to prevent the amendment of the pressure signal. The second problem is common to all measurements with a remote pressure transducer and relates to the possibility of the damping of the dynamic pressure signal. Hutchinson (1979) reports that if the length of tubing is restricted to 1m or less dynamic pressure response is maintained up to 15 Hz. In the present study the practical range of frequencies (including higher-order oscillations) is well within this limit and preliminary experiments with various lengths of tubing gave no evidence of any damping.

For a single transducer connected to a pressure tapping by a length of tubing the calibration is achieved in situ by introduction of a branch of tubing which is open to the atmosphere. Isolation of the pressure tapping by clamping the nylon tubing does not affect the head of water in the calibtation branch so that the output signal from the transducer is also unaffected. With the transducer subject to the same static head as for pressure measurement the calibration procedure is executed by movement of the branch of tubing through a sequence of known vertical distances. For pressure measurement the calibration branch is closed to the atmosphere. Typical results of detailed calibration tests are given in Figure 5.3.3 for two different ranges of pressure.

For the calibration of the four transducers used in the measurement of the pressures on the submerged cylinder the procedure is identical to that which is described above for the single transducer with the exception that the calibration branches are connected so that the transducers are calibrated simultaneously.

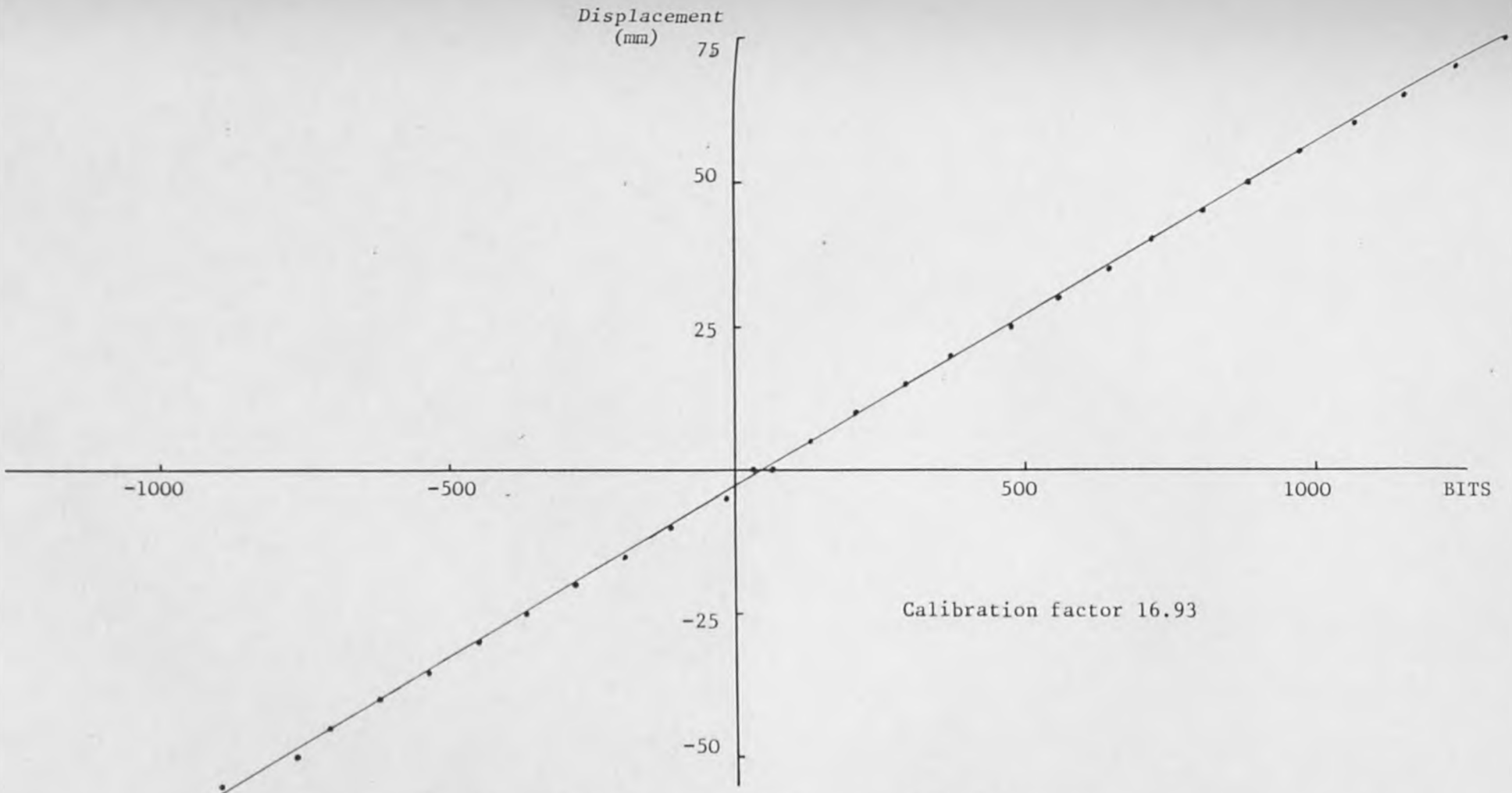

Figure 5.3.3a Pressure Transducer Calibration

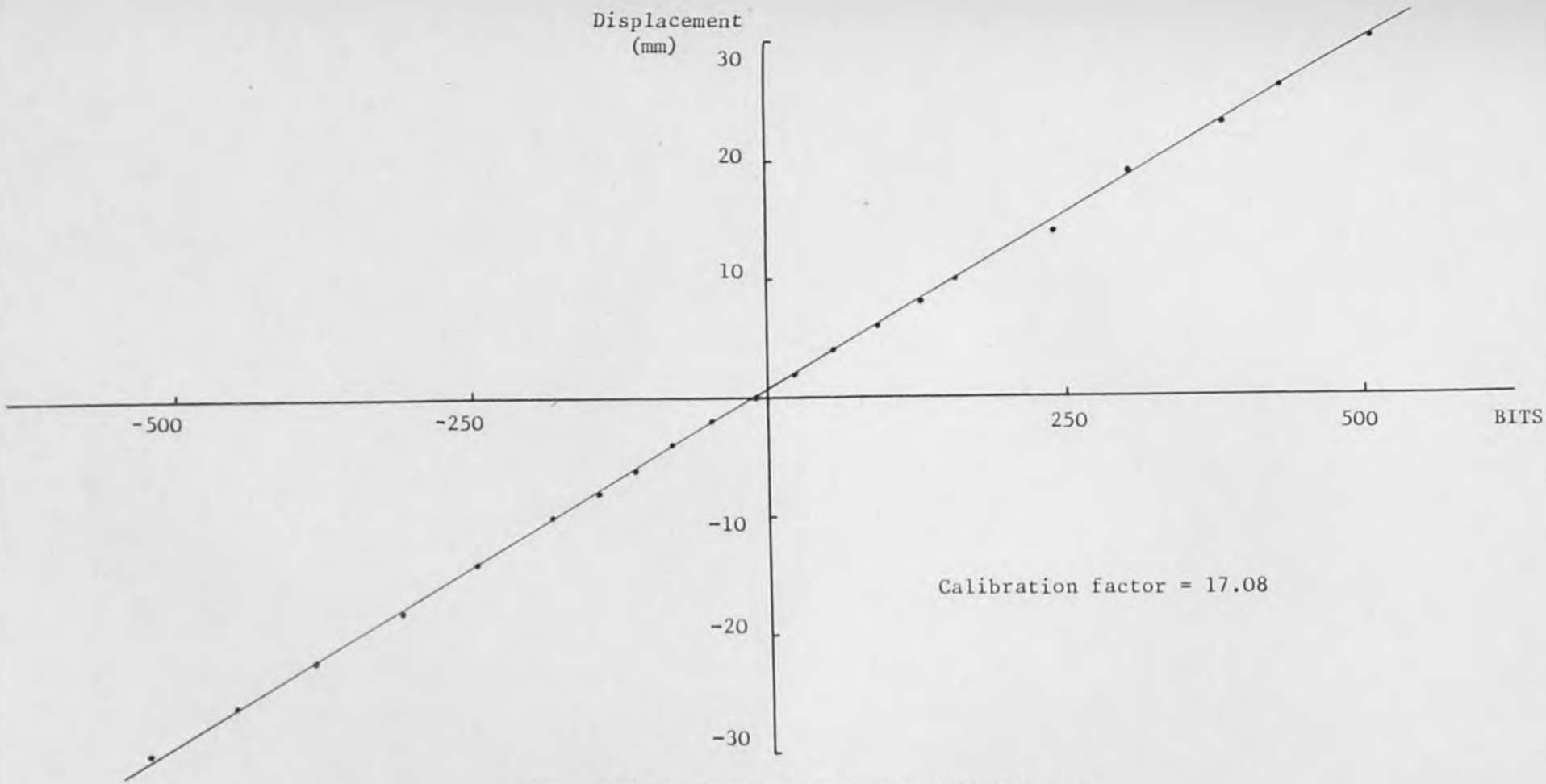

Figure 5.3.3b Pressure Transducer Calibration

For the measurement of pressures under a wave in the absence of a cylinder a pressure plate has been constructed. The plate has been designed to restrict deformation of the wave motion to a minimum and to ensure that any such deformation is restricted to regions away from the point of measurement. This is achieved by locating a pressure tapping at the centre of a flat circular plate of 310mm diameter (approximately 4 x maximum amplitude of particle oscillation) with bevelled edges and all attachments and connections located behind the measurement face. A sketch of this arrangement is given in figure 5.3.4 which indicates that the pressure tubing is braced to the support arm to prevent movement of the tubing and possible modification of the pressure signal.

5.3.4 Data Collection and Analysis

The fluctuating voltage signals from the wave probe and pressure transducer amplifiers are fed into a scanner module which performs an analogue to digitial conversion. The software available on the Digital pdp-11 micro computer permits scanning of the signal at intervals which are multiples of the mains frequency and the data is written to a disc file. The data obtained in this way is in binary form and must be converted to decimal form and calibrated before analysis.

A number of software packages have been developed for scanning, conversion, calibration and analysis of data which permit interactive use of the computing facility while performing the experiments. All of the analysis in this study has been

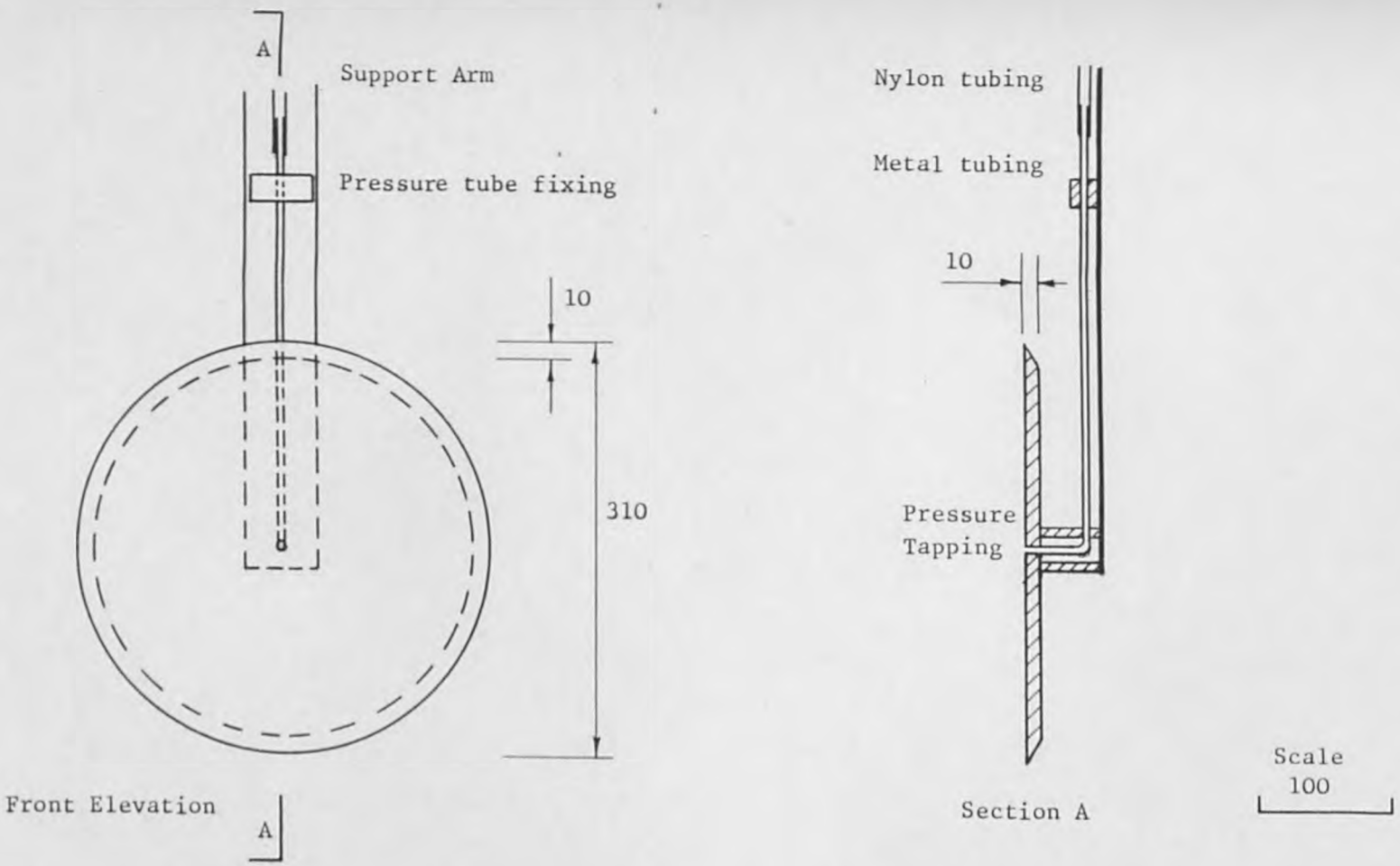

Figure 5.3.4 Pressure Plate

performed on the micro computer but the 'link' with the university main frame computer has been used to obtain graphical output where necessary. A flow diagram indicating the various stages in the collection and analysis of data is given in figure 5.3.5.

Analysis of the data collected to obtain values for the wave height and pressure is achieved by using a fast Fourier transform software package mounted on the mico-computer. The method permits the evaluation of the coefficients in the Fourier series.

$$s = a_o + a_1\cos\omega t + b_1\sin\omega t + a_2\cos 2\omega t + b_2\sin 2\omega t + \ldots\ldots \qquad 5.3.3$$

where s is the input signal. The magnitude of the signal at any frequency is obtained by the expression

$$s_n = \sqrt{a_n^2 + b_n^2} \qquad 5.3.4$$

In this study the values of interest are the oscillations at the fundamental or wave frequency and at twice this frequency and oscillations at higher frequencies are generally negligible. The constant coefficient, a_o, is potentially a valuable source of information for non-linear wave interaction problems but in this study the value can not be used. This is because the zero value of the voltage output 'drifts' during the course of the testing so that although oscillatory values may be evaluated with confidence the measurement of changes in mean values is subject to errors which are not much smaller than the quantities to be measured.

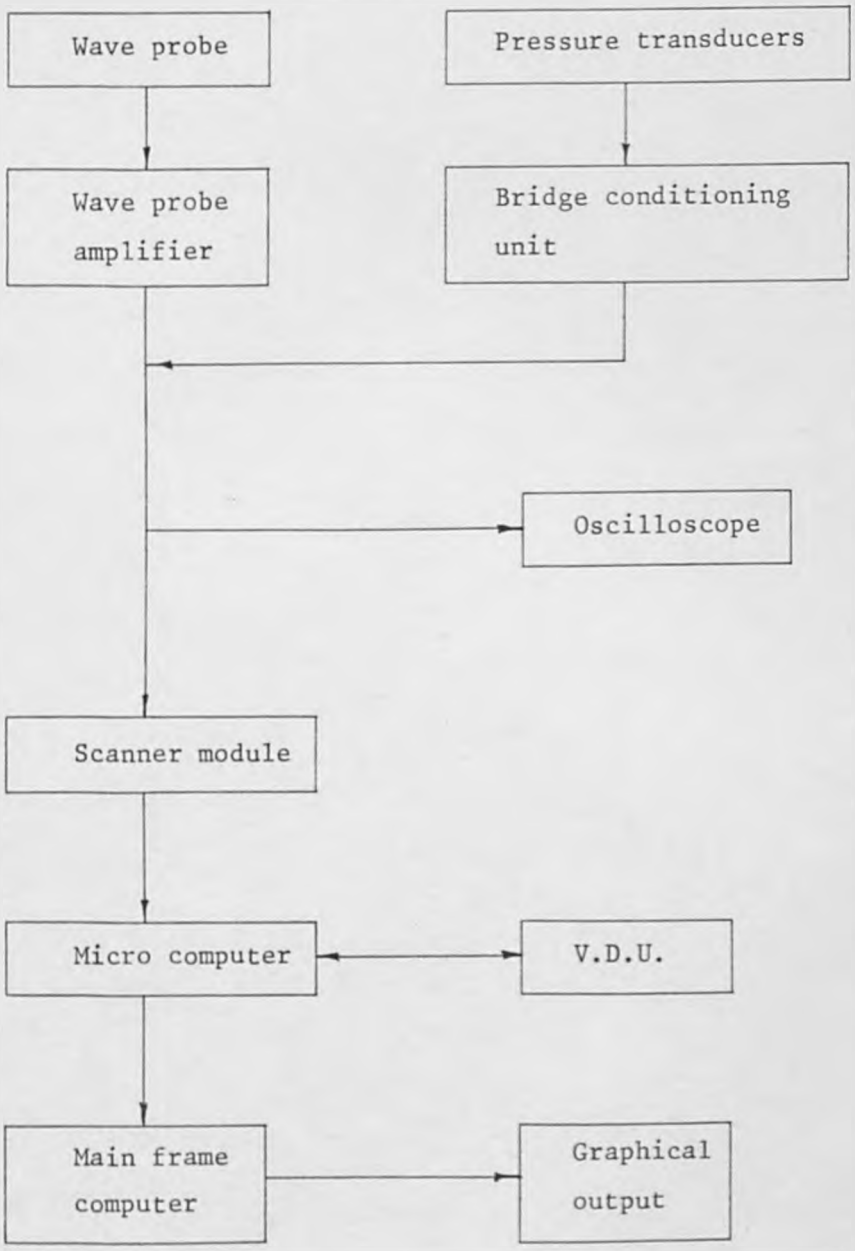

5.3.5 Collection and analysis of experimental data

The accurate prediction of pressures under a wave by linear wave theory or the prediction of pressures on a submerged obstacle by the diffraction computer program depends on the measurement of the wave height. It is therefore important to obtain a precise measurement of the wave travelling in the flume.

If the free surface displacement η is measured at any single location the oscillation may consist of a number of components. If it is initially assumed that all oscillations at frequencies other than the wave frequency may be neglected the problem is reduced considerably and only two components must be considered: the incident and the reflected wave. The free surface displacement may therefore be expressed as

$$\eta = \frac{H_I}{2} (\cos(kx - \omega t + \alpha) + R \cos(kx + \omega t + \beta)) \qquad 5.3.5$$

where H_I is the incident wave height, R the reflection coefficient and α and β are phase shifts.

Equation 5.3.5 may be taken as a complete description of wave motion in two dimensions because if more than one dispersive wave of the same frequency is travelling in the same direction the sum of the two waves may be expressed in the same form. This is best appreciated by reference to the experimental set up. If the oscillation of the wedge gives rise to a wave of height H_1 and a wave travelling in the direction opposite to this wave is reflected at the wedge giving rise to a second wave of height H_2 travelling in the same direction as the first the sum of these two wave will be

$$\frac{H_1}{2} \cos(kx - \omega t + \alpha_1) + \frac{H_2}{2} \cos(kx - \omega t + \alpha_2)$$

$$= \frac{H_I}{2} \cos(kx - \omega t + \alpha) \qquad 5.3.6$$

where $H_I^2 = (H_1 + H_2)^2((\sin\alpha_1 + \sin\alpha_2)^2 + (\cos\alpha_1 + \cos\alpha_2)^2)$ 5.3.7a

and $$\tan\alpha = \frac{\sin\alpha_1 + \sin\alpha_2}{\cos\alpha_1 + \cos\alpha_2} \qquad 5.3.7b$$

This is the wave much must be taken as the incident wave and is in agreement with equation 5.3.5. If two waves travel in the opposite direction, say waves reflected by the beach and an obstacle, the same sort of summation occurs and again equation 5.3.5 describes completely the reflected wave motion.

It is necessary to employ a method by which the incident wave height, H_I, and the reflection coefficient, R, can be measured and clearly the information provided by a single measurement at a fixed location does not provide sufficient information. Goda and Suzuki (1976) have reported the use of a method in which the oscillations of the free surface at two points separated by a known distance are measured and a fast Fourier transform is employed to separate waves travelling in opposite directions over a range of frequencies. This method has been tested but has been found to give unreliable results.

The method adopted for evaluation of H_I and R takes advantage of the spatial variation of the free surface displacement. Modification of equation 5.3.5 is required to demonstrate this feature

$$\eta = \frac{H_I}{2} (\cos(kx + \alpha)\cos\omega t + \sin(kx + \alpha)\cos\omega t$$

$$+ R\cos(kx + \beta)\cos\omega t - R \sin(kx + \beta)\sin\omega t)$$

$$= \frac{H_I}{2} ((\cos(kx + \alpha) + R\cos(kx + \beta))\cos\omega t$$

$$+ (\sin(kx + \alpha) - R\sin(kx + \beta))\sin\omega t)$$

$$= \frac{H_I}{2} A(kx)\cos(\delta(kx) - \omega t) \qquad 5.3.8$$

where $$A^2(kx) = 1 + R^2 + 2R \cos(2kx + \alpha + \beta) \qquad 5.3.9a$$

$$\tan(\delta(kx)) = \frac{\sin(kx + \alpha) - R\sin(kx + \beta)}{\cos(kx + \alpha) + R\cos(kx + \beta)} \qquad 5.3.9b$$

Equation 5.3.8 with equation 5.3.9 indicates that there is a variation of the first-order wave height along the length of the wave flume and that the maximum and minimum values are

$$H_{max} = (1 + R) H_I \qquad 5.3.10a$$

$$H_{min} = (1 - R) H_I \qquad 5.3.10b$$

Examination of equation 5.3.9 indicates that there is a sinusoidal variation of wave height with a wavelength equal to L/2 and a wave height of $R\ H_I$. On the basis of these results it is possible to evaluate the wave height and the reflection coefficient if the maximum and minimum values of the wave height are measured. The relevent equations are

$$H_I = \frac{1}{2} (H_{max} + H_{min}) \qquad 5.3.11a$$

$$R = \frac{H_{max} - H_{min}}{H_{max} + H_{min}} \qquad 5.3.11b$$

One method which has been adopted in some studies for the measurement of the wave height and reflection coefficients employs two wave probes. The wavelength is measured and then the probes are separated by a distance L/4 which is the distance between the maximum and minimum wave heights. The two probes are then moved until the difference between the two signals is maximised and the required values are then obtained by application of equation 3.5.11. This method is subject to one minor objection concerning the separation of the probes. For steeper waves the wavelength is modified and is different from the value obtained by application of the linear dispersion equation so that the separation of probes by a distance L/4 will not correspond exactly to a separation by half the beat wavelength.

The method used in this thesis requires the measurement of the oscillation of the free surface with a single probe at a number of locations over a distance greater than L/2. The fast Fourier transform technique is then applied to obtain a value for the magnitudes of the oscillations at the wave frequency and equation 5.3.11 is applied to obtain the required values (H_I and R). A typical plot of the results is given in figure 5.3.6 and it may be noted that this method has been chosen because it not only satisfies the requirement that the incident wave height is measured accurately, but also permits the determination of the magnitudes of the components of the wave which oscillate at twice the wave frequency.

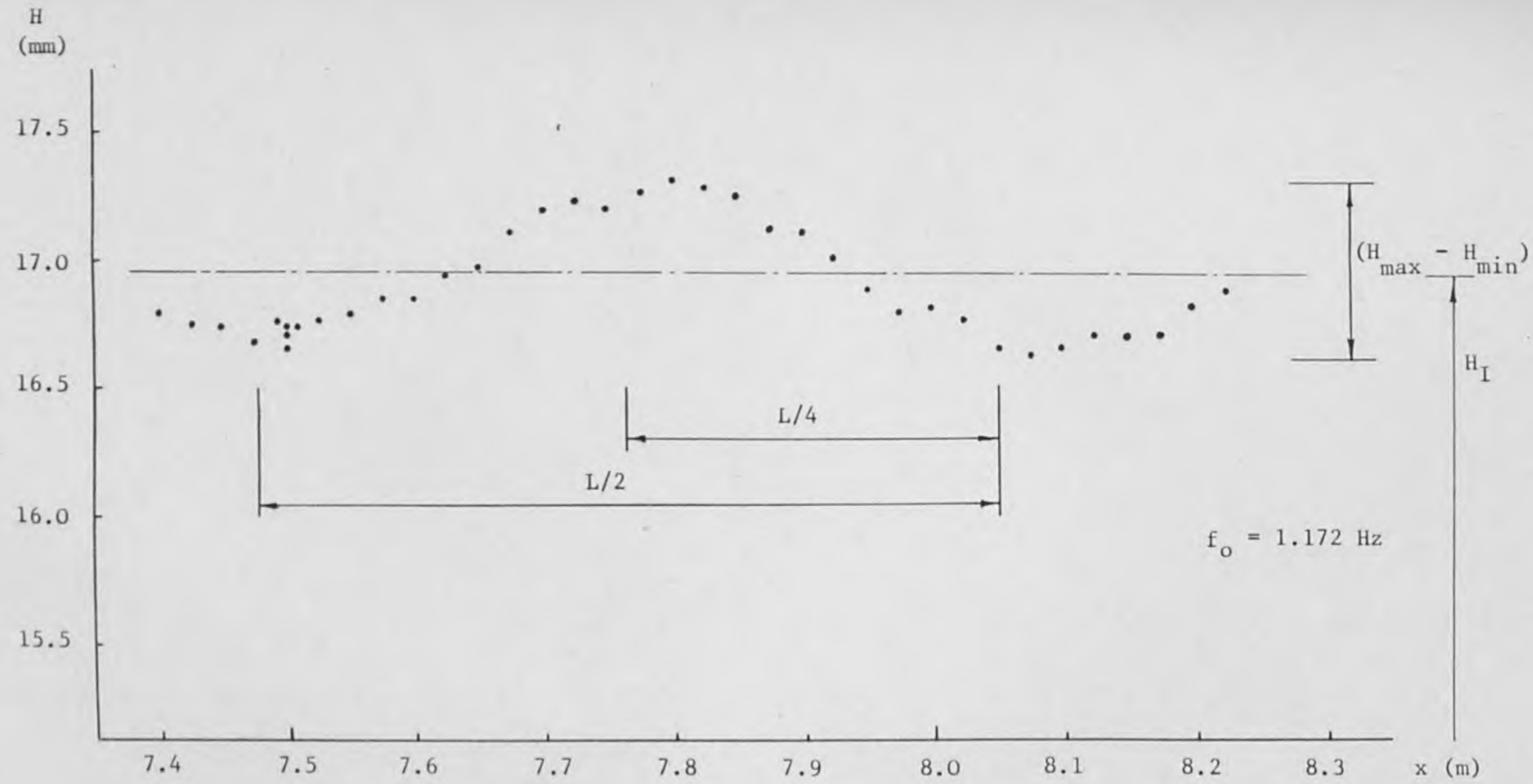

Figure 5.3.6 Variation of wave height

Having determined the magnitude of the incident wave height it then becomes possible to obtain a prediction of the pressure on the surface of a submerged obstacle from the values predicted by the diffraction computer program. The theoretical pressure amplitude, p_t, is given by

$$p_t = \frac{H_I}{2} \bar{p} \qquad 5.3.12$$

where $\bar{p}$ is the non-dimensional value obtained from the program. It is emphasised that the linear theory can only predict oscillations at the wave frequency, f_o, and in this study the theoretical pressure p_t is therefore compared with the amplitude of the measured pressure oscillation at this frequency. Employing the Fourier series as written in equation 5.3.3 the measure pressure amplitude, p_m, is given by

$$p_m = \sqrt{(a_1^2 + b_1^2)} \qquad 5.3.13$$

and this use of the fast Fourier transform technique might be regarded as a filtering procedure.

A second value of the use of the fast Fourier transform technique in measuring the free surface oscillation is that the magnitudes of the components of the wave at twice the wave frequency may be evaluated. Four components are expected to exist: a fixed wave which travels with the main wave, a free wave which travels independently of main wave and reflected waves corresponding to these two components. The reflected waves may be neglected in this study since their magnitude is small and therefore of no physical

significance but it may be noted that Ellix and Arumugam (1983) have used the data provided by the measurement of the free surface oscillations at several locations to evaluate the reflected wave amplitude at twice the wave frequency.

In the present study there are two problems for which knowledge of the magnitudes of these components is instructive. Firstly, if the fixed and free components at twice the fundamental frequency in the indicent wave may be evaluated it may be established whether or not the cylinder responds to a monochromatic wave and then by comparison of the measured pressure oscillations at the same frequency it may be established whether these are due to a non-linear interaction or are simply a linear response to the free wave. Secondly, the evaluation of the fixed and free second-order components in the diffracted wave, which in the case of the horizontal cylinder is the transmitted wave, provides useful information for comparison with the theoretical second-order formulation of chapter 3.

At any point along the wave flume the oscillation of the free surface at twice the wave frequency, η_2, may be expressed in the form

$$\eta_2 = \frac{H_{21}}{2} \cos(2kx - 2\omega t + \alpha) + \frac{H_{22}}{2} \cos(k_2 x - 2\omega t + \beta_2) \qquad 5.3.14$$

where H_{21} is the height of the fixed wave and H_{22} is the height of the free wave, α_2 and β_2 are phase shifts and k_2 satisfies the dispersion equation

$$\left(\frac{2\omega}{g}\right)^2 = k_2 \tanh k_2 h \qquad 5.3.15$$

Comparison of equations 5.3.14 and equation 5.3.5 indicates that the first component on the right hand side is locked into the fluctuation of the incident wave at the wave frequency, hence the reference to this component as a fixed wave. The technique employed to distinguish between the two components at twice the wave frequency requires that the data recorded commences exactly at a wave crest in order that the amplitude of the oscillation at the wave frequency is given by the coefficient a_1 in equation 5.3.3 with $b_1 = 0$. Measurement of the free surface oscillation at a number of locations along the wave flume provides data from which the magnitudes of the fixed and free waves may be evaluated. The quadrature component of the oscillation at twice the wave frequency (the coefficient b_2 in equation 5.3.5) gives the spatial variation of the free wave from which the amplitude may be obtained. The in-phase component will give approximately the same magnitude of spatial variation but this variation will be about a mean position which gives the amplitude of the fixed wave. These features may be expressed by the formulae

$$\frac{H_{22}}{2} = \frac{1}{2}(a_{2max} - a_{2min}) = b_{2max} \qquad 5.3.16a$$

$$\frac{H_{21}}{2} = \frac{1}{2}(a_{2max} + a_{2min}) \qquad 5.3.16b$$

where a_{2max} and a_{2min} are the maximum and minimum values in the spatial variation of the in-phase Fourier component and b_{max} is the maximum value of the quadrature component.

5.3.5 Test Cylinder

A circular cylindrical model has been constructed for use in two sets of experiments. In the first set the diffracted wave is measured and in the second set pressures and measured at four locations on the cylinder surface. A sketch of the cylinder is given in figure 5.3.7 and the following requirements were considered in design and construction:

1) The cylinder diameter should be appropriate for testing of wave diffraction.

2) The cylinder should be rigidly fixed with the axis parallel with the still water level.

3) The supporting rig should permit location of the cylinder at any required depth of submergence.

4) The cylinder should span the entire width of the channel.

5) Pressure tappings should be remote from any local disturbances due to the passage of tubing through the wave and therefore the tubes are located at one end of the cylinder and the tappings are located centrally.

6) Pressure tubing should be rigid and must be restrained from moving in response to the wave motion. The small bore metal tubing is therefore fixed to the support arm.

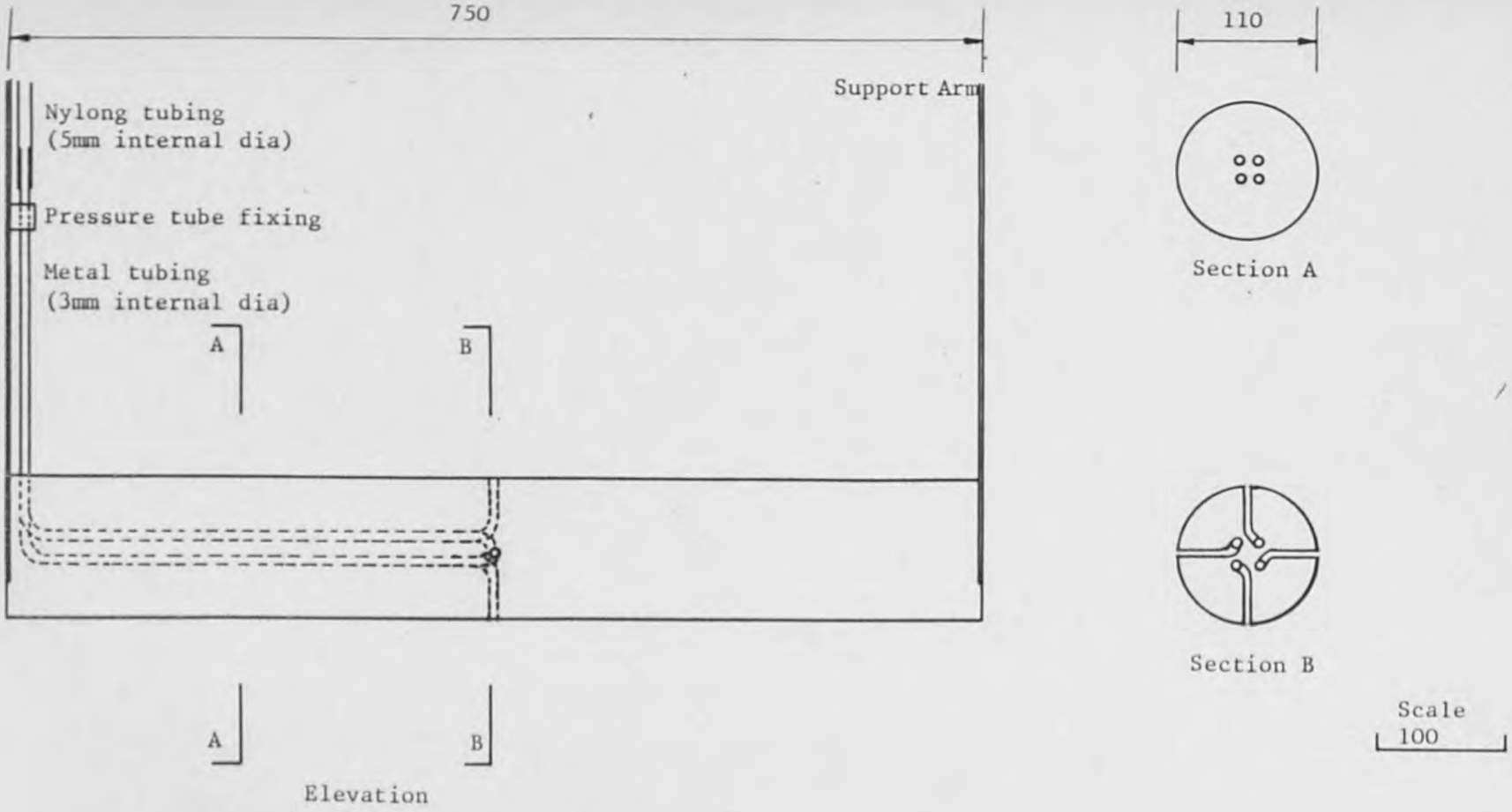

Figure 5.3.7 Experimental Model

5.3.6 Accuracy of Measurements

If a meaningfull comparison is to be made between experimental and theoretical results it is necessary to consider the possible sources of error in the measurement system. Determination of an estimate of the magnitude of the experimental error permits the identification of genuine discrepancies between the results of the mathematical model and results obtained by measurement. The various errors which occur in the measurement system are now considered in turn.

Evaluation of calibration factors for the wave probe and each of the pressure transducers is a source of small errors. Random errors may be identified in the data from which values of the calibration factors are obtained (figures 5.3.1 and 5.3.3) but these errors, which are in fact small, are only relevent to a consideration of the accuracy of the measurement system if they lead to an error in evaluation of the calibration factor. The data is sufficient to permit a very accurate calibration of the wave probe and all the pressure transducers and the assumption of linear response is clearly satisfactory.

The only other source of error in the calibration system is associated with the failure of the wave probe static calibration procedure to provide an accurate factor which may be applied to a fluctuating signal. Because this problem is due to the limitations of the 'home made' amplifier it is not anticipated that similar problems occur in calibration of the pressure transducers. The series of tests performed to determine the variation of the dynamic

calibration correction factor indicate that the empirical formula provides a good model for oscillations of similar amplitude and frequency to those for which measurements have been made.

It may therefore be concluded that significant errors in individual measurement of wave height and pressure due to poor calibration are unlikely but that small systematic errors are inevitable and will contribute to the overall error in the measurement system.

A second type of error in the measurements of wave height and pressure is associated with the small amount of irregularity in the wave motion and in the mechanisms of interaction. Such errors are random and are minimized by taking several measures to ensure that the final recorded values are a good average representation of the amplitudes of the fluctuating quantities. For the wave height and pressure amplitude measurements data is recorded for a minimum of ten cycles of the wave motion so that application of the fast Fourier transform package has an averaging effect. This accounts for the good agreement which has been obtained for any repeated measurements. The method which is used to evaluate the magnitude of the incident wave also results in a reduction in the importance of random errors and all pressure measurements are repeated so that the values presented in the next section of this chapter are the average of two measurements.

It is also possible that errors are introduced due to the use of the results of the fast Fourier transform technique. The software has been extensively tested for harmonic data and the possibility of errors is concerned with the relevence of applying

the method to oscillations which depart from the simple harmonic form. In order to test the method a number of the measurements obtained by the fast Fourier transform technique are compared with the peak to peak value obtained from the same data file. Agreement was found to be good (±2% in general) if the data is collected for conditions where non-linear effects are small for fluctuations of the pressures which include oscillations at multiples of the fundamental wave frequency. However, comparisons for pressure oscillations recorded when non-linear effects are of significance are less satisfactory.

Errors in the measurement system are clearly small and it is suggested that the errors which will be incurred are less than ±5% of the measured values. The measurement of smaller quantities may be subject to a greater uncertainty due to the fluctuating level of noise within the system but these errors are still small. It seems that it is possible to measure quantities which are as small as 0.5mm with reasonable accuracy.

5.4 Presentation of Results

5.4.1 Incident wave motion

Before commencing the experimental investigation of waves interacting with a submerged horizontal cylinder a set of experiments were performed in which the pressure at points in the fluid beneath a progressive wave were measured. The purpose of these tests was to determine the accuracy with which small amplitude wave theory

predicts the pressure field beneath waves of finite height for the same range of waves which are employed in the subsequent experiments for wave cylinder interaction.

A similar set of experiments has been reported for waves in the same wave flume by Coates (1982) who measured the pressure at a fixed location 399 mm above the bed of the flume for a water depth of 523mm. These experiments used a pressure transducer which was a great deal less sensitive than that which has been used in the present study and therefore the calibration proved difficult and was noted to be a possible source of error. If the results are corrected for the dynamic calibration of the wave probes the measured results lie within ±10% of the predicted value. The author concluded that in view of the possible errors in the measurement procedure (high noise levels and calibration difficulties) there is nothing to suggest that the linear wave theory is inadequate.

There are two main differences between the study of Coates and the present study. The availability of a more sensitive pressure transducer gives an improved measurement system and the use of the fast Fourier transform technique permits the determination of the spectral composition of the pressure signal.

The choice of waves has been governed by a number of considerations which may be listed as follows:

1) In order to obtain results for which wave scattering effects are significant it is necessary to choose higher frequency waves.

2) In order to minimise the effects of refraction it is

necessary to generate waves for $h/L > 0.5$ and because of the limitation imposed on the value of the water depth, h, by the flume it is required that wavelengths are short and frequencies correspondingly high.

3) In order to obtain results for a wide range of wave steepness it is necessary to generate waves which are of shorter wavelength because it is for these conditions that the efficiency of the wedge type generator is maximised.

4) It is convenient to choose a frequency which corresponds exactly with the frequency bands at which the fast Fourier transform package gives results.

5) It is necessary to generate waves which are of sufficient amplitude to permit accurate measurement of pressure and therefore the very short waves which may be generated in the flume are unsuitable because they are only stable for small wave heights.

The waves which have been used in this study have already been described (Section 5.2.2) and the choices largely satisfy the requirements outlined above. The waves chosen are higher frequency waves but because the maximum water depth in the tank requires that $L > 1.110$m for deep water conditions ($h/L > 0.5$), the lowest frequency waves are in water of finite depth ($h/L = 0.35$). The significance of the bottom is not however great and this is demonstrated by examination of the particle orbits at the various cylinder locations. The minimum value of the ratio of the minor and major axes of the elliptical orbit is 0.8 so that there is a close resemblence to the circular orbit of a particle in a deep water wave.

An additional advantage in choosing waves which are in the deep water range is that the theoretical pressure value obtained by Stokes' wave theory is correct to the second-order and if this is confirmed in the experiments by the absence of pressures oscillating at twice the wave frequency then the occurence of any higher frequency oscillations in the pressure measurements on the obstacle surface must be due to non-linear wave obstacle interaction.

The theoretical pressure amplitude, p_t, for waves in water of finite depth is given, correct to second-order, by

$$p_t = \rho g \frac{H}{2} \frac{\cosh k(h + y)}{\cosh kh} \cos(kx - \omega t) \qquad 5.4.1$$

$$+ 3\rho g \frac{H}{2} \frac{\pi H}{2L} \frac{1}{\sinh(2kh)} \left[\frac{\cosh 2k(h + y)}{\sinh^2 kh} - \frac{1}{3} \right] \cos 2(kx - \omega t)$$

$$- \rho g \frac{H}{2} \frac{\pi H}{2L} \frac{1}{\sinh(2kh)} (\cosh 2k(h + y) - 1)$$

The changes in the steady pressure as given by the third component on the right hand side of equation 5.4.1 are not measured in this study and computation of the pressure fluctuations at twice the wave frequency for the range of waves used in this study indicates that theoretical values are very much smaller than any value which can be measured. Therefore, the theoretical pressure for comparison with measured values is given by the first component on the right hand side of equation 5.4.1.

For the study of pressures in the incident wave it is

not necessary to obtain a value for the incident wave height, H_I, and the local measured wave height, H_m, is used to obtain a theoretical estimation of the pressure amplitude. This is because the pressure fluctuations are in phase with the free surface fluctuations and if the local wave height is the sum of an incident and a reflected wave the pressure below that point will be due to the addition of the pressures for each of the waves.

The results of the tests for a range of waves with measurements at a number of depths are presented in table 5.4.1. The measured pressure amplitude is denoted by p_m and the value s_2 includes components due to the Stokes' correction and the free wave which cannot be separated by a single measurement. No measured values of the pressure amplitude at twice the wave frequency are given because no values were obtained which could be distinguished from the noise on the spectrum and therefore these values are always less than 2% of the measured pressure amplitude at the wave frequency.

For the intermediate frequency (f_o = 1.172) the variation of the measured pressure with depth compared with the theoretical variation is presented in figure 5.4.1. Examination of table 5.4.1 and figure 5.4.1 indicates that small amplitude wave theory gives results which for the range of waves tested underestimates the pressure under a wave. It may be noted that agreement is best for waves of small steepness and that the discrepancies are often greater than the expected experimental error.

$\frac{y_o}{L}$	$\frac{H}{2}$ (mm)	$\frac{H}{L}$	$\frac{s_2}{H}$	P_t (mm)	P_m (mm)	$\frac{P_m}{P_t}$	Error (mm)
.15	8.9	.021	.04	3.5	3.9	1.12	0.4
.15	19.4	.046	.07	7.6	7.2	.95	0.4
.15	39.5	.095	.11	15.4	18.0	1.17	2.6
.30	8.5	.020	.05	1.3	1.5	1.16	0.2
.30	19.4	.046	.07	3.0	3.4	1.15	0.4
.30	38.3	.092	.14	5.9	7.2	1.23	1.3

Frequency, f_o = 1.367 Hz Wavelength, L = 0.835 m

Table 5.4.1a Incident wave pressure measurements

$\frac{y_o}{L}$	$\frac{H}{2}$ (mm)	$\frac{H}{L}$	$\frac{s_2}{H}$	P_t (mm)	P_m (mm)	$\frac{P_m}{P_t}$	Error (mm)
.08	17.8	.031	-	10.6	11.4	1.08	0.8
.09	17.7	.031	-	10.0	10.6	1.07	0.6
.10	17.7	.031	-	9.5	10.2	1.08	0.7
.11	7.6	.013	-	3.8	4.1	1.08	0.3
.11	17.6	.031	-	8.9	9.8	1.10	0.9
.11	30.6	.053	.08	15.4	16.6	1.08	1.2
.11	42.9	.076	.17	21.6	24.6	1.14	3.0
.12	17.7	.031	-	8.4	9.2	1.09	0.8
.13	17.7	.031	-	8.0	8.7	1.08	0.7
.14	17.6	.031	-	7.5	8.1	1.08	0.6
.15	17.6	.031	-	7.1	7.8	1.09	0.7
.17	17.6	.031	-	6.2	6.8	1.09	0.6
.19	17.5	.031	-	5.4	5.9	1.09	0.5
.21	17.6	.031	-	4.8	5.2	1.07	0.4
.22	7.6	.013	-	2.0	2.1	1.07	0.1
.22	17.7	.031	-	4.6	4.9	1.07	0.3
.22	30.1	.053	.10	7.8	8.6	1.10	0.8
.22	42.6	.076	.17	11.0	12.5	1.14	1.5
.23	17.6	.031	-	4.2	4.5	1.06	0.3

Frequency, f_o = 1.172 Hz Wavelength, L = 1.132 m

Table 5.4.1b Incident wave pressure measurements

$\frac{y_o}{L}$	$\frac{H}{2}$ (mm)	$\frac{H}{L}$	$\frac{s_2}{H}$	P_t (mm)	P_m (mm)	$\frac{P_m}{P_t}$	Error (mm)
.08	14.6	.018	-	9.1	9.5	1.04	0.4
.08	29.6	.037	.09	19.0	19.1	1.01	0.1
.08	48.9	.062	.10	30.5	32.4	1.06	1.9
.16	14.6	.018	-	5.9	6.1	1.04	0.2
.16	29.6	.037	.07	11.9	12.5	1.05	0.6
.16	49.4	.062	.10	19.8	21.5	1.08	1.7

Frequency, f_o = 0.977 Hz Wavelength, L = 1.595 m

Table 5.4.1c Incident wave pressure measurements

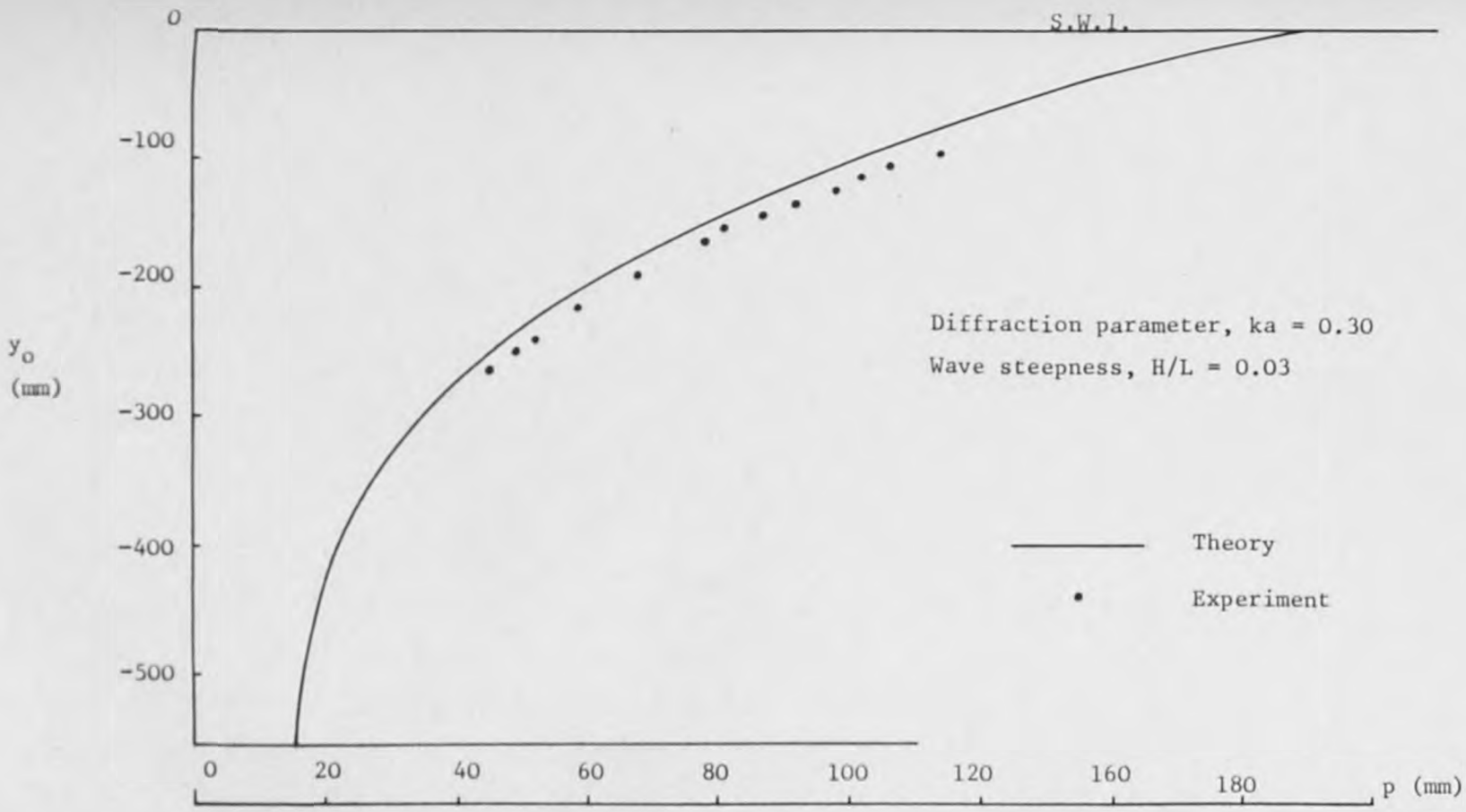

Figure 5.4.1 Variation of Pressure with Depth

5.4.2 Reflection and Transmission of Waves

The classical diffraction theory (John, 1950) predicts that the total wave motion for waves interacting with a submerged obstacle may be regarded as the linear superposition of three component motions. The three components are the primary or incident wave, the secondary wave and the local wave. For the two dimensional problem, which is the subject of this study, the secondary wave travels away from the obstacle combining with the primary wave downstream of the cylinder to make up the transmitted wave. Upstream of the cylinder the secondary wave travels in the opposite direction to the primary wave and the waves beat. The form of the local wave must be determined by a theoretical analysis and for the present problem the diffraction computer program is used to evaluate the magnitude of the free surface oscillations in the vicinity of the cylinder as well as in the far-field.

The detailed measurements of the wave motion have been obtained at the same frequencies as in the study of pressures on the cylinder surface. However, the cylinder locations and wave heights are different. The cylinder was located at a single depth for all the measurements so that the cylinder depth parameter has values $0.044 < (y_o-a)/L < 0.084$ and the range of wave steepness is $0.015 < H_I/L < 0.087$. Therefore, although the values of the cylinder submergence and wave steepness parameters differ from the values which have been set for the study reported in the next section there is a clear similarity. This means that any physical mechanisms identified in the present study will occur in the subsequently reported study and may be of assistance in explaining

discrepancies between theoretical and experimental pressure magnitudes.

In order to determine the form of the wave motion in both the far-field and near-field measurements of the free surface oscillations at a large number of locations have been obtained for ten waves. The fast Fourier transform technique has been employed to determine the magnitude of the oscillation at the wave frequency and the results have been plotted together with the linear theory predictions in figures 5.4.2a - j. Details of the diffracted wave are given in table 5.4.2 but before considering the results for wave transmission and energy loss which are included in this table a detailed examination of the graphical results is made.

The numerical results for the spatial variation of wave height demonstrate that the linear theory predictions do take the form described by John (1950). The reflected wave is clearest for f_o = 0.977 Hz when finite depth effects are significant (figures 5.4.2a - c) and all the graphs indicate that the transmitted wave is of constant amplitude. The numerical results for f_o = 1.172 and 1.367 Hz are in very close agreement with the result of Dean (1948) who demonstrated that for a wave in deep water interacting with a submerged circular cylinder there is no reflected wave and the transmitted wave has the same amplitude as the incident wave.

Theoretical results for the wave motion in the far-field due to interaction of waves with submerged obstacles have often been obtained but results for wave motion in the near field are less numerous. The results presented in figures 5.4.2 indicate that for

a cylinder located at x = 0 there is a local standing wave motion for $-L < x < L$ which combines with the progressive wave motion to give an increased amplitude of motion above and close to the cylinder. This occurence of a standing wave motion might have been proposed by a consideration of the possible deformation of the orbital motions due to the introduction of a circular obstacle. It would appear that this local wave motion becomes more significant for shallower cylinder submergence.

To permit a comparison of experimental measurements with theoretical predictions a small amplitude wave was generated at each of the three frequencies and these results are presented in figures 5.4.2a, d and h. The same comparison for steeper waves is given in figures 5.4.2b, e and i and the remaining figures (5.4.2c, f, g and j) are for steeper waves which give some indication of breaking. It must be remembered that all the results presented in this manner will be obscured to some extent by the tank reflection and the coefficient R has been recorded in table 5.4.2.

There are three aspects of the wave motion which are now considered in turn: the agreement between theory and experiment for motion in the far-field, the agreement in the near-field and the generation of free waves oscillating at multiples of the wave frequency.

The consideration of the agreement between theory and experiment for motion in the far-field requires two separate examinations of the plotted and tabulated results. Firstly the form of the reflected wave must be considered and then the form of the transmitted wave.

For each of the waves generated the measurement of the reflected wave motion is in close agreement with theory. The beating of waves is generally quite clear, particularly for the small amplitude motions, but it is never possible to identify any small amount of cylinder reflection which might occur because of the amplitude of the tank reflection.

The value of the transmission coefficient T_1, for harmonic waves oscillating at the fundamental frequency, f_o, have been taken from figure 5.4.2 and entered into table 5.4.2. For the small amplitude waves agreement with theory is reasonable but agreement for steeper waves is less good and particularly poor for some cases when wave breaking has been induced. The departure of the transmission coefficient T_1 from the theoretical value of unity indicates that there is an energy loss in the system. The energy loss coefficient P_1 may be defined as

$$P_1 = 1 - R_1^2 - T_1^2 \qquad 5.4.2$$

where R_1 is the cylinder reflection coefficient. Values of the energy loss coefficient, P_1, entered in table 5.4.2 indicate that for small amplitude waves between 5 and 10% of the energy in the system has been dissipated in the wave obstacle interaction. For steeper waves the loss is between 7½% and 11½% and for the steepest waves energy losses are as much as 20%.

Comparison of local wave measurements with the theoretical predictions is difficult for two reasons. The major difficulty

is in distinguishing between tank reflection and local wave effects. The second difficulty is in the shortage of results very close to the cylinder location. It is unfortunately not possible to obtain measurements above the cylinder because the wave probes must be submerged to half of their length to give a linear response. In spite of these difficulties it is possible to identify some agreement between theory and experiment for local wave motion.

Agreement is best for small amplitude waves and even for steeper waves and breaking waves there is evidence of agreement in the local wave motion upstream of the cylinder. However, for steeper waves and breaking waves the local wave downstream of the cylinder has a smaller amplitude of oscillation than the predicted value.

There is a significant free wave component in the transmitted wave. The amplitude of the free wave oscillating at twice the wave frequency may be isolated by the method described in section 5.3.4. A second harmonic transmission coefficient, T_2 is defined by

$$T_2 = \frac{H_{22}}{H_I} \qquad 5.4.3$$

and the measured values have been entered in table 5.4.2. The value of this transmission coefficient is greatest for the steeper waves for which breaking has not commenced.

In a similar manner it is possible to define a third harmonic transmission coefficient, T_3, so that

$$T_3 = \frac{s_3}{H_I} \qquad 5.4.4$$

and the values of T_3 which have been entered in table 5.4.2 must be due to free waves generated in the interaction.

The values of the energy loss coefficient, P_1 have indicated a loss of energy in the system. This result is obtained by a linear analysis and it is possible to include the second harmonic free wave in the energy analysis to account for the transfer of energy which must have taken place in generating this wave. A corrected energy loss coefficient P_2 is defined by

$$P_2 = P_1 - \frac{c_{g_2}}{c_{g1}} T_2^2 \qquad 5.4.5$$

where C_{g1} is the group velocity of the main wave and C_{g2} is the group velocity of the free second harmonic wave.

The correction of the energy loss coefficient does not have a significant effect even when the free waves are large and it is therefore clear that the transfer of energy to free waves at multiples of the wave frequency does not account for the loss of energy in the system.

f_o (Hz)	$\frac{(y_o-a)}{L}$	$H_I/2$ (mm)	H_I/L	R	T_1	P_1	T_2	P_2	T_3
1.367	.084	9.6	.012	.02	.97	.060	.17	.046	.04
1.367	.084	19.7	.047	.04	.96	.076	.23	.049	.09
1.367	.084	36.2	.087	.01	.89	.204	.16	.192	.05
1.172	.062	8.5	.015	.03	.99	.013	.12	.005	.06
1.172	.062	17.6	.031	.02	.96	.078	.20	.059	.04
1.172	.062	30.9	.055	.02	.94	.116	.17	.102	.05
1.172	.062	43.5	.077	.03	.90	.185	.11	.179	.07
0.977	.044	14.8	.019	.03	.97	.055	.16	.043	.08
0.977	.044	28.5	.036	.02	.95	.091	.18	.076	.09
0.977	.044	47.5	.060	.04	.97	.061	.15	.050	.06

Table 5.4.2 Diffracted Wave Results

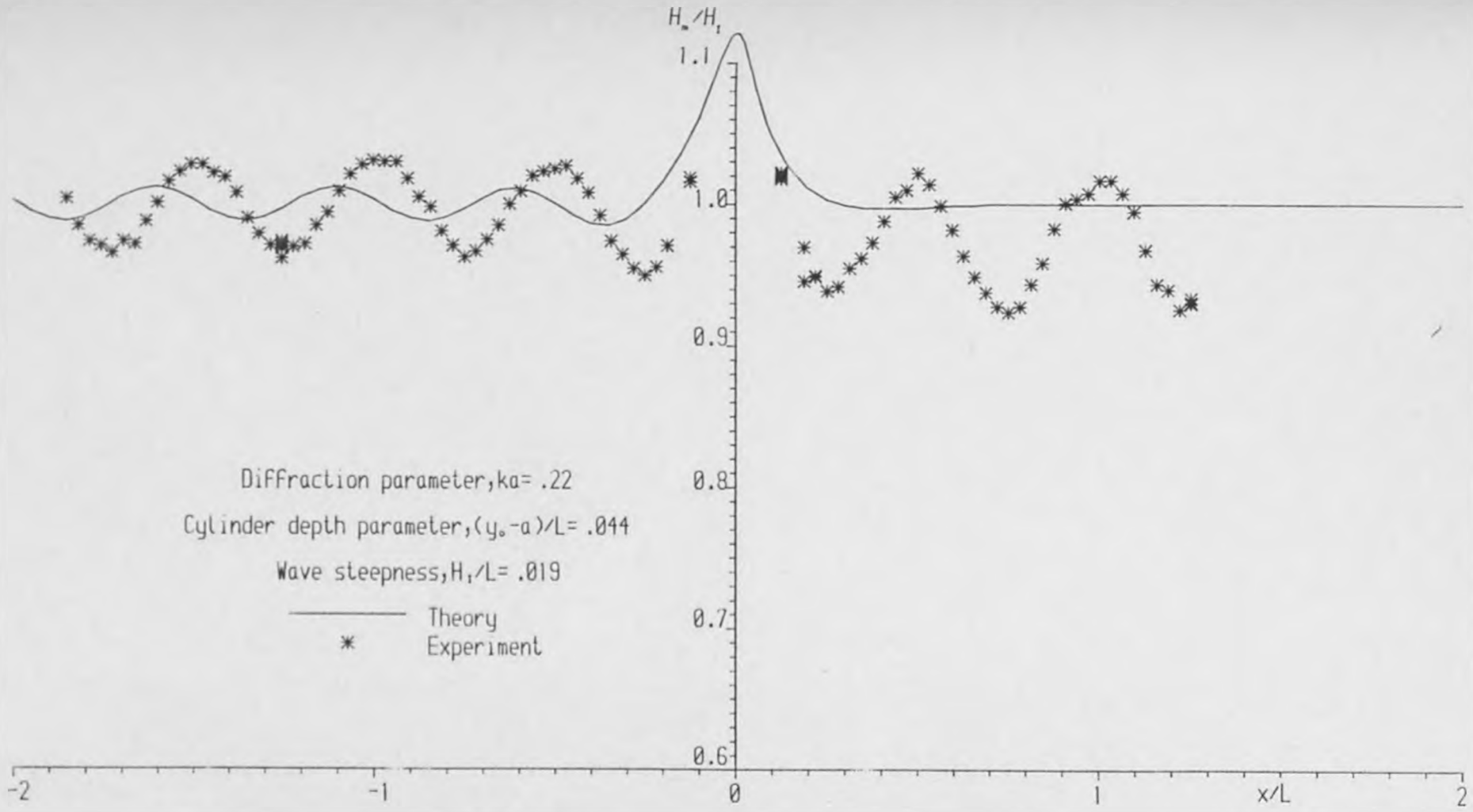

Figure 5.4.2a Spatial variation of wave height

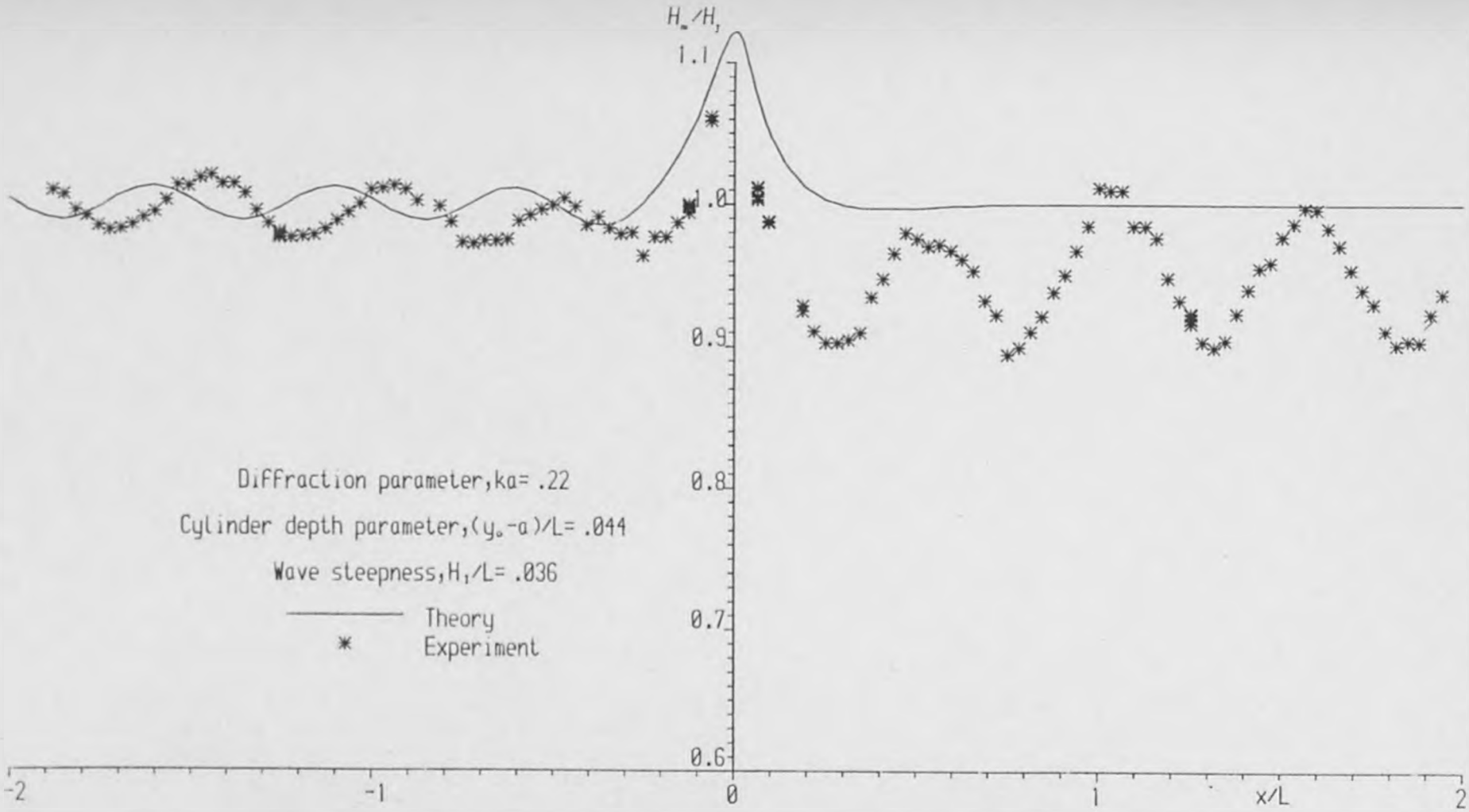

Figure 5.4.2b Spatial variation of wave height

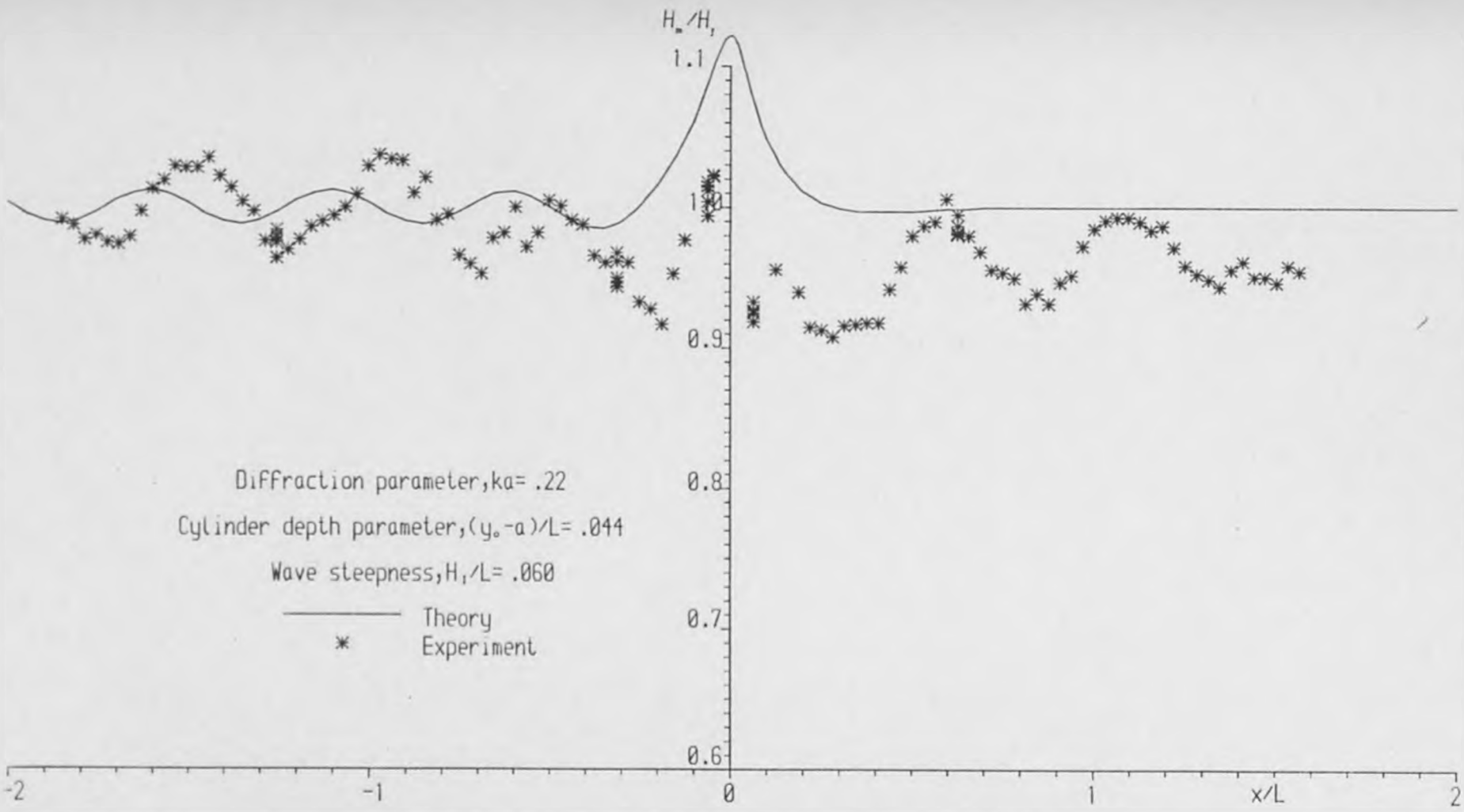

Figure 5.4.2c Spatial variation of wave height

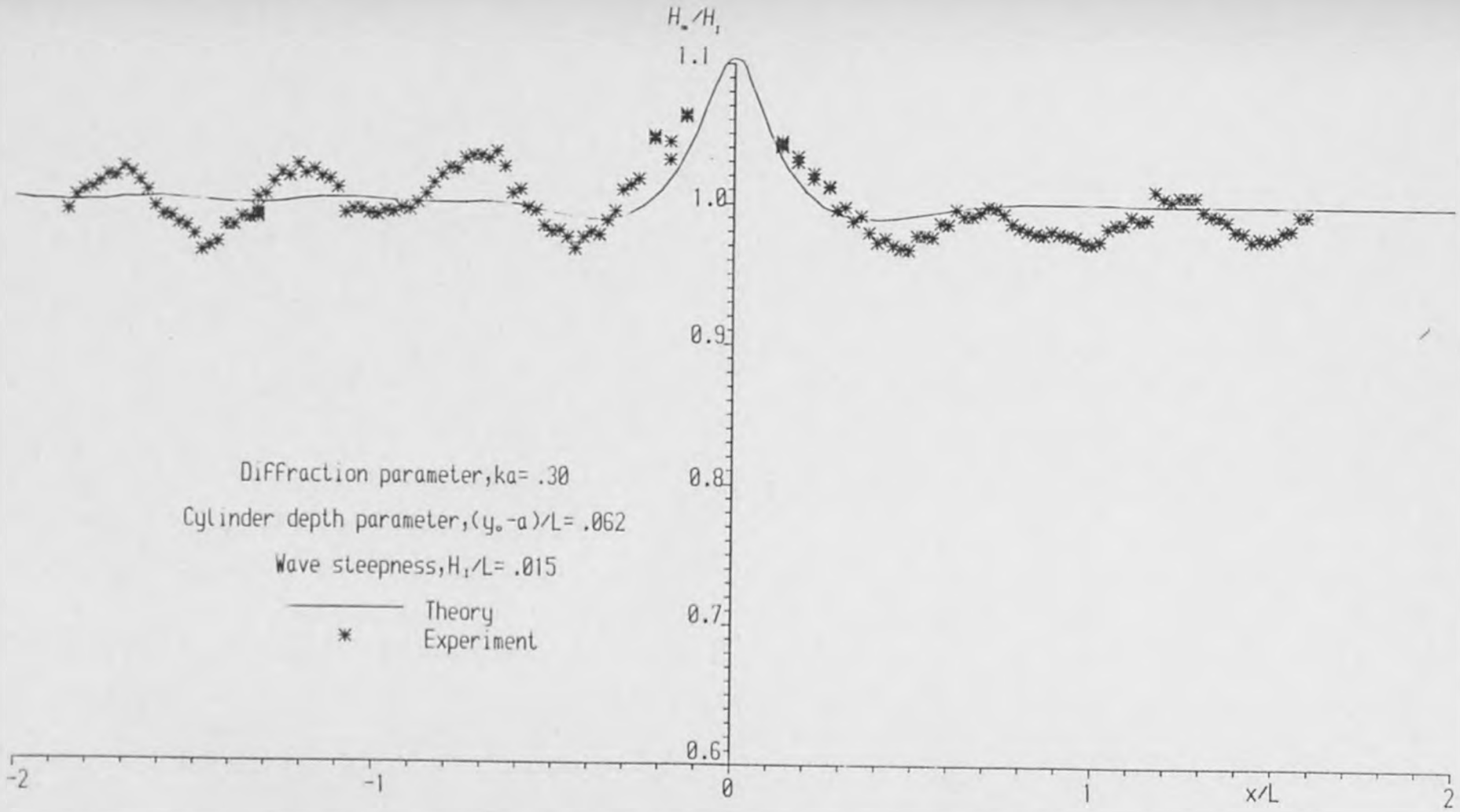

Figure 5.4.2d Spatial variation of wave height

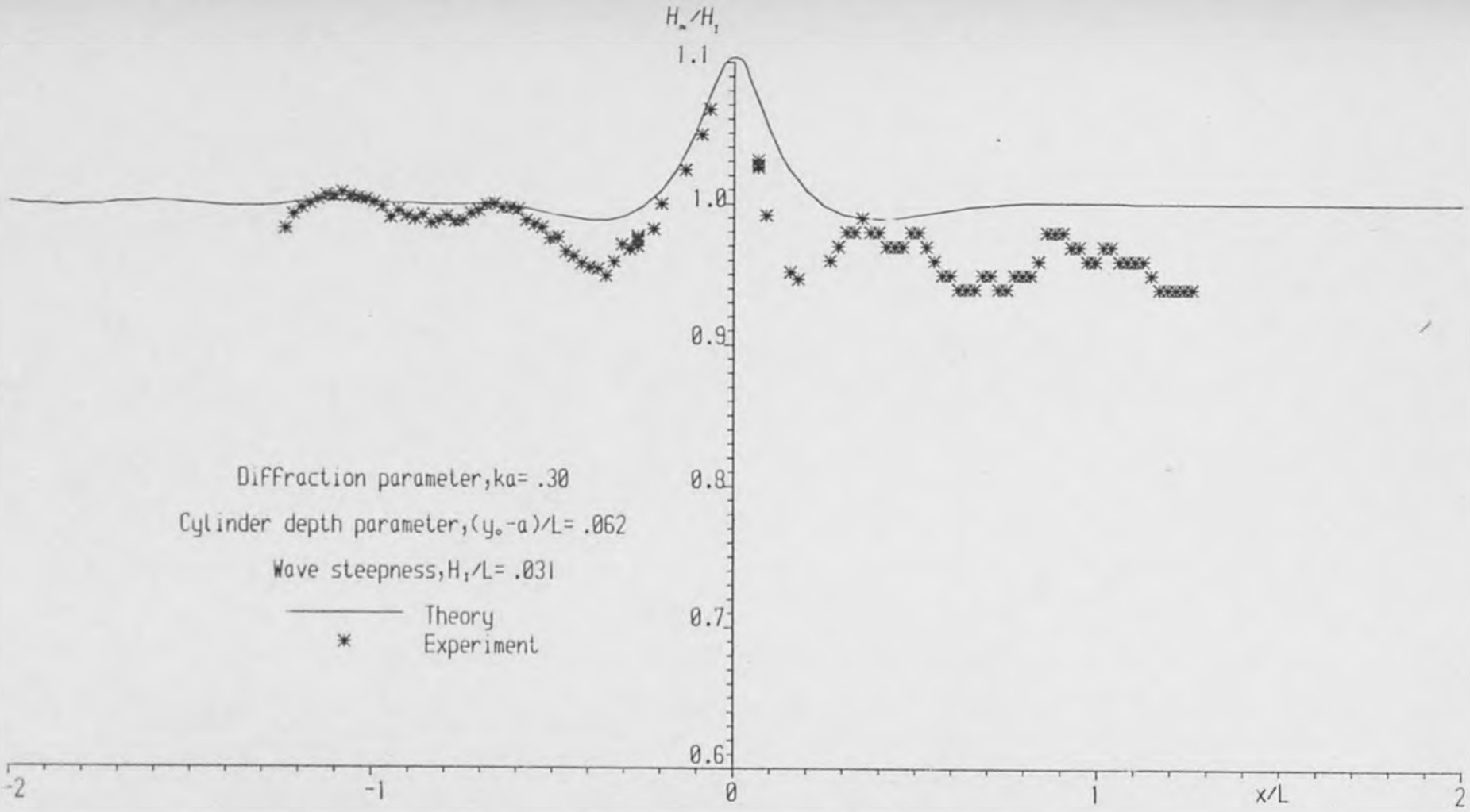

Figure 5.4.2e Spatial variation of wave height

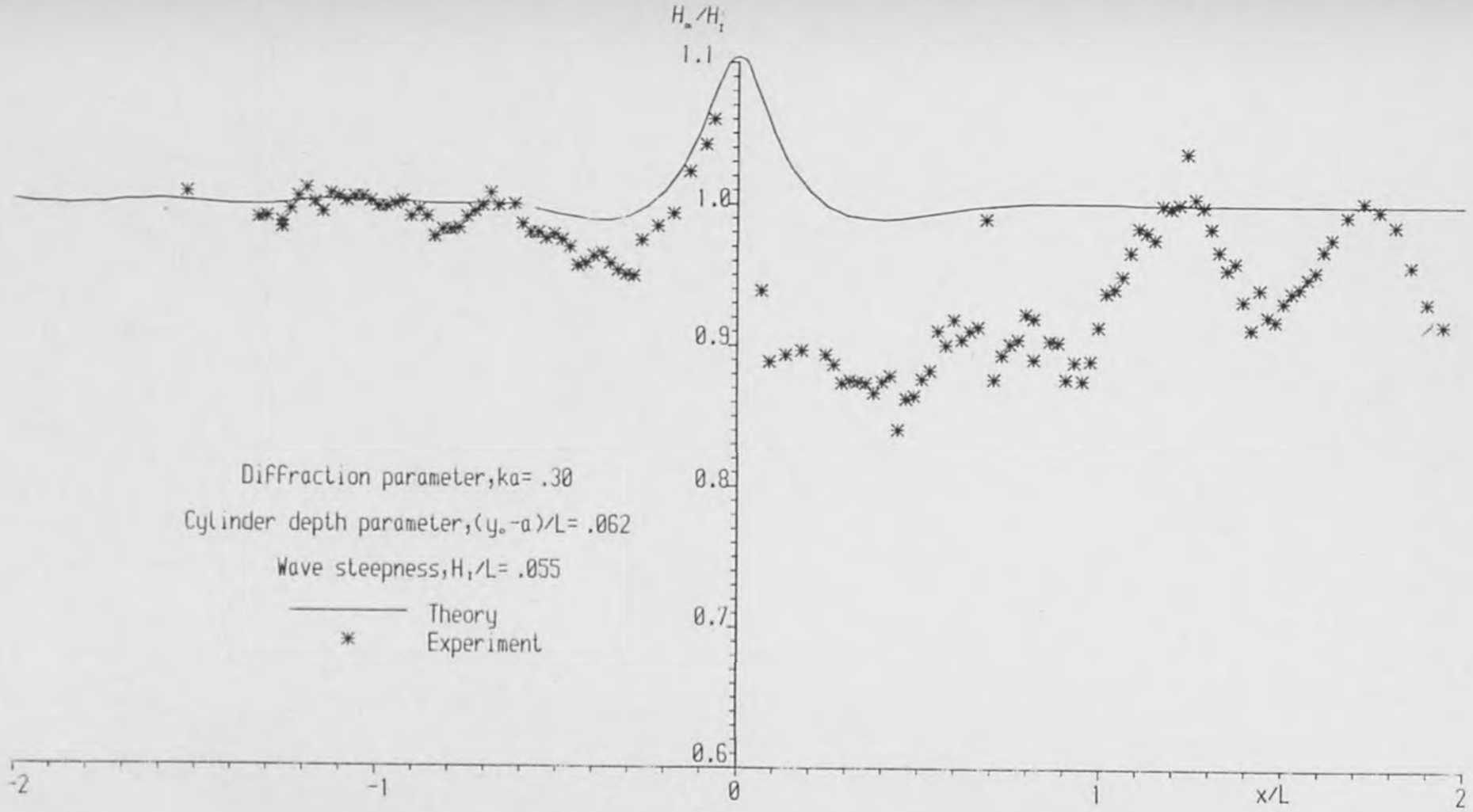

Figure 5.4.2f Spatial variation of wave height

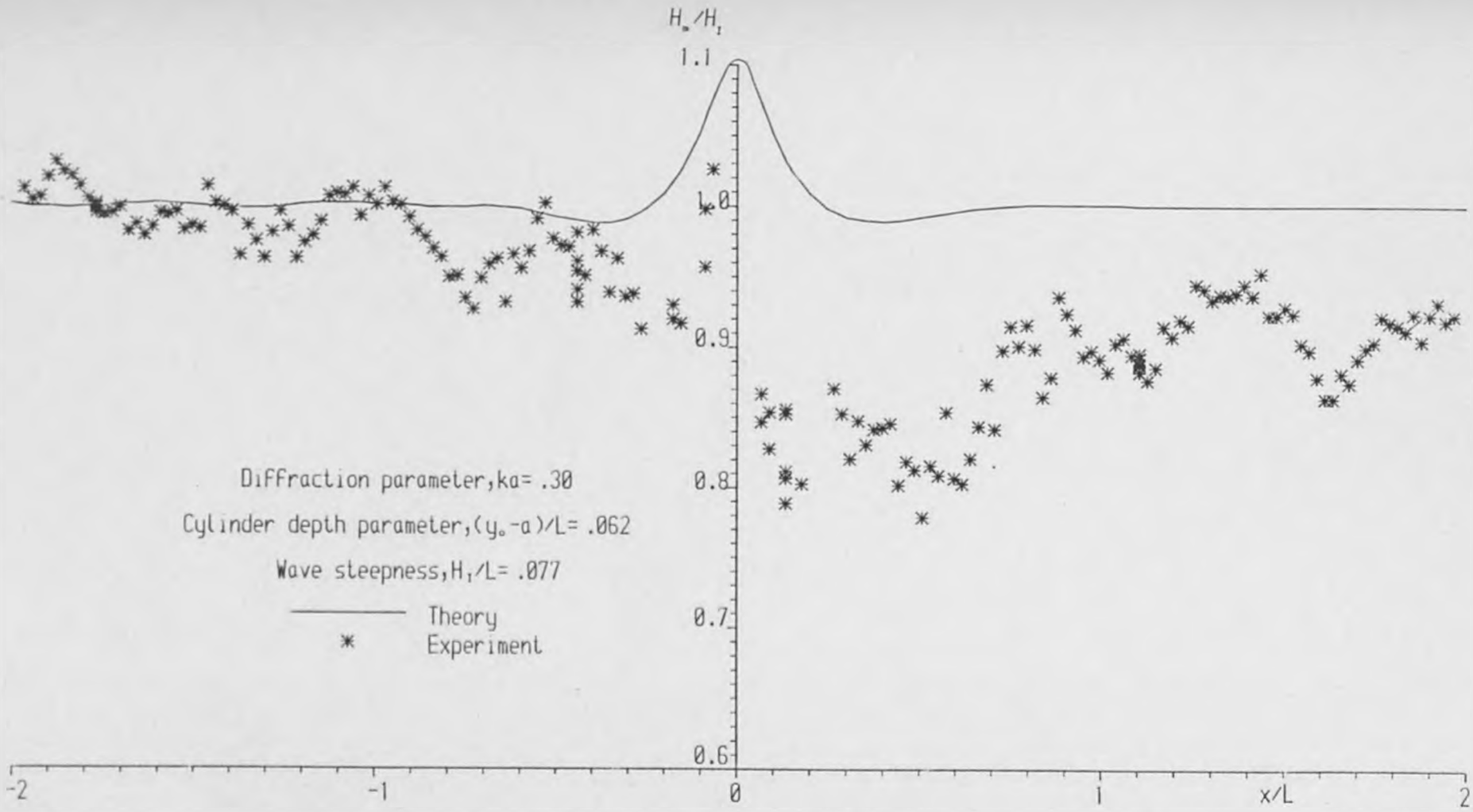

Figure 5.4.2g Spatial variation of wave height

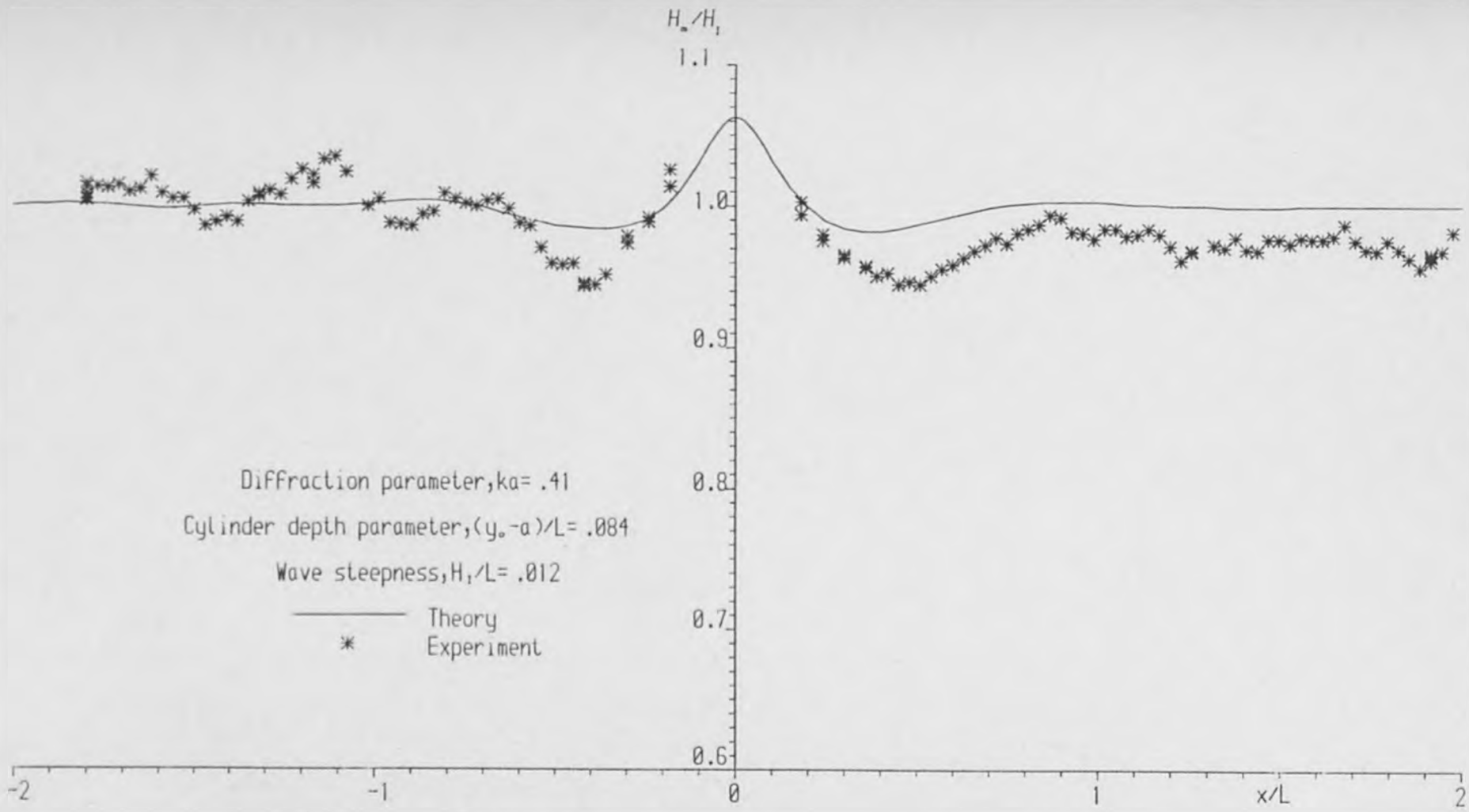

Figure 5.4.2h Spatial variation of wave height

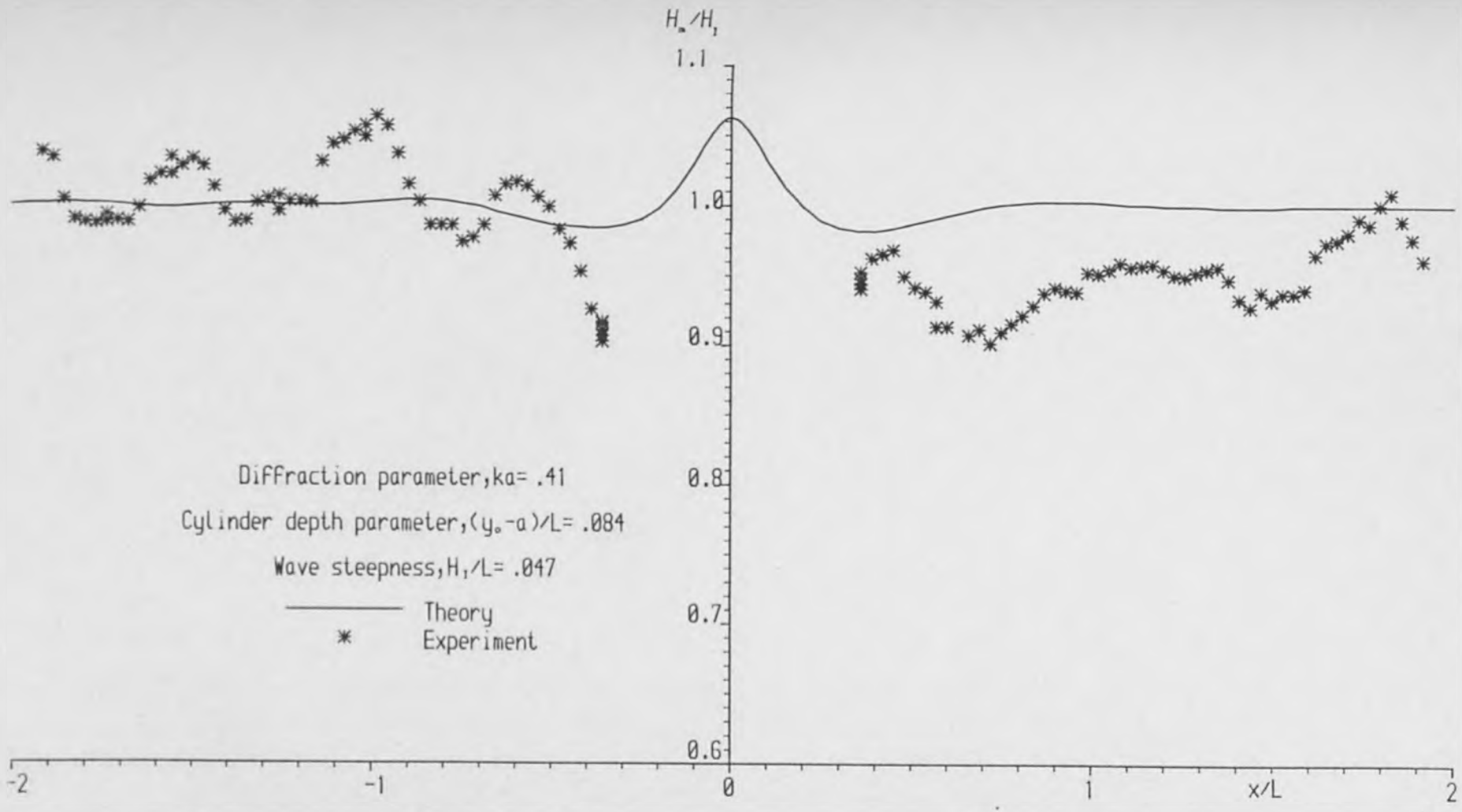

Figure 5.4.2i Spatial variation of wave height

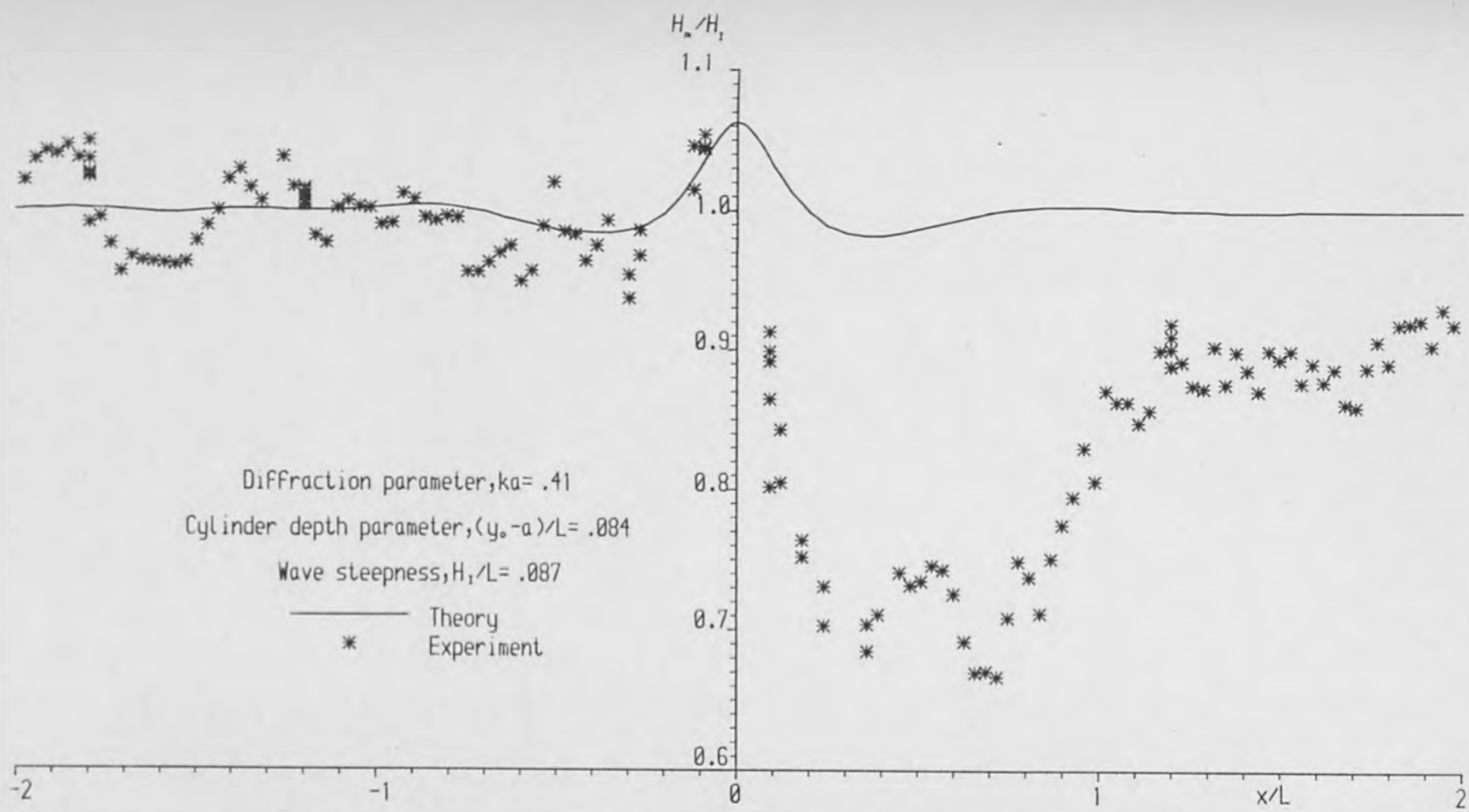

Figure 5.4.2j Spatial variation of wave height

5.4.3 Pressure Measurements on the Cylinder

Results for the pressures at four locations on the cylinder surface have been obtained for a range of waves and a range of cylinder locations. The pressure tappings are located at quarter points on the cylinder half way along the cylinder length (see figure 5.3.7). Pressure tapping 1 is located on the side of the cylinder facing the beach (downstream face) and pressure tapping 2 is at the top of the cylinder. Pressure tapping 3 is on the side of the cylinder facing the wedge (upstream face) and pressure tapping 4 is at the bottom of the cylinder.

The values of the cylinder submergence and diffraction parameters which have been set for these experiments have been given in section 5.2.2. The three values of each parameter make up the nine test cases for which results have been obtained. For each of the combinations results have been collected for a set of waves of varying steepness. The upper limit on the wave steepness is set both by the flume capacity and by the need to ensure that the cylinder remains submerged for all locations. The lower limit is set by the need to maintain pressure oscillations of a sufficiently large magnitude to avoid the introduction of errors.

As in the results for wave motion reported in the previous section there are occasions when a small amount of breaking can be detected in the free surface. This feature has only been observed for the steeper waves at the shallowest of the cylinder locations.

The details of the incident wave motion have been recorded in table 5.4.3. Values are given for the incident wave amplitude, $H_I/2$ and the wave steepness H_I/L plus the tank reflection coefficient R. Table 5.4.3 also includes the results of the analysis of the wave motion at multiples of the wave frequency. The agreement between the measured amplitude of the fixed wave, $H_{21}/2$, fluctuating at twice the wave frequency and the Stokes' second-order correction to the free surface displacement, $H_{2t}/2$, given by equation 3.3.9, is excellent over the range of wave steepness. The amplitude of the free wave at twice the wave frequency, $H_{22}/2$, is always smaller than the fixed component at this frequency and is never large enough to result in measurable pressures on the cylinder. The amplitude of the fluctuation of the free surface at three times the wave frequency, s_3, has also been included in the table and the recorded values confirm that the wave height for the oscillations at the wave frequency will be in good agreement with the peak to peak value.

The measurements of pressure at the four locations on the cylinder are recorded in table 5.4.4. The reference number given in the first column is stated to permit the identification of the incident wave as given in table 5.4.3. For pressure amplitudes at multiples of the wave frequency the absence of entries in the tables indicates that the measured quantities are very small and are generally not distinguishable from the noise in the measurement system.

To permit an examination of the pressure measurements the results given in table 5.4.4 have been plotted in figures 4.5.3 to 4.5.6. These graphs are in four sets each of which is now considered in turn.

The first set of graphs (figures 5.4.3a - c) gives plots of the ratio of measured to theoretical pressure, p_m/p_t, against wave steepness, H_I/L, for the four pressure tapping locations. Each of the three graphs in this first set give results for a different value of the diffraction parameter and include results for each of the different cylinder locations. These graphs will therefore indicate the significance of the finite height of waves for shallow and deep cylinder submergence. The vertical scales of the graphs in each figure vary for the pressure tapping locations which is an indication that the extent of departure from the linear theory predictions varies with position on the cylinder.

The pressure measurements at pressure tapping locations 1, 2 and 3 demonstrate reasonable agreement between experiment and theory for the cylinder locations which are more remote from the free surface over the full range of wave steepness. These measurements generally lie between $\pm$5% of the theoretical value although the discrepancy is sometimes a little greater for the steeper waves. The differences between theory and experiment are noticably greater for the cylinder nearer to the free surface and in this case the measured values for small amplitude waves demonstrate poor agreement in some instances and the measured values for the steepest waves are occasionally very different from the theoretical values. The pressure amplitude ratio is very much larger for measurements at location 4 over the full range of wave steepness. The greater discrepancies at this location for waves of small amplitude may be attributed in part to experimental error because the amplitudes of oscillations are small. However, the differences for the larger amplitude waves is an indication of substantial disagreement between theory and experiment.

The second set of graphs (figures 5.4.4a - c) which are presented in this section gives the results for the ratio of the pressure amplitude at twice the wave frequency to the measured pressure at the wave frequency (p_{2m}/p_m) plotted against wave steepness, H_I/L. Two trends which have been anticipated are confirmed by these results: firstly, that the oscillation at twice the wave frequency demonstrates a gradual increase with wave steepness at all depths of submergence and secondly, that the values of this pressure ratio is larger for smaller depths of submergence.

The values of the ratio p_{2m}/p_m are quite similar for each of the four pressure tapping locations at any one value of the diffraction parameter, ka. The occurence of oscillations at twice the wave frequency is itself a departure from a linear theory prediction. However, these oscillations are only of real significance if they are sufficiently large to modify the peak to peak oscillation. The measured amplitudes of oscillation at twice the wave frequency are never very much more than 20% of the fundamental pressure oscillation and do not therefore modify the peak to peak value.

The results plotted in figures 5.4.3 and 5.4.4 demonstrate clearly that finite wave height and shallow cylinder submergence are important effects which cause departure from linear theory predictions. To permit a further examination of the pressure results the data which has been presented in figures 5.4.3 and 5.4.4 is replotted in figures 5.4.5 and 5.4.6. In these figures the quantities p_m/p_t and p_{2m}/p_m are again plotted against wave steepness, H_I/L but in this case each graph includes the results for a particular value of the cylinder submergence parameter, $(y_o-a)/L$. The purpose of this

replot is to determine whether there is any identifiable difference between the results at different values of the diffraction parameter, ka, and also to permit conclusions to be drawn concerning the extent of the disagreement between the measured values and the linear diffraction theory predictions for each of the cylinder locations.

There is some evidence to suggest that the discrepancies between measured and theoretical pressure fluctuations at higher values of the diffraction parameter are greater than at lower values. This is a little clearer in the results for the two deeper locations of the cylinder for which results vary more consistently. It is also noticable that the pressure amplitude which oscillates at twice the wave frequency is generally a larger proportion of the oscillation at the wave frequency for higher values of the diffraction parameter at all cylinder locations.

The results obtained for the deepest cylinder submergence as plotted in figures 5.4.5a and 5.4.6a demonstrate the validity of linear diffraction theory for small amplitude waves interacting with a submerged circular cylindrical obstacle. For this cylinder location the measured results are consistently larger than theory. At pressure tapping location 1 agreement is good over the whole range of wave steepness (5% difference) and for locations 2 and 3 the differences are a little larger (10% for steeper waves). The greatest differences between theory and experiment are for location 4. At this location it is only for small amplitude waves that the measured results are within 10% of linear theory predictions for all values of the diffraction parameter.

The results for the pressure ratio p_{2m}/p_m plotted in figure 5.4.6a and the absence of values for p_{3m}/p_m in table 5.4.4 at the deepest cylinder submergence demonstrate that higher frequency oscillations will not in general ammend the peak to peak pressure. The only exception is for results at the bottom pressure tapping and these modifications would be of small magnitude.

For the intermediate value of the cylinder submergence parameter results are not greatly dissimilar to those obtained for the deepest submergence. However, for the shallowest cylinder submergence agreement between theory and experiment is less good. It is important to notice that for the largest value of the diffraction parameter the linear theory predictions are quite poor even for the smallest values of the wave steepness parameter. For steeper waves there is significant disagreement between the theoretical and measured pressure amplitudes at all locations on the cylinder and the results at the top and bottom pressure tapping locations are poorest.

The values of the pressure ratios p_{2m}/p_m and p_{3m}/p_m (figure 5.4.6c and table 5.4.4) for the shallowest cylinder submergence indicate that there are some occasions when pressure oscillations at multiples of the wave frequency will modify the peak to peak pressure value. This result is only of minor significance because when these higher-order pressures are important the disagreement between theory and pressure is larger and the discrepancies would not have been very different if the peak to peak measurement had been presented.

In general it may be concluded that small amplitude wave theory gives a good representation of the physics of wave obstacle

interaction for waves of small steepness at larger depths of submergence but that non-linear effects due to the finite height of waves result in poor agreement between experiment and theory.

Reference Number	$\frac{(y_o-a)}{L}$	$\frac{H_I}{2}$ (mm)	$\frac{H_I}{L}$	R (%)	$\frac{H_{21}}{H_I}$	$\frac{H_{2t}}{H_I}$	$\frac{H_{22}}{H_2}$	$\frac{s_3}{H_I}$
1	0.15	14.0	.018	4	.05	.03	.05	.04
2	0.15	26.1	.033	3	.04	.06	.03	.03
3	0.15	36.0	.046	2	.08	.08	.04	.03
4	0.15	45.3	.059	3	.11	.10	.02	.04
5	0.15	56.1	.072	3	.12	.12	.05	.03
6	0.10	14.4	.018	3	.03	.03	.04	
7	0.10	25.7	.033	3	.05	.06	.03	
8	0.10	36.6	.047	2	.07	.08	.03	.02
9	0.10	46.1	.059	2	.10	.10	.02	.02
10	0.10	57.2	.072	3	.12	.12	.02	.03
11	0.05	14.5	.019	3	.03	.03	.04	
12	0.05	25.7	.033	2	.05	.06	.02	
13	0.05	36.6	.047	2		.08		
14	0.05	47.0	.060	2		.10		
15	0.05	56.9	.073	2		.12		

Table 5.4.3a Incident wave characteristics at f_o = 0.98 Hz

Reference Number	$\frac{(y_o-a)}{L}$	$\frac{H_I}{2}$ (mm)	$\frac{H_I}{L}$	R (%)	$\frac{H_{21}}{H_I}$	$\frac{H_{2t}}{H_I}$	$\frac{H_{22}}{H_I}$	$\frac{s_3}{H_I}$
16	0.15	7.9	.014	2		.02		
17	0.15	17.4	.031	1	.03	.05		
18	0.15	26.4	.046	2	.06	.07	.02	
19	0.15	35.4	.062	2	.11	.10	.03	.02
20	0.15	43.5	.077	1	.12	.12	.05	.03
21	0.15	50.2	.088	2	.14	.13	.02	.05
22	0.15	55.8	.098	2	.15	.15	.04	.04
23	0.10	8.3	.015	2		.02		
24	0.10	18.4	.032	1	.03	.05		
25	0.10	27.3	.048	1	.09	.07	.03	.02
26	0.10	35.0	.062	2	.10	.09	.05	.03
27	0.10	43.5	.077	2	.14	.12	.06	.04
28	0.10	50.2	.088	2	.13	.13	.03	.05
29	0.10	56.7	.100	4	.15	.15	.03	.05
30	0.05	7.7	.013	2		.02		
31	0.05	18.5	.033	1	.05	.05	.03	.03
32	0.05	27.1	.048	1	.07	.07	.02	.02
33	0.05	35.6	.063	2	.09	.10	.03	.03
34	0.05	44.2	.078	3	.11	.12	.04	.04
35	0.05	50.6	.089	2	.15	.14	.05	.05
36	0.05	56.8	.100	1	.16	.15	.05	.05

Table 5.4.3b Incident wave characteristics at f_o = 1.17 Hz

Reference Number	$\frac{(y_o-a)}{L}$	$\frac{H_I}{2}$ (mm)	$\frac{H_I}{L}$	R (%)	$\frac{H_{21}}{H_I}$	$\frac{H_{2t}}{H_I}$	$\frac{H_{22}}{H_I}$	$\frac{s_3}{H_I}$
37	0.15	9.1	.022	3		.03		
38	0.15	15.4	.037	2	.04	.06	.04	
39	0.15	20.1	.048	2	.09	.07	.03	
40	0.15	25.1	.060	2	.10	.09	.03	.03
41	0.15	29.8	.071	3	.09	.11	.03	.03
42	0.15	34.0	.082	2	.12	.12	.04	.04
43	0.15	37.6	.090	3	.14	.14	.06	.05
44	0.10	9.2	.022	3	.10	.03	.05	
45	0.10	15.1	.036	2	.03	.06		
46	0.10	19.9	.048	2	.07	.07	.04	.03
47	0.10	24.7	.059	3	.07	.09	.03	.02
48	0.10	30.1	.072	2	.09	.11	.04	.02
49	0.10	34.3	.082	1	.09	.12	.05	.03
50	0.10	38.4	.092	2	.11	.14	.07	.04
51	0.05	9.6	.023	1	.14	.03	.07	
52	0.05	14.3	.034	2	.03	.05	.12	
53	0.05	20.4	.049	0	.08	.07	.04	.04
54	0.05	26.2	.063	1	.10	.09	.04	.03
55	0.05	30.0	.072	3	.12	.11	.04	.03
56	0.05	34.0	.081	2	.12	.12	.04	.04

Table 5.4.3c Incident wave characteristics at f_o = 1.37 Hz

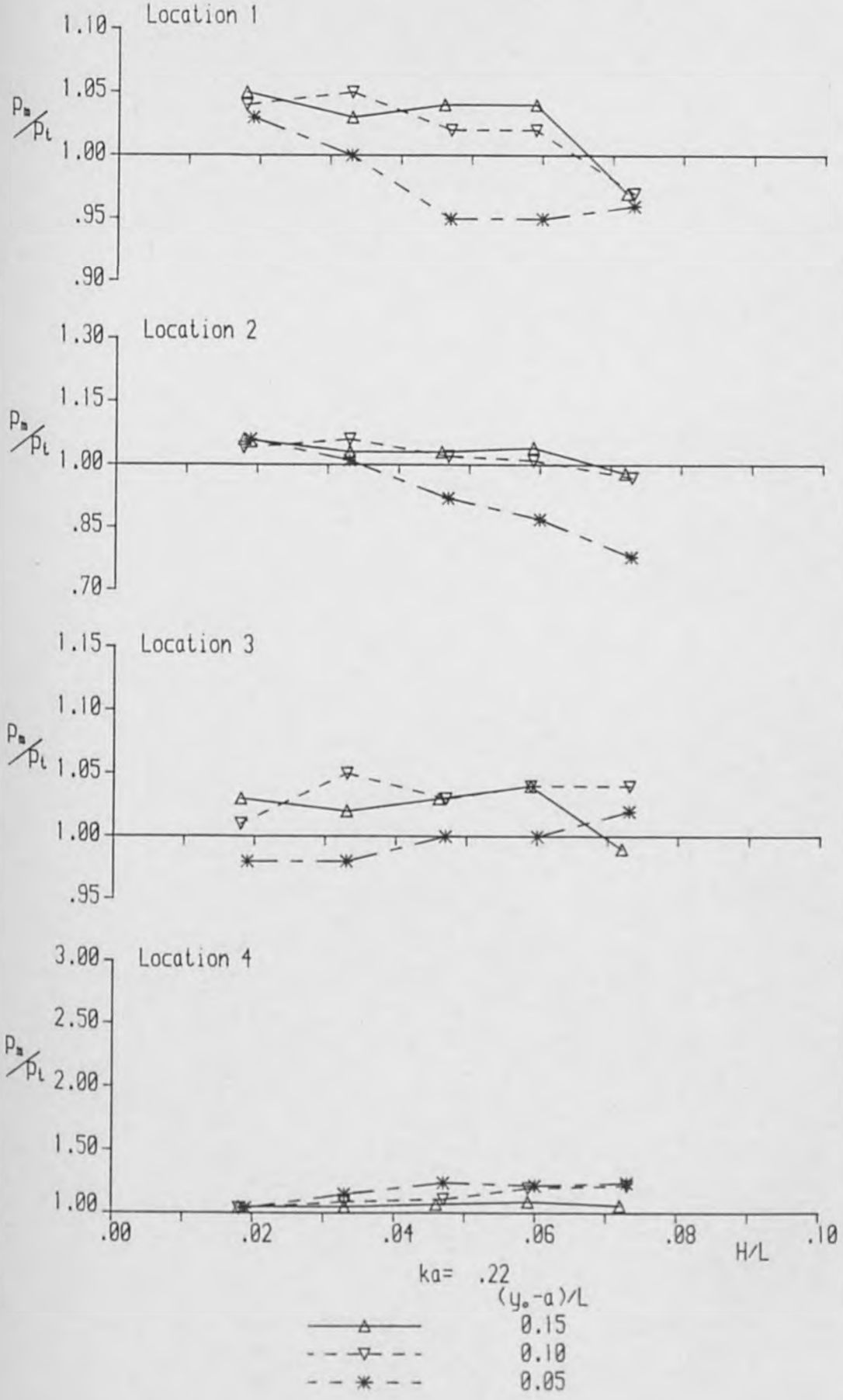

Figure 5.4.3a Ratio of measured and theoretical pressure amplitudes

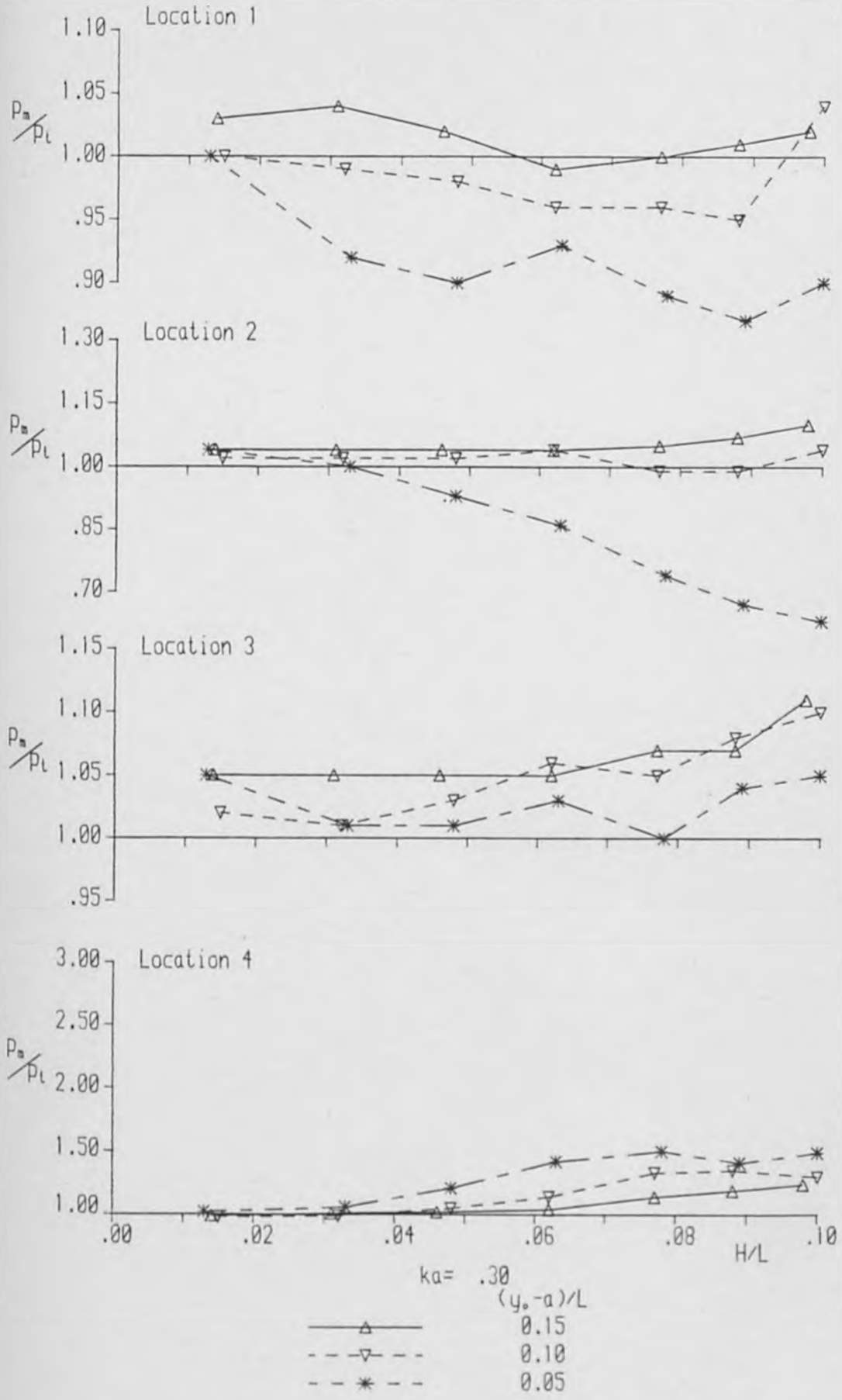

Figure 5.4.3b Ratio of measured and theoretical pressure amplitudes

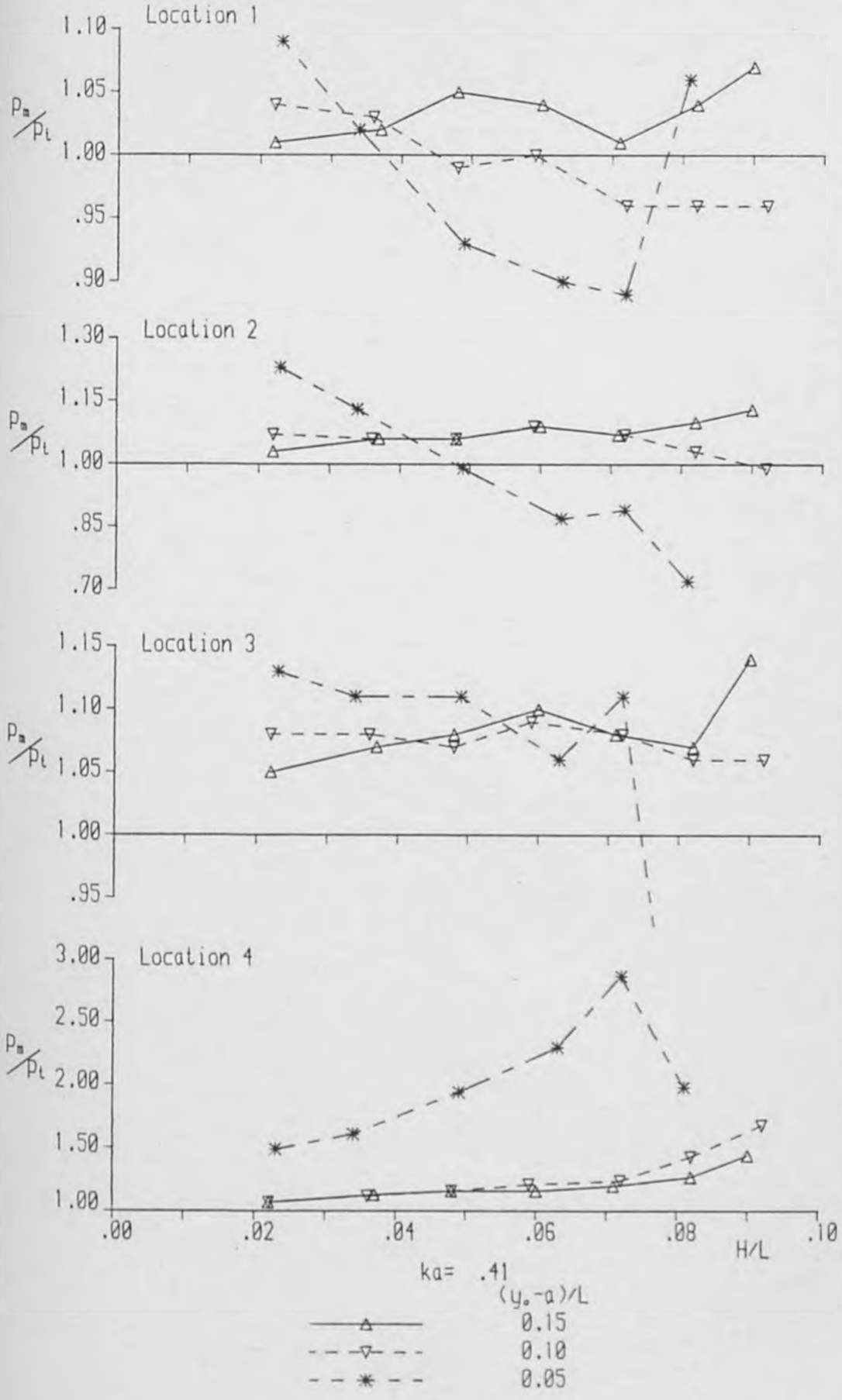

Figure 5.4.3c Ratio of measured and theoretical pressure amplitudes

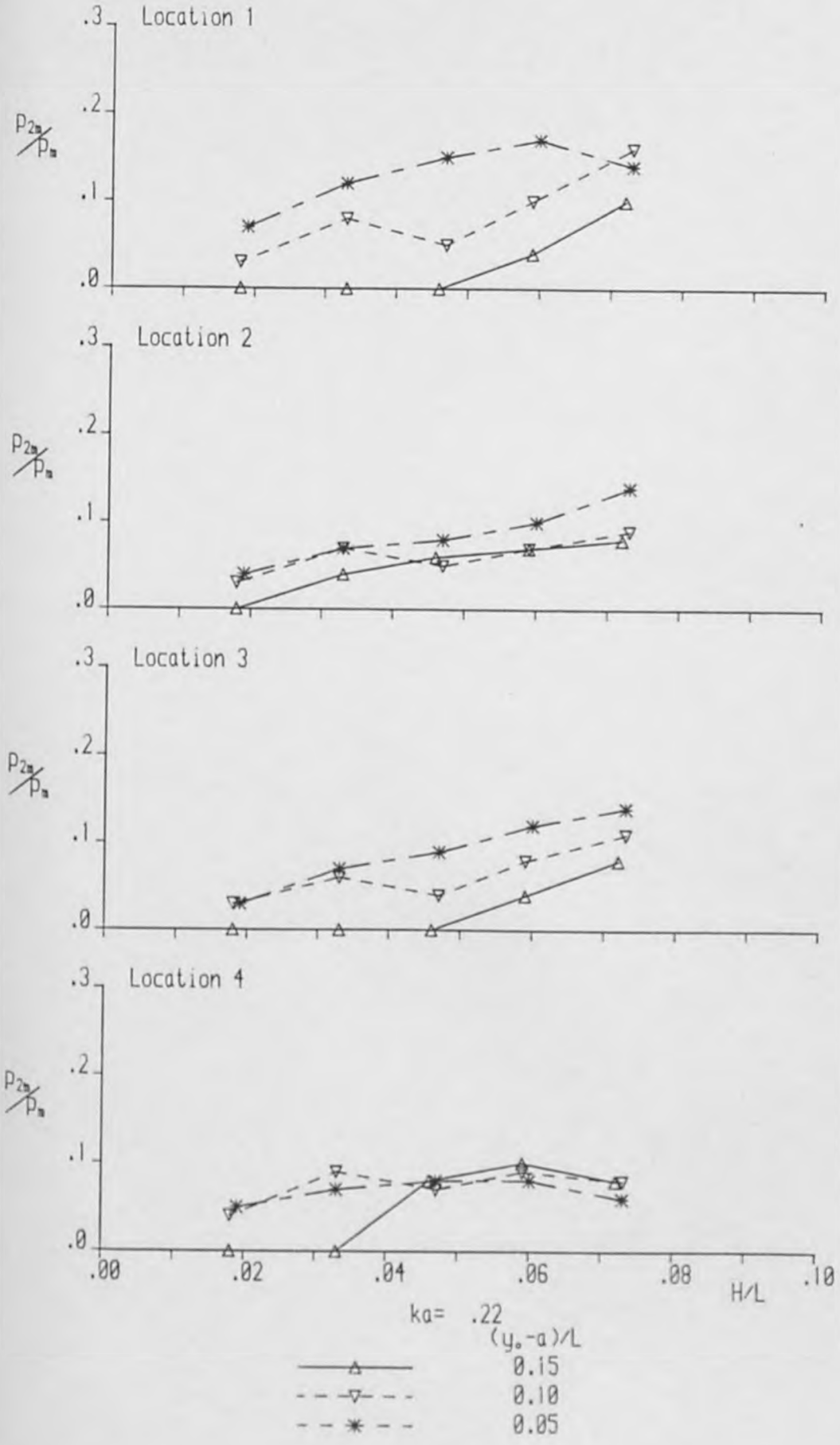

Figure 5.4.4a Pressure amplitude at twice the wave frequency

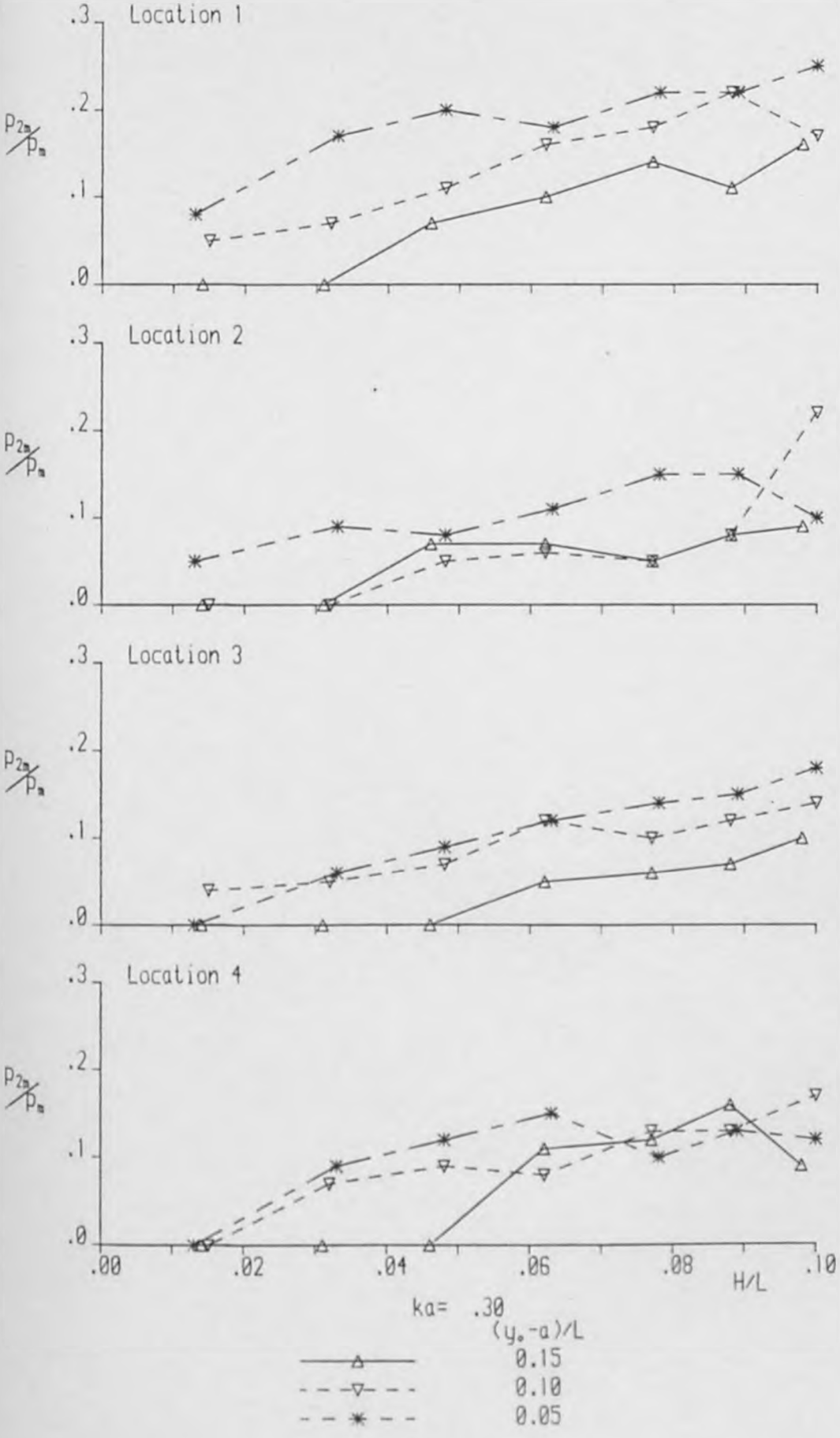

Figure 5.4.4b Pressure amplitude at twice the wave frequency

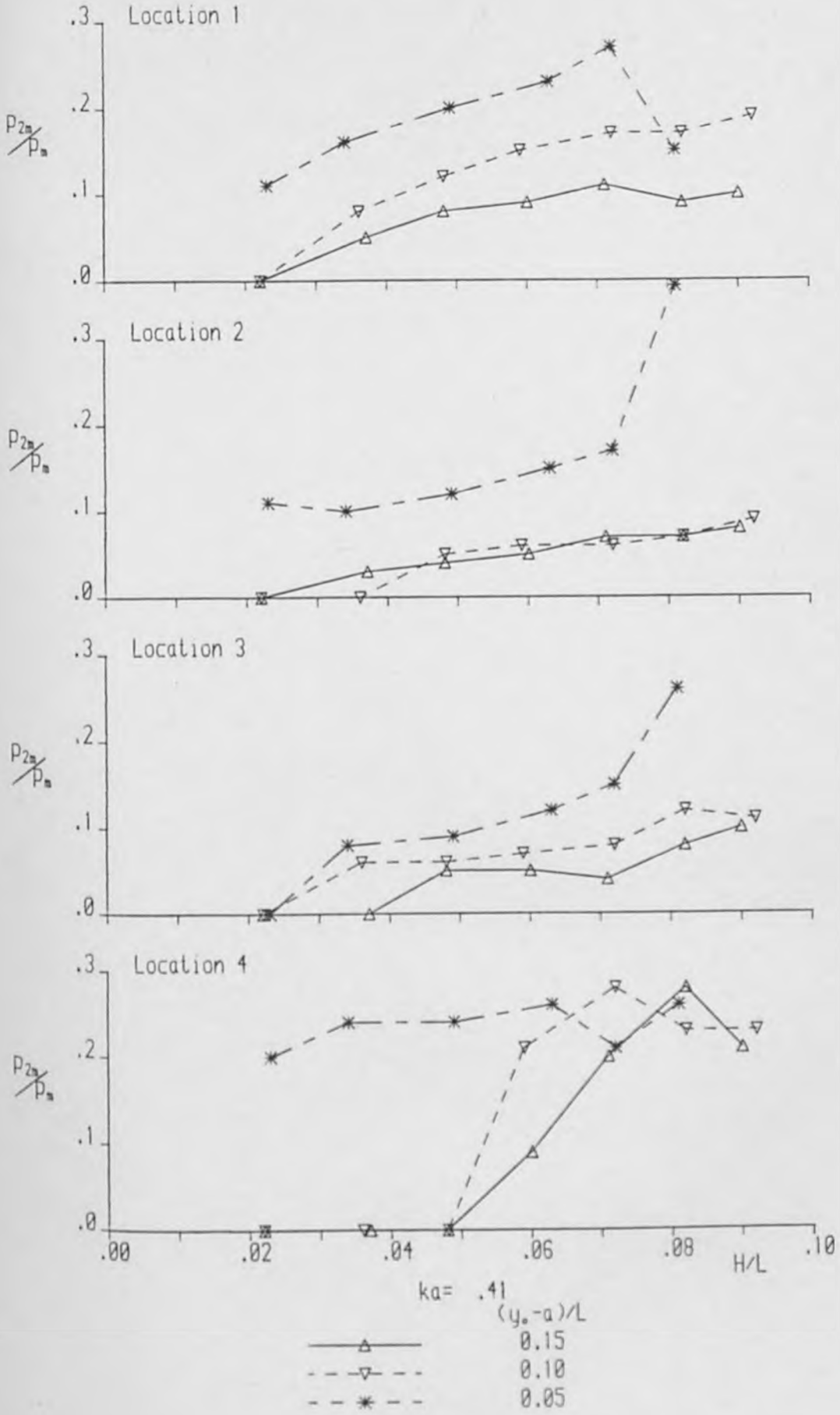

Figure 5.4.4c Pressure amplitude at twice the wave frequency

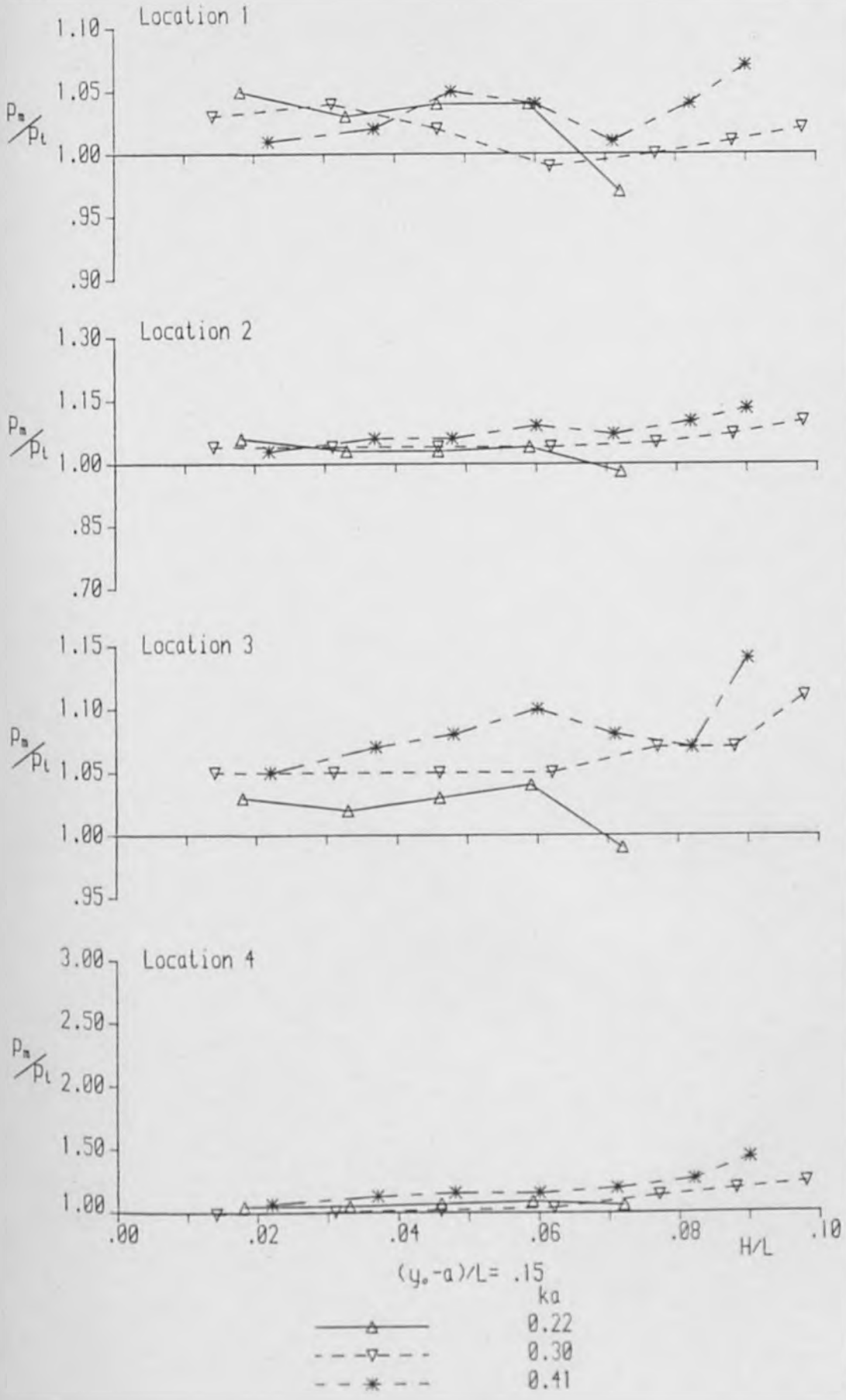

Figure 5.4.5a Ratio of measured and theoretical pressure amplitudes

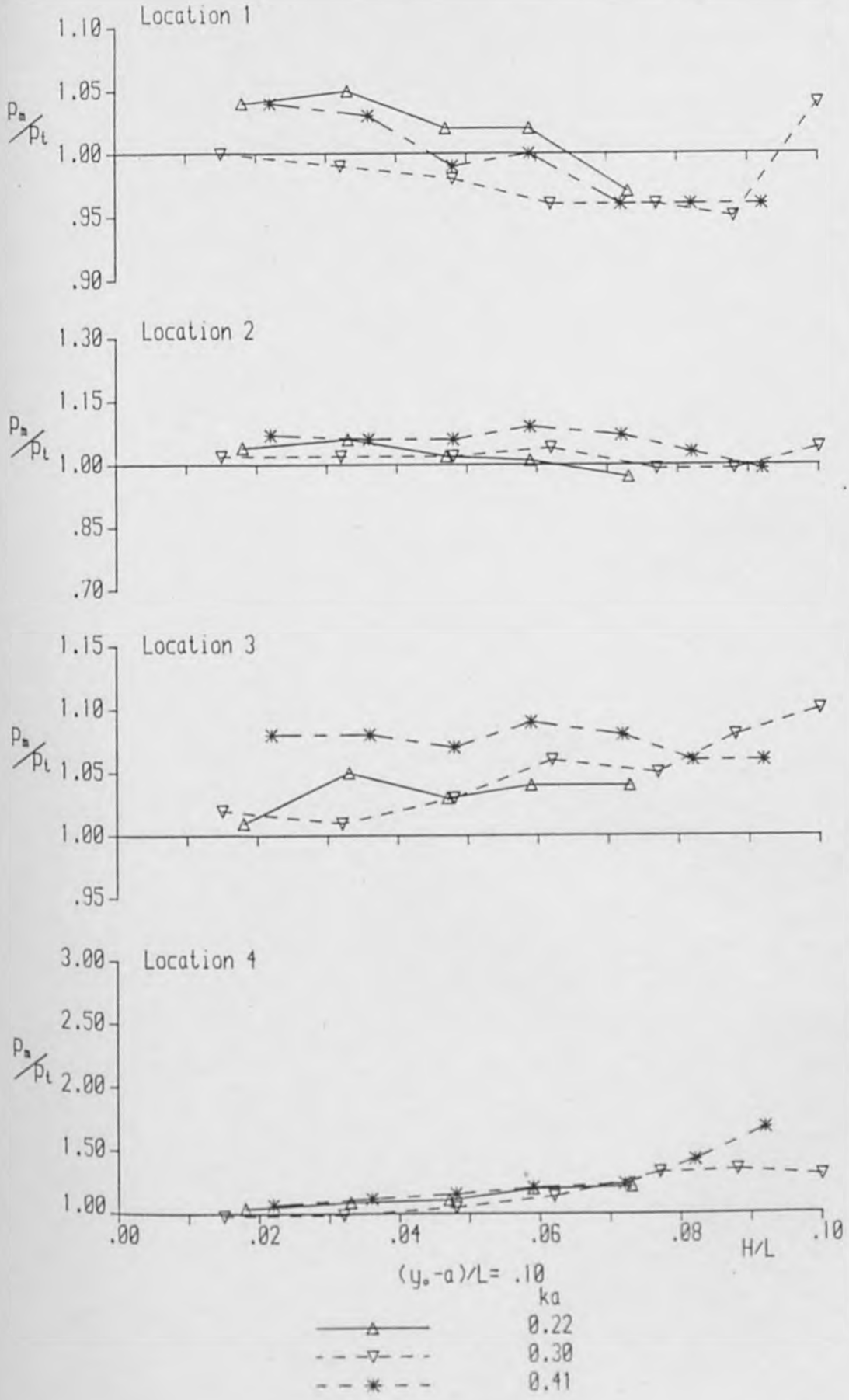

Figure 5.4.5b Ratio of measured and theoretical pressure amplitudes

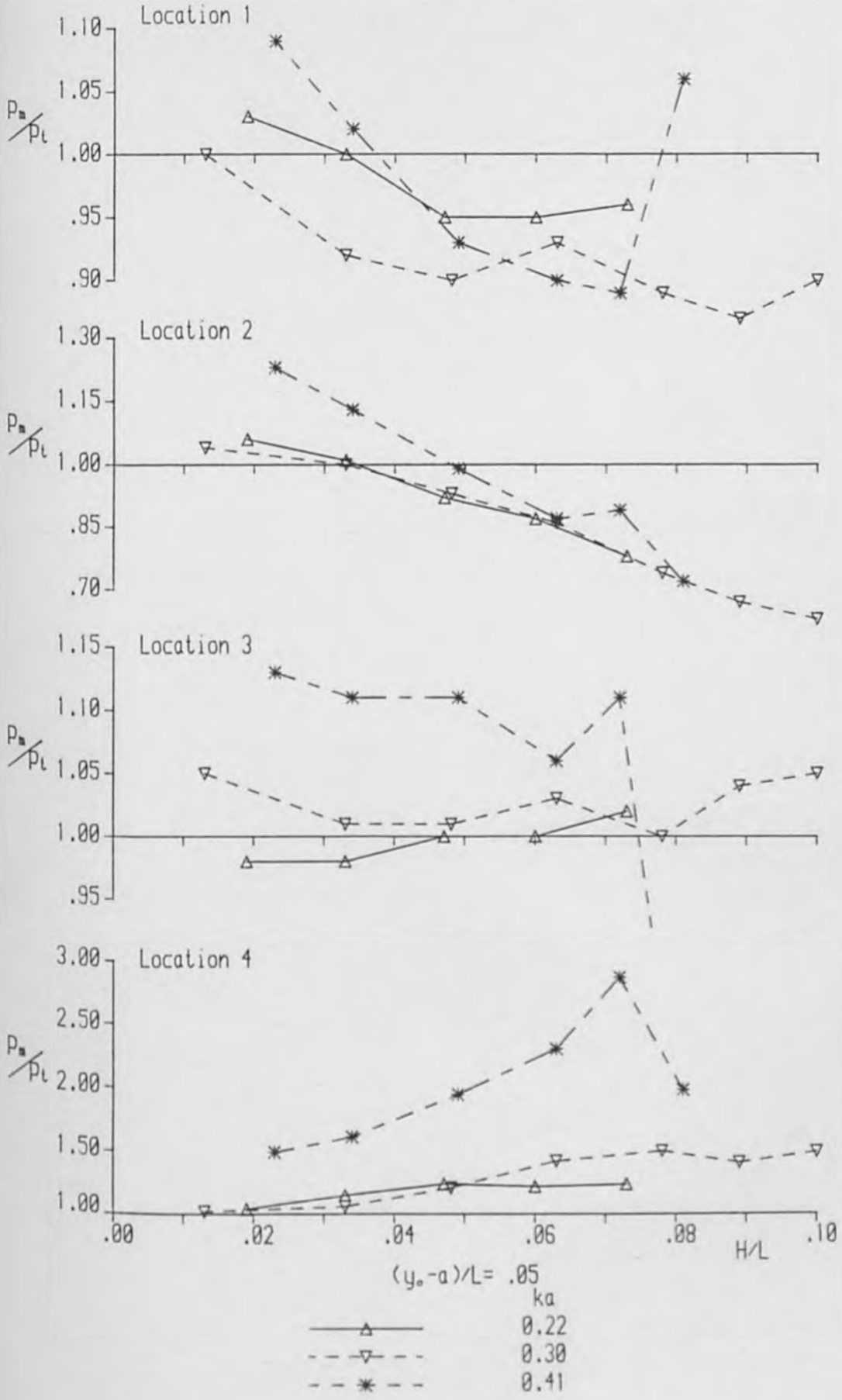

Figure 5.4.5c Ratio of measured and theoretical pressure amplitudes

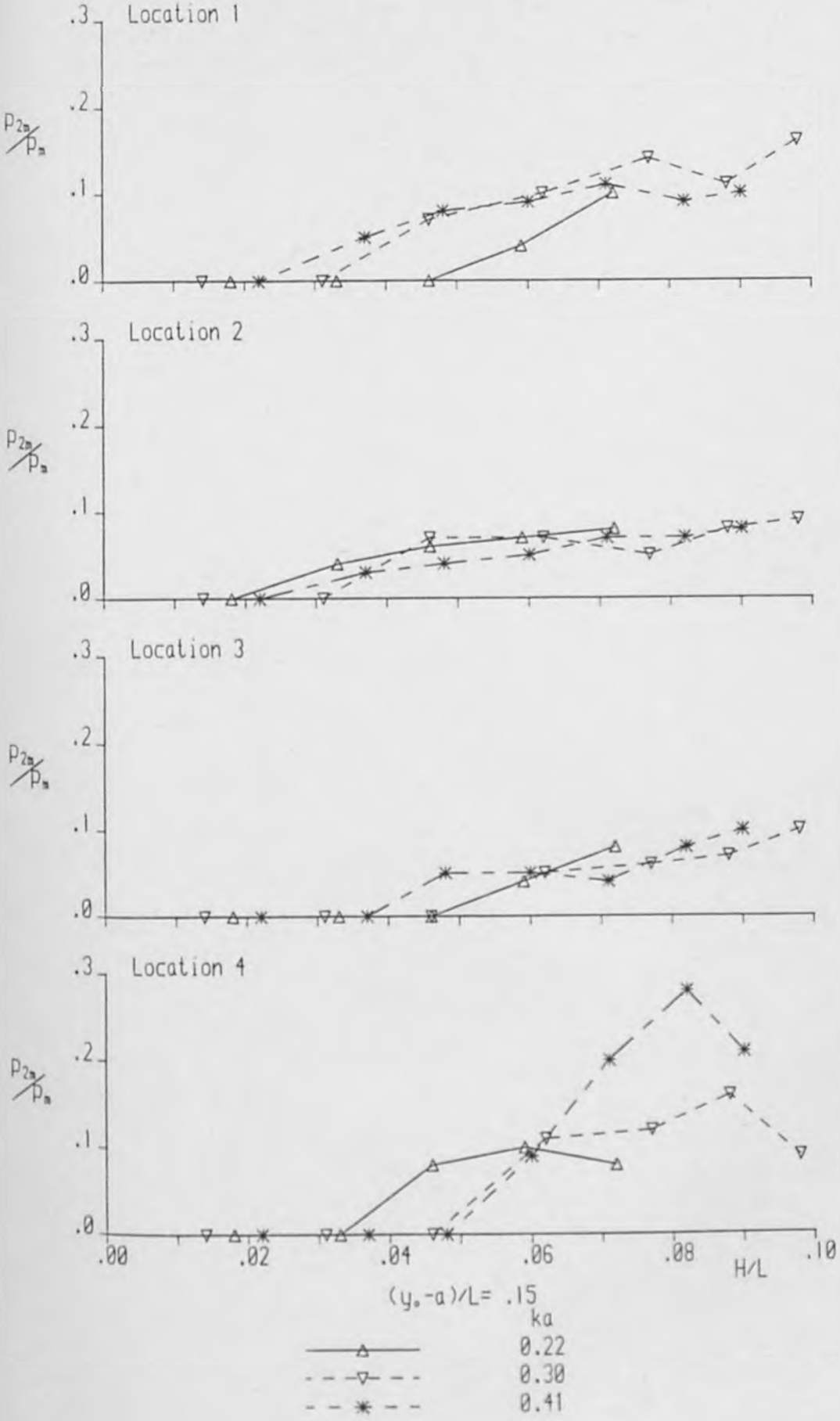

Figure 5.4.6a Pressure amplitude at twice the wave frequency

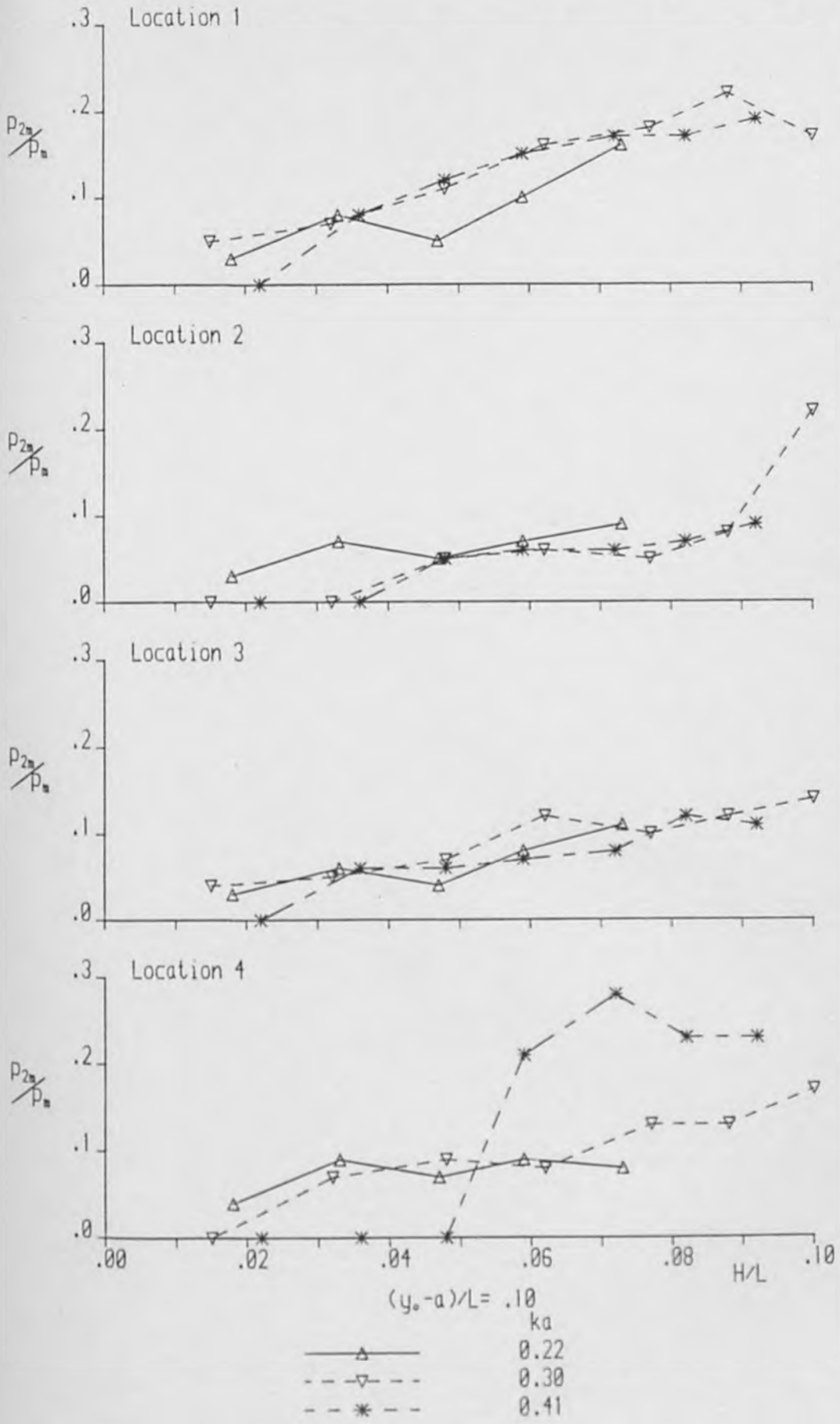

Figure 5.4.6b Pressure amplitude at twice the wave frequency

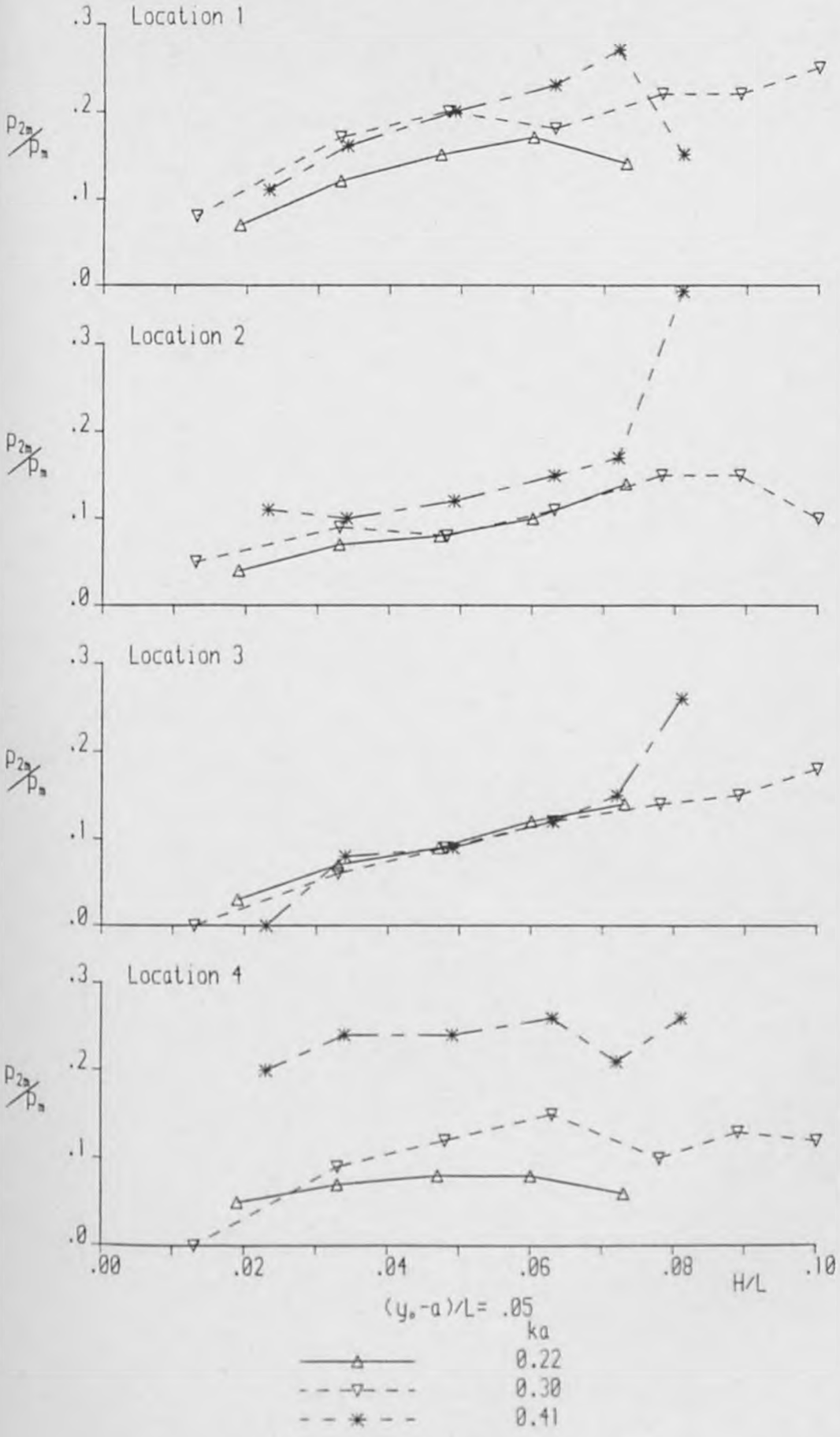

Figure 5.4.6c Pressure amplitude at twice the wave Frequency

Reference number	p_t (mm)	p_m (mm)	$\frac{p_m}{p_t}$	Error (mm)	p_{2m} (mm)	$\frac{p_{2m}}{p_m}$	p_{3m} (mm)	$\frac{p_{3m}}{p_m}$
1	5.0	5.2	1.05	0.2				
2	9.2	9.5	1.03	0.3				
3	12.7	13.2	1.04	0.5				
4	16.2	16.8	1.04	0.6	0.7	0.04		
5	19.8	19.1	0.97	-0.7	1.9	0.10		
6	6.6	6.9	1.04	0.3	0.2	0.03		
7	11.8	12.3	1.05	0.5	1.0	0.08		
8	16.7	17.1	1.02	0.4	0.9	0.05		
9	21.0	21.5	1.02	0.5	2.2	0.10	0.4	0.02
10	26.1	25.4	0.97	-0.7	4.1	0.16	0.5	0.02
11	9.0	9.2	1.03	0.2	0.6	0.07		
12	15.9	15.8	1.00	0.1	1.9	0.12	0.5	0.03
13	22.6	21.6	0.95	-1.0	3.2	0.15	0.6	0.03
14	29.0	27.5	0.95	-1.0	4.7	0.17	1.1	0.04
15	35.1	33.7	0.96	-1.4	4.7	0.14	2.0	0.06

Table 5.4.4a Pressure measurements at location 1

Reference number	p_t (mm)	p_m (mm)	$\frac{p_m}{p_t}$	Error (mm)	p_{2m} (mm)	$\frac{p_{2m}}{p_m}$	p_{3m} (mm)	$\frac{p_{3m}}{p_m}$
1	6.7	7.1	1.06	0.4				
2	12.4	12.9	1.03	0.5				
3	17.1	17.7	1.03	0.6	1.1	0.06		
4	21.8	22.6	1.04	0.8	1.6	0.07		
5	26.6	26.1	0.98	-0.5	2.1	0.08		
6	9.2	9.6	1.04	0.4	0.3	0.03		
7	16.4	17.4	1.06	1.0	1.2	0.07		
8	23.3	23.8	1.02	0.5	1.2	0.05		
9	29.3	29.5	1.01	0.2	2.1	0.07		
10	36.3	35.1	0.97	-1.2	3.2	0.09	1.1	0.03
11	13.0	13.7	1.06	0.7	0.5	0.04		
12	22.9	23.2	1.01	0.3	1.6	0.07	0.5	0.02
13	32.6	30.2	0.92	-2.4	2.4	0.08	0.9	0.03
14	41.8	36.3	0.87	-5.5	3.6	0.10	1.5	0.04
15	50.6	39.6	0.78	-10.4	5.5	0.14	2.0	0.05

Table 5.4.4b Pressure measurements at location 2

Reference number	p_t (mm)	p_m (mm)	$\frac{p_m}{p_t}$	Error (mm)	p_{2m} (mm)	$\frac{p_{2m}}{p_m}$	p_{3m} (mm)	$\frac{p_{3m}}{p_m}$
1	5.0	5.2	1.03	0.2				
2	9.3	9.5	1.02	0.2				
3	12.9	13.2	1.03	0.3				
4	16.4	17.0	1.04	0.6	0.7	0.04		
5	20.0	19.8	0.99	-0.2	1.6	0.08		
6	6.7	6.7	1.01	0.0	0.2	0.03		
7	11.9	12.5	1.05	0.6	0.8	0.06		
8	16.9	17.3	1.03	0.4	0.7	0.04		
9	21.2	22.2	1.04	1.0	1.8	0.08		
10	26.3	27.4	1.04	1.1	3.0	0.11		
11	9.4	9.2	0.98	-0.2	0.3	0.03		
12	16.0	16.4	1.02	0.4	1.1	0.07		
13	22.8	22.9	1.00	0.1	2.1	0.09		
14	29.3	29.3	1.00	0.0	3.5	0.12		
15	35.4	36.1	1.02	0.7	5.1	0.14		

Table 5.4.4c Pressure measurements at location 3

Reference number	p_t (mm)	p_m (mm)	$\frac{p_m}{p_t}$	Error (mm)	p_{2m} (mm)	$\frac{p_{2m}}{p_m}$	p_{3m} (mm)	$\frac{p_{3m}}{p_m}$
1	3.3	3.5	1.05	0.2				
2	6.1	6.4	1.05	0.3				
3	8.5	9.1	1.07	0.6	0.7	0.08		
4	10.8	11.8	1.09	1.0	1.2	0.10		
5	13.2	13.9	1.06	0.7	1.1	0.08		
6	4.1	4.2	1.04	0.1	0.2	0.04		
7	7.2	7.9	1.09	0.7	0.7	0.09		
8	10.3	11.5	1.11	1.2	0.8	0.07		
9	12.9	15.5	1.20	2.6	1.4	0.09		
10	16.1	19.6	1.22	3.5	1.6	0.08		
11	5.2	5.4	1.04	0.2	0.3	0.05		
12	9.1	10.5	1.15	1.4	0.7	0.07		
13	13.1	16.2	1.24	3.1	1.3	0.08		
14	16.7	20.4	1.22	3.7	1.6	0.08	0.4	0.02
15	20.2	25.1	1.24	4.9	1.5	0.06		

Table 5.4.4d Pressure measurements at location 4

Reference number	p_t (mm)	p_m (mm)	$\frac{p_m}{p_t}$	Error (mm)	p_{2m} (mm)	$\frac{p_{2m}}{p_m}$	p_{3m} (mm)	$\frac{p_{3m}}{p_m}$
16	2.4	2.5	1.03	0.1				
17	5.2	5.4	1.04	0.2				
18	7.9	8.0	1.02	0.1				
19	10.6	10.5	0.99	-0.1	0.6	0.07		
20	13.0	12.9	1.00	0.1	1.8	0.14		
21	15.0	15.2	1.01	0.2	1.7	0.11		
22	16.8	17.2	1.02	0.4	2.8	0.16		
23	3.3	3.3	1.00	0.0	0.2	0.05		
24	7.4	7.4	0.99	0.0	0.5	0.07		
25	11.0	10.8	0.98	-0.2	1.2	0.11		
26	14.2	13.6	0.96	-0.6	2.2	0.16		
27	17.6	16.9	0.96	-0.7	3.0	0.18		
28	20.3	19.3	0.95	-1.0	4.2	0.22		
29	22.9	23.9	1.04	1.0	4.1	0.17		
30	4.3	4.3	1.00	0.0	0.3	0.08		
31	10.4	9.6	0.92	-0.8	1.6	0.17		
32	15.1	13.6	0.90	-1.5	2.7	0.20	0.5	0.04
33	20.0	18.5	0.93	-1.5	3.3	0.18	0.9	0.05
34	24.7	22.0	0.89	-2.7	4.8	0.22	1.3	0.06
35	28.2	24.5	0.87	-3.7	5.4	0.22	1.7	0.07
36	31.7	28.6	0.90	-3.1	7.2	0.25	1.1	0.04

Table 5.4.4e Pressure measurements at location 1

Reference number	p_t (mm)	p_m (mm)	$\frac{p_m}{p_t}$	Error (mm)	p_{2m} (mm)	$\frac{p_{2m}}{p_m}$	p_{3m} (mm)	$\frac{p_{3m}}{p_m}$
16	3.8	3.9	1.04	0.1				
17	8.3	8.6	1.04	0.3				
18	12.5	13.0	1.04	0.5	0.9	0.07		
19	16.7	17.4	1.04	0.7	1.2	0.07		
20	20.6	21.6	1.05	1.0	1.1	0.05		
21	23.7	25.4	1.07	1.7	2.0	0.08		
22	26.5	29.2	1.10	2.7	2.6	0.09		
23	5.4	5.5	1.02	0.1				
24	12.0	12.0	1.02	0.2				
25	17.7	18.1	1.02	0.4	0.9	0.05		
26	22.8	23.8	1.04	1.0	1.4	0.06		
27	28.3	27.9	0.99	-0.4	1.4	0.05		
28	32.6	32.3	0.99	-0.3	2.6	0.08		
29	36.9	38.5	1.04	1.6	8.5	0.22		
30	7.1	7.4	1.04	0.3	0.4	0.05		
31	17.3	17.2	1.00	0.1	1.5	0.09		
32	25.3	23.5	0.93	-1.8	1.9	0.08	1.2	0.05
33	33.2	28.5	0.86	-4.7	3.1	0.11	3.4	0.12
34	41.2	30.5	0.74	-10.7	4.6	0.15	3.7	0.12
35	47.1	31.4	0.67	-15.7	4.7	0.15	2.8	0.09
36	52.9	33.4	0.63	-19.5	3.3	0.10	3.3	0.10

Table 5.4.4f Pressure measurements at location 2

Reference number	p_t (mm)	p_m (mm)	$\frac{p_m}{p_t}$	Error (mm)	p_{2m} (mm)	$\frac{p_{2m}}{p_m}$	p_{3m} (mm)	$\frac{p_{3m}}{p_m}$
16	2.4	2.5	1.05	0.1				
17	5.2	5.5	1.05	0.3				
18	7.9	8.3	1.05	0.4				
19	10.6	11.1	1.05	0.5	0.6	0.05		
20	13.0	14.0	1.07	1.0	0.8	0.06		
21	15.1	16.1	1.07	1.0	1.1	0.07		
22	16.8	18.7	1.11	1.9	1.9	0.10		
23	3.4	3.4	1.02	0.0	0.1	0.04		
24	7.5	7.6	1.01	0.1	0.4	0.05		
25	11.0	11.4	1.03	0.4	0.8	0.07		
26	14.2	15.1	1.06	0.9	1.8	0.12		
27	17.6	18.6	1.05	1.0	1.9	0.10		
28	20.3	21.9	1.08	1.6	2.6	0.12		
29	23.0	25.2	1.10	2.2	3.5	0.14		
30	4.3	4.5	1.05	0.2				
31	10.4	10.5	1.01	0.1	0.6	0.06		
32	15.2	15.3	1.01	0.1	1.4	0.09		
33	19.9	20.5	1.03	0.6	2.5	0.12		
34	24.7	24.8	1.00	0.1	3.5	0.14		
35	28.3	29.3	1.04	1.0	4.4	0.15		
36	31.7	33.2	1.05	1.5	6.0	0.18	1.0	0.03

Table 5.4.4g Pressure measurements at location 3

Reference number	p_t (mm)	p_m (mm)	$\frac{p_m}{p_t}$	Error (mm)	p_{2m} (mm)	$\frac{p_{2m}}{p_m}$	p_{3m} (mm)	$\frac{p_{3m}}{p_m}$
16	1.1	1.0	0.99	-0.1				
17	2.2	2.3	1.01	0.1				
18	3.3	3.4	1.02	0.1				
19	4.5	4.7	1.04	0.2	0.5	0.11		
20	5.5	6.3	1.14	0.8	0.8	0.12		
21	6.4	7.6	1.19	0.8	1.2	0.16		
22	7.1	8.8	1.24	1.7	0.8	0.09		
23	1.3	1.3	0.98	0.0				
24	3.0	2.9	0.99	-0.1	0.2	0.07		
25	4.4	4.6	1.05	0.2	0.4	0.09		
26	5.7	6.4	1.14	0.7	0.5	0.08		
27	7.0	9.3	1.33	2.3	1.2	0.13		
28	8.1	10.9	1.35	2.8	1.4	0.13		
29	9.1	11.9	1.30	2.8	2.0	0.17		
30	1.5	1.6	1.02	0.1				
31	3.7	4.0	1.06	0.3	0.4	0.09		
32	5.5	6.6	1.21	1.1	0.8	0.12		
33	7.2	10.2	1.42	3.0	1.5	0.15		
34	8.9	13.3	1.50	4.4	1.3	0.10		
35	10.2	14.3	1.41	4.1	1.9	0.13		
36	11.4	17.0	1.49	5.6	2.0	0.12		

Table 5.4.4h Pressure measurements at location 4

Reference number	p_t (mm)	p_m (mm)	$\frac{p_m}{p_t}$	Error (mm)	p_{2m} (mm)	$\frac{p_{2m}}{p_m}$	p_{3m} (mm)	$\frac{p_{3m}}{p_m}$
37	2.5	2.5	1.01	0.0				
38	4.2	4.3	1.02	0.1	0.2	0.05		
39	5.4	5.7	1.05	0.3	0.5	0.08		
40	6.8	7.0	1.04	0.2	0.6	0.09		
41	8.1	8.1	1.01	0.0	0.9	0.11		
42	9.2	9.5	1.04	0.3	0.9	0.09		
43	10.2	10.9	1.07	0.7	1.1	0.10		
44	3.3	3.5	1.04	0.2				
45	5.5	5.6	1.03	0.1	0.4	0.08		
46	7.2	7.2	0.99	0.0	0.9	0.12		
47	8.9	8.9	1.00	0.0	1.3	0.15		
48	10.9	10.5	0.96	-0.4	1.8	0.17		
49	12.4	11.9	0.96	-0.5	2.0	0.17		
50	13.9	13.4	0.96	-0.5	2.5	0.19		
51	4.8	5.2	1.09	0.4	0.8	0.11		
52	7.1	7.3	1.02	0.2	1.2	0.16		
53	10.1	9.4	0.93	-0.7	1.9	0.20		
54	13.1	11.7	0.90	-1.4	2.7	0.23	0.7	0.06
55	14.9	13.3	0.89	-2.6	3.6	0.27	0.8	0.06
56	16.9	18.0	1.06	1.1	2.7	0.15	1.3	0.07

Table 5.4.4i Pressure measurements at location 1

Reference number	p_t (mm)	p_m (mm)	$\frac{p_m}{p_t}$	Error (mm)	p_{2m} (mm)	$\frac{p_{2m}}{p_m}$	p_{3m} (mm)	$\frac{p_{3m}}{p_m}$
37	4.4	4.5	1.03	0.1				
38	7.5	7.9	1.06	0.4	0.2	0.03		
39	9.7	10.4	1.06	0.7	0.4	0.04		
40	12.2	13.3	1.09	1.1	0.7	0.05		
41	14.5	15.6	1.07	1.1	1.1	0.07		
42	16.6	18.1	1.10	1.5	1.3	0.07		
43	18.3	20.6	1.13	2.3	1.6	0.08		
44	6.1	6.5	1.07	0.4	0.3	0.05		
45	9.9	10.5	1.06	0.6				
46	13.1	13.9	1.06	0.8	0.7	0.05		
47	16.3	17.7	1.09	1.4	1.1	0.06		
48	19.9	21.2	1.07	1.3	1.3	0.06		
49	22.6	23.3	1.03	0.7	1.6	0.07		
50	25.4	25.2	0.99	-0.2	2.3	0.09		
51	9.1	11.2	1.23	2.1	1.2	0.11		
52	13.7	15.5	1.13	1.8	1.6	0.10		
53	19.4	19.3	0.99	-0.1	2.3	0.12		
54	25.1	21.9	0.87	-3.2	3.3	0.15	1.8	0.08
55	28.6	25.6	0.89	-3.0	4.4	0.17	3.3	0.13
56	32.5	23.3	0.72	-9.2	8.4	0.36	4.2	0.18

Table 5.4.4j Pressure measurements at location 2

Reference number	p_t (mm)	p_m (mm)	$\frac{p_m}{p_t}$	Error (mm)	p2m (mm)	$\frac{p2m}{p_m}$	p3m (mm)	$\frac{p3m}{p_m}$
37	2.5	2.7	1.05	0.2				
38	4.2	4.5	1.07	0.3				
39	5.4	5.9	1.08	0.5	0.3	0.05		
40	6.8	7.5	1.10	0.7	0.4	0.05		
41	8.1	8.7	1.08	0.6	0.3	0.04		
42	9.2	9.9	1.07	0.7	0.8	0.08		
43	10.2	11.6	1.14	1.4	1.2	0.10		
44	3.3	3.6	1.08	0.3				
45	5.5	5.9	1.08	0.4	0.4	0.06		
46	7.2	7.7	1.07	0.5	0.5	0.06		
47	8.9	9.8	1.09	0.9	0.7	0.07		
48	10.9	11.8	1.08	0.9	0.9	0.08		
49	12.4	13.1	1.06	0.7	1.6	0.12		
50	13.9	14.8	1.06	0.9	1.6	0.11		
51	4.8	5.4	1.13	0.6				
52	7.1	7.9	1.11	0.8	0.6	0.08		
53	10.1	11.2	1.11	1.1	1.0	0.09		
54	13.0	13.9	1.06	0.9	1.7	1.09		
55	14.9	16.5	1.11	1.6	2.5	0.15		
56	16.9	12.7	0.75	-4.2	3.3	0.26	1.0	0.08

Table 5.4.4k Pressure measurements at location 3

Reference number	p_t (mm)	p_m (mm)	$\frac{p_m}{p_t}$	Error (mm)	p2m (mm)	$\frac{p2m}{p_m}$	p3m (mm)	$\frac{p3m}{p_m}$
37	0.5	0.6	1.07	0.1				
38	0.9	1.0	1.13	0.1				
39	1.1	1.3	1.16	0.2				
40	1.4	1.6	1.16	0.2	0.4	0.09		
41	1.7	2.0	1.26	0.3	0.4	0.26		
42	1.9	2.4	1.27	0.5	0.7	0.28		
43	2.1	3.0	1.44	0.9	0.6	0.21		
44	0.6	.7	1.07	0.1				
45	1.0	1.1	1.12	0.1				
46	1.3	1.6	1.16	0.3				
47	1.7	2.0	1.21	0.3	0.4	0.21		
48	2.0	2.5	1.24	0.5	0.7	0.28		
49	2.3	3.3	1.43	1.0	0.8	0.23		
50	2.6	4.3	1.68	1.7	1.0	0.23		
51	0.6	0.9	1.49	0.3	0.2	0.20		
52	0.9	1.4	1.61	0.5	0.3	0.24		
53	1.3	2.5	1.94	1.2	0.6	0.24		
54	1.6	3.8	2.30	2.2	1.0	0.26		
55	1.9	5.3	2.87	3.4	1.1	0.21		
56	2.1	4.2	1.98	2.1	1.1	0.26		

Table 5.4.41 Pressure measurements at location 4

CHAPTER 6 - DISCUSSION

6.1 Introduction

The discussion of the main results of this thesis commences with a consideration of the formulation and numerical solution of the linear potential theory problem of wave scattering. The numerical results which have been obtained in this study by solution of the regular kernel integral equation formulation and by the application of higher-order discretisation techniques for both the singular and regular kernel methods are used to indicate which of the alternative integral equation methods and which of the different numerical schemes provides the most reliable and efficient means of evaluating the response of an obstacle to wave motion.

Detailed numerical results have only been obtained for the particular case of a submerged circular cylinder in a two dimensional domain, although some results have been computed for a semi-immersed cylinder (Appendix A.8). It is therefore necessary to extend the present study to include a greater range of problems if the potentially advantageous regular kernel method is to be regarded as a reliable alternative to the established methods. Recommendations are made concerning the extension of the test programme.

The validation of potential theory results under controlled laboratory conditions is very important if numerical methods are to be employed with confidence. The experimental study reported in this thesis has not beenrestricted to the problem for small amplitude waves and

attempts have been made to determine how well the linear theory predicts the physics of wave obstacle interaction for conditions when wave height effects are expected to be significant. The physical mechanisms which are not accommodated in the linear diffraction theory model are considered in an attempt to explain discrepancies between theory and experiment.

The discussion of the results of this thesis is concluded by considering the possibility of developing non-linear analysis methods. The alternative possibilities are discussed with regard to the possibility of implementation and then consideration is given to the possibility of using these methods to improve the agreement between theoretical predictions and the experimental results obtained in this study.

6.2 Discussion of Numerical Results

If the potential theory problem of small amplitude waves interacting with submerged obstacles is to be solved there are a number of alternative numerical schemes which might be employed. The finite element method, the multipole method, the integral equation methods and hybrid methods have all been used to varying extents and each has peculiar advantages and disadvantages.

If a general formulation is required the multipole method would be discarded because for this method the obstacle geometry must be a simple two dimensional shape which may be conformally mapped

onto a circle. There are difficulties associated with the use of the finite element method in exterior domains which reduce the usefulness of this method for the type of problem under consideration and it would seem that the best use of the finite element method would be as part of a hybrid element solution scheme. It is therefore reasonable to suggest that the integral equation methods are the most suitable for this type of problem and this is supported by the widespread use of these methods in research and design.

If the integral equation methods are to be regarded as the most suitable methods for the numerical solution of wave obstacle interaction problems it is relevent to consider which of the various formulations is to be preferred. In developing an integral equation formulation there are three basic choices which must be made. The first choice is concerned with the type of fluid singularity to be used and the second choice requires the selection of any one of three alternative representations of the unknown scattered wave velocity potential. Of the six possible formulations three have been the subject of extensive investigations. The earliest solutions were published for the wave source indirect formulation and subsequently results have appeared for the wave source and the simple source direct formulations. Most authors have preferred the wave source (Green's function) formulations because they result in a much smaller system of equations and some have preferred the direct formulation. This preference is supported as the best of the above-mentioned integral equation methods particularly if the principle of energy conservation is used to give a check on the solution.

This thesis includes an investigation of results obtained for the alternatives of the third type of choice which is concerned with the location of the source distributions. Conventionally the formulations have been obtained for sources located on the cylinder boundary and the studies which employ a separated source boundary are scarce. However, it is possible to obtain indirect formulations for simple sources or wave sources located on boundaries which are external to the fluid domain.

For a distribution of wave sources over a boundary which is inside the obstacle it has been demonstrated that the resulting regular kernel integral equation formulation is amenable to numerical solution. The results obtained for the particular problem of a submerged circular obstacle in a two dimensional domain indicate that for a range of waves and a range of cylinder locations the regular kernel method is the most efficient scheme. It has been identified that the results obtained are sensitive to the location of the 'source boundary' relative to the obstacle boundary and that greater separations give more rapid convergence to a final solution as the level of discretisation is varied. It has also been identified that for more precise discretisations ill-conditioning in the system of algebraic equations gives rise to some unreliability. This problem does not preclude the suggestion that this method is the most suitable of the integral equation methods for the particular problem of waves interacting with submerged circular cylinders because more precise discretisations are always unnecessary. However, this type of failure must be investigated further if the method is to be applied to problems which do require more precise discretisation or require the solution of larger systems of algebraic equations.

Before computing the results for the regular kernel method it was anticipated that the use of higher-order discretisation schemes would permit a reduction in the level of discretisation giving a reduction in the size of the system of equations. This attempt to reduce the possibility of ill-conditioning was unsuccessful in that the results obtained with higher-order elements in the regular kernel method were never considerably better than the results obtained by the simple discretisation scheme. However, as well as being unsucessful the attempts proved to be unnecessary because the results obtained by the simple scheme proved to be quite adequate.

A secondary purpose for including the higher-order discretisation schemes in the computer program was to permit the investigation of the suitability of such schemes for use with the singular kernel method. No consistent improvement was obtained although some results demonstrated considerable improvements when compared with results obtained by the simple scheme which has been used in nearly all published studies. It is suspected that the occasional failure of the higher-order techniques is associated with the gradual variation of the quantities which the refinements are intended to model making the techniques superfluous and leading to a delay in the convergence to the final solution. The modelling of the variation of source density within an element and the variation of the Green's function value on an element must therefore be given proper consideration before a choice of discretisation scheme is made. This suggestion illustrates that there has been no detailed study of the possible sources of error due to the simple discretization scheme which would be useful if the limitations are to be better understood.

There are two ways in which the numerical study reported in this thesis might be extended. The first type of extension would involve the improvement of the existing computer program by implementing some modifications and including a number of additional options and the second type would require a considerable extension of the range of problems tested.

The improvements which might be made to the computer program may be listed as follows:

(i) Inclusion of the Green's function expressions for infinite water depth.

(ii) Amendment of the subroutines for the compilation of the kernel matrix to permit utilization of symmetry thereby reducing the number of Green's function evaluations.

(iii) Implementing a more efficient solution subroutine which employs a series of matrix operations for the solution of two simultaneous complex matrix equations in the manner described in Chapter 4.

(iv) Inclusion of an iterative procedure in the solution subroutine. This iterative procedure assists in the solution of slightly ill-conditioned systems of equations.

(v) Extension of the solution subroutine to include a conditioning number (Hearn, Donati and Mahendran, 1982), which assists in the identification of unsuitable discretisation schemes.

The extensions of the second type are of greater importance and the additional investigations recommended are:

(i) The examination of the form of the source density function to assist in the choice of relevent discretisation schemes.

(ii) The solution of problems for multiple bodies in two dimensional domains in order to determine the significance of ill-conditioning schemes for larger systems of equations.

(iii) The solution of problems of various geometries and locations in two dimensional domains to examine whether the regular kernel integral equation method is suitable for non-circular obstacles and also to determine whether or not the higher-order elements assist in modelling more difficult obstacle geometries. Particular consideration should be given to the solution of problems in which the discretised boundary includes corners.

(iv) The solution of three dimensional problems of various geometries and locations to supplement the results of Coates (1982) for the problem of a surface piercing circular cylinder in water of finite depth.

(v) The extension of the program to include evaluation of the radiation potentials for each degree of freedom and evaluation of the added mass and damping coefficients. It is anticipated that the results obtained for the body in motion by the regular kernel method will also be obtained for reduced computational requirements. This should be confirmed for the range of problems outlined above.

This recommended programme of tests is quite extensive but is obviously very necessary if the regular kernel integral equation method is to be used with confidence for the solution of wave obstacle interaction problems. Even if the regular kernel method is found to be unsuitable for more demanding problems it may be convenient to include the regular kernel option in a program so that it is possible to obtain solutions at the 'irregular frequencies' for obstacles of simple geometry in the free surface. It may be noted that the modifications to established computer programs which would be required for the implementation of the regular kernel method are only minor.

In concluding this section of the discussion it is noted that the regular kernel integral equation results in significant savings in computer core and time requirements. This method is therefore potentially very useful for more demanding problems of analysis because the savings may prove to be much greater. The most trivial example of increased reduction in computer requirements would be the repeated use of the two dimensional model with a strip theory and the most obvious example would be the application of the method to the analysis of three dimensional problems.

6.3 Discussion of Experimental Results

It must be remembered that in attempting to improve the numerical methods employed for the solution of the potential theory problems of wave hydrodynamics, the aim of the engineer is not to

obtain solutions to a high degree of accuracy but rather to establish methods which ensure that a specified accuracy is achieved for a reduced demand on computational resources.

For submerged obstacles in a two dimensional domain there are a variety of robust numerical methods which may be used to provide accurate predictions of physically significant quantities. These methods may be used to obtain solutions which are accurate in the sense that they are in close agreement with the true solution of the boundary value problems as posed. It is stressed that these results are only likely to be an accurate representation of the physics of the problem if the physical conditions closely resemble the boundary conditions of the mathematical model.

An obvious departure of the physical conditions from the conditions assumed in the formulation of the boundary value problem is due to waves of finite height interacting with an obstacle. The extent of the departure is of engineering significance because waves in the ocean are often of considerable steepness whereas the only design tools available for the solution of wave scattering or radiation problems are based on the assumption of small amplitude motion.

It has also been anticipated that the physical conditions will differ from the mathematical conditions for obstacles located at small depths below the free surface. This is because finite wave height is of greater significance in the local shallow water region above the obstacle.

Before giving detailed consideration to the experimental results obtained in this study the importance of experimental study in engineering research is emphasised. The available computer programs permit evaluation of potential theory results for objects of any geometry at any location within the wave field. However, experimental results for the various problems may, as a result of different physical mechanisms, depart from the predicted values by a different amount. This point is best illustrated by reference to the studies of Dean and Ursell (1960) and Yu and Ursell (1961) for the semi-immersed circular cylinder. The first study was performed for regular waves interacting with a fixed cylinder and the second for the vertical oscillation of the cylinder in otherwsie calm water and the discrepancy between theoretical and experimental values for wave height were different for the two problems. This is a little surprising because the object geometry is identical in both problems and it is noted that the difference in the discrepancy may prove to be greater if the amplitudes of motion are larger. It is therefore clear that if any of the numerical methods are to be used with confidence in engineering design there must be substantial experimental evidence to demonstrate the validity of the linear boundary value problem for the particular physical problem. This not only requires extensive collection of data for small amplitude wave obstacle interaction but should include investigation of important features such as finite wave height, currents and modification of waves, and therefore of wave obstacle interaction, due to wind.

The experimental results for the diffraction of waves due to interaction with a submerged horizontal circular cylinder have been obtained for small depths of submergence only. It has been found

that linear theory predictions are in good agreement with experimental measurements for small amplitude wave motion and that the theoretical result of no reflection for deep water waves is confirmed for small amplitude and finite amplitude waves. However, the amplitude of the transmitted wave and its harmonic composition are very different from the theoretical prediction when finite height waves interact with the cylinder.

The most significant result is the reduction in the amplitude of oscillation of the transmitted finite height wave. The measurement of the local wave motion just downstream of the cylinder demonstrates the greatest reduction and there is then an increase in the amplitude further downstream. A free wave oscillating at twice the wave frequency has been identified in the transmitted wave but this does not account for the energy deficit in the system. It is therefore clear that the loss of energy which is demonstrated by the reduced wave height in the far-field transmitted wave must be due to the occurrence of viscous effects. One viscous mechanism which is easily identified and which must be responsible for a large proportion of the energy dissipation is the spilling of the wave surface which occurs just after the wave crest has passed the cylinder. However, wave breaking does not provide a complete explanation for the energy deficit because losses are also identified for the steep waves which are transmitted without any distortion of the wave crest.

The local reduction in the amplitude of the wave motion downstream of the cylinder is not easily explained because of the partial recovery of wave amplitude which is identified in the far-field

motion. It is suggested that two local effects might explain this apparent loss and then recovery of energy. The first possible explanation is that the loss in the amplitude of oscillation occurs because the energy is sustaining a change in mean water level and the second possibility is that there is a local increase in wave velocity so that a greater proportion of the wave energy is being transported as kinetic energy.

The existence of a free wave oscillating at twice the wave frequency in the transmitted wave is of interest because it provides some experimental confirmation for the second-order diffraction analysis (sections 3.9 and 3.10). Computation of a second-order transmission coefficient would permit quantitative comparison with the experimental results and for waves of intermediate steepness (before breaking becomes significant) might provide for a reasonable estimation of the magnitude of the mean force (Longuet-Higgins, 1977).

Comparison of the measured pressure oscillations at the wave frequency with the results of the linear theory diffraction computer program establishes that for the interaction of finite height waves with a submerged circular cylinder located just below the free surface the agreement beween experiment and theory is poor. The results for the measurements of the diffracted wave motion and the pressures under the wave in the absence of the cylinder are of assistance when attempts are made to explain why these differences occur.

The conditions when the measured pressures disagree with theory are very similar to the conditions when the wave motion departs

from the theoretical form. The inducement of high particle velocities in the local shallow water region above the cylinder, the reduced amplitude of oscillation downstream of the cylinder and the failure to sustain the local standing wave motion and the occurrence of wave breaking for the steepest waves are mechanisms which might be responsible for the departure of the measured results from the theoretical predictions. The consistent theoretical underestimation of pressures which was identifies in the pressure measurements below the wave are not always so evident in the measurements of pressure on the cylinder. It is suggested that this may be partly due to the loss of energy in the system.

The occurrence of pressure oscillations at twice the wave frequency is in agreement with the second-order analysis which was outlined towards the end of chapter 3, (sections 3.9 and 3.10). It may therefore be possible to obtain theoretical results which demonstrate agreement with the measured values but this line of further investigation is inappropriate. This is because in the presenty study the oscillations are not large enough to affect the peak to peak pressure oscillations and also because the major discrepancy between theory and experiment are in the amplitudes of the pressure and free surface oscillations at the wave frequency.

There are a number of extensions to this particular experimental study of wave obstacle interaction which may be of value. In all of the suggested extensions which follow the collection of results for a range of wave steepnesses and cylinder locations should be continued because a greater understanding of non-linear interaction is required.

It is suggested that pressure measurements should be collected for a wider range of values of the diffraction parameter. This could be achieved both by the construction of additional test cylinders of different diameters and by increasing the range of wave frequency for tests with the existing cylinder. The aim of extending the experimental study in this way is to establish how well the mathematical model represents the physics of wave scattering. Results cited in the literature survey (section 2.5) and the experimental results obtained in this study appear to demonstrate that good agreement between theory and experiment is obtained when diffraction effects are small or when the loading is entirely inertial but that as diffraction effects become more significant the discrepancy between theory and experiment increases.

An additional reason for this first type of extension would be to determine whether or not fluid separation effects become significant at the same time as wave scattering effects. Preliminary calculations and tests demonstrate that this is possible for cylinders at very small depths of submergence even if the Keulegan-Carpenter number is small because the very much higher velocities which are induced above the cylinder may result in separation downstream of the cylinder. The presence of a wake may be established by obtaining pressure measurements at a large number of locations on a single cross-section and comparison of the measured pressure distribution with the theoretical distribution at a number of instants in a period will permit identification of the development of a fluid wake.

The measurement of pressure at four locations on the cylinder has proved sufficient for the present study since it has permitted comparison between theory and experiment to establish the importance of wave nonlinearity and small cylinder submergence. Although several studies have already been completed for the measurement of forces on submerged horizontal circular cylinders in waves, it is suggested that additional force measurements should be obtained for a range of cylinder locations and wave steepnesses. In some of the suggested studies which follow force measurements may prove to be preferable to pressure measurements because they give a more general impression of the agreement between experiment and theory. However, pressure measurements may be of assistance in identification of the mechanisms responsible for the discrepancies so that the best procedure would be to collect a large amount of force data supplemented by more detailed pressure measurements when larger discrepancies occur.

In the present study the deformation of the incident waves as they pass over the 'double beach' has proved to be of importance when cylinder submergence is small. For smaller cylinders located near the free surface there are visually identifiable deformations of the free surface. It is therefore suggested that wave obstacle interaction should be investigated for cylinders which are subject to inertia and drag loading when located near the free surface. It would be surprising if force predictions obtained by Morison's equation with coefficient values obtained from experiments at larger depths of submergence (Koterayama , 1979) provide a good representation for the measured force when finite height free surface effects are large. It is less likely that coefficient values derived from

oscillatory flow tests will provide accurate predictions.

For shallow cylinder submergence the considerable difference between the predicted and measured wave motion just downstream of the cylinder suggests that if two bodies are separated by a small distance the departure from theory for force and pressure measurement may be great. It would be of interest to perform a study which is similar to the one reported in this thesis for two cylinders.

The experimental study which has been performed has not only attempted to provide for the validation of linear wave theory for small amplitude waves but has sought to investigate the importance of phenomena of engineering significance. The remaining suggestions for the extension of the experimental study are all concerned with providing conditions which resemble ocean conditions more closely.

The investigation of the effects of currents would be worthwhile and in this case it would be possible to modify the theoretical model. Investigation of wind effects would also be of interest but there is no simple extension of the theoretical model for this type of problem. The final suggestion is that interaction of irregular waves with submerged obstacles should be studied particularly when non-linear effects are known to be important for monochromatic waves.

6.4 Discussion of Higher-Order Theory

The necessity for a higher-order numerical solution is demonstrated by the failure of the linear theory to predict the experimental results in this study and will be of importance in a number of different problems when wave steepness and local shallow water effects become significant. Higher-order theory will also be necessary if accurate numerical modelling is required for ship-motion problems when the amplitude of oscillation of the body becomes large.

There appear to be two alternative approches in the development of a non-linear theory for wave obstacle interaction problems. The first resembles the Stokes' wave formulation and if numerical solutions can be computed this method would provide second-order solutions for wave diffraction and radiation problems. The second approach employs a time-stepping procedure in which the development of the free surface is followed. The results obtained by this time-stepping method have been referred to as numerically exact solutions because the complete non-linear boundary condition is applied at the moving free surface.

There are two different methods which may yield numerical solutions for the second-order wave obstacle interaction problem. The most complete approach is the one which has been presented in this thesis (sections 3.9 and 3.10) and it is suggested that the improved efficiency which may be achieved by application of the regular kernel integral equation method makes the numerical solution of the second-order boundary value problem a less formidable task.

The alternative method adopts the approach suggested by Lighthill (1979) in which the second-order force on a fixed obstacle is evaluated by solving a linear radiation problem and evaluating an integral over the free surface. The advantage of Lighthill's method is that the second-order potential does not need to be evaluated.

It has been demonstrated that the second-order boundary value problem predicts that wave obstacle interaction gives rise to wave and pressure oscillations at twice the fundamental frequency. This has been confirmed experimentally but is not of great significance in the present study because the amplitudes of these oscillations are not sufficiently large to be of importance. Further, for the steeper waves interacting with a cylinder located near the free surface the discrepancy between experiment and theory would not be reduced by this type of theoretical refinement because it is the amplitudes of the fundamental oscillations of the free surface and the pressure which demonstrate poor agreement with theory.

Although the second-order theory is of little value for the range of experimental data covered in this study it may be of value for a different range of data and may be suitable for solution of ship-motion problems. It is suggested that results of a second-order theory may prove to be adequate for any obstacle geometry or location for which local shallow water effects are absent because it is these effects which give rise to the large discrepancies between experiment and theory for submerged horizontal cylinders.

If accurate numerical modelling of wave obstacle interaction is required for obstacles submerged just below the free surface the time-stepping methods are the only possibility. Recent developments in the application of these methods are reported by Vinje, Maogang and Brevig (1982) and Lau (1983). The methods are potentially very useful because they permit modelling of steep waves and breaking waves but a considerable amount of further investigation is required before it can be concluded that these numerical methods provide an accurate prediction of the physics of wave obstacle interaction.

CHAPTER 7 - CONCLUSIONS

The integral equation formulations of potential theory problems have been considered and have been applied to the particular problem of small amplitude waves interacting with submerged obstacles in a two dimensional domain. Conventionally the integral equation formulations for wave obstacle interaction are the result of fictitious distributions of fluid singularities throughout the fluid domain and over its boundaries. The outcome of this abstact procedure is that the velocity potential of the unknown motion is represented by a distribution of sources over the boundary of the fluid domain. The extent of this boundary is often reduced by choice of an appropriate Green's function but each of the various formulations results in a formulation which is a Fredholm equation of the second kind with a singular kernel.

It has been demonstrated that if the fictitious distribution of sources is extended to include a portion of the infinite domain which is external to the fluid domain the resulting formulation is a Fredholm equation of the first kind with a regular kernel. For the problem of wave scattering by submerged obstacles this alternative formulation may be regarded conceptually as the generation of the scattered wave motion by the continuous distribution of fluid singularities over a boundary which lies outside the fluid domain. The regular kernel integral equation obtained in this manner is an indirect formulation and it has been demonstrated that direct formulations always give integral equations with singular kernels.

The numerical solution of indirect integral equation formulations has been investigated by solving a series of test problems by the singular and regular kernel methods. The integral equation which was chosen for numerical analysis included the 'wave function' and the problem was therefore reduced to the discretisation of integral equations and integrals on the boundary of the obstacle or on a separate 'source boundary'. The numerical techniques which have been used most often in the solution of integral equations of this type are simple and methods have been described which involve the refinement of the discretisation procedure and may therefore result in an improved efficiency in solution.

Results obtained by using the simple discretisation procedure have demonstrated that the regular kernel integral equation formulation is amenable to numerical solution and that for the problems tested this method is generally more efficient and occasionally very much more efficient than the conventionally employed singular kernel method. It is important to note that the efficiency and reliability of the method are sensitive to the location of the source boundary and it is concluded that the most rapid convergence to the final solution is obtained for source distributions which are located on boundaries which are remote from the obstacle boundary but that the results obtained for such distributions are unreliable for more precise discretisations due to ill-conditioning in the system of algebraic equations.

The regular kernel integral equation method is a potentially advantageous alternative to the conventional singular kernel integral

equation methods. The results of this study together with results obtained in earlier studies demonstrate that for a given level of discretisation the regular kernel method provides more accurate results than the singular kernel method. Therefore, if results are required to a specified accuracy the use of the regular kernel method permits a reduction in the level of discretisation which results in an improvement in computational efficiency. For the problems tested ill-conditioning has only been identified for unnecessarily fine discretisations and does not therefore diminish the usefulness of the regular kernel method.

For the regular kernel method the results obtained by application of the higher-order discretisation techniques never indicated any marked improvement in efficiency. There were however some occasions when the use of the higher-order techniques gave improved convergence to the final solution for the singular kernel methods but for other examples the method indicated that the techniques are detrimental to efficiency. It is concluded that the application of higher-order elements is not well understood and that further investigations are required to determine their usefulness.

The experimental study was designed to permit validation of the linear potential theory results for small amplitude waves interacting with a submerged horizontal circular cylinder and to examine the extent to which the measured results depart from the theoretical predictions when non-linear effects due to finite wave height and shallow cylinder submergence become important.

The measurements obtained for the wave motion indicate that the linear diffraction theory provides a good representation of the physical motion due to interaction when wave steepness is small. Even when wave steepness is large the linear potential theory result of no reflection holds but the transmitted wave does not agree with theory and demonstrates a loss of energy in the system. Free waves oscillating at multiples of the fundamental frequency are generated by the wave cylinder interaction but analysis demonstrates that this energy transfer is small and does not account for the lost energy. This energy loss is greatest when wave breaking is induced but other mechanisms are also responsible for the dissipation.

Theoretical and experimental results for the wave motion in the near-field have also been presented and again agreement is reasonable for small amplitude waves but deteriorates as wave steepness increases and is particularly poor when wave breaking occurs.

Comparison of pressure measurements with linear theory predictions indicates that there is good agreement for small amplitude waves when the cylinder is located at larger depths of submergence. When wave steepness or local shallow water effects become significant the pressure measurements do not agree so well and agreement is particularly poor for the steepest waves at the shallowest submergence.

The results of the experimental study demonstrate the value of the linear diffraction theory for the prediction of physically significant quantities for the interaction of monochromatic small

amplitude waves with a submerged horizontal circular cylinder. Wave steepness and local shallow water effects result in discrepancies between and experiment and theory which are often very large and these results indicate that the theoretical model must be extended to a higher order if the physics of wave cylinder interaction is to be accurately modelled.

APPENDIX A.1 THE FREDHOLM INTEGRAL EQUATION

Many excellent texts have been written in which the theory of integral equations is comprehensively treated and this appendix is intended only to introduce the subject and to define the terms used in the text of the thesis. The interested reader should refer to Petrovskii (1957) or Smithies (1958) for a full account.

The integral equation is one in which the unknown function occurs under the integral sign. The equation

$$\alpha(\underline{x})\phi(\underline{x}) + f(\underline{x}) = \int_{\Gamma} K(\underline{x},\underline{\xi})\phi(\underline{\xi})d\Gamma \qquad \text{A.1.1}$$

is an integral equation in the function $\phi(\underline{\xi})$, where $\alpha(\underline{x})$, $f(\underline{x})$ and $K(\underline{x},\underline{\xi})$ are known functions and $\phi(\underline{\xi})$ is to be determined. Γ is a region of the $\underline{\xi}=\xi,\eta$ plane and $\underline{x}=x,y$ is a point of Γ. The equation is linear and $K(\underline{x},\underline{\xi})$ is referred to as the kernel. Provided $\alpha(\underline{x})$ never vanishes equation A.1.1 may be written

$$\phi(\underline{x}) = \int_{\Gamma} K(\underline{x},\underline{\xi})\phi(\underline{\xi})d\Gamma + f(\underline{x}) \qquad \text{A.1.2}$$

which is a Fredholm equation of the second kind and if $f(\underline{x}) = 0$ this equation is said to be homogenous. If the function $\alpha(x) = 0$ in equation A.1.1

$$f(\underline{x}) = \int_{\Gamma} K(\underline{x},\underline{\xi})\phi(\underline{\xi})d\Gamma \qquad \text{A.1.3}$$

and equation A.1.3 is a Fredholm equation of the first kind.

The classical Fredholm theory is concerned with equations of the second kind and no general theory for equations of the first kind is available. The theory is concerned with equation A.1.2 written in the form

$$\phi(x) = \lambda \int_{\Gamma} K(\underline{x},\underline{\xi})\phi(\underline{\xi})d\Gamma + \phi(x) \qquad \text{A.1.4}$$

and the basic concept is to regard equation A.1.4 as the limiting form of a finite system of linear equations in a finite number of variables. This is Fredholm's (1903) celebrated discretisation scheme which, incidentially, forms the basis for the solution of such equations. This was not, however, appreciated at the time of introduction and the purpose was to establish a theory for the integral equation by carrying over the known theorems about linear algebraic equations.

Of the Fredholm theorems it is sufficient here to state only the first which reads

> Either the given non-homogenous integral equation of the second kind has one and only one solution for every function $f(\underline{x})$, or the corresponding homogenous equation has at least one non-trivial solution, that is one that is not identically zero.

The significance of this theorem is that under certain circumstances an integral equation formulation of a potential theory problem has no solution. This does not mean that no solution to the problem exists, but that the integral equation is, in such cases, an unsuitable formulation. It may be noted that the occurrence of such a breakdown is, in practice, rare.

The classical Fredholm theory is, strictly speaking, only applicable for non-singular kernels. However, if the kernel is weakly singular the Fredholm theory may be applied if the integral operator remains non-singular. This situation bears a certain similarity to the definition of a Cauchy principal value integral. In the text of the thesis we are concerned with a Fredholm equation of the first kind with a non-singular or regular kernel and a Fredholm equation of the second kind with a logarithmic singularity in the kernel. The corresponding systems of linear algebraic equations may therefore be written, in matrix form, as

$$(\underline{A} - \alpha \underline{I})\underline{x} = \underline{b} \qquad \text{A.1.5}$$

where $\underline{A}$ is the kernel matrix, $\underline{I}$ is the unit matrix, $\underline{b}$ is a vector containing known values and $\underline{x}$ is the unknown vector. The constant α is zero for the Fredholm equation of the first kind and is given for equations of the second kind.

APPENDIX A.2 DETAILS OF THE SECOND-ORDER INTEGRAL EQUATION FORMULATION

The following equations are required for the application of the boundary condition at the free surface in the integral equation formulation of the second-order diffraction boundary value problem.

$$\phi^{(1)}(\underline{x},t) = \Phi_w^{(1)}(\underline{x},t) + \int_\Gamma \sigma(\xi)\phi^*(\underline{x},\underline{\xi},t)d\Gamma \qquad \text{A.2.1}$$

$$\frac{\partial\Phi}{\partial x}^{(1)}(\underline{x},t) = \frac{\partial\Phi_w^{(1)}}{\partial x}(\underline{x},t) + \int_\Gamma \sigma(\underline{\xi})\ \frac{\partial\Phi}{\partial x}^*(\underline{x},\underline{\xi},t)d\Gamma + \beta\sigma(\underline{x})\exp(-i\omega t) \qquad \text{A.2.2}$$

$$\frac{\partial\phi}{\partial y}^{(1)}(\underline{x},t) = \frac{\partial\Phi_w^{(1)}}{\partial y}(\underline{x},t) + \int_\Gamma \sigma(\underline{\xi})\ \frac{\partial\phi}{\partial y}^*(\underline{x},\underline{\xi},t)d\Gamma + \beta\sigma(\underline{x})\exp(-i\omega t) \qquad \text{A.2.3}$$

$$\frac{\partial^2\phi}{\partial x\partial t}^{(1)}(\underline{x},t) = -i\omega\ \frac{\partial\phi}{\partial x}^{(1)}(\underline{x},t) \qquad \text{A.2.4}$$

$$\frac{\partial^2\phi}{\partial y\partial t}^{(1)}(\underline{x},t) = -i\omega\ \frac{\partial\phi}{\partial y}^{(1)}(\underline{x},t) \qquad \text{A.2.5}$$

$$\frac{\partial\phi}{\partial t}^{(1)}(\underline{x},t) = -i\omega\ \phi^{(1)}(\underline{x},t) \qquad \text{A.2.6}$$

$$\frac{\partial^3\phi}{\partial y\partial t^2}^{(1)}(\underline{x},t) = (-i\omega)^2\ \frac{\partial\phi}{\partial y}^{(1)}(\underline{x},t) \qquad \text{A.2.7}$$

$$\frac{\partial^2\phi}{\partial y^2}^{(1)}(\underline{x},t) = \frac{\partial^2\Phi_w^{(1)}}{\partial y^2}(\underline{x},t) + \int_\Gamma \sigma(\underline{\xi})\ \frac{\partial^2\phi}{\partial y^2}^*(\underline{x},\underline{\xi},t)d\Gamma \qquad \text{A.2.8}$$

where $\phi^*(\underline{x},\underline{\xi},t) = \phi^*(\underline{x},\underline{\xi})\exp(-i\omega t)$ A.2.9

and no singular term arises in equation A.2.8 since the singularity

is stronger and causes the integration over a semi-circle to vanish.

APPENDIX A.3 NUMERICAL DETAILS

A.3.1 Lagrangian Interpolation and Boundary Elements

The aim of interpolation in classical numerical analysis is to evaluate the value of a function at certain points within an interval when the value of the function is known at a number of tabular points. The many sophisticated interpolation techniques which have been developed are now generally redundant due to the advent of the digital computer since it is usually more convenient to evaluate the function directly. It is, however, occasionally advantageous to employ simple interpolation techniques.

The finite element and boundary element methods developed in recent years for the numerical solution of differential and integral equations respectively, require that the governing equations and the boundary conditions are satisfied at a finite number of nodal points on a number of elements. The elements are obtained by subdivision of the original volume, area or line and it is often advantageous to choose elements with more than one node since this avoids the necessity for a more precise subdivision of the original domain or boundary. Each element may therefore be regarded as analogous to the tabular problems for which interpolation techniques have been developed with the distinction that the values of the function at the nodal or tabular points are initially unknown. The interpolation techniques are therefore first employed not to evaluate the value of the function but to describe the variation of the function within each element. However, once the problem has

been constructed and solved to obtain the values of the unknown function at the nodal points the interpolation techniques may be employed in a more conventional manner to obtain the values of the required function at points throughout the domain.

The problem which is the subject of the text of the thesis is reduced to a one-dimensional problem and the boundary elements are simple lines. Since the object is circular the boundary elements, whether coincident with the cylinder boundary or not, are arcs of a circle. In this and subsequent appendices an element coordinate system is employed and the results given must therefore be transformed into the cartesian coordinate system before they are employed in the assembly of the required matrix equations.

A representation for the variation of a function $f(\zeta)$ within an element $\Delta\zeta$ is required. The basis of interpolation is to replace the function, f, by an approximation to it denoted by $h(\zeta)$ where

$$h(\zeta) = N_k(\zeta)f(\zeta_k) + E(\zeta), \quad k=1,.....,n \qquad \text{A.3.1}$$

where ζ_k are the nodal or tabular points and the repeated index implies summation. Since the values of the functions h and f are required to be identical at the nodal points so that $E(\zeta) = 0$

$$N_k(\zeta_j) = \delta_{jk} \qquad j,k = 1,.....,n \qquad \text{A.3.2}$$

where δ_{jk} is the Kronecker delta defined by

$$\delta_{jk} = 1 \qquad j = k, \qquad \text{A.3.3a}$$

$$\delta_{jk} = 0 \qquad j \neq k. \qquad \text{A.3.3b}$$

The polynomials $N_k(\zeta)$ are given by

$$N_k(\zeta) = \frac{(\zeta - \zeta_1).....(\zeta - \zeta_{k-1})(\zeta - \zeta_{k+1}).....(\zeta - \zeta_n)}{(\zeta_k - \zeta_1).....(\zeta_k - \zeta_{k-1})(\zeta_k - \zeta_{k+1}).....(\zeta_k - \zeta_n)} \qquad \text{A.3.4}$$

and are referred to as the Lagrangian interpolation polynomials.

The interpolation polynomials employed in the writing of the diffraction program are for two or three nodal points per element, (n=2 and n=3). The variation of the unknown function is therefore approximated by either a linear or a quadratic function within the element since equation A.3.4 gives a polynomial of order (n-1). For n=2 equation A.3.1 is written

$$h(\zeta) = \frac{(\zeta - \zeta_2)}{(\zeta_1 - \zeta_2)} f(\zeta_1) + \frac{(\zeta - \zeta_1)}{(\zeta_2 - \zeta_1)} f(\zeta_2) \qquad \text{A.3.5}$$

and for n=3

$$h(\zeta) = \frac{(\zeta - \zeta_2)(\zeta - \zeta_3)}{(\zeta_1 - \zeta_2)(\zeta_1 - \zeta_3)} f(\zeta_1) + \frac{(\zeta - \zeta_1)(\zeta - \zeta_3)}{(\zeta_2 - \zeta_1)(\zeta_2 - \zeta_3)} f(\zeta_2)$$

$$+ \frac{(\zeta - \zeta_1)(\zeta - \zeta_2)}{(\zeta_3 - \zeta_1)(\zeta_3 - \zeta_2)} f(\zeta_3) \qquad \text{A.3.6}$$

If the element $\Delta\zeta$ is given by $-1 \leq \zeta \leq 1$ equations A.3.5 and A.3.6 may be written

$$h(\zeta) = \frac{(\zeta-1)}{2} f(\zeta_1) + \frac{(\zeta+1)}{2} f(\zeta_2) \qquad \text{A.3.7a}$$

$$h(\zeta) = \frac{\zeta}{2}(\zeta-1) f(\zeta_1) + (\zeta+1)(\zeta-1) f(\zeta_2) + \frac{\zeta}{2}(\zeta+1) f(\zeta_3) \qquad \text{A.3.7b}$$

and equation A.3.7 is employed in subroutine VARN.

A.3.2 Legendre-Gauss Quadrature

The general form for a quadrature formula within the interval $a \leq \mu \leq b$ is

$$\int_a^b I(\mu)\, d\mu = H_j\, I(\mu_j) + E\ , \quad j=1,\ldots.n \qquad \text{A.3.8}$$

where the repeated index implies summation. An equation of this type might be derived by integration of the Lagrangian interpolation formula given in equation A.3.1. This procedure is not carried out but indicates that the error E can be made zero for n abscissas, μ_j, and n weights, H_j, if the polynomial is chosen to be of order 2n-1. The degree of this polynomial may then be referred to as the order of accuracy of the quadrature formula.

The quadrature formula employed in the diffraction program is the Legendre-Gauss quadrature formula so-called because the abscissas are chosen to be the zeros of the Legendre polynomial or order n. The Legendre-Gauss formula is written for an interval $-1 \leq \mu \leq +1$

$$\int_{-1}^{+1} I(\mu)d\mu = H_j I(\mu_j) \qquad \text{A.3.9}$$

and the values of the abscissas and weights for $n \leq 4$ is given in Table A.3.1.

n	Abscissas μ_j	Weights H_j
2	±0.577350	1
3	0	0.888889
	±0.774597	0.555556
4	±0.538469	0.652145
	±0.906180	0.347855

Table A.3.1 Quadrature Data

In the main text of the thesis it has been stated that the abscissas of the Guassian quadrature correspond to the points at which a number of discrete sources are located. This is conceptually convenient but might be regarded in an alternative manner. If it is assumed that a continuous distribution of sources is located on each individual element, the choice of the order of the quadrature formula determines whether this source distribution is to be represented by a constant, linear, quadratic or higher-order variation. The order of the variation is identical to the number of quadrature points and therefore the statement that the source variation within each element is quadratic is equivalent to stating that two discrete sources are located on each element.

The interval for which the quadrature formula is stated is identical to the "element" interval chosen for equation A.3.7 and therefore the evaluation of the integrals in equation 4.2.9 is straightforward provided the source point coordinates, $\underline{\xi}_j$, are specified to correspond with the abscissas, μ_j. It may be noted that since the elements are arcs of a circle the Jacobian $|J|$ is not required and the transformation of equations A.3.7 and A.3.9 into the global cartesian coordinate system is complete if an element length factor is included and the nodal labeling is transformed.

A.3.3 Integration of the normal gradient of the logarithmic singularity

The integral to be considered may be identified as a component of the integral written in equation 4.2.7 and is of the form

$$\int_{\Delta\Gamma} \frac{\partial}{\partial m} \log \left|\underline{x} - \underline{\xi}\right| \cdot N_k (\underline{\xi}) \, d\Gamma \qquad \text{A.3.10}$$

If equation A.3.10 is rewritten for an element coordinate system similar to that adopted in the previous sections of this appendix and if the nodal point $\underline{x}$ is chosen to coincide with the origin of this coordinate system there are two locations of the nodal point which are significant. The first is the central location indicated in Figure A.3.1a and in this case equation A.3.10 is rewritten in the form

$$\int_{-1}^{+1} \frac{\partial}{\partial m} \log \mu \cdot N(\mu) d\mu \qquad \text{A.3.11}$$

where $$\frac{\partial}{\partial m} \log \mu = \frac{\partial}{\partial m} \log \mu \cdot \frac{\partial \mu}{\partial m} = \frac{1}{\mu} \qquad \text{A.3.12}$$

hence $$\int_{-1}^{+1} \frac{1}{\mu} N(\mu) d\mu \qquad \text{A.3.13}$$

where the integral must be evaluated in the Cauchy principal value sense. This central location of the node is significant if either a constant or quadratic variation of source density is assumed on the

element. Since in both cases the interpolation function N is an even function within the chosen coordinate system and the function $1/\mu$ is odd the integrand must be an odd function and the result of the integral A.3.13 zero.

The second choice of nodal location is a point at the end of an element and is indicated in Figure A.3.1b

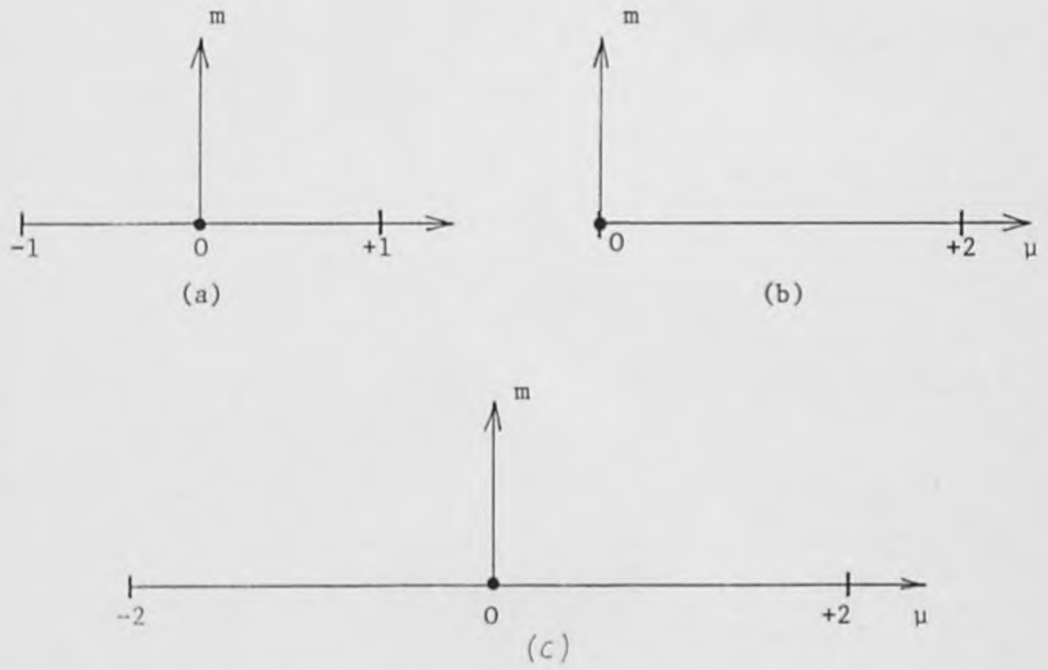

Figure A.3.1 Nodal Locations on an Element

In this case, with the evaluation of the gradient as in equation A.3.12, equation A.3.10 must be rewritten

$$\lim_{\varepsilon \to 0} \int_{-2}^{-\varepsilon} \frac{1}{\mu} N'(\mu) d\mu + \lim_{\varepsilon \to 0} \int_{\varepsilon}^{+2} \frac{1}{\mu} N(\mu) d\mu \qquad \text{A.3.15}$$

where the element configuration is indicated in Figure A.3.1c and the interpolation function N' refers to the additional element. The integration in equation A.3.15 is again a Cauchy principal value integral and examination of the interpolation functions in equations A.3.7a and A.3.7b indicates that the interpolation functions give an even function so that the integral vanishes.

It must be emphasised that these integral results only apply to the cases in which the nodal point and the source distribution occur on the same element and therefore do not apply when the source boundary is separated from the physical boundary.

A.3.4 Numerical Solution of the Dispersion Equation

The dispersion equation for progressive gravity waves in water of finite depth, h, may be written in the form

$$m \tanh (mh) = \nu \qquad \text{A.3.16}$$

where m are the required roots. The real roots of the equation are $m = \pm k$, where k is the wave number which may be evaluated directly from the data supplied to the program. The imaginary roots are obtained by making the substitution m = ic and equation A.3.16 is written

$$ic \tanh (ich) = \nu \qquad \text{A.3.17}$$

and the identity $\tanh(i\theta) = i\tan(\theta)$ gives

$$c \tan(ch) = -\nu \qquad \text{A.3.18}$$

which is identical to equation 3.4.16. The roots of the dispersion equation are then completely expressed by

$$m = \pm c_i, \qquad i = 0,1,2,.... \qquad \text{A.3.19}$$

where $c_o = k$. In evaluating the wave function and the gradient of the wave function by the series expressions the positive roots of the dispersion equation are taken and since the series is to be truncated only a finite number of roots are to be evaluated.

Equation A.3.18 has been solved by applying the Newton-Raphson iterative method in the following manner. The Newton-Raphson formula may be expressed in the form

$$c_{n+1} = c_n - \frac{f(c_n)}{f'(c_n)} \qquad \text{A.3.20}$$

where the prime denotes differentiation, the suffix indicates successive approximations to the root and

$$f(c) = c \tan(ch) + \nu \qquad \text{A.3.21}$$

Therefore,

$$f'(c) = \text{cosech}^2(ch) + \tan(ch) \qquad \text{A.3.22}$$

and after a little algebra

$$c_{n+1} = \frac{2c_n^2 h - 2\nu\cos^2(c_n h)}{\sin(2c_n h) + 2c_n h} \qquad \text{A.3.23}$$

It is now required that suitable trial values are chosen and that the required roots of equation A.3.18 are obtained to a specified accuracy.

The choice of trial values is best demonstrated by rewriting equation A.3.21 in the form

$$f(c) = \tan(ch) + \frac{\nu}{c} \qquad \text{A.3.24}$$

If the components of f(c) are plotted (Figure A.3.2) the points of

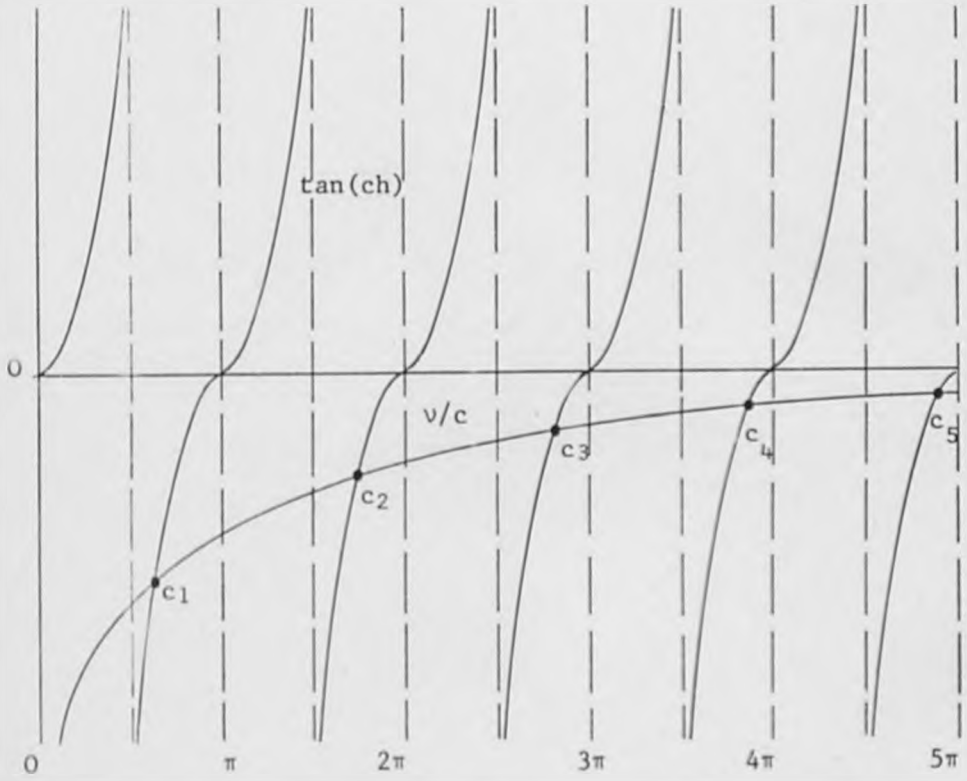

Figure A.3.2 Roots of Dispersion Equation

intersection indicate the values of the roots of equation A.3.18 and it is clear that

$$c_i \in ((2i - 1)\pi/2, \quad (2i + 1)\pi/2), \; i=1,2,... \qquad \text{A.3.25}$$

For the first root the trial value is taken to be $(\Pi/2 + \varepsilon)$ where ε is a small positive value chosen to ensure that $(\Pi/2 + \varepsilon) < c_1$, thereby guaranteeing convergence to the root. Each successive root is greater than the previous root by $(\Pi + \delta)$ where δ is a small positive value and the i^{th} root is obtained by applying the Newton-Raphson formula (equation A.3.23) with a trial value $(c_{i-1} + \Pi)$. For each evaluation iteration proceeds until the required accuracy is achieved.

The computation of this iterative procedure is contained within subroutine DISP.

A.3.5 Integration of logarithmic singularity

The procedure of this section closely resembles that which has been adopted in section A.3.3 for the normal gradient of the logarithmic singularity. The integrals to be considered for the possible nodal location which arise in assuming constant, linear or quadratic variation of source density may be written in the general form

$$\int_{\Delta\Gamma} \log |\underline{x} - \underline{\xi}| \cdot N_k(\underline{\xi}) d\Gamma \qquad \text{A.3.26}$$

and the particular integrals in question are those for which $\underline{x}$ and $\underline{\xi}$ both lie within $\Delta\Gamma$.

Each integral of this type must be evaluated analytically for inclusion in the diffraction program since a numerical integration of

these integrals would yield poor results. The first integral to be evaluated is for the case of an assumed constant variation of source density on the element and the origin of the local coordinate system coincides with the central node as illustrated in Figure A.3.1a with the exception that it is more convenient in this case to introduce the element length, ℓ, which gives an interval $(-\ell/2, \ell/2)$. The interpolation function $N_k (k = 1)$ has the value of unity over the element and the required integral is of the form

$$\int_{-\ell/2}^{+\ell/2} \log \mu \, d\mu \qquad \text{A.3.26}$$

This integral together with each of the integrals introduced in this section must be evaluated in the Cauchy principal value sense and for integrals in which the node is centrally located it is convenient to evaluate the integral over half of the element. The integral evaluation of A.3.26 is as follows

$$\begin{aligned}
\int_{-1}^{+1} \log \mu \, d\mu &= 2 \lim_{\varepsilon \to 0} \int_{\varepsilon}^{+\ell/2} \log \mu \, d\mu \\
&= 2 \lim_{\varepsilon \to 0} \left[\mu \log \mu \right]_{\varepsilon}^{+\ell/2} + \lim_{\varepsilon \to 0} \int_{\varepsilon}^{\ell/2} d\mu \\
&= \ell \log(\ell/2) + \lim_{\varepsilon \to 0} \left[\mu \right]_{\varepsilon}^{\ell/2} \\
&= \ell(\log(\ell/2) + 1/2) \qquad \text{A.3.27}
\end{aligned}$$

For the assumed linear variation of source density, two

integrals must be evaluated one for each of the interpolation functions which are given by

$$N_1 = (1 - \mu/\ell), \quad N_2 = \mu/\ell \qquad \text{A.3.28}$$

The two integrals and their results may be written

$$\lim_{\varepsilon \to 0} \int_{\varepsilon}^{\ell} (1 - \mu/\ell) \log \mu \, d\mu = \frac{\ell}{2} \log \ell - \frac{3\ell}{4} \qquad \text{A.3.29a}$$

$$\lim_{\varepsilon \to 0} \int_{\varepsilon}^{\ell} \frac{\mu}{\ell} \log \mu \, d\mu = \frac{\ell}{2} \log \ell - \frac{\ell}{4} \qquad \text{A.3.29b}$$

and evaluation of the results of these integrals is similar to the evaluation given in A.3.27.

The interpolation functions for the assumed quadratic variation of source density take different forms depending on the location of the node and therefore the location of the origin of the local coordinate system. For a node located at the end of the element the interpolation functions are written

$$N_1 = (1 - 2\mu/\ell)(1 - \mu/\ell), \qquad \text{A.3.30a}$$

$$N_2 = 4\mu(1 - \mu/\ell)/\ell \qquad \text{A.3.30b}$$

$$N_3 = \mu(2\mu/\ell - 1)/\ell \qquad \text{A.3.30c}$$

and the integrals to be evaluated with the results are

$$\lim_{\varepsilon\to 0}\int_{\varepsilon}^{\ell}(1-2\mu/\ell)(1-\mu/\ell)\log\mu\,d\mu=\frac{\ell}{6}\log\ell-\frac{17}{36}\ell \qquad \text{A.3.31a}$$

$$\lim_{\varepsilon\to 0}\int_{\varepsilon}^{\ell}(4\mu(1-\mu/\ell)/\ell)\log\mu\,d\mu=\frac{2\ell}{3}\log\ell-\frac{5}{9}\ell \qquad \text{A.3.31b}$$

$$\lim_{\varepsilon\to 0}\int_{\varepsilon}^{\ell}(\mu(2\mu/\ell-1)/\ell)\log\mu\,d\mu=\frac{\ell}{6}\log\ell+\frac{\ell}{36} \qquad \text{A.3.31c}$$

For a centrally located node the interpolation functions are

$$N_1 = 2(\mu/\ell)^2-(\mu/\ell) \qquad \text{A.3.32a}$$

$$N_2 = 1-4(\mu/\ell)^2 \qquad \text{A.3.32b}$$

$$N_3 = 2(\mu/\ell)^2+(\mu/\ell) \qquad \text{A.3.32c}$$

and as stated above it is convenient to evaluate the integrals over half of the element and these integrals with the results are

$$\lim_{\varepsilon\to 0}\int_{\varepsilon}^{\ell/2}(2(\mu/\ell)^2-(\mu/\ell))\log\mu\,d\mu=\ell(5/6-\log(\ell/2))/24 \qquad \text{A.3.33a}$$

$$\lim_{\varepsilon\to 0}\int_{\varepsilon}^{\ell/2}(1-4(\mu/\ell)^2)\log\mu\,d\mu=\ell(6\log(\ell/2)-8)/18 \qquad \text{A.3.33b}$$

$$\lim_{\varepsilon\to 0}\int_{\varepsilon}^{\ell/2}(2(\mu/\ell)^2+(\mu/\ell))\log\mu\,d\mu=\ell(5\log(\ell/2)-13/6)/24 \qquad \text{A.3.33c}$$

and the results for integration over the whole element are obtained by adding the results of equations A.3.33a and A.3.33c to obtain the integrals which include the interpolation functions N_1 and N_3

and doubling the result of equation A.3.33b for the integral which includes N_2. This approach might at first appear incorrect or at best inconsistent but is justified by the fact that the origin of the local coordinate system may in this case be regarded as the origin of a source so that the above equations in μ are strictly speaking equations in $|\mu|$.

The results of this appendix are evaluated by the diffraction program in subroutine ELINT and it may be noted that the results for sources at the ends of the element are doubled to account for the contribution from the source distributions on each of the adjacent elements.

The methods employed for integral evaluation in this appendix have all been discussed for a straight element. The methods explained and the results obtained may in the special case of a circular cylinder be applied directly since this is equivalent to evaluating the integrals within the polar coordinate system with it's origin at the centre of the cylinder. This would also be the case if a more general object geometry had been chosen and only constant or linear variation of source density were to be assumed. However, if a quadratic variation is assumed the curvature of the element must be included in the evaluations, that is, the Jacobian (included in the expression given in equation 4.2.9) must be incorporated in the integrand. The Jacobian is given by

$$d\Gamma = |J| \, d\mu \qquad \text{A.3.34}$$

with

$$|J| = \left[\left(\frac{dx}{d\mu}\right)^2 + \left(\frac{dy}{d\mu}\right)^2 \right]^{\frac{1}{2}} \qquad \text{A.3.35}$$

where $d\Gamma$ is a small increment of length in the cartesian coordinate system and $d\mu$ a small increment of length within the element coordinate system. The significance of this transformation is that for more general curved surfaces the results of equations A.3.31 and A.3.33 can not be used and a numerical quadrature must be performed. If this is the case the numerical quadrature formula to be used is one in which the weights and abscissas automatically take into consideration the logarithmic singularity.

A.3.6 Evaluation of the reflection and transmission coefficients

Expressions for the free surface displacement have been given in section 3.10 and the relationship between the reflection coefficient R, the transmission coefficient T and the scattered wave free surface displacement has been demonstrated. In this appendix expressions for the reflection and transmission coefficients have been derived by introducing an expression for the wave function for large separations of the source and field points.

The expression for the wave function is not different from that which has been given in section 3.4 and is obtained from equations 3.4.10, 3.4.12, 3.4.13 and 3.4.14. Examination of equation 3.4.14 indicates that the series decays with increasing separation of the source point $\underline{\xi}$ and the field point $\underline{x}$ and may therefore be regarded as a local wave which will vanish for sufficiently large values of $|\underline{x} - \underline{\xi}|$. This may be expressed by writing the wave function in the form

$$\lim_{x\to\pm\infty} g(\underline{x},\underline{\xi}) = -g_o(y,\eta)(i\exp(\pm ik(x-\xi))) \qquad \text{A.3.36}$$

where g_o is as given in equation 3.4.13.

The total free surface displacement has been given in equations 3.10.8 and 3.10.9 but it is advantageous in computational work to employ non-dimensional values for the free surface displacement and the potential function. The non-dimensional free surface displacement $\bar{\eta}$ is therefore given by

$$\bar{\eta}(\underline{x},t) = \frac{\eta}{H/2}(\underline{x},t) = i\bar{\phi}(\underline{x})\exp(-i\omega t) \qquad \text{A.3.37}$$

where $\bar{\phi} = \phi/(gH/2\sigma)$ is the non-dimensional total velocity potential. Expressing the non-dimensional potential as the sum of incident and scattered components

$$\bar{\eta}(\underline{x},t) = i\,(\bar{\phi}_w(\underline{x}) + \bar{\phi}_s(\underline{x}))\exp(-i\omega t) \qquad \text{A.3.38}$$

where $$\bar{\phi}_w(\underline{x}) = i\exp(ikx) \qquad \text{A.3.39}$$

and $$\bar{\phi}_s(\underline{x}) = \int_\Gamma \sigma(\underline{\xi})g(\underline{x},\underline{\xi})d\Gamma \qquad \text{A.3.40}$$

Substitution of equations A.3.39 and A.3.40 in A.3.38 with the result for the wave function given in equation A.3.40 gives after a little algebra the results

$$\bar{\eta}^+ = i(1 + I_1)\exp(i(kx - \omega t)) \qquad \text{A.3.41a}$$

$$\bar{\eta}^- = i(\exp(i(kx - \omega t)) + I_2\exp(-i(kx + \omega t))) \qquad \text{A.3.41b}$$

where $\bar{\eta}^+$ and $\bar{\eta}^-$ are the non-dimensional free surface displacements far upstream and far downstream of the obstacle and

$$I_1 = -i \int_\Gamma \sigma g_o \exp(-ik\xi) d\Gamma \qquad \text{A.3.42a}$$

$$I_2 = -i \int_\Gamma \sigma g_o \exp(ik\xi) d\Gamma \qquad \text{A.3.42b}$$

Comparison of equations A.3.41 and A.3.42 with equations 3.10.11 and 3.10.12 gives the following expressions for the complex quantities R and T

$$R = I_2 \qquad \text{A.3.43a}$$

$$T = I_1 + 1 \qquad \text{A.3.43b}$$

This scheme forms the basis of subroutines CREFL and REFL which employ the same discretisation schemes as the subroutines CSRCDEN and SRCDEN. The results

$$|R|^2 + |T|^2 = 1 \qquad \text{A.3.44a}$$

and $$|\text{Arg}(R) - \text{Arg}(T)| = (\Pi/2) \text{ modulo } \Pi \qquad \text{A.3.44b}$$

which have been proved by Newman (1975) have been incorporated in the subroutines and provide a useful check on the solution of the integral equation for the source density function.

APPENDIX A.4 INTEGRAL EQUATION SUBROUTINES

This appendix contains the listings of the subroutines required for the compilation and numerical solution of the integral equation. The subroutines have been written to accommodate a number of alternative discretisation schemes and the source distribution boundary may be chosen either to coincide with the object boundary or to be positioned outside the fluid domain. These listings form the first part of the diffraction program and many of the values set are also required for the evaluation of the wave function values and evaluation of the pressure, force and free surface values.

The following variable names have been used in the diffraction program subroutines. Wherever possible variable names are chosen to coincide with the symbols employed in the text of the thesis but the use of mnemonics is frequently necessary

CA	Cylinder radius, r_n.
EL	Element length, $\Delta\Gamma$.
GRAV	Acceleration of gravity, g.
IROUT	Test value to determine the final form of wave function.
NE	Number of elements, q.
NN	Number of nodes, n.
NNEL	Number of nodes per element, p.
NQ	Number of sources, m x q.
NQEL	Number of sources per element, m.
NTESTEL	Test value to identify location of node on element for quadratic variation of source density.

NVARN Test value to distinguish between constant and linear variation of source density.

PI $\pi = 3.1416$

RAT Ratio of source boundary radius, r_s, and object boundary radius, r_n. ($RAT = r_s/r_n$).

TESTRAT Test value to determine whether source and object boundaries are coincident or not.

V $\nu = \omega^2/g$.

WD Water depth, h.

WK Wave number, k.

WL Wavelength, L.

YO Depth of cylinder axis, y_o.

The following arrays have been declared for use in the diffraction program.

A(2n,2n) Kernel matrix, $\underline{A}$ (equation 4.2.1)

AN(p,m) Interpolation function values at abscissas.

C(2n,1) Vector containing incident wave potential gradient $\partial\phi_w/\partial m$.

CHI(mxq) Source point coordinates, ξ.

ETA(mxq) Source point coordinates, η.

F(2n,1) Vector containing source density function after solution of matrix equation

GP(m) Gauss abscissas

GW(m) Gauss weights

TH(n) Angle denoting direction of normal gradient at nodal points, $\underline{x}$.

XN(n) Nodal point coordinate, x.

YN(n) Nodal point coordinate, y.

Computer program (pp. 345-352) has been removed for copyright reasons

APPENDIX A.5 WAVE FUNCTION EVALUATION SUBROUTINES

This appendix contains listings of the subroutines written for the evaluation of the real and imaginary parts of the wave function and the normal gradient of the wave function on the object boundary. The following variable names have been used and are additional to those identified in Appendix A.4.

ACCI,ACCIXY	Accuracy test values for integral evaluations.
ACCS,ACCSXY	Accuracy test values for series evaluations.
C	Variable in integration, μ.
CON1	= kh cosh(kh) + (1 - νh)sinh(kh)
CON2	= (η + h)
CON3	= (y + h)
CONØ4	= (x - ξ)
CON4	= |x - ξ|
CLIM(=2.5k)	Maximum value in interval for principal value integral.
CMAX	Maximum value in interval for remainder integral.
DG1,DG2	Real and imaginary parts of normal gradient of wave function $\partial g_1/\partial m$ and $\partial g_2/\partial m$.
G1,G2	Real and imaginary parts of wave function g_1 and g_2.
HI	Length of interval for Simpson's rule.
NCK	Number of roots of dispersion equation evaluated.
NHI	Number of intervals in Simpson's rule evaluation.
NHIM	Maximum number of intervals permitted
PVI,PVIX,PVIY	Results of principal value integrals
QI,QIX,QIY	Results of remainder integrals
R1LOG,RLOG,RILOGX,R1LOGY,RLOGX,RLOGY,RLOGN	Logarithmic terms.

The following arrays have also been assigned:

CK(NCK) Roots of dispersion equation

Cl(NCK) = C_i (equations 4.3.4 and 3.4.16).

Computer program (pp. 355-368) has been removed for copyright reasons

APPENDIX A.6 WAVE FUNCTION EVALUATIONS

The wave function evaluation subroutines have been written for inclusion in the diffraction program and therefore the numerical results have been tested for the same data that has been used to test the diffraction program. The published results of Naftzger and Chakrabarti (1979) for a submerged circular cylinder in water of finite depth and Martin and Dixon (1983) for a semi-immersed circular cylinder in water of infinite depth have been used in this thesis for comparison purposes but if the test data is chosen to cover a sufficient range of waves it is sufficient to test the wave function evaluation for the submerged case only. A definition sketch for the submerged circular cylinder is given in Figure A.6.1 and the evaluations are tested for a range of waves with the variation described by the non-dimensional group ka where k is the wave number ($k = 2\Pi/L$) and a the cylinder radius.

The parameters chosen by Naftzger and Chakrabarti (1979) to describe the diffraction refraction problem completely are the water depth parameter, h/a, the cylinder depth parameter y_o/a and the diffraction parameter ka. The water depth and the cylinder depth parameters have been set at $h/a = 2.5$ and $y_o/a = 1.25$ for these tests and the diffraction parameter has been varied over a range ($0.2 < ka < 2.0$) which includes the shallow water depth range ($h/L < 0.05$), the intermediate water depth range ($0.05 < h/L < 0.5$) and the deep water depth range ($h/L > 0.5$).

The wave function test program has been written in a similar form to the diffraction program and nodal and source coordinates are

generated within the program. The results given in this appendix have been obtained for a ninety-six node linear discretisation with a single source located centrally on each element and the node and source locations are specified in accordance with Figure A.6.2. The test data has been designed to establish the accuracy with which the alternative wave function evaluations are made for a range of source node locations $(\underline{x},\underline{\xi})$ and the results of the tests may therefore be regarded as applicable to a coarse discretisation or a distribution of sources on a separate boundary. A range of wave data has been chosen ka = 0.2, 0.5, 1.0, 1.5, 2.0 and results have been obtained for two nodal points for small, intermediate and large source node separation (i=13, j=13,17,29,49, i=61, j=61,49,25).

The first set of wave function tests are for the series evaluations obtained by subroutines GRNSER and DGRNSER. The convergence test has been constructed so that the part of the function which decays is compared with a specified test value. For the evaluation of the wave function (G1) the expression

$$\frac{1}{c_i} C_i \exp(- c_i |x - \xi|) \qquad \text{A.6.1}$$

is compared with the value of ACCS and for the evaluation of the gradient (DG1) the expression

$$C_i \exp(- c_i |x - \xi|) \qquad \text{A.6.2}$$

is compared with the value of ACCSXY. The number of terms which must

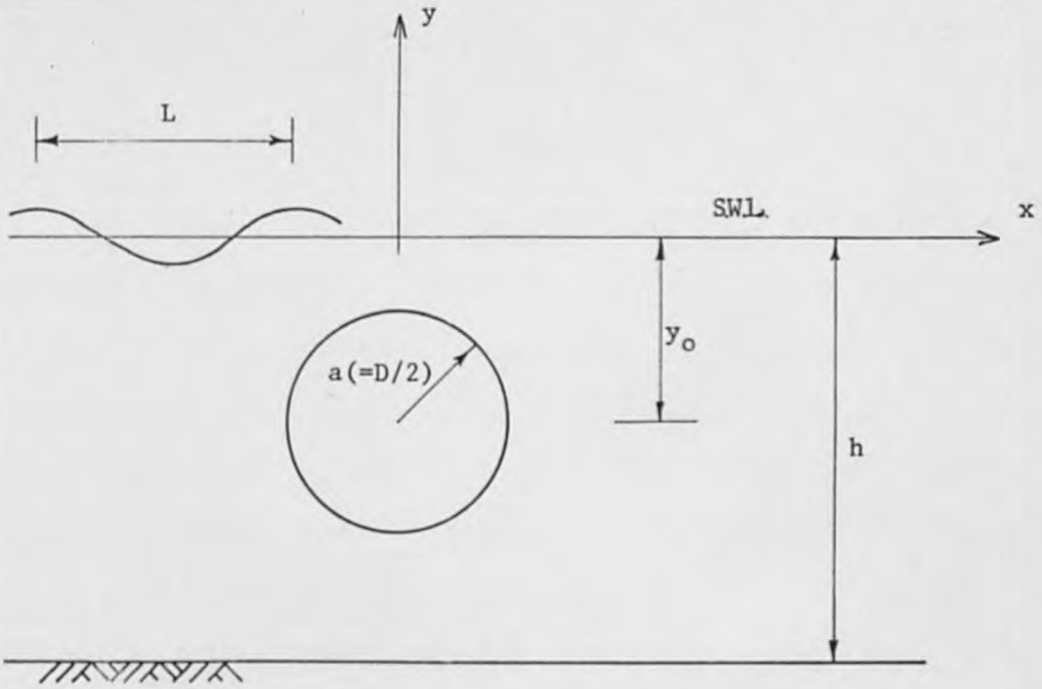

Figure A.6.1 Submerged Cylinder Geometry

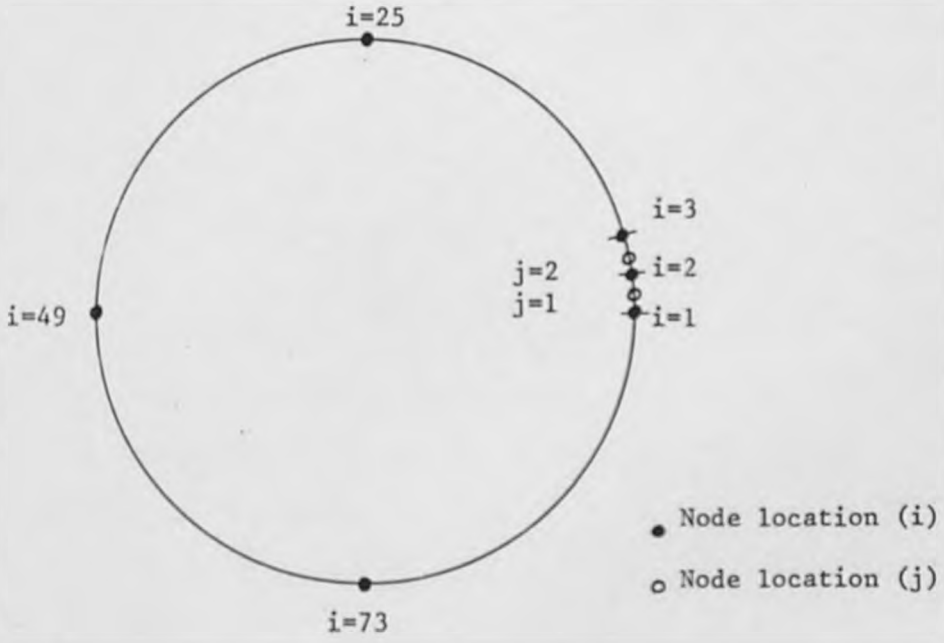

Figure A.6.2 Node and Source Locations

be included in the series to satisfy the tests for the wave function and it's gradient are NS and NSXY respectively.

The results for the test for a range of ACCS and ACCSXY are given in table A.6.1 and it is clear that there is a direct relationship between the accuracy test values and the extent to which the answers have converged. The accuracy test value determines that the evaluation is correct to a certain number of decimal places and for the wave function and it's gradient a convergence to the third decimal place will guarantee that the results of the diffraction program will not be subject to error due to the evaluations. The test results indicate that values of ACCS = 0.0001 and ACCSXY = 0.00001 are sufficient for this purpose.

The results of these tests also indicate that the number of terms which must be included to obtain the required accuracy is dependent entirely upon the horizontal separation of the source and nodal points and this feature has been used as the basis for the choice between a series or integral evaluation in the diffraction program.

Three tests have been constructed to determine the accuracy with which integral evaluations are made. The purpose of the first test is to determine the extent of the interval for which the second integration must be performed. In this test an approximate area ratio is compared with the specified accuracy test values (ACCI, ACCIXY) and a value of μ_{max} is set when the test is satisfied. The second test, which for convenience employs the same test values, determines whether the results of the iterative Simpson's rule have converged

to the required accuracy and the third test gives a maximum number of terms (NHIM) for which the iterative procedure is to continue. This final test is a precautionary measure designed to avoid excessive computational labour.

Preliminary tests have indicated that the total number of evaluations over the interval $(0,\mu_{max})$ is minimised if the interval for the principal value integral is chosen as (0,2.5k) and the results of tests performed under these conditions are given in tables A.6.2 and A.6.3. In evaluating the wave function it is necessary to include double precision since failure to do so results in incorrect evaluations for ka < 0.7 (in this problem). Double precision has therefore been employed throughout the diffraction program except when inclusion results in an unacceptable increase in the program memory requirement.

Comparison of the results of tables A.6.2 and A.6.3 with the corresponding series evaluations given in table A.6.1 indicates that there is general agreement and that the integral evaluation provides a result which is correct to the third decimal place for accuracy test values of ACCI = ACCIXY = 0.0001 and NHIM = 64 with the additional test value NHIM appearing to be of little significance for the settings used.

The computational efficiency for the wave function evaluations is directly related to the number of terms required in the series or the number of intervals required in the integral evaluation. While an exact comparison is not possible based simply on the values NSXY and (NHIM1 + NHIM2) from tables A.6.1,

A.6.2 and A.6.3 an approximate comparison indicates that the integral evaluation is best suited for the smaller source node separations and the series evaluation for the larger. Further examination of tables A.6.2 and A.6.3 indicates that the number of intervals to obtain the required accuracy and the length of the interval for integration are larger for the source located near the free surface for any particular value of ka and that for the same location the number of intervals and the interval for integration are larger for shallower water.

In order to demonstrate the behaviour of the integrand for the integral evaluations a number of plots have been made and are given in Figure A.6.3. The numerical results corresponding to each of the graphs are contained in tables A.6.2 and A.6.3 and the functions FI, FIX and FIY are the integrands of equations 3.4.11 and 4.3.8 and the functions VI, VIX and VIY correspond to the modified integrands due to treatment for singular behaviour as given in equation 4.3.11. The main feature of the graphs is that the singular behaviour of the integrands FI, FIX and FIY has clearly been removed. The graphs also indicate the trends which have been identified for the length of the interval in tables A.6.2 and A.6.3 where the C/WK axis is equivalent to μ/k. It is clear that the interval is larger for shallower water depths and for the source location nearer to the free surface. This trend continues if the source location is moved nearer towards the free surface and may therefore be expected to be larger for the case of the semi-immersed cylinder. However, this does not effect the accuracy of the evaluations unless the length of the interval gives arguments of hyperbolic or

exponential functions which are too large for computation in which case the program run will cease. This has been avoided in the integral subroutines INT3 and INT4 by imposing a maximum interval length of 50k. In the evaluation of results for the semi-immersed cylinder given in Appendix A.8 it has been found that a maximum interval length of 10k must be artificially imposed but the errors introduced are not considered to be significant.

DIFFRACTION PARAMETER (2*PI*CA/WL) 0.20
CYLINDER DEPTH PARAMETER (YO/WL) 0.04
WATER DEPTH PARAMETER (WD/WL) 0.08

I	J	ACCS	NS	G1	ACCSXY	NSXY	DG1
13	13	0.1E-01	20	-0.4270E 00	0.1E-01	69	0.1124E 00
13	13	0.1E-02	59	-0.4709E 00	0.1E-02	147	-0.1084E-01
13	13	0.1E-03	114	-0.4652E 00	0.1E-03	224	-0.8909E-03
13	13	0.1E-04	177	-0.4644E 00	0.1E-04	302	-0.8721E-03
13	13	0.1E-05	244	-0.4644E 00	0.1E-05	380	-0.9796E-03
13	14	0.1E-01	13	-0.2960E 00	0.1E-01	23	0.4009E-01
13	14	0.1E-02	29	-0.2976E 00	0.1E-02	48	-0.3343E-02
13	14	0.1E-03	48	-0.2948E 00	0.1E-03	74	-0.6108E-03
13	14	0.1E-04	69	-0.2947E 00	0.1E-04	99	-0.4276E-03
13	14	0.1E-05	91	-0.2948E 00	0.1E-05	124	-0.4700E-03
13	15	0.1E-01	10	-0.2163E 00	0.1E-01	14	0.2369E-01
13	15	0.1E-02	20	-0.2196E 00	0.1E-02	29	-0.6108E-03
13	15	0.1E-03	31	-0.2179E 00	0.1E-03	44	0.2730E-03
13	15	0.1E-04	44	-0.2179E 00	0.1E-04	58	0.4384E-03
13	15	0.1E-05	57	-0.2179E 00	0.1E-05	73	0.4114E-03
13	16	0.1E-01	8	-0.1738E 00	0.1E-01	10	0.1561E-01
13	16	0.1E-02	15	-0.1694E 00	0.1E-02	21	0.9696E-03
13	16	0.1E-03	24	-0.1679E 00	0.1E-03	31	0.1525E-02
13	16	0.1E-04	32	-0.1678E 00	0.1E-04	41	0.1721E-02
13	16	0.1E-05	41	-0.1678E 00	0.1E-05	51	0.1713E-02
13	17	0.1E-01	7	-0.1303E 00	0.1E-01	8	0.2189E-01
13	17	0.1E-02	13	-0.1313E 00	0.1E-02	16	0.3137E-02
13	17	0.1E-03	19	-0.1302E 00	0.1E-03	24	0.3359E-02
13	17	0.1E-04	26	-0.1301E 00	0.1E-04	32	0.3445E-02
13	17	0.1E-05	33	-0.1301E 00	0.1E-05	39	0.3446E-02
13	25	0.1E-01	4	0.6541E-01	0.1E-01	4	0.2534E-01
13	25	0.1E-02	6	0.6771E-01	0.1E-02	6	0.2242E-01
13	25	0.1E-03	8	0.6765E-01	0.1E-03	9	0.2236E-01
13	25	0.1E-04	10	0.6767E-01	0.1E-04	11	0.2231E-01
13	25	0.1E-05	13	0.6768E-01	0.1E-05	14	0.2231E-01
13	49	0.1E-01	3	0.3439E 00	0.1E-01	2	0.2799E-01
13	49	0.1E-02	4	0.3443E 00	0.1E-02	4	0.2854E-01
13	49	0.1E-03	5	0.3443E 00	0.1E-03	5	0.2853E-01
13	49	0.1E-04	6	0.3443E 00	0.1E-04	6	0.2852E-01
13	49	0.1E-05	7	0.3443E 00	0.1E-05	7	0.2852E-01
61	61	0.1E-01	20	-0.4520E 00	0.1E-01	69	0.1125E 00
61	61	0.1E-02	59	-0.4961E 00	0.1E-02	147	-0.1219E-01
61	61	0.1E-03	114	-0.4905E 00	0.1E-03	224	-0.1962E-02
61	61	0.1E-04	177	-0.4896E 00	0.1E-04	302	-0.1984E-02
61	61	0.1E-05	244	-0.4897E 00	0.1E-05	380	-0.2086E-02
61	49	0.1E-01	7	0.7421E-01	0.1E-01	7	0.9978E-02
61	49	0.1E-02	11	0.6912E-01	0.1E-02	13	0.2948E-02
61	49	0.1E-03	16	0.6990E-01	0.1E-03	19	0.2360E-02
61	49	0.1E-04	22	0.6988E-01	0.1E-04	26	0.2389E-02
61	49	0.1E-05	27	0.6988E-01	0.1E-05	32	0.2392E-02
61	25	0.1E-01	4	0.2388E 00	0.1E-01	4	0.1622E-01
61	25	0.1E-02	6	0.2373E 00	0.1E-02	7	0.1865E-01
61	25	0.1E-03	9	0.2373E 00	0.1E-03	9	0.1871E-01
61	25	0.1E-04	11	0.2373E 00	0.1E-04	12	0.1867E-01
61	25	0.1E-05	14	0.2373E 00	0.1E-05	15	0.1867E-01

Table A.6.1a Series Evaluation of Wave Function Values

DIFFRACTION PARAMETER (2*PI*CA/WL) 0.50
CYLINDER DEPTH PARAMETER (YO/WL) 0.10
WATER DEPTH PARAMETER (WD/WL) 0.20

I	J	ACCS	NS	G1	ACCSXY	NSXY	DG1
13	13	0.1E-01	20	-0.3811E 00	0.1E-01	69	0.1161E 00
13	13	0.1E-02	59	-0.4249E 00	0.1E-02	147	-0.7131E-02
13	13	0.1E-03	114	-0.4192E 00	0.1E-03	224	0.2814E-02
13	13	0.1E-04	177	-0.4183E 00	0.1E-04	302	0.2833E-02
13	13	0.1E-05	244	-0.4184E 00	0.1E-05	380	0.2726E-02
13	14	0.1E-01	13	-0.2486E 00	0.1E-01	23	0.4359E-01
13	14	0.1E-02	29	-0.2502E 00	0.1E-02	48	0.2213E-03
13	14	0.1E-03	48	-0.2475E 00	0.1E-03	74	0.2957E-02
13	14	0.1E-04	69	-0.2474E 00	0.1E-04	99	0.3140E-02
13	14	0.1E-05	91	-0.2474E 00	0.1E-05	124	0.3098E-02
13	15	0.1E-01	10	-0.1675E 00	0.1E-01	14	0.2716E-01
13	15	0.1E-02	20	-0.1709E 00	0.1E-02	29	0.2963E-02
13	15	0.1E-03	31	-0.1693E 00	0.1E-03	44	0.3852E-02
13	15	0.1E-04	44	-0.1693E 00	0.1E-04	58	0.4018E-02
13	15	0.1E-05	57	-0.1693E 00	0.1E-05	73	0.3991E-02
13	16	0.1E-01	8	-0.1239E 00	0.1E-01	10	0.1931E-01
13	16	0.1E-02	15	-0.1194E 00	0.1E-02	21	0.4731E-02
13	16	0.1E-03	24	-0.1179E 00	0.1E-03	31	0.5283E-02
13	16	0.1E-04	32	-0.1178E 00	0.1E-04	41	0.5480E-02
13	16	0.1E-05	41	-0.1178E 00	0.1E-05	51	0.5472E-02
13	17	0.1E-01	7	-0.7904E-01	0.1E-01	8	0.2603E-01
13	17	0.1E-02	13	-0.7976E-01	0.1E-02	16	0.7251E-02
13	17	0.1E-03	19	-0.7863E-01	0.1E-03	24	0.7473E-02
13	17	0.1E-04	26	-0.7854E-01	0.1E-04	32	0.7559E-02
13	17	0.1E-05	33	-0.7855E-01	0.1E-05	39	0.7560E-02
13	25	0.1E-01	4	0.1355E 00	0.1E-01	4	0.3578E-01
13	25	0.1E-02	6	0.1378E 00	0.1E-02	6	0.3313E-01
13	25	0.1E-03	8	0.1377E 00	0.1E-03	9	0.3308E-01
13	25	0.1E-04	10	0.1378E 00	0.1E-04	11	0.3303E-01
13	25	0.1E-05	13	0.1378E 00	0.1E-05	14	0.3303E-01
13	49	0.1E-01	3	0.3261E 00	0.1E-01	3	0.3376E-01
13	49	0.1E-02	4	0.3263E 00	0.1E-02	4	0.3451E-01
13	49	0.1E-03	5	0.3263E 00	0.1E-03	5	0.3448E-01
13	49	0.1E-04	6	0.3263E 00	0.1E-04	6	0.3447E-01
13	49	0.1E-05	7	0.3263E 00	0.1E-05	7	0.3447E-01
61	61	0.1E-01	20	-0.5258E 00	0.1E-01	69	0.1093E 00
61	61	0.1E-02	59	-0.5701E 00	0.1E-02	147	-0.1538E-01
61	61	0.1E-03	114	-0.5644E 00	0.1E-03	224	-0.5150E-02
61	61	0.1E-04	177	-0.5636E 00	0.1E-04	302	-0.5173E-02
61	61	0.1E-05	244	-0.5637E 00	0.1E-05	380	-0.5274E-02
61	49	0.1E-01	7	0.2487E-01	0.1E-01	7	0.8696E-02
61	49	0.1E-02	11	0.1970E-01	0.1E-02	13	0.1576E-02
61	49	0.1E-03	16	0.2049E-01	0.1E-03	19	0.9855E-03
61	49	0.1E-04	22	0.2047E-01	0.1E-04	26	0.1014E-02
61	49	0.1E-05	27	0.2047E-01	0.1E-05	32	0.1018E-02
61	25	0.1E-01	4	0.2585E 00	0.1E-01	4	0.1180E-01
61	25	0.1E-02	6	0.2572E 00	0.1E-02	7	0.1402E-01
61	25	0.1E-03	9	0.2572E 00	0.1E-03	9	0.1409E-01
61	25	0.1E-04	11	0.2572E 00	0.1E-04	12	0.1404E-01
61	25	0.1E-05	14	0.2572E 00	0.1E-05	15	0.1404E-01

Table A.6.1b Series Evaluation of Wave Function Values

DIFFRACTION PARAMETER (2*PI*CA/WL) 1.00
CYLINDER DEPTH PARAMETER (YO/WL) 0.20
WATER DEPTH PARAMETER (WD/WL) 0.40

I	J	ACCS	NS	Gl	ACCSXY	NSXY	DGl
13	13	0.1E-01	20	-0.2972E 00	0.1E-01	69	0.1353E 00
13	13	0.1E-02	59	-0.3409E 00	0.1E-02	147	0.1209E-01
13	13	0.1E-03	114	-0.3352E 00	0.1E-03	224	0.2204E-01
13	13	0.1E-04	177	-0.3344E 00	0.1E-04	302	0.2206E-01
13	13	0.1E-05	244	-0.3345E 00	0.1E-05	380	0.2195E-01
13	14	0.1E-01	13	-0.1579E 00	0.1E-01	23	0.6261E-01
13	14	0.1E-02	29	-0.1598E 00	0.1E-02	48	0.1934E-01
13	14	0.1E-03	48	-0.1570E 00	0.1E-03	74	0.2208E-01
13	14	0.1E-04	69	-0.1569E 00	0.1E-04	99	0.2226E-01
13	14	0.1E-05	91	-0.1570E 00	0.1E-05	124	0.2222E-01
13	15	0.1E-01	10	-0.7069E-01	0.1E-01	14	0.4615E-01
13	15	0.1E-02	20	-0.7443E-01	0.1E-02	29	0.2213E-01
13	15	0.1E-03	31	-0.7276E-01	0.1E-03	44	0.2303E-01
13	15	0.1E-04	44	-0.7275E-01	0.1E-04	58	0.2320E-01
13	15	0.1E-05	57	-0.7277E-01	0.1E-05	73	0.2317E-01
13	16	0.1E-01	8	-0.2198E-01	0.1E-01	10	0.3868E-01
13	16	0.1E-02	15	-0.1726E-01	0.1E-02	21	0.2416E-01
13	16	0.1E-03	24	-0.1578E-01	0.1E-03	31	0.2471E-01
13	16	0.1E-04	32	-0.1570E-01	0.1E-04	41	0.2491E-01
13	16	0.1E-05	41	-0.1573E-01	0.1E-05	51	0.2490E-01
13	17	0.1E-01	7	0.2772E-01	0.1E-01	8	0.4593E-01
13	17	0.1E-02	13	0.2749E-01	0.1E-02	16	0.2713E-01
13	17	0.1E-03	19	0.2865E-01	0.1E-03	24	0.2736E-01
13	17	0.1E-04	26	0.2873E-01	0.1E-04	32	0.2744E-01
13	17	0.1E-05	33	0.2872E-01	0.1E-05	39	0.2744E-01
13	25	0.1E-01	4	0.2620E 00	0.1E-01	4	0.6012E-01
13	25	0.1E-02	6	0.2641E 00	0.1E-02	6	0.5804E-01
13	25	0.1E-03	8	0.2639E 00	0.1E-03	9	0.5799E-01
13	25	0.1E-04	10	0.2639E 00	0.1E-04	11	0.5794E-01
13	25	0.1E-05	13	0.2640E 00	0.1E-05	14	0.5794E-01
13	49	0.1E-01	3	0.1774E 00	0.1E-01	3	0.2165E-01
13	49	0.1E-02	4	0.1771E 00	0.1E-02	4	0.2269E-01
13	49	0.1E-03	5	0.1771E 00	0.1E-03	5	0.2266E-01
13	49	0.1E-04	6	0.1771E 00	0.1E-04	6	0.2264E-01
13	49	0.1E-05	7	0.1771E 00	0.1E-05	7	0.2264E-01
61	61	0.1E-01	20	-0.6726E 00	0.1E-01	69	0.1064E 00
61	61	0.1E-02	59	-0.7169E 00	0.1E-02	147	-0.1831E-01
61	61	0.1E-03	114	-0.7113E 00	0.1E-03	224	-0.8080E-02
61	61	0.1E-04	177	-0.7104E 00	0.1E-04	302	-0.8102E-02
61	61	0.1E-05	244	-0.7105E 00	0.1E-05	380	-0.8204E-02
61	49	0.1E-01	7	-0.9842E-01	0.1E-01	7	0.7248E-02
61	49	0.1E-02	11	-0.1037E 00	0.1E-02	13	-0.1534E-04
61	49	0.1E-03	16	-0.1029E 00	0.1E-03	19	-0.6106E-03
61	49	0.1E-04	22	-0.1029E 00	0.1E-04	26	-0.5821E-03
61	49	0.1E-05	27	-0.1029E 00	0.1E-05	32	-0.5783E-03
61	25	0.1E-01	4	0.2085E 00	0.1E-01	4	-0.2481E-02
61	25	0.1E-02	6	0.2074E 00	0.1E-02	7	-0.6720E-03
61	25	0.1E-03	9	0.2075E 00	0.1E-03	9	-0.5999E-03
61	25	0.1E-04	11	0.2075E 00	0.1E-04	12	-0.6486E-03
61	25	0.1E-05	14	0.2075E 00	0.1E-05	15	-0.6497E-03

Table A.6.1c Series Evaluation of Wave Function Values

DIFFRACTION PARAMETER (2*PI*CA/WL) 1.50
CYLINDER DEPTH PARAMETER (Y0/WL) 0.30
WATER DEPTH PARAMETER (WD/WL) 0.60

I	J	ACCS	NS	G1	ACCSXY	NSXY	DG1
13	13	0.1E-01	20	-0.2863E 00	0.1E-01	69	0.1524E 00
13	13	0.1E-02	59	-0.3299E 00	0.1E-02	147	0.2926E-01
13	13	0.1E-03	114	-0.3242E 00	0.1E-03	224	0.3920E-01
13	13	0.1E-04	177	-0.3233E 00	0.1E-04	302	0.3922E-01
13	13	0.1E-05	244	-0.3234E 00	0.1E-05	380	0.3911E-01
13	14	0.1E-01	13	-0.1411E 00	0.1E-01	23	0.7959E-01
13	14	0.1E-02	29	-0.1430E 00	0.1E-02	48	0.3642E-01
13	14	0.1E-03	48	-0.1403E 00	0.1E-03	74	0.3917E-01
13	14	0.1E-04	69	-0.1402E 00	0.1E-04	99	0.3935E-01
13	14	0.1E-05	91	-0.1402E 00	0.1E-05	124	0.3931E-01
13	15	0.1E-01	10	-0.4867E-01	0.1E-01	14	0.6288E-01
13	15	0.1E-02	20	-0.5263E-01	0.1E-02	29	0.3902E-01
13	15	0.1E-03	31	-0.5097E-01	0.1E-03	44	0.3993E-01
13	15	0.1E-04	44	-0.5096E-01	0.1E-04	58	0.4009E-01
13	15	0.1E-05	57	-0.5098E-01	0.1E-05	73	0.4007E-01
13	16	0.1E-01	8	0.4000E-02	0.1E-01	10	0.5525E-01
13	16	0.1E-02	15	0.8850E-02	0.1E-02	21	0.4077E-01
13	16	0.1E-03	24	0.1031E-01	0.1E-03	31	0.4131E-01
13	16	0.1E-04	32	0.1039E-01	0.1E-04	41	0.4151E-01
13	16	0.1E-05	41	0.1037E-01	0.1E-05	51	0.4150E-01
13	17	0.1E-01	7	0.5672E-01	0.1E-01	8	0.6210E-01
13	17	0.1E-02	13	0.5696E-01	0.1E-02	16	0.4334E-01
13	17	0.1E-03	19	0.5814E-01	0.1E-03	24	0.4356E-01
13	17	0.1E-04	26	0.5823E-01	0.1E-04	32	0.4365E-01
13	17	0.1E-05	33	0.5822E-01	0.1E-05	39	0.4365E-01
13	25	0.1E-01	4	0.2688E 00	0.1E-01	4	0.6304E-01
13	25	0.1E-02	6	0.2704E 00	0.1E-02	6	0.6158E-01
13	25	0.1E-03	8	0.2703E 00	0.1E-03	9	0.6152E-01
13	25	0.1E-04	10	0.2703E 00	0.1E-04	11	0.6147E-01
13	25	0.1E-05	13	0.2703E 00	0.1E-05	14	0.6147E-01
13	49	0.1E-01	3	0.4042E-01	0.1E-01	3	0.4184E-02
13	49	0.1E-02	4	0.3952E-01	0.1E-02	4	0.5480E-02
13	49	0.1E-03	5	0.3958E-01	0.1E-03	5	0.5430E-02
13	49	0.1E-04	6	0.3959E-01	0.1E-04	6	0.5417E-02
13	49	0.1E-05	7	0.3959E-01	0.1E-05	7	0.5417E-02
61	61	0.1E-01	20	-0.7487E 00	0.1E-01	69	0.1069E 00
61	61	0.1E-02	59	-0.7931E 00	0.1E-02	147	-0.1785E-01
61	61	0.1E-03	114	-0.7874E 00	0.1E-03	224	-0.7624E-02
61	61	0.1E-04	177	-0.7866E 00	0.1E-04	302	-0.7646E-02
61	61	0.1E-05	244	-0.7867E 00	0.1E-05	380	-0.7748E-02
61	49	0.1E-01	7	-0.1776E 00	0.1E-01	7	0.7479E-02
61	49	0.1E-02	11	-0.1830E 00	0.1E-02	13	0.9296E-04
61	49	0.1E-03	16	-0.1822E 00	0.1E-03	19	-0.5060E-03
61	49	0.1E-04	22	-0.1822E 00	0.1E-04	26	-0.4777E-03
61	49	0.1E-05	27	-0.1822E 00	0.1E-05	32	-0.4739E-03
61	25	0.1E-01	5	0.1213E 00	0.1E-01	4	-0.8340E-02
61	25	0.1E-02	7	0.1217E 00	0.1E-02	7	-0.6957E-02
61	25	0.1E-03	9	0.1215E 00	0.1E-03	9	-0.6880E-02
61	25	0.1E-04	11	0.1216E 00	0.1E-04	12	-0.6931E-02
61	25	0.1E-05	14	0.1216E 00	0.1E-05	15	-0.6932E-02

Table A.6.1d Series Evaluation of Wave Function Values

DIFFRACTION PARAMETER (2*PI*CA/WL) 2.00
CYLINDER DEPTH PARAMETER (Y0/WL) 0.40
WATER DEPTH PARAMETER (WD/WL) 0.80

I	J	ACCS	NS	G1	ACCSXY	NSXY	DG1
13	13	0.1E-01	20	-0.3111E 00	0.1E-01	69	0.1613E 00
13	13	0.1E-02	59	-0.3546E 00	0.1E-02	147	0.3816E-01
13	13	0.1E-03	114	-0.3489E 00	0.1E-03	224	0.4810E-01
13	13	0.1E-04	177	-0.3480E 00	0.1E-04	302	0.4812E-01
13	13	0.1E-05	244	-0.3481E 00	0.1E-05	380	0.4801E-01
13	14	0.1E-01	13	-0.1627E 00	0.1E-01	23	0.8819E-01
13	14	0.1E-02	29	-0.1648E 00	0.1E-02	48	0.4512E-01
13	14	0.1E-03	48	-0.1621E 00	0.1E-03	74	0.4787E-01
13	14	0.1E-04	69	-0.1620E 00	0.1E-04	99	0.4805E-01
13	14	0.1E-05	91	-0.1620E 00	0.1E-05	124	0.4801E-01
13	15	0.1E-01	10	-0.6787E-01	0.1E-01	14	0.7096E-01
13	15	0.1E-02	20	-0.7202E-01	0.1E-02	29	0.4725E-01
13	15	0.1E-03	31	-0.7037E-01	0.1E-03	44	0.4817E-01
13	15	0.1E-04	44	-0.7036E-01	0.1E-04	58	0.4834E-01
13	15	0.1E-05	57	-0.7038E-01	0.1E-05	73	0.4831E-01
13	16	0.1E-01	8	-0.1376E-01	0.1E-01	10	0.6275E-01
13	16	0.1E-02	15	-0.8820E-02	0.1E-02	21	0.4828E-01
13	16	0.1E-03	24	-0.7375E-02	0.1E-03	31	0.4882E-01
13	16	0.1E-04	32	-0.7300E-02	0.1E-04	41	0.4902E-01
13	16	0.1E-05	41	-0.7322E-02	0.1E-05	51	0.4901E-01
13	17	0.1E-01	7	0.3937E-01	0.1E-01	8	0.6848E-01
13	17	0.1E-02	13	0.4007E-01	0.1E-02	16	0.4981E-01
13	17	0.1E-03	19	0.4128E-01	0.1E-03	24	0.5003E-01
13	17	0.1E-04	26	0.4136E-01	0.1E-04	32	0.5012E-01
13	17	0.1E-05	33	0.4136E-01	0.1E-05	39	0.5012E-01
13	25	0.1E-01	4	0.2097E 00	0.1E-01	4	0.4654E-01
13	25	0.1E-02	6	0.2107E 00	0.1E-02	6	0.4573E-01
13	25	0.1E-03	8	0.2105E 00	0.1E-03	9	0.4565E-01
13	25	0.1E-04	10	0.2105E 00	0.1E-04	11	0.4560E-01
13	25	0.1E-05	13	0.2105E 00	0.1E-05	14	0.4560E-01
13	49	0.1E-01	3	-0.1207E-01	0.1E-01	3	0.1946E-02
13	49	0.1E-02	4	-0.1354E-01	0.1E-02	4	0.3442E-02
13	49	0.1E-03	5	-0.1346E-01	0.1E-03	5	0.3378E-02
13	49	0.1E-04	6	-0.1344E-01	0.1E-04	6	0.3365E-02
13	49	0.1E-05	7	-0.1344E-01	0.1E-05	7	0.3365E-02
61	61	0.1E-01	20	-0.7825E 00	0.1E-01	69	0.1075E 00
61	61	0.1E-02	59	-0.8269E 00	0.1E-02	147	-0.1723E-01
61	61	0.1E-03	114	-0.8213E 00	0.1E-03	224	-0.7001E-02
61	61	0.1E-04	177	-0.8204E 00	0.1E-04	302	-0.7024E-02
61	61	0.1E-05	244	-0.8205E 00	0.1E-05	380	-0.7125E-02
61	49	0.1E-01	7	-0.2162E 00	0.1E-01	7	0.7933E-02
61	49	0.1E-02	11	-0.2217E 00	0.1E-02	13	0.4369E-03
61	49	0.1E-03	16	-0.2209E 00	0.1E-03	19	-0.1657E-03
61	49	0.1E-04	22	-0.2209E 00	0.1E-04	26	-0.1375E-03
61	49	0.1E-05	27	-0.2209E 00	0.1E-05	32	-0.1336E-03
61	25	0.1E-01	5	0.6674E-01	0.1E-01	4	-0.7148E-02
61	25	0.1E-02	7	0.6691E-01	0.1E-02	7	-0.6197E-02
61	25	0.1E-03	9	0.6679E-01	0.1E-03	9	-0.6113E-02
61	25	0.1E-04	11	0.6680E-01	0.1E-04	12	-0.6167E-02
61	25	0.1E-05	14	0.6681E-01	0.1E-05	15	-0.6168E-02

Table A.6.1e Series Evaluation of Wave Function Values

DIFFRACTION PARAMETER (2*PI*CA/WL) 0.20
CYLINDER DEPTH PARAMETER (YO/WL) 0.04
WATER DEPTH PARAMETER (WD/WL) 0.08

I	J	ACCIXY	NHIM	NHI1	NHI2	CMAX	DG1
13	13	0.1E 00	16	1	1	5.0	0.6150E-02
13	13	0.1E-01	32	2	2	7.5	0.3002E-02
13	13	0.1E-02	64	2	4	17.5	-0.6117E-03
13	13	0.1E-03	128	4	32	27.5	-0.9194E-03
13	13	0.1E-04	256	8	64	40.0	-0.9643E-03
13	14	0.1E 00	16	2	1	5.0	0.6348E-02
13	14	0.1E-01	32	2	2	12.5	0.5500E-03
13	14	0.1E-02	64	4	16	22.5	-0.3581E-03
13	14	0.1E-03	128	8	32	35.0	-0.4643E-03
13	14	0.1E-04	256	16	128	45.0	-0.4677E-03
13	15	0.1E 00	16	2	1	5.0	0.6669E-02
13	15	0.1E-01	32	2	4	15.0	0.8281E-03
13	15	0.1E-02	64	4	16	27.5	0.4031E-03
13	15	0.1E-03	128	8	64	37.5	0.4058E-03
13	15	0.1E-04	256	16	128	50.0	0.4101E-03
13	16	0.1E 00	16	2	2	7.5	0.4286E-02
13	16	0.1E-01	32	2	4	17.5	0.1613E-02
13	16	0.1E-02	64	4	16	27.5	0.1644E-02
13	16	0.1E-03	128	8	64	40.0	0.1700E-02
13	16	0.1E-04	256	16	128	52.5	0.1711E-02
13	17	0.1E 00	16	2	2	7.5	0.4984E-02
13	17	0.1E-01	32	2	8	20.0	0.3108E-02
13	17	0.1E-02	64	4	32	30.0	0.3343E-02
13	17	0.1E-03	128	8	64	42.5	0.3431E-02
13	17	0.1E-04	256	16	256	57.5	0.3444E-02
13	25	0.1E 00	16	2	2	12.5	0.1846E-01
13	25	0.1E-01	32	2	16	30.0	0.2254E-01
13	25	0.1E-02	64	8	64	47.5	0.2230E-01
13	25	0.1E-03	128	16	128	55.0	0.2231E-01
13	25	0.1E-04	256	16	256	62.5	0.2231E-01
13	49	0.1E 00	16	2	4	10.0	0.2859E-01
13	49	0.1E-01	32	4	8	15.0	0.2856E-01
13	49	0.1E-02	64	8	32	22.5	0.2851E-01
13	49	0.1E-03	128	16	128	30.0	0.2852E-01
13	49	0.1E-04	256	32	256	35.0	0.2852E-01
61	61	0.1E 00	16	1	1	5.0	-0.2205E-02
61	61	0.1E-01	32	1	1	5.0	-0.2205E-02
61	61	0.1E-02	64	2	2	7.5	-0.2086E-02
61	61	0.1E-03	128	4	4	10.0	-0.2074E-02
61	61	0.1E-04	256	8	16	12.5	-0.2075E-02
61	49	0.1E 00	16	2	1	5.0	0.2325E-02
61	49	0.1E-01	32	2	2	10.0	0.2402E-02
61	49	0.1E-02	64	4	8	12.5	0.2393E-02
61	49	0.1E-03	128	8	32	17.5	0.2393E-02
61	49	0.1E-04	256	16	64	20.0	0.2393E-02
61	25	0.1E 00	16	2	2	10.0	0.1860E-01
61	25	0.1E-01	32	2	8	15.0	0.1866E-01
61	25	0.1E-02	64	8	32	20.0	0.1867E-01
61	25	0.1E-03	128	16	64	22.5	0.1867E-01
61	25	0.1E-04	256	16	128	30.0	0.1867E-01

Table A.6.2a Integral Evaluation of Wave Function Values

DIFFRACTION PARAMETER (2*PI*CA/WL) 0.50
CYLINDER DEPTH PARAMETER (Y0/WL) 0.10
WATER DEPTH PARAMETER (WD/WL) 0.20

I	J	ACCIXY	NHIM	NHI1	NHI2	CMAX	DG1
13	13	0.1E 00	16	1	1	5.0	0.3965E-02
13	13	0.1E-01	32	2	2	7.5	0.3020E-02
13	13	0.1E-02	64	4	4	10.0	0.2802E-02
13	13	0.1E-03	128	8	16	15.0	0.2743E-02
13	13	0.1E-04	256	16	32	20.0	0.2738E-02
13	14	0.1E 00	16	2	1	5.0	0.4466E-02
13	14	0.1E-01	32	2	2	10.0	0.2915E-02
13	14	0.1E-02	64	4	8	12.5	0.3106E-02
13	14	0.1E-03	128	8	32	17.5	0.3100E-02
13	14	0.1E-04	256	16	64	22.5	0.3100E-02
13	15	0.1E 00	16	2	2	7.5	0.4069E-02
13	15	0.1E-01	32	4	4	10.0	0.3973E-02
13	15	0.1E-02	64	8	16	15.0	0.3984E-02
13	15	0.1E-03	128	8	32	20.0	0.3989E-02
13	15	0.1E-04	256	16	64	22.5	0.3990E-02
13	16	0.1E 00	16	2	2	7.5	0.5308E-02
13	16	0.1E-01	32	4	4	10.0	0.5355E-02
13	16	0.1E-02	64	8	16	15.0	0.5451E-02
13	16	0.1E-03	128	16	32	20.0	0.5468E-02
13	16	0.1E-04	256	16	128	25.0	0.5471E-02
13	17	0.1E 00	16	2	2	7.5	0.7063E-02
13	17	0.1E-01	32	4	4	10.0	0.7312E-02
13	17	0.1E-02	64	8	16	17.5	0.7545E-02
13	17	0.1E-03	128	16	32	20.0	0.7555E-02
13	17	0.1E-04	256	16	128	27.5	0.7559E-02
13	25	0.1E 00	16	2	4	12.5	0.3317E-01
13	25	0.1E-01	32	4	16	15.0	0.3308E-01
13	25	0.1E-02	64	8	32	22.5	0.3302E-01
13	25	0.1E-03	128	16	128	27.5	0.3303E-01
13	25	0.1E-04	256	32	256	32.5	0.3303E-01
13	49	0.1E 00	16	2	2	7.5	0.3452E-01
13	49	0.1E-01	32	4	8	10.0	0.3447E-01
13	49	0.1E-02	64	8	16	12.5	0.3447E-01
13	49	0.1E-03	128	16	64	15.0	0.3447E-01
13	49	0.1E-04	256	32	128	17.5	0.3447E-01
61	61	0.1E 00	16	1	1	5.0	-0.5194E-02
61	61	0.1E-01	32	2	1	5.0	-0.5255E-02
61	61	0.1E-02	64	2	1	5.0	-0.5255E-02
61	61	0.1E-03	128	4	4	7.5	-0.5262E-02
61	61	0.1E-04	256	8	8	7.5	-0.5262E-02
61	49	0.1E 00	16	2	1	5.0	0.1024E-02
61	49	0.1E-01	32	2	2	7.5	0.1024E-02
61	49	0.1E-02	64	4	4	7.5	0.1019E-02
61	49	0.1E-03	128	8	16	10.0	0.1018E-02
61	49	0.1E-04	256	16	32	10.0	0.1018E-02
61	25	0.1E 00	16	2	2	7.5	0.1411E-01
61	25	0.1E-01	32	4	8	10.0	0.1404E-01
61	25	0.1E-02	64	8	16	10.0	0.1404E-01
61	25	0.1E-03	128	16	32	12.5	0.1404E-01
61	25	0.1E-04	256	32	64	15.0	0.1404E-01

Table A.6.2b Integral Evaluation of Wave Function Values

DIFFRACTION PARAMETER (2*PI*CA/WL) 1.00
CYLINDER DEPTH PARAMETER (Y0/WL) 0.20
WATER DEPTH PARAMETER (WD/WL) 0.40

I	J	ACCIXY	NHIM	NHI1	NHI2	CMAX	DG1
13	13	0.1E 00	16	1	1	5.0	0.1952E-01
13	13	0.1E-01	32	4	1	5.0	0.2192E-01
13	13	0.1E-02	64	8	4	7.5	0.2196E-01
13	13	0.1E-03	128	16	8	10.0	0.2196E-01
13	13	0.1E-04	256	32	32	12.5	0.2196E-01
13	14	0.1E 00	16	2	1	5.0	0.2178E-01
13	14	0.1E-01	32	4	2	7.5	0.2208E-01
13	14	0.1E-02	64	16	8	10.0	0.2222E-01
13	14	0.1E-03	128	16	16	12.5	0.2222E-01
13	14	0.1E-04	256	32	32	12.5	0.2222E-01
13	15	0.1E 00	16	2	1	5.0	0.2268E-01
13	15	0.1E-01	32	8	2	7.5	0.2306E-01
13	15	0.1E-02	64	16	8	10.0	0.2317E-01
13	15	0.1E-03	128	32	32	12.5	0.2317E-01
13	15	0.1E-04	256	32	64	15.0	0.2317E-01
13	16	0.1E 00	16	2	1	5.0	0.2431E-01
13	16	0.1E-01	32	8	4	7.5	0.2486E-01
13	16	0.1E-02	64	16	8	10.0	0.2489E-01
13	16	0.1E-03	128	32	32	12.5	0.2490E-01
13	16	0.1E-04	256	64	64	15.0	0.2490E-01
13	17	0.1E 00	16	4	1	7.5	0.2675E-01
13	17	0.1E-01	32	8	4	7.5	0.2739E-01
13	17	0.1E-02	64	16	16	10.0	0.2744E-01
13	17	0.1E-03	128	32	32	12.5	0.2744E-01
13	17	0.1E-04	256	64	64	15.0	0.2744E-01
13	25	0.1E 00	16	2	2	7.5	0.5781E-01
13	25	0.1E-01	32	8	8	10.0	0.5793E-01
13	25	0.1E-02	64	16	16	12.5	0.5794E-01
13	25	0.1E-03	128	32	64	15.0	0.5794E-01
13	25	0.1E-04	256	64	128	17.5	0.5794E-01
13	49	0.1E 00	16	4	1	5.0	0.2274E-01
13	49	0.1E-01	32	8	4	7.5	0.2266E-01
13	49	0.1E-02	64	16	8	7.5	0.2264E-01
13	49	0.1E-03	128	32	32	10.0	0.2264E-01
13	49	0.1E-04	256	32	32	10.0	0.2264E-01
61	61	0.1E 00	16	1	1	5.0	-0.6540E-02
61	61	0.1E-01	32	4	1	5.0	-0.8189E-02
61	61	0.1E-02	64	8	1	5.0	-0.8191E-02
61	61	0.1E-03	128	8	1	5.0	-0.8191E-02
61	61	0.1E-04	256	16	1	5.0	-0.8192E-02
61	49	0.1E 00	16	4	1	5.0	-0.5755E-03
61	49	0.1E-01	32	8	1	5.0	-0.5776E-03
61	49	0.1E-02	64	8	1	7.5	-0.5776E-03
61	49	0.1E-03	128	16	8	7.5	-0.5780E-03
61	49	0.1E-04	256	32	16	7.5	-0.5780E-03
61	25	0.1E 00	16	4	1	5.0	-0.5904E-03
61	25	0.1E-01	32	8	4	7.5	-0.6439E-03
61	25	0.1E-02	64	16	8	7.5	-0.6492E-03
61	25	0.1E-03	128	32	16	7.5	-0.6496E-03
61	25	0.1E-04	256	64	64	10.0	-0.6496E-03

Table A.6.2c Integral Evaluation of Wave Function Values

DIFFRACTION PARAMETER (2*PI*CA/WL) 1.50
CYLINDER DEPTH PARAMETER (Y0/WL) 0.30
WATER DEPTH PARAMETER (WD/WL) 0.60

I	J	ACCIXY	NHIM	NHI1	NHI2	CMAX	DG1
13	13	0.1E 00	16	2	1	5.0	0.3743E-01
13	13	0.1E-01	32	8	1	5.0	0.3904E-01
13	13	0.1E-02	64	16	2	7.5	0.3905E-01
13	13	0.1E-03	128	32	8	7.5	0.3912E-01
13	13	0.1E-04	256	32	16	10.0	0.3913E-01
13	14	0.1E 00	16	4	1	5.0	0.3903E-01
13	14	0.1E-01	32	8	1	7.5	0.3890E-01
13	14	0.1E-02	64	16	4	7.5	0.3930E-01
13	14	0.1E-03	128	32	16	10.0	0.3931E-01
13	14	0.1E-04	256	64	32	10.0	0.3931E-01
13	15	0.1E 00	16	4	1	5.0	0.3979E-01
13	15	0.1E-01	32	8	2	7.5	0.3998E-01
13	15	0.1E-02	64	16	8	7.5	0.4006E-01
13	15	0.1E-03	128	32	16	10.0	0.4007E-01
13	15	0.1E-04	256	64	32	10.0	0.4007E-01
13	16	0.1E 00	16	4	1	5.0	0.4123E-01
13	16	0.1E-01	32	8	2	7.5	0.4143E-01
13	16	0.1E-02	64	16	8	7.5	0.4150E-01
13	16	0.1E-03	128	32	16	10.0	0.4150E-01
13	16	0.1E-04	256	64	64	12.5	0.4150E-01
13	17	0.1E 00	16	4	1	5.0	0.4337E-01
13	17	0.1E-01	32	8	4	7.5	0.4363E-01
13	17	0.1E-02	64	16	8	10.0	0.4365E-01
13	17	0.1E-03	128	32	16	10.0	0.4365E-01
13	17	0.1E-04	256	64	64	12.5	0.4365E-01
13	25	0.1E 00	16	4	1	7.5	0.6345E-01
13	25	0.1E-01	32	16	4	7.5	0.6148E-01
13	25	0.1E-02	64	32	16	10.0	0.6147E-01
13	25	0.1E-03	128	32	32	12.5	0.6147E-01
13	25	0.1E-04	256	64	64	15.0	0.6147E-01
13	49	0.1E 00	16	8	1	5.0	0.5404E-02
13	49	0.1E-01	32	16	1	7.5	0.5361E-02
13	49	0.1E-02	64	16	8	7.5	0.5417E-02
13	49	0.1E-03	128	32	16	7.5	0.5417E-02
13	49	0.1E-04	256	64	16	7.5	0.5417E-02
61	61	0.1E 00	16	1	1	5.0	-0.5114E-02
61	61	0.1E-01	32	1	1	5.0	-0.5114E-02
61	61	0.1E-02	64	8	1	5.0	-0.7736E-02
61	61	0.1E-03	128	16	1	5.0	-0.7736E-02
61	61	0.1E-04	256	16	1	5.0	-0.7736E-02
61	49	0.1E 00	16	8	1	5.0	-0.4729E-03
61	49	0.1E-01	32	8	1	5.0	-0.4729E-03
61	49	0.1E-02	64	16	1	5.0	-0.4735E-03
61	49	0.1E-03	128	32	1	5.0	-0.4736E-03
61	49	0.1E-04	256	64	4	7.5	-0.4735E-03
61	25	0.1E 00	16	4	1	5.0	-0.6817E-02
61	25	0.1E-01	32	8	1	5.0	-0.6919E-02
61	25	0.1E-02	64	16	2	7.5	-0.6930E-02
61	25	0.1E-03	128	32	8	7.5	-0.6932E-02
61	25	0.1E-04	256	64	16	7.5	-0.6932E-02

Table A.6.2d Integral Evaluation of Wave Function Values

DIFFRACTION PARAMETER (2*PI*CA/WL) 2.00
CYLINDER DEPTH PARAMETER (Y0/WL) 0.40
WATER DEPTH PARAMETER (WD/WL) 0.80

I	J	ACCIXY	NHIM	NHI1	NHI2	CMAX	DG1
13	13	0.1E 00	16	2	1	5.0	0.4430E-01
13	13	0.1E-01	32	8	1	5.0	0.4793E-01
13	13	0.1E-02	64	16	1	7.5	0.4784E-01
13	13	0.1E-03	128	32	4	7.5	0.4802E-01
13	13	0.1E-04	256	64	16	7.5	0.4803E-01
13	14	0.1E 00	16	4	1	5.0	0.4739E-01
13	14	0.1E-01	32	16	1	5.0	0.4797E-01
13	14	0.1E-02	64	32	4	7.5	0.4801E-01
13	14	0.1E-03	128	32	8	7.5	0.4801E-01
13	14	0.1E-04	256	64	32	10.0	0.4801E-01
13	15	0.1E 00	16	4	1	5.0	0.4773E-01
13	15	0.1E-01	32	16	1	5.0	0.4828E-01
13	15	0.1E-02	64	32	4	7.5	0.4831E-01
13	15	0.1E-03	128	64	8	7.5	0.4831E-01
13	15	0.1E-04	256	64	32	10.0	0.4831E-01
13	16	0.1E 00	16	4	1	5.0	0.4846E-01
13	16	0.1E-01	32	16	1	7.5	0.4898E-01
13	16	0.1E-02	64	32	4	7.5	0.4900E-01
13	16	0.1E-03	128	64	16	7.5	0.4901E-01
13	16	0.1E-04	256	64	32	10.0	0.4901E-01
13	17	0.1E 00	16	4	1	5.0	0.4961E-01
13	17	0.1E-01	32	16	2	7.5	0.5011E-01
13	17	0.1E-02	64	32	8	7.5	0.5012E-01
13	17	0.1E-03	128	64	16	10.0	0.5012E-01
13	17	0.1E-04	256	64	32	10.0	0.5012E-01
13	25	0.1E 00	16	4	1	5.0	0.4558E-01
13	25	0.1E-01	32	8	4	7.5	0.4560E-01
13	25	0.1E-02	64	32	8	7.5	0.4560E-01
13	25	0.1E-03	128	32	32	10.0	0.4560E-01
13	25	0.1E-04	256	64	64	12.5	0.4560E-01
13	49	0.1E 00	16	16	1	5.0	0.3390E-02
13	49	0.1E-01	32	32	1	5.0	0.3371E-02
13	49	0.1E-02	64	32	2	7.5	0.3369E-02
13	49	0.1E-03	128	64	8	7.5	0.3365E-02
13	49	0.1E-04	256	64	32	7.5	0.3365E-02
61	61	0.1E 00	16	1	1	5.0	-0.4541E-02
61	61	0.1E-01	32	1	1	5.0	-0.4541E-02
61	61	0.1E-02	64	16	1	5.0	-0.7113E-02
61	61	0.1E-03	128	16	1	5.0	-0.7113E-02
61	61	0.1E-04	256	32	1	5.0	-0.7113E-02
61	49	0.1E 00	16	8	1	5.0	-0.1292E-03
61	49	0.1E-01	32	16	1	5.0	-0.1331E-03
61	49	0.1E-02	64	32	1	5.0	-0.1332E-03
61	49	0.1E-03	128	32	1	5.0	-0.1332E-03
61	49	0.1E-04	256	64	1	5.0	-0.1332E-03
61	25	0.1E 00	16	8	1	5.0	-0.6135E-02
61	25	0.1E-01	32	16	1	5.0	-0.6166E-02
61	25	0.1E-02	64	32	1	5.0	-0.6168E-02
61	25	0.1E-03	128	64	2	7.5	-0.6168E-02
61	25	0.1E-04	256	64	8	7.5	-0.6168E-02

Table A.6.2e Integral Evaluation of Wave Function Values

DIFFRACTION PARAMETER (2*PI*CA/WL) 0.20
CYLINDER DEPTH PARAMETER (YO/WL) 0.04
WATER DEPTH PARAMETER (WD/WL) 0.08

I	J	ACCI	NHIM	NHI1	NHI2	CMAX	G1
13	13	0.1E-01	16	4	8	10.0	-0.4571E 00
13	13	0.1E-02	32	8	32	17.5	-0.4637E 00
13	13	0.1E-03	64	16	64	25.0	-0.4644E 00
13	13	0.1E-04	128	32	128	32.5	-0.4644E 00
13	13	0.1E-05	256	32	256	42.5	-0.4644E 00
13	14	0.1E-01	16	4	8	12.5	-0.2910E 00
13	14	0.1E-02	32	8	32	17.5	-0.2938E 00
13	14	0.1E-03	64	16	64	25.0	-0.2946E 00
13	14	0.1E-04	128	32	128	35.0	-0.2948E 00
13	14	0.1E-05	256	32	256	45.0	-0.2948E 00
13	15	0.1E-01	16	4	8	12.5	-0.2139E 00
13	15	0.1E-02	32	8	32	17.5	-0.2169E 00
13	15	0.1E-03	64	16	64	27.5	-0.2179E 00
13	15	0.1E-04	128	32	128	35.0	-0.2179E 00
13	15	0.1E-05	256	32	256	45.0	-0.2179E 00
13	16	0.1E-01	16	4	8	12.5	-0.1638E 00
13	16	0.1E-02	32	8	32	20.0	-0.1675E 00
13	16	0.1E-03	64	16	64	27.5	-0.1678E 00
13	16	0.1E-04	128	32	128	35.0	-0.1678E 00
13	16	0.1E-05	256	32	256	42.5	-0.1678E 00
13	17	0.1E-01	16	4	8	12.5	-0.1263E 00
13	17	0.1E-02	32	8	32	20.0	-0.1299E 00
13	17	0.1E-03	64	16	64	27.5	-0.1301E 00
13	17	0.1E-04	128	32	128	35.0	-0.1301E 00
13	17	0.1E-05	256	32	256	40.0	-0.1301E 00
13	25	0.1E-01	16	4	8	12.5	0.6238E-01
13	25	0.1E-02	32	8	32	15.0	0.6395E-01
13	25	0.1E-03	64	16	64	32.5	0.6768E-01
13	25	0.1E-04	128	32	128	37.5	0.6772E-01
13	25	0.1E-05	256	32	256	55.0	0.6768E-01
13	49	0.1E-01	16	4	8	10.0	0.3442E 00
13	49	0.1E-02	32	8	16	10.0	0.3442E 00
13	49	0.1E-03	64	16	64	17.5	0.3443E 00
13	49	0.1E-04	128	32	128	25.0	0.3443E 00
13	49	0.1E-05	256	32	256	27.5	0.3443E 00
61	61	0.1E-01	16	4	4	7.5	-0.4881E 00
61	61	0.1E-02	32	8	16	12.5	-0.4896E 00
61	61	0.1E-03	64	16	32	15.0	-0.4897E 00
61	61	0.1E-04	128	16	128	20.0	-0.4897E 00
61	61	0.1E-05	256	32	256	22.5	-0.4897E 00
61	49	0.1E-01	16	4	8	10.0	0.7028E-01
61	49	0.1E-02	32	8	16	12.5	0.6996E-01
61	49	0.1E-03	64	16	64	17.5	0.6988E-01
61	49	0.1E-04	128	32	128	20.0	0.6988E-01
61	49	0.1E-05	256	32	256	25.0	0.6988E-01
61	25	0.1E-01	16	4	8	10.0	0.2377E 00
61	25	0.1E-02	32	8	16	12.5	0.2373E 00
61	25	0.1E-03	64	16	64	17.5	0.2373E 00
61	25	0.1E-04	128	32	128	20.0	0.2373E 00
61	25	0.1E-05	256	32	256	20.0	0.2373E 00

Table A.6.3a Integral Evaluation of Wave Function Values

DIFFRACTION PARAMETER (2*PI*CA/WL) 0.50
CYLINDER DEPTH PARAMETER (Y0/WL) 0.10
WATER DEPTH PARAMETER (WD/WL) 0.20

I	J	ACCI	NHIM	NHI1	NHI2	CMAX	G1
13	13	0.1E-01	16	2	4	7.5	-0.4176E 00
13	13	0.1E-02	32	4	8	10.0	-0.4183E 00
13	13	0.1E-03	64	8	32	15.0	-0.4184E 00
13	13	0.1E-04	128	16	64	17.5	-0.4184E 00
13	13	0.1E-05	256	32	128	22.5	-0.4184E 00
13	14	0.1E-01	16	2	4	7.5	-0.2465E 00
13	14	0.1E-02	32	4	16	12.5	-0.2474E 00
13	14	0.1E-03	64	8	32	15.0	-0.2474E 00
13	14	0.1E-04	128	16	128	20.0	-0.2474E 00
13	14	0.1E-05	256	32	256	22.5	-0.2474E 00
13	15	0.1E-01	16	2	4	10.0	-0.1694E 00
13	15	0.1E-02	32	4	16	12.5	-0.1692E 00
13	15	0.1E-03	64	8	32	15.0	-0.1693E 00
13	15	0.1E-04	128	16	128	20.0	-0.1693E 00
13	15	0.1E-05	256	32	256	22.5	-0.1693E 00
13	16	0.1E-01	16	2	8	10.0	-0.1175E 00
13	16	0.1E-02	32	4	16	12.5	-0.1178E 00
13	16	0.1E-03	64	8	32	15.0	-0.1178E 00
13	16	0.1E-04	128	16	128	17.5	-0.1178E 00
13	16	0.1E-05	256	32	256	20.0	-0.1178E 00
13	17	0.1E-01	16	2	8	10.0	-0.7835E-01
13	17	0.1E-02	32	4	16	12.5	-0.7855E-01
13	17	0.1E-03	64	8	32	15.0	-0.7856E-01
13	17	0.1E-04	128	16	128	17.5	-0.7856E-01
13	17	0.1E-05	256	32	256	25.0	-0.7855E-01
13	25	0.1E-01	16	2	4	7.5	0.1358E 00
13	25	0.1E-02	32	4	32	15.0	0.1378E 00
13	25	0.1E-03	64	8	64	17.5	0.1378E 00
13	25	0.1E-04	128	16	128	22.5	0.1378E 00
13	25	0.1E-05	256	32	256	25.0	0.1378E 00
13	49	0.1E-01	16	4	2	5.0	0.3264E 00
13	49	0.1E-02	32	8	8	7.5	0.3263E 00
13	49	0.1E-03	64	16	32	12.5	0.3263E 00
13	49	0.1E-04	128	16	64	12.5	0.3263E 00
13	49	0.1E-05	256	32	128	15.0	0.3263E 00
61	61	0.1E-01	16	4	1	7.5	-0.5659E 00
61	61	0.1E-02	32	8	4	7.5	-0.5637E 00
61	61	0.1E-03	64	8	16	10.0	-0.5637E 00
61	61	0.1E-04	128	16	32	10.0	-0.5637E 00
61	61	0.1E-05	256	32	64	12.5	-0.5637E 00
61	49	0.1E-01	16	4	2	7.5	0.2002E-01
61	49	0.1E-02	32	8	8	7.5	0.2047E-01
61	49	0.1E-03	64	8	16	10.0	0.2047E-01
61	49	0.1E-04	128	16	64	12.5	0.2047E-01
61	49	0.1E-05	256	32	64	12.5	0.2047E-01
61	25	0.1E-01	16	2	4	7.5	0.2575E 00
61	25	0.1E-02	32	8	8	7.5	0.2572E 00
61	25	0.1E-03	64	16	16	10.0	0.2572E 00
61	25	0.1E-04	128	16	32	10.0	0.2572E 00
61	25	0.1E-05	256	32	128	12.5	0.2572E 00

Table A.6.3b Integral Evaluation of Wave Function Values

DIFFRACTION PARAMETER (2*PI*CA/WL) 1.00
CYLINDER DEPTH PARAMETER (Y0/WL) 0.20
WATER DEPTH PARAMETER (WD/WL) 0.40

I	J	ACCI	NHIM	NHI1	NHI2	CMAX	GI
13	13	0.1E-01	16	4	2	7.5	-0.3353E 00
13	13	0.1E-02	32	8	4	7.5	-0.3345E 00
13	13	0.1E-03	64	16	16	10.0	-0.3345E 00
13	13	0.1E-04	128	32	32	12.5	-0.3345E 00
13	13	0.1E-05	256	64	64	12.5	-0.3345E 00
13	14	0.1E-01	16	4	2	7.5	-0.1578E 00
13	14	0.1E-02	32	8	8	7.5	-0.1570E 00
13	14	0.1E-03	64	16	16	10.0	-0.1570E 00
13	14	0.1E-04	128	32	64	12.5	-0.1570E 00
13	14	0.1E-05	256	64	128	15.0	-0.1570E 00
13	15	0.1E-01	16	4	2	7.5	-0.7369E-01
13	15	0.1E-02	32	8	8	7.5	-0.7279E-01
13	15	0.1E-03	64	16	16	10.0	-0.7277E-01
13	15	0.1E-04	128	32	64	12.5	-0.7277E-01
13	15	0.1E-05	256	64	128	15.0	-0.7277E-01
13	16	0.1E-01	16	4	4	7.5	-0.1611E-01
13	16	0.1E-02	32	8	8	10.0	-0.1577E-01
13	16	0.1E-03	64	16	16	10.0	-0.1573E-01
13	16	0.1E-04	128	32	64	12.5	-0.1573E-01
13	16	0.1E-05	256	64	128	15.0	-0.1573E-01
13	17	0.1E-01	16	4	4	7.5	0.2831E-01
13	17	0.1E-02	32	8	8	7.5	0.2868E-01
13	17	0.1E-03	64	16	16	10.0	0.2872E-01
13	17	0.1E-04	128	32	64	12.5	0.2872E-01
13	17	0.1E-05	256	64	128	15.0	0.2872E-01
13	25	0.1E-01	16	4	2	7.5	0.2632E 00
13	25	0.1E-02	32	8	8	10.0	0.2639E 00
13	25	0.1E-03	64	16	32	12.5	0.2640E 00
13	25	0.1E-04	128	32	64	15.0	0.2640E 00
13	25	0.1E-05	256	64	128	17.5	0.2640E 00
13	49	0.1E-01	16	8	1	5.0	0.1774E 00
13	49	0.1E-02	32	16	8	7.5	0.1771E 00
13	49	0.1E-03	64	32	16	7.5	0.1771E 00
13	49	0.1E-04	128	32	32	10.0	0.1771E 00
13	49	0.1E-05	256	64	64	10.0	0.1771E 00
61	61	0.1E-01	16	8	1	5.0	-0.7105E 00
61	61	0.1E-02	32	8	1	5.0	-0.7105E 00
61	61	0.1E-03	64	16	4	7.5	-0.7105E 00
61	61	0.1E-04	128	32	8	7.5	-0.7105E 00
61	61	0.1E-05	256	64	16	7.5	-0.7105E 00
61	49	0.1E-01	16	8	1	5.0	-0.1030E 00
61	49	0.1E-02	32	8	1	7.5	-0.1031E 00
61	49	0.1E-03	64	16	8	7.5	-0.1029E 00
61	49	0.1E-04	128	32	16	7.5	-0.1029E 00
61	49	0.1E-05	256	64	32	10.0	-0.1029E 00
61	25	0.1E-01	16	4	1	5.0	0.2075E 00
61	25	0.1E-02	32	8	1	5.0	0.2074E 00
61	25	0.1E-03	64	16	8	7.5	0.2075E 00
61	25	0.1E-04	128	32	16	7.5	0.2075E 00
61	25	0.1E-05	256	64	32	10.0	0.2075E 00

Table A.6.3c Integral Evaluation of Wave Function Values

DIFFRACTION PARAMETER (2*PI*CA/WL) 1.50
CYLINDER DEPTH PARAMETER (YO/WL) 0.30
WATER DEPTH PARAMETER (WD/WL) 0.60

I	J	ACCI	NHIM	NHI1	NHI2	CMAX	G1
13	13	0.1E-01	16	8	1	5.0	-0.3237E 00
13	13	0.1E-02	32	16	4	7.5	-0.3235E 00
13	13	0.1E-03	64	32	8	7.5	-0.3234E 00
13	13	0.1E-04	128	64	32	10.0	-0.3234E 00
13	13	0.1E-05	256	128	64	10.0	-0.3234E 00
13	14	0.1E-01	16	8	1	5.0	-0.1406E 00
13	14	0.1E-02	32	16	4	7.5	-0.1403E 00
13	14	0.1E-03	64	32	8	7.5	-0.1402E 00
13	14	0.1E-04	128	64	32	10.0	-0.1402E 00
13	14	0.1E-05	256	128	64	10.0	-0.1402E 00
13	15	0.1E-01	16	8	1	7.5	-0.5243E-01
13	15	0.1E-02	32	16	4	7.5	-0.5102E-01
13	15	0.1E-03	64	32	8	7.5	-0.5098E-01
13	15	0.1E-04	128	64	32	10.0	-0.5098E-01
13	15	0.1E-05	256	128	64	10.0	-0.5098E-01
13	16	0.1E-01	16	8	1	7.5	0.8862E-02
13	16	0.1E-02	32	16	4	7.5	0.1032E-01
13	16	0.1E-03	64	32	8	7.5	0.1036E-01
13	16	0.1E-04	128	64	32	10.0	0.1037E-01
13	16	0.1E-05	256	128	64	12.5	0.1037E-01
13	17	0.1E-01	16	8	1	7.5	0.5672E-01
13	17	0.1E-02	32	16	4	7.5	0.5817E-01
13	17	0.1E-03	64	32	8	7.5	0.5821E-01
13	17	0.1E-04	128	64	32	10.0	0.5822E-01
13	17	0.1E-05	256	128	64	12.5	0.5822E-01
13	25	0.1E-01	16	8	2	7.5	0.2703E 00
13	25	0.1E-02	32	16	4	7.5	0.2703E 00
13	25	0.1E-03	64	32	8	10.0	0.2703E 00
13	25	0.1E-04	128	64	16	10.0	0.2703E 00
13	25	0.1E-05	256	128	32	12.5	0.2703E 00
13	49	0.1E-01	16	16	1	5.0	0.3965E-01
13	49	0.1E-02	32	32	8	7.5	0.3960E-01
13	49	0.1E-03	64	64	16	7.5	0.3959E-01
13	49	0.1E-04	128	128	16	7.5	0.3959E-01
13	49	0.1E-05	256	256	32	10.0	0.3959E-01
61	61	0.1E-01	16	8	1	5.0	-0.7866E 00
61	61	0.1E-02	32	16	1	5.0	-0.7867E 00
61	61	0.1E-03	64	32	1	5.0	-0.7867E 00
61	61	0.1E-04	128	64	2	7.5	-0.7867E 00
61	61	0.1E-05	256	64	8	7.5	-0.7867E 00
61	49	0.1E-01	16	16	1	5.0	-0.1821E 00
61	49	0.1E-02	32	16	1	5.0	-0.1822E 00
61	49	0.1E-03	64	32	1	5.0	-0.1822E 00
61	49	0.1E-04	128	64	4	7.5	-0.1822E 00
61	49	0.1E-05	256	128	16	7.5	-0.1822E 00
61	25	0.1E-01	16	8	1	5.0	0.1216E 00
61	25	0.1E-02	32	8	1	5.0	0.1216E 00
61	25	0.1E-03	64	32	2	7.5	0.1216E 00
61	25	0.1E-04	128	32	8	7.5	0.1216E 00
61	25	0.1E-05	256	64	16	7.5	0.1216E 00

Table A.6.3d Integral Evaluation of Wave Function Values

DIFFRACTION PARAMETER (2*PI*CA/WL) 2.00
CYLINDER DEPTH PARAMETER (YO/WL) 0.40
WATER DEPTH PARAMETER (WD/WL) 0.80

I	J	ACCI	NHIM	NHI1	NHI2	CMAX	G1
13	13	0.1E-01	16	16	1	5.0	-0.3485E 00
13	13	0.1E-02	32	16	1	7.5	-0.3485E 00
13	13	0.1E-03	64	32	8	7.5	-0.3481E 00
13	13	0.1E-04	128	64	16	7.5	-0.3481E 00
13	13	0.1E-05	256	128	32	10.0	-0.3481E 00
13	14	0.1E-01	16	16	1	5.0	-0.1624E 00
13	14	0.1E-02	32	16	2	7.5	-0.1622E 00
13	14	0.1E-03	64	32	8	7.5	-0.1620E 00
13	14	0.1E-04	128	64	16	7.5	-0.1620E 00
13	14	0.1E-05	256	128	32	10.0	-0.1620E 00
13	15	0.1E-01	16	16	1	5.0	-0.7081E-01
13	15	0.1E-02	32	32	2	7.5	-0.7051E-01
13	15	0.1E-03	64	32	8	7.5	-0.7038E-01
13	15	0.1E-04	128	64	16	7.5	-0.7038E-01
13	15	0.1E-05	256	128	64	10.0	-0.7038E-01
13	16	0.1E-01	16	16	1	5.0	-0.7771E-02
13	16	0.1E-02	32	32	4	7.5	-0.7360E-02
13	16	0.1E-03	64	32	8	7.5	-0.7325E-02
13	16	0.1E-04	128	64	16	7.5	-0.7322E-02
13	16	0.1E-05	256	128	64	10.0	-0.7322E-02
13	17	0.1E-01	16	16	1	5.0	0.4090E-01
13	17	0.1E-02	32	32	2	7.5	0.4123E-01
13	17	0.1E-03	64	32	8	7.5	0.4135E-01
13	17	0.1E-04	128	64	32	10.0	0.4136E-01
13	17	0.1E-05	256	128	64	10.0	0.4136E-01
13	25	0.1E-01	16	16	1	5.0	0.2105E 00
13	25	0.1E-02	32	32	8	7.5	0.2105E 00
13	25	0.1E-03	64	32	8	7.5	0.2105E 00
13	25	0.1E-04	128	64	32	10.0	0.2105E 00
13	25	0.1E-05	256	128	64	10.0	0.2105E 00
13	49	0.1E-01	16	16	1	5.0	-0.1317E-01
13	49	0.1E-02	32	32	1	5.0	-0.1342E-01
13	49	0.1E-03	64	64	4	7.5	-0.1344E-01
13	49	0.1E-04	128	128	16	7.5	-0.1344E-01
13	49	0.1E-05	256	256	32	7.5	-0.1344E-01
61	61	0.1E-01	16	16	1	5.0	-0.8202E 00
61	61	0.1E-02	32	32	1	5.0	-0.8205E 00
61	61	0.1E-03	64	32	1	5.0	-0.8205E 00
61	61	0.1E-04	128	64	1	5.0	-0.8205E 00
61	61	0.1E-05	256	128	1	5.0	-0.8205E 00
61	49	0.1E-01	16	16	1	5.0	-0.2207E 00
61	49	0.1E-02	32	32	1	5.0	-0.2209E 00
61	49	0.1E-03	64	64	1	5.0	-0.2209E 00
61	49	0.1E-04	128	64	1	5.0	-0.2209E 00
61	49	0.1E-05	256	128	2	7.5	-0.2209E 00
61	25	0.1E-01	16	8	1	5.0	0.6685E-01
61	25	0.1E-02	32	16	1	5.0	0.6681E-01
61	25	0.1E-03	64	32	1	5.0	0.6681E-01
61	25	0.1E-04	128	64	2	7.5	0.6681E-01
61	25	0.1E-05	256	128	8	7.5	0.6681E-01

Table A.6.3e Integral Evaluation of Wave Function Values

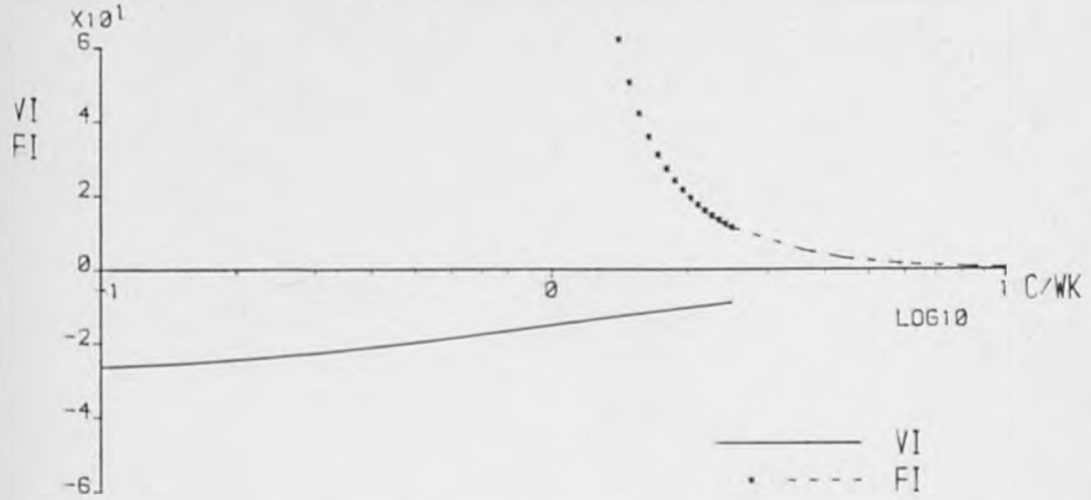

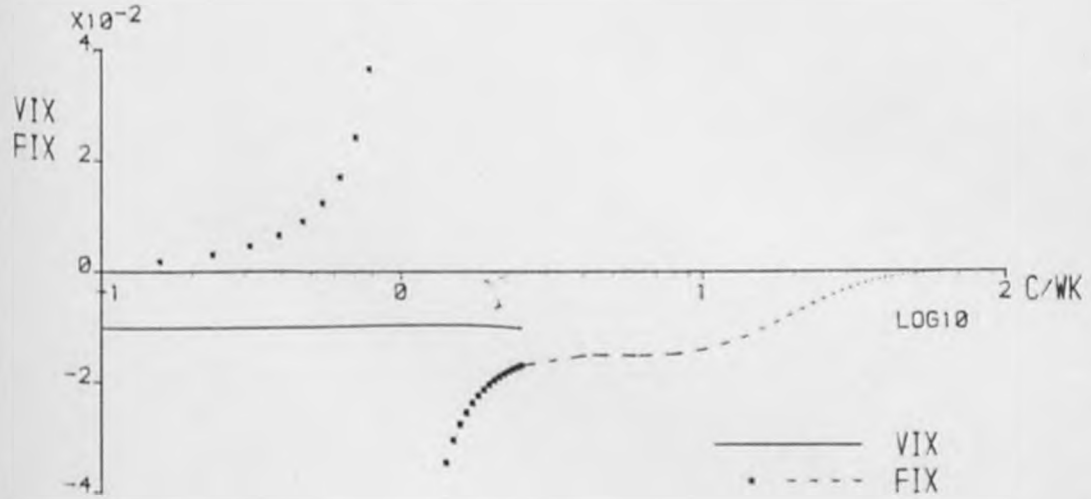

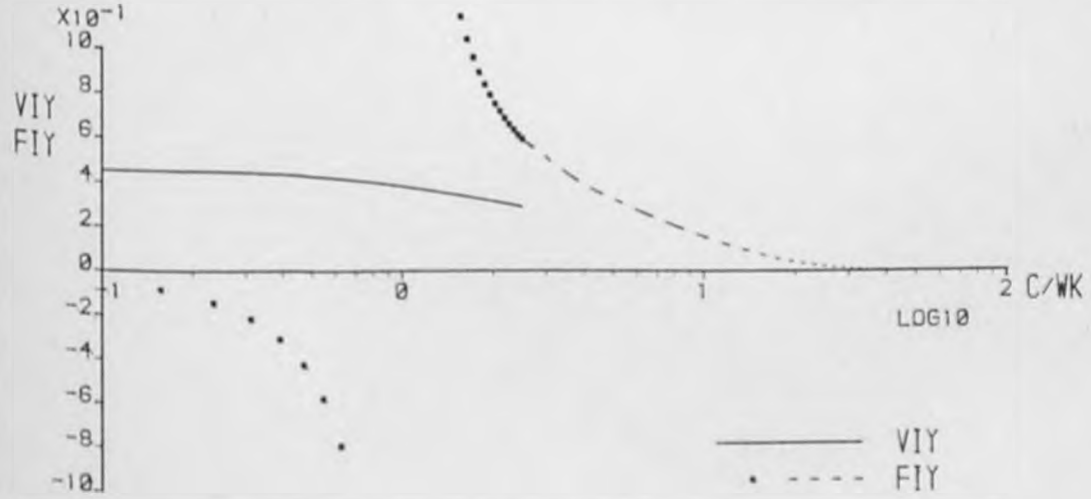

Diffraction Parameter (2xPIxCA/WL)	.20
Cylinder Depth Parameter (Y0/WL)	.04
Water Depth Parameter (WD/WL)	.08

Number of Nodes=96 Nodal point, I=13 Source point, J=13

Figure A.6.3a Numerical Integration

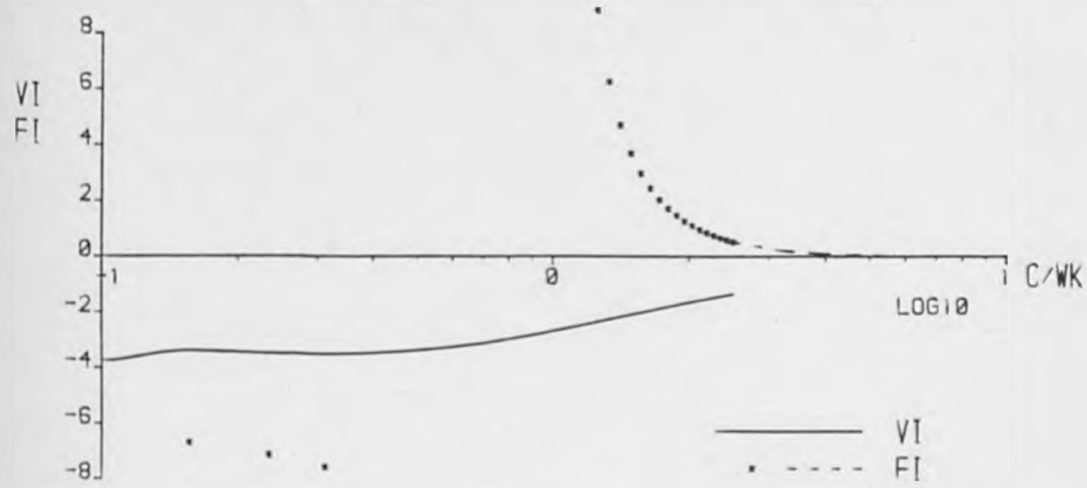

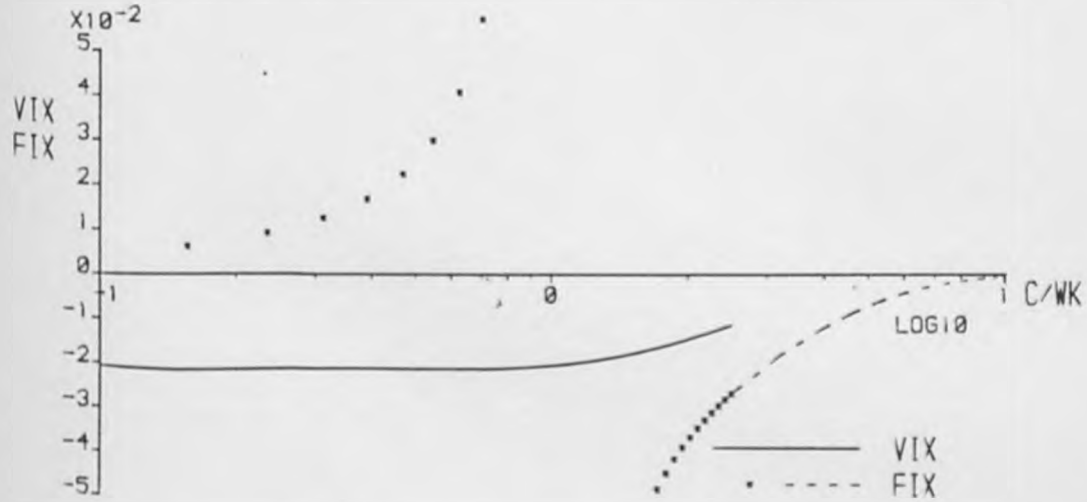

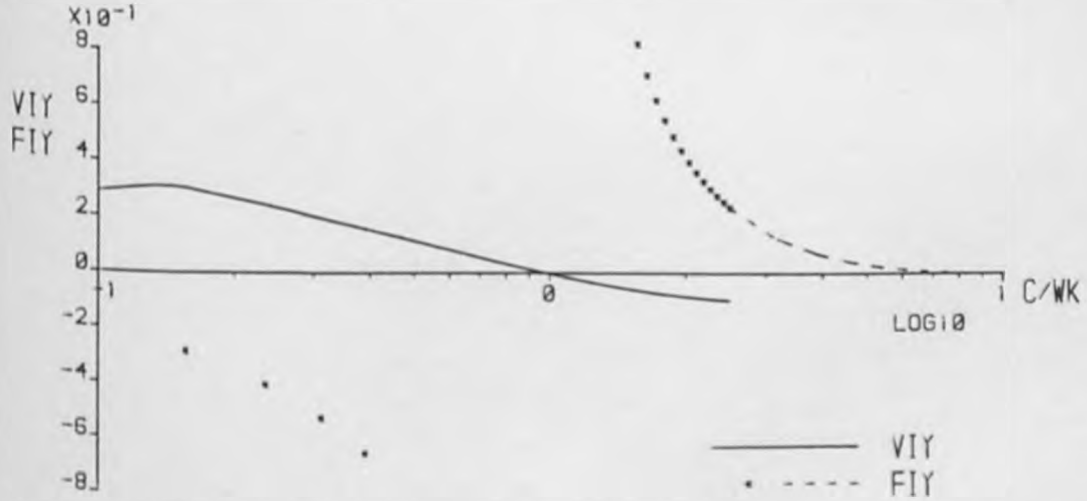

Diffraction Parameter (2xPIxCA/WL)	1.00
Cylinder Depth Parameter (Y0/WL)	.20
Water Depth Parameter (WD/WL)	.40

Number of Nodes=96 Nodal point, I=13 Source point, J=13

Figure A.6.3b Numerical Integration

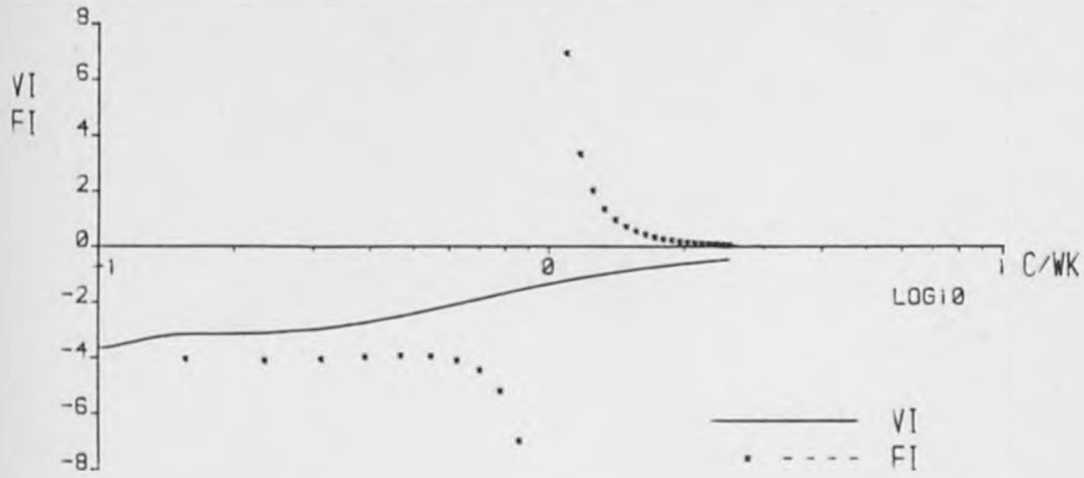

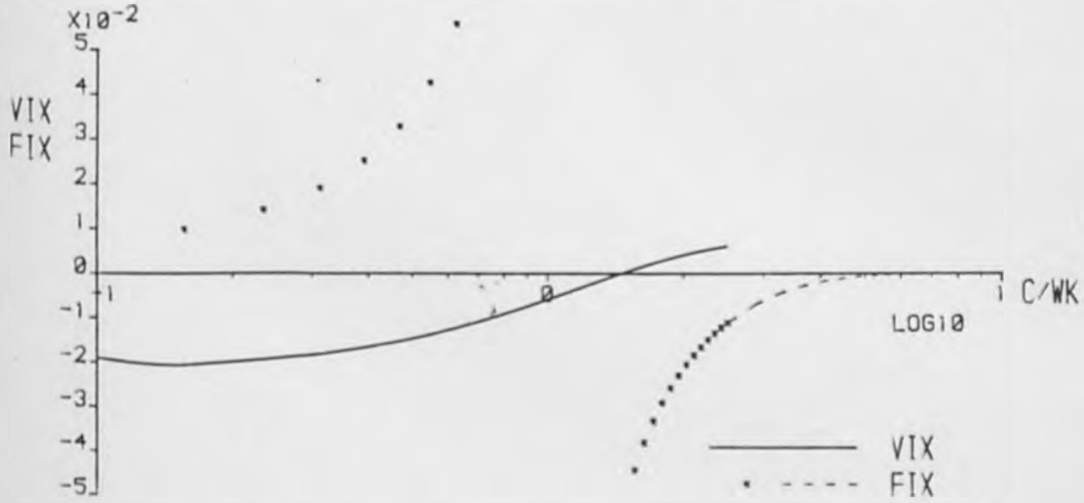

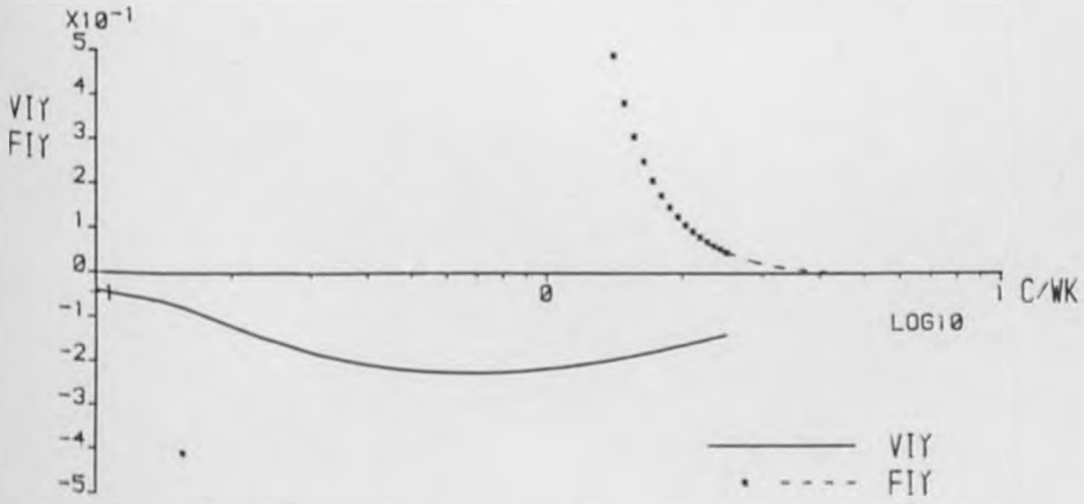

Diffraction Parameter (2xPIxCA/WL)	2.00
Cylinder Depth Parameter (Y0/WL)	.40
Water Depth Parameter (WD/WL)	.80

Number of Nodes=96 Nodal point, I=13 Source point, J=13

Figure A.6.3c Numerical Integration

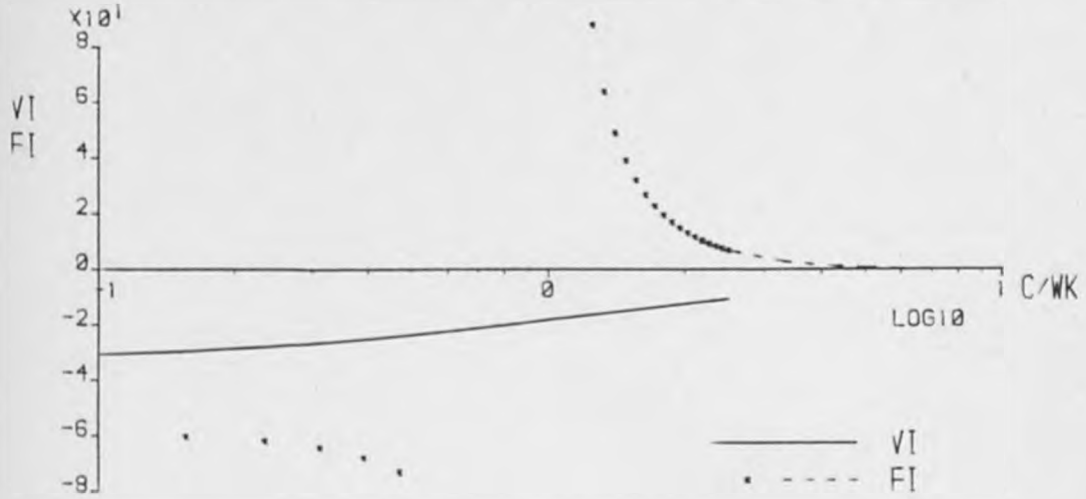

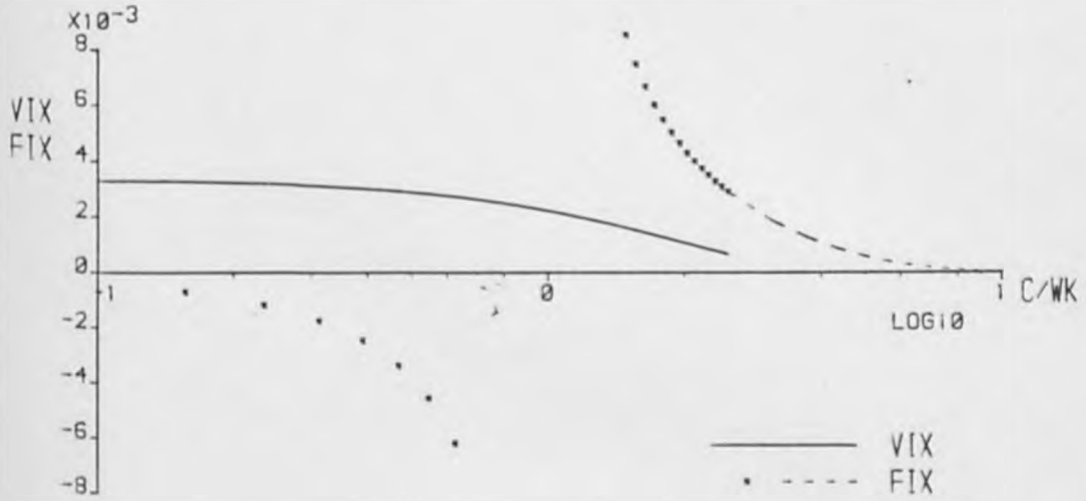

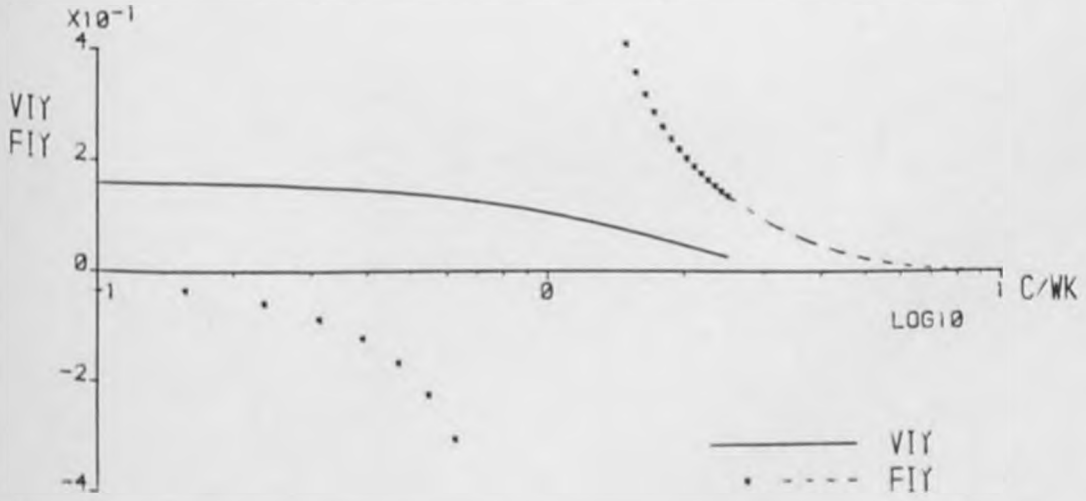

Diffraction Parameter (2xPIxCA/WL) .20
Cylinder Depth Parameter (Y0/WL) .04
Water Depth Parameter (WD/WL) .08

Number of Nodes=96 Nodal point, I=61 Source point, J=61

Figure A.6.3d Numerical Integration

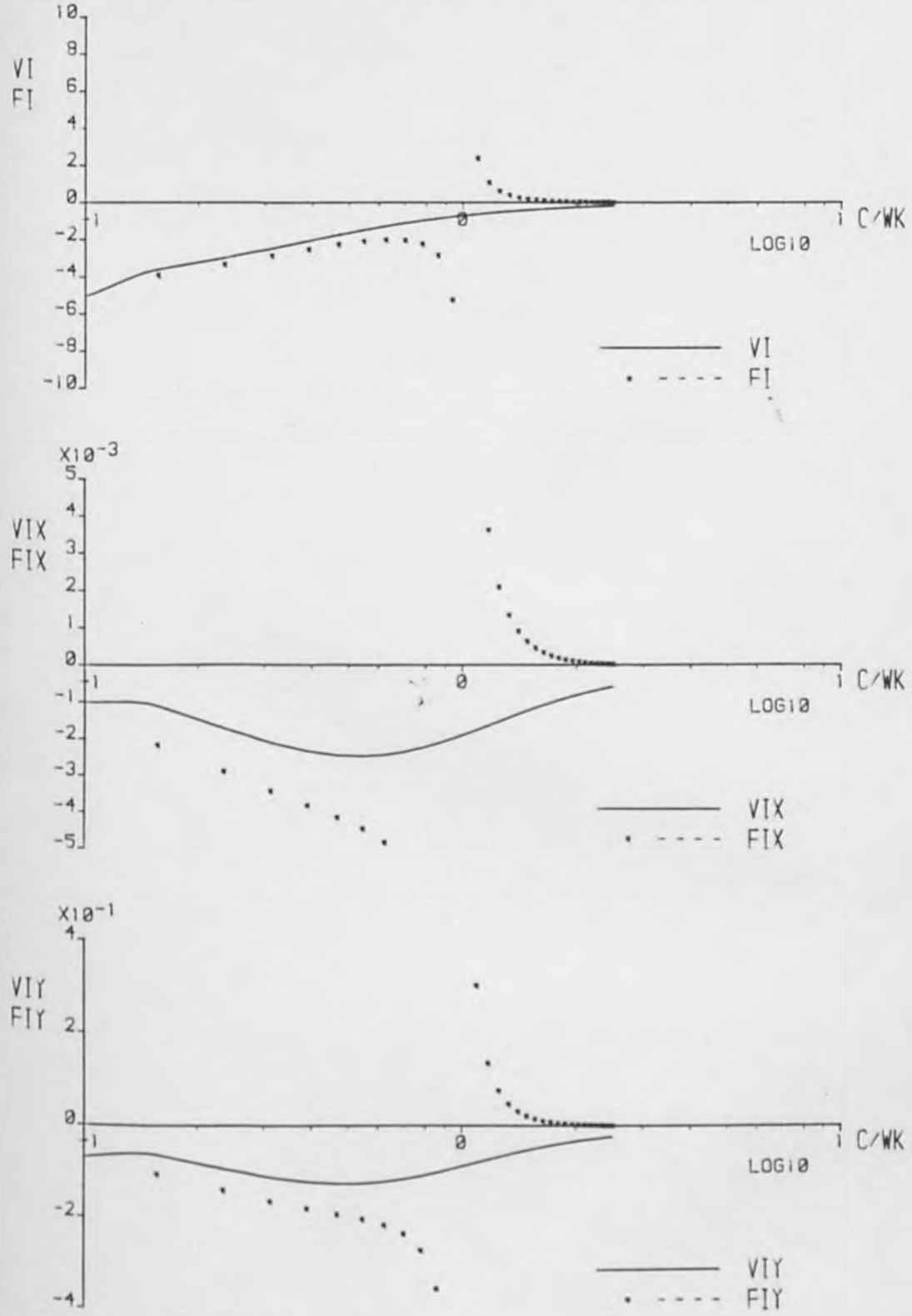

Diffraction Parameter (2xPIxCA/WL)	1.00
Cylinder Depth Parameter (Y0/WL)	.20
Water Depth Parameter (WD/WL)	.40

Number of Nodes=96 Nodal point, I=61 Source point, J=61

Figure A.6.3e Numerical Integration

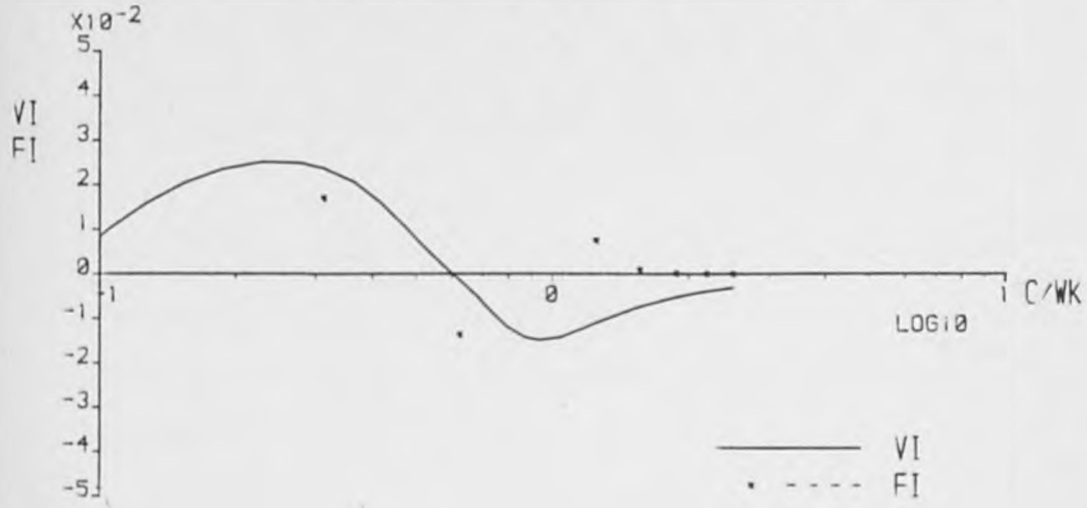

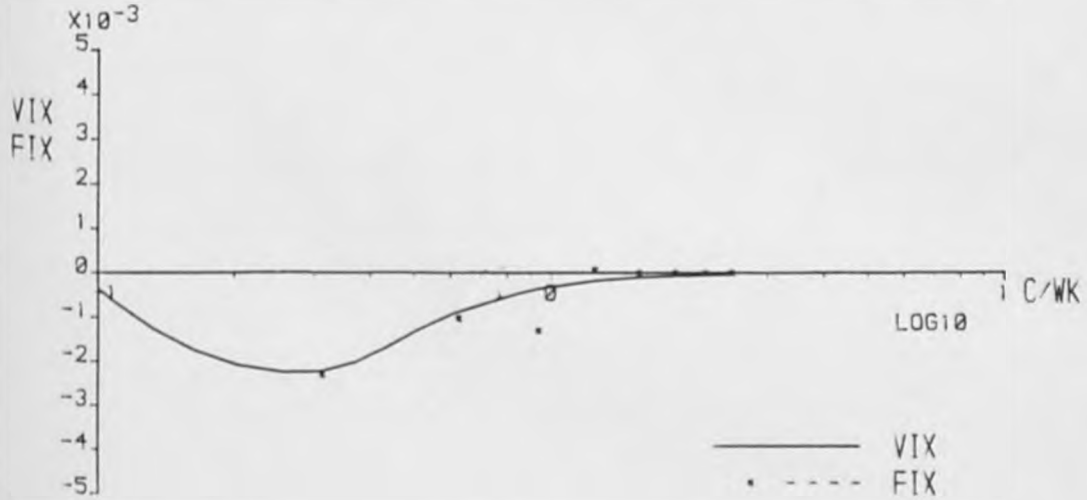

Diffraction Parameter (2xPIxCA/WL)	2.00
Cylinder Depth Parameter (Y0/WL)	.40
Water Depth Parameter (WD/WL)	.80

Number of Nodes=96 Nodal point, I=61 Source point, J=61

Figure A.6.3F Numerical Integration

APPENDIX A.7 PRESSURE, FORCE AND WAVE SUBROUTINES

This appendix includes a listing of the main segment of the diffraction program and the subroutine DATA written to read data from a prepared file plus the subroutines referred to in section 4.4 of the thesis.

The variable names which have not been included in the previous appendices are

BETAR,BETAT	Arguments of complex reflection and transmission coefficients, R,T.
BETAX,BETAY	Arguments of complex total force components, f_x,f_y.
CX,CY	Horizontal and vertical diffraction coefficients, C_x,C_y.
EI	Results of analytic integration of logarithmic singularity for constant variation of source density.
EI1,EI2	Results of analytic integration of logarithmic singularity for linear variation of source density.
FX,FY	Moduli of complex total force components, f_x,f_y.
FXW,FYW	Moduli of complex Froude Krylov force components, f_{kx},f_{ky}.
GQ1 to GQ5	Results of analytic integration of logarithmic singularity for quadratic variation of source density.
PA	Modulus of complex total pressure on object boundary, p.
PW	Modulus of complex incident wave pressure on object boundary, p_w.
R	Modulus of complex reflection coefficient, R.
RES	Residual to determine whether the principle of energy conservation is satisfied RES = $1 - R^2 - T^2$.

T — Modulus of complex transmission complex, T.

A number of the previously declared arrays are allocated new values in this part of the diffraction program and the new assignments are

A(2n,2n) — Matrix $\underline{A}$ in matrix evaluation equation (equation 4.2.3)

C(2n,1) — Vector containing scattered wave and incident wave pressures, p_s and p_w, in turn.

The arrays declared in this section of the program which have not been required previously are

BETASP(ns),BETASN(ns) — Arguments of complex free surface displacements, η_s^+ and η_s^-.

BETATP(ns),BETATN(ns) — Arguments of complex free surface displacements, η^+ and η^-.

YSP(ns),YSN(ns) — Moduli of complex free surface displacements, η_s^+ and η_s^-.

YTP(ns),YTN(ns) — Moduli of complex free surface displacements, η^+ and η^-.

where ns is the number of points at which the quantities are to be evaluated. It may be noted that the subroutine SGRNFN has been called in subroutines WAVE and CWAVE, this subroutine is, with the exception of very minor differences, the same as subroutine GRNFN and is therefore not listed.

Computer program (pp. 399-411)
has been removed
for copyright reasons

APPENDIX A.8 THE SEMI-IMMERSED CIRCULAR CYLINDER

As an additional test for the numerical solution of the regular kernel integral equation formulation of the linear wave diffraction problem the diffraction program has been used to obtain results for the case of the semi-immersed circular cylinder. These additional tests are valuable for a number of reasons. Firstly it is possible that with the object located in the free surface the problem may prove to be more numerically demanding, secondly the geometry of this problem more closely resembles that of ship problems and, thirdly, results have been published for this problem in tabular form.

Martin and Dixon (1983) have applied Ursell's multipole method to obtain numerical solutions for the semi-immersed circular cylinder in water of infinite depth. Results have been given in tabular form for four complex quantities: the horizontal and vertical components of force F_x and F_y and the reflection and transmission coefficients R and T.

Results have been obtained using the diffraction program for the same range of the diffraction parameter, ka, as in the testing of the submerged obstacle but in these tests the water depth parameter, kh, has been fixed to give deep water over the whole range of ka. The effects of refraction have therefore been eliminated. It has been found that the evaluation of the integral form of the wave function can only be achieved if the interval is restricted to (0,10k) but tests in which the series evaluation was preferred have demonstrated that this does not affect the accuracy of the results.

The geometry of this problem introduces a number of discretisation difficulties which are absent for the submerged cylinder problem. These difficulties are concerned with the introduction of higher order elements and in particular with the elements at the cylinder free surface junction each of which has a "free" node. This should not lead to any numerical problems but requires that several minor modifications are made to the diffraction program to include the results of the analytical integrations for sources on elements at the correct addresses in the matrix if higher-order elements are to be employed. These amendements do not, however, alter the general form of the program and the listings are therefore not given.

The modified form of the diffraction program has been used to obtain results for this problem using assumed constant and assumed linear distribution of source density on each element with a single source located centrally on each element. Results for the horizontal and vertical components of force and reflection coefficient for a distribution of wave functions on the cylinder boundary are given in Figures A.8.1 to A.8.6 and the corresponding results for sources distributed over a boundary located on a concentric semi-circle with radius $r_s = 0.7r_n$ are given in Figures A.8.7 to A.8.12. The results given by Martin and Dixon are reproduced in table A.8.1 and the results used to plot Figures A.8.1 to A.8.12 are recorded in Tables A.8.2 to A.8.13.

The results obtained for the singular kernel constant element method demonstrate good agreement with the results of Martin and Dixon and also rapid convergence to the final solutions for coarse

discretisations over the full range of ka. Implementation of the linear element method with sources located on the source boundary does not give markedly different results but results at certain ka give an indication of reduced accuracy. These results are therefore in general agreement with those presented in section 4.5.

Location of the source boundary outside the fluid domain with a constant element discretisation gives poor results for the horizontal force at lower ka but with this exception results are in better agreement with the results of Martin and Dixon than those obtained by the singular kernel method. The results obtained by the regular kernel method with linear elements are poor for the full range of discretisation and this trend is different from that identified in the submerged cyliner problem as reported in section 4.5. It may be noted that the poorest results are often due to the most precise disretisations and therefore that the problem is associated with the ill-conditioning of the system of equations.

With regard to the efficiency these results do not indicate that the regular kernel method offers the opportunity of employing a coarser discretisation and the comparison of the execution times included in the tables indicate that the savings identified in section 4.5 are not so significant for the semi-immersed cylinder.

However, the results given in this appendix so confirm the results of section 4.5 in that the regular kernel integral equation provides satisfactory results for a constant element discretisation. One advantage of the regular kernel method which is relevent for surface piercing cylinders but not for submerged bodies is that

since the Fredholm integral equation is of the first kind the difficulties due to the breakdown of the integral equation method at frequencies which correspond to eigen values of the homogenous equation are not encountered.

ka	Mod(R)	Mod(Fx)	Mod(Fy)
0.1	0.194	0.317	1.651
0.2	0.396	0.627	1.470
0.3	0.586	0.888	1.335
0.4	0.737	1.065	1.224
0.5	0.840	1.156	1.129
0.6	0.905	1.186	1.046
0.7	0.943	1.180	0.971
0.8	0.965	1.154	0.905
0.9	0.978	1.121	0.844
1.0	0.986	1.108	0.789
2.0	1.000	0.777	0.436

Results obtained by Martin and Dixon (1983) using the multipole method for waves in fluid of infinite depth.

Table A.8.1 Diffraction Results for a Semi-immersed Cylinder

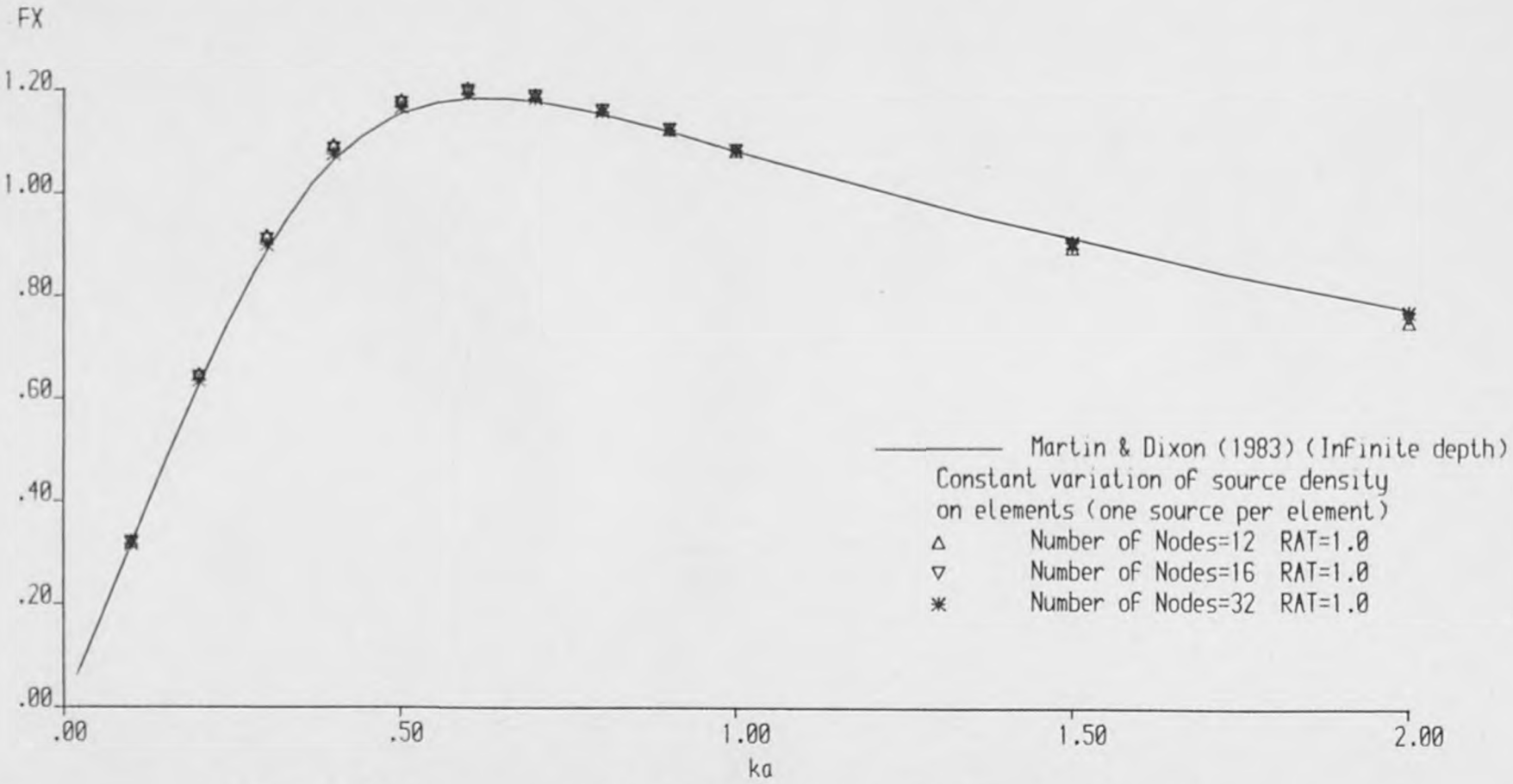

Figure A.8.1 Maximum horizontal force on a semi-immersed cylinder

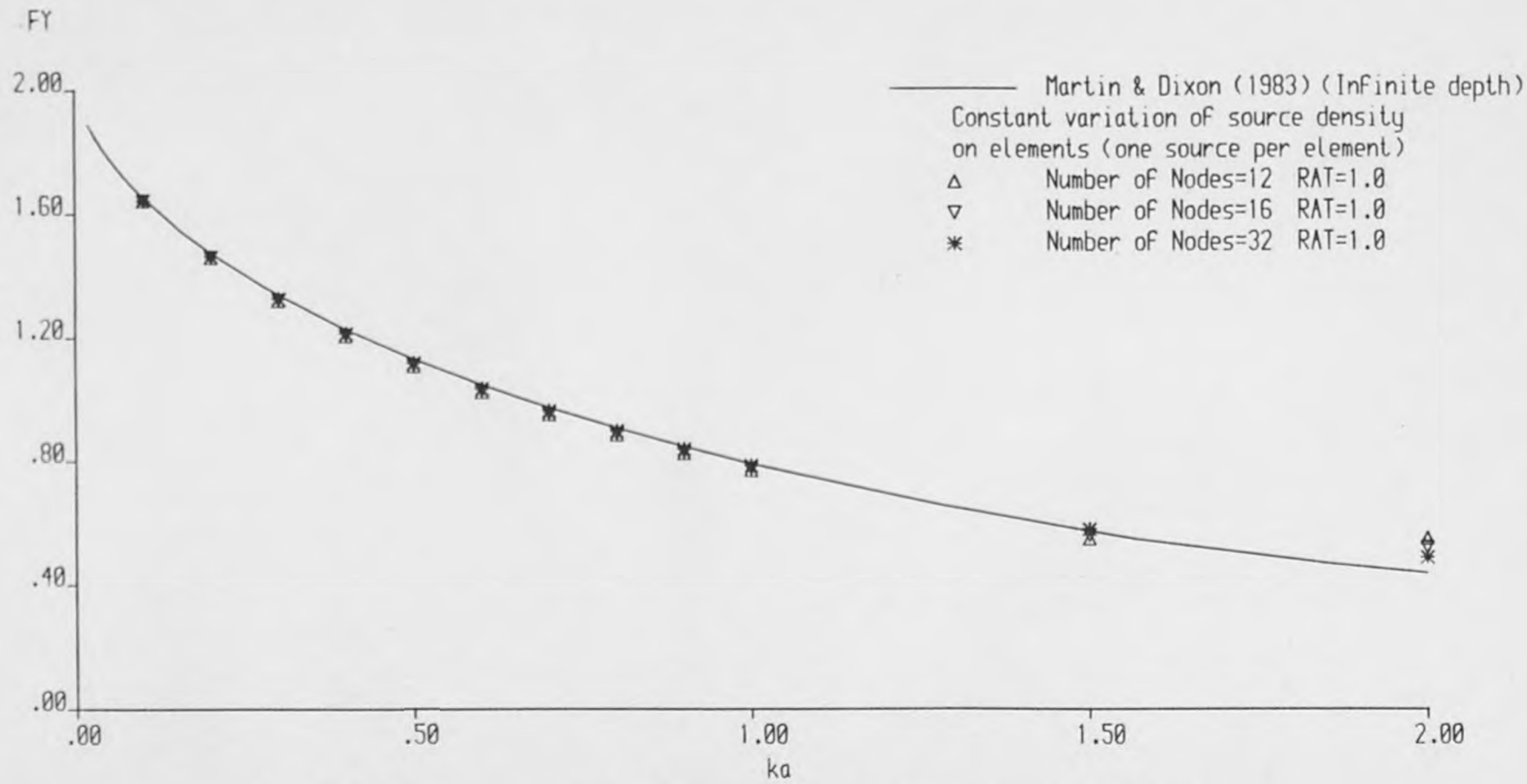

Figure A.8.2 Maximum vertical force on a semi-immersed cylinder

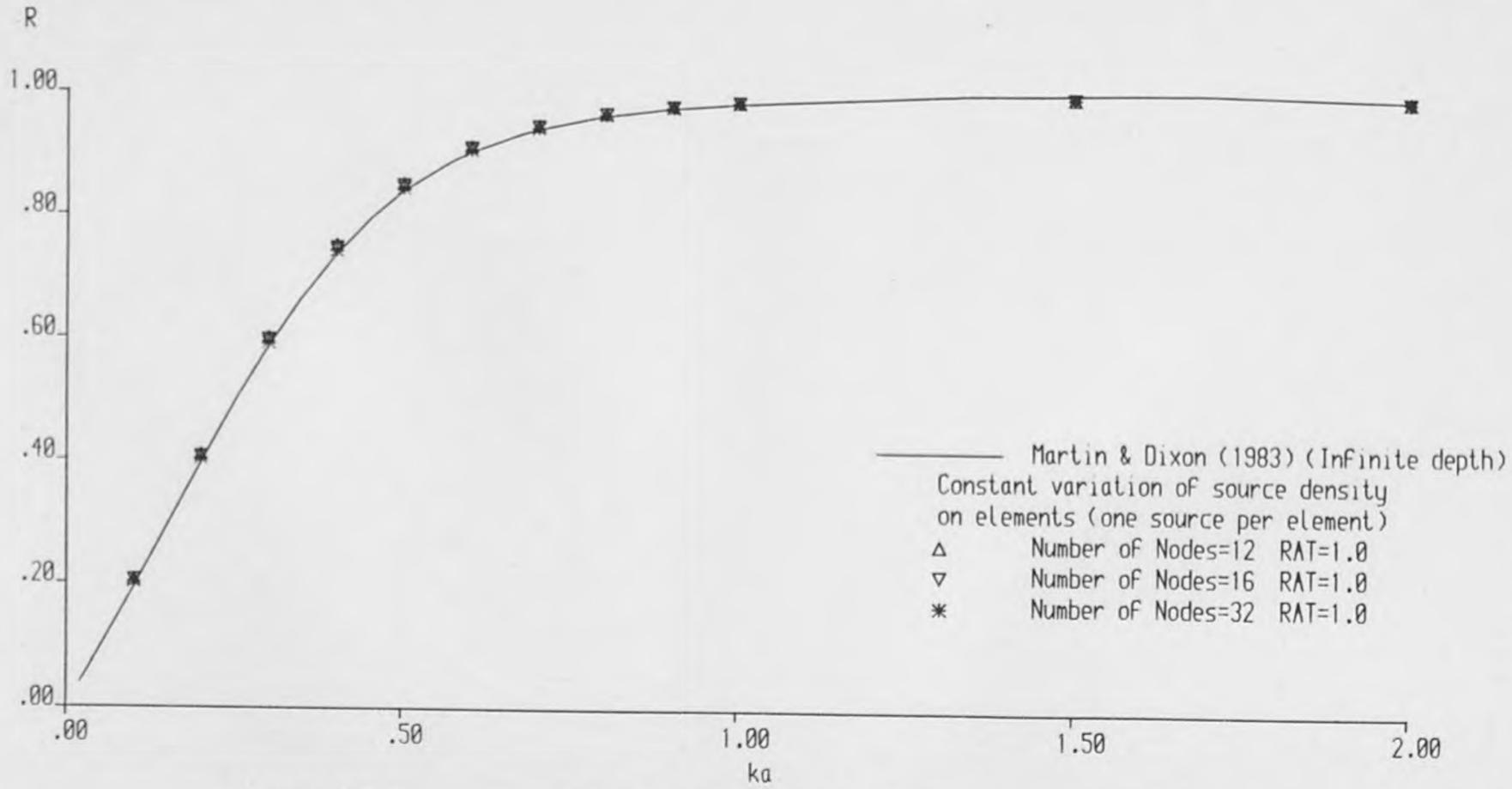

Figure A.8.3 Reflection coefficient for a semi-immersed cylinder

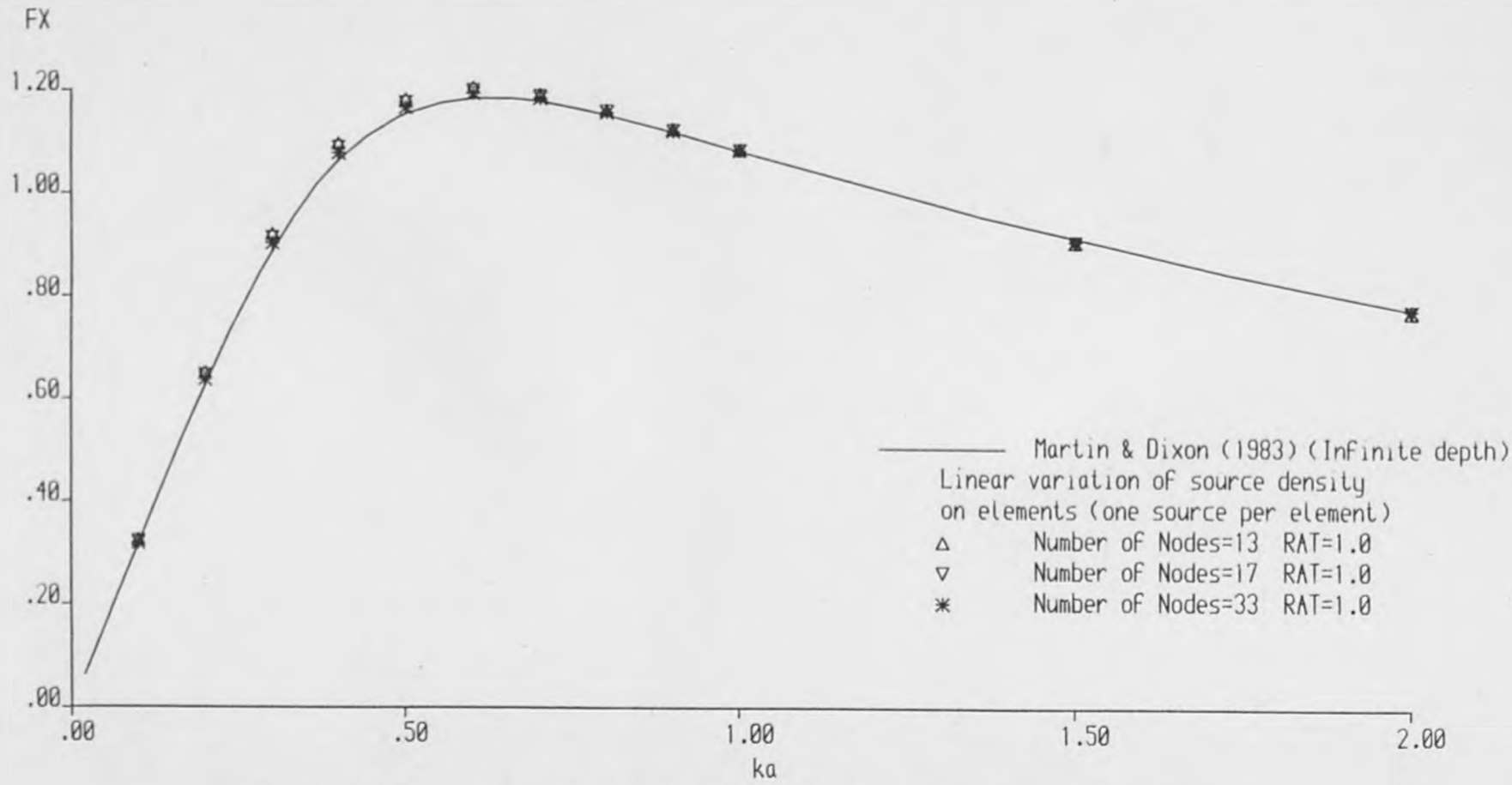

Figure A.8.4 Maximum horizontal force on a semi-immersed cylinder

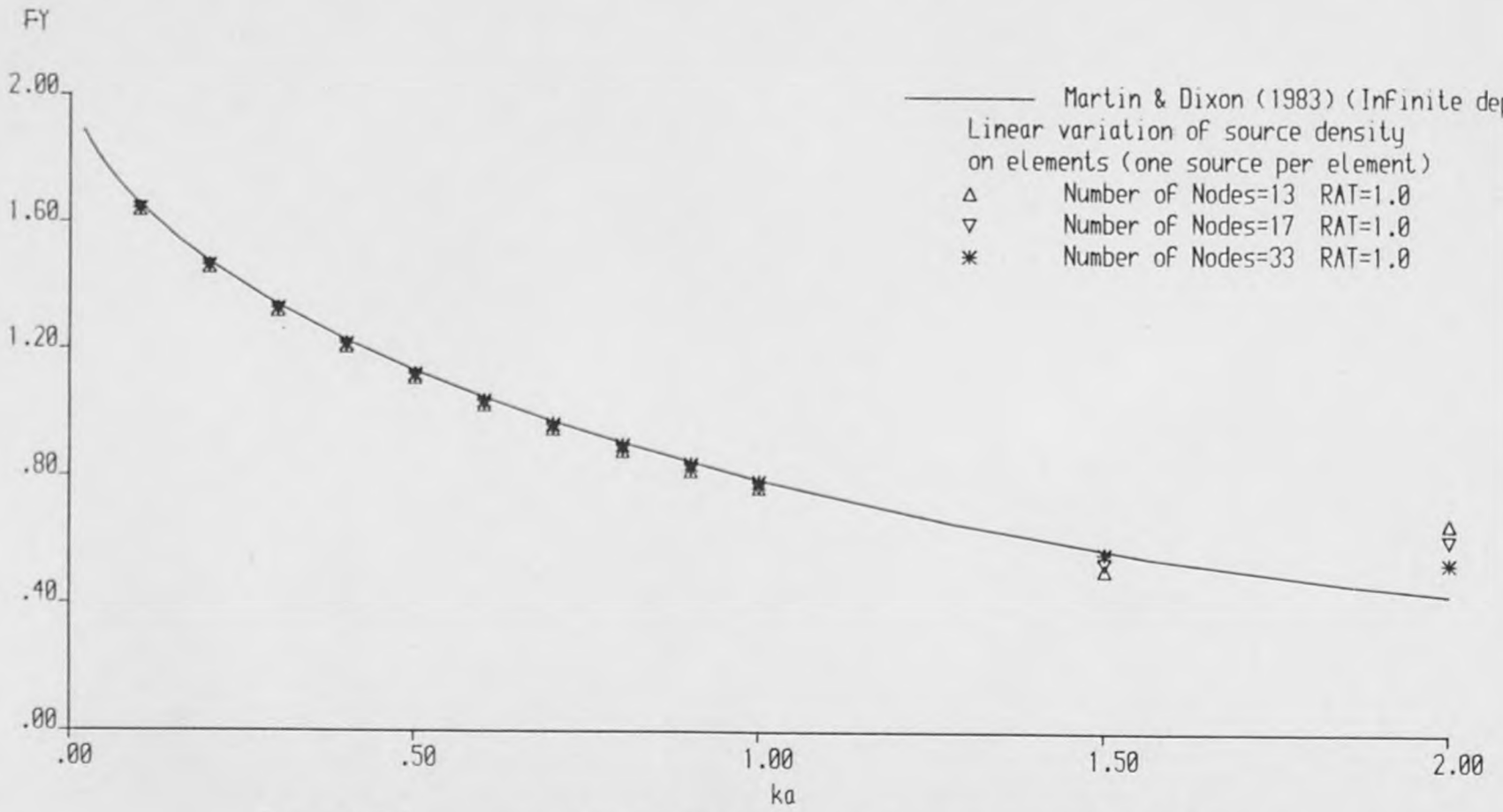

Figure A.8.5 Maximum vertical force on a semi-immersed cylinder

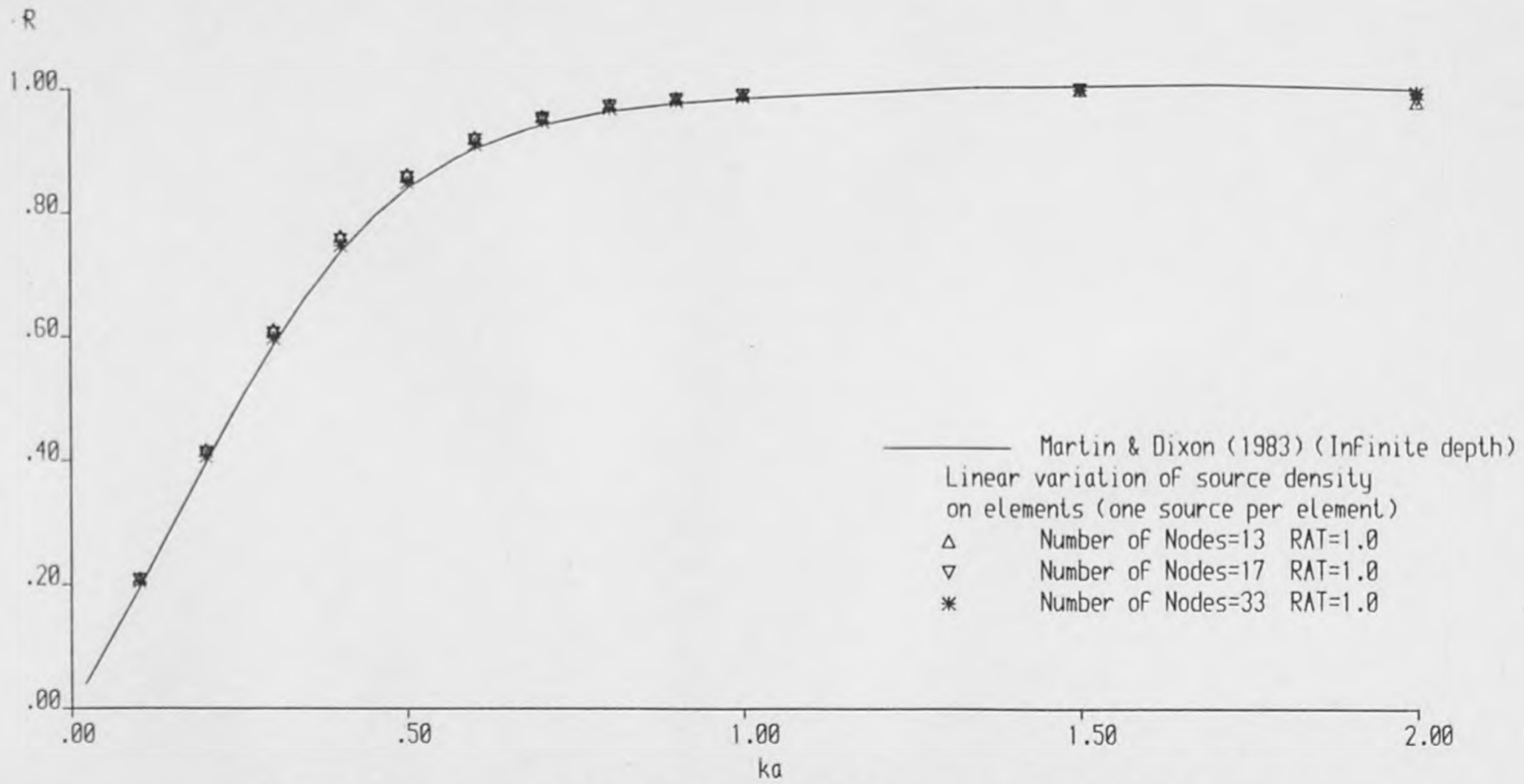

Figure A.8.6 Reflection coefficient for a semi-immersed cylinder

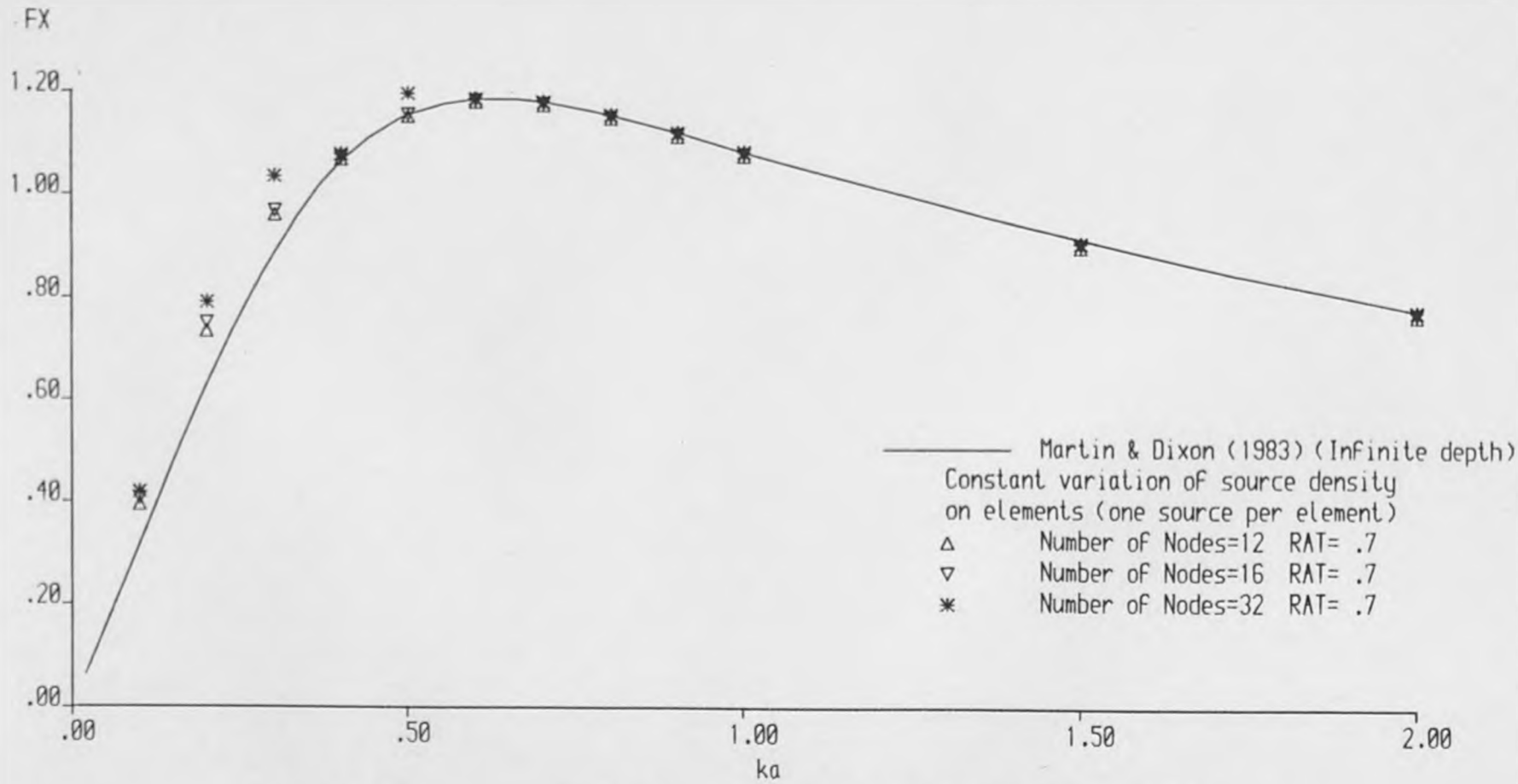

Figure A.8.7 Maximum horizontal force on a semi-immersed cylinder

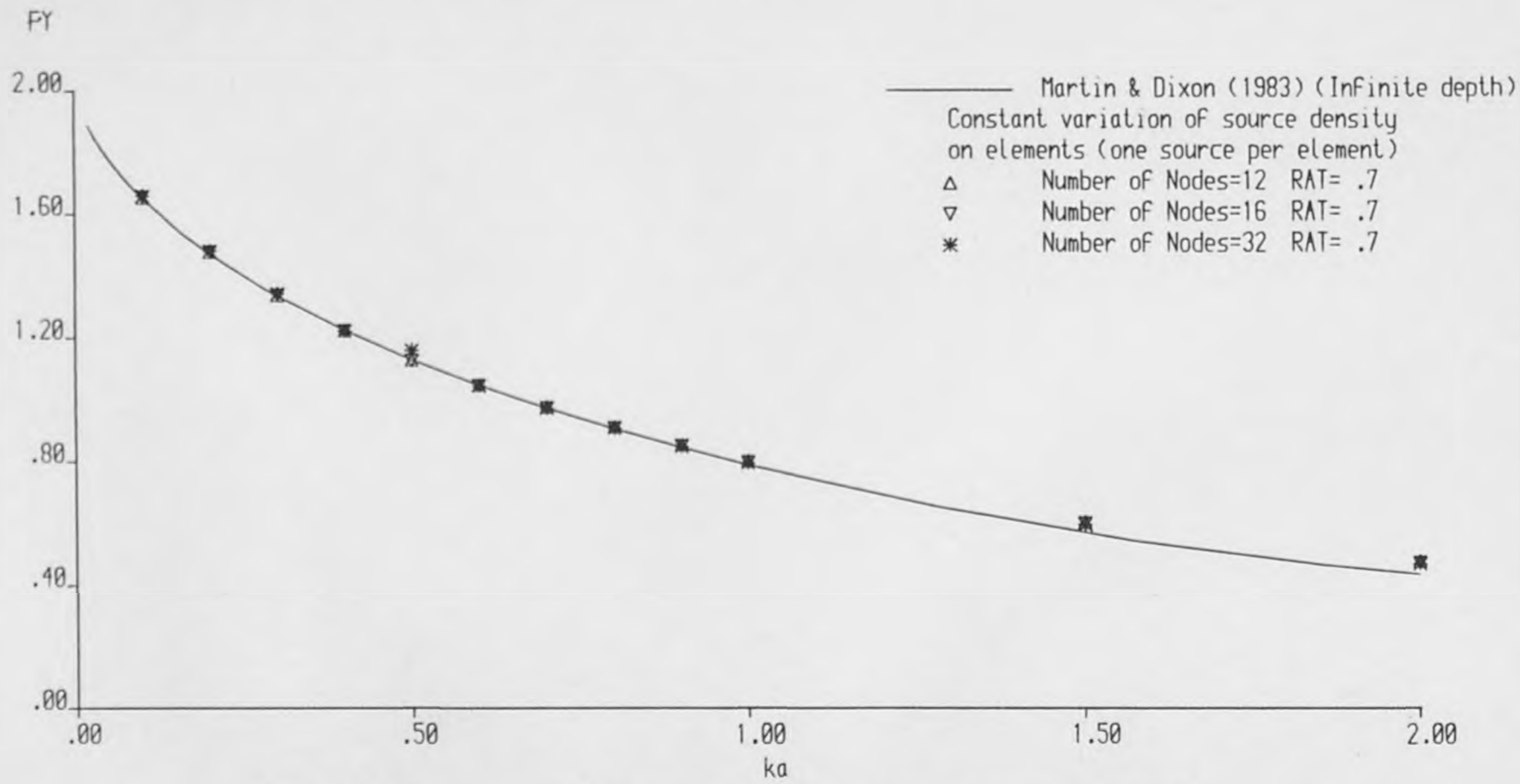

Figure A.8.8 Maximum vertical force on a semi-immersed cylinder

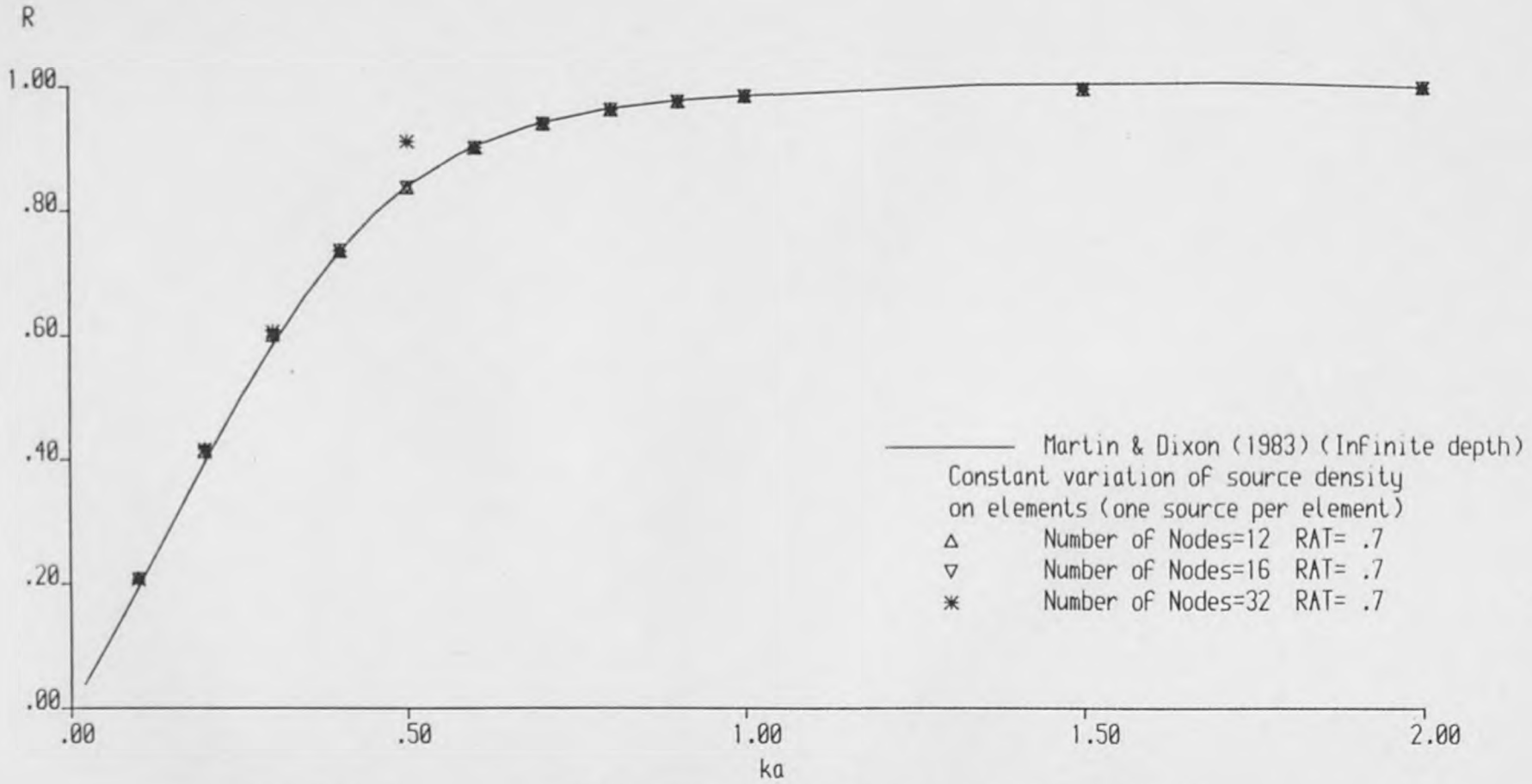

Figure A.8.9 Reflection coefficient for a semi-immersed cylinder

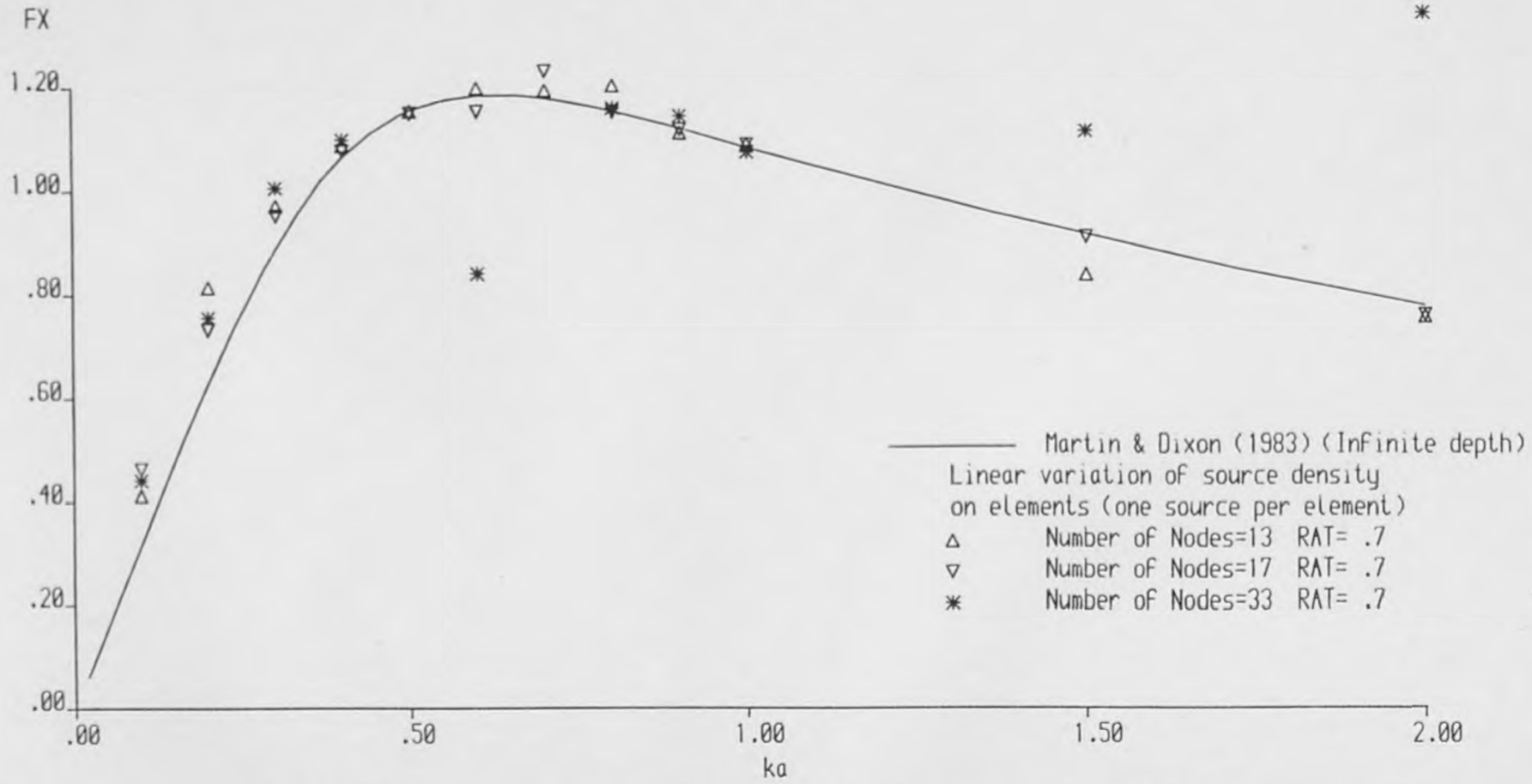

Figure A.8.10 Maximum horizontal force on a semi-immersed cylinder

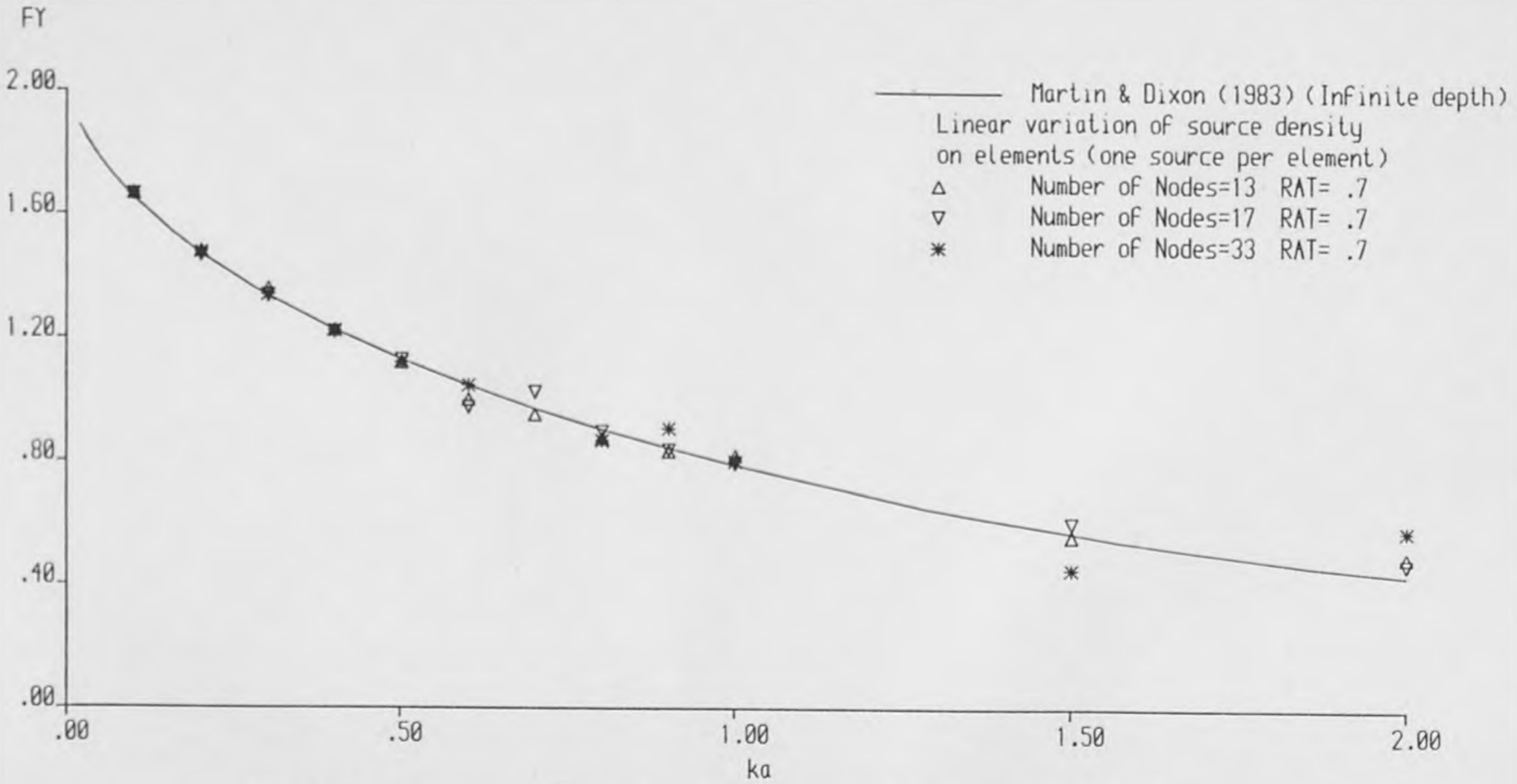

Figure A.8.11 Maximum vertical force on a semi-immersed cylinder

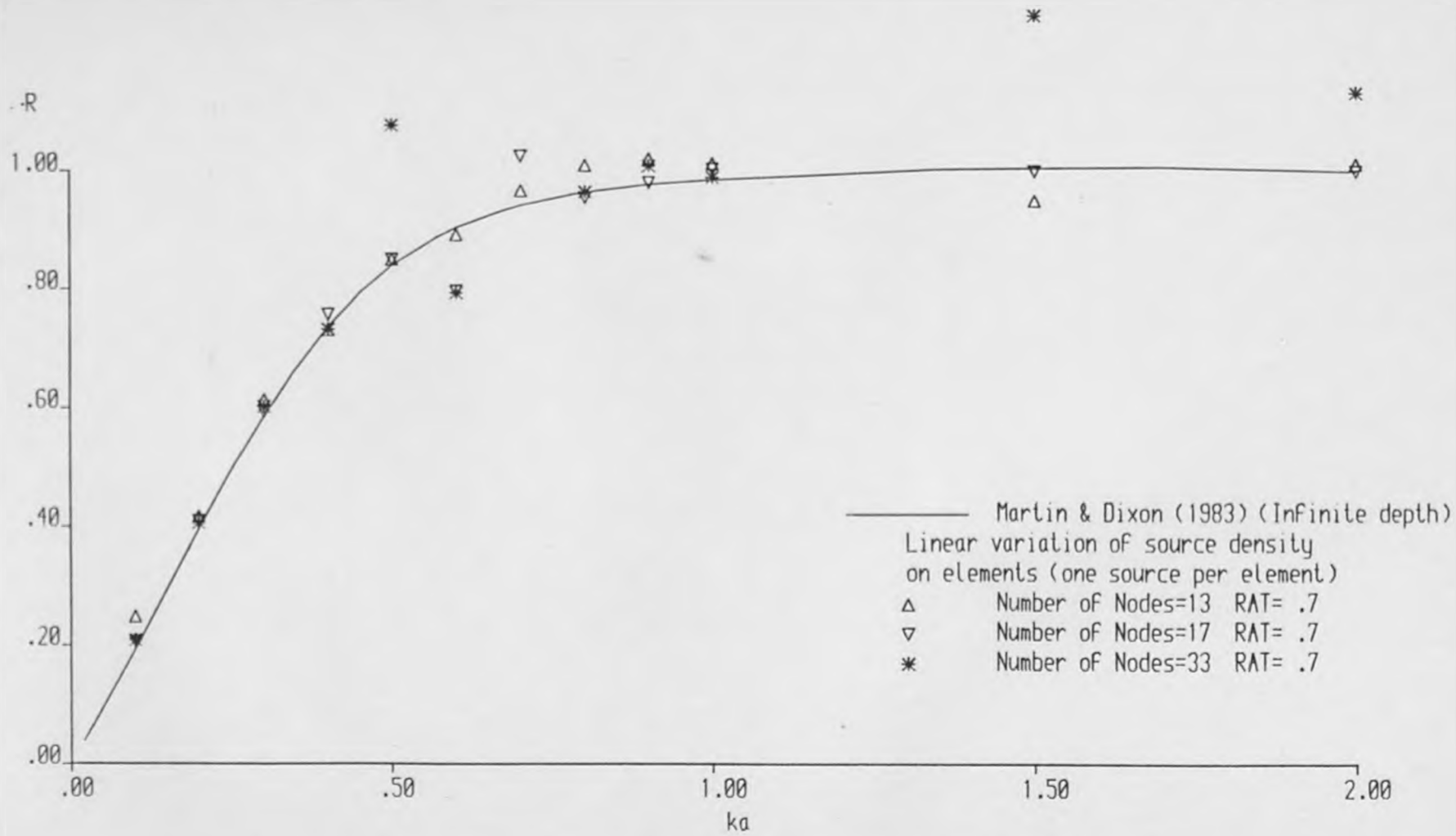

Figure A.8.12 Reflection coefficient for a semi-immersed cylinder

SOURCES DISTRIBUTED ON CYLINDER BOUNDARY
NO NODES= 12 (CONSTANT ELEMENTS)
ONE-POINT GAUSS QUADRATURE

ka	h/L	Mod(R)	Arg(R)	RES	Mod(Fx)	Arg(Fx)	Mod(Fy)	Arg(Fy)
0.10	0.75	0.206	0.455	0.2E-09	0.322	0.033	1.641	1.396
0.20	0.75	0.409	0.438	0.3E-09	0.647	0.113	1.457	1.262
0.30	0.75	0.600	0.431	0.6E-08	0.917	0.214	1.317	1.141
0.40	0.75	0.751	0.425	0.3E-08	1.094	0.306	1.204	1.028
0.50	0.75	0.851	0.410	0.8E-08	1.181	0.368	1.107	0.920
0.60	0.75	0.913	0.386	0.2E-07	1.205	0.395	1.023	0.816
0.70	0.75	0.948	0.352	0.2E-07	1.193	0.392	0.949	0.715
0.80	0.75	0.969	0.312	0.3E-07	1.163	0.365	0.883	0.615
0.90	0.75	0.981	0.266	0.2E-07	1.125	0.321	0.823	0.516
1.00	0.75	0.988	0.217	0.3E-08	1.084	0.264	0.768	0.417
1.50	0.75	0.999	-0.064	0.2E-06	0.897	-0.120	0.547	-0.082
2.00	0.75	0.998	-0.343	0.2E-08	0.753	-0.571	0.547	-0.507

Processor time=0.0317

Table A.8.2 Diffraction Results for a Semi-immersed Cylinder

SOURCES DISTRIBUTED ON CYLINDER BOUNDARY
NO NODES= 16 (CONSTANT ELEMENTS)
ONE-POINT GAUSS QUADRATURE

ka	h/L	Mod(R)	Arg(R)	RES	Mod(Fx)	Arg(Fx)	Mod(Fy)	Arg(Fy)
0.10	0.75	0.205	0.455	0.2E-08	0.320	0.032	1.641	1.397
0.20	0.75	0.406	0.438	0.5E-08	0.642	0.112	1.458	1.264
0.30	0.75	0.597	0.432	0.1E-07	0.910	0.212	1.320	1.143
0.40	0.75	0.747	0.425	0.7E-09	1.087	0.304	1.207	1.031
0.50	0.75	0.849	0.411	0.3E-08	1.176	0.367	1.111	0.924
0.60	0.75	0.911	0.387	0.2E-07	1.201	0.395	1.027	0.821
0.70	0.75	0.947	0.354	0.5E-10	1.191	0.393	0.953	0.720
0.80	0.75	0.968	0.314	0.3E-09	1.162	0.367	0.887	0.621
0.90	0.75	0.980	0.269	0.4E-07	1.125	0.324	0.828	0.522
1.00	0.75	0.988	0.220	0.2E-08	1.085	0.268	0.774	0.424
1.50	0.75	0.999	-0.060	0.2E-07	0.902	-0.114	0.559	-0.073
2.00	0.75	0.997	-0.337	0.3E-07	0.762	-0.565	0.518	-0.494

Processor time=0.0635

Table A.8.3 Diffraction Results for a Semi-immersed Cylinder

SOURCES DISTRIBUTED ON CYLINDER BOUNDARY
NO NODES= 32 (CONSTANT ELEMENTS)
ONE-POINT GAUSS QUADRATURE

ka	h/L	Mod(R)	Arg(R)	RES	Mod(Fx)	Arg(Fx)	Mod(Fy)	Arg(Fy)
0.10	0.75	0.202	0.455	0.4E-08	0.317	0.032	1.641	1.399
0.20	0.75	0.403	0.438	0.4E-04	0.635	0.110	1.460	1.267
0.30	0.75	0.592	0.432	0.1E-07	0.900	0.210	1.324	1.147
0.40	0.75	0.742	0.425	0.2E-07	1.077	0.301	1.212	1.035
0.50	0.75	0.844	0.412	0.2E-07	1.167	0.364	1.117	0.929
0.60	0.75	0.907	0.388	0.3E-07	1.195	0.393	1.034	0.827
0.70	0.75	0.944	0.356	0.5E-07	1.186	0.392	0.961	0.727
0.80	0.75	0.966	0.317	0.4E-07	1.159	0.367	0.895	0.628
0.90	0.75	0.979	0.272	0.1E-07	1.124	0.325	0.836	0.531
1.00	0.75	0.987	0.224	0.3E-07	1.085	0.270	0.783	0.434
1.50	0.75	0.999	-0.053	0.3E-07	0.907	-0.108	0.577	-0.057
2.00	0.75	0.998	-0.334	0.2E-06	0.772	-0.558	0.486	-0.492

Processor time=0.2224

Table A.8.4 Diffraction Results for a Semi-immersed Cylinder

SOURCES DISTRIBUTED ON CYLINDER BOUNDARY
NO NODES= 13 (LINEAR ELEMENTS)
ONE-POINT GAUSS QUADRATURE

ka	h/L	Mod(R)	Arg(R)	RES	Mod(Fx)	Arg(Fx)	Mod(Fy)	Arg(Fy)
0.10	0.75	0.209	0.454	0.2E-08	0.326	0.034	1.635	1.394
0.20	0.75	0.416	0.438	0.5E-08	0.651	0.116	1.454	1.259
0.30	0.75	0.610	0.432	0.4E-08	0.921	0.222	1.318	1.137
0.40	0.75	0.762	0.427	0.2E-07	1.098	0.318	1.205	1.023
0.50	0.75	0.862	0.413	0.4E-08	1.184	0.383	1.108	0.915
0.60	0.75	0.922	0.389	0.5E-08	1.207	0.413	1.023	0.810
0.70	0.75	0.956	0.356	0.1E-07	1.194	0.411	0.948	0.708
0.80	0.75	0.975	0.316	0.2E-07	1.164	0.385	0.879	0.608
0.90	0.75	0.986	0.270	0.2E-07	1.127	0.341	0.817	0.507
1.00	0.75	0.992	0.221	0.1E-07	1.087	0.285	0.765	0.410
1.50	0.75	1.000	-0.069	0.5E-07	0.908	-0.099	0.509	-0.118
2.00	0.75	0.980	-0.287	0.7E-05	0.773	-0.552	0.659	-0.350

Processor time=0.0392

Table A.8.5 Diffraction Results for a Semi-immersed Cylinder

SOURCES DISTRIBUTED ON CYLINDER BOUNDARY
NO NODES= 17 (LINEAR ELEMENTS)
ONE-POINT GAUSS QUADRATURE

ka	h/L	Mod(R)	Arg(R)	RES	Mod(Fx)	Arg(Fx)	Mod(Fy)	Arg(Fy)
0.10	0.75	0.207	0.455	0.2E-09	0.323	0.033	1.637	1.395
0.20	0.75	0.412	0.438	0.1E-07	0.646	0.115	1.457	1.261
0.30	0.75	0.605	0.432	0.2E-08	0.914	0.219	1.320	1.139
0.40	0.75	0.756	0.426	0.9E-08	1.091	0.313	1.209	1.026
0.50	0.75	0.857	0.413	0.2E-07	1.178	0.378	1.113	0.919
0.60	0.75	0.918	0.389	0.2E-07	1.202	0.407	1.027	0.815
0.70	0.75	0.953	0.356	0.1E-07	1.191	0.405	0.952	0.713
0.80	0.75	0.973	0.316	0.3E-07	1.162	0.380	0.885	0.613
0.90	0.75	0.984	0.271	0.6E-08	1.125	0.336	0.824	0.514
1.00	0.75	0.991	0.221	0.5E-07	1.086	0.280	0.768	0.414
1.50	0.75	1.000	-0.066	0.5E-08	0.908	-0.103	0.529	-0.106
2.00	0.75	0.985	-0.299	0.4E-07	0.775	-0.556	0.605	-0.384

Processor time=0.0648

Table A.8.6 Diffraction Results for a Semi-immersed Cylinder

SOURCES DISTRIBUTED ON CYLINDER BOUNDARY
NO NODES= 33 (LINEAR ELEMENTS)
ONE-POINT GAUSS QUADRATURE

ka	h/L	Mod(R)	Arg(R)	RES	Mod(Fx)	Arg(Fx)	Mod(Fy)	Arg(Fy)
0.10	0.75	0.204	0.455	0.1E-08	0.319	0.032	1.640	1.398
0.20	0.75	0.406	0.438	0.7E-09	0.638	0.112	1.460	1.265
0.30	0.75	0.597	0.432	0.1E-07	0.903	0.213	1.325	1.144
0.40	0.75	0.747	0.426	0.3E-07	1.079	0.306	1.214	1.032
0.50	0.75	0.849	0.412	0.2E-07	1.168	0.369	1.119	0.926
0.60	0.75	0.911	0.389	0.1E-07	1.195	0.398	1.036	0.823
0.70	0.75	0.948	0.356	0.1E-07	1.186	0.397	0.962	0.722
0.80	0.75	0.969	0.317	0.5E-07	1.159	0.372	0.897	0.623
0.90	0.75	0.981	0.272	0.2E-07	1.123	0.330	0.837	0.525
1.00	0.75	0.988	0.223	0.3E-07	1.085	0.274	0.783	0.427
1.50	0.75	1.000	-0.058	0.2E-07	0.909	-0.106	0.560	-0.078
2.00	0.75	0.994	-0.319	0.1E-09	0.777	-0.558	0.534	-0.444

Processor time=0.2401

Table A.8.7 Diffraction Results for a Semi-immersed Cylinder

SOURCES DISTRIBUTED ON INTERNAL BOUNDARY, RS= 0.70*CA
NO NODES= 12 (CONSTANT ELEMENTS)
ONE-POINT GAUSS QUADRATURE

ka	h/L	Mod(R)	Arg(R)	RES	Mod(Fx)	Arg(Fx)	Mod(Fy)	Arg(Fy)
0.10	0.75	0.210	0.463	0.4E-08	0.394	0.048	1.654	1.407
0.20	0.75	0.413	0.454	0.1E-07	0.734	0.141	1.479	1.286
0.30	0.75	0.601	0.445	0.3E-07	0.959	0.236	1.339	1.162
0.40	0.75	0.736	0.425	0.3E-07	1.068	0.296	1.225	1.039
0.50	0.75	0.838	0.409	0.1E-07	1.152	0.354	1.130	0.932
0.60	0.75	0.902	0.386	0.2E-08	1.180	0.383	1.048	0.830
0.70	0.75	0.940	0.354	0.1E-07	1.173	0.382	0.976	0.730
0.80	0.75	0.963	0.315	0.3E-08	1.148	0.358	0.911	0.631
0.90	0.75	0.976	0.271	0.2E-07	1.113	0.316	0.853	0.534
1.00	0.75	0.985	0.222	0.2E-08	1.076	0.261	0.801	0.437
1.50	0.75	0.997	-0.051	0.8E-07	0.900	-0.117	0.604	-0.045
2.00	0.75	0.999	-0.349	0.4E-07	0.767	-0.567	0.478	-0.530

Processor time=0.0331

Table A.8.8 Diffraction Results for a Semi-immersed Cylinder

SOURCES DISTRIBUTED ON INTERNAL BOUNDARY, RS= 0.70*CA
NO NODES= 16 (CONSTANT ELEMENTS)
ONE-POINT GAUSS QUADRATURE

ka	h/L	Mod(R)	Arg(R)	RES	Mod(Fx)	Arg(Fx)	Mod(Fy)	Arg(Fy)
0.10	0.75	0.208	0.466	0.6E-08	0.406	0.051	1.656	1.413
0.20	0.75	0.414	0.457	0.5E-08	0.750	0.146	1.479	1.291
0.30	0.75	0.600	0.447	0.6E-07	0.967	0.239	1.339	1.166
0.40	0.75	0.737	0.427	0.8E-08	1.073	0.299	1.223	1.042
0.50	0.75	0.838	0.411	0.2E-07	1.156	0.357	1.128	0.933
0.60	0.75	0.902	0.387	0.2E-07	1.184	0.385	1.046	0.831
0.70	0.75	0.940	0.355	0.4E-07	1.177	0.384	0.973	0.731
0.80	0.75	0.963	0.316	0.1E-07	1.151	0.361	0.908	0.633
0.90	0.75	0.976	0.272	0.1E-07	1.117	0.319	0.850	0.536
1.00	0.75	0.985	0.224	0.3E-07	1.080	0.265	0.798	0.440
1.50	0.75	0.997	-0.048	0.2E-06	0.904	-0.112	0.600	-0.041
2.00	0.75	0.999	-0.345	0.5E-07	0.771	-0.560	0.473	-0.525

Processor time=0.0635

Table A.8.9 Diffraction Results for a Semi-immersed Cylinder

SOURCES DISTRIBUTED ON INTERNAL BOUNDARY, RS= 0.70*CA
NO NODES= 32 (CONSTANT ELEMENTS)
ONE-POINT GAUSS QUADRATURE

ka	h/L	Mod(R)	Arg(R)	RES	Mod(Fx)	Arg(Fx)	Mod(Fy)	Arg(Fy)
0.10	0.75	0.207	0.469	0.7E-06	0.419	0.056	1.660	1.418
0.20	0.75	0.417	0.465	0.6E-07	0.790	0.160	1.482	1.301
0.30	0.75	0.607	0.465	0.1E-05	1.035	0.271	1.344	1.190
0.40	0.75	0.736	0.428	0.2E-07	1.078	0.301	1.222	1.044
0.50	0.75	0.912	0.422	0.2E-03	1.197	0.451	1.161	0.875
0.60	0.75	0.902	0.388	0.2E-06	1.187	0.387	1.044	0.833
0.70	0.75	0.941	0.356	0.1E-05	1.180	0.386	0.971	0.733
0.80	0.75	0.963	0.318	0.6E-06	1.155	0.363	0.907	0.635
0.90	0.75	0.977	0.274	0.8E-04	1.121	0.322	0.848	0.538
1.00	0.75	0.985	0.226	0.5E-06	1.084	0.267	0.795	0.442
1.50	0.75	0.998	-0.046	0.4E-06	0.908	-0.107	0.596	-0.037
2.00	0.75	0.999	-0.342	0.2E-05	0.776	-0.554	0.469	-0.519

Processor time=0.2269

Table A.8.10 Diffraction Results for a Semi-immersed Cylinder

SOURCES DISTRIBUTED ON INTERNAL BOUNDARY, RS= 0.70*CA
NO NODES= 13 (LINEAR ELEMENTS)
ONE-POINT GAUSS QUADRATURE

ka	h/L	Mod(R)	Arg(R)	RES	Mod(Fx)	Arg(Fx)	Mod(Fy)	Arg(Fy)
0.10	0.75	0.249	0.460	0.5E-02	0.413	0.114	1.667	1.432
0.20	0.75	0.416	0.467	0.4E-02	0.814	0.165	1.482	1.306
0.30	0.75	0.613	0.442	0.5E-01	0.970	0.200	1.360	1.134
0.40	0.75	0.731	0.431	0.1E-01	1.087	0.285	1.226	1.060
0.50	0.75	0.850	0.417	0.7E-03	1.154	0.382	1.122	0.927
0.60	0.75	0.892	0.381	0.6E-01	1.200	0.404	1.002	0.838
0.70	0.75	0.967	0.360	0.3E-01	1.195	0.393	0.953	0.738
0.80	0.75	1.010	0.299	0.6E-01	1.204	0.363	0.877	0.606
0.90	0.75	1.021	0.242	0.1E 00	1.112	0.251	0.835	0.488
1.00	0.75	1.013	0.246	0.5E-01	1.091	0.284	0.821	0.510
1.50	0.75	0.950	-0.013	0.8E-01	0.838	-0.091	0.560	-0.010
2.00	0.75	1.012	-0.319	0.3E-01	0.756	-0.485	0.498	-0.481

Processor time=0.0355

Table A.8.11 Diffraction Results for a Semi-immersed Cylinder

SOURCES DISTRIBUTED ON INTERNAL BOUNDARY, RS= 0.70*CA
NO NODES= 17 (LINEAR ELEMENTS)
ONE-POINT GAUSS QUADRATURE

ka	h/L	Mod(R)	Arg(R)	RES	Mod(Fx)	Arg(Fx)	Mod(Fy)	Arg(Fy)
0.10	0.75	0.207	0.476	0.5E-02	0.464	0.085	1.665	1.429
0.20	0.75	0.409	0.440	0.3E-01	0.733	0.068	1.469	1.294
0.30	0.75	0.594	0.446	0.3E-02	0.951	0.236	1.337	1.164
0.40	0.75	0.757	0.426	0.5E-01	1.077	0.291	1.220	1.046
0.50	0.75	0.850	0.410	0.2E-01	1.150	0.356	1.130	0.923
0.60	0.75	0.797	0.436	0.2E 00	1.155	0.583	0.977	0.820
0.70	0.75	1.026	0.382	0.2E 00	1.233	0.415	1.027	0.764
0.80	0.75	0.955	0.322	0.2E-01	1.154	0.373	0.900	0.642
0.90	0.75	0.981	0.274	0.9E-02	1.119	0.325	0.840	0.541
1.00	0.75	1.004	0.228	0.4E-01	1.090	0.251	0.796	0.466
1.50	0.75	1.000	-0.043	0.9E-03	0.910	-0.089	0.603	-0.053
2.00	0.75	1.000	-0.327	0.2E-02	0.759	-0.520	0.474	-0.492

Processor time=0.0607

Table A.8.12 Diffraction Results for a Semi-immersed Cylinder

SOURCES DISTRIBUTED ON INTERNAL BOUNDARY, RS= 0.70*CA
NO NODES= 33 (LINEAR ELEMENTS)
ONE-POINT GAUSS QUADRATURE

ka	h/L	Mod(R)	Arg(R)	RES	Mod(Fx)	Arg(Fx)	Mod(Fy)	Arg(Fy)
0.10	0.75	0.209	0.478	0.8E-02	0.442	0.069	1.667	1.421
0.20	0.75	0.406	0.454	0.4E-02	0.756	0.140	1.478	1.289
0.30	0.75	0.602	0.457	0.4E-04	1.005	0.256	1.341	1.180
0.40	0.75	0.732	0.439	0.5E-02	1.098	0.319	1.224	1.063
0.50	0.75	1.078	-0.484	0.2E 00	3.478	0.591	1.121	0.945
0.60	0.75	0.794	0.366	0.4E-01	0.841	0.227	1.048	0.896
0.70	0.75	4.969	0.255	0.3E 02	5.711	0.778	2.904	0.908
0.80	0.75	0.965	0.323	0.2E-02	1.160	0.400	0.870	0.634
0.90	0.75	1.009	0.279	0.6E-01	1.145	0.327	0.909	0.520
1.00	0.75	0.990	0.234	0.2E-01	1.075	0.312	0.803	0.456
1.50	0.75	1.264	-0.110	0.8E 00	1.115	-0.528	0.452	0.065
2.00	0.75	1.133	-0.384	0.3E 00	1.343	-0.455	0.582	-0.895

Processor time=0.2516

Table A.8.13 Diffraction Results for a Semi-immersed Cylinder

APPENDIX A.9 DIMENSIONAL ANALYSIS

This appendix contains the details of a dimensional analysis of the diffraction problem for a two dimensional obstacle of characteristic dimension, D, at a depth y_o. For wave motion in water of finite depth four independent variables are sufficient to describe the motion completely and the choices made in this analysis are the wave height H, the wavelength, L, the water depth, h and the acceleration of gravity, g. The final variables which must be included are the fluid density and kinematic viscosity.

The force, F, per unit length, ℓ, may be expressed as

$$\frac{F}{\ell} = f(\rho,\nu,D,y_o,H,L,h,g) \qquad A.9.1$$

The force per unit length may then be expressed in series form by

$$\frac{F}{\ell} = \Sigma C(\rho^a \nu^b D^c y_o^d H^e L^f h^i g^j) \qquad A.9.2$$

where C is a constant and a,b,c,d,e,f,i and j are indices. It is required that equation A.9.2 is balanced dimensionally and by inserting the dimensions of each variable an equation in the three primary dimensions mass M, length L and time T is obtained.

$$(MLT^{-2}L^{-1}) = (ML^{-3})^a (L^2T^{-1})^b (L)^c (L)^d (L)^e (L)^f (L)^i (LT^{-2})^j \qquad A.9.3$$

Collecting the indices of M, L and T three equations are obtained

for M $\quad 1 = a$ A.9.4a

for L $\quad 0 = -3a + 2b + c + d + e + f + i + j$ A.9.4b

for T $\quad -2 = - b - j$ A.9.4c

Elimination of the indices a,b & j in equation A.9.2 by substituting from equations A.9.4 gives

$$\frac{F}{\ell} = \Sigma C\rho(\nu^{2-2(1+c+d+e+f+i)/3} D^{c} y_o^{d} H^{e} L^{f} h^{i} g^{(1+c+d+e+f+i)/3}) \qquad \text{A.9.5}$$

which after a little algebra reduces to

$$\frac{F}{\ell} = \Sigma C\rho gDH(\nu^{-2/3} Dg^{1/3})^{c-1}(\nu^{-2/3} y_o g^{1/3})^{d}(\nu^{-2/3} Hg^{1/3})^{e-1}$$

$$X(\nu^{-2/3} Lg^{1/3})^{f}(\nu^{-2/3} hg^{1/3})^{i} \qquad \text{A.9.6}$$

From equation A.9.6 it is clear that the non-dimensional force may be expressed in the form $F/(\ell\rho gDH)$ but in determining the non-dimensional groups which may be obtained from the right hand side some choice may be exercised. Five non-dimensional groups are to be obtained from the right hand side of equation A.9.6 and the groups chosen are the diffraction parameter D/L, the cylinder depth parameter y_o/h, the wave steepness parameter, H/L and the water depth parameter h/L. Rearrangement of equation A.9.6 to obtain the required groupings gives

$$\frac{F}{\ell} = \Sigma C\rho gDH(D/L)^{c-1-f}(y_o/h)^{d-f}(H/L)^{e-1-f}(h/L)^{2i-f}(\nu^{-2/3} Lg^{1/3})^{4f}$$

A.9.7

If alternative groupings had been chosen for the water depth or cylinder depth parameter the final non-dimensional number ($\nu^{-2/3} Lg^{1/3}$) remains unchanged. This non-dimensional number may be written as

$$\nu^{-2/3} Lg^{1/3} = (L\sqrt{gL}/\nu)^{2/3} \qquad \text{A.9.8}$$

and introduction of a characteristic velocity U indicates that this group is the ratio of two non-dimensional groups

$$\frac{L\sqrt{gL}}{\nu} = \frac{UL}{\nu} \Big/ \frac{U}{\sqrt{gL}} \qquad \text{A.9.9}$$

where the numerator is the Reynolds number and the denominator is the square root of the Froude number. Finally the non-dimensional force may be expressed as

$$\frac{F}{\ell\rho gDH} = f(D/L,\ y_o/h,\ H/L,\ h/L,\ R_e/\sqrt{F_r}) \qquad \text{A.9.10}$$

It may be noted that if diffraction effects are expected to be small and the effects of flow separation significant the diffraction parameter, D/L, may be replaced by the Keulegan/Carpenter number, K. However, in general a dimensional analysis for objects which are small compared with the incident wavelength commences with the choice of different independent variables and the results is quite different and may be quoted in the form

$$\frac{F}{\ell\rho DU_m^{\,2}/2} = f(K,\ R_e,\ y_o/D,\ H/L,\ h/L) \qquad \text{A.9.11}$$

APPENDIX A.10 NOMENCLATURE

This appendix contains a list of the main symbols which are used in the text of the thesis. Any additional symbols which are used in the appendices are defined where they first occur.

$\underline{A}$	Kernel matrix
$\underline{A}_1, \underline{A}_2$	Real and imaginary kernel matrices
a	Radius of circular cylinder
a_n	Coefficients in Fourier series
$\underline{b}$	Vector containing known quantities in matrix equation
$\underline{b}_1, \underline{b}_2$	Real and imaginary parts of $\underline{b}$
b_n	Coefficients in Fourier series
C_i	Component of series form of Green's function
C_x, C_y	Horizontal and vertical components of the diffraction coefficient
c_{g1}	Group velocity of wave
c_{g2}	Group velocity of free wave oscillating at twice the wave frequency
c_i	Real positive roots of dispersion equation
D	Diameter of circular cylinder
F	Force
$F(t)$	Arbitrary function of time
F_r	Froude number
f_o	Fundamental frequency of wave
$f(\mu)$	Integrand of principal value integral
f_d	Second-order drift force
f_{kx}, f_{ky}	Components of Froude-Krylov force
f_x, f_y	Horizontal and vertical components of force

$G(\underline{x},\underline{\xi},t)$	Green's function
g	Acceleration of gravity
$g(\mu)$	Component of integrand of principal value integrand
$g(\underline{x},\underline{\xi})$	Spatial component of Green's function
g_o	Component of Green's function
g_1, g_2	Real and imaginary parts of spatial component of Green's function
H	Wave height
H_I	Incident wave height
H_i	Weights in quadrature formula
H_m	Measured wave height
H_s	Scanned wave height
H_{21}	Wave height of "fixed" second harmonic wave
H_{22}	Wave height of "free" second harmonic wave
H_{2t}	Theoretical wave height of "fixed" second harmonic wave
h	Water depth
$h(\mu)$	Component of integrand of principal value integral
$\underline{I}$	Unit matrix
$I(\mu)$	Component of integrand in principal value integral
$i = \sqrt{-1}$	
$i=1,....n$	Nodal numbering system
$\|J\|$	Jacobian
$j=i,....m$	Numbering system for sources on element
$k = 2\pi/L$	Wave number
k_2	Solution of dispersion equation for free second harmonic wave
$k=1,....p$	Numbering system for nodes on an element
L	Wavelength
L	Primary dimension of length
ℓ	Length of circular cylinder

$\ell=1,.....q$	Element numbering system
M	Primary dimension of mass
m	Number of sources per element
$\underline{m}(\partial/\partial x, \partial/\partial y) = \partial/\partial m$	Normal gradient on obstacle boundary at nodal location
$N_k(\underline{\xi})$	Lagrangian interpolation function of order k
n	Number of nodes in discretisation
$\underline{n} = (\partial/\partial x, \partial/\partial y) = \partial/\partial n$	Normal gradient on obstacle boundary at source loaction
n_x, n_y	Direction cosines for evaluation of forces
P_1	Energy loss coefficient
P_2	Energy loss coefficient corrected to account for free second harmonic wave
p	Pressure
p	Superfix indicating order of function in perturbation analysis
p	Number of nodes per element
p_m	Measured pressure amplitude
p_{2m}	Measured pressure amplitude at twice the wave frequency
p_{3m}	Measured pressure amplitude at three times the wave frequency
p_s	Scattered wave pressure amplitude
p_t	Theoretical pressure amplitude
p_w	Incident wave pressure amplitude
$Q(\underline{x},t)$	Right hand side of second-order free surface boundary condition
$q(\underline{x})$	Spatial component of $Q(\underline{x},t)$
q	Number of elements in discretisation scheme
R	Reflection coefficient
R	Tank reflection coefficient
R_1	Cylinder reflection coefficient for a wave oscillating at fundamental frequency

R_e	Reynolds' number
$R=\|\underline{x}-\underline{\xi}\|$	
$RAT=r_s/r_n$	
$r=\|x-\xi\|$	
r_n	Radius of obstacle of circular geometry
r_s	Radius of source boundary
$s_n\sqrt{a_n^2 + b_n^2}$	Amplitude of oscillation at frequency nf_o
T	Primary dimension of time
T	Transmission coefficient
T_1	Transmission coefficient for a wave oscillating at the fundamental frequency
T_2	Second-harmonic transmission coefficient
T_3	Third-harmonic transmission coefficient
t	Time variable
$\underline{x}=(x,y)$	Cartesian coordinates of field point
$\underline{x}$	Unknown vector in matrix equation
$\underline{x}_1, \underline{x}_2$	Real and imaginary part of unknown matrix
y_o	Depth of cylinder axis below still water level
$\Gamma(\underline{x})$	Source boundary
$\Gamma_o(\underline{x})$	Obstacle boundary
Γ_ε	Small circular boundary around field point
Γ_F	Fluid boundary
$\delta(\underline{x}-\underline{\xi})$	Dirac delta function
ε	Perturbation series parameter
ε	Radius of small circle about field point
$\eta(\underline{x},t)$	Free surface displacement
η_s	Free surface displacement of scattered wave
η_w	Free surface displacement of incident wave
μ	Doublet moment

μ	Local element coordinate system
μ	Variable in principal value integral
$\nu = \omega^2/g$	
$\underline{\xi} = (\xi,\eta)$	Source point
ρ	Fluid density
σ	Source density
$\sigma(\underline{x})$	Source density function
$\Phi(\underline{x},t)=\phi(\underline{x})e^{-i\omega t}$	Velocity potential
$\Phi_s(\underline{x},t)=\phi_s(\underline{x})e^{-i\omega t}$	Scattered wave velocity potential
$\Phi_w(\underline{x},t)=\phi_w(\underline{x})e^{-i\omega t}$	Incident wave velocity potential
$\phi^*(\underline{x},\underline{\xi})$	Singular harmonic function
$\phi_o^*(\underline{x},\underline{\xi})$	Regular harmonic function
$\psi(\underline{x})$	Potential function
Ω	Domain
Ω_F	Fluid domain
$\omega = 2\pi f_o$	Angular frequency

APPENDIX A.11 REFERENCES

Au, M.C. and Brebbia, C.A., 1982. Numerical prediction of wave forces using the boundary element method. Applied Mathematical Modelling, Vol. 6, pp. 218-228.

Bai, K.J. and Yeung, R., 1974. Numerical solutions of free surface problems. Proc. 10th Symp. Naval Hydrodyn., Cambridge, Mass., pp. 609-647.

Banerjee, P.K. and Butterfield, R., 1979. Developments in boundary element methods. Vol. 1, Applied Science (Development Series), London.

Banerjee, P.K. and Shaw, R.P., 1982. Developments in boundary element methods. Vol. 2, Applied Science (Development Series), London.

Bidde, D., 1971. Laboratory study of lift forces on circular piles. J. Wat.Ways Harb.Div. ASCE, Vol. 97, WW4, pp. 595-614.

Bird, H.W.K. and Shepherd, R., 1982. Wave interaction with large submerged structures. J. Wat.Ways Harb. Div. Am. Soc. Civ. Engrs., Vol. 10, WW2, May, pp. 146-162.

Boreel, L.J., 1974. Wave action on large offshore structures. Proc. Inst. Civil Eng. Conf. on Offshore Structures, London, pp. 7-14.

Chakrabarti, S.K., 1973. Wave forces on submerged objects of symmetry. J. Waterways Harbors and Coastal Eng. Div., ASCE, Vol. 99, No.WW2, pp. 147-164.

Coates, L.E., 1983. Wave forces on vertical cylinders - A numerical and experimental investigation. Ph.D. thesis. The City University, London.

Dean, R.G., 1965. Stream function representation of non-linear ocean waves. J. Geophys. Res., Vol. 70, No. 18, Sept., 4561.

Dean R.G. and Ursell, F., 1959. Interaction of a fixed, semi-immersed circular cylinder with a train of surface waves. Hydrodynamics Lab., M.I.T., Tech. Rept. No. 37, Mass.

Dean, W.R., 1948. On the reflection of surface waves by a submerged circular cylinder. Proc. Camb. Phil. Soc. Vol. 44, pp. 483-491.

Dixon, A.G., 1980. Wave forces on cylinders, Ph.D. thesis, University of Edinburgh.

Eatock Taylor, R., 1982. Developments in boundary element methods, Vol. 2, (Ed. Banerjee, P.K. and Shaw, R.P.). Applied Science (Development Series), London.

Ellix, D.M. and Arumugam, K., 1983. An experimental study of waves generated by an oscillating wedge. Paper submitted to the Journal of the International Association of Hydraulics Research.

Frank, W., 1967. Oscillations of cylinders in or below the free surface of deep fluids. Naval Ship Research and Development Center, Washington, D.C. Report 2375.

Fredholm, I., 1903. Sur une classe d'equations fonctionelles. Acta. Math. Vol. 27, pp. 365-390.

Garrison, C.J. and Chow, P.Y., 1972. Wave forces on submerged bodies. J. Waterways Harbors and Coastal Eng. Div., ASCE, Vol. 98, No. WW3, pp. 375-392.

Goda, Y. and Suzuki, Y., 1976. Estimation of Incident and Reflected Waves in Random Wave Experiments. Proc. 15th Coastal Eng. Conf., Honolulu, Vol. I, pp. 828-845.

Graham, J.M.R., 1979. Analytical methods of representing wave-induced forces on cylinders. in Mechanics of Wave-Induced Forces on Cylinders, (ed. T.L. Shaw), Pitman Advanced Publishing Program, London, pp. 133-151.

Havelock, T.H., 1929. Phil. Mag., Series 7, Vol. 8, pp. 569-576.

Havelock, T.H., 1940. The pressure of water waves upon a fixed obstacle. Proc. Royal Soc., London, Ser. A, Vol. 963, pp. 175-190.

Hearn, G.E. and Donati, E., 1981. Seakeeping theories - applying some choice. Trans. NECIES. Vol. 97, pp. 53-72.

Hearn, G.E., Donati, E and Mahendran, I.K., 1982. Prediction, measurement and comparison of fluid-structure interaction using mathematical and experimental models. Preprint of report. Dept. of Naval Arch., Univ. of Newcastle upon Tyne.

Hogben, N., 1974. Fluid loading on offshore structures, a state-of-the-art appraisal: wave loads. Maritime Tech. Monograph, No. 1, RINA.

Hogben, N., Miller B.L., Searle, J.W., and Ward, G., 1977. Estimation of fluid loading on offshore structures, Proc. Inst. Civil Eng., Vol. 63, pp. 515-562.

Hogben, N. and Standing R.G., 1974. Wave loads on large bodies. Proc. Int. Symp. on the Dynamics of Marine Vehicles and Structures in Waves, Univ. College, London, pp. 258-277.

Hunt, J.N. and Baddour, R.E., 1980a. Nonlinear standing waves bounded by cylinders. Quarterly Jornal of Mechanics and Applied Mathematics, Vol. 33, Part 3, pp. 357-371.

Hunt, J.N. and Baddour, R.E., 1980b. Second-order standing waves bounded by circular cylinders. Journal of the Waterways, Port, Coastal and Ocean Division, ASCE, Vol. 106, No. WW1, Proc. Paper 15166, Feb., pp. 122-127.

Hunt, J.N. and Baddour, R.E., 1981. The diffraction of nonlinear progressive waves by a vertical cylinder. Quarterly Journal of Mechanics and Applied Mathematics, Vol. 34, Part 1, pp. 69-87.

Hunt, J.N. and Baddour, R.E., 1982. Second-order wave forces on vertical cylinders. Journal of the Waterway, Port, Coastal and Ocean Division, ASCE, Vol. 108, No. WW3, pp. 430-434.

Hutchinson, R.S., 1979. An experimental investigation of wave-induced pressures on a vertical cylinder. Mechanics of Wave-Induced Forces on Cylinders (ed. T.L. Shaw), Pitman, London, pp.302-313.

Isaacson, M. de St. Q., 1974. The forces on circular cylinders in waves. Ph.D. Thesis submitted to the Department of Engineering, Univ. of Cambridge.

Isaacson, M. de St. Q., 1977a. Shallow wave diffraction around large cylinder. J. Waterway Port Coastal and Ocean Div., ASCE, Vol. 103, No. WW1, pp. 69-82.

Isaacson, M. de St. Q., 1977b. Nonlinear wave forces on large offshore structures. J. Waterway Port Coastal and Ocean Div. ASCE, Vol. 103, No. WW1, pp. 100-104.

Isaacson, M. de St. Q. and Maull, D.J., 1976. Transverse Forces on Vertical Cylinders in Waves. ASCE, Vol. 102, WW1, Paper No. 11934, pp. 49-60.

Jaswon, M.A., 1964. Integral equation methods in potential theory I. Proc. Royal Soc., Ser. A, Vol. 275, pp. 23-32.

Jaswon, M.A. and Symm, G.T., 1977. Integral Equation Methods in Potential Theory and Elastostatics. Academic Press, London.

Jeffrey, D.C., Richmond, D.J.E., Salter, S.H. and Taylor, J.R.M., 1976. 2nd Year Interim Rep. on Edinburgh Wave Power Project, Dept. of Mech. Eng., Univ. of Edinburgh.

John F., 1950. On the motion of floating bodies, II. Comm. Pure and Applied Mathematics, Vol. 3, pp.45-101.

Keulegan, G.H. and Carpenter, L.H., 1958. Forces on cylinders and plates in an oscillating fluid. J. Res. Nat. Bureau of Standards, Vol. 60, No. 5, pp. 423-440.

Kim, W.D., 1965. On the harmonic oscillation of a rigid body on a free surface. J.F.M., Vol. 21, pp. 427-451.

Korteweg, D.J. and De Vries, G., 1895. On the change of form of long waves advancing in a rectangular canal, and on a new type of long stationary waves. Phil. Mag., 5th Series, Vol. 39, pp.422-443.

Koterayama, W., 1979. Wave forces exerted on submerged circuler cylinders fixed in deep water. Reports on Research Institute of Applied Mechanics, Kyushu, Univ. Vol. 27, No. 84, pp. 25-46.

Lamb, Sir Horace, 1932. Hydrodynamics. (6th ed.), Dover Publications, New York.

Lau, C.S. 1983. Ph.D thesis, The City University, London. To be submitted.

Lighthill, J., 1979. Waves and hydrodynamic loading. Proc. 2nd Int. Conf. on the Behaviour of Off-Shore Structures, BOSS '79, London, Vol. I, pp. 1-40.

Longuet-Higgins, M.S. 1977. The Mean Forces Exerted by Waves on Floating or Submerged Bodies with Applications to Sand Bars and Wave Power Machines. Proc. Roy. Soc., London, Ser. A, Vol. 352, pp. 463-480.

Longuet-Higgins, M.S. and Cokelet, E.D., 1976. The deformation of steep surface waves on water. 1. A numerical method of computation. Proc. Roy. Soc., Ser. A., Vol. 350, pp. 1-25.

MacCamy , R.C. and Fuchs, R.A., 1954. Wave forces on piles: A diffraction theory. U.S. Army Corps of Engineers, Beach Erosion Board, Tech. Momo No. 69.

Maeda, H., 1974. Hydrodynamical forces on a cross section of a stationary structure. Proc. In. Symp. on the Dynamics of Marine Vehilces and Structures in Waves, Univ. College, London, pp. 80-90.

Martin, P.A., and Dixon, A.G., 1983. The scattering of regular surface waves by a fixed, half-immersed, circular cylinder. Applied Ocean Research, Vol. 5, No. 1, pp. 13-23.

Maull, D.J. and Norman, S.G., 1979. A horizontal circular cylinder under waves. Mechanics of wave-induced forces on cylinders (ed. T.L. Shaw), Pitman, London, pp. 359-378.

Miloh, T., 1980. Irregularities in solutions of nonlinear wave diffraction problem by vertical cylinder. Journal of the Waterway, Port, Coastal and Ocean Division, ASCE, Vol. 106, No. WW2, Proc. Paper 15385, May, pp. 279-284.

Mogridge, G.R. and Jamieson, W.W., 1975. Wave Forces on A Circular Caisson: Theory and Experiment. Can. J. Civil Eng., Vol. 2, pp. 540-548.

Monacella, V.J., 1966. The disturbance due to a slender ship oscillating in waves in fluid of finite depth. J. Ship Res., Vol. 10., p. 242.

Morison, J.R., O'Brien, M.P., Johnson, J.W. and Schaaf, S.A., 1950. The forces exerted by surface waves on piles. Petrol Trans., AIME, Vol. 189, pp. 149-154.

Murphy, J.E., 1978. Integral equation failure in wave calculations. J. Waterway Port Coastal and Ocean Div., ASCE, Vol. 104, No. WW4, pp. 330-334.

Naftzger, R.A. and Chakrabarti, S.K., 1979. Scattering of Waves by Two-Dimensional Circular Obstacles in Finite Water Depths, J. Ship Research, Vol. 23, pp. 32-42.

Newman, J.N., 1975. Ineraction of waves with two-dimensional obstacles: A relation between the radiation and scattering problems. JFM, Vol. 71, pp. 273-282.

Odabasi, A.Y. and Hearn, G.E., 1978. Seakeeping Theories - What is the choice? Trans. NECIES. Vol. 94, pp. 53-84.

Ogilvie, T.F., 1963. First and Second Order Forces on a Cylinder Submerged under a Free Surface, JFM, Vol. 16, pp. 451-472.

Oliveira, E.R.A., 1968. Plane stress analysis by general integral equation method. J. Eng. Mech. Div. ASCE, EM1, pp. 79-101.

Petrovski, I.G., 1957. Lectures on the theory of integral equations. Graylock Press, N.Y.

Patterson, C., and Sheikh, M.A., 1982. A regular boundary element method for fluid flow. Int. J. for Num. Meth. in Fluids, Vol. 2, pp. 239-251.

Salvesen, N., 1969. On higher-order theory for submerged two-dimensional bodies. JFM, Vol. 38, part 2, pp. 415-432.

Salvesen, N., 1974. Discussion of paper by Bai and Yeung (1974), see above.

Sarpkaya, T., 1976. Vortex shedding and resistance in harmonic flow about smooth and rough circular cylinders at high Reynolds numbers. Report No. NPS-59SL76021, Naval Posgraduate School, Monterey, CA.

Sarpkaya, T. and Isaacson, M. de St. Q., 1981. Mechanics of wave forces on offshore structures. Van Nostrand Reinhold Co., New York.

Schiller, F.C., 1971. Wave forces on a submerged horizontal cylinder, Master's thesis, Naval Postgraduate School, Monterey, Calif., Report No. AD 727 691, 99 pp.

Smithies, F., 1958. Integral Equations. University Press, Cambridge. (Cambridge tracts in mathematics and mathematical physics, No. 49).

Standing, R.G., Dacunha, N.M.C. and Matten, R.B., 1981. Mean wave drift forces: theory and experiment. National Maritime Institute. NMI R 124.OT-R-8175.

Stokes, G.G., 1847. On the theory of oscillating waves. Trans. Camb. Phil. Soc., Vol. 8, pp. 441-455. Also Math. Phys. Papers, Vol. 1, Camb. Univ. Press, 1880.

Symm, G.T., 1964. Integral equation methods in potential theory II. Proc. Roy. Soc., Ser. A, Vol. 275, pp. 33-46.

Thorne, R.C., 1953. Multipole expansion in the theory of surface waves, Proc. Cambridge Phil. Soc., Vol. 49, p. 707.

Tuck, E.O., 1965. The effect of non-linearity at the free surface on flow past a submerged cylinder. JFM, Vol. 22, Part 2, pp. 401-414.

Ursell, F., 1948. On the heaving motion of a circular cylinder on the surface of a fluid, Quart. J. Mech. Appl. Math., Vol. 2, p.218.

Ursell, F., 1950a. Surface waves on deep water in the presence of a submerged circular cylinder,I. Proc. Camb. Phil. Soc., Vol. 46, pp. 141-152.

Ursell, F., 1950b. Surface waves on deep water in the presence of a submerged circular cylinder, II. Proc. Camb. Phil. Soc., Vol. 46, pp. 153-158.

Ursell, F., 1953. Short surface waves due to an oscillating immersed body. Proc. Royal Soc. of London, Series A, Vol. 220, p. 90.

Ursell, F., Dean, R., and Yu, Y., 1960. Forced small amplitude water waves; a comparison of theory and experiment, JFM, Vol. 7, pp. 33-52.

Van Oortmerssen, G., 1972. Some aspects of very large offshore structures. Proc. 9th Symp. Naval Hydrodynamics, Paris, pp. 957-1001.

Vinje, Maogang, Brevig, 1982. A numerical approach to non-linear ship motion. Fourteenth symposion on Naval Hydrodynamics. University of Michigan.

Wehausen, J.V., 1971. The motion of floating bodies. Ann. Rev. Fluid Mech., Vol. 3, pp. 237-268.

Wehausen, J.V. and Laitone, E.V., 1960. Surface waves. In Handbuch der Physik, ed. S. Flugge, Springer-Verlag, Berlin, Vol. IX, pp. 446-778.

Whitham, G.B., 1962. Mass, momentum and energy flux in water waves. JFM, Vol. 12, pp. 135-147.

Yu, Y.S. and Ursell, F., 1961. Surface waves generated by an oscillating circular cylinder on water of finite depth: Theory and experiment. JFM, Vol. 11, pp. 529 - 551.